Sara E. Monaco
Lisa A. Teot *Editors*

# Pediatric Cytopathology

## A Practical Guide

Springer

# Pediatric Cytopathology

Sara E. Monaco • Lisa A. Teot
Editors

# Pediatric Cytopathology

## A Practical Guide

Springer

*Editors*
Sara E. Monaco, MD
Associate Professor
Director of Fine Needle Aspiration
Biopsy Service, Children's Hospital
of Pittsburgh of UPMC
Department of Pathology
University of Pittsburgh Medical Center
(UPMC)
Pittsburgh, PA, USA

Lisa A. Teot, MD
Department of Pathology
Boston Children's Hospital
Boston, MA, USA

ISBN 978-3-662-53439-7 ISBN 978-3-662-53441-0 (eBook)
DOI 10.1007/978-3-662-53441-0

Library of Congress Control Number: 2016958612



Printed on acid-free paper

This Springer imprint is published by Springer Nature
The registered company is Springer-Verlag GmbH Germany
The registered company address is: Heidelberger Platz 3, 14197 Berlin, Germany

*Sara E. Monaco, MD*
*To my parents, husband, and children Eddie, Julia,*
*and Nicholas for their endless love and support.*

*Lisa A. Teot, MD*
*To my parents, for their love and for always believing in me,*
*and to Mark, for his love, quiet support,*
*and calm understanding.*

# Foreword

Pediatric cytopathology is so much more than just another area of our expanding specialty. It is as heavily dominated by tumor diagnosis as other branches, but, involving children and teenagers as it does, this arena evokes a heightened sense of crisis to parents, patients, and ourselves as practitioners. Most pediatric tumors are potentially lethal if left untreated, and many of them present acutely. At the same time, prospects of cure or at least significant remission with appropriate therapy are generally far greater than encountered with most common tumors of adults. This is therefore an area wide open for early, quick, and accurate cytodiagnosis to enable rapid determination of tumor type, with molecular and genetic characteristics. At the same time, exclusion of malignancy by confident demonstration of benign lesions, many of them inflammatory, enables rapid institution of appropriate treatment and gives relief to all that neoplasia is not involved.

With this in mind, it may appear that there would be a plethora of texts on pediatric cytopathology. This is not the case; pediatric tumors are generally uncommon in the population at large; few generalists are able to develop daily expertise in all but a few tumor types. Into this significant gap comes the awaited text by Dr. Sara Monaco, of the Children's Hospital, University of Pittsburgh, and Dr. Lisa Teot of Boston Children's Hospital. Both authors draw on a wealth of experience and involvement in pediatric cytopathology. It is clear that they both embody enviable expertise, gained over time at their large academic institutions with active pediatric programs. Not only are they immersed in microscopy but also in active collection of cytologic material from young and apprehensive patients, often accompanied by parents, the latter experiencing one of the most grave circumstances a child's parent may know. This is a fraught environment many pathologists never encounter.

This major text will be a standard and a benchmark in cytopathology. It will serve all practitioners in this most necessary of specialty areas. It combines basic experience with up-to-date concepts in an accessible and readable text, generously illustrated with clear color images. The chapters are well ordered and fully comprehensive, incorporating not only microscopic diagnoses but immunochemical and molecular data as well.

A significant feature of this book is the inclusion of numerous informative tables, enabling the practitioner to readily view comprehensive differential diagnoses in an easily accessible format. The authors have created these new clear and concise aids which perfectly complement both the text and the images. With this format, the book presents itself both as a reliable reference

and as a ready desk handbook to be used at the microscope when viewing unusual and challenging entities.

This new text is an essential addition to every cytopathology departmental library and is geared for use by cytopathologists and cytotechnologists alike. Moreover, for surgical pathologists tasked with looking at rare pediatric tumors, the book enables knowledgeable viewing of unusual entities. Sara Monaco and Lisa Teot have given us an important and much anticipated volume which will be used for years to come.

Gladwyn Leiman, MD
University of Vermont Medical Center
Burlington, VT, USA

# Preface

Pediatric cytopathology is a challenging area of anatomic pathology. This is due in part to the limited use of cytology as a diagnostic modality in the pediatric age group, particularly in North America, and in part to the different spectra of diseases encountered in this population as compared to adults. With the increased use of minimally invasive techniques to obtain diagnostic specimens from pediatric patients, the need has evolved for a current reference focused on the cytopathology of entities that are either unique to or more common in children and adolescents.

The aim of this book is to provide an up-to-date reference focusing on the cytomorphology of the common and uncommon entities encountered in the pediatric population, richly illustrated with full-color, high-resolution images. Challenges and diagnostic pitfalls are also highlighted. Each chapter includes tables which summarize key points, as well as features used to resolve the differential diagnosis.

This book is intended to be a concise yet comprehensive reference for practicing pathologists and cytopathologists, pediatric pathology fellows, cytopathology fellows, residents in anatomic pathology, pediatricians, and pediatric subspecialists. We hope that it will serve as a practical and useful guide and enhance the skills of those involved in the practice of pediatric cytopathology.

Sara E. Monaco, MD
Children's Hospital of Pittsburgh of UPMC
Pittsburgh, PA, USA

Lisa A. Teot, MD
Boston Children's Hospital
Boston, MA, USA

# Acknowledgements

We acknowledge the hard work and dedication of our cytopathology laboratories, in Pittsburgh and Boston, including our cytotechnologists and trainees, in addition to the efforts of our clinicians and technical staff.

# Contents

# Contributors

**Michelle Dubb, MBBCh, FCPath, FRCPath** Cytology Unit, Department of Anatomical Pathology, Faculty of Health Sciences, University of the Witwatersrand and National Health Laboratory Service, Johannesburg, South Africa

**Samir B. Kahwash, MD** Department of Pathology and Laboratory Medicine, Nationwide Children's Hospital, Columbus, OH, USA

Department of Pathology, The Ohio State University College of Medicine, Columbus, OH, USA

**Pamela Michelow, MBBCh, MSc (Med Sci)** Cytology Unit, Department of Anatomical Pathology, Faculty of Health Sciences, University of the Witwatersrand and National Health Laboratory Service, Johannesburg, South Africa

**Sara E. Monaco, MD** Department of Pathology, University of Pittsburgh Medical Center (UPMC) & Children's Hospital of Pittsburgh of UPMC, Pittsburgh, PA, USA

**Christopher R. Pierson, MD, PhD** Department of Pathology and Laboratory Medicine, Nationwide Children's Hospital, Columbus, OH, USA

Department of Pathology, The Ohio State University College of Medicine, Columbus, OH, USA

Department of Biomedical Education and Anatomy, The Ohio State University College of Medicine, Columbus, OH, USA

**Anita L. Sengupta, MD** Department of Pathology, Children's Medical Center, Dallas, TX, USA

**Lisa A. Teot, MD** Department of Pathology, Boston Children's Hospital, Harvard Medical School, Boston, MA, USA

# Introduction

1

Sara E. Monaco and Lisa A. Teot

## 1.1 Introduction

Fine needle aspiration (FNA) is a reliable, minimally invasive, cost effective technique for obtaining samples from superficial and deep mass lesions for pathologic evaluation. Despite these advantages, physicians in the USA have been slow to embrace FNA as a primary diagnostic modality in the pediatric population. Obstacles to the acceptance and use of FNA include diagnostic challenges posed by the overall rarity and spectrum of tumors seen in children and adolescents, the experience and biases of clinicians and pathologists, and practical and technical considerations. Cytopathologists who are experienced in the performance and interpretation of FNAs may have limited familiarity with the spectrum and morphologic appearances of tumors seen in the pediatric population. Conversely, pediatric pathologists who are familiar with the histologic features and differential diagnosis of tumors encountered in children and adolescents often have little experience performing and/or interpreting FNAs. Likewise, clinicians who have extensive experience performing endoscopic or endobronchial ultrasound guided FNAs may have little experience with endoscopy or bronchoscopy of pediatric patients, and vice versa. These factors can impact the quality of the specimen and/or interpretation and lead to the need for a second procedure in order to arrive at a definitive diagnosis, thereby limiting the value of FNA as a diagnostic modality. Practical considerations include the cognitive and emotional maturity of the child or adolescent, and the need for immobilization, sedation, or anesthesia. Alone or in combination, these and other challenges and limitations have contributed to reluctance on the part of both pathologists and clinicians to promote the use of FNA as a primary diagnostic modality in the pediatric population. In contrast, exfoliative cytology is routinely used in the evaluation of cerebrospinal fluid and respiratory tract specimens from children and adolescents, and smears and crush preparations are standard methods for intraoperative assessment of pediatric central nervous system lesions.

## 1.2 Spectrum of Practice

The use of FNA as a primary diagnostic modality in the pediatric population varies with geographic location, practice setting, and clinical environment (Table 1.1) [1]. With respect to geographic

S.E. Monaco, MD (✉)
Department of Pathology, University of Pittsburgh Medical Center (UPMC) & Children's Hospital of Pittsburgh of UPMC, Pittsburgh, PA, USA
e-mail: monacose@upmc.edu

L.A. Teot, MD
Department of Pathology, Boston Children's Hospital, Harvard Medical School,
300 Longwood Avenue, Boston, MA 02115, USA
e-mail: Lisa.Teot@childrens.harvard.edu



S.E. Monaco, L.A. Teot (eds.), *Pediatric Cytopathology*, DOI 10.1007/978-3-662-53441-0_1

**Table 1.1** Factors influencing the use of FNA in the pediatric population

| |
|---|
| • Geographic location (resource-limited, resource-rich) |
| • Type of practice (academic, community) |
| • Presence of a free-standing pediatric hospital |
| • Organization of practice (subspecialty based or general pathology) |
| • Clinical environment (experience with and acceptance of FNA, referral patterns) |
| • Availability of physicians trained in performance and interpretation of fine needle aspiration |
| • Sensitivity and performance of fine needle aspiration (diagnostic vs. inadequate or non-diagnostic specimens, definitive or narrowed diagnoses that effectively guide management vs. nonspecific diagnoses/need for additional biopsy) |

location, 86 % of the world's pediatric population lives in resource-limited or developing countries where malignancies in children and adolescents comprise a greater percent of all cancers and have a higher mortality rate than in the USA and Europe [2]. In countries where access to medical care, diagnostic imaging, and more invasive procedures such as core or excisional biopsy is limited, FNA is routinely used for the primary evaluation of suspected malignancies in the pediatric population and has proven to be an accurate diagnostic tool [3, 4]. In contrast, FNA is rarely used for the primary diagnosis of pediatric malignancies in the USA where there is widespread access to more invasive diagnostic modalities and where risk stratification and treatment are often based on histologic diagnosis.

Within the USA and other resource-rich countries, the volume of pediatric FNAs can also vary greatly in different practice settings. Clinicians who have had positive experiences with FNA as a diagnostic modality are more likely to consider referring patients for FNA or to recommend the use of FNA to their colleagues, than those who have had negative experiences. Acquisition of an adequate specimen, appropriate triage, and diagnostic expertise are all required for providing a high quality FNA service. Adequate samples can be obtained by pathologists, interventional radiologists, and/or clinicians with appropriate training and expertise in performing FNAs. However, within a given institution, the type(s) and availability of qualified physicians impacts whether FNAs are performed in inpatient and/or outpatient settings, or not at all, and whether the lesions sampled are superficial and/or deep. Appropriate triage of the specimen is essential when ancillary studies are needed for a definitive or narrowed differential diagnosis. Rapid on site evaluation (ROSE) not only allows assessment of adequacy, but also guides appropriate triage of the specimen. However, ROSE can be time consuming and is deemed economically impractical in some practice settings. The availability of pathologists and/or cytotechnologists to perform ROSE can have a significant impact on whether the procedure results in a definitive or narrowed differential diagnosis and thus, on the use of FNA rather than a more invasive core or open biopsy for the primary evaluation of a mass lesion in a child or adolescent. Finally, the expertise required for accurate cytologic diagnosis of pediatric lesions is more likely to be found in settings with subspecialty-trained cytopathologists and pediatric pathologists, and can have a positive impact on the use of FNA. In general, the key elements for the acceptance and successful use of FNA as a diagnostic modality in the pediatric population are more likely to be found in an academic institution than in a community hospital.

Geographic location and practice setting also influence the type and pathologic spectrum of pediatric lesions evaluated by FNA. In resource-limited countries, malignancies comprise the majority of lesions diagnosed by FNA [4], while in resource-rich countries benign processes predominate [1]. Moreover, in resource-limited countries, a greater proportion of malignancies diagnosed by FNA are primary and/or deep-seated tumors than in resource-rich countries. In the USA, primary cytologic diagnosis of malignancies is rare; rather, FNA is primarily used for the evaluation of superficial masses, the majority of which are benign and located in the head and neck [1]. It is important to note that this

pattern is observed even in institutions with robust pediatric FNA services and, in part, reflects the fact that Children's Oncology Group therapeutic protocols are based on histologic diagnosis and associated biologic studies require frozen or formalin-fixed tissue.

## 1.3 Diagnostic Considerations

Mass lesions in children and adolescents raise different diagnostic considerations than those in adults. In the pediatric population, malignancies are rare and comprised predominantly of hematolymphoid and central nervous system neoplasms. In contrast, in the adult population, cancer is common and epithelial neoplasms account for the vast majority of malignancies. Unlike in adults, small changes in age can significantly alter the differential diagnostic considerations in the pediatric population [5]. Table 1.2 lists the three most common types of malignancies in different age groups, and illustrates the changes observed with small increments of age. The types of tumors seen in a given anatomic site also vary with age. In the kidney, for example, mesoblastic nephroma is usually diagnosed in the first 3 months of life, whereas Wilms tumor is most common in children under 5 years of age, and renal cell carcinoma primarily affects adolescents. A variety of genetic syndromes are also associated with increased risk of developing certain pediatric tumors, as illustrated by the increased risk of Wilms tumor in children with Beckwith–Wiedemann, WAGR (Wilms tumor, aniridia, genitourinary malformation, and mental retardation), and Denys–Drash syndromes. Awareness of the types of tumors that arise at different ages in various anatomic locations and of the associations between genetic syndromes and certain types of tumors is important for accurate cytologic diagnosis of pediatric mass lesions.

**Table 1.2** Cancer incidence by age group in children based on data from the Automated Childhood Cancer Information System ([5], adopted from ref. [2])

| Age group | Tumor category |
|---|---|
| Infants (less than 1 y.o.) | #1: Sympathetic nervous system tumors |
| | #2: Leukemia |
| | #3: CNS tumors |
| Young children (1–4 y.o.) | #1: Leukemias |
| | #2: CNS tumors |
| | #3: Renal tumors |
| School-age children (5–9 y.o.) | #1: CNS tumors |
| | #2: Leukemias |
| | #3: Lymphomas |
| Older school-age children or young adolescents (10–14 y.o.) | #1: Lymphomas |
| | #2: Leukemias |
| | #3: CNS tumors |
| Older adolescents (15–19 y.o.) | #1: Lymphomas |
| | #2: Carcinomas |
| | #3: Germ cell tumors |

In addition to these considerations, morphologic similarities between pediatric malignancies can pose diagnostic challenges. Many of the most common pediatric malignancies are small round blue cell tumors, while a variety of benign and malignant neoplasms have spindle cell morphology. Ancillary studies, such as immunoperoxidase stains, flow cytometry, fluorescence in situ hybridization, and/or other molecular tests, are usually required for definitive diagnosis, thereby making appropriate triage of these specimens critical. Treatments for many of these tumors vary considerably and thus, an accurate, specific diagnosis is essential. In contrast, for benign and low-grade spindle cell neoplasms for which treatment consists of surgical excision and for non-rhabdomyosarcomatous high-grade spindle cell sarcomas for which chemotherapy is the same, it may be sufficient to exclude certain entities and provide a narrowed differential diagnosis.

## 1.4 Conclusion

This book will provide a practical reference for pathologists evaluating cytologic specimens from pediatric patients. It is organized in an organ-based manner to address the spectrum of lesions seen in this population, and highlights important ancillary studies and differential diagnostic considerations.

## References

1. Monaco SE, Teot LA. Cytopathology of pediatric malignancies: where are we today with fine-needle aspiration biopsies in pediatric oncology? Cancer Cytopathol. 2014;122:322–36.
2. Sullivan R, Kowalczyk JR, Agarwal B, et al. New policies to address the global burden of childhood cancers. Lancet Oncol. 2013;14:e125–35.
3. Drut R, Drut RM, Pollono D, et al. Fine-needle aspiration biopsy in pediatric oncology patients: a review of experience with 829 patients (899 biopsies). J Pediatr Hematol Oncol. 2005;27:370–6.
4. Razack R, Michelow P, Leiman G, et al. An interinstitutional review of the value of FNAB in pediatric oncology in resource-limited countries. Diagn Cytopathol. 2012;40:770–6.
5. Steliarova-Foucher E, Stiller C, Kaatsch P, et al. Geographical patterns and time trends of cancer incidence and survival among children and adolescents in Europe since the 1970s (the ACCIS project): an epidemiological study. Lancet. 2004;364:2097–105.

# Fine Needle Aspiration in Pediatric Patients: Approach and Technique

2

Sara E. Monaco and Lisa A. Teot

## 2.1 Introduction

The statement "children are not just small adults" applies not only to clinical medicine, but also to pathology, as evidenced by formal recognition of pediatric pathology as a subspecialty. Successful use of fine needle aspiration (FNA) for the pathological evaluation of pediatric lesions poses special challenges and requires consideration of the patient's level of cognitive and emotional maturity, awareness of the diseases that occur in this population, and knowledge of the cytological features of those entities.

In children and adolescents, as in adults, FNA has the advantage of being a minimally invasive technique for obtaining diagnostic material from mass lesions. In experienced hands and in the appropriate clinical context, FNA has a sensitivity of approximately 97–98 % and a specificity of 93–97 % [1, 2]. In the pediatric population, use of FNA is particularly beneficial for evaluation of superficial lesions, many of which are reactive or infectious in origin. In this setting, FNA can confirm the benignity of the lesion and in some cases, provide a specific diagnosis through the use of ancillary studies, while avoiding the greater risks of core or open biopsy. For both benign and malignant lesions, on-site evaluation at the time of the procedure is important and can help to ensure adequacy, guide appropriate triage and, thereby, minimize the likelihood of a non-diagnostic specimen. When the FNA is performed by someone other than the pathologist, on-site evaluation also affords an opportunity to provide important feedback to the proceduralist and, for suboptimal specimens, may allow conversion to core biopsy, thereby averting the need for a second diagnostic procedure at a later time. While it is desirable to avoid the need for a repeat FNA or additional biopsy irrespective of the patient's age, subjecting a child or adolescent to a second procedure may be particularly burdensome to the patient and family in terms of emotional distress, the costs associated with time away from school, work, and caring for siblings and, in some cases, the need for sedation or anesthesia, none of which is trivial.

This chapter will highlight some of the key factors to consider when performing FNAs on pediatric patients.

S.E. Monaco, MD (✉)
Department of Pathology, University of Pittsburgh Medical Center (UPMC) & Children's Hospital of Pittsburgh of UPMC, Pittsburgh, PA, USA
e-mail: monacose@upmc.edu

L.A. Teot, MD
Department of Pathology, Boston Children's Hospital, Harvard Medical School,
300 Longwood Avenue, Boston, MA 02115, USA
e-mail: Lisa.Teot@childrens.harvard.edu



S.E. Monaco, L.A. Teot (eds.), *Pediatric Cytopathology*, DOI 10.1007/978-3-662-53441-0_2

## 2.2 Pre-procedural Evaluation

The pathologist who performs an FNA serves as a consultant to the referring clinician and therefore, usually meets the patient and parent(s) or legal guardian for the first time at the time of the FNA. Ideally, the referring physician or physician extender communicates to the pathologist in writing his or her clinical suspicions and any pertinent history, physical findings, laboratory results, and/or imaging studies on which they are based, as well as any relevant pending studies. This can occur through a medical record to which the pathologist has access or through a letter or written request for consultation in cases in which the medical records are inaccessible to the pathologist. Oral communication initiated either by the clinician at the time of referral or by the pathologist when written communication from the referring clinician is lacking is an acceptable alternative, although less desirable due to the possibility of errors. The pathologist should review the patient's medical record when it is accessible, irrespective of any communication with the referring clinician. Ideally, information from the referring clinician and/or medical record provides the pathologist with important background data that may or may not be elicited at the time of FNA, but is not intended to replace communication between the pathologist and the patient and parent(s) or legal guardian. In addition to conveying important medical information, communication between the referring clinician and pathologist provides an opportunity to address key issues related to consent, such as who a minor child's legal guardian is and the need for an interpreter (see Sect. 2.3).

### 2.2.1 Clinical History

As noted above, the initial encounter between the pathologist performing an FNA and the child and parent(s) or legal guardian is usually at the time of the procedure. A successful interaction with the child and parent(s) or legal guardian requires appreciation of the child's level of apprehension, which may range from virtually absent to intense and is shaped by cognitive and emotional maturity, prior experiences with medical personnel and vaccinations, the degree to which the child has been prepared for the FNA, and his or her expectations around the procedure. Wearing street clothes rather than a white coat, and engaging the child in age appropriate conversation or other interactions prior to obtaining a clinical history and performing a physical examination can help to establish rapport with the child, as well as the parent(s) or legal guardian. At each stage of the encounter, it is important to include the child in the conversation at his or her cognitive level and talk with the child at his or her eye level, rather than simply talking about the child with the parent(s) or legal guardian. This is particularly important when the patient is a school age child or adolescent.

Clinical history is helpful for formulating a differential diagnosis and can provide important clues to the correct diagnosis. It is important to obtain a clinical history directly from the patient and/or parent(s) or legal guardian, rather than simply relying on information communicated by the referring clinician and/or contained in the medical record. Beyond helping to establish rapport with the patient and parent(s) or legal guardian, this allows the pathologist to validate the clinical history provided elsewhere and resolve any potentially important discrepancies or omissions. For example, when a child is referred with lymphadenopathy, there should be a discussion about exposure to cats or other animals, as well as any recent travel. The qualities of the lesion and how they have changed over time are also important. A mass lesion that has persisted and enlarged over a short period of time is more concerning for a malignancy than a lymph node that fluctuates in size over time. Results of laboratory tests, serologic studies, and microbiologic cultures can also be helpful. For example, in developed countries, many children and adolescents presenting with persistent lymphadenopathy will have had a tuberculin skin test, monospot test, Epstein–Barr virus (EBV) IgM and IgG titers, and *Bartonella* titers. Having the results of these tests can be very helpful when approaching the evaluation of these cases, although results may

not be available at the time of the procedure or may not have been conveyed to the parent(s) or legal guardian by the ordering clinician.

### 2.2.2 Physical Examination

After obtaining a history, a directed physical examination establishes the size of the lesion, its mobility (freely mobile or fixed), contour (ill- or well-defined), texture (soft, doughy/cystic, or firm), and any associated tenderness. This tactile contact with the patient not only allows the pathologist to guage the patient's level of anxiety about the procedure, but may also help the patient to feel more comfortable with the pathologist. When examining a school age child or adolescent, especially of the opposite gender, it is suggested that the pathologist be accompanied by a nurse or other health care assistant. Parents can be asked to leave or may stay, depending on the preference of the child.

## 2.3 Informed Consent

Prior to performing the FNA, informed consent is obtained. This includes an explanation of the procedure, its benefits, potential complications, and risks, including a non-diagnostic aspirate and the need for a second diagnostic procedure, and alternatives to FNA. The consent form is signed and dated by the physician and the patient's legal guardian, which in most cases is the parent. The consent form becomes part of the medical record. For children under the age of 18, who cannot legally consent to undergoing a procedure, it is imperative that the pathologist confirm prior to the appointment who will be accompanying the child and who the legal guardian is. If someone other than the legal guardian or parent will accompany the child, then it is important to obtain informed consent from the legal guardian or parent beforehand, usually by telephone with at least one witness. This occurs most often when a child who is in a foster home or other institution is accompanied by someone other than the legal guardian, but can also arise when a child is accompanied by a relative, such as a grandparent, who is not the legal guardian. A social worker or risk management personnel can usually help to determine and, if necessary, locate the legal guardian. However, this can take time and may delay or necessitate rescheduling of the procedure if not done beforehand. Of note, the consent laws of about 30 states and the District of Columbia give patients who are minors but are parents, married, or pregnant the legal capacity to consent for a procedure, while the remaining states have no explicit policy or law [3]. It is also recommended that, as part of the consent process, assent be obtained from school age children and adolescents to confirm that they are willing to undergo the FNA and to ease their anxiety. When obtaining consent and/or assent, it is important to be at eye level, to turn off all electronic devices that could be a distraction, to use basic language rather than medical terminology, and to make sure that the parent(s) or legal guardian and child understand what they have been told, are given the opportunity to ask questions and that their questions are answered to their satisfaction. When necessary, an interpreter employed by the facility in which the FNA is performed should be provided to ensure that the parent(s) or legal guardian and child understand the pathologist's explanations, have had their questions answered satisfactorily and are truly giving informed consent.

## 2.4 Equipment

The equipment required for the FNA procedure includes syringes, needles (22–27G), a syringe holder, such as the Cameco Syringe Pistol, glass slides, pencil or permanent marking pen, spray fixative or Coplin jar with 95 % alcohol, slide folders or plastic slide holders, staining solutions, sterile tubes, formalin-filled containers, alcohol wipes, gauze, band-aids, and personal protective equipment (Figs. 2.1 and 2.2). In the pediatric setting, it can be helpful to have colorful band-aids with patterns, superheroes, or other characters that children can identify with. These items can be stored in a labeled basket or cart for convenience

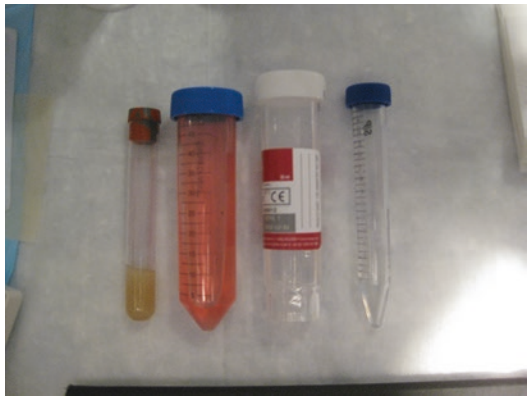

**Fig. 2.1** Supplies for pediatric FNAs. Multiple supplies are needed during pediatric FNAs because of the variety of ancillary studies that may be required. It is usually helpful to have a variety of different containers (shown from *right* to *left*), including sterile tube for microbial cultures (*right*), liquid based cytology containers (e.g., Thin Prep™; *middle right*), container with fresh cold Roswell Park Memorial Institute (RPMI) media for flow cytometry (*middle left*), and tiger-top blood collection tubes (*left*) for tapping needles that have clotted material.


**Fig. 2.3** An FNA basket utilized to carry materials to procedures. A crate or sturdy plastic tool box can be used to hold the materials needed for an FNA and allows the pathologist to be mobilized quickly to perform an FNA on a child in an outpatient clinic, operating room, or inpatient setting. An opaque container also maintains patient confidentiality when carrying materials back to the cytology laboratory after a procedure.

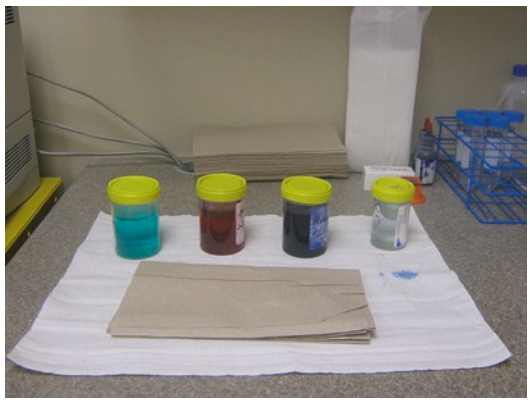

**Fig. 2.2** Diff-Quik staining supplies. If on-site evaluation is performed, a rapid stain is necessary, such as a Romanowsky-type stain, like Diff-Quik. The staining takes less than 1 minute and is performed on air-dried smears. These slides can be examined without coverslipping.

(Figs. 2.3 and 2.4). If on-site evaluation and preliminary diagnosis are desired, then a microscope is also required, which can be placed on a mobile cart or in a permanent location in sites where FNAs are frequently performed (Fig. 2.4). A papoose or large blanket to wrap a child's extremities can also be very helpful to immobilize the non-sedated patient who is unable to cooperate (Fig. 2.5).

**Fig. 2.4** FNA cart utilized for on-site evaluations. If on-site evaluation of an FNA is required, then an FNA cart stocked with a microscope and all necessary supplies is important.


**Fig. 2.5** Papoose for immobilization of non-sedated pediatric patients. These immobilization devices allow the child to lie down on the flat board, while soft cloth arms are wrapped and secured around the child's arms and legs to prevent them from moving during the FNA procedure.

## 2.5 Fine Needle Aspiration Procedure

FNAs are performed by pathologists and other physicians in a variety of locations, including outpatient clinics, the operating room, at the bedside of hospitalized patients, and in the radiology suite. For non-palpable masses detected by imaging, CT or ultrasound (US) guidance should be used to perform the FNA. In addition to interventional radiologists, some pathologists are qualified to perform US-guided FNAs and may use portable ultrasound equipment in the clinic, operating room, or at the bedside. The techniques involved in US-guided FNA are beyond the scope of this discussion, which will be confined to FNA of palpable lesions. Prior to beginning the FNA, a "time out" is performed and documented to confirm the procedure, the patient's name and unique identifiers, and the location (anatomic site and laterality) of the FNA. This pause allows everyone to confirm that the correct procedure is performed on the correct patient and the correct lesion.

### 2.5.1 Palpation and Immobilization of the Lesion

The first steps in performing an FNA are palpation and immobilization of the lesion. Palpation is performed at the time of physical examination to investigate the size, mobility, contour and consistency of the mass, and presence or absence of associated tenderness. It is repeated prior to sampling primarily to confirm the location and accessibility of the lesion. Before proceeding with immobilization and sampling of the lesion, children who are developmentally unable to cooperate and are not under general anesthesia must be securely positioned with a nurse and/or parent helping to immobilize their arms and legs. If the child is strong or there are not enough people to assist with the procedure, then a papoose can be utilized to secure the child (Fig. 2.5). In some cases the FNA is performed under conscious sedation or general anesthesia at the request of the parent and/or discretion of the clinician. An ideal time to perform an FNA is when the child is undergoing general anesthesia for another procedure (e.g., FNA of an enlarged cervical lymph node during anesthesia for placement of myringotomy tubes) and can be optimally positioned with no movement; however, this is not an option in all cases. Once the patient is immobilized, the lesion itself can be immobilized with the fingers of the non-dominant hand, usually the index and middle fingers in order to reserve the thumb for stabilizing the needle and syringe holder. In young or anxious patients, topical anesthetic, such as 4 % topical lidocaine cream, can be applied prior to the procedure to decrease discomfort during the FNA and is typically tolerated better than subcutaneous injection of 1 % lidocaine with 1:100,000 epinephrine.

### 2.5.2 Performing the Fine Needle Aspiration

An FNA typically involves 3–5 needle passes with 22, 23, 25, or 27 gauge disposable hypodermic needles with long bevels. If aspiration is used, a syringe holder is helpful because it allows one to aspirate with one hand and stabilize the target with the other. Most syringe holders accommodate a 10cc syringe, which is easier to manage than those designed for 20cc syringes. Once the lesion is immobilized, the skin overlying the aspiration site is disinfected with an alcohol swab or iodine scrub. The needle is then inserted and a sweeping motion back and forth within the lesion is utilized for about 15 quick excursions or until material appears in the hub of the needle. FNAs can be performed with or without suction. A comparison of these methods is summarized in Table 2.1. FNAs utilizing suction are helpful for obtaining more abundant material for ancillary studies and for draining cystic lesions; however, the increased distance between the aspirating hand and the lesion limits the fine motor control and the size of the device may increase the patient's apprehension (Fig. 2.6). FNAs performed without suction (capillary method, Zajdela technique, French method, or "non-aspiration aspiration") usually yield less material, but the aspirates tend to be less bloody and relatively more cellular making it ideal for sampling highly vascular lesions, such as thyroid nodules (Fig. 2.7). This approach may also cause less anxiety for a young patient because the equipment is limited to a small needle, which is more modest in scale and can be hidden discretely in the operator's hand. It also offers better fine motor control because of the shorter distance between the lesion and the operator's hand. This makes it the optimal technique for sampling small, mobile lesions or lesions in non-sedated or anxious patients who are likely to move during the procedure.

**Fig. 2.6** FNA performed with suction (Swedish technique). This FNA is performed with a syringe holder containing a 10cc syringe, which allows the operator to use negative pressure during the aspirate with one hand, while the non-dominant hand stabilizes the lesion and the patient.

**Table 2.1** Comparison of FNA techniques with and without suction

| | Fine needle aspiration without suction | Fine needle aspiration with suction |
|---|---|---|
| Other terminology | French, Zjadela technique, fine needle non-aspiration aspiration, capillary method | Swedish technique |
| Uses | • Vascular lesions<br>• Small lesions<br>• Lesions that are very mobile and require optimal fine motor control<br>• Pediatric patients or anxious patients that are not under anesthesia | • Cysts<br>• Cases requiring material for ancillary studies<br>• Cases with low yield using non-aspiration techniques in order to try to obtain greater cellularity |
| Advantages | • Better fine motor control<br>• Concentrated specimen with less blood (qualitative)<br>• Absence of syringe holder may decrease anxiety for the patient | • Cystic lesions (to drain material)<br>• Can obtain more material (quantitative) |
| Disadvantages | • Less material and potentially dry tap<br>• Cannot drain a cystic lesion | • Greater chance of peripheral blood dilution<br>• Less fine motor control<br>• Syringe holder may create anxiety for patient |

**Fig. 2.7** FNA performed without suction (non-aspiration method). This FNA is performed with the needle only, without a syringe, thereby allowing for better fine motor control and possibly, decreasing the patient's anxiety.

## 2.6 Slide Preparation andTriaging Material for Ancillary Studies

After performing each pass, the aspirated material is expelled onto a labeled glass slide(s) using a syringe filled with air and is then smeared to create a monolayer or near monolayer of cells that can be stained and examined (Fig. 2.8). The smearing technique involves sliding a second clean glass slide on top of the slide containing the aspirated material. The preparation of optimal smears takes time and practice, as too much material on a slide results in a thick smear that is difficult to interpret, too much pressure may cause crushing of fragile cells, and improper fixation can lead to artifactual changes limiting the morphological evaluation (Figs. 2.9 and 2.10). If smears are to be alcohol fixed, then submersion in the fixative should be immediate to avoid air-drying artifact. Papanicolaou staining is superior for nuclear detail and to identify squamous cells. However, Romanowsky-type stains enhance nuclear pleomorphism due to slight nuclear enlargement with air-drying, and highlight background (extracellular) elements like mucin and stromal material. Romanowsky-type stains are usually preferred for rapid on-site evaluation in the pediatric setting because they are take less than a minute to perform and are especially useful for evaluation of lymphoid morphology and

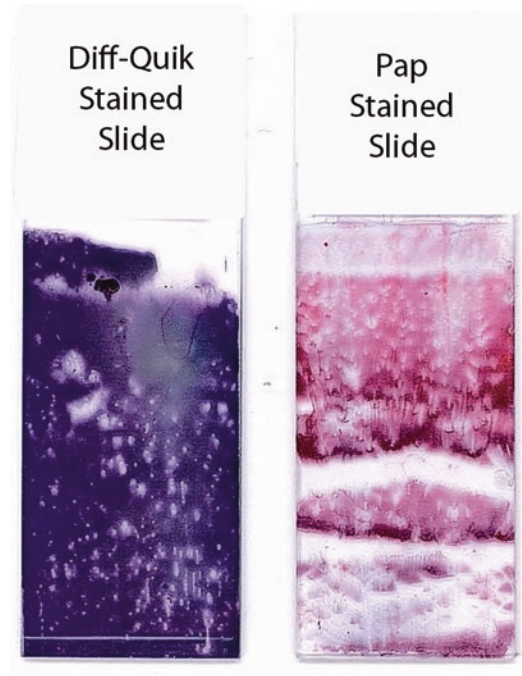


**Fig. 2.8** Aspirate smears from FNA. Once material is aspirated, it is expelled onto a slide and spread into a monolayer or near monolayer for staining and evaluation with a variety of different stains.

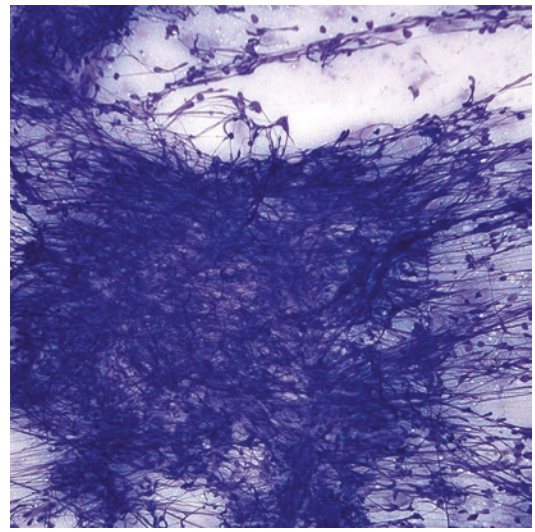

**Fig. 2.9** Artifactual changes in lymphoid cells (Diff-Quik stain, medium power). The act of smearing and other preparation-related issues can cause crush artifact, which is most pronounced in fragile cells, such as lymphocytes, and this is sometimes called a "lymphoid tangle".

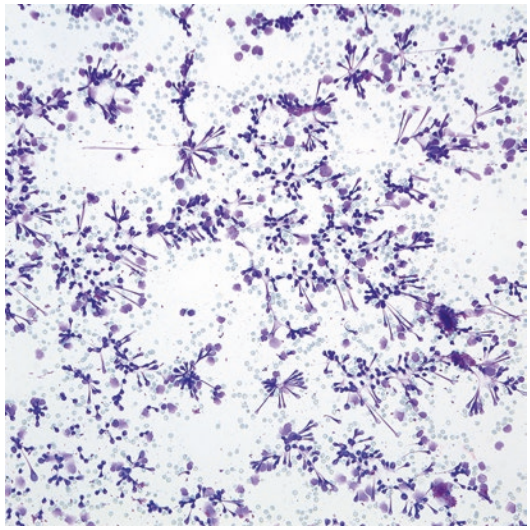

**Fig. 2.10** Artifactual changes in lymphoid cells (Diff-Quik stain, medium power). The act of smearing and other preparation-related issues can cause artifactual changes, which are most pronounced in fragile cells, such as lymphocytes, and can make the cytological evaluation difficult.

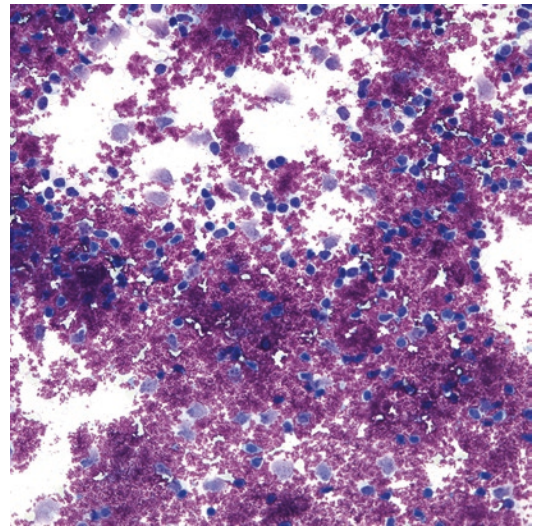

**Fig. 2.11** Ultrasound gel artifact (Diff-Quik stain, high power). In ultrasound-guided FNAs, if there is residual gel on the needle that is not wiped off before smearing, the gel can appear as metachromatic, crystalline-like material that obscures the cells of interest.

discrimination of lymphoid proliferations from other small round cell tumors. In US-guided FNAs, the ultrasound gel can obscure the smears and make interpretation difficult (Fig. 2.11). Thus, wiping the excess gel from the needle prior to expelling the material can be helpful.

Following expulsion of material onto slides, the needles are rinsed in RPMI, phosphate buffered saline or a fixative such as formalin or CytoLyt™. RPMI and phosphate buffered saline allow eventual triage of material to flow cytometry and/or cytogenetics, as well as cell block preparation, and therefore, are suggested media for rinsing needle(s) prior to on-site evaluation. Following on-site evaluation, needles from additional and/or dedicated passes can be rinsed in the medium or media deemed most appropriate for triaging the specimen.

## 2.7 Documentation

At the conclusion of the FNA, the pathologist should complete, date, and sign a note documenting the procedure and, if performed, on-site evaluation. In addition, appropriate requisition form(s) should be completed and accompany the slides and any additional samples for ancillary studies. A sample intraoperative procedure note is presented in Table 2.2.

## 2.8 Post-procedure Laboratory Handling of the FNA Specimen

When the FNA procedure is complete, all slides and containers should be labeled clearly with at least two patient identifiers and the type of specimen (site and laterality). In addition, all paperwork should be completely filled out and signed in the appropriate places.

The material obtained by FNA typically includes aspirate smears that either need to be coverslipped (Romanowsky-type stained slides) or stained and coverslipped (alcohol-fixed slides). The needle rinses and/or the material obtained from dedicated passes for ancillary studies can be triaged in a variety of ways, depending on the differential diagnosis. For example, if a lesion yields

**Table 2.2** Sample intraoperative procedure note for pediatric FNA biopsies

| *Pre-procedural information* |
|---|
| Topical lidocaine cream was applied 30 minute prior to the procedure by the nursing team.<br>The patient was seen and examined by _____.<br>Physical examination: # cm lesion noted to be mobile/fixed, soft/firm, tender/non-tender, round/ill-defined, in the _____location.<br>The potential risks of the procedure including infection, bleeding, bruising, and inadequate sampling with the possibility of additional diagnostic procedures were explained to the patient's parent/guardian by Dr._____. Informed consent was obtained from the patient's parent/guardian by Dr._____ and witnessed by _____. Assent was obtained from the patient. |
| *Procedural information* |
| A time out was performed prior to the procedure and documented by Dr._____.<br>Procedure: FNAB, # passes with #G needle measuring # in. in length.<br># air-dried and # wet-fixed smears were prepared.<br>Needles were rinsed in saline/RPMI/formalin [Free text for additional triaging of specimens]. Patient tolerated procedure well. No complications.<br>The findings were communicated to and confirmed by the [Physician/Physician extender] at the conclusion of the procedure on [date] at [time].<br><br>Signature of physician performing the FNA, date, time. |
| *Immediate On-site evaluation reporting* |
| Date: mm/dd/yyyy Time stamp: hh:mm<br>Part #, Pass #<br>Site, Laterality, Procedure:<br>A. Adequacy determination: Adequate/Less than optimal/Inadequate<br>B. Primary Interpretation: Non-diagnostic/Benign/Defer/Malignant<br>C. Free text<br>D. Reason for terminating procedure: Adequate material obtained/Other.<br><br>The findings in this case were communicated to and confirmed by [Physician/ Physician Extender] at the conclusion of the procedure on [date] at [time].<br><br>Signature of physician performing the on-site evaluation, date, time. |

**Fig. 2.12** FNA with suppurative material from a patient with a soft tissue abscess. The material aspirated is thick, turbid, yellow pus from the site of infection, and can be triaged for microbial cultures and determination of antibiotic sensitivities.

suppurative material, then material is usually reserved in sterile tubes to be sent to microbiology for culture and antibiotic sensitivities (Fig. 2.12). Needle rinses from worrisome hematolymphoid proliferations can be sent for flow cytometry to immunophenotype the cells, establish clonality, and aid in subclassification of a hematolymphoid malignancy. Cell blocks can also be prepared from residual material and can be used for hematoxylin and eosin-stained slides, special stains, immunostains, or molecular studies. Liquid based cytology (LBC) preparations, such as ThinPrep™ and SurePath™, are helpful for hypocellular aspirates, bloody aspirates, and cyst fluids in order to maximize the cellular yield and decrease obscuring blood. Hypocellular cyst aspirates in children can be difficult to classify without the presence of cyst lining cells, and LBC can be very helpful in these scenarios (Figs. 2.13 and 2.14).

## 2.9 Final Interpretation

After review of the slides and results of ancillary studies, a diagnosis is rendered and verified by the pathologist. It is important to correlate the results of ancillary studies with the morphological findings

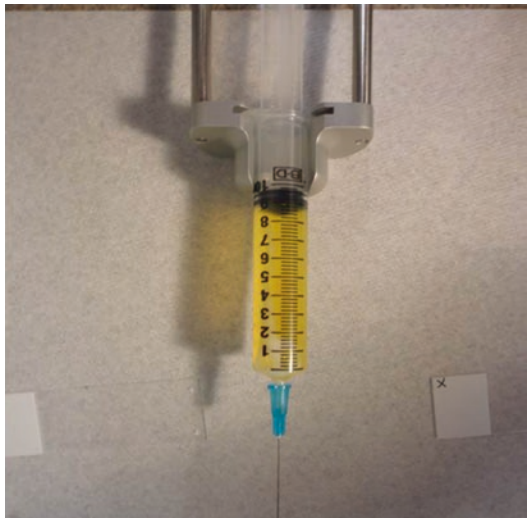

**Fig. 2.13** FNA of cyst contents from a cystic neck mass. The fluid aspirated from this cystic lesion is translucent and yellow. These tend to be very hypocellular, and the use of liquid based cytology may improve the ability to concentrate the specimen and identify cyst lining cells.

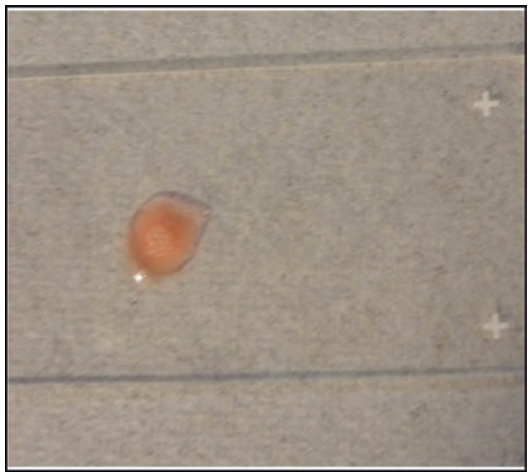

**Fig. 2.14** FNA material from a branchial cleft cyst. Aspirate material from a branchial cleft cyst is expelled onto a slide and appears more watery, thin, and translucent than the suppurative material seen in Fig. 2.12.

to arrive at a definitive cytologic diagnosis or, when that is not possible, a differential diagnosis and to provide the referring clinician with as much information as possible. Furthermore, when the pathologist renders a diagnosis of a malignancy or other neoplasm, it is helpful to discuss the case directly with the referring physician in order to ensure that he or she receives the results in a timely fashion and is able to expedite notification of the family.

## 2.10 Conclusions

The approach to FNA in the pediatric population differs from that in adults, as highlighted in this chapter. Awareness of special considerations, including obtaining consent for an FNA, approaching the patient in a way that minimizes anxiety, and establishing appropriate immobilization of the patient, can help to maximize the success of a pediatric FNA. As illustrated, cytological material can be utilized for almost any ancillary study, and thus, knowledge of the differential diagnosis and what testing is required to arrive at a diagnosis are critical for optimizing one's yield from these procedures.

## References

1. Drut R, Drut RM, Pollono D, et al. Fine-needle aspiration biopsy in pediatric oncology patients: a review of experience with 829 patients (899 biopsies). J Pediatr Hematol Oncol. 2005;27:370–6.
2. Razack R, Michelow P, Leiman G, et al. An interinstitutional review of the value of FNAB in pediatric oncology in resource-limited countries. Diagn Cytopathol. 2012;40:770–6.
3. State policies in brief: an overview of minors' consent law. 2015. http://www.guttmacher.org/statecenter/spibs/spib_OMCL.pdf

# Lymph Nodes

3

Sara E. Monaco

## 3.1 Introduction

Fine needle aspiration (FNA) cytology offers a minimally invasive modality for evaluating lymphadenopathy in pediatric patients. In the majority of children and adolescents, lymphadenopathy is due to reactive lymphoid hyperplasia or infection and in this setting, the use of FNA can avoid more invasive and unnecessary core or open biopsies, provide a relatively rapid diagnosis, and by confirming benignity, alleviate the anxiety of patients and/or families [1–5]. Moreover, when coupled with appropriate ancillary studies, FNA allows specific diagnosis of many benign and malignant causes of lymphadenopathy. Overall, the diagnostic accuracy for lymph node FNAs has been reported to be approximately 90 %, with a sensitivity of about 85–95 % and specificity of 98–100 % [4–6].

S.E. Monaco, MD (✉)
Department of Pathology, University of Pittsburgh Medical Center (UPMC) & Children's Hospital of Pittsburgh of UPMC, Pittsburgh, PA, USA
e-mail: monacose@upmc.edu

## 3.2 Approach to the Evaluation of Lymphadenopathy in Children and Adolescents

### 3.2.1 Gross Examination

At the time of FNA, note the color, consistency and amount of aspirated material, and the presence or absence of fluid indicative of a cystic lesion. If cystic fluid is obtained, note whether it appears purulent, suggesting an infectious process, and in this scenario, material should be reserved for microbial cultures. Mucoid, watery, or bloody aspirates are more suggestive of a non-lymphoid lesion. Non-diagnostic aspirates often yield a dry tap or bloody material, whereas adequate lymphoid aspirates usually are composed of finely granular, opaque material that is easy to smear.

### 3.2.2 Low Power Microscopic Examination

Dyscohesion is characteristic of benign and malignant lymphoid populations (Fig. 3.1), but does not exclude non-lymphoid entities. Any clustering raises the possibility of metastatic non-lymphoid malignancy, granulomatous inflammation, germinal center fragments, or technical artifacts, such as a thick smear, suboptimal spreading technique, or blood clot [7] (Fig. 3.2).



S.E. Monaco, L.A. Teot (eds.), *Pediatric Cytopathology*, DOI 10.1007/978-3-662-53441-0_3

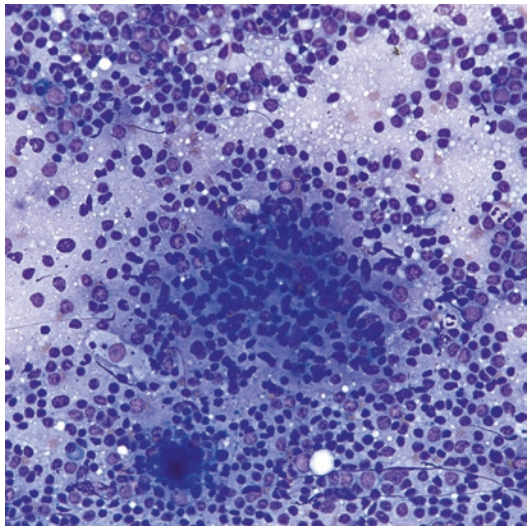

**Fig. 3.1** Reactive lymphadenopathy (Diff-Quik stain, medium power). This case of reactive lymphadenopathy shows a follicle-like organization, in which the lymphoid cells cluster together with tingible body macrophages. The lymphoid population appears polymorphous, which is helpful in excluding a lymphoid malignancy.

### 3.2.3 High Power Microscopic Examination

The presence of lymphoglandular bodies is an important diagnostic feature of benign and malignant lymphoid populations (Fig. 3.1). When lymphoglandular bodies are present supporting a lymphoid proliferation, the next step is to assess the homogeneity or heterogeneity of the constituent cells, the size(s) of the cells, and the presence or absence of tingible body macrophages. The size of lymphoid cells is usually described in relation to a histiocyte nucleus or 2–3 red blood cells, with small, intermediate and large lymphoid cells being smaller than, the same size as, and larger than the nucleus of a histiocyte, respectively. The size of the predominant population helps to narrow the differential diagnosis. Features suggestive of malignancy include a homogeneous lymphoid population, predominance of large cells, marked pleomorphism, and/or an absence of tingible body macrophages, and should prompt collection of additional material for flow cytometry, cell block, and/or fluorescence in situ hybridization (FISH). In the setting of clinical findings suggestive of lymphoma, such as extensive lymphadenopathy or an elevated LDH, the presence of numerous mitotic figures and tingible body macrophages should also lead one to consider a high-grade lymphoma, such as Burkitt lymphoma. In contrast, features of reactive lymphoid proliferations include a heterogeneous population of cells with a predominance of small mature lymphocytes, lymphohistiocytic aggregates, and scattered tingible body macrophages (Fig. 3.1). Other features that provide important clues to the differential diagnosis include the presence or absence of other hematolymphoid cells (including eosinophils, neutrophils, plasma cells and histiocytes), granulomas, necrosis, and non-hematolymphoid cells.

#### Differential Diagnosis

Causes of lymphadenopathy in children and adolescents are summarized in Table 3.1, which categorizes the entities based on whether they are benign or malignant and common or uncommon (Figs. 3.3, 3.4, and 3.5). Differential diagnostic considerations based on eight morphologic patterns are listed in Table 3.2 and those based on the size of the predominant population are listed in Table 3.3. Primary lymphoid malignancies must be distinguished from metastatic small round cell tumors, which are summarized in Table 3.4.

#### Pearls

- Avoid examination of areas on a slide with artifactual distortion, such as crush artifact or air-drying artifact, where the cells appear poorly preserved and/or pale (Fig. 3.2).
- The key features to evaluate in lymph node aspirates from children and adolescents include: presence or absence of cohesion; the type of lymphoid population (heterogeneous versus homogeneous); the size(s) of the constituent cells; the presence or absence of certain cell types (macrophages and/or granulomas, plasma cells, immunoblasts, eosinophils, neutrophils, and non-hematolymphoid cells); and the background (clean versus necrotic).

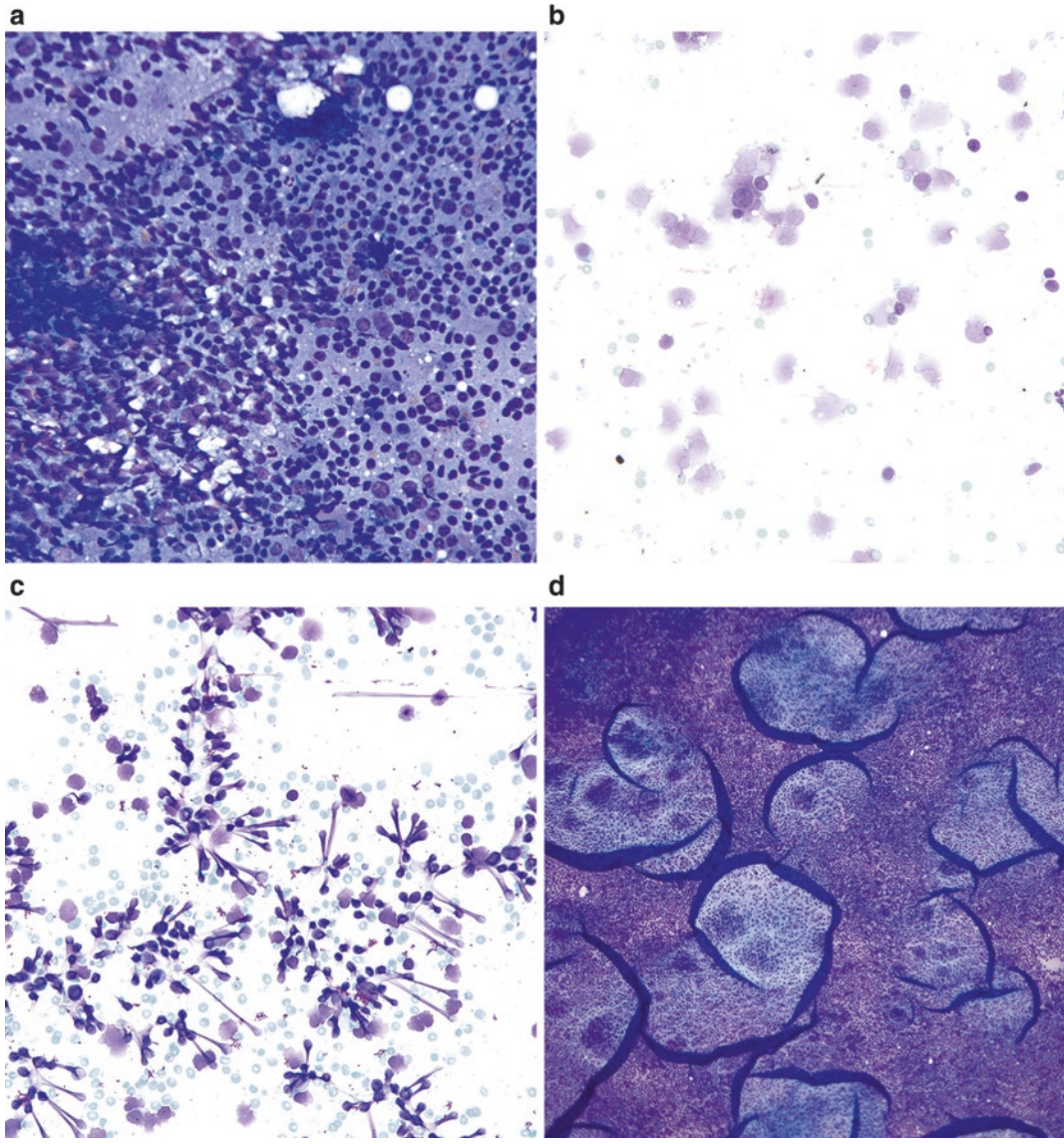


**Fig. 3.2** Reactive lymphoid hyperplasia with artifact (**a**–**c**. Diff-Quik stain, medium power; **d**. Diff-Quik stain, low power). Some cases of reactive lymphoid hyperplasia have artifactual changes such as air-drying artifact (**a**, **b**) and crush artifact (**c**), that can make the cells appear, paler (**a**), blown up (**b**) or spindled (**c**), and may raise concern for a metastatic neoplasm or lymphoproliferative disorder. In addition, when smears are too thick, the cytological features and lymphoglandular bodies may be difficult to identify (**d**).

## 3.3 Mimics of Lymphadenopathy

Some lesions, particularly superficial masses in the head and neck, mimic a lymph node clinically and/or radiologically due to their well-circumscribed nature and location, but prove to be other structures or processes on pathological examination. It is important to be aware of these entities and recognize their cytological features to ensure appropriate management. Pediatric head and neck lesions that can mimic lymphadenopathy are listed in Table 3.5 and selected lesions are illustrated in Fig. 3.6. Aspirates from ectopic thymic tissue yield a lymphoid population with a predominance of small lymphocytes,

**Table 3.1** Summary of benign and malignant causes of lymphadenopathy in children and adolescents

| | | |
|---|---|---|
| Benign | Common | • Reactive lymphoid hyperplasia<br>• Acute suppurative and/or granulomatous lymphadenitis<br>• Infection, including Epstein–Barr virus, *Bartonella* (cat scratch disease), atypical mycobacteria, and *M. tuberculosis* |
| | Uncommon | • Sinus histiocytosis with massive lymphadenopathy (Rosai-Dorfman Disease)<br>• Dermatopathic lymphadenitis<br>• Histiocytic necrotizing lymphadenitis (Kikuchi disease)<br>• HIV-associated lymphadenopathy<br>• Drugs (e.g., Dilantin, methotrexate)<br>• Vaccines<br>• Foreign body/iatrogenic<br>• Metabolic/storage disorders<br>• Autoimmune disease, including systemic lupus erythematosus, rheumatoid arthritis, autoimmune lymphoproliferative syndrome<br>• Chronic granulomatous disease<br>• Nodal extramedullary hematopoiesis<br>• Fungal or parasitic infection |
| Malignant | Common | • Acute lymphoblastic leukemia/lymphoma<br>• Hodgkin lymphoma<br>• Non-Hodgkin lymphomas, including diffuse large B- cell lymphoma, Burkitt lymphoma, and T-cell lymphomas |
| | Uncommon | • Small B-cell non-Hodgkin lymphoma<br>• Metastatic malignancies |

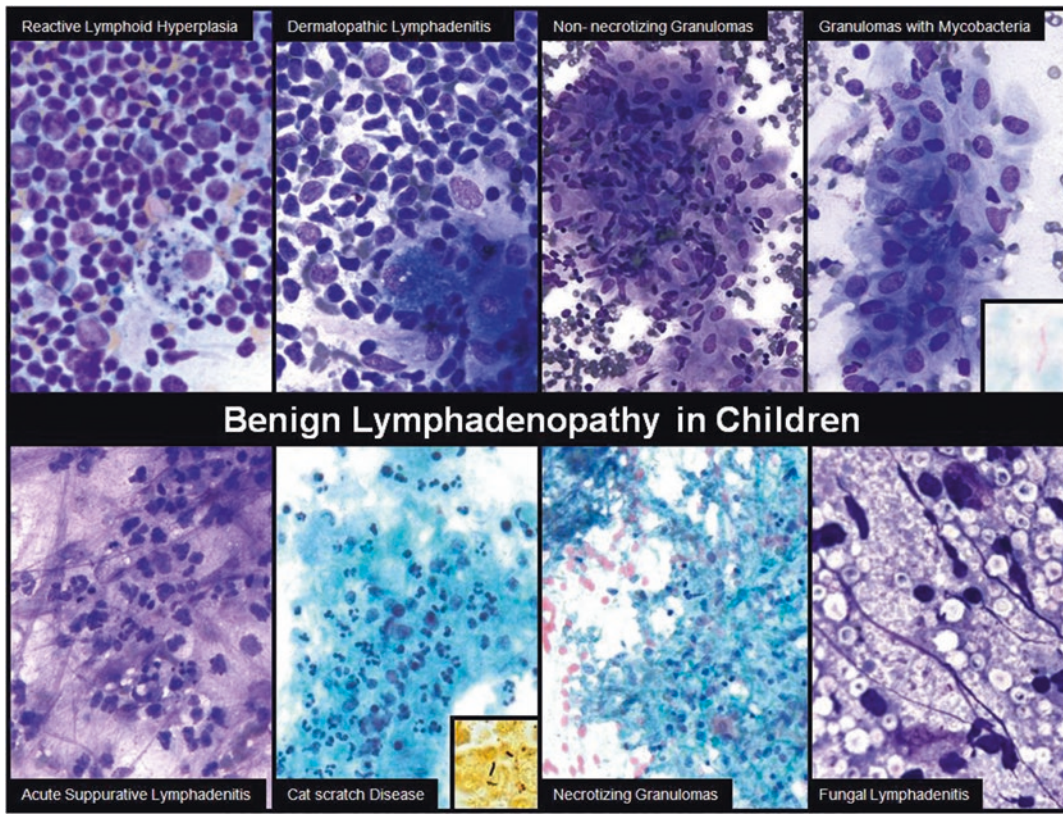


**Fig. 3.3** Composite of benign causes of pediatric lymphadenopathy.

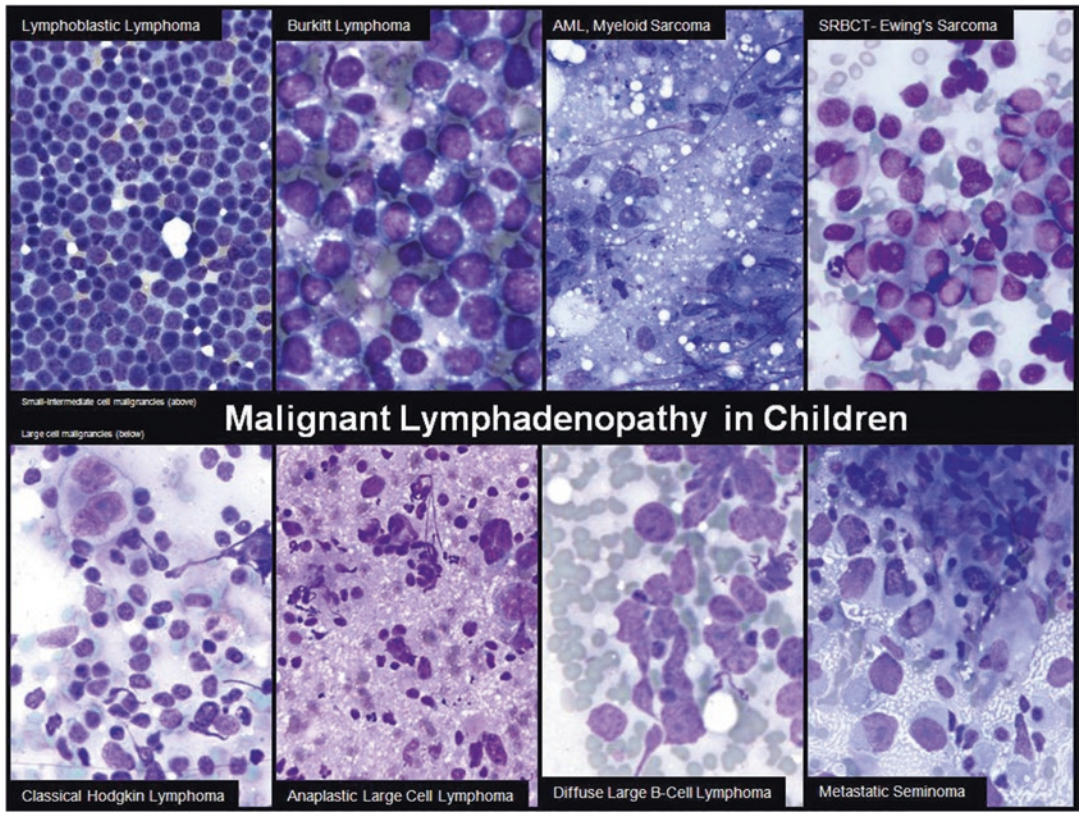


**Fig. 3.4** Composite of malignant causes of pediatric lymphadenopathy.

which can be particularly challenging to distinguish from true lymphadenopathy. However, thymic aspirates are characterized by a variable number of larger epithelial cells, and if flow cytometry is performed, there is a maturational spectrum from immature to maturing T-cells (Fig. 3.7).

## 3.4 Benign Entities

### 3.4.1 Reactive Lymphoid Hyperplasia

#### Clinical Features

Reaactive lymphoid hyperplasia (RLH), characterized by follicular hyperplasia, paracortical hyperplasia and/or sinus histiocytosis, is the most common cause of lymphadenopathy in the pediatric population, accounting for approximately 75 % or more of cases. The high incidence of RLH in this population is largely attributable to the repeated antigenic stimulation of naïve immune systems. On physical examination, benign, reactive lymph nodes usually measure less than 3 cm in greatest dimension and most commonly involve the head and neck, axilla, or inguinal region. RLH resolves spontaneously and can be followed clinically. However, lymphadenopathy that persists for more than 3–6 months or has features inconsistent with RLH may prompt an initial or repeat cytologic evaluation.

#### Cytological Features

RLH is characterized by a heterogeneous lymphoid population spanning the spectrum from immunoblasts to plasma cells, but dominated by small mature lymphocytes with round nuclei and condensed dark chromatin (Fig. 3.1). In addition, scattered tingible body macrophages, lymphohistiocytic aggregates, and follicular dendritic cells are usually seen.

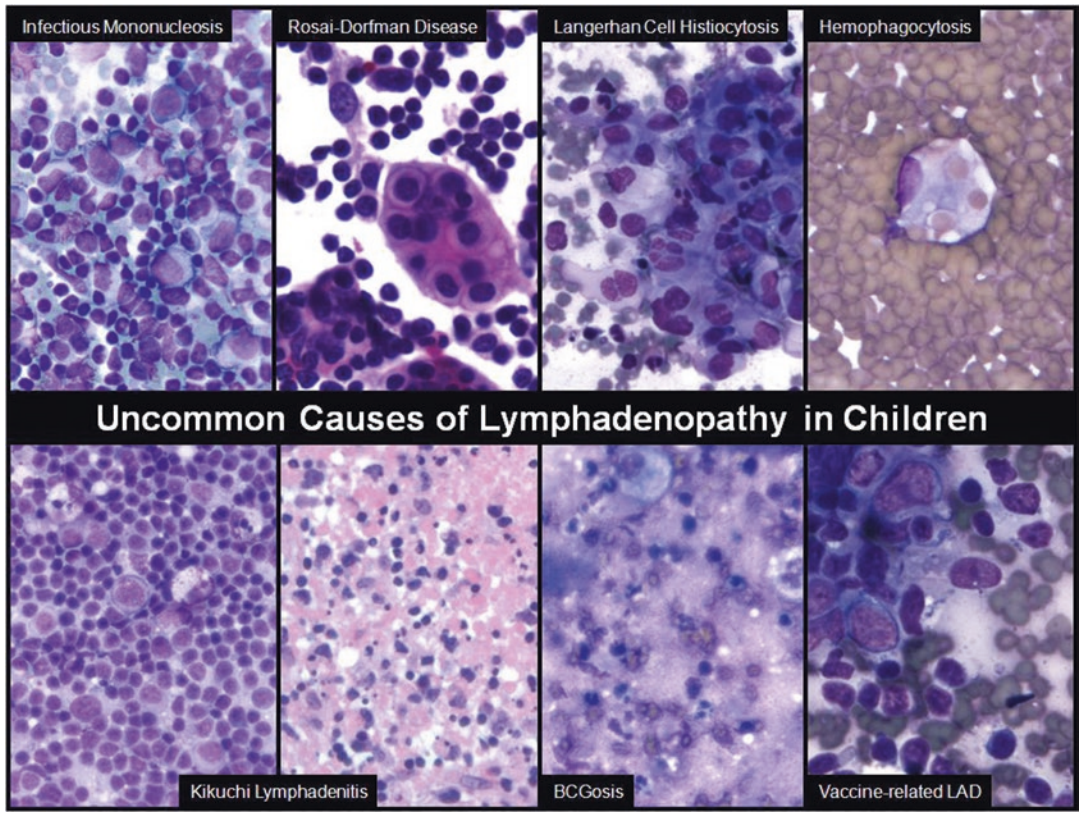


**Fig. 3.5** Composite of uncommon causes of pediatric lymphadenopathy.

**Table 3.2** Diagnostic patterns in pediatric lymph node cytopathology

| |
|---|
| Pattern 1: Heterogeneous lymphoid population with clean background<br>• Reactive lymphoid hyperplasia<br>• Drugs<br>• Vaccines<br>• Autoimmune disease<br>• Progressive transformation of germinal centers<br>• Infection (early stages of infection or chronic infection)<br>• Nodal extramedullary hematopoiesis<br>• Neoplasms (e.g., classical Hodgkin lymphoma with paucity of Reed–Sternberg cells, post-transplant lymphoproliferative disorder, T-cell lymphoma) |
| Pattern 2: Heterogeneous lymphoid population with numerous histiocytes or granulomas<br>• Infection (e.g., mycobacteria, fungi, toxoplasmosis)<br>• Sinus histiocytosis with massive lymphadenopathy (Rosai-Dorfman Disease)<br>• Langerhans cell histiocytosis<br>• Foreign body or iatrogenic related lymphadenopathy<br>• Hemophagocytosis and hemophagocytic lymphocytosis (hemophagocytic syndrome)<br>• Metabolic or storage diseases<br>• Chronic granulomatous disease<br>• Sarcoid |
| Pattern 3: Heterogeneous lymphoid population with increased plasma cells<br>• Castleman disease<br>• Autoimmune diseases<br>• IgG4 related lymphadenopathy<br>• Infection (e.g., toxoplasmosis)<br>• Neoplastic entities (e.g., plasmablastic or plasmacytoid lymphoma) |

(continued)

**Table 3.2** (continued)

| |
|---|
| Pattern 4: Heterogeneous lymphoid population with increased eosinophils<br>• Kimura disease<br>• Langerhans cell histiocytosis<br>• Hypereosinophilia syndrome<br>• Drugs<br>• Infection (e.g., parasites)<br>• Neoplastic entities (e.g., Classical Hodgkin lymphoma, T-cell lymphoma) |
| Pattern 5: Heterogeneous lymphoid population and intracellular or extracellular pigment<br>• Dermatopathic lymphadenitis<br>• Tattoo<br>• Nodal nevi<br>• Metastatic malignant melanoma<br>• Contamination (e.g., lead from pencil, metallic pigment from stylet for needles) |
| Pattern 6: Heterogeneous lymphoid population with dirty/necrotic background<br>• Acute suppurative lymphadenitis<br>• Infection (e.g., cat scratch disease, mycobacteria, pneumocystis, herpes simplex virus)<br>• Histiocytic necrotizing lymphadenitis (Kikuchi-Fujimoto disease or Kikuchi disease)<br>• Autoimmune disease (Systemic lupus erythematosus related lymphadenopathy)<br>• Chronic granulomatous disease<br>• Lymph node infarction<br>• Drug or treatment-related changes<br>• High-grade malignancy (hematolymphoid or metastasis) |
| Pattern 7: Homogeneous population, small-to-intermediate cell predominant<br>• Infectious mononucleosis<br>• Acute lymphocytic or myeloid leukemia<br>• Non-Hodgkin lymphoma (e.g., lymphoblastic or Burkitt lymphoma)<br>• Metastatic small round cell malignancies |
| Pattern 8: Homogeneous population, large cell predominant<br>• Classical Hodgkin lymphoma with numerous Reed–Sternberg cells<br>• Non-Hodgkin lymphoma (e.g., Burkitt lymphoma, diffuse large B-cell lymphoma, anaplastic large cell lymphoma)<br>• Non-hematopoietic malignancy (e.g., metastatic sarcoma, germ cell tumor, or melanoma) |

**Table 3.3** Size-based differential diagnosis for lymph node aspirates in children and adolescents

| *Small cell population* | *Intermediate cell population* |
|---|---|
| Reactive lymphoid hyperplasia | Reactive immunoblastic proliferations |
| Early infection | Infectious mononucleosis |
| Hodgkin lymphoma with paucity of Reed–Sternberg cells | Lymphoblastic lymphoma |
| Leukemia or myeloid/granulocytic sarcoma | Burkitt lymphoma |
| Small B-cell lymphoma (rare) | T-cell lymphoma |
| T-cell lymphoma | Leukemia or myeloid/granulocytic sarcoma |
| Non-lymphoid small round cell tumors | Non-lymphoid small round cell tumors |
| *Monomorphic large cell population* | *Pleomorphic large cell population* |
| Diffuse large B-cell lymphoma | Diffuse large B-cell lymphoma (e.g., anaplastic) |
| Anaplastic large cell lymphoma | Anaplastic large cell lymphoma |
| Hodgkin lymphoma, with predominance of Reed–Sternberg cells) | Germ cell tumors |
| Germ cell tumors | High-grade sarcomas |
| Sarcomas | Malignant melanoma |
| Malignant melanoma | |

## Differential Diagnosis

The main diagnostic considerations include Hodgkin lymphoma, T-cell lymphoma, partial lymph node involvement by a lymphoid or non-lymphoid malignancy, post-transplant lymphoproliferative disorder, and early infection, as well as other possibilities (Tables 3.1, 3.2, and 3.3). Although rare in the pediatric population, some

**Table 3.4** Differential diagnosis of small round cell tumors (adapted from Monaco SE and Teot LA. Cancer Cytopathol 2014) [8]

| | Cytomorphology | Immunophenotype | Genetics |
|---|---|---|---|
| Wilms' Tumor | Blastema +/− epithelial component +/− stroma<br>Rarely, anaplasia | + WT1<br>+ EMA, Cytokeratin (epithelial component)<br>− Synaptophysin, chromogranin | Mutations of *WT1, WT2* |
| Neuroblastoma | Neuropil, rosettes,<br>+/− ganglion cells,<br>+/− schwannian stroma,<br>+/− calcification | + synaptophysin, chromogranin, CD56, PGP9.5<br>− S100, CD99, desmin, myogenin, lymphoid markers | +/− *N-MYC* amplification |
| Rhabdomyosarcoma | Rhabdomyoblastic differentiation subtle to obvious<br>+/− Floret cells, +/− strap cells | + Myogenin, myoD1, desmin<br>− TLE1<br>+/− aberrant CD99, cytokeratin, EMA, neural markers | Alveolar subtype:<br>t(2;13)(q35;14)<br>t(1:13)(p36;q14) |
| Ewing sarcoma/ primitive neuroectodermal tumor (PNET) | +/− Rosettes, +/− neuropil<br>+/− Tigroid background | +CD99, FLI-1<br>+/− Synaptophysin, PGP9.5, CD56<br>− Desmin, myogenin, CD45, TLE-1, EMA, cytokeratins | t(11;22)(q24;q12) (>90 %)<br>t(21;22)(q12;q12), t(2;22)(q33;q12)<br>Others (rare) |
| Synovial sarcoma (poorly differentiated round cell) | +/− Metachromatic stroma,<br>+/− calcifications | + TLE-1, +EMA, +/− cytokeratin, +/− CD99<br>− Myogenin, myoD1, desmin | t(X;18) (p11.2;q11) |
| Lymphoid malignancies | Morphology varies with type<br>Lymphoglandular bodies | Varies with lineage and type (B-cell, T-cell)<br>+TdT (Lymphoblastic lymphoma) | Burkitt: *MYC* translocations, t(8;14)(q24;q32) and less commonly, t(2;8)(p12;q24), t(8;22)(q24;q11) |

**Table 3.5** Mimics of lymphadenopathy in children and adolescents

- Thyroid lesions/neoplasms
- Salivary gland lesions/neoplasms
- Cystic head and neck lesions (e.g., branchial cleft cyst, thyroglossal duct cyst, other developmental cysts)
- Extranodal inflammatory lesions (e.g., abscess)
- Fibrous hamartoma of infancy
- Pilomatrixoma
- Mesenchymal lesions/neoplasms (e.g., lymphangioma/hemangioma, fat necrosis, lipoma, fibromatosis, solitary myofibroma, rhabdomyosarcoma)
- Neural neoplasms (e.g., schwannoma, neurofibroma, ganglioneuroma)
- Germ cell tumors (e.g., cervical teratoma)
- Odontogenic or bone lesions (e.g., odontogenic cyst, fibrous dysplasia)
- Thymic tissue or lesion (e.g., undescended thymus)
- Benign soft tissue elements (e.g., skeletal muscle, adipose tissue)

B-cell non-Hodgkin lymphomas, including marginal zone, low grade follicular, and T-cell rich large B-cell lymphomas, have a heterogeneous population of cells dominated by small cells. However, in contrast to RLH, the spectrum of cells in these malignancies is usually limited. Atypical cells should raise the possibility of a malignant process, but may be few in number in T-cell rich large B-cell lymphoma, Hodgkin lymphoma with a paucity of Reed–Sternberg cells, or partial replacement of a lymph node by a primary lymphoid or metastatic non-lymphoid malignancy. In some early infections, particularly mycobacteria and *Bartonella*, the characteristic granulomatous and/or neutrophilic inflammation may be absent or poorly developed, and therefore, aspirates from these lymph nodes may mimic non-specific RLH. A rare but important cause of reactive-appearing lymphadenopathy in the

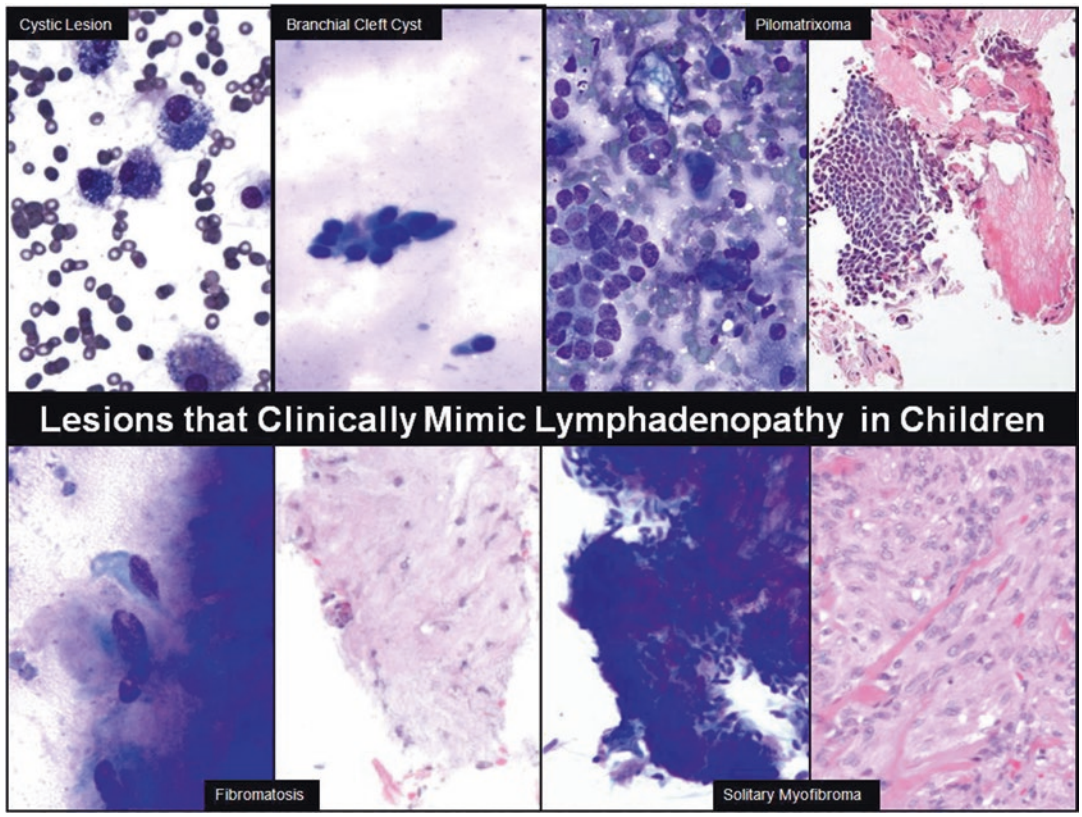


**Fig. 3.6** Composite of mimics of lymphadenopathy in children and adolescents.

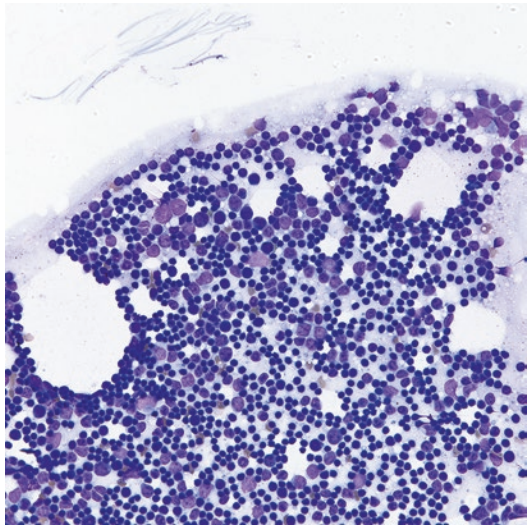

**Fig. 3.7** Ectopic thymic tissue (Diff-Quik stain, high power). Thymic tissue can be present in the neck and mimic a lymph node clinically and cytologically. Although there is a predominance of small lymphocytes, larger epithelial cells are also present and flow cytometry or immunohistochemical stains can help to confirm the presence of immature and maturing T-cells.

pediatric population is autoimmune lymphoproliferative syndrome (ALPS). This inherited disorder is characterized by defects in Fas/CD95/Apo-1 mediated apoptosis, which lead to childhood onset of generalized lymphadenopathy, hypergammaglobulinemia, lymphocytosis, splenomegaly, and autoimmune phenomena. Flow cytometry performed on lymph nodes from ALPS patients shows an increase in CD4, CD8 double negative, T-cell receptor (TCR)-alpha beta T-cells, ranging from 27 to 54 % of mononuclear cells, and representing 51–78 % of alpha beta T-cells [9].

## Pearls

- Collection of additional material for ancillary studies, such as microbial cultures, special stains, flow cytometry, FISH, and immunohistochemical stains, should be considered when the clinical or microscopic features are concerning for infection, a lymphoproliferative disorder or a metastatic malignancy.

- Use of a needle alone, without an attached syringe or suction (fine needle non-aspiration technique), can help to optimize control and sampling of small, mobile lymph nodes, and may also decrease anxiety for the patient.

### 3.4.2 Suppurative Lymphadenitis

#### Clinical Features

Acute suppurative lymphadenitis usually presents as tender, erythematous, superficial lymph nodes, and is most often due to infection with bacteria such as *Staphylococcus*, *Streptococcus*, and gram-negative organisms. Cat scratch disease due to *Bartonella henselae* infection should be considered, particularly if there is a history of a cat scratch or bite or simply the presence of a cat in the patient's home environment. Although rare, fungal infections can also cause suppurative lymphadenitis. Empiric treatment with antibiotics results in resolution of acute lymphadenitis in many cases and therefore, cytologic evaluation is usually reserved for those cases in which the lymphadenopathy persists despite therapy.

#### Cytological Features

Aspirates from acute suppurative lymphadenitis yield yellow-tinged, thick, turbid material. Microscopically, numerous neutrophils, as well as variable numbers of lymphocytes and histiocytes, are present in a dirty background of granular and cellular debris (Fig. 3.8). In some cases, intracellular and/or extracellular microorganisms can be identified on routine stains, and are usually more apparent on modified Giemsa than on Papanicolaou-stained smears. The presence of granulomas in addition to suppurative inflammation is suggestive of cat scratch disease (Fig. 3.9) or mycobacterial infection. Special stains, such as Gram, methenamine silver, Steiner, Warthin–Starry, and acid fast, and/or an immunohistochemical stain for *Bartonella* may be helpful for demonstrating the presence of microorganisms.

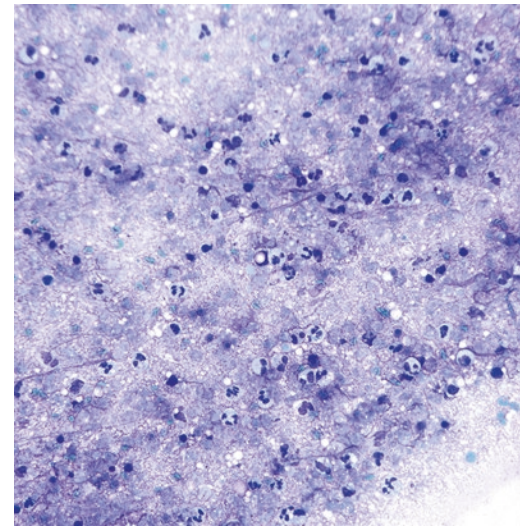

**Fig. 3.8** Acute suppurative lymphadenitis (Diff-Quik stain, high power). Aspirates from suppurative lymphadenitis show granular necrotic and karyorrhectic debris and neutrophils.

#### Differential Diagnosis

The main differential diagnostic considerations include necrotizing granulomatous lymphadenitis, systemic lupus erythematosus (SLE), Kikuchi disease, lymph node infarction, and necrotic tumor. Although a dirty background with necrosis is characteristic of these entities, in contrast to acute suppurative lymphadenitis, neutrophils are usually absent, or if present, not a prominent feature. Other distinguishing features include the presence of granulomas in necrotizing granulomatous inflammation, hematoxylin bodies and LE cells in SLE, crescentic histiocytes in Kikuchi disease, and malignant cells in necrotic tumors.

#### Pearls

- Material should be obtained for cultures to establish the specific identity of the causative organism, as well as to determine susceptibility and resistance to antimicrobial agents.
- High quality aspirate smears may be superior to a diluted or limited cell block, particularly if there are few organisms.
- Serology can be used to confirm the presence of *Bartonella* infection and may be particularly warranted when cat scratch disease is suspected

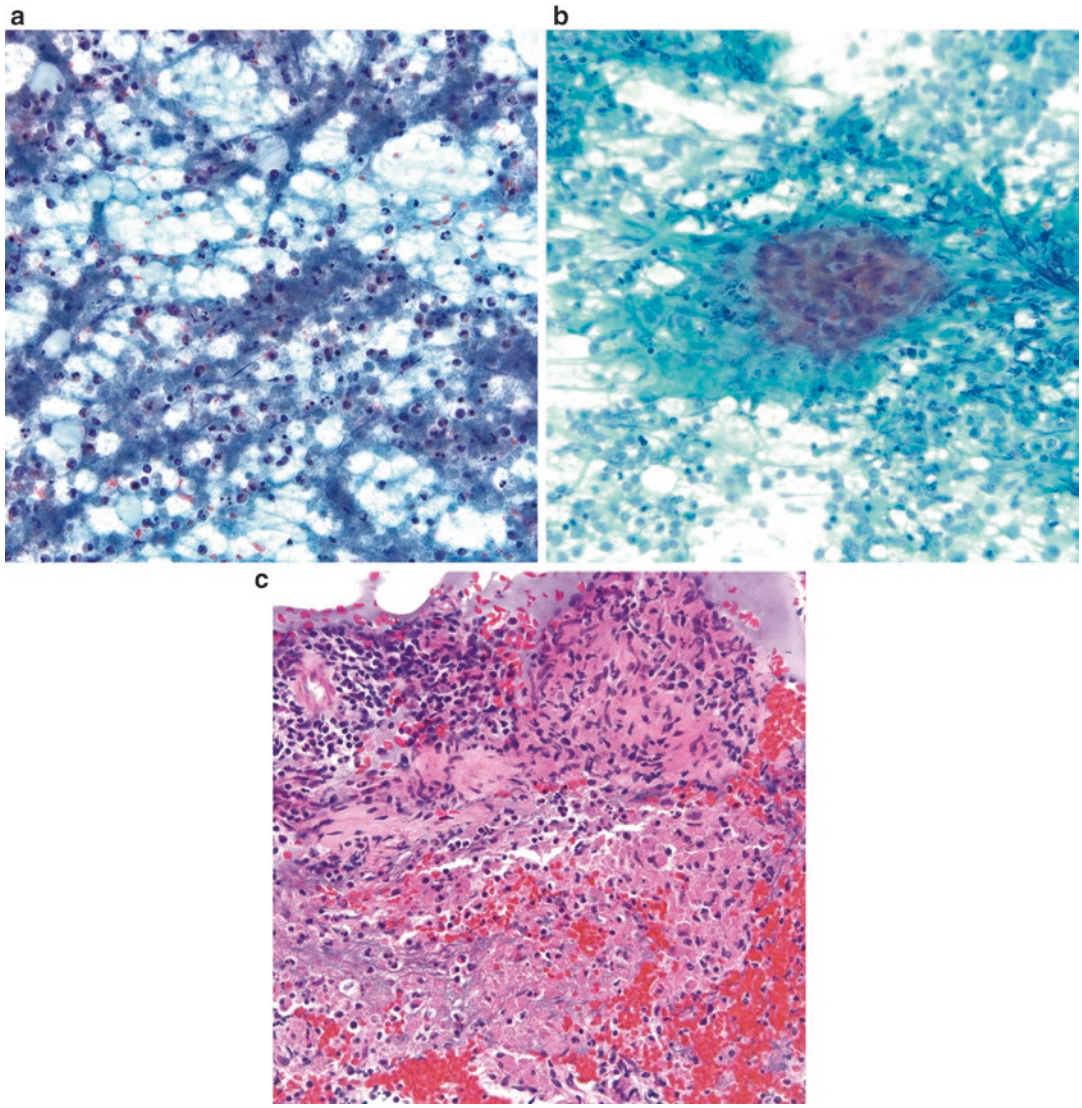


**Fig. 3.9** Cat scratch disease (**a**, **b**. Papanicolaou stain, high power; **c**. H&E stain, medium power). Some lymph nodes with suppurative changes (**a**) also have granulomas (**b**). Acute suppurative and granulomatous inflammation should raise concern for cat scratch disease (**c**).

clinically and/or cytologically, but organisms are not identified with Steiner, Warthin–Starry or immunohistochemical stains, and mycobacterial infection has been excluded.

- When acid fast organisms are seen or when no organisms are seen but the clinical suspicion of mycobacterial infection is high, polymerase chain reaction (PCR)-testing can be performed on material from the cell block to confirm the presence and subtype of mycobacteria.

### 3.4.3 Granulomatous Lymphadenitis

#### Clinical Features

Granulomatous lymphadenitis is associated with mycobacterial, fungal, bacterial and parasitic infections, foreign body reactions, drugs, sarcoid, and malignancy, as well as a variety of other causes. Beyond the presence of lymphadenopathy, the clinical presentation depends on and may provide important clues to the underlying etiology.

Clinical history, such as exposure to infectious individuals, pets, travel, implanted medical devices or prostheses, innate or acquired immunodeficiency, or malignancy, is also key. Diagnostic evaluation usually includes exclusion of treatable infectious etiologies, and even in the setting of a non-infectious cause of granulomatous lymphadenitis, superimposed infection should be considered.

### Cytological Features

The characteristic cytological finding is the presence of nodular clusters of epithelioid histiocytes with syncytial-appearing cytoplasm, oval, reniform or spindled nuclei, fine chromatin and small, distinct nucleoli (Figs. 3.10, 3.11, 3.12, and 3.13). Intermixed small mature lymphocytes are present in the clusters. Multinucleated giant cells may be present in variable numbers or absent. Granulomatous inflammation is classified as necrotizing or non-necrotizing, based on the presence or absence of necrosis, and necrotizing granulomatous inflammation is further divided into suppurative and non-suppurative types, based on the presence or absence of neutrophilic inflammation. These features provide important clues to the differential diagnosis. Special stains, including acid fast, methenamine silver, Steiner, Warthin–Starry, and Gram, and/or an immunohistochemical stain for *Bartonella* may be helpful for demonstrating the presence of microorganisms. In longstanding granulomatous

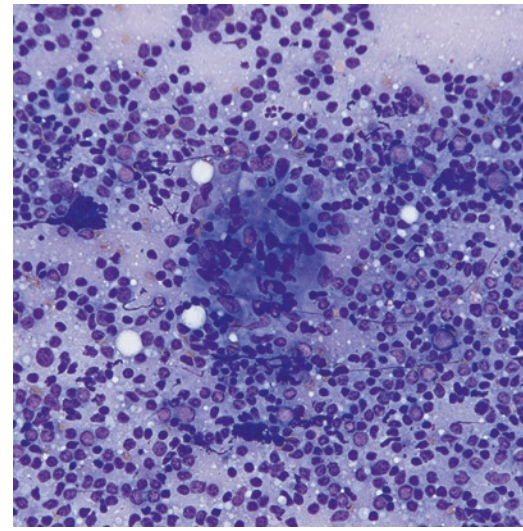

**Fig. 3.10** Granulomatous lymphadenitis (Diff-Quik stain, medium power). This case shows a heterogeneous lymphoid population with a cluster of epithelioid histiocytes with intermixed lymphocytes, compatible with granuloma.

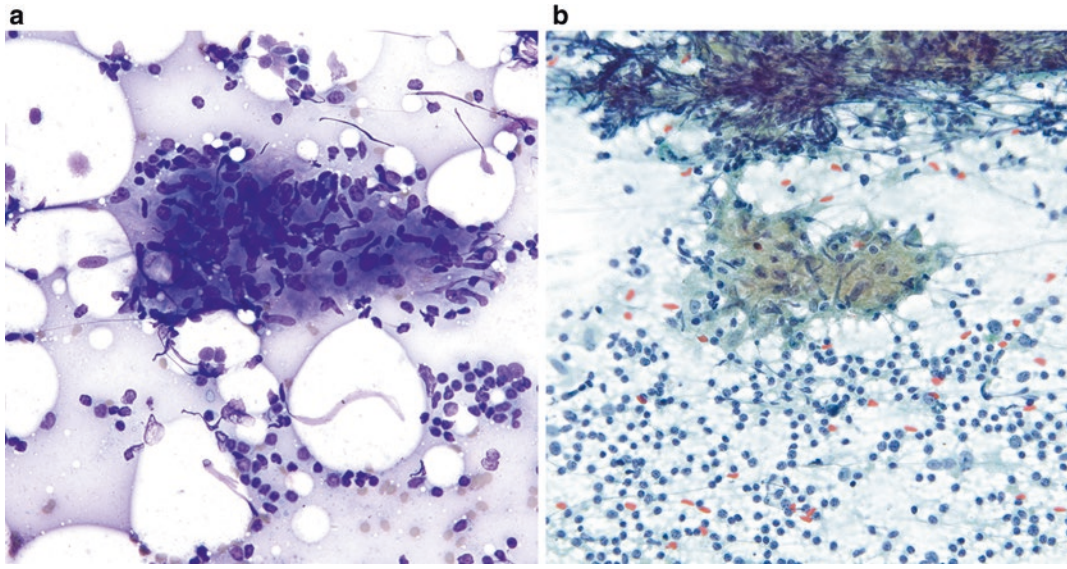


**Fig. 3.11** Non-necrotizing granulomatous inflammation (**a**. Diff-Quik stain, high power; **b**. Papanicolaou stain, medium power). These aspirates show well-defined granulomas within a clean background of heterogeneous lymphoid cells.

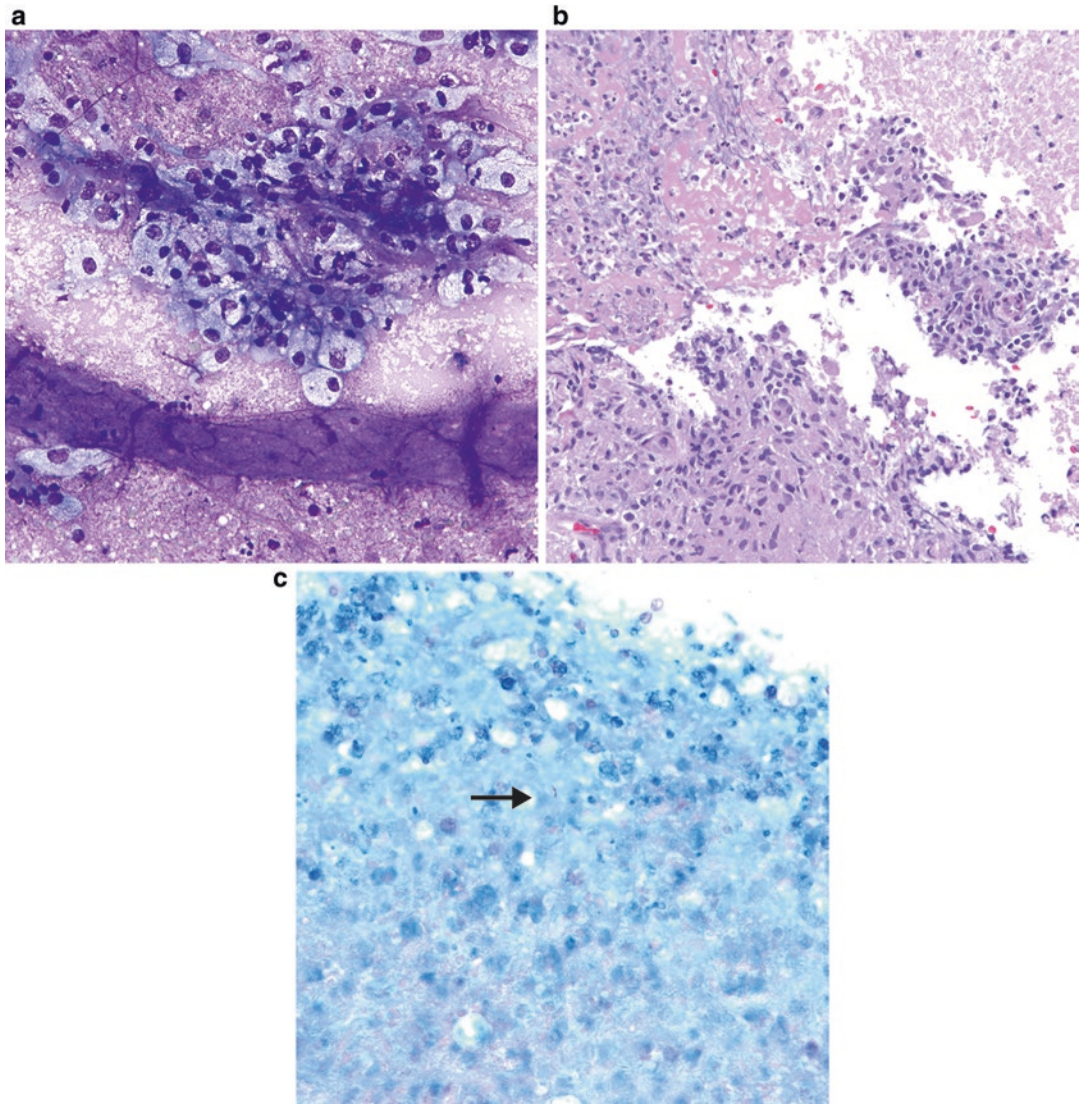


**Fig. 3.12** Necrotizing granulomatous inflammation (**a**. Diff-Quik stain, high power; **b**. H&E stain, high power; **c**. Acid fast stain, high power). In this a case of lymphadenitis due to atypical mycobacteria, clusters of epithelioid histiocytes with foamy cytoplasm are seen within a background of necrosis. Neutrophils are also present, characteristic of suppurative granulomatous inflammation. The acid fast stain highlights rare acid fast bacilli (**c**, *arrow*).

inflammation, the presence of fibrosis and hyalinization may result in paucicellular, non-diagnostic aspirates. Other cytological features that may be seen in a subset of cases are included in discussion of the differential diagnosis.

## Differential Diagnosis

As noted above, the differential diagnostic considerations for granulomatous lymphadenitis include a wide variety of infectious and non-infectious processes. In the pediatric population, the most common causes of suppurative necrotizing granulomatous lymphadenitis are atypical mycobacterial or *Bartonella* infection, while non-suppurative necrotizing granulomatous lymphadenitis is most often due to infection with *M. tuberculosis* and fungi. In developing countries where use of the BCG (Bacille de Calmette et Guérin) vaccine is common, necrotizing granulomatous inflammation can be seen in newborns

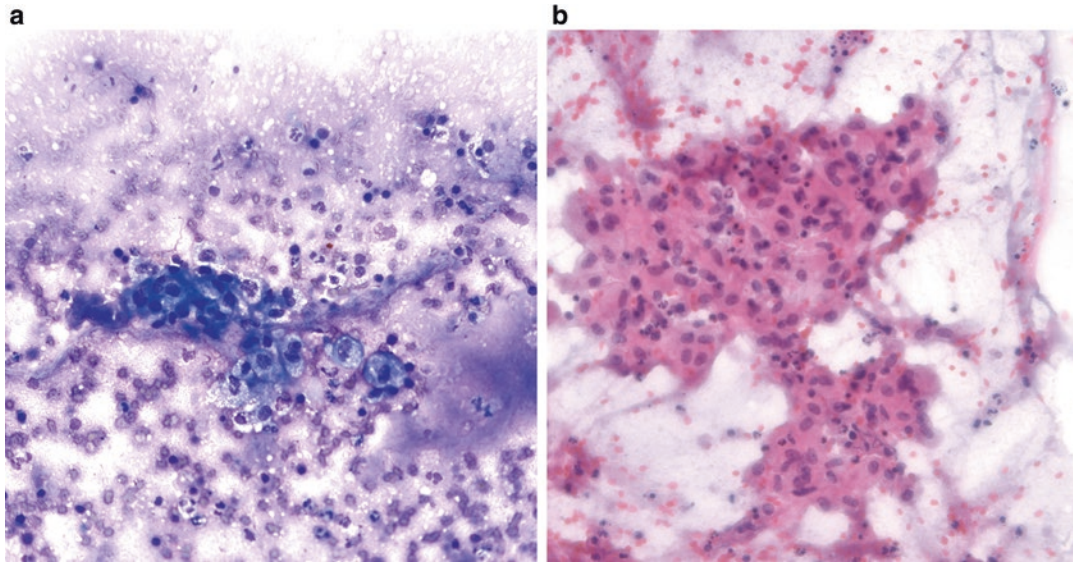


**Fig. 3.13** BCGosis (**a**. Diff-Quik stain, high power; **b**. H&E stain, high power). Newborns and children vaccinated with the BCG (Bacille de Calmette et Guérin) vaccine may develop ipsilateral lymphadenopathy from the attenuated live *Mycobacterium bovis* in the vaccine. The lymphadenitis appears similar to *Mycobacterium tuberculosis* with necrotizing granulomatous inflammation. (Images taken from slides provided by Dr. Pamela Michelow).

or older children in the lymph nodes draining the site of vaccination (Fig. 3.13). Necrotizing granulomatous inflammation may also be seen in some malignancies, such as Hodgkin and T-cell lymphomas, and if exuberant may obscure the diagnostic malignant cells. Causes of non-necrotizing granulomatous lymphadenitis include toxoplasmosis, early mycobacterial infection, foreign body reaction, drug reaction, and sarcoid, among others. Foreign body reactions are characterized by clusters of histiocytes, foamy histiocytes, and variable numbers of interspersed multinucleated giant cells with engulfed debris (the so-called foreign body giant cells), and may be due to a variety of causes, such as sclerosing agents for vascular anomalies, talc or other crystalline carriers from intravenous drug abuse, and silicone from breast augmentation. Lipogranulomas can be seen in lymph nodes in response to endogenous or exogenous lipids, and oil droplets from lymphangiography. Sarcoid is characterized by tight, single and confluent, non-necrotizing granulomas, and an absence or paucity of multinucleated giant cells. Asteroid bodies (star-shaped), Hamazaki-Wesenberg inclusions (periodic acid-Schiff positive yellow-brown inclusions), and Schaumann bodies (concentrically laminated spherules composed of calcium and iron) may also be seen in sarcoid, but are not specific for that entity. Occasionally, central necrosis, characterized by granular eosinophilic debris is present in sarcoidal granulomas, but such cases lack the dirty background of necrotizing granulomatous processes. Other causes of lymphadenopathy associated with histiocytic proliferations that may mimic granulomatous inflammation include Langerhans cell histiocytosis (LCH), metabolic and storage disorders, hemophagocytosis and familial hemophagocytic syndrome, and sinus histiocytosis with massive lymphadenopathy (Rosai-Dorfman disease). In Gaucher disease, the most common lysosomal storage disease, the histiocytes are enlarged with abundant crinkled tissue paper-like cytoplasm (Gaucher cells) [10]. Gaucher-like cells have also been reported in extramedullary hematopoietic tumors, chronic myeloid leukemia, and crystal storage histiocytosis [11]. Gaucher and Gaucher-

like cells may be confused with histiocytes from granulomatous inflammation due to atypical mycobacteria in which negative-images of the mycobacteria impart a striped or wrinkled appearance to the cytoplasm in modified Giemsa-stained preparations. Hemophagocytic disorders, LCH, and sinus histiocytosis with massive lymphadenopathy are discussed below in Sects. 3.4.4, 3.4.5, and 3.4.8.

#### Pearls

- Material should be obtained for cultures to establish the specific identity of the causative organism, as well as to determine susceptibility and resistance to antimicrobial agents.
- High quality aspirate smears may be superior to a diluted or limited cell block, particularly if there are few organisms.
- Serology can be used to confirm the presence of *Bartonella* infection and may be particularly warranted when cat scratch disease is suspected clinically and/or cytologically, but organisms are not identified with Steiner, Warthin–Starry, or immunohistochemical stains, and mycobacterial infection has been excluded.
- When acid fast organisms are seen or when no organisms are seen but the clinical suspicion of mycobacterial infection is high, polymerase chain reaction (PCR)-testing can be performed on material from the cell block to confirm the presence and subtype of mycobacteria.

### 3.4.4 Hemophagocytic Lymphohistiocytosis and Hemophagocytosis

#### Clinical Features

Hemophagocytic lymphocytosis (HLH) is a rare, life-threatening condition that can be primary due to inherited defects in NK cells (familial hemophagocytic lymphohistiocytosis), or acquired after strong immunologic activation by infection, particularly herpes viruses, autoimmune disease, or malignancy. HLH is a hyperinflammatory, uncontrolled, ineffective, immune response with clinical features attributable to high levels of cytokines and chemokines. In contrast, hemophagocytosis outside the context of HLH is a non-specific finding that is often associated with viral infections and pursues a benign course. In both HLH and non-specific hemophagocytosis, activated macrophages in various organs phagocytize other hematolymphoid cells, such as erythrocytes and lymphocytes [12].

#### Cytological Features

The key cytological finding is the presence of macrophages with engulfed erythrocytes or white blood cells, which are typically surrounded by a thin halo (Fig. 3.14). The histiocytes are positive for CD68 and S100, but are negative for CD1a.

#### Differential Diagnosis

The main differential diagnostic considerations include sinus histiocytosis with massive lymphadenopathy, which is discussed in Sect. 3.4.8, and other histiocytic processes, as summarized in Table 3.2. In addition, an associated lymphoma, particularly T-cell lymphomas, should be excluded.

#### Pearls

Although hemophagocytosis may be non-specific and pursue a benign course, its presence should prompt consideration of HLH, as well as lymphoma or leukemia.

### 3.4.5 Langerhans Cell Histiocytosis (Histiocytosis X, Letterer–Siwe Disease, Hand–Schuller–Christian Disease, Eosinophilic Granuloma)

#### Clinical Features

Langerhans cell histiocytosis (LCH) is a clinically heterogeneous disease, characterized by clonal proliferation of Langerhans cells. Multifocal multisystem LCH (Letterer–Siwe disease) presents in infancy and preferentially

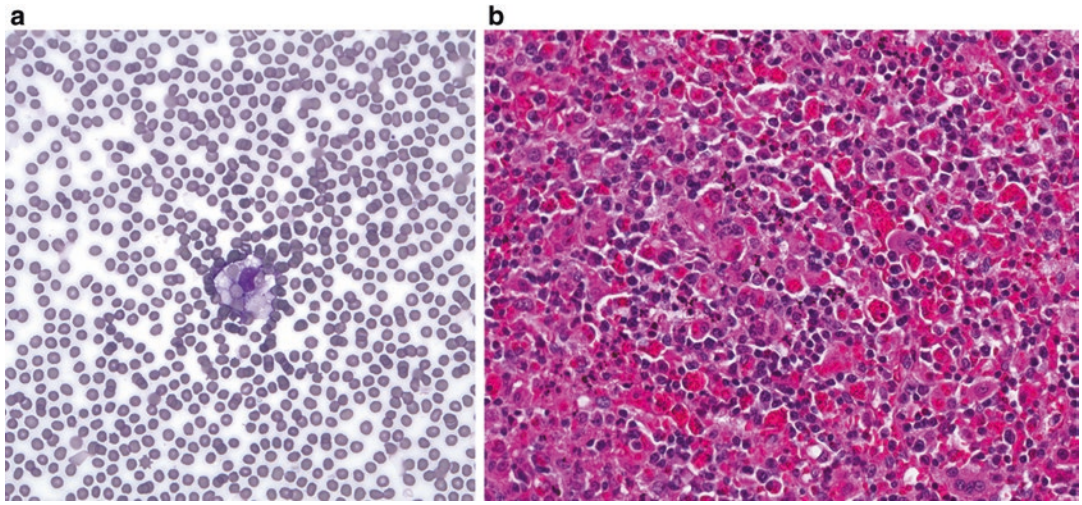


**Fig. 3.14** Viral associated hemophagocytosis (**a**. Wright-Giemsa stain, high power; **b**. H&E stain, medium power). The aspirate (**a**) and biopsy (**b**) showed histiocytes with prominent erythrophagocytosis.

involves skin, bone, liver, spleen, and bone marrow, whereas multifocal unisystem LCH (Hand–Schuller–Christian disease) affects young children and typically involves bone and adjacent soft tissue. Unifocal unisystem LCH (eosinophilic granuloma) usually presents in older children and adults as a lytic bone lesion with or without involvement of the adjacent soft tissue, or less commonly in lymph node, skin, or lung. Males are more commonly affected than females. Whereas unifocal unisystem LCH follows a benign course in virtually all cases, multifocal multisystem disease is associated with a high mortality rate, particularly in patients who fail to respond promptly to therapy [13].

### Cytological Features

Approximately 85 % of cases of LCH can be correctly diagnosed by FNA cytology [14]. The key feature is the presence of LCH cells, which are oval, intermediate-sized cells with moderately abundant cytoplasm, and grooved, folded, or indented nuclei with delicate chromatin and inconspicuous nucleoli (Fig. 3.15). In addition to small lymphocytes, the background has variable numbers of eosinophils, histiocytes, multinucleated giant cell of both histiocytic and LCH cell origin, and neutrophils. Eosinophilic microabscesses are present in some cases. Late lesions may be fibrotic and have a paucity of LCH cells. LCH cells are positive for CD68, S100, CD1a, langerin, and fascin [13, 14].

### Differential Diagnosis

The main differential diagnostic considerations include dermatopathic lymphadenitis, sinus histiocytosis with massive lymphadenopathy (Rosai-Dorfman disease), hemophagocytic disorders, lymphoma, and malignant histiocytosis. In dermatopathic lymphadenitis, the accumulation of Langerhans cells that are morphologically indistinguishable from LCH cells and are positive for CD68, S100, CD1a, and langerin, as well as the presence of eosinophils in some cases, can lead to confusion with LCH. However, histiocytes with engulfed pigment are present in dermatopathic lymphadenitis and help to distinguish this entity from LCH [15, 16]. Lymphomas and malignant histiocytosis can be distinguished from LCH by the presence of morphologically malignant cells. Features of sinus histiocytosis with massive lymphadenopathy and hemophagocytic disorders are discussed in Sects. 3.4.8 and 3.4.4, respectively. Additional diagnostic considerations include infections due to parasites or fungus, Kimura disease, Hodgkin lymphoma,

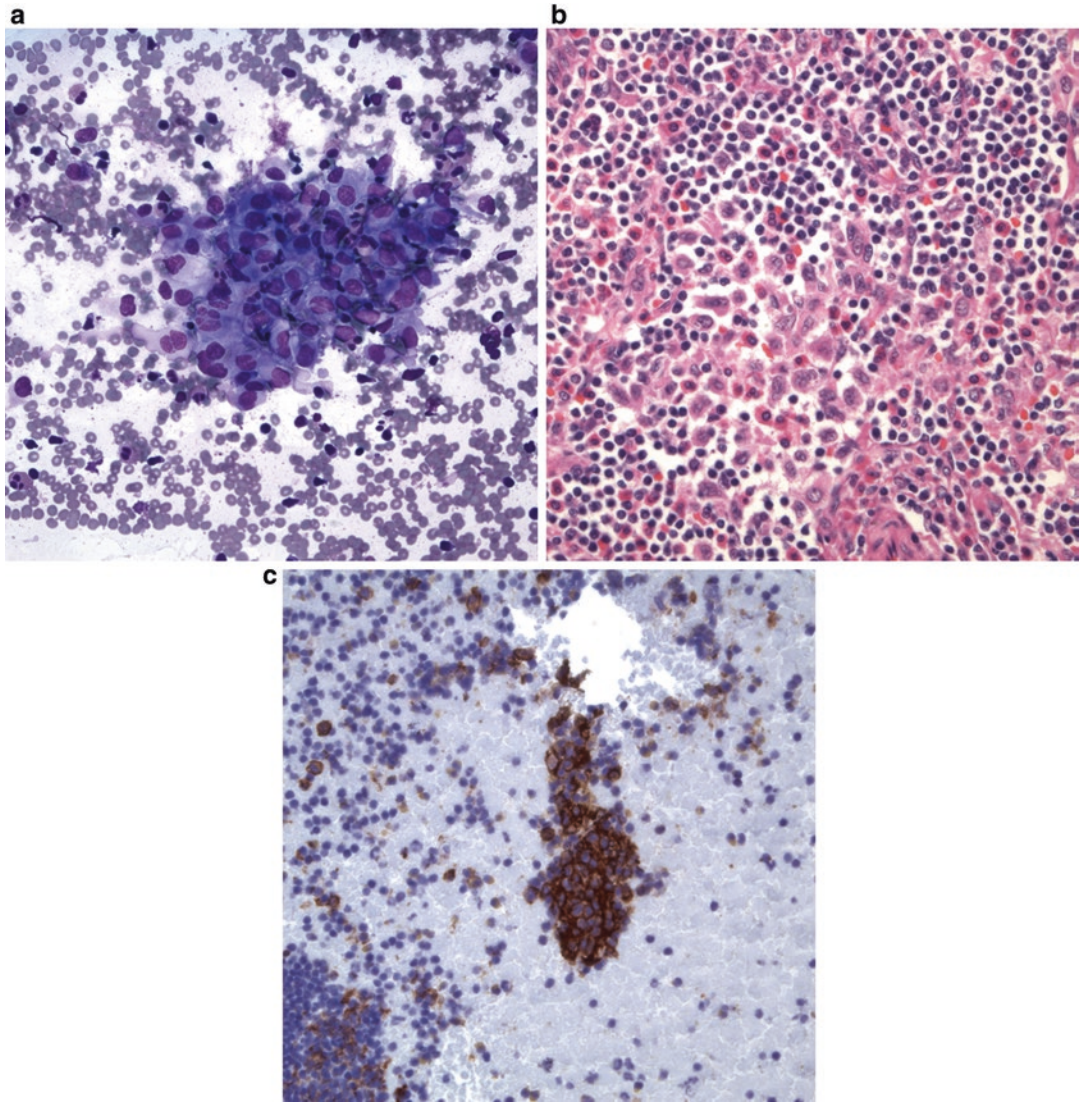


**Fig. 3.15** Langerhans cell histiocytosis. (**a**. Diff-Quik stain, high power; **b**. H&E stain, high power; **c**. CD1a stain, high power). The aspirate (**a**) and biopsy (**b**) from this cervical lymph node shows LCH cells with irregular, grooved, or folded nuclei. Deep clefts give some nuclei multilobated appearance. Lymphocytes and eosinophils are present in the background. CD1a staining on the cell block (**c**) is strongly positive in these Langerhans cells.

and T-cell lymphoma, due to the presence of eosinophils in those entities.

### Pearls

- The distinct nuclear morphology of LCH cells, positivity for CD1a and absence of engulfed cells, help to distinguish LCH from most other histiocytic processes.
- Dermatopathic lymphadenitis may closely mimic LCH due to the presence of Langerhans cells that are morphologically indistinguishable from LCH cells and positive for CD68, S100, CD1a, and langerin, and in some cases, they have associated eosinophils. Histiocytes with intracellular pigment provide an important clue to the correct diagnosis.

### 3.4.6 Histiocytic Necrotizing Lymphadenitis (Kikuchi-Fujimoto Disease or Kikuchi Disease)

#### Clinical Features

This is a benign, self-limited condition of unclear etiology that occurs most often in young Asian women and presents with fever, night sweats, and painless cervical lymphadenopathy [17]. However, in children, there tends to be a male predominance. The condition usually resolves spontaneously within 6 months of the diagnosis.

#### Cytological Features

The cytological diagnosis can be challenging, with a reported accuracy of about 56% in one retrospective study [18]. Smears are characterized by heterogeneous lymphoid cells in a granular, necrotic background containing abundant karyorrhectic debris. Typically there are increased histiocytes and an absence of neutrophils. Histiocytes with peripherally situated, crescent-shaped nuclei and engulfed cellular debris (so-called crescentic histiocytes) are also characteristic, in addition to increased numbers of plasmacytoid dendritic cells, which co-express CD68 and CD123 and are negative for fascin, in the background [17, 18]. The background lymphocytes are predominantly CD8-positive T-cells.

#### Differential Diagnosis

The differential diagnostic considerations include necrotizing lymphadenitis related to autoimmune disease, such as systemic lupus erythematosus (SLE), herpes viruses, or other infections, as well as infarction and malignancy. Features of SLE that are not seen in histiocytic necrotizing lymphadenitis (HNL) are hematoxylin bodies, which are periodic acid Schiff (PAS)-positive amorphous extracellular structures composed of DNA and immunoglobulin, LE cells which are neutrophils with engulfed hematoxylin bodies, and increased plasma cells. The presence of characteristic viral inclusions supports a diagnosis of herpes simplex virus, which can be confirmed by immunohistochemical stains. Infectious mononucleosis is discussed in Sect. 3.4.7. Granulomas, which are a key feature of necrotizing granulomatous lymphadenitis due to mycobacterial and other infections, are absent in HNL.

#### Pearls

- Crescentic histiocytes and plasmacytoid dendritic cells are characteristic of HNL, but are non-specific and can be seen in smaller numbers in other disorders.
- Neutrophils are absent in HNL; however, the abundant karyorrhectic debris may mimic the multilobulated nuclei of neutrophils, leading to misinterpretation as suppurative inflammation.

### 3.4.7 Infectious Mononucleosis

#### Clinical Features

Infectious mononucleosis (IM) is an acute illness characterized by marked cervical lymphadenopathy, fatigue, fever, pharyngitis, and hepatomegaly, splenomegaly or both. Epstein–Barr virus (EBV) is the most common cause, but other viruses, particularly cytomegalovirus (CMV) and human immunodeficiency virus (HIV), can produce clinically indistinguishable disease. IM can mimic lymphoma clinically, especially when the lymphadenopathy is pronounced or asymmetrical and associated with constitutional symptoms, and the heterophile antibody test is negative, thereby prompting pathological evaluation. Serological studies for specific causative viruses confirm the diagnosis, but may not be available at the time of presentation for an FNA.

#### Cytological Features

Aspirates are composed of a heterogeneous population of lymphocytes with increased intermediate-sized to large immunoblasts with nuclear enlargement, prominent nucleoli, and basophilic cytoplasm (Fig. 3.16). In cases due to EBV infection, lymphocytes throughout the spectrum are positive for EBV-encoded RNA (EBER) by in situ hybridization. Large CD30-positive binucleate immunoblasts mimicking Reed–Sternberg (RS) cells are present in some cases; however, in contrast to RS cells, these cells are positive for CD20 and negative for CD15 [19]. Eosinophils and/or necrosis are also present in some cases. Triage in these cases usually includes collection of additional material for flow cytometry to exclude a lymphoproliferative

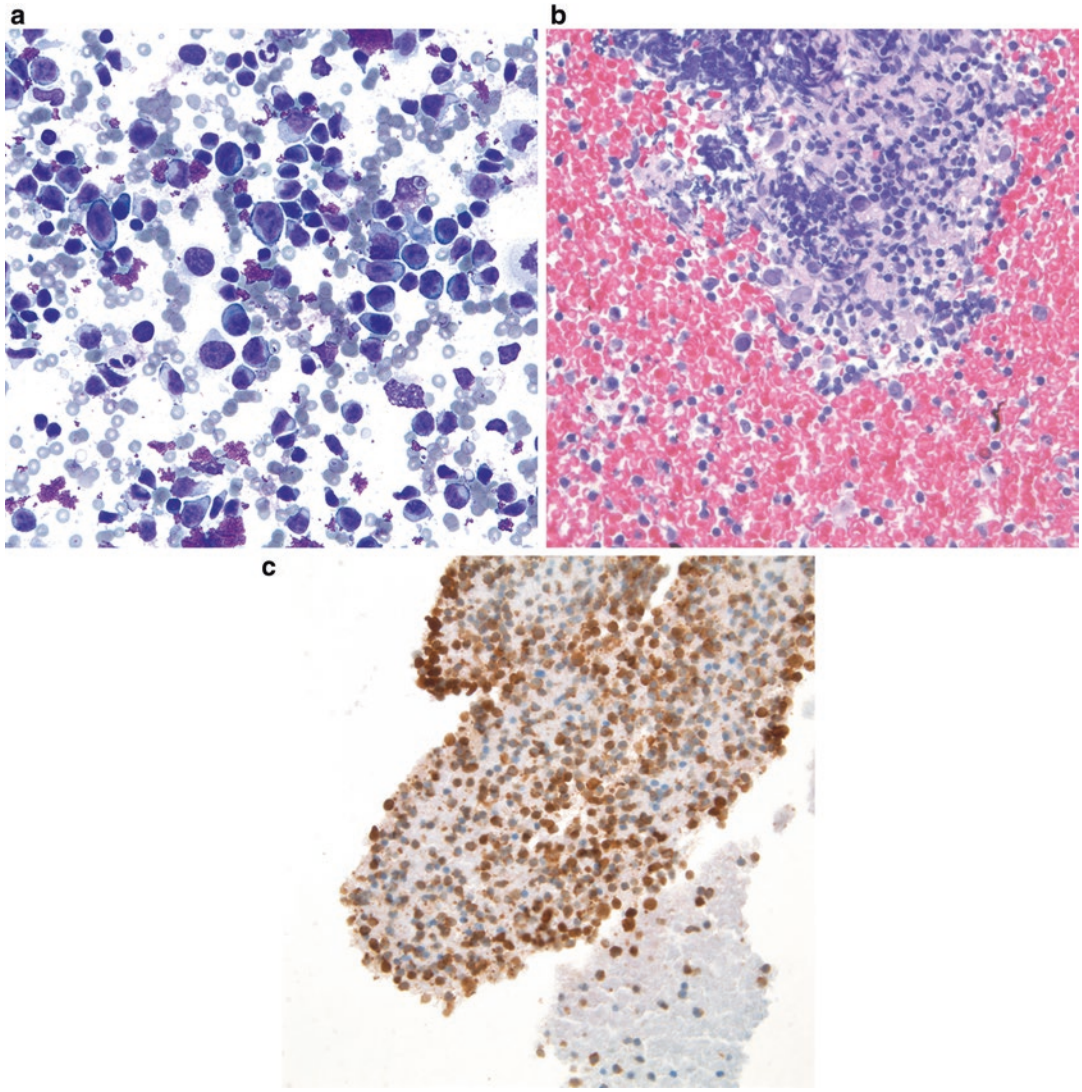


**Fig. 3.16** Infectious mononucleosis. (**a**. Diff-Quik stain, high power; **b**. H&E stain, high power; **c**. EBER in situ hybridization). These aspirates show a shift to intermediate-sized to large immunoblastic cells with immature-appearing chromatin, prominent nucleoli, and basophilic cytoplasm. EBV in situ hybridization (EBER) performed on a cell block is positive (**c**).

disorder and a cell block for immunohistochemical stains and EBER in situ hybridization.

### Differential Diagnosis

The main differential diagnostic considerations include drug-related lymphadenopathy, post-vaccine lymphadenopathy, other infections, such as toxoplasmosis, and lymphoproliferative disorders. The heterogeneous lymphoid population in IM helps to distinguish this entity from non-Hodgkin lymphomas, which are composed of a relatively homogenous population of cells. Distinction between classical Hodgkin lymphoma (CHL) and IM can be challenging as both have a heterogeneous population of cells, RS and RS-like cells are morphologically similar, and in some cases, EBER is positive in RS cells. Eosinophils may be present but are not usually a prominent feature of IM and as previously noted, RS-like cells are CD15 negative. In

addition, RS-like cells are usually positive for BOB.1 and OCT-2, which helps to distinguish IM from the infrequent cases of classical Hodgkin lymphoma.

**Pearls**

Ancillary studies, including flow cytometry, immunohistochemical stains, and in situ hybridization for EBER, are important for confirming the diagnosis and excluding malignancies, particularly in cases with atypical clinical presentations.

### 3.4.8 Sinus Histiocytosis with Massive Lymphadenopathy (Rosai-Dorfman Disease)

**Clinical Features**

SHML is a rare histiocytic disorder of uncertain etiology that most often presents with bulky, bilateral, painless cervical lymphadenopathy in children, but can occur in any node, in extranodal sites, and at any age. It is a benign, self-limited condition, although the course may be protracted [20].

**Cytological Features**

The characteristic finding in SHML is the presence of emperipolesis, which is the engulfment of benign lymphocytes and erythrocytes by histiocytes. The cells are markedly enlarged with abundant pale cytoplasm containing intact engulfed cells surrounded by a thin halo. Nuclei are round to oval with smooth nuclear contours, fine chromatin, and small but conspicuous nucleoli. The histiocytes are positive for CD68, S100, and fascin, but are negative for CD1a [20]. The background lymphoid population is heterogeneous. Eosinophils are usually absent.

**Differential Diagnosis**

The main differential diagnostic considerations are hemophagocytic lymphohistiocytosis and Langerhans cell histiocytosis, which are discussed in Sects. 3.4.4 and 3.4.5, respectively.

**Pearls**

In emperipolesis, the histiocytes can be distinguished from tingible body macrophages by the presence of intact engulfed lymphocytes and erythrocytes rather than cellular debris.

## 3.5 Malignant Entities

### 3.5.1 Hodgkin Lymphoma

**Clinical Features**

Classical Hodgkin lymphoma (CHL) accounts for 95 % of Hodgkin lymphomas and has a bimodal age distribution, with the earlier peak occurring in adolescence and young adulthood. Patients usually present with cervical or mediastinal lymphadenopathy, and may have B symptoms, including fever, night sweats, and weight loss. Nodular lymphocyte-predominant Hodgkin lymphoma (NLPHL) accounts for approximately 5 % of Hodgkin lymphomas and primarily affects 30- to 50-year-old males. The majority of patients present with localized peripheral adenopathy [21].

**Cytological Features**

CHL is characterized by variable numbers of Reed–Sternberg (RS) cells within a polymorphous background containing increased eosinophils (Fig. 3.17). Classical RS cells are large cells with abundant cytoplasm and two nuclei or nuclear lobes. Nuclei are with irregular membranes, pale chromatin, and a single eosinophilic nucleolus surrounded by a clear halo in each nucleus or lobe. Mononuclear variants (Hodgkin cells) and mummified cells are also present. The malignant cells comprise a small minority of the cells, and are positive for CD30 in a Golgi and membranous pattern, CD15, MUM-1, and PAX5 (weak), and negative for OCT-2 and/or BOB.1 [21]. Granulomas may also be seen. NLPHL is characterized by a predominant population of small lymphocytes with admixed histiocytes and scattered malignant cells. Lymphocyte-predominant (LP) or so-called popcorn cells are large with scant cytoplasm and a single convoluted or multilobated nucleus with multiple, basophilic nuclei that are smaller than those in

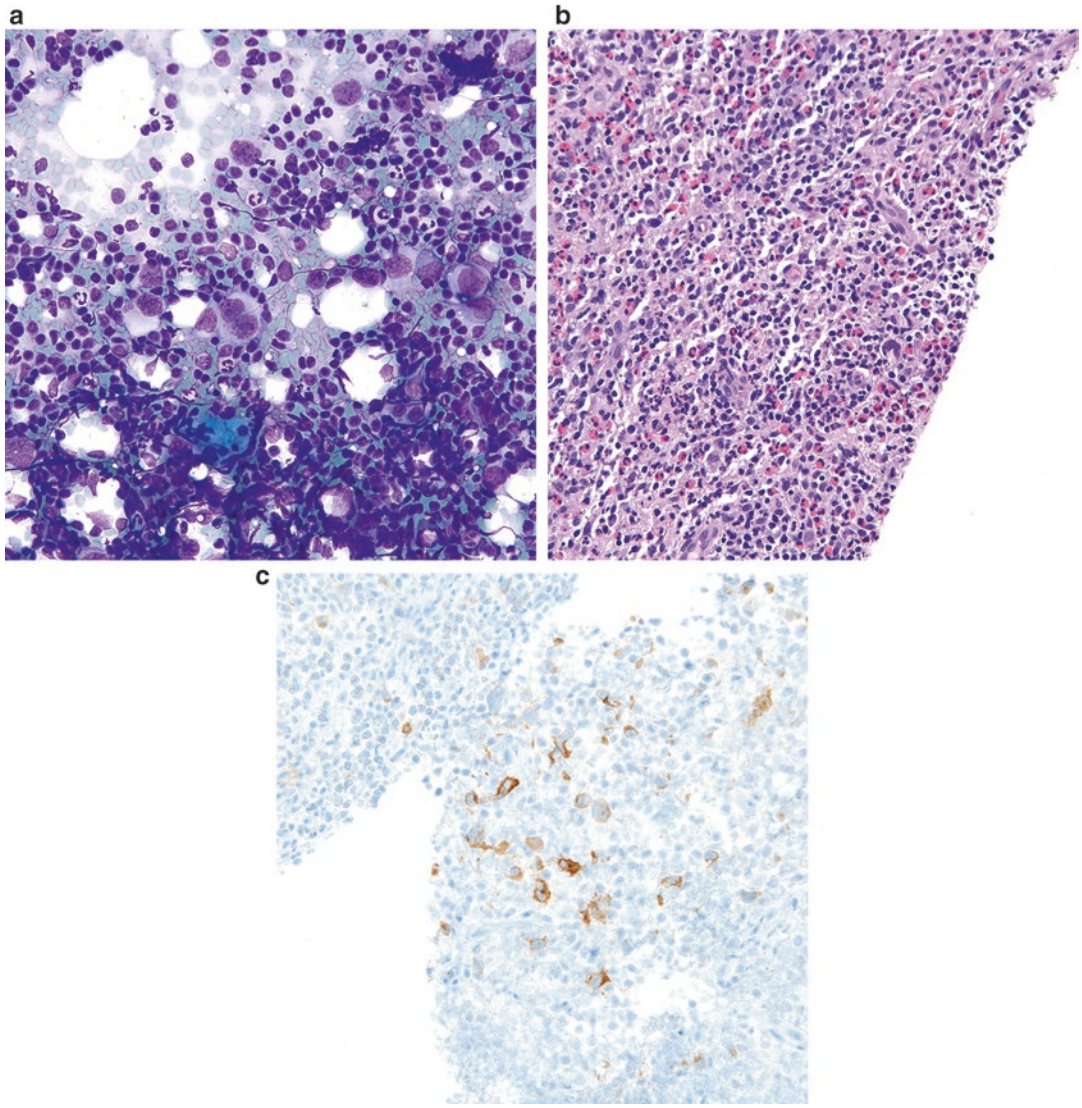


**Fig. 3.17** Classical Hodgkin lymphoma (**a**. Diff-Quik stain, high power; **b**. H&E stain, medium power; **c**. CD30 stain, medium power). The aspirates reveal Reed–Sternberg (RS) cells with binucleation and prominent nucleoli, within a polymorphous background of lymphocytes and eosinophils (**a**, **b**). CD30 (**c**) is positive in the large RS cells.

RS cells. Occasional LP cells are morphologically indistinguishable from RS cells. However, in contrast to RS cells, LP cells are positive for CD20, CD79a, BCL6, OCT-2, and BOB.1, and negative for CD30 and CD15 [21].

### Differential Diagnosis

The main differential diagnostic considerations are reactive lymphoid proliferations, infectious mononucleosis, and other viral infections that may have large immunoblastic cells that mimic RS cells, anaplastic large T-cell lymphoma (ALCL) and other large cell non-Hodgkin lymphomas, and metastatic malignancies such as seminoma and melanoma.

### Pearls

- Immunohistochemical stains are critical for confirming the diagnosis of Hodgkin lymphoma given the wide variety of different

entities in the differential diagnosis, some of which are also CD30-positive.
- Flow cytometry shows a reactive pattern and therefore is non-contributory.

### 3.5.2 Lymphoblastic Leukemia/ Lymphoma

#### Clinical Features

Acute lymphoblastic leukemia (ALL) comprises about 75 % of all acute leukemias in the pediatric population, and is also one of the most curable based on modern treatments [22]. These malignancies can be of B (B-ALL) or T (T-ALL) cell origin. B-ALL accounts for 85 % of pediatric ALL and the majority of cases occur in children under 5 years of age [22]. In contrast, T-ALL comprises approximately 15 % of pediatric ALL, is more common in older children and adolescents, and affects males more often than females. Lymph node involvement is common in ALL, whereas primary lymphoblastic lymphoma (LBL) without leukemia occurs less often [22, 23]. B-LBL comprises approximately 10 % of primary lymphoblastic lymphomas and like B-ALL occurs in children. They often present in the head and neck, and patients are usually asymptomatic with limited disease. In contrast, T-LBL comprises 85–90 % of primary lymphoblastic lymphomas, and like T-ALL occurs more frequently in adolescent males. Patients often present with a large mediastinal mass, and may have tracheal compression, superior vena cava syndrome, and/or pleural effusions. B-ALL and B-LBL have favorable prognoses, whereas T-ALL and T-LBL have less favorable outcomes and require more aggressive treatment [22, 23, 24]. Risk stratification is used to determine treatment and is based on clinical, laboratory, and genetic findings.

#### Cytological Features

B-ALL/LBL and T-ALL/LBL are morphologically indistinguishable. They are characterized by a homogenous population of intermediate-sized lymphoblasts with scant cytoplasm, round, oval or irregular nuclei, dispersed, finely granular chromatin, and prominent nucleoli. Mitotic figures and tingible body macrophages are present and may be numerous, similar to Burkitt lymphoma. The lymphoblasts in both T- and B-ALL/LBL are TdT-positive by flow cytometry or immunohistochemistry. In addition, T-ALL/LBL shows variable expression of CD1a and T-cell markers, as well as clonal rearrangement of T-cell receptor genes [23]. B-ALL/LBL is usually positive for CD19, CD10, and PAX5, is variably positive for CD20 and CD34, and also expresses the myeloid markers CD13 and CD33. Of note, T-cell receptor gene rearrangements may be seen in up to 70 % of B-ALL/LBL and thus are not useful for determination of lineage [22]. Various cytogenetic and molecular abnormalities are present, some of which define specific subtypes of ALL/LBL.

#### Differential Diagnosis

The main diagnostic considerations: Burkitt lymphoma, diffuse large B-cell lymphoma, thymoma, and reactive immunoblastic proliferations, such as infectious mononucleosis. Burkitt lymphoma and diffuse large B-cell lymphoma are discussed in Sect. 3.5.4.

#### Pearls

- When the clinical or cytological features are suspicious for lymphoma, it is essential to collect adequate additional material for flow cytometry, immunohistochemistry, FISH, and molecular studies.
- Thin, evenly spread, cellular smears may be preferable to sections from a cell block for molecular studies.
- Aspirates targeting a mediastinal mass may inadvertently sample normal thymic tissue. Normal immature T-cells maturing in the thymus are phenotypically similar to a T-LBL with positivity for TdT, CD3, and CD1a. Flow cytometry of a sample derived from thymic tissue shows a heterogeneous population of T-cells encompassing the maturation spectrum, whereas a clonal population of immature T-cells is present in T-LBL.

### 3.5.3 Acute Non-Lymphocytic Leukemia

#### Clinical Features

Acute leukemias of non-lymphoid origin comprise about 20 % of pediatric leukemias, except in newborns where they are more common than lymphoblastic leukemia. In children less than 2 years of age, monocytic leukemias tend to be the most common, whereas in older children, myeloblastic and myelomonocytic leukemias predominate. When non-lymphoid leukemic cells form a mass lesion, it is referred to as a granulocytic/myeloid sarcoma or chloroma; however, this is rare in children and most often these leukemias will present in the peripheral blood or bone marrow, and never undergo FNA evaluation.

#### Cytological Features

The morphologic features of the blasts vary, depending on the degree of maturation and type of cell. Myeloid blasts tend to have round, ovoid, or irregular nuclei similar to those seen in ALL/LBL, whereas myelomonocytic and monocytic leukemias tend to have either round or more convoluted nuclei. The blasts are intermediate to large in size with scant-to-abundant cytoplasm with or without vacuoles, granules, or Auer rods, depending on the type of cells. Nuclei have pale, delicate, or lacey chromatin with one or more nucleoli. Flow cytometry and immunohistochemical stains are important for determining maturation and cell lineage markers.

#### Differential Diagnosis

The main differential diagnostic considerations include lymphoblastic or other non-Hodgkin lymphoma, as well as other malignancies such as germ cell tumors, melanoma, and sarcomas with epithelioid morphology.

#### Pearls

- Leukemias are rarely seen in FNA specimens, except for myeloid/granulocytic sarcomas that present with a mass lesion. Although rare, these tumors should be considered when a sample consists of a monomorphous population of intermediate to large, dyscohesive epithelioid cells.
- According the 2008 World Health Organization (WHO) classification, the term myeloid sarcoma should be used, opposed to previously used terms like chloroma and granulocytic sarcoma.

### 3.5.4 Other Non-Hodgkin Lymphomas

#### Clinical Features

In addition to lymphoblastic lymphomas (described above), the most common non-Hodgkin lymphomas (NHLs) in the pediatric population include Burkitt lymphoma, large B-cell lymphomas including diffuse (DLBCL) and primary mediastinal (thymic) PMBL, and anaplastic large cell lymphoma (ALCL) [24]. Of these, Burkitt lymphoma is the most common, comprising 50–60 % of NHL children and adolescents, may be endemic related to EBV infection or sporadic, and usually presents in head and neck or abdomen [25]. Large B-cell lymphomas account for approximately 10–15 % of pediatric NHLs, occur more frequently in adolescents than younger children, and include DLBCL and PMBL subtypes [26, 27]. DLBCL can present with nodal and/or extranodal disease. PBML is likely of thymic origin and by definition arises in the anterior mediastinum without evidence of lymphoma elsewhere. ALCL comprises 10–20 % of childhood NHLs, has a peak incidence in the second decade of life, and often presents with nodal and extranodal disease and B symptoms [28]. Small B-cell lymphomas, which are common in adults, are rare in children.

#### Cytological Features

These NHLs are characterized by homogeneous populations of intermediate to large malignant cells and, with the exception of PMBL, typically yield highly cellular cytologic specimens.

In Burkitt lymphoma, the cells are intermediate in size, have scant, deeply basophilic cytoplasm with "punched-out" vacuoles, and round or slightly irregular nuclei with clumped, dispersed chromatin, and multiple nucleoli. Numerous mitoses, apoptotic bodies, and tingible body macrophages are present (Fig. 3.18).

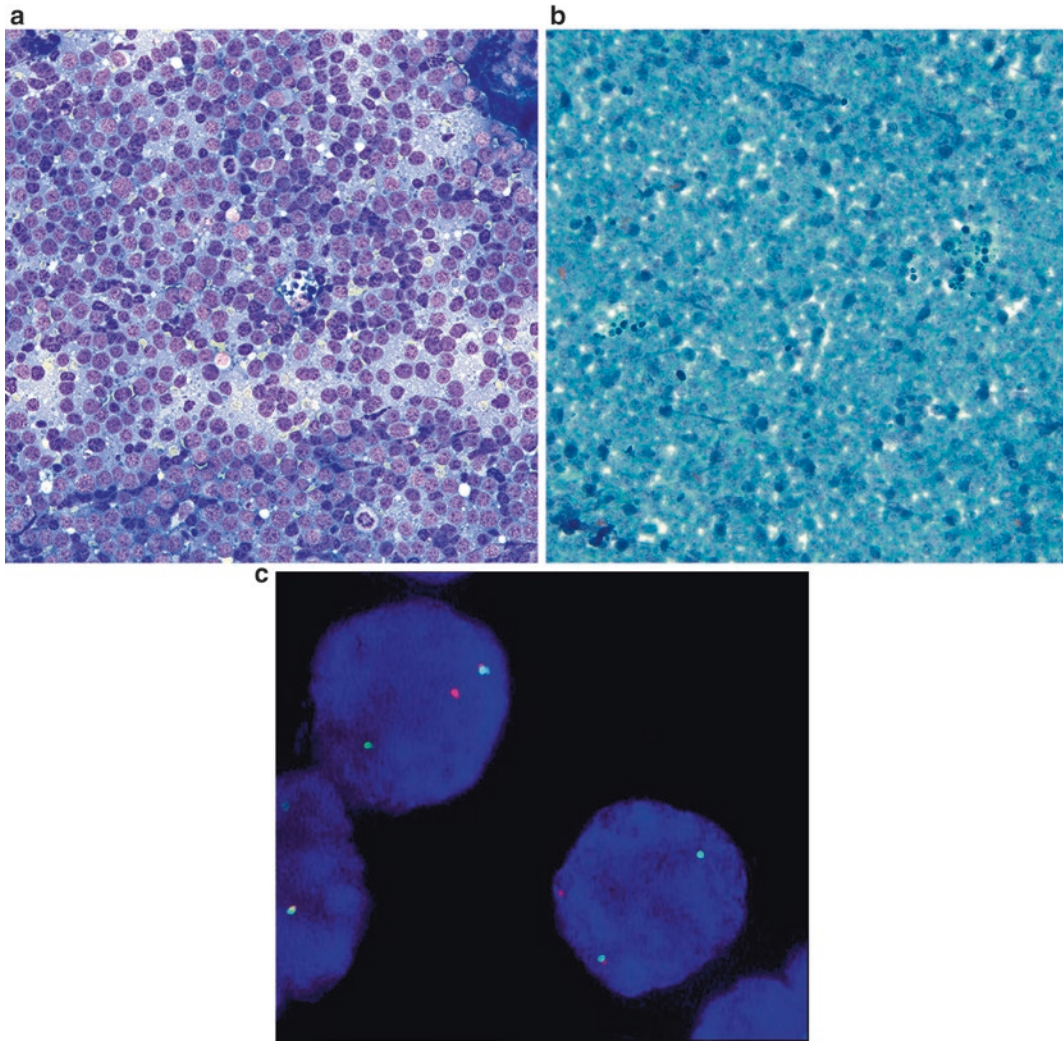


**Fig. 3.18** Burkitt lymphoma (**a**. Diff-Quik stain, high power; **b**. Papanicolaou stain, high power; **c**. FISH with the *CMYC* breakapart probe). This aspirate from a 14-year-old girl with Burkitt lymphoma presenting as a neck mass shows a uniform intermediate-sized lymphoid population with mitoses and tingible body macrophages (**a**, **b**), which had a high proliferation index on Ki-67. FISH studies confirmed a *CMYC* gene rearrangement (**c**).

The cells have a mature B-cell phenotype and are positive for CD10, CD19, CD20, CD79a, Bcl-6, and surface immunoglobulin, and negative for TdT and MUM1. Ki-67 (MIB1) is positive in virtually 100 % of cells. In situ hybridization for EBER is positive in all endemic and up to 30 % of sporadic cases. Translocations involving the *MYC* gene on chromosome 8 and an *IG* gene, usually *IGH* on chromosome 14, are present in almost 100 % of cases [24, 25].

DLBCLs are morphologically diverse tumor with three main variants recognized. Centroblastic, the most common variant, is composed of large cells with scant cytoplasm and round, irregular, or lobated vesicular nuclei with fine chromatin and multiple nucleoli. Immunoblastic DLBCL is composed of large cells with moderate to abundant cytoplasm, and round, oval, or irregular nuclei with a single, prominent central nucleolus. Anaplastic DLBCL is composed of pleomorphic, large, round, oval, or polygonal cells with bizarre nuclei and/or multinucleation, and may resemble Hodgkin lymphoma and/or ALCL. Mitotic figures, apoptoses, and variable numbers of tingible body macrophages are present. DLBCLs have a mature B-cell phenotype and are positive for

CD19, CD20, CD79a, variably positive for CD10, Bcl-6, and surface immunoglobulin, usually negative for MUM1 and negative for TdT. CD30 is often positive, particularly in the anaplastic variant. Many DLBCL have translocations involving *IGH* and various partner genes, including *BCL6* (up to 30%), *BCL2* (20–30%), and *MYC* (6%) [24, 26]. In addition, some tumors have morphologic features intermediate between Burkitt lymphoma (BL) and DLBCL, and for these, immunophenotyping and genetic analysis are essential for diagnosis and treatment, as these tumors may represent BL, DLBCL, or B-cell lymphoma, unclassifiable, with features intermediate between DLBCL and BL [29].

PMBLs typically yield paucicellular specimens with poorly preserved large cells with a spectrum of morphologies similar to those seen in DLBCL. On corresponding biopsies distinctive compartmentalizing thin fibrous bands are

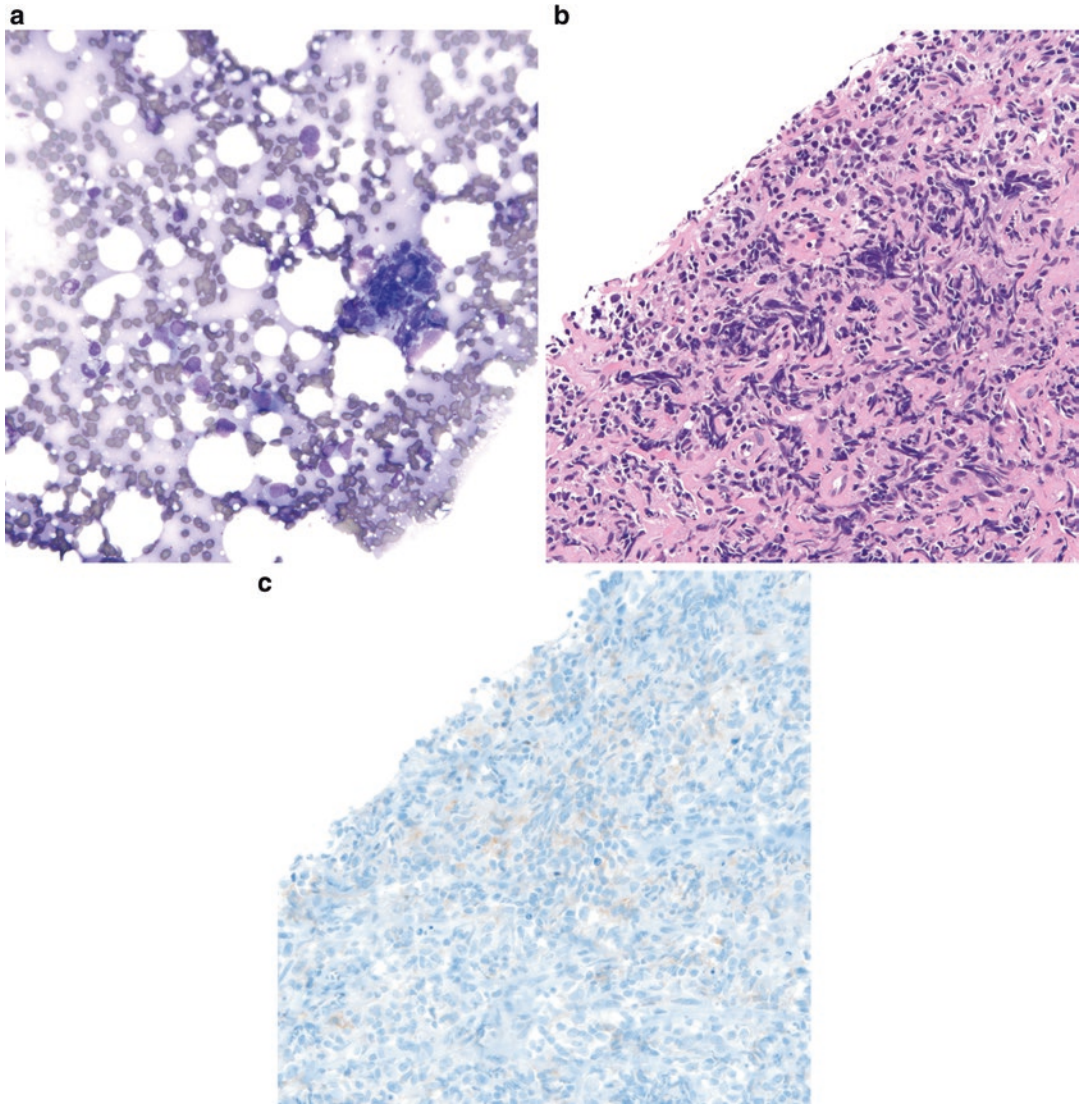


**Fig. 3.19** Mediastinal thymic large B-cell lymphoma (**a**. Diff-Quik stain, high power; **b**. H&E stain, high power; **c**. CD30 stain, high power). This lymphoma typically has intermediate-to-large lymphoid cells with artifactual distortion and limited aspirates due to the interlacing fibrosis. The core biopsy highlights the compartmentalizing fibrosis and the CD30 shows the weak but diffuse staining that is usually seen in these tumors.

present throughout (Fig. 3.19). The cells are positive for CD19, CD20, CD79a, and MUM1, variably positive for Bcl-6 and CD30, usually negative for CD10, and negative for surface immunoglobulin and TdT [27].

Like DLBCL, ALCL is morphologically heterogeneous, with common, lymphohistiocytic, small cell, Hodgkin-like, and composite patterns. Common to all patterns is the presence of variable numbers of the so-called hallmark cells, which have eccentric, reniform, or U-shaped nuclei. ALCLs are positive for CD30 and ALK, usually positive for EMA, variably positive for T-cell antigens, and negative for CD15 and B-cell markers. Of note approximately 75% of ALCLs are CD3 negative. Some ALCLs have an apparent null cell phenotype due to loss of multiple pan T-cell antigens, but are positive for cytotoxic markers such as

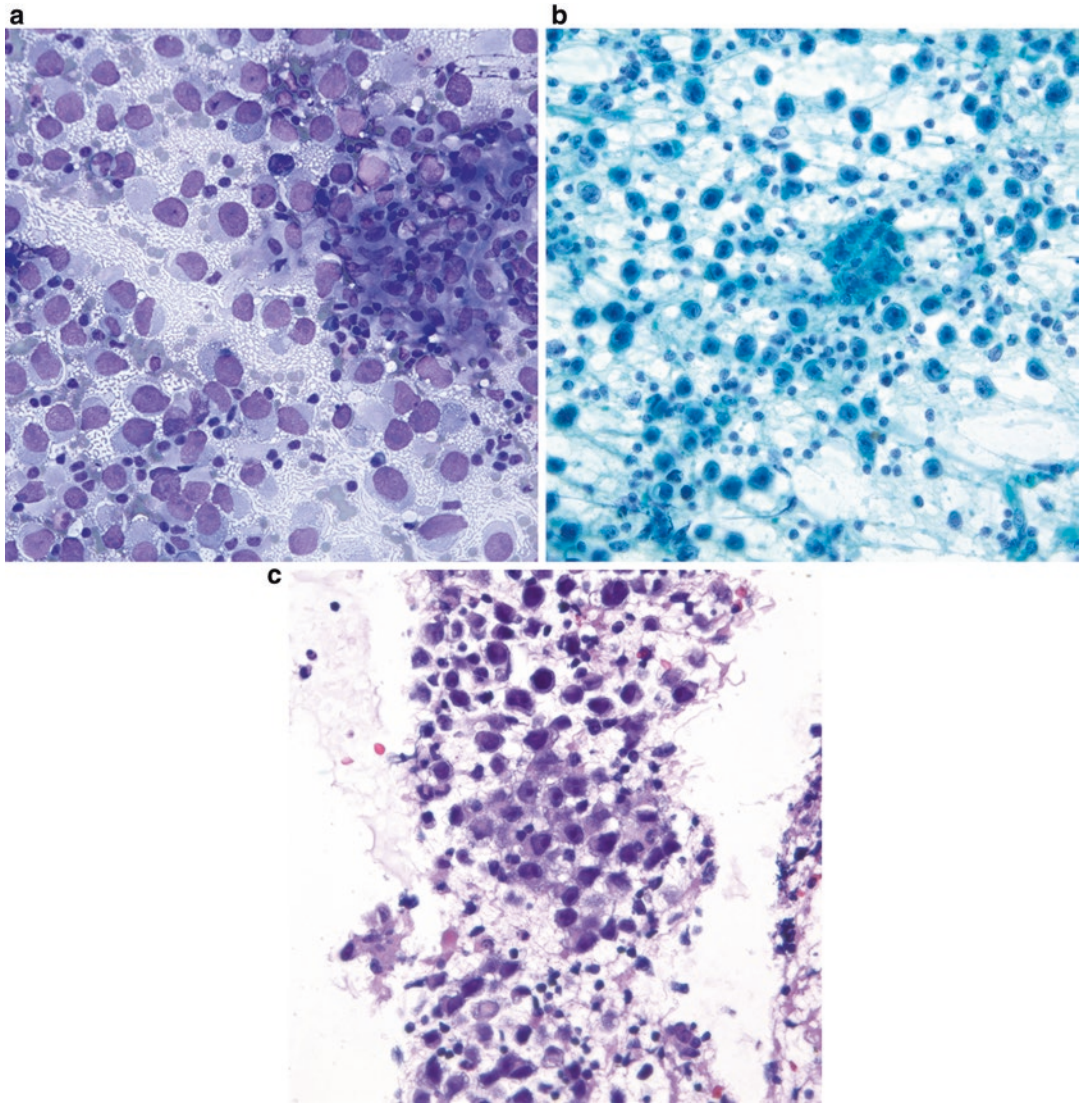


**Fig. 3.20** Metastatic seminoma (**a**. Diff-Quik stain, high power; **b**. Papanicolaou stain, high power; **c**. H&E stain, high power). Seminomas show a discohesive pattern of cells with prominent nucleoli and a tigroid background on modified Giemsa-stained slides (**a**) due to the glycogen in the cells. There is also a lymphohistiocytic background, often with granulomas (**a**–**c**). The tigroid background is not typically seen in alcohol fixed material (**b**, **c**).

perforin, granzyme B, and TIA-1. *ALK* rearrangements are present in over 90 % of cases [28].

### Differential Diagnosis

The differential diagnosis varies depending on the type of non-lymphoblastic NHL, but in general includes Hodgkin lymphoma, lymphoblastic lymphoma, and metastatic melanoma, sarcoma, germ cell tumors, carcinoma, and pediatric round blue cell tumors. Ancillary studies are required to distinguish between these entities.

### Pearls

- Collection of additional material for flow cytometry, immunohistochemical studies, and FISH is essential.
- Cellular, evenly spread unstained smears, may be preferable to sections from a cell block for FISH.
- CD30 positivity is present in many tumors in the differential diagnosis, and therefore must be interpreted in the context of other immunophenotypic and molecular findings.

## 3.5.5 Other Malignancies

In the pediatric population, the more common non-lymphoid malignancies metastatic to lymph nodes include small round cell tumors, germ cell tumors (Fig. 3.20), malignant melanoma, and several carcinomas, including papillary thyroid carcinoma, medullary carcinoma, and nasopharyngeal carcinoma. Non-lymphoid small round cell malignancies are summarized in Table 3.4.

## References


1. Cardillo MR. Fine-needle aspiration cytology of superficial lymph nodes. Diagn Cytopathol. 1989;5:166–73.
2. Rimm DL, Stastny JF, Rimm EB, Ayer S, Frable WJ. Comparison of the costs of fine needle aspiration and open surgical biopsy as methods for obtaining a pathologic diagnosis. Cancer. 1997;81:51–6.
3. Steel BL, Schwartz MR, Ramzy I. Fine needle aspiration biopsy in the diagnosis of lymphadenopathy in 1103 patients: role, limitations, and analysis of diagnostic pitfalls. Acta Cytol. 1995;39:76–81.
4. Lioe TF, Elliott H, Allen DC, Spence RAJ. The role of fine needle aspiration cytology (FNAC) in the investigation of superficial lymphadenopathy: uses and limitations of the technique. Cytopathology. 1999;10:291–7.
5. Prasad RR, Narasimhan R, Sankaran V, Veliath AJ. Fine-needle aspiration cytology in the diagnosis of superficial lymphadenopathy: an analysis of 2,418 cases. Diagn Cytopathol. 1996;15:382–6.
6. Thomas JO, Adeyi D, Amanguno H. Fine-needle aspiration in the management of peripheral lymphadenopathy in a developing country. Diagn Cytopathol. 1999;21:159–62.
7. O'Dowd GJ, Frable WJ, Behm FG. Fine needle aspiration cytology of benign lymph node hyperplasia: diagnostic significance of lymphohistiocytic aggregates. Acta Cytol. 1985;29:554–8.
8. Monaco SE, Teot LA. Cytopathology of pediatric malignancies: where are we today with fine-needle aspiration biopsies in pediatric oncology? Cancer Cytopathol. 2014;122:322–36.
9. Lim MS, Straus SE, Dale JK, Fleisher TA, Stetler-Stevenson M, Strober W, Sneller MC, Puck JM, Lenardo MJ, Elenitoba-Johnson KSJ, Lin AY, Raffeld M, Jaffe ES. Pathological findings in human autoimmune lymphoproliferative syndrome. Am J Pathol. 1998;153:1541–50.
10. Chen M, Wang J. Gaucher disease: review of the literature. Arch Pathol Lab Med. 2008;132:851–3.
11. Mokhtari M, Kumar PV, Talei AR. Gaucher-like cells in retroperitoneal extramedullary hematopoietic tumor diagnosed by fine needle aspiration: a case report. Acta Cytol. 2010;54:903–6.
12. Janka GE, Lehmberg K. Hemophagocytic syndromes—an update. Blood Rev. 2014;28:135–42.
13. Swerdlow S, Campo E, Harris N, et al. WHO classification of tumors of hematopoietic and lymphoid tissue. 4th ed. Lyons: IARC Press; 2008. p. 358–60.
14. Kakkar S, Kapila K, Verma K. Langerhans cell histiocytosis in lymph nodes: cytomorphologic diagnosis and pitfalls. Acta Cytol. 2001;45:327–32.
15. Sudilovsky D, Cha I. Fine needle aspiration cytology of dermatopathic lymphadenitis. Acta Cytol. 1998;42:1341–7.
16. Iyer VK, Kapila K, Verma K. Fine-needle aspiration cytology of dermatopathic lymphadenitis. Acta Cytol. 1998;42:1347–51.
17. Tong TR, Chan OW, Lee KC. Diagnosing Kikuchi disease on fine needle aspiration biopsy: a retrospective study of 44 cases diagnosed by cytology and 8 by histopathology. Acta Cytol. 2001;45:953–7.
18. Deaver D, Horna P, Cualing H, Sokol L. Pathogenesis, diagnosis and management of Kikuchi-Fujimoto disease. Cancer Control. 2014;21:313–21.
19. Louissnat A, Ferry JA, Soupir CP, et al. Infectious mononucleosis mimicking lymphoma: distinguishing morphological and immunophenotypic features. Mod Pathol. 2012;25:1149–59.

20. Shi Y, Griffin AC, Zhang PJL, et al. Sinus histiocytosis with massive lymphadenopathy (Rosai-Dorfman disease): a case report and review of 49 cases with fine needle aspiration cytology. CytoJournal. 2011;8:3.
21. Swerdlow S, Campo E, Harris N, et al. WHO classification of tumors of hematopoietic and lymphoid tissue. 4th ed. Lyons: IARC Press; 2008. p. 323–30.
22. Swerdlow S, Campo E, Harris N, et al. WHO classification of tumors of hematopoietic and lymphoid tissue. 4th ed. Lyons: IARC Press; 2008. p. 168–70.
23. Swerdlow S, Campo E, Harris N, et al. WHO classification of tumors of hematopoietic and lymphoid tissue. 4th ed. Lyons: IARC Press; 2008. p. 176–8.
24. Minard-Colin V, Brugières L, Reiter A, et al. Non-Hodgkin lymphoma in children and adolescents: progress through effective collaboration, current knowledge, and challenges ahead. J Clin Oncol. 2015;33:2963–74.
25. Swerdlow S, Campo E, Harris N, et al. WHO classification of tumors of hematopoietic and lymphoid tissue. 4th ed. Lyons: IARC Press; 2008. p. 262–4.
26. Swerdlow S, Campo E, Harris N, et al. WHO classification of tumors of hematopoietic and lymphoid tissue. 4th ed. Lyons: IARC Press; 2008. p. 233–7.
27. Swerdlow S, Campo E, Harris N, et al. WHO classification of tumors of hematopoietic and lymphoid tissue. 4th ed. Lyons: IARC Press; 2008. p. 250–1.
28. Swerdlow S, Campo E, Harris N, et al. WHO classification of tumors of hematopoietic and lymphoid tissue. 4th ed. Lyons: IARC Press; 2008. p. 312–6.
29. Swerdlow S, Campo E, Harris N, et al. WHO classification of tumors of hematopoietic and lymphoid tissue. 4th ed. Lyons: IARC Press; 2008. p. 267–8.

# Head and Neck

# 4

Anita L. Sengupta

## 4.1 Introduction

Fine needle aspirations (FNAs) of the head and neck can be divided into five categories: thyroid, salivary gland, lymph nodes, skin (acquired and congenital lesions), and bone/soft tissue (everything else). Each of these categories is discussed in this chapter, with the exception of lymph nodes (Chap. 3) and bone/soft tissue (Chap. 5), which are covered in greater detail in separate chapters.

The vast majority of mass lesions in the head and neck region are benign and amenable to FNA given their superficial nature; however, 5 % of pediatric neoplasms occur in the head and neck region [1, 2]. Clinical information, including the age of the patient and the location of the lesion, and radiologic findings are helpful for narrowing the differential diagnosis.

## 4.2 Thyroid

Palpable thyroid nodules are uncommon in children with a prevalence of 0.2–1.4 % [3, 4]. Older studies show a rate of malignancy ranging from 9 to 70 % [3], but more recent studies have shown a narrower range of 20–35 % [3, 5–9]. Some of the decrease noted in the upper limit of the range may be attributable to a decrease in the use of radiation therapy to the head and neck and a resulting decline in secondary cancers. Thyroid FNA is considered the gold standard for preoperative evaluation of thyroid nodules. One meta-analysis showed a sensitivity of 82 % and a specificity of 91 % in the pediatric population [9].

### 4.2.1 Benign Thyroid Nodules

#### Clinical Features

The vast majority of pediatric thyroid nodules are benign (up to 65–80 %) [3, 5–9]. Most are benign follicular or hyperplastic nodules. Follicular adenoma, a benign neoplastic proliferation of follicular cells, is uncommon in the pediatric population. Chronic lymphocytic thyroiditis (Hashimoto's thyroiditis), a benign thyroid disease associated with elevated antithyroid serum antibodies, is also relatively common in the pediatric population. Chronic lymphocytic thyroiditis typically has a heterogeneous appearance on ultrasound examination.

#### Cytological Features

Benign thyroid nodules typically have abundant colloid with scant to moderate follicular epithelial cells. Some cases have cystic change, manifested by a background rich in hemosiderin-laden macrophages and debris (Fig. 4.1). The epithelial cells are seen in variably sized clusters and

A.L. Sengupta, MD (✉)
Department of Pathology, Children's Medical Center, Dallas, Texas 75235, USA
e-mail: anita.sengupta@utsouthwestern.edu



S.E. Monaco, L.A. Teot (eds.), *Pediatric Cytopathology*, DOI 10.1007/978-3-662-53441-0_4

two-dimensional sheets with evenly spaced round nuclei, and may have oncocytic features (Hürthle cell change) (Figs. 4.2 and 4.3). Occasionally, the follicular cells have an eosinophilic accentuation of the peripheral cytoplasm, so-called flame cells, which may be related to overproduction of thyroid hormone (Fig. 4.2). In chronic lymphocytic thyroiditis, follicular cell groups, often with oncocytic features, are seen in a background of small lymphocytes, plasma cells, and lymphohistiocytic aggregates or germinal center fragments.

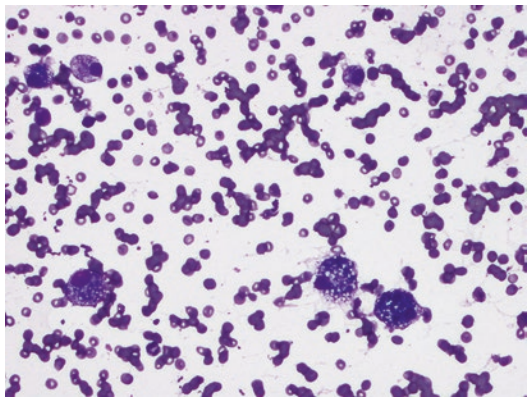

**Fig. 4.1** Thyroid cyst fluid (Diff-Quik stain, high power). Hemosiderin-laden macrophages in a background of watery colloid. Note that hemosiderin stains deep blue with Diff-Quik stain.

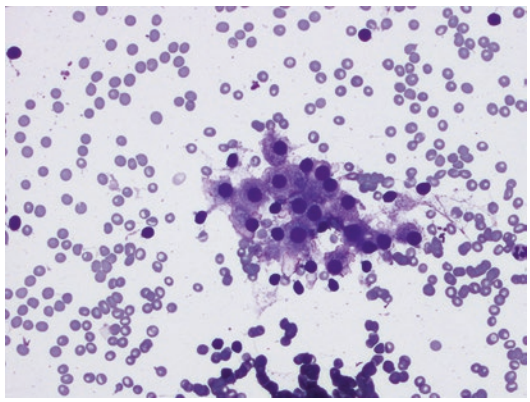

**Fig. 4.2** Benign follicular/colloid nodule with "flame cells" (Diff-Quik stain, high power). In this example of a benign colloid nodule, "flame" cells with cytoplasmic vacuoles are seen. These cells are primarily seen in benign nodules with an overproduction of thyroid hormone.

## Triage

Benign nodules that are hypocellular or have a predominance of cyst contents may benefit from liquid based cytology to facilitate identification of follicular cells. In cases with a prominent lymphoid population, cytological or clinical features that are concerning for a lymphoproliferative disorder should prompt collection of additional material for flow cytometry. Some laboratories allocate material for molecular studies on all thyroid FNAs at the time of the procedure, in case the final diagnosis is indeterminate.

## Differential Diagnosis

The main differential diagnostic consideration is a papillary thyroid carcinoma (PTC) with colloid or cystic changes. Nuclear features help to differentiate benign entities from PTC and are best appreciated on alcohol-fixed material. Lymphocytic thyroiditis also raises the possibility of ectopic cervical thymic tissue or a lymphoproliferative disorder.

## Pearls

- According to The Bethesda System for Reporting Thyroid Cytology (TBSRTC) [10], which is discussed in detail below, cases with abundant colloid, focal atypia, or features of lymphocytic thyroiditis do not require six groups of ten cells for adequacy. Thus, these cases should not be reported as non-diagnostic,

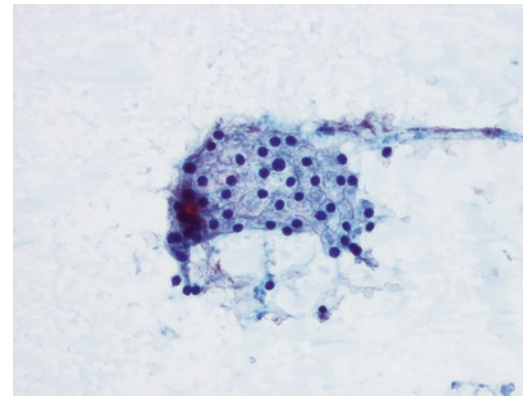

**Fig. 4.3** Benign follicular/colloid nodule (Papanicolaou stain, high power). Honeycomb arrangement of follicular cells with evenly spaced, round nuclei and no nuclear features of papillary thyroid carcinoma.

but rather benign (for abundant colloid and features of lymphocytic thyroiditis) or atypia/follicular lesion of undetermined significance (for focal atypia).
- In contrast, cases with abundant cyst contents should be meticulously examined and if there are insufficient follicular cells, they should be classified as non-diagnostic with a note that PTC with cystic changes cannot entirely be excluded.
- Imaging studies are an important part of the evaluation of a thyroid lesion. When the cytological findings do not correlate with the radiological impression, failure to sample the targeted lesion should be considered.

### 4.2.2 Malignant Thyroid Nodules

#### Clinical Features

The main thyroid malignancies in the pediatric population include PTC, follicular carcinoma, Hürthle cell or follicular oncocytic carcinoma, medullary thyroid carcinoma, and lymphoma. Metastatic neoplasms are more common in adults, but can rarely be seen in children as well. PTC accounts for the vast majority (80–95 %) of pediatric thyroid malignancies, and is the third most common solid tumor in the pediatric population. Previous radiation is a risk factor for development of PTC and 7–11 % of patients have a history of previous radiation [11, 12]. Up to 40–80 % of pediatric patients have metastatic disease at presentation, [6, 12, 13] and FNA of radiologically suspicious lymph nodes is frequently performed prior to surgery, and occasionally concurrently with the thyroid FNA to guide decisions regarding dissection of the lymph node chains. Follicular carcinoma accounts for most of the remainder of malignancies (5–15 %). Medullary thyroid carcinoma is uncommon (3–5 %), and frequently associated with familial cancer syndromes [3, 6, 8]. Multiple Endocrine Neoplasia (MEN) Types 2A and 2B are characterized by point mutations in the *RET* proto-oncogene and patients develop medullary thyroid carcinoma and pheochromocytoma. MEN 2A patients also have hyperparathyroidism, while MEN 2B patients have mucosal ganglioneuromas and Marfanoid habitus. Patients with MEN2 inevitably develop medullary thyroid carcinoma and thus, prophylactic thyroidectomy is recommended in early childhood.

#### Cytological Features

Follicular carcinomas show predominantly microfollicular architecture with scant colloid and high cellularity. Nuclear features of PTC are not seen in these tumors. Since vascular and capsular invasion cannot be assessed on FNA specimens, these cases are typically classified as suspicious for follicular neoplasm by TBSRTC [10] (Fig. 4.4).

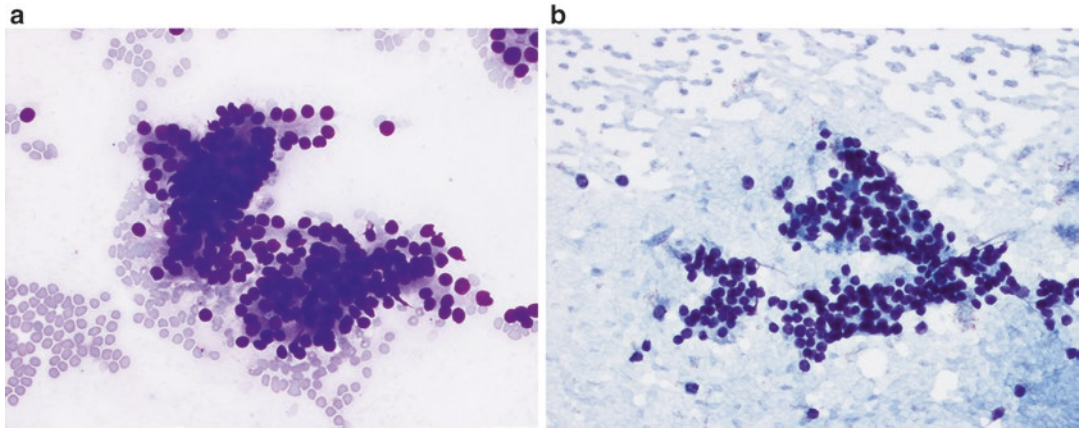


**Fig. 4.4** Suspicious for follicular neoplasm (**a**. Diff-Quik stain, high power; **b**. Papanicolaou stain, high power). Cellular clusters with prominent microfollicles and overlapping nuclei, seen in a background of scant colloid. This was follicular carcinoma on excision.

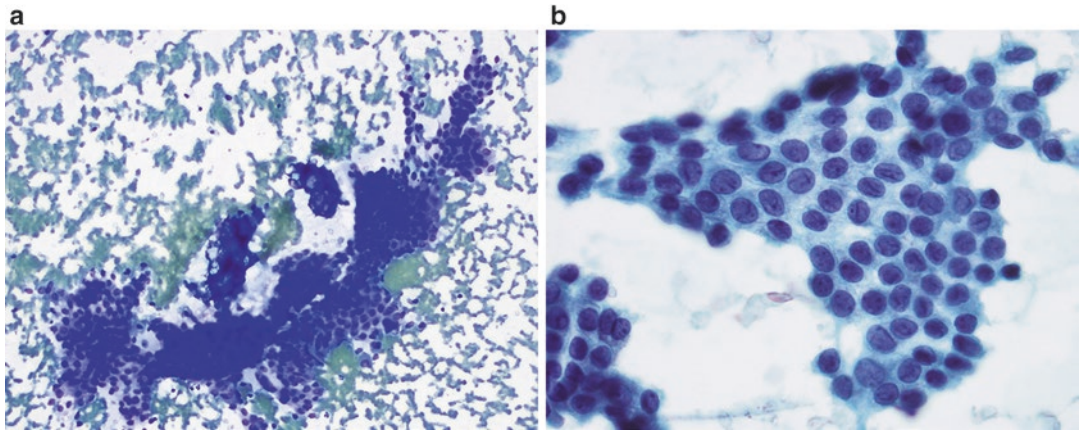


**Fig. 4.5** Papillary thyroid carcinoma (**a**. Diff-Quik stain, low power; **b**. Papanicolaou stain, high power). Papillary tissue fragments composed of crowded follicular cells with oval nuclei. The Papanicolaou stain (**b**) highlights prominent nuclear grooves, powdery chromatin and small nucleoli.

Classic PTC is more common in the pediatric population and may show true papillary tissue fragments with dyscohesive tumor cells surrounding a fibrovascular core, in addition to cells in sheets and follicular arrangements. The nuclear features include pale, evenly dispersed, fine chromatin, nuclear grooves, intranuclear pseudoinclusions, and small peripherally placed nucleoli (Fig. 4.5). In contrast to classic PTC, the follicular variant of PTC (FVPTC) and non-invasive follicular thyroid neoplasm with papillary-like nuclear features (NIFTP) lack true papillary fragments, and often has a greater number of microfollicles. Nuclear features of PTC may be subtle or absent in FVPTC and NIFTP. The background may have thick colloid, multinucleated giant cells, and/or atypical histiocytoid cells with cytoplasmic vacuolization.

Medullary thyroid carcinoma typically yields cellular aspirates with loosely cohesive and isolated tumor cells. The tumor cells are most often plasmacytoid, but spindled and/or round forms may also be seen. The cells have abundant granular cytoplasm and round to spindle nuclei with stippled chromatin (Fig. 4.6). Amyloid, which is indistinguishable from thick colloid on Papanicolaou-stained smears and may be metachromatic on modified Giemsa-stained preparations, may also be present in the background. Medullary thyroid carcinoma is positive for synaptophysin, calcitonin, TTF1, and carcinoembryonic antigen (CEA), while negative for thyroglobulin.

## Triage

Some thyroid malignancies may benefit from molecular studies. In addition, molecular studies may be helpful prior to resection, especially if there is an indeterminate cytological diagnosis. If medullary carcinoma is suspected, a cell block should be prepared to facilitate confirmatory special and immunohistochemical stains.

## Differential Diagnosis

The possibility of a hyperplastic colloid nodule should be considered in cases with abundant colloid and little cytological atypia. In PTC with cystic changes, the epithelial cells may have small cytoplasmic vacuoles and atypical nuclear features, thereby mimicking histiocytes (e.g., atypical histiocytoid cells), but are positive for TTF-1 and cytokeratin, and negative for CD68 [13]. Similarly, PTCs, especially those metastatic to lymph nodes, can mimic clusters of histiocytes, reactive germinal centers, and granulomatous inflammation. However, in this setting, the presence of nuclear features of PTC helps to exclude these entities. In addition, immunohistochemical stains help to confirm the diagnosis of a thyroid malignancy, and distinguish it from other benign and malignant processes.

## Pearl

In aspirates from lymph nodes lateral to the jugular vein, benign-appearing thyroid elements (colloid and follicular cells) should prompt serious

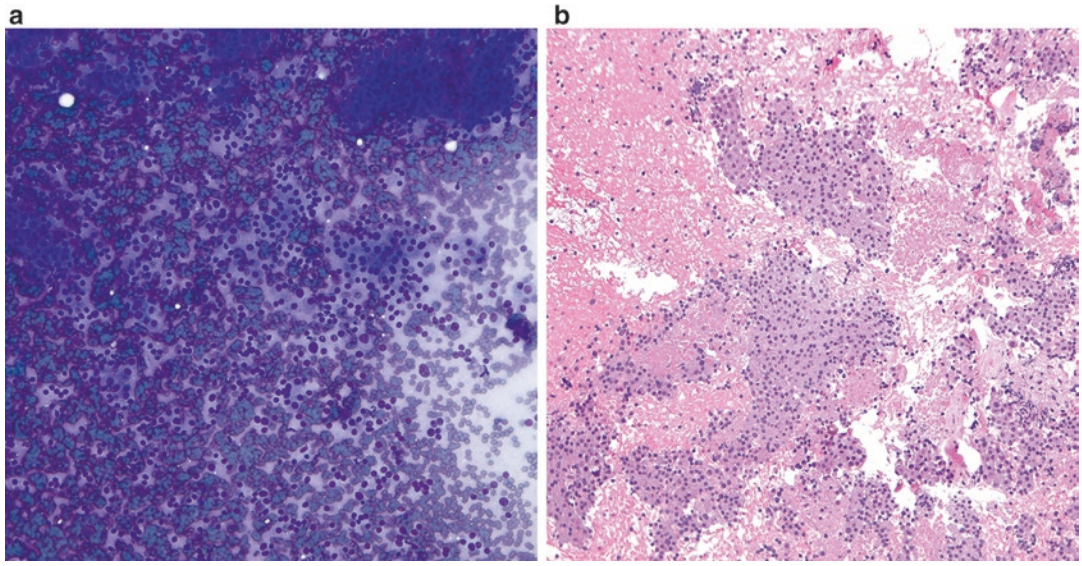


**Fig. 4.6** Medullary thyroid carcinoma (**a**. Diff-Quik stain, low power; **b**. H&E stain, low power). The tumor cells in this case of medullary carcinoma are relatively monomorphic, epithelioid and plasmacytoid. On the cell block (**b**), they appear oncocytic. Strong positive staining for calcitonin and neuroendocrine markers, in addition to positivity for a *RET* gene mutation, solidified the diagnosis of medullary thyroid carcinoma arising in the setting of multiple endocrine neoplasia (MEN). (Image courtesy of Dr. Sara Monaco).

consideration of a metastatic PTC, even if nuclear features of PTC are not clearly identified. However, in aspirates obtained from what radiologically appears to be a lymph node more medially in the neck, benign-appearing thyroid elements may represent rests of thyroid tissue along the embryological path of descent and warrant cautious interpretation. Similarly, in patients with dyshormonogenetic goiter, a portion of the multilobulated thyroid gland may be radiologically interpreted as a separate discrete mass or "lymph node," leading to misdiagnosis of metastatic carcinoma.

### 4.2.3 Reporting of Thyroid FNAs

The Bethesda System for Reporting Thyroid Cytopathology (TBSRTC) was developed in 2007–2010 as a standardized system of reporting thyroid fine needle aspiration biopsies with an implied risk of malignancy and recommended clinical management [10]. The system consists of six diagnostic categories with further descriptive diagnoses: Non-diagnostic, Benign, Atypia of Undetermined Significance or Follicular Lesion of Undetermined Significance, Follicular or Oncocytic Neoplasm or Suspicious for a Follicular or Oncocytic Neoplasm, Suspicious for Malignant Cells, and Malignant.

Although TBSRTC was largely developed based on adult data, there are two studies evaluating the application of TBSRTC to the pediatric population, which have shown an incremental increase in the risk of malignancy among the categories [7, 14]. However, in each category, the risk of malignancy is higher in the pediatric population. This is due to an overall higher incidence of malignancy (10–14 % in adults vs 20–35 % in children [3, 7]) and a lower incidence of benign neoplastic nodules (Table 4.1).

#### 4.2.3.1 Summary of TBSRTC Diagnostic Categories

In order to be adequate, an FNA must have a minimum of six groups of cells with at least ten follicular cells per group. Exceptions include cases with cytologic atypia in evaluable cells, nodules in a background of lymphocytic thyroiditis, and colloid nodules showing abundant colloid. A summary of TBSRTC categories is seen in Table 4.2.

**Table 4.1** Correlation of diagnostic categories by TBSRTC with the risk of malignancy overall and in studies restricted to pediatric populations

| Diagnostic category | Risk of malignancy (%)[a] | Risk of malignancy in children (%)[b] |
|---|---|---|
| Benign | 0–3 | 2–7 |
| Atypia of undetermined significance (AUS/FLUS) | 5–15 | 28–40 |
| Suspicious for follicular or oncocytic neoplasm | 15–30 | 58–100 |
| Suspicious for malignant cells | 60–75 | 40–100 |
| Positive for malignant cells | 97–99 | 100 |

[a]Adapted from Ali SZ and Cibas ES, eds. The Bethesda System for Reporting Thyroid Cytopathology [10]
[b]Adapted from Gupta et al. [7] and Monaco et al. [14]

### 4.2.4 Molecular Testing in Thyroid FNA

In the adult population, molecular testing is performed on cytological specimens from the thyroid in order to refine the cytologic diagnosis and thereby aid in management. In the case of an indeterminate cytologic diagnosis (e.g., AUS/FLUS, suspicious for follicular neoplasm, or suspicious for malignancy), the presence of mutations common in malignancy, particularly the *BRAF* mutation, may lead to more aggressive follow-up or surgical therapy. However, the distribution of genetic mutations is different in the children and adolescents than in the adults, and the utility of genetic testing in the pediatric population is unclear [11, 15–17].

#### 4.2.4.1 *BRAF* Mutations

Mutations in the *BRAF* gene, virtually all the 1799 T>A point mutation resulting in the V600E single amino acid substitution, are seen in up to 70 % of adult PTC and are associated with a more aggressive clinical course. Accordingly, testing for this mutation is increasingly offered in adult thyroid aspirates. However, this mutation is reported to be much less frequent in the pediatric population, being seen in 0–20 % (overall 7 %) of pediatric cases [16].

#### 4.2.4.2 *RET/PTC* Rearrangements

Translocations of the *RET* proto-oncogene on chromosome 10 are seen in 40–70 % of sporadic pediatric PTC, compared to less than 40 % in adults [11, 15]. There are three common translocations referred to as *RET/PTC1, RET/PTC2,* and *RET/PTC3*. Some studies have indicated a higher incidence of *RET/PTC1* in sporadic PTC and a higher incidence of *RET/PTC3* in radiation induced carcinoma [15]. Currently genetic testing for these translocations is performed in the clinical setting in some laboratories.

#### 4.2.4.3 *PAX8/PPAR* Gamma Rearrangements and *RAS* Mutations

A translocation between the *PAX8* gene and the *PPAR* gamma gene is seen in 20–50 % of adult follicular carcinoma of the thyroid [16]. Follicular carcinomas that do not have this translocation are frequently associated with *RAS* mutations. However, these changes are also seen in follicular adenomas and are not specific for carcinoma. Genetic testing for these changes is not commonly performed on aspirates in the clinical setting.

## 4.3 Salivary Gland

Lesions in the salivary glands include neoplasms, congenital vascular or cystic masses, and inflammatory lesions. True salivary gland epithelial neoplasms are rare in the pediatric population, but are largely benign. Intraparotid lymph nodes may present as a palpable mass or incidental radiologic finding. In addition, tumors of the connective tissues including benign lesions such as nodular fasciitis and solitary fibrous tumor or malignant lesions such as malignant peripheral nerve sheath tumor and rhabdomyosarcoma can involve the salivary glands (Personal archives, 19). Pilomatrixoma or other lesions of the skin or soft tissue overlying the parotid have also been mistaken for parotid masses.

**Table 4.2** Diagnostic categories for the Bethesda System for Reporting Thyroid Cytopathology

| Category | Cytological features | Recommended management |
|---|---|---|
| Unsatisfactory/ Non-diagnostic | Inadequate samples include cases with fewer than six groups of ten cells each (acellular or hypocellular), cases with technical problems limiting interpretation (staining, preservation, obscuring artifacts), and cases with cyst fluid only. | Repeat FNA after 3 months. However, if the cyst is drained upon aspiration and there is no remaining nodule, then a non-diagnostic FNA may be presumably negative for malignant cells, but radiological correlation is essential. |
| Benign | Aspirates typically show abundant colloid and moderate cellularity with follicular cells arranged in a two-dimensional sheets (benign colloid nodule, hyperplastic colloid nodule), or features of lymphocytic thyroiditis. Pediatric follicular cells may show a tighter arrangement than adult benign tissue, but an orderly arrangement without overlapping of nuclei should be visible. | Clinical follow-up, as needed. However, most studies report a 1–3 % false negative rate for benign thyroid FNAs, thus radiological correlation is essential with a negative diagnosis. |
| Atypia of undetermined significance/follicular lesion of undetermined significance (AUS/FLUS) | Cases with cytologic atypia or architectural atypia that is insufficient for a definitive diagnosis of suspicious for follicular neoplasm or malignancy. This includes cases with prominent microfollicles in a case that is otherwise benign or scantly cellular, cases that show predominantly oncocytic cells in a benign background, cases with cellular crowding due to clotting artifact or other obscuring factors, and cases with focal cytological atypia suggestive of papillary thyroid carcinoma. | Repeat FNA in 3–6 months. However, in the pediatric population, up to 40 % of these cases are malignant on excision [7, 14]. Thus, in conjunction with the clinical and radiological picture, some clinicians may choose to take the patient directly to surgery, especially if the patient has two AUS/FLUS diagnoses where the risk of malignancy approaches that of the suspicious for follicular neoplasm category. |
| Suspicious for follicular or oncocytic neoplasm | More cellular smears with significant crowding and overlapping of nuclei. There may be significant microfollicle formation. The nuclei are monotonous and slightly hyperchromatic. The key to diagnosis is the cellularity of the samples, lack of colloid, and the architecture of the clusters. In adults, the majority of cases with this diagnosis turn out to be follicular adenomas or follicular variant of papillary thyroid carcinoma, with a smaller proportion of follicular carcinomas. In the pediatric population, 60–100 % of these cases are malignant, usually papillary thyroid carcinoma [7, 14]. | Partial thyroidectomy is recommended for this category given the risk of malignancy. However, due to the high rate of malignancy in the pediatric population, clinicians may request molecular testing and based on the results, may choose to go directly to total thyroidectomy. |
| Suspicious for malignant cells | Most of the cases in this category are suspicious for papillary thyroid carcinoma; however, cases can also be suspicious for lymphoma, medullary thyroid carcinoma, metastatic carcinoma, or other malignancies. These cases usually quantitatively or qualitatively fall short of being diagnostic of malignancy. | Recommended management for cases suspicious for papillary thyroid carcinoma is usually a total thyroidectomy. Cases suspicious for lymphoma or metastatic neoplasms typically undergo repeat biopsy. |
| Positive for malignant cells (papillary carcinoma, medullary carcinoma, metastatic malignancy, lymphoma) | Cases of papillary thyroid carcinoma show abundantly cellular smears with characteristic nuclear features, including intranuclear inclusions, nuclear grooves, chromatin clearing. Cases of medullary carcinoma, metastatic malignancies, or lymphoma, are likewise highly cellular with morphologic and immunophenotypic features characteristic of the particular entity. | Recommended management for papillary thyroid carcinoma is total thyroidectomy. In the pediatric population, lymph node sampling should be considered due to the high rate of metastasis at the time of diagnosis. |

### 4.3.1 Benign Salivary Gland Lesions

#### Clinical Features

Most of the benign salivary gland lesions can be grouped into lymphoid or inflammatory lesions and cystic lesions. Benign lymphoid lesions include chronic sialadenitis, lymphoepithelial cysts, and intraparenchymal lymph nodes. Inflammatory lesions include acute sialadenitis or sialolithiasis, and chronic fibrosing sialadenitis (Kuttner tumor).

#### Cytological Features

Benign intrasalivary lymph nodes and chronic inflammatory processes are characterized by variable amounts of benign salivary tissue in a background of a heterogeneous lymphoid population with a predominance of small lymphocytes and intermixed histiocytes. Squamous or mucinous metaplasia may be present. Chronic sialadenitis can be associated with dense fibrosis, which clinically presents as a hard tumor-like mass, and may yield scantly cellular aspirates with stromal fragments. Acute sialadenitis has abundant neutrophils and inflammatory debris, and special stains for organisms should be performed in these cases. Cystic lesions include sialoceles and lymphoepithelial cysts, as well as extrasalivary cystic lesions such as thyroglossal duct cyst or branchial cleft cyst. Meticulous examination for the presence and type of cyst lining cells and correlation with radiology is essential.

#### Triage

A cell block can be prepared from the needle rinses or additional dedicated passes, and can be used for special stains, such as for microorganisms, or immunohistochemical stains. If a lymphoid lesion is concerning for lymphoma, additional material should be collected for flow cytometry. Acute inflammatory lesions should prompt collection of additional material for microbial cultures.

#### Differential Diagnosis

The main differential diagnostic considerations for lymphocytic lesions include reactive lymphoid processes in extrasalivary lymph nodes or adjacent soft tissues and lymphomas. In addition, lymphocyte-rich aspirates with a dirty background should raise the possibility of Warthin tumor, although this entity is exceedingly rare in the pediatric population. Acute sialadenitis can mimic an abscess or acute suppurative lymphadenitis.

#### Pearls

Many benign or inflammatory salivary gland lesions can be associated with metaplastic changes, such as squamous or mucinous metaplasia, which may raise concern for neoplasms such as low grade mucoepidermoid carcinoma. A conservative approach is recommended if mucinous and/or squamous features are focal, to avoid an erroneous diagnosis of malignancy.

### 4.3.2 Salivary Gland Neoplasms

#### 4.3.2.1 Introduction and Classification

#### Clinical Features

Salivary gland neoplasms are rare in the pediatric population, accounting for 3–8 % of all salivary gland neoplasms and 0.5 % of all pediatric malignancies [19, 20]. Most pediatric salivary gland lesions are benign (60–75 %) with pleomorphic adenoma comprising the vast majority of benign neoplasms (>90 %) [18, 19, 21, 22]. Scattered cases of myoepithelioma, Warthin tumor, and sebaceous lymphadenoma have been reported [19, 21]. Malignant lesions of the salivary gland are much less common, comprising 25–40 % of cases. The majority of these cases (50–80 %) are mucoepidermoid carcinoma, followed by a smaller proportion of acinic cell carcinoma (13–25 %) [18, 19, 21, 22]. Most lesions occur in adolescents; less than 10 % of patients are less than 10 years old at diagnosis [19, 21]. There is a slight female predominance. Tumors in very young patients (<5 years old) may include metastatic or mesenchymal malignancies, of which neuroblastoma, rhabdomyosarcoma, undifferentiated sarcoma, and epithelioid sarcoma have been reported [24, 25]. The parotid gland is most often affected (45–80 %), followed by the submandibular gland (10–25 %) [19, 22].

### Cytological Features

Salivary gland neoplasms are best characterized by the type of cells present, the degree of atypia, and the presence or absence of stromal material. Cases with cells and stroma, so-called biphasic lesions, should describe the qualities of the cells (e.g., basaloid with scant cytoplasm, oncocytic with moderate-to-abundant granular cytoplasm, or pleomorphic with marked nuclear pleomorphism) and the qualities of the mesenchymal material (e.g., fibrillary, dense/hyaline, or rounded globules). If mucin is present, this should also be noted. A summary of the differential diagnosis for the various cytomorphological patterns described in the literature is seen in Table 4.3 [23].

### Triage

Preparation of a cell block may be helpful for visualizing small tissue fragments or for performing immunohistochemical stains to confirm specific diagnoses. In general, immunohistochemical stains are not usually required for the evaluation of salivary gland epithelial neoplasms, as the morphological features often allow either a specific diagnosis or categorization of a lesion as benign or malignant, and definitive classification can be made on the surgical specimen. However, immunohistochemical stains are often very helpful for the diagnosis of primary non-epithelial salivary neoplasms or metastatic malignancies. Fluorescent in situ hybridization (FISH) tests are emerging as one of the most helpful ancillary studies for salivary gland neoplasms with characteristic translocations of *MAML2* seen in mucoepidermoid carcinomas, *HMGA2* and *PLAG1* rearrangements in pleomorphic adenomas, *MYB-NFIB* fusions in adenoid cystic carcinoma, and the *ETV6-NTRK3* rearrangement (t(12;15)) seen in mammary analog secretory carcinoma (MASC).

**Table 4.3** Correlation of cytomorphological pattern with morphological features and differential diagnosis in salivary gland lesions

| Cytomorphological pattern | Cytomorphology | Differential diagnosis |
|---|---|---|
| Basaloid neoplasm without stroma | Cellular smears with monomorphic cells containing scant cytoplasm. The cells should show at least some cohesion, but also can be seen as single, plasmacytoid or spindled cells. | • Cellular monomorphic adenoma<br>• Basal cell adenoma/carcinoma<br>• Basaloid squamous cell carcinoma<br>• Lymphoma<br>• Neuroendocrine tumors<br>• Pilomatrixoma<br>• Metastatic round blue cell neoplasm |
| Basaloid neoplasm with stroma (Biphasic neoplasm) | Cellular smears with monomorphic cells with scant cytoplasm, within a background of metachromatic stromal material such as fibrillary fragments or dense hyaline globules. | • Pleomorphic adenoma<br>• Adenoid cystic carcinoma<br>• Polymorphous low grade adenocarcinoma<br>• Mammary analog secretory carcinoma<br>• Mesenchymal neoplasms (e.g., solitary myofibroma) |
| Oncocytic neoplasm | Cellular smears with monomorphic cells with moderate-to-abundant granular cytoplasm. Background may show lymphoid cells in the setting of Warthin tumor. | • Oncocytoma<br>• Warthin tumor<br>• Acinic cell carcinoma<br>• Salivary duct carcinoma |
| Pleomorphic neoplasm | Cellular smears with malignant cells with marked nuclear pleomorphism. | • Salivary duct carcinoma<br>• Squamous cell carcinoma<br>• High grade lymphoma<br>• Sarcoma (e.g., MPNST)<br>• Metastatic malignancy |
| Lymphocyte-rich lesion or neoplasm | Cellular smears with discohesive cells with scant cytoplasm within a background of lymphoglandular bodies. | • Lymphoepithelial cyst<br>• Warthin tumor<br>• Intraparotid lymph node<br>• Lymphoma<br>• Metastatic round blue cell tumor<br>• Acinic cell carcinoma<br>• Mucoepidermoid carcinoma |

### Differential Diagnosis

Chronic fibrosing sialadenitis (Kuttner tumor) often presents as a mass clinically and radiologically and can mimic biphasic salivary gland neoplasms cytologically. The key findings in these benign lesions are the relatively scant cellularity and the presence of chronic inflammation. An edematous background in chronic fibrosing sialadenitis can also mimic mucin in a mucoepidermoid carcinoma or a cystic lesion. In addition to the lesions listed in Table 4.3, mesenchymal lesions, such as a solitary myofibroma, should also be in the differential diagnosis of salivary gland neoplasms.

## 4.3.2.2 Pleomorphic Adenoma

### Clinical Features

Pleomorphic adenoma is the most common pediatric salivary gland neoplasm and comprises up to 70% of all neoplasms. Pleomorphic adenomas are benign, but may recur if incompletely excised (4.5% in one series [22]). Malignant transformation (carcinoma ex pleomorphic adenoma) has been reported in a pediatric case, but is exceedingly rare [26]. These tumors present as a slowly growing painless mass, most commonly in the parotid gland (~67.5%) and when they involve the tail of the parotid may present as a preauricular mass [19, 21, 22].

### Cytological Features

Grossly the smears may appear mucoid or gel-like. Microscopically, the most recognizable element is the fibrillary stroma, which is metachromatic with a rich magenta color on modified Giemsa stains. The cellular component may be variable, but usually shows epithelial cells which are small and uniform with bland round nuclei. Myoepithelial cells are frequently present and may be spindled, stellate, or plasmacytoid (Fig. 4.7). The majority of these tumors have rearrangement of *PLAG1* or *HMGA2* and are positive for PLAG1 by immunohistochemistry.

### Triage

A cell block can be useful for identification of small tissue fragments (mini-biopsies) and thereby provide additional architectural information, and in challenging cases, can be used for immunohistochemical stains.

### Differential Diagnosis

Cellular pleomorphic adenomas may have a paucity of characteristic stroma and may mimic other epithelial or small round cell neoplasms. However, they usually show cohesive clusters and some cytoplasmic development, which help

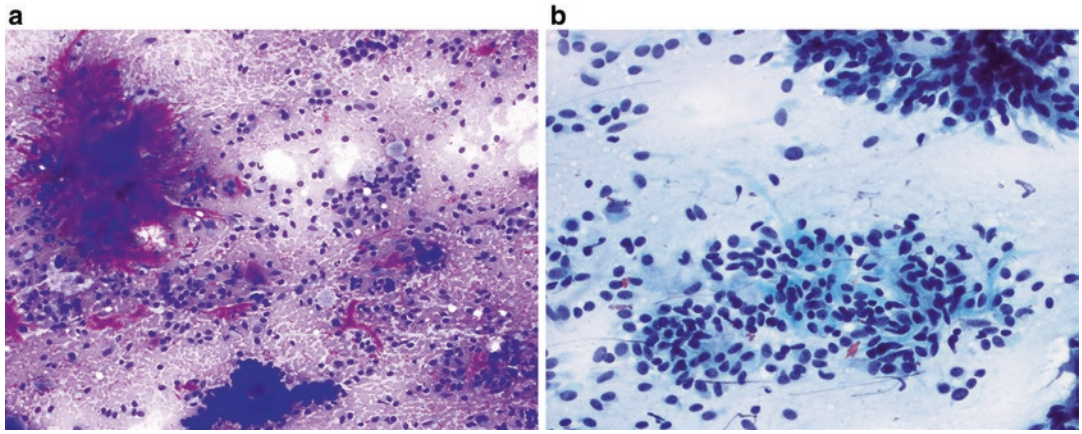


**Fig. 4.7** Pleomorphic adenoma (**a**. Diff-Quik stain, low power; **b**. Papanicolaou stain, high power). Metachromatic magenta fibrillary stroma (**a**) in a background of abundant discohesive plasmacytoid myoepithelial cells and clusters of basaloid epithelial cells (**a**, *bottom*). The fibrillary stroma is pale blue and less prominent on Papanicolaou stain (**b**). Plump spindled stromal cells adhere to the fragments. Scattered myoepithelial cells are present in the background.

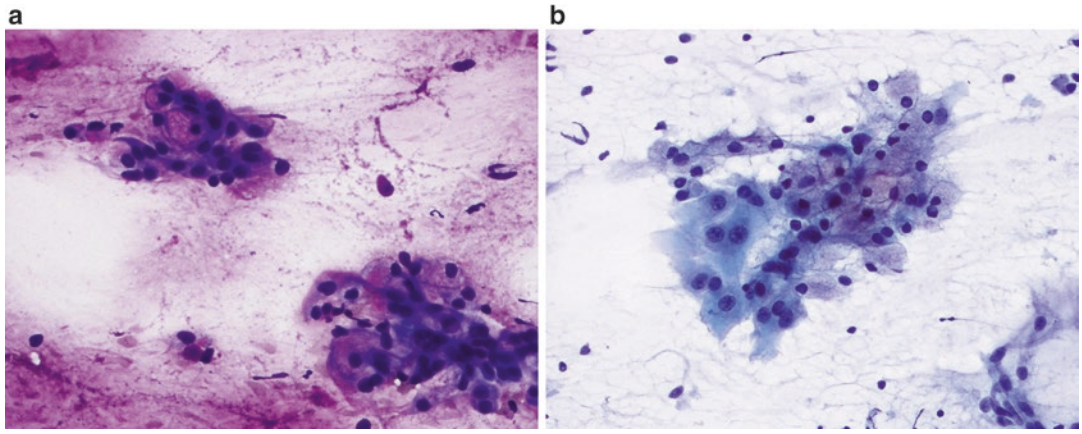


**Fig. 4.8** Mucoepidermoid carcinoma (**a**. Diff-Quik stain, high power; **b**. Papanicolaou stain, high power). Tissue fragments with goblet cells (**a**, *upper left*) in a background of abundant mucus, and squamoid cells (**b**, *left*) with enlarged nuclei and prominent nucleoli adjacent to mucous cells (**b**, *right*).

to rule out lymphoma and primitive neoplasms. Immunohistochemical stains may be helpful to confirm the presence of myoepithelial cells (e.g., S100, p63) and to exclude other mimics.

#### 4.3.2.3 Mucoepidermoid Carcinoma

**Clinical Features**

Mucoepidermoid carcinoma (MEC) is the most common pediatric salivary gland malignancy, accounting for 50–80 % of salivary gland malignancies in this population. These tumors may present as a second malignancy in patients with a history of radiation or chemotherapy, up to 61 % in one series [27]. These tumors usually present as a painless mass that may be fixed to the surrounding tissues. Although these tumors most commonly occur in the parotid gland (67.6 %), they may also occur in minor salivary glands [19, 21, 22]. MEC can be classified into low and high grade types, but most cases in the pediatric population fall into the low grade, cystic category.

**Cytological Features**

The key diagnostic feature of MEC carcinoma is a mixture of epithelial cells including glandular, intermediate, and squamous cells. Glandular cells predominate in low grade MEC and show vacuolated cytoplasm and large nuclei with conspicuous nucleoli. In solid, high grade MEC, intermediate and/or squamous cells usually comprise the majority of cells, while mucous cells may be few, inconspicuous, and identified only with mucin stains. Variable amounts of mucin may be seen in the background, but is most abundant in low grade cystic MEC (Fig. 4.8). A prominent lymphoid infiltrate is present in some cases.

**Triage**

Cystic, low grade MEC may yield hypocellular specimens and benefit from liquid based cytology. In addition, preparation of a cell block or unstained smears is useful for performing FISH for the *MAML2* rearrangement.

**Differential Diagnosis**

The main differential diagnostic considerations in the pediatric population include a benign mucous retention cyst or mucocele, mucinous or squamous metaplasia in inflammatory conditions, chronic fibrosing sialadenitis, reactive lymphoid hyperplasia or lymphoma in an intrasalivary lymph node, and acinic cell carcinoma. Muciphages in mucoceles may resemble lesional mucous cells, but lack the cytological atypia seen in MEC, and are positive for CD68 and negative for cytokeratin. Metaplasia in the setting of chronic inflammation is a potential pitfall as both mucous and squamous cells may be present; however, in contrast to MEC,

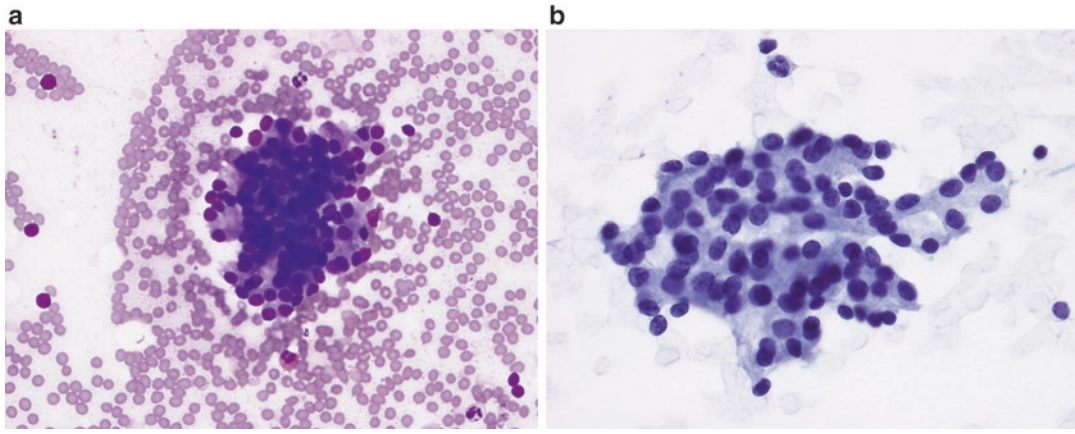


**Fig. 4.9** Acinic cell carcinoma (**a**. Diff-Quik stain, high power; **b**. Papanicolaou stain, high power) Disorganized clusters of small cells with frothy cytoplasm, small round nuclei and vague acinar formation. The cells have granular cytoplasm and bland round nuclei with granular chromatin.

the metaplastic cells lack significant cytological atypia, and are intimately associated with other benign salivary elements. A primary inflammatory or lymphoproliferative process can usually be excluded by a careful search for abnormal mucous, intermediate and/or squamous cells.

#### 4.3.2.4 Acinic Cell Carcinoma

**Clinical Features**

Acinic cell carcinoma is the second most common malignancy in the pediatric population, in contrast to adults in whom adenoid cystic carcinoma is more common. The majority of acinic cell carcinomas present in the parotid gland (~64 %) with a smaller number appearing in minor salivary glands (~14 %) [19, 21, 22]. These tumors present as a slowly enlarging, unfixed mass. In lesions of longer duration, the patient may present with pain due to perineural invasion.

**Cytological Features**

The neoplastic cells of acinic cell carcinoma mimic normal acinar cells. They often have abundant granular cytoplasm and small to medium sized, relatively bland nuclei. Abnormal architecture is an important clue to diagnosis, as the cells tend to form sheets and unorganized clusters. Although there may be a suggestion of acinar formation, the small, well-formed acini in grape-like clusters surrounding ducts that are seen in normal salivary gland tissue are absent (Fig. 4.9). Numerous naked nuclei are often present in the background. As in mucoepidermoid carcinoma, aspirates from acinic cell carcinoma may have numerous lymphocytes in the background.

**Triage**

Allocating material for a cell block can be helpful for supporting special and immunohistochemical stains.

**Differential Diagnosis**

The differential diagnosis includes normal salivary gland, particularly in a well-differentiated tumor, chronic sialadenitis in tumors with a prominent lymphocytic component, and mucoepidermoid carcinoma. The monotony of the cells and lack of stromal and ductal elements, as well as architectural features help to support a diagnosis of acinic cell carcinoma, and exclude normal salivary gland and chronic sialadenitis. In poorly differentiated tumors, the malignant acinic cells may be confused with mucin-poor glandular cells or intermediate cells in MEC; however, the absence of squamous cells in acinic cell carcinoma helps to resolve the diagnosis. Oncocytic (Warthin) tumor is an additional consideration, but is

exceedingly rare in pediatric patients. These tumors can often be distinguished morphologically on cell block and confirmed with a PAS stain which is positive in acinic cell carcinoma and negative in Warthin tumor.

#### 4.3.2.5 Adenoid Cystic Carcinoma

**Clinical Features**
Although adenoid cystic carcinoma is the most common malignancy of non-parotid salivary gland tissue in the adult, it is rare in the pediatric population. These tumors present as a slowly growing mass, followed by pain due to perineural invasion.

**Cytological Features**
Smears from adenoid cystic carcinoma are cellular and classically show small cohesive clusters of deceptively bland basaloid epithelial cells. The cells frequently surround tight globules of glassy hyaline stromal material that appears metachromatic on modified Giemsa stains.

**Triage**
A cell block can be useful for identifying small tissue fragments, as well as for special or immunohistochemical stains. Adenoid cystic carcinomas have been reported to show positivity for MYB and KIT immunostains.

**Differential Diagnosis**
Pleomorphic adenoma and polymorphous low grade adenocarcinoma may also have circumscribed hyaline globules mimicking those of adenoid cystic carcinoma, and in addition, pleomorphic adenoma may have a dominant population of basaloid cells. However, absence of larger plasmacytoid, spindle or epithelial cells and fibrillary stroma, as well as lack of staining for PLAG1 and myoepithelial markers, helps to exclude a diagnosis of pleomorphic adenoma. Similarly, the monotonous population of small basaloid cells excludes polymorphous low grade tumor, which is characterized by a heterogeneous population of neoplastic cells. When the characteristic hyaline globules are absent or inconspicuous, other small round cell tumors, including lymphoma, enter the differential; however, these can usually be excluded using immunohistochemical stains.

## 4.4 Lymphadenopathy in the Head and Neck

Approximately half of all children have benign palpable cervical lymphadenopathy that is not associated with systemic disease or known infection. As a result, reactive lymph nodes comprise the majority (50–75%) of FNA biopsies of the head and neck in the USA, although numbers vary by region and clinical demand [28–30]. Lymph node cytology is discussed in detail in Chap. 3. However, some features about cervical lymphadenopathy that are worth highlighting include the fact that infectious etiologies (e.g., mycobacteria, bacteria) are common, while metastatic malignancies are rare, which is different from adulthood. Although metastases are rare, if they are seen, the most common metastatic tumor to involve the head and neck lymph nodes in children and adolescents is PTC (Fig. 4.10). Mediastinal/thoracic tumors and occasionally abdominal tumors, including neuroblastoma and germ cell tumors, can present with metastases to the cervical lymph nodes (Fig. 4.11). Lymphomas are also relatively common, with Hodgkin lymphoma, lymphoblastic lymphoma, Burkitt lymphoma, diffuse large B-cell lymphoma, and ALK-positive anaplastic large cell lymphoma being more common in the pediatric age group than the small B-cell non-Hodgkin lymphomas seen in adults.

## 4.5 Skin and Congenital Lesions

Although most skin lesions are diagnosed clinically, FNA may be requested in some cases, particularly those presenting as a subcutaneous mass. In addition, skin lesions occasionally masquerade as lesions of underlying organs such as salivary glands or thyroid. Congenital lesions, particularly vascular neoplasms, are also relatively common in children, but are usually diagnosed clinically and not aspirated.

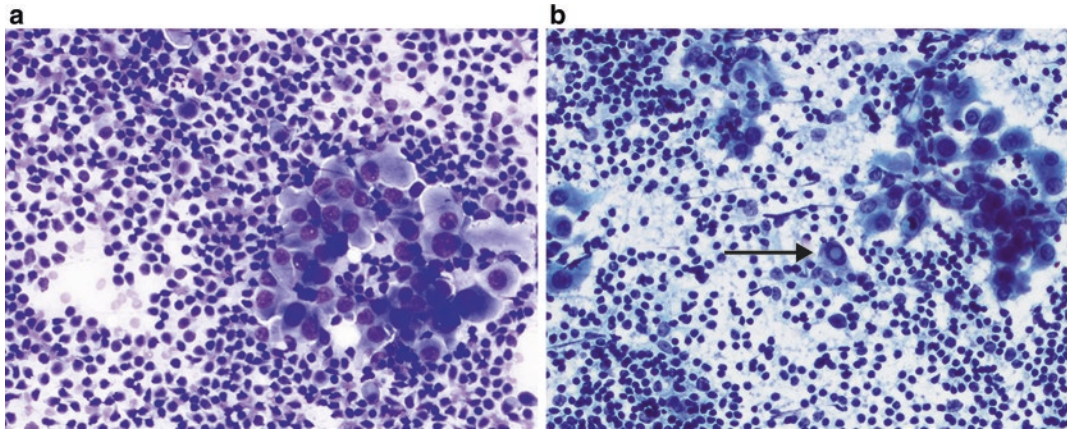


**Fig. 4.10** Metastatic papillary thyroid carcinoma (**a**. Diff-Quik stain, high power; **b**. Papanicolaou stain, high power). Cohesive cluster of follicular cells in a background of small lymphocytes. The follicular cells have nuclear features of papillary thyroid carcinoma with powdery chromatin, fine nuclear grooves, and small nucleoli. A cell with an intranuclear pseudoinclusion is seen in the center of the field (**b**, *arrow*).

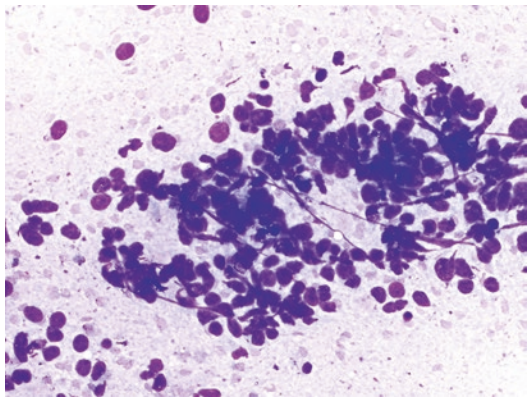

**Fig. 4.11** Metastatic neuroblastoma in cervical lymph node (Diff-Quik stain, high power). Cohesive clusters of small round cells with nuclear molding and focal rosette formation.

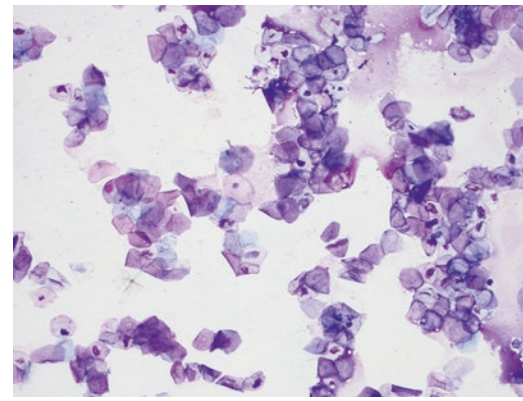

**Fig. 4.12** Epidermal inclusion cyst (Diff-Quik stain, high power). Abundant anucleate and nucleated squamous cells are seen in these aspirates, consistent with an epidermal inclusion cyst.

### 4.5.1 Epidermal Cysts

#### Clinical Features

This category encompasses epidermal inclusion cysts and dermoid cysts. Dermoid cysts arise congenitally along lines of skin closure, have adnexal structures, and may present at an earlier age. Occasionally, dermoid cysts present as a mass lesion within salivary glands. In contrast, epidermal inclusion cysts are acquired. Both are located in the superficial dermis and present as a non-fixed, ovoid-to-irregular mass. When large, they may be clinically mistaken for a reactive lymph node.

#### Cytological Features

These cystic lesions show abundant discohesive anucleate squamous cells with keratin debris, and a smaller component of nucleated squamous cells (Fig. 4.12). Rarely, clusters of stratified squamous epithelium may be present. Acute and/or chronic inflammation may be present, and in addition, there may be evidence of rupture, including a prominent granulomatous inflammatory response, with macrophages and multinucleated giant cells containing engulfed keratin debris. Since the center of the cyst, not the lining, is usually sampled during aspiration, differentiation between these entities is not possible on FNA.

### Triage

Liquid based cytology may be beneficial for evaluation of hypocellular cystic specimens.

### Differential Diagnosis

Other cystic lesions with squamous elements such as pilomatrixoma, branchial cleft cysts, and thyroglossal duct cysts may show similar cytology, and differentiation may not be possible on FNA alone. However, the benignity of the lesion is usually apparent and should allow for appropriate management. Squamous cell carcinoma is rare in the pediatric population and is characterized by the presence of overtly malignant squamous cells.

## 4.5.2 Pilomatrixoma (Calcifying Epithelioma of Malherbe)

### Clinical Features

Pilomatrixoma classically presents as a firm, mobile lesion in the cheek of a young child, but may also occur overlying the parotid or in the supraclavicular fossa. The benign neoplasms are located in the superficial dermis and appear fixed to the skin.

### Cytological Features

During aspiration, the lesions may feel "gritty" as the needle brushes against calcifications within the lesion. Aspirates show a biphasic population comprised of sheets and clusters of abundant anucleate squamous cells with "ghost" nuclei and cohesive clusters of bland basaloid cells. The basaloid cells are small with high nuclear to cytoplasmic ratios and show an orderly arrangement without crowding or overlapping of nuclei. Multinucleated foreign body-type giant cells are also present and calcifications may be seen in the background (Fig. 4.13). One of the key features, which is best seen in tissue fragments in the cell block, is an abrupt transition between the basaloid cells and anucleate ghost cells, without intervening maturing squamous cells or a granular cell layer.

### Triage

A cell block is often helpful for identifying small tissue fragments that highlight the abrupt keratinization.

### Differential Diagnosis

Differential diagnostic considerations include small round cell neoplasms that may mimic

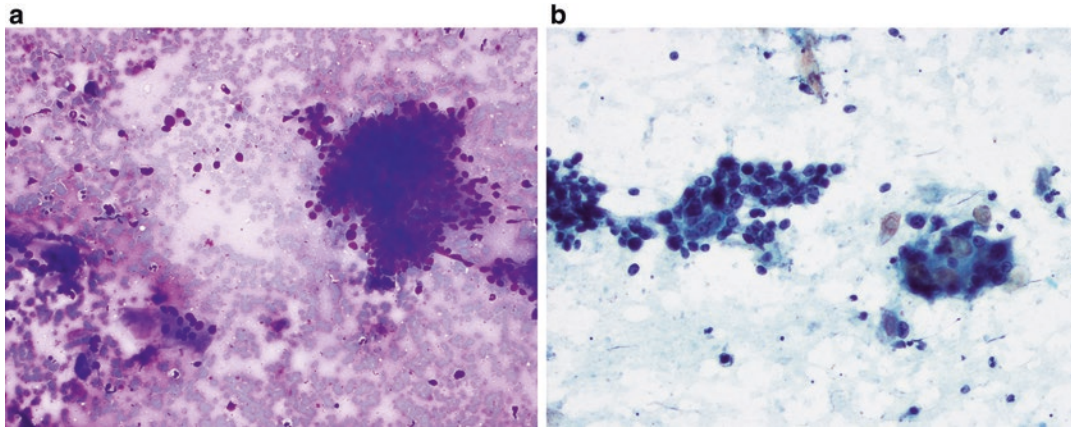


**Fig. 4.13** Pilomatrixoma (**a**. Diff-Quik stain, low power; **b**. Papanicolaou stain, low power). Basaloid cells with orderly arrangement (*right*). A multinucleated giant cell is present in lower left (**a**). Scattered anucleate "ghost cells" are present (**b**).

basaloid cells, or, when the mass overlies the parotid gland of an older child or adolescent, a cellular monomorphic adenoma or less likely, an adenoid cystic carcinoma. The presence of squamous ghost cells supports the diagnosis of pilomatrixoma and in difficult cases, immunohistochemical stains can also be used to exclude small round cell tumors. Smears with abundant foreign body giant cell reaction may be mistaken for granulomatous inflammation, but the presence of basaloid and squamous ghost cells and keratin debris is indicative of pilomatrixoma. In addition, the keratin debris and ghost cells may raise the possibility of a dermoid or epidermal inclusion cyst, however basaloid cells are absent in those entities.

#### Pearl

Pilomatrixoma is one of the most notorious benign mimickers of malignant small round cell neoplasms, given the basaloid cells and dirty background that can be mistaken for necrosis [31].

### 4.5.3 Branchial Remnants

#### Clinical Features

Incomplete fusion of the branchial arches results in the formation of cysts, sinuses, and fistulas. Cysts of the second branchial arch are the most common branchial anomaly, accounting for 90 % of cervical cysts [32]. Branchial remnants present as masses along the lateral neck. Superficial lesions are located along the anterior border of the sternocleidomastoid muscle. Deep lesions usually have sinus tracts that course posterior to the submandibular gland toward the tonsillar fossa. These commonly are identified in small children, but may be undetected until they become infected at an older age. The presence of pain and/or tenderness is suggestive of infection. Although branchial remnants are usually diagnosed clinically, branchial cysts that are mistaken for lymph nodes may undergo FNA.

#### Cytological Features

Smears may have squamous, ciliated respiratory and/or mucinous epithelium, and some cases are characterized by abundant anucleate squamous cells. Acute and chronic inflammatory cells may also be present.

#### Triage

Liquid based cytology may be useful for identifying ciliated cells in hypocellular aspirates and thereby suggesting the diagnosis of a branchial cleft cyst.

#### Differential Diagnosis

Cystic lesions of the neck arise from a variety of different organs and embryologic remnants in addition to the branchial apparatus, including thyroid, salivary gland, parathyroid, thyroglossal duct and skin, and it may be difficult or impossible to differentiate between these lesions based on cytology alone. However, the benignity of the lesion is usually obvious, allowing for appropriate management.

### 4.5.4 Thyroglossal Duct Cysts

#### Clinical Features

Thyroglossal duct cysts form along the line of embryological migration of the thyroid and are the second most common congenital pediatric neck mass [32]. The cysts are located in the anterior midline of the neck anywhere from the base of the tongue to the thyroid gland. Like branchial cysts, these may not become apparent until they become swollen and tender after infection. The typical presentation is a midline or near midline mass in the neck above the level of the thyroid gland.

#### Cytological Features

FNA smears of non-inflamed cysts usually show abundant mucus and scattered fragments of ciliated respiratory epithelium (Fig. 4.14). Squamous epithelium may be present and if extensive, the squamous cells may be the only component seen

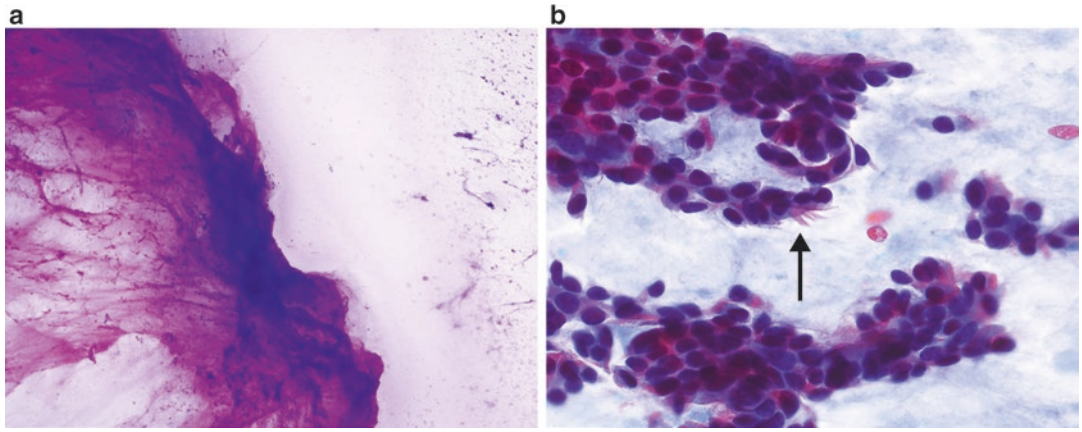


**Fig. 4.14** Thyroglossal duct cyst (**a**. Diff-Quik stain, low power; **b**. Papanicolaou stain, high power). Abundant thick mucoid material with scant cells (**a**). Clusters of basal and columnar cells with cilia (**b**, *arrow*).

on smears. Inflammation may or may not be present. Although thyroid tissue may be seen histologically, it is usually not sampled by FNA.

### Differential Diagnosis

The main differential diagnostic considerations include other cystic lesions of the neck, particularly branchial cleft cysts. A midline anatomic location supports a diagnosis of thyroglossal duct cyst, but does not exclude other entities; lesions in which smears are comprised predominantly of squamous cells may be difficult or impossible to distinguish from epidermal cysts or branchial anomalies. Fragments of respiratory epithelium that contain basal cells may show mild pleomorphism and overlapping (stratification) of the nuclei, which may raise the possibility of malignancy; however, absence of overtly malignant nuclear features helps to confirm the benignity of the lesion.

## 4.5.5 Vascular Malformations

### Clinical Features

Vascular malformations, including hemangiomas, lymphangiomas, and cystic hygromas, are most commonly seen in the neck, but may occur in the face or oral cavity. Superficial vascular malformations are usually diagnosed clinically and rarely undergo FNA. Subcutaneous lymphangiomas are usually diagnosed by radiologic imaging, but clinically ambiguous lesions, such as those that are small and firm on palpation, are occasionally aspirated. Although the lesions are usually present at birth, they may not be apparent clinically until later in life. The presence of thrombosis may result in an increase in the size of the lesion and also give the radiologic impression of a mass, prompting FNA.

### Cytological Features

Aspirates are characterized by abundant clear to serosanguineous to brown fluid, depending on the type of vascular lesion and presence or absence of old blood. Smears vary from acellular to having variable amounts of old blood, which is distinguished from fresh hemorrhage or vascular puncture by the absence of neutrophils and presence of pale or crenated red cells and often, hemosiderin-laden macrophages (Fig. 4.15). Rare clusters of endothelial cells (simple squamoid cells) may also be present. Lymphangiomas are characterized by scattered lymphoid cells and proteinaceous fluid, and often disappear upon aspiration.

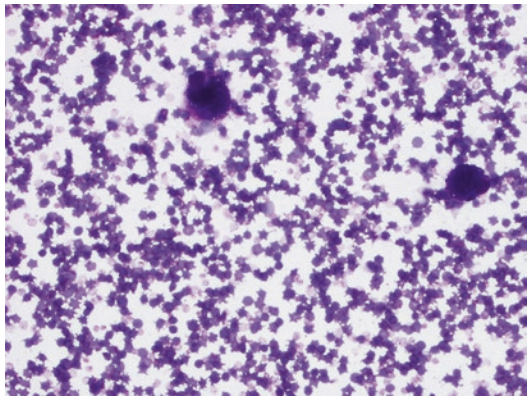

**Fig. 4.15** Vascular malformation (Diff-Quik stain, high power). Old blood with crenelated red blood cells and hemosiderin-laden macrophages.

#### Triage

Liquid based cytology can be helpful for identifying cellular elements, as it decreases the obscuring blood and concentrates the specimen.

#### Differential Diagnosis

The differential diagnosis includes fresh blood from a vascular puncture and/or an inadequate, hemodilute sample. Hemosiderin-laden macrophages are an important clue to the vascular nature of the lesion. The watery, clear fluid obtained from some lymphangiomas can mimic a parathyroid cyst. Analysis of the fluid for parathyroid hormone (PTH) resolves the diagnosis.

## 4.6 Bone and Soft Tissue

FNA of pediatric bone and soft tissue lesions is covered in Chap. 5. The discussion here will be limited to the incidence and distribution of the more common cases in the head and neck region. Sarcomas, in general, account for 14 % of malignancies of the head and neck region [33]. Bone lesions are not commonly subjected to FNA biopsy unless there is destruction/erosion of the cortex or soft tissue extension allowing access to the lesional tissue. Additionally, the bones of the head and neck are frequently either difficult to approach (facial bones and spine) or covering sensitive areas (calvarium). Bone sarcomas are infrequently seen in the head and neck. However, approximately 10 % of osteosarcomas present in the head and neck, more commonly as a secondary malignancy in patients who received prior radiation than as primary tumors. Osteosarcomas in the head and neck most commonly involve the mandible and maxilla, are more likely to be chondroblastic, and are often low to intermediate grade [33].

### 4.6.1 Ewing Sarcoma/Primitive Neuroectodermal Tumor (PNET)

#### Clinical Features

Ewing sarcoma/PNET is the second most common sarcoma in the pediatric population. However, less than 10 % of cases occur in head and neck. Unlike osteosarcoma, Ewing sarcoma is more likely to involve the calvarium.

#### Cytological Features

These tumors are characterized by a monomorphous population of single and loosely cohesive small round cells with scant cytoplasm and finely granular chromatin. Lighter (viable) and darker (degenerating) cells are usually evident. Pseudorosettes are seen in some tumors. In air-dried smears, the background may appear tigroid due to the presence of glycogen released from disrupted cells.

#### Triage

Collection of additional material for a cell block is critical, as immunostains and FISH are needed to support the diagnosis and exclude other small round cell tumors. High quality unstained smears may be preferable to sections of the cell block for FISH studies looking for an *EWS* gene rearrangement.

#### Differential Diagnosis

The differential diagnosis includes other small round cell tumors of childhood.

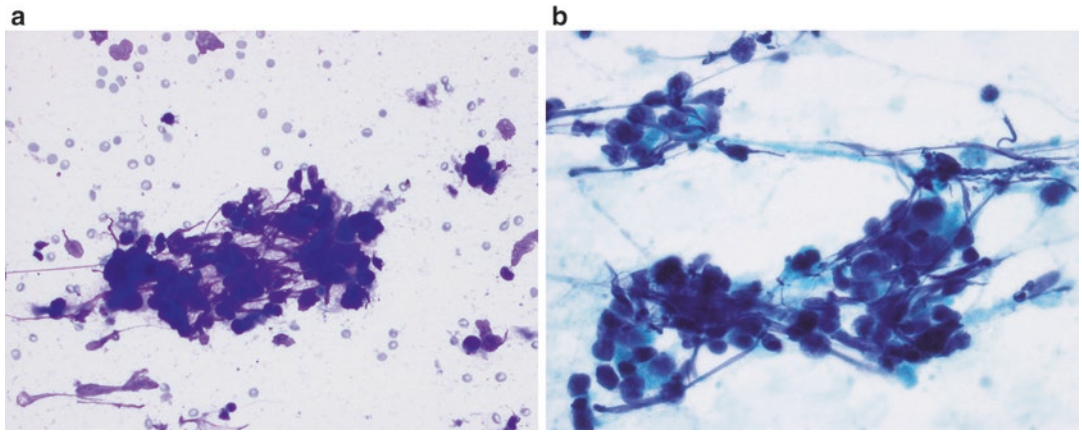


**Fig. 4.16** Rhabdomyosarcoma (**a**. Diff-Quik stain, high power; **b**. Papanicolaou stain, high power.) Pleomorphic cells with varying amounts of dense blue cytoplasm. A "tadpole" cell is seen at the bottom of the cluster (**a**). Pleomorphic nuclei with uneven granular chromatin (**b**).

### 4.6.2 Rhabdomyosarcoma

Rhabdomyosarcoma (RMS) is the most common sarcoma of the head and neck region. One third of all rhabdomyosarcomas occur in the head and neck and 25–35 % of these arise in the orbit or periorbital region. Embryonal rhabdomyosarcoma is more common, accounting for up to 90 % of cases in the orbit/periorbital region [33, 34]. Depending on histologic subtype, the tumors may be composed of round, spindled, or anaplastic cells. Evidence of rhabdomyoblastic differentiation is variable, but is usually more prominent in embryonal and spindle cell RMS than in alveolar RMS (Fig. 4.16). Immunohistochemical stains are important for distinguishing RMS from other small round cell or spindle cell tumors, and cytogenetic or molecular studies are needed to distinguish *FOXO1* fusion positive and negative cases. These tumors are discussed in greater detail in Chap. 5.

### 4.6.3 Neuroblastoma

Primary neuroblastoma of the head and neck is rare, accounting for <5 % of all neuroblastoma [34]. Primary neuroblastoma arises from the sympathetic ganglia and forms masses in the lateral neck and retropharyngeal space. The head and neck is much more commonly involved with metastatic disease to the cervical lymph node chains or periorbital soft tissue. Cytologic specimens are characterized by the presence of small round cells and/or cells with ganglionic differentiation in a background of variable amounts of neuropil and/or schwannian stroma. Pseudorosettes may also be present (Fig. 4.11). Neuroblastoma is discussed in greater detail in Chap. 7.

### 4.6.4 Desmoid Fibromatosis

#### Clinical Features

Desmoid fibromatosis is a locally aggressive fibroblastic tumor. The head and neck is the primary site in up to 10–15 % of cases [33]. Patients generally present with a painless, firm, deep seated, slowly growing mass. In general, desmoid fibromatosis, like most fibrous lesions, yields paucicellular specimens and is not well suited for FNA. However, occasionally, smaller desmoid tumors are clinically indistinguishable from other head and neck masses, particularly when overlying or adjacent to the salivary glands or thyroid, and thus, are subjected to FNA. In such cases, recognition of the lesion as a low grade spindle cell proliferation is often sufficient for guiding surgical management.

### Cytological Features

Due to the fibrous nature of the lesion, FNAs tend to be paucicellular, and may consistent only of blood. Lesional tissue is composed of bland spindled cells lying singly or enmeshed in fibrous stroma. The nuclei are usually uniform and elongated without tapered ends. Occasional fragments of dense fibrous matrix may be also present (Fig. 4.17).

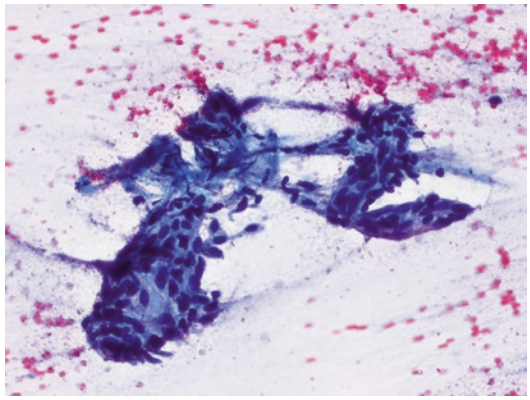

**Fig. 4.17** Desmoid fibromatosis (Papanicolaou stain, medium power). Cohesive cellular tissue fragment composed of slender uniform spindled cells. A scant amount of fibrous stroma is present.

### Differential Diagnosis

The differential diagnosis is broad and includes many benign and low grade spindle cell lesions. Precise classification of these lesions often requires core biopsy or surgical excision.

## 4.6.5 Nodular Fasciitis

### Clinical Features

Nodular fasciitis is a benign fibroblastic proliferation of the connective tissues. While the most common location across all ages is in the upper extremities, in the pediatric population the head and neck is a common location, comprising up to 40 % of cases in one pediatric series [35–37]. Patients present with a rapidly growing solitary mass. In the pediatric population there is often no history of trauma.

### Cytological Features

Smears are usually paucicellular with scattered cohesive clusters of uniform, plump, spindled cells with oval to round nuclei and pale cytoplasm. There is often a myxoid background which appears metachromatic magenta on modified Giemsa stains (Fig. 4.18).

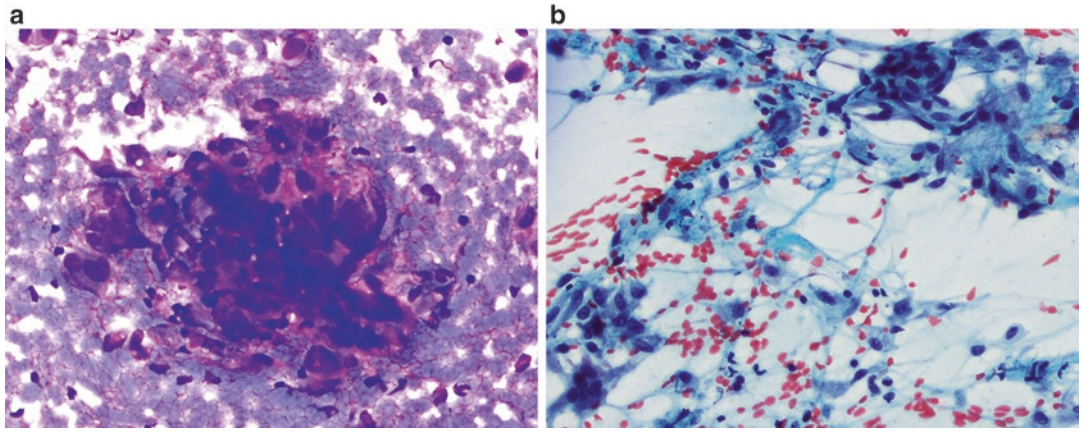


**Fig. 4.18** Nodular fasciitis (**a**. Diff-Quik stain, high power, **b**. Papanicolaou stain, high power). Loose tissue fragment with plump spindled cells surrounding a fibrous matrix. Scattered inflammatory cells are seen within the matrix.

### Differential Diagnosis

Due to the metachromatic matrix, nodular fasciitis presenting in the region of the parotid gland may mimic pleomorphic adenoma, but can be distinguished from that entity by the absence of epithelial and myoepithelial cells [37]. A variety of spindle cell lesions also enter the differential diagnosis. Desmoid fibromatosis usually presents as larger lesions with smaller, more slender nuclei. Neural tumors (schwannoma/neurofibroma) typically have thin wavy nuclei with tapered ends, and are positive for S100.

### Pearls

Recently, a recurrent somatic gene fusion, *MYHP-USP6*, was discovered in cases of nodular fasciitis, which may help in diagnosis.

## 4.7 Other Head and Neck Tumors

### 4.7.1 Nasopharyngeal Carcinoma

### Clinical Features

Nasopharyngeal carcinoma (NPC) is one of the few carcinomas seen in children. NPC accounts for 1–5 % of all pediatric cancers, but 20–50 % of all cancers in the nasopharynx. In pediatric patients, virtually all cases are associated with Epstein–Barr virus infection. There is a prominent ethnic and geographic distribution with endemic areas in China, Southeast Asia, the Mediterranean and Alaska. There is a bimodal distribution with an early peak at 10–20 years in addition to the adult peak at 40–60 years. In the USA, children under 16 account for 10 % of all cases of NPC [38]. Patients may complain of nasal symptoms including obstruction and bloody discharge, or present with bulky lymphadenopathy from metastatic disease. Up to 80 % of pediatric patients with NPC present with regional metastasis. In some cases, the initial diagnosis is made on cervical lymph nodes involved by metastatic disease.

### Cytological Features

Cytologically, these tumors yield cellular smears with sheets and clusters of large epithelial cells in a background of necrosis. The cells show large oval nuclei with hyperchromatic chromatin and prominent macronucleoli (Fig. 4.19). The cytoplasmic borders may be indistinct, giving a syncytial appearance. The clusters of epithelioid cells may also show squamoid features. A prominent lymphoid infiltrate is often present, even in the primary tumor.

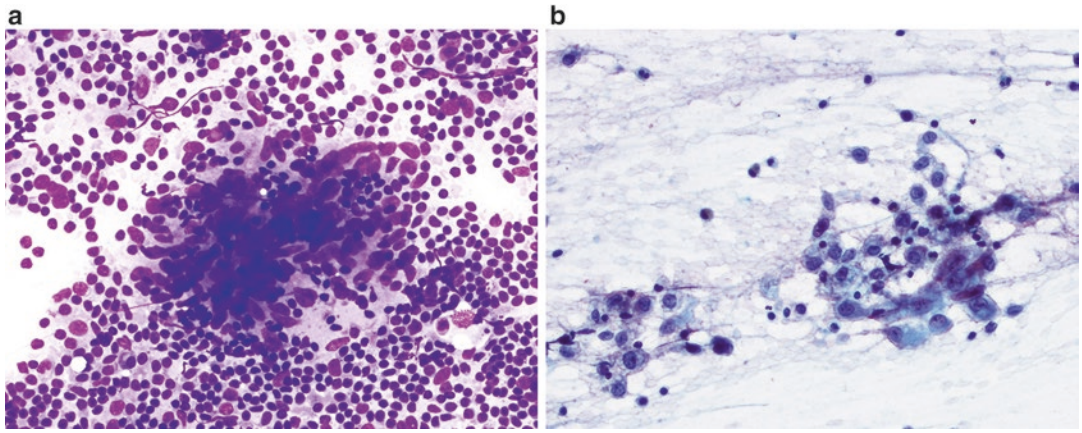


**Fig. 4.19** Nasopharyngeal carcinoma, metastatic to lymph node (**a**. Diff-Quik stain, high power; **b**. Papanicolaou stain, high power). Large cells with mildly pleomorphic oval nuclei in cohesive clusters in a background of mixed lymphocytes.

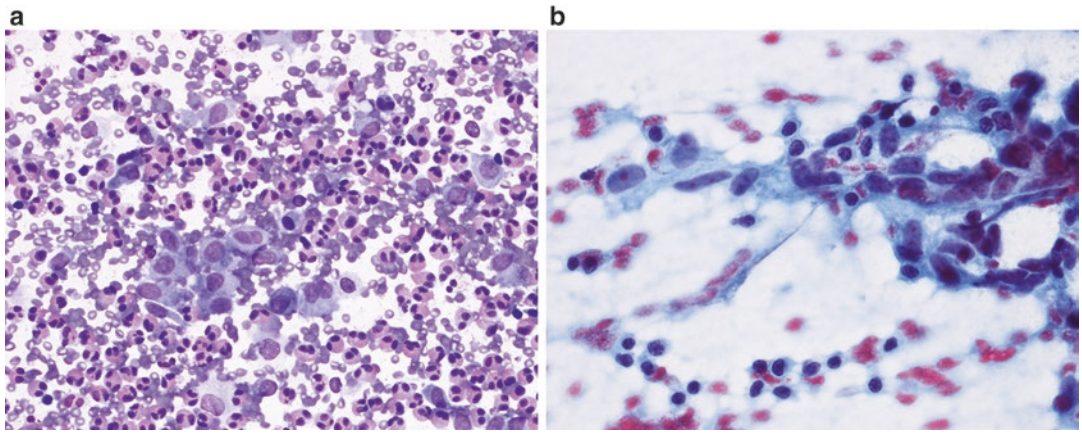


**Fig. 4.20** Langerhans cell histiocytosis (Papanicolaou stain, high power). Large cells with folded nuclei and abundant cytoplasm in a background of abundant eosinophils. Background eosinophils have brown granules on Papanicolaou stain.

### Triage

Material should be obtained for a cell block for immunohistochemical stains and in situ hybridization for EBV (EBER).

### Differential Diagnosis

NPCs can mimic basaloid neoplasms of the salivary gland, squamous cell carcinoma, and other epithelioid and round cell tumors. When present, the clinical history of a nasopharyngeal mass is an important clue to the correct diagnosis. In the aspirates obtained from cervical lymph nodes, other large cell malignancies, such as Hodgkin disease, large cell lymphomas, and metastatic melanoma or seminoma, also enter the differential. Cohesive clusters of malignant cells are an important morphological clue to the diagnosis of NPC and help to distinguish it from these entities.

## 4.7.2 Langerhans Cell Histiocytosis

### Clinical Features

Langerhans cell histiocytosis (LCH) is a neoplastic proliferation of histiocytes that has been shown to have *BRAF* mutations, and is described in more detail in Chapter 3 (Lymph nodes) [39]. Common sites of involvement include skin, bone, and the adjacent soft tissue and lymph nodes. It is characterized by lytic lesions in the bone and is frequently diagnosed radiologically. Occasionally, solitary lesions of the calvarium with extension into the scalp tissues may undergo FNA, which allows confirmation of the diagnosis without the need for neurosurgery.

### Cytological Features

Smears show a mixed population of Langerhans histiocytes (LCH cells), eosinophils, other inflammatory cells, and multinucleated giant cells. The LCH cells have moderately abundant cytoplasm and characteristic grooved or folded nuclei with fine chromatin and small or inconspicuous nucleoli (Fig. 4.20).

### Triage

Collection of material for a cell block is important in order to demonstrate the characteristic immunophenotype of the LCH cells, which are positive for CD68, CD1a, langerin, fascin, and S100. Molecular studies could also be performed to demonstrate a *BRAF* mutation, but at this time are not routinely used in evaluation of these lesions [39].

### Differential Diagnosis

LCH may be confused with osteomyelitis, or other reactive bony processes. In addition, other histiocytic disorders should be considered. Identification of the classic nuclear features of LCH cells provides an important clue to the correct diagnosis.

## References


1. Liu ES, Bernstein JM, Sculerati N, Wu HC. Fine needle aspiration biopsy of pediatric head and neck masses. Int J Pediatr Otorhinolaryngol. 2001;60: 135–40.
2. Goins MR, Beasley MS. Pediatric neck masses. Oral Maxillofac Surg Clin North Am. 2012;24:457–68.
3. Osipoff JN, Wilson TA. Consultation with the specialist: thyroid nodules. Pediatr Rev. 2012;33:75–81.
4. Rallison ML, Dobyns BM, Meikle AW, Bishop M, Lyon JL, Stevens W. Natural history of thyroid abnormalities: prevalence, incidence, and regression of thyroid diseases in adolescents and young adults. Am J Med. 1991;91:363–70.
5. Corrias A, Mussa A, Baronio F, Arrigo T, Salerno M, Segni M, et al. Diagnostic features of thyroid nodules in pediatrics. Arch Pediatr Adolesc Med. 2010;164:714–9.
6. Dinauer C, Francis GL. Thyroid cancer in children. Endocrinol Metab Clin North Am. 2007;36:779–806.
7. Gupta A, Ly S, Castroneves LA, Frates MC, Benson CB, Feldman HA, et al. A standardized assessment of thyroid nodules in children confirms higher cancer prevalence than in adults. J Clin Endocrinol Metab. 2013;98:3238–45.
8. Scholz S, Smith JR, Chaignaud B, Shamberger RC, Huang SA. Thyroid surgery at Children's Hospital Boston: a 35-year single-institution experience. J Pediatr Surg. 2011;46:437–42.
9. Stevens C, Lee JKP, Sadatsafavi M, Blair GK. Pediatric thyroid fine-needle aspiration cytology: a meta-analysis. J Pediatr Surg. 2009;44:2184–91.
10. Ali SZ, Cibas ES, editors. The Bethesda system for reporting thyroid cytopathology. New York: Springer; 2010.
11. Bently AA, Gillespie C, Malis D. Evaluation and management of a solitary thyroid nodule in a child. Otolaryngol Clin North Am. 2003;36:117–28.
12. La Quaglia MP, Black T, Holcomb GW, Sklar C, Azizkhan RG, Haase GM, et al. Differentiated thyroid cancer: clinical characteristics, treatment, and outcome in patients under 21 years of age who present with distant metastases. A Report from the Surgical Discipline Committee of the Children's Cancer Group. J Pediatr Surg. 2000;35:955–60.
13. Harshan M, Crapanzano JP, Aslan DL, Vazquez MF, Saqi A. Papillary thyroid carcinoma with atypical histiocytoid cells on fine-needle aspiration. Diagn Cytopathol. 2009;37:244–50.
14. Monaco SE, Pantanowitz L, Khalbuss WE, Benkovich VA, Ozolek J, Nikoforova MN, et al. Cytomorphological and molecular genetic findings in pediatric thyroid fine-needle aspiration. Cancer Cytopathol. 2012;120: 342–50.
15. Fenton CL, Lukes Y, Nicholson D, Dinauer CA, Francis GL, Tuttle RM. The ret/PTC mutations are common in sporadic papillary thyroid carcinoma of children and young adults. J Clin Endocrinol Metab. 2000;85:1170–5.
16. Niedziela M. Pathogenesis, diagnosis and management of thyroid nodules in children. Endocr Relat Cancer. 2006;13:427–53.
17. Penko K, Livezey J, Fenton C, Patel A, Nicholson D, Flora M, et al. BRAF mutations are uncommon in papillary thyroid cancer of young patients. Thyroid. 2005;15:320–5.
18. Orvidas LJ, Kasperbauer JL, Lewis JE, Olsen KD, Lesnick TG. Pediatric parotid masses. Arch Otolaryngol Head Neck Surg. 2000;126:177–84.
19. Deng R, Huang X, Hao J, Ding J, Hu Q. Salivary gland neoplasms in children. J Craniofac Surg. 2013;24:5111–3.
20. Sultan I, Rodriguez-Galindo C, Al-Sharabati S, Guzzo M, Casanova M, Ferrari A. Salivary gland carcinomas in children and adolescents: a population-based study, with comparison to adult cases. Head Neck. 2011;33:1476–81.
21. Fang Q, Shi S, Li Z, Zhang X, Liu F, Sun C. Epithelial salivary gland tumors in children: a twenty-five-year experience of 122 patients. Int J Pediatr Otorhinolaryngol. 2013;77:1252–4.
22. Guzzo M, Ferrari A, Marcon I, Collini P, Gandola L, Pizzi N, et al. Salivary gland neoplasms in children: the experience of the istituto nazionale tumori of Milan. Pediatr Blood Cancer. 2006;47:806–10.
23. Griffith CC, Pai RK, Schneider F, Duvvuri U, Ferris RL, Johnson JT, Seethala RR. Salivary gland tumor fine-needle aspiration cytology: a proposal for a risk stratification classification. Am J Clin Pathol. 2015;143:839–53.
24. Jaryszak EM, Shah RK, Bauman NM, Howell RJ, Rossi CT, Preciado DA. Unexpected pathologies in pediatric parotid lesions: management paradigms revisited. Int J Pediatr Otorhinolaryngol. 2011;75:558–63.
25. Keelawat S, Shuangshoti S, Kittikowit W, Lerdlum S, Thorner PS. Epithelioid sarcoma of the parotid gland of a child. Pediatr Dev Pathol. 2009;12(4): 301–6.
26. Liu B, Liu JY, Zhang WF, Jia J. Pediatric parotid tumors: clinical review of 24 cases in a Chinese population. Int J Pediatr Otorhinolaryngol. 2012;76: 1007–11.
27. Vedrine PO, Coffinet L, Temam S, Montagne K, Lapeyre M, Oberlin O, et al. Mucoepidermoid carcinoma of salivary glands in the pediatric age group: 18 clinical cases including 11 second malignant neoplasms. Head Neck. 2006;28:827–33.
28. Anne S, Teot LA, Mandell DL. Fine needle aspiration biopsy: role in diagnosis of pediatric head and neck masses. Int J Pediatr Otorhinolaryngol. 2008;72:1547–53.
29. Liu ES, Bernstein JM, Sculerati N, Wu HC. Fine needle aspiration biopsy of pediatric head and neck masses. Int J Pediatr Otorhinolaryngol. 2001;60:135–40.
30. Rapkiewicz A, Le BT, Simsir A, Cangiarella J, Levine P. Spectrum of head and neck lesions diagnosed by fine-needle aspiration cytology in the

pediatric population. Cancer Cytopathol. 2007; 111(4):242–51.
31. Thapliyal N, Joshi U, Vaibhav G, Sayana A, Srivastava AK, Jha RS. Pilomatrixoma mimicking small round cell tumor on fine needle aspiration cytology: a case report. Acta Cytol. 2008;52:627–30.
32. Goins MR, Beasley MS. Pediatric neck masses. Oral Maxillofac Surg Clin North Am. 2012;24:457–68.
33. Huh WW, Fitzgerald N, Mahajan A, Sturgis EM, Raney RB, Anderson PM. Pediatric sarcomas and related tumors of the head and neck. Cancer Treat Rev. 2011;37:431–9.
34. Dickson PV, Davidoff AM. Malignant neoplasms of the head and neck. Semin Pediatr Surg. 2006;15:92–8.
35. Matusik J, Wiberg A, Sloboda J, Anderson O. Fine needle aspiration in nodular fasciitis of the face. Cytopathology. 2002;13:128–32.
36. Bemrich-Stolz CJ, Kelly DR, Meunsterer OJ, Pressey JG. Single institution series of nodular fasciitis in children. J Pediatr Hematol Oncol. 2010;32:354–7.
37. Saad RS, Takei H, Lipscomb J, Ruiz B. Nodular fasciitis of parotid region: a pitfall in the diagnosis of pleomorphic adenomas on fine-needle aspiration cytology. Diagn Cytopathol. 2005;33:191–4.
38. Ayan I, Kaytan E, Ayan N. Childhood nasopharyngeal carcinoma: from biology to treatment. Lancet Oncol. 2003;4:12–21.
39. Badalian-Very G, Vergilio JA, Degar BA, MacConaill LE, Brandner B, Calicchio ML, Kuo FC, Ligon AH, Stevenson KE, Kehoe SM, Garraway LA, Hahn WC, Meyerson M, Fleming MD, Rollins BJ. Recurrent BRAF mutations in Langerhans cell histiocytosis. Blood. 2010;116: 1919–23.

# Bone and Soft Tissue

# 5

Lisa A. Teot

## 5.1 Introduction

A wide variety of bone and soft tissue lesions are seen in children and adolescents, including benign and malignant neoplasms, as well non-neoplastic processes. Evaluation of these lesions traditionally has included open biopsy to establish a diagnosis prior to definitive treatment. With the development of increasingly sophisticated imaging techniques that allow accurate localization and sampling of these lesions, fine needle aspiration (FNA) and small biopsies are assuming an increasingly important role in the diagnosis of pediatric musculoskeletal lesions [1–6]. This is particularly true in light of the trend toward less invasive and more cost-effective diagnostic procedures. Although limitations and pitfalls exist, FNA is a valuable tool for the diagnosis of pediatric bone and soft tissue lesions, and can often provide information on which to base further diagnostic and therapeutic decisions [1–6]. In many cases, FNA allows accurate diagnosis of primary or metastatic lesions of bone and soft tissue, thereby obviating the need for a more invasive and significantly more expensive diagnostic biopsy. In other cases, although a definite diagnosis is not possible, FNA is useful for ruling out specific processes or for narrowing the diagnostic considerations, and in the appropriate clinical setting, this information may be sufficient for initiation of therapy. When a definitive cytologic diagnosis cannot be rendered and/or additional information is needed prior to therapy, material should be obtained for histologic evaluation. In such cases, rapid on site evaluation of an FNA can help to confirm that viable, diagnostic tissue is being sampled and guide triage of concurrent core biopsies.

It is important to note that FNA is not an appropriate tool for the evaluation of certain pediatric bone and soft tissue lesions. Some bone tumors have highly characteristic features on imaging studies that, when present, are virtually diagnostic and obviate the need for a pathologic diagnosis prior to definitive treatment. In addition, with some exceptions, benign bone lesions typically have intact overlying cortical bone and are not easily sampled by FNA or small biopsy. As treatment for many of these lesions is curettage with or without bone grafting or cementation, intraoperative frozen section or touch preparation is often the preferred method for confirming benignity and/or establishing a diagnosis, as well as guiding surgical management. Similarly, despite having a broad differential diagnosis, many benign-appearing soft tissue masses are treated by simple excision irrespective of the specific diagnosis, thereby making preoperative pathologic diagnosis unnecessary.

L.A. Teot, MD (✉)
Department of Pathology, Boston Children's Hospital, Harvard Medical School,
300 Longwood Avenue, Boston, MA 02115, USA
e-mail: lisa.teot@childrens.harvard.edu



S.E. Monaco, L.A. Teot (eds.), *Pediatric Cytopathology*, DOI 10.1007/978-3-662-53441-0_5

Accurate interpretation of FNAs of bone and soft tissue lesions is best accomplished using an integrated approach in which the cytologic findings are correlated with the clinical data and imaging studies prior to rendering a final diagnosis. Integrated assessment of the clinical presentation, radiographic features, presence or absence of matrix production, and cytologic features usually allows the cytopathologist to generate a limited differential diagnosis, and in many instances, a specific diagnosis. In some cases, additional studies, such as histochemical and immunoperoxidase stains, flow cytometry, molecular studies, electron microscopy, or cultures, are needed for a definitive diagnosis. In other cases, the differential diagnosis can be resolved based on further correlation with clinical and radiographic data. In such cases, the final cytologic diagnosis is phrased to reflect this fact, e.g., "Atypical cartilaginous proliferation, consistent with the clinical and radiographic impression of digital enchondroma." This chapter describes the cytologic features of various common and uncommon neoplastic and non-neoplastic lesions of bone and soft tissue that are encountered in the pediatric population, as well as key clinical and radiologic features of these entities and differential diagnostic considerations.

## 5.2 Bone Lesions

Primary bone tumors, whether benign or malignant, are more common in the pediatric population than in adults. In children under 10 years of age, approximately 75% of bone tumors are benign, whereas malignant neoplasms comprise close to 50% of bone tumors in older children and adolescents. Some genetic disorders are also associated with increased risk of developing certain bone tumors; for example, patients with germline mutations in *TP53* or *RB1* are predisposed to the development of osteosarcoma.

As already noted, correlation with imaging studies is essential when evaluating an FNA from a pediatric bone lesion. Particular types of tumors tend to occur at specific sites within long bones, and thus, the site of involvement (epiphyseal, metaphyseal or diaphyseal; cortical or medullary) narrows the differential diagnosis. The presence or absence of matrix and its appearance also provide important diagnostic clues. Benign osseous lesions are characterized by orderly ossification, while malignant neoplasms have ill-defined cloud-like calcifications. Chondroid matrix appears as stippled or flocculent densities. The pattern of growth is also important and as a general rule is indicative of biological potential and behavior. The hallmark of a benign process is containment of the lesion by a rim of reactive host bone. In a slowly growing lesion, the rim of reactive bone often becomes thickened or sclerotic. Lesions with this pattern of growth are well circumscribed and have pushing rather than infiltrative margins. A periosteal reaction is usually absent, and if present, has a solid appearance. In contrast, infiltration of the surrounding bone is typical of an aggressive or malignant lesion that has the potential for local recurrence and/or distant metastasis. Permeation and destruction of the bone by a rapidly growing lesion result in ill-defined or "moth-eaten" borders. In addition, rapid erosion and significant weakening of the cortical bone induces a periosteal reaction, which appears as a complex pattern of either layering parallel to the cortical surface ("onion skin") or spiculation perpendicular to the cortical surface ("sunburst" or "hair on end"). Another radiographic hallmark of aggressive lesions is Codman's triangle, an incomplete triangle formed by periosteum at the interface between a growing tumor and the normal host bone. A comparison of the key radiographic features of benign and malignant skeletal lesions is listed in Table 5.1.

A microscopically useful and clinically relevant way of classifying lesions of bone is based on evidence of matrix production. In general, destructive processes in the skeleton can be divided into those that show evidence of matrix production, both radiographically and microscopically, and those that do not. The former are further subdivided based on the type of matrix produced, i.e., osteoid, chondroid, chondromyxoid, or myxoid matrix, or fibrous stroma. Matrix producing lesions of bone and soft tissue can be non-neoplastic or neoplastic, and benign or malignant.

**Table 5.1** Radiographic features of benign versus malignant lesions of bone

| Feature | Benign lesions | Malignant lesions |
|---|---|---|
| **Pattern of growth** | Pushing | Infiltrative |
| | No extension or penetration into surrounding bone | Permeation and destruction of surrounding bone |
| **Borders of lesion** | Well circumscribed | Ill-defined, moth-eaten |
| | Sclerotic rim or "rind" separates lesion from adjacent bone | Infiltration of adjacent host bone |
| **Periosteal reaction** | Absent or solid | Complex ("onion skin" or "hair on end") |
| | | Codman's triangle |

**Table 5.2** Osteoid producing lesions of bone

| Benign lesions | Malignant lesions |
|---|---|
| Osteoblastoma | Osteosarcoma |
| Osteoid osteoma | Conventional |
| Fracture callus | Surface (parosteal, periosteal, high grade) |
| | Telangiectatic |
| Aneurysmal bone cyst with reactive bone formation | Small cell |
| | Low grade central |

In cytologic specimens, matrix is best appreciated in air-dried, modified Giemsa-stained preparations, and is often readily apparent at scanning power. Osteoid appears as irregular fragments of opaque, intensely metachromatic stroma, often arrayed in branched or interlacing cords or strands. The edges of the fragments may be sharply defined or have a frayed, fibrillar appearance. Variable numbers of benign or malignant osteoblasts are present within and/or at the periphery of the fragments. Fibrous matrix is also metachromatic, and varies from dense and opaque to pale and finely fibrillar or wispy. Fragments can be large or small, and have well-defined, smooth edges or be frayed and irregular. The fragments may be acellular or have variable numbers of benign or malignant spindle cells of fibroblastic or myofibroblastic origin embedded within the stroma. Due to biochemical and staining similarities, acellular or relatively hypocellular fragments of dense collagen may be difficult or impossible to distinguish from osteoid. Chondroid, chondromyxoid, and myxoid matrices, like osteoid, are intensely metachromatic, but in contrast to osteoid, often occur in large, sheet-like fragments or clumps. The matrix can appear opaque, or have a fibrillar or filmy quality, and the borders are often relatively well defined. The fragments can be acellular, or have variable numbers of benign or malignant cells embedded in the stroma. Because these matrices are essentially identical, the principal feature that distinguishes the various chondroid, chondromyxoid, and myxoid lesions from each other is the type(s) of benign or malignant mesenchymal cells associated with the matrix.

### 5.2.1 Osteoid Producing Lesions

A number of lesions of bone produce osteoid and its mineralized end product, woven bone. Production of lamellar bone, which is the mature, highly organized matrix of the skeleton, is seen only in osteoma and enostosis (bone islands). Osteoid is the unmineralized, protein matrix produced by osteoblasts. This matrix consists of type I collagen (approximately 90%) and a number of non-collagenous proteins, including osteocalcin, osteopontin, osteonectin, and various growth factors. The morphologic separation of osteoid from fibroblastic collagen is often qualitative; however, this distinction is important diagnostically. Fibroblastic collagen is laid down by flattened or spindle shaped fibroblasts and has a distinctly fibrillar, longitudinal arrangement. In contrast, osteoid forms irregular, amorphous masses that have a hard, waxy quality. Osteoid appears bright magenta in air-dried, modified Giemsa-stained smears, and green-blue in wet-fixed, Papanicolaou-stained preparations. Osteoblasts, that may be benign or malignant, become entrapped in the matrix, creating a lacy, interwoven pattern. The major osteoid producing lesions of bone that are encountered in the pediatric population are listed in Table 5.2.

#### 5.2.1.1 Osteoblastoma

**Clinical Features**

Osteoblastoma (OB) is a rare benign neoplasm, accounting for approximately 1 % of primary bone tumors. Most patients are less than 30 years old, with a peak incidence in the second decade of life. Patients typically present with local pain.

**Location**

OB may arise in any portion of the skeleton, but has a distinct predilection for the axial skeleton, particularly the spine.

**Radiographic Appearance**

OB is typically intramedullary, although occasional intracortical examples occur. In long bones, OB arises in the metaphysis, whereas vertebral OB is usually located in the posterior elements. OB produces a uniform, sharply circumscribed, expansile lesion that is usually radiolucent. Periosteal reaction is generally absent. Calcification of the matrix may be present or absent radiographically.

**Cytological Features**

FNA yields moderately cellular smears composed of a polymorphous population of benign mesenchymal cells, and irregular fragments of osteoid and woven bone [7, 8]. Osteoblasts, osteoclasts, and fibrovascular stroma comprise the mesenchymal elements. Osteoblasts are plump, round, or polygonal cells with well-defined cellular borders, abundant cytoplasm, and eccentric, round nuclei with evenly dispersed chromatin and a single, round, often prominent nucleolus. The osteoblasts occur as individually dispersed cells or in rows "rimming" the fragments of osteoid. Individually dispersed, true osteoclasts are also present, and characteristically exhibit variation in size, shape, and number of benign nuclei. Benign spindle cells of fibroblastic and endothelial origin are arrayed within irregular fragments of fibrous stroma, and also occur singly. The background is usually bloody, reflecting the richly vascular nature of OB.

**Differential Diagnosis**

Differential diagnostic considerations include osteoid osteoma, fracture callus, and osteosarcoma. Usually, these entities can be distinguished from each other based on imaging characteristics. Moreover, neither osteoid osteoma nor fracture callus is likely to undergo FNA. Occasionally OB has an aggressive appearance on imaging studies, raising concern for osteosarcoma. However, the cytologically benign appearance of the cells in OB helps to distinguish this entity from osteosarcoma.

**Pearls**

Occasional OBs have atypical cytological features that may lead to misdiagnosis as osteosarcoma, particularly when combined with an aggressive radiologic appearance. Because osteosarcoma is the most common primary bone tumor in the second decade of life and is far more common than OB irrespective of the patient's age, histologic evaluation of tumors with atypical features is imperative to avoid misdiagnosis and guide appropriate treatment.

#### 5.2.1.2 Osteoid Osteoma

**Clinical Features**

The majority of cases of osteoid osteoma (OO) occur in the second decade of life. OO is usually associated with marked pain that is worse at night and relieved with aspirin.

**Location**

OO may arise in any portion of the skeleton, and almost always involves cortical bone. Occasional subchondral and intramedullary lesions occur.

**Radiographic Appearance**

The characteristic radiographic appearance of intracortical OO is that of a well-circumscribed, lytic lesion surrounded by excessive sclerosis and reactive bone formation. The central lytic region, termed the nidus, is almost always less than 1 cm in diameter and by definition, less than 2 cm. Although periosteal new bone formation is characteristic, a true periosteal reaction is absent.

### Cytological Features

To our knowledge, cytologic diagnosis of OO by FNA has not been reported. The diagnosis is usually apparent from the clinical history and radiographic findings, and this, combined with the characteristic intracortical location and extensive peripheral sclerosis, makes aspiration of OO highly unlikely.

## 5.2.1.3 Conventional Osteosarcoma

### Clinical Features

Osteosarcoma (OS) is the most common primary malignant tumor of bone and more than 60 % of patients present in the second decade of life. While most osteosarcomas are sporadic, there is an increased incidence of this tumor in patients with hereditary retinoblastoma, Li–Fraumeni syndrome, and Rothmund–Thomson syndrome. Secondary or post-irradiation osteosarcoma may also occur in childhood. Primary conventional osteosarcoma is 1.5 times more frequent in males than females. The usual presenting symptom is pain with or without swelling that can be present for weeks or months. Pathologic fractures are present in 5–10 % of patients.

### Location

OS has a predilection for the metaphyseal portion of long bones, particularly the distal femur, proximal tibia, and proximal humerus.

### Radiographic Appearance

OS characteristically appears as a large, poorly defined, infiltrative, metaphyseal lesion arising in the medullary bone and extending through the cortex to form a large soft tissue mass. A periosteal reaction, usually of the hair on end, sunburst or onion skin type, and Codman's triangle are present. Lesions are usually mixed lytic and blastic, the latter feature reflecting matrix production. Occasionally, OS is purely lytic.

### Cytological Features

OS has a spectrum of cytologic appearances, reflecting the histologic variability of these neoplasms [7, 9–11]. FNA of conventional OS yields variably cellular smears, depending on the amount of matrix within the area sampled. Aspirates are composed of varying proportions of malignant osteoblasts, spindle cells and bizarre, multinucleated tumor giant cells (Fig. 5.1a). In addition, scattered osteoclast-like giant cells are often present.

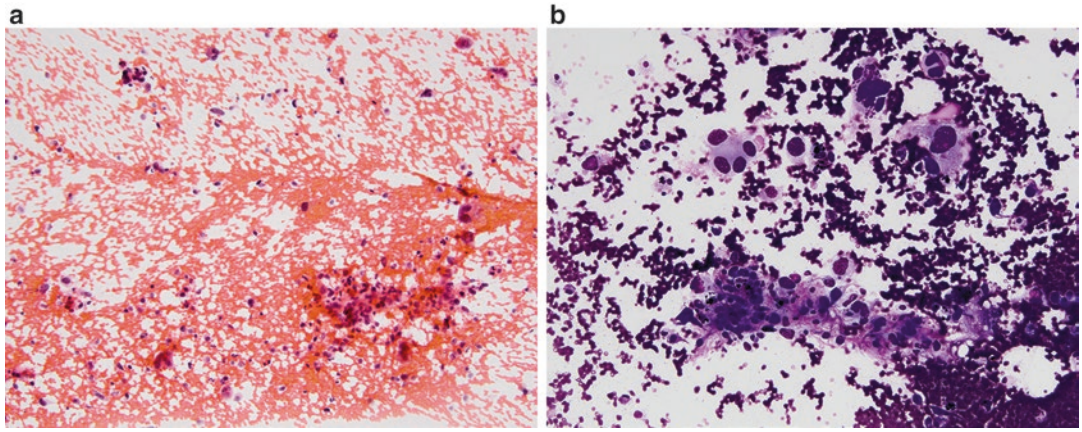


**Fig. 5.1** Conventional osteosarcoma, osteoblastic subtype (**a**. Papanicolaou stain, medium power; **b**. Diff-Quik stain, medium power). Osteosarcoma is composed of obviously malignant osteoblasts and spindle cells, with occasional bizarre multinucleated giant cells and osteoclastic giant cells. The cells occur singly and in loosely cohesive clusters (**a**). Marked anisocytosis and nuclear pleomorphism are evident in this example of osteosarcoma. Magenta-colored matrix is present between and around some of the tumor cells in the cluster (**b**).

The malignant cells show considerable anisocytosis, nuclear pleomorphism, and increased nuclear to cytoplasmic ratios. Nuclei are characterized by absolute enlargement, irregular contours, coarsely clumped chromatin, and prominent, irregular nucleoli. The malignant cells occur as individually dispersed elements, in irregular aggregates, and in association with osteoid or other matrix (Fig. 5.1b).

The amount of osteoid varies considerably, and may dominate the smears or be exceedingly scant and focal. Osteoid can be distinguished from dense collagen in the air-dried, modified Giemsa-stained smears by its amorphous, lace-like quality in combination with the presence of entrapped or individually dispersed malignant cells reminiscent of osteoblasts. In cases lacking these features, osteoid may be difficult or impossible to distinguish from dense collagen. In addition to osteoid, chondroid and fibrous matrices may be present in aspirates from chondroblastic [12] and fibroblastic OS, respectively (Fig. 5.2).

#### Differential Diagnosis

The overtly malignant nature of these tumors is usually apparent thereby limiting differential diagnostic considerations, particularly when osteoid is evident. In the absence of convincing osteoid, cytologic distinction from chondrosarcoma and fibrosarcoma may be difficult or impossible [12].

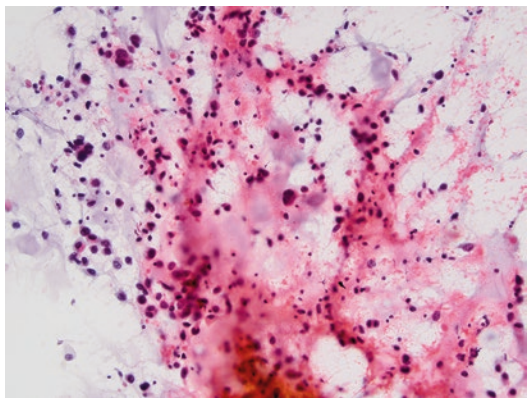

**Fig. 5.2** Conventional osteosarcoma, chondroblastic subtype (Papanicolaou stain, medium power). Irregular fragments of chondroid matrix are present in this smear comprised of highly pleomorphic, overtly malignant cells.

#### Pearls

Preparation of a cell block can be helpful for identifying osteoid matrix (Fig. 5.3). In osteoid poor tumors, an immunoperoxidase stain for SATB2 can help to confirm the osteoblastic origin of the neoplasm; however, other immunoperoxidase stains are not helpful as OS can be positive for a variety of mesenchymal, as well as epithelial markers. Cytogenetics reveals a numerically and structurally complex karyotype and may help to distinguish OS from tumors characterized by recurrent translocations.

### 5.2.1.4 Other Variants of Osteosarcoma

Although a detailed discussion of the different variants of OS is beyond the scope of this chapter, cytopathologists should be aware of these entities.

#### Small Cell Osteosarcoma

This variant of OS comprises less than 2 % of OS and, as the name implies, is composed of small round cells. Osteoid matrix can be exceedingly scant, and rare examples may also have focal chondroid matrix. The cytologic features of small cell OS are considerably different from those of other types. Aspirates are composed of small round or ovoid cells with scant cytoplasm, oval to elongate nuclei with finely dispersed or clumped

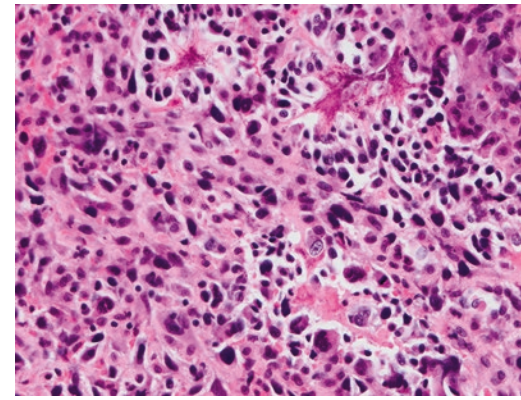

**Fig. 5.3** Conventional osteosarcoma (Cell block, H&E stain, high power). Cell block preparations can help to confirm the presence of osteoid, which may be inconspicuous in smears. Delicate osteoid with focal evidence of calcification is evident between and around cells in this fragment of tissue from an osteosarcoma.

chromatin, and very high nuclear to cytoplasmic ratios. Nuclear pleomorphism is present, but may not be marked. Cells occur singly and in cohesive fragments. When osteoid is scant or absent in aspirate smears, small cell OS may be mistaken for Ewing sarcoma or metastasis from a pediatric small round cell tumor. Immunoperoxidase stains and fluorescent in situ hybridization for *EWSR1, FOXO1,* and *SS18(SYT)* can be helpful for excluding these entities.

#### Telangiectatic Osteosarcoma

This variant, which comprises less than 4% of OS, is a high grade intramedullary tumor with prominent intralesional blood-filled spaces and scant evidence of osteoid formation. Radiographically, these lesions are purely lytic with extensive destruction of bone and often, soft tissue extension. Aspirates are usually bloody and may have a paucity of diagnostic malignant cells, thereby mimicking aneurysmal bone cyst or a vascular lesion.

#### Low Grade Central Osteosarcoma

This rare variant, which comprises 1–2% of OS, lacks the marked nuclear pleomorphism that characterizes conventional OS. Tumors are composed of hypocellular fibrous tissue with variable amounts of osteoid and woven, or occasionally lamellar, bone, and due to the bland appearance of the malignant cells, may be confused with fibrous dysplasia. This variant typically progresses more slowly than conventional OS and has a better prognosis. Low-grade central osteosarcomas have also been shown to have *MDM2* amplifications, which can help to distinguish it from benign mimics.

#### Juxtacortical Osteosarcomas (Parosteal, Periosteal, and High Grade Surface)

These tumors originate from the periosteal surface of the bone and typically grow outward as well as into the cortex, with minimal or no involvement of the underlying medullary bone. High grade surface OS accounts for less than 1% of OS and is morphologically and biologically indistinguishable from conventional OS. In contrast, parosteal and periosteal OS are characterized by slow growth and have a better prognosis than conventional OS. Parosteal OS accounts for approximately 4% of OS and is characterized by a proliferation of spindle cells within a predominantly fibrous stroma with well-formed bony trabeculae in parallel array. The spindle cells tend to show minimal cytologic atypia. Periosteal OS comprises less than 2% of OS and usually appears as a lytic lesion with scalloping of the outer cortex. This variant of demonstrates abundant cartilaginous matrix. The cytologic features are those of an intermediate grade malignant neoplasm.

### 5.2.1.5 Fracture Callus

On occasion, an early or incipient fracture can mimic a sarcoma both clinically and pathologically. In addition, benign as well as malignant lesions of bone can lead to pathologic fracture, and the presence of fracture callus can make interpretation of the FNA or small biopsy difficult. For these reasons and to avoid false positive diagnoses, it is important that one be familiar with the pathology of fracture callus.

In an acute fracture, there are hemorrhage, variable tissue damage, and necrosis of adjacent bone and marrow. The hematoma and necrosis stimulate rapid proliferation of mitotically active, spindled mesenchymal cells that appear atypical. After approximately 1 week, primitive osteoid and chondroid matrices are produced by the cells of the callus. This early osteoid and chondroid is disorganized and at this stage, is most likely to be confused with an OS. By the second week, the osteoblasts begin to appear in single rows along the periphery of osteoid, a phenomenon known as "osteoblastic rimming." The osteoblasts are plump and uniform, and appear to be at the same maturational stage. The islands of cartilaginous matrix show gradual transition to osteoid at their periphery (chondro-osseous bone). The orderly arrangement of osteoblasts in rows, the uniformity of the cells, and the gradual transition from one matrix type to another without a change in the appearance of the cells distinguish this process from sarcoma.

As evident from the previous discussion, the features of fracture callus in FNA vary with age of the fracture. Aspirates from acute fractures

may contain old blood, spicules of necrotic lamellar bone, fragments of necrotic tissue, and highly atypical spindled mesenchymal cells occurring singly and in irregular fragments. In maturing fractures, fragments of osteoid, chondroid, and eventually chondro-osseous bone are also present, while the number of primitive spindled mesenchymal cells decreases. Preparation of a cell block can help to distinguish fragments of fracture callus from more ominous lesions.

### 5.2.2 Chondroid Producing Lesions

Cartilaginous tumors of the skeleton are a major source of diagnostic difficulty, in both cytologic and histologic specimens. This is due, in part, to the tremendous amount of overlap in the morphologic spectrum of these lesions [13]. But in addition, considerable histologic variation often exists within a single tumor. In lesions that are deemed malignant, grading is sometimes difficult and is more subjective than in other neoplasms. Fortunately, differentiating low grade lesions with minimal risk of metastasis from high grade lesions is usually not a problem, and clinically, is the most relevant distinction.

It is critically important to include the clinical data, particularly the presence or absence of pain, and the radiographic findings in the evaluation of cartilaginous tumors. The plain films provide crucial information regarding the bone involved and the pattern of growth, both of which are important predictors of benign or malignant behavior. Tumors of the pelvis, axial skeleton and proximal ends of long bones are more likely to behave in a malignant fashion than lesions in the distal extremities and tubular bones of the hands and feet. When different patterns of growth are evident, the radiographic studies also guide the selection of the most appropriate area of the lesion to sample. Heavily calcified areas are more likely to be benign or low grade, whereas purely lytic areas usually represent a higher grade malignancy. The major chondroid producing lesions of bone are listed in Table 5.3.

**Table 5.3** Chondroid producing lesions of bone

| Benign lesions | Malignant lesions |
|---|---|
| Enchondroma | Chondrosarcoma<br>Grade I, II, & III<br>De-differentiated<br>Mesenchymal |
| Osteochondroma | Secondary low grade chondrosarcoma arising within osteochondroma |
| Periosteal chondroma (Juxtacortical chondroma) | Periosteal osteosarcoma |
| | Periosteal chondrosarcoma |
| Chondromyxoid fibroma | Myxoid chondrosarcoma |
| Chondroblastoma | Clear cell chondrosarcoma |
| Synovial chondromatosis | |
| Fracture callus | |

#### 5.2.2.1 Enchondroma

**Clinical Features**

Enchondroma (EC) is a common benign bone tumor that occurs over a broad age range. Most solitary lesions in the pediatric population present in the second decade of life, whereas those associated with enchondromatosis syndromes manifest in infancy or early childhood. Most of the solitary tumors are asymptomatic and are incidental findings, or present after pathologic fracture. In contrast, enchondromatosis syndromes (Ollier disease, Maffucci syndrome) are characterized by multiple enchondromas involving multiple sites. The resulting skeletal deformities and symptoms vary depending on the sites involvement. Enchondromatosis is also associated with increased risk of malignant degeneration of EC.

**Location**

The most common location of EC is in the tubular bones of the hands. EC is also seen in the proximal humerus, proximal femur, distal femur and other locations, particularly in enchondromatosis.

**Radiographic Appearance**

EC arises in the medullary space, usually in the metaphysis. Most solitary lesions are small, lytic, and expansile, with well-demarcated borders.

Calcifications, that are described as rings, flocculent, fluffy, or popcorn-like, are characteristic and often, abundant. Cortical destruction or a soft tissue mass is unusual, and should raise the possibility of malignancy.

### Cytological Features

FNA of enchondroma yields paucicellular smears dominated by mature cartilaginous matrix (Fig. 5.4). The benign chondroid has a filmy or granular quality, appears bright magenta to purple in air-dried, modified Giemsa-stained and blue-green to blue-gray in Papanicolaou-stained preparations. Fragments of matrix occasionally have a lobulated appearance that recapitulates the histologic pattern. Embedded in the matrix are variable numbers of uniform, round or ovoid cells, usually within lacunar spaces. Cells have small, round, dark nuclei without nucleoli. Nuclear detail is typically difficult to discern. Binucleated cells are rare. Multinucleated forms and mitotic figures are absent. Cells occur singly, as doublets, or occasionally as clusters within the lacunae. Individually dispersed cells may also be identified. Foci of calcification within the matrix are often, but not always, evident. In contrast to EC arising in other sites, digital EC often shows hypercellularity and cytologic atypia.

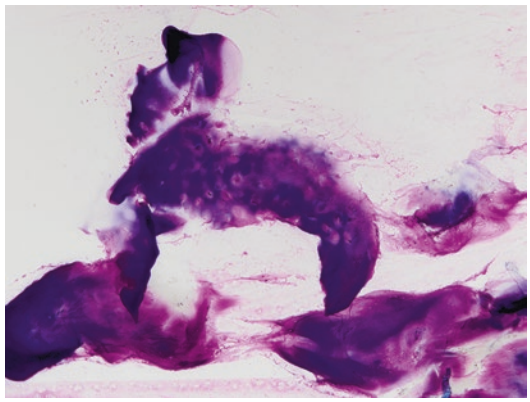

**Fig. 5.4** Enchondroma (Diff-Quik stain, medium power). Irregular fragments of hyaline-type cartilage are present in this aspirate from a digital enchondroma. Although the cellularity is mildly increased, cytologic atypia is absent.

### Differential Diagnosis

The major differential diagnostic consideration is low grade chondrosarcoma. Because hypercellularity and mild cytologic atypia are characteristic of digital EC, it is important not to overinterpret these findings as indicative of malignancy in lesions arising in the fingers and toes. Regardless of site, both significant myxoid degeneration and necrosis should be absent, and if present, should arouse suspicion of malignant transformation. Table 5.4 summarizes the features that help to distinguish enchondroma from low grade chondrosarcoma.

**Table 5.4** Useful features for distinguishing enchondroma from low grade chondrosarcoma

| Feature | Enchondroma | Low grade chondrosarcoma |
|---|---|---|
| Binucleated cells | Occasional (EC < LCS) | Occasional to frequent (LCS > EC) |
| Cellular morphology | Small, bland cells | Larger, "plump" cells |
| | Don't fill lacunar space | Tend to fill lacunae |
| | Atypia absent or minimal except in digital EC | Mild atypia |
| Nuclear morphology | Small, round nuclei | Larger, round nuclei |
| | Dark, pyknotic-appearing nuclei, chromatin detail absent | ± evenly dispersed open chromatin |
| | | ± small nucleoli |
| Pattern of growth | Well circumscribed | Infiltrative |
| | Usually surrounded by a rim of trabecular bone | Invades/surrounds host bone |
| | Lobulated architecture | Erodes and destroys cortex |
| | | Architecture is less organized |
| Skeletal location | Small bones hand and feet, long bones especially femur and humerus | Pelvis, axial skeleton, proximal long bones |
| Clinical history | Painless, usually asymptomatic | Usually painful (± night or rest pain) |
| | Most often discovered incidentally or after pathologic fracture | |

**Pearl**

The radiographic appearance of EC is often diagnostic and treatment is curettage; thus, these lesions are rarely sampled by FNA.

### 5.2.2.2 Chondromyxoid Fibroma

**Clinical Features**

Chondromyxoid fibroma (CMF) is a very rare benign bone tumor. The vast majority of patients are between 5 and 30 years of age at presentation. CMF is usually asymptomatic, but may present with long standing, intermittent pain. When lesions occur in the small bones of the hand or feet, local swelling may be noted.

**Location**

CMF most often arises in the lower extremities, particularly the proximal tibia.

**Radiographic Appearance**

CMF is an eccentric, metaphyseal, lytic lesion with sharply circumscribed, sclerotic margins. The borders typically have a scalloped appearance. Cortical thinning is typical and may be marked. If present, cortical expansion is usually minimal. Periosteal reaction is absent.

**Cytological Features**

FNA of CMF yields mildly to moderately cellular smears composed of fragments of chondromyxoid matrix admixed with stellate, spindled, and round cells [14]. The stellate and spindled cells may be mildly pleomorphic, with variably shaped nuclei and finely clumped to dark chromatin. Binucleated and multinucleated forms may be identified. The stellate and spindled cells appear to float in the chondromyxoid matrix, and also occur as individually dispersed elements. Variable numbers of uniform, small, round to ovoid cells that are morphologically similar or identical to chondroblasts are also present, either singly or in small clusters. These cells have dense, well-defined cytoplasm and relatively uniform, round to ovoid nuclei with pale, finely dispersed chromatin. Nuclear grooves or convolutions may be seen. Mitotic figures are absent. The chondromyxoid matrix has a watery or filmy quality, and appears magenta or pale purple in air-dried modified Giemsa-stained smears and pale blue-green or gray-blue in Papanicolaou-stained preparations.

**Differential Diagnosis**

Differential diagnostic considerations include chondromyxoid fibroma-like conventional osteosarcoma and a chondrosarcoma. In contrast to CMF, these entities have aggressive radiographic appearances and are characterized by a greater degree of cytologic atypia.

### 5.2.2.3 Chondroblastoma

**Clinical Features**

Although chondroblastoma occurs over a wide age range, approximately 75 % of patients present in the second decade of life. CB is rare in patients less than 10 years old. Patients typically present with gradually increasing pain of long duration. Swelling and decreased range of motion may occur, but are usually late symptoms.

**Location**

CB is most often located in the proximal humerus, distal femur, or proximal tibia.

**Radiographic Appearance**

CB is located within the epiphysis or apophysis. Lesions are small, lytic defects with sharply circumscribed, sclerotic borders. Speckled calcifications may be present.

**Cytological Features**

FNA of CB yields variably cellular smears dominated by small, mononuclear cells occurring singly and in small clusters, admixed with osteoclast-like giant cells and fragments of chondroid matrix (Fig. 5.5) [15, 16]. The mononuclear cells have dense cytoplasm, sharp cytoplasmic borders, and eccentric, round to oval nuclei with finely dispersed chromatin, and absent or inconspicuous nucleoli. Nuclei often have longitudinal grooves or convolutions. The fragments of chondroid matrix are typically small, have an amorphous or fibrillar quality, and may be calcified. Cellular aggregates in which matrix surrounds individual mononuclear

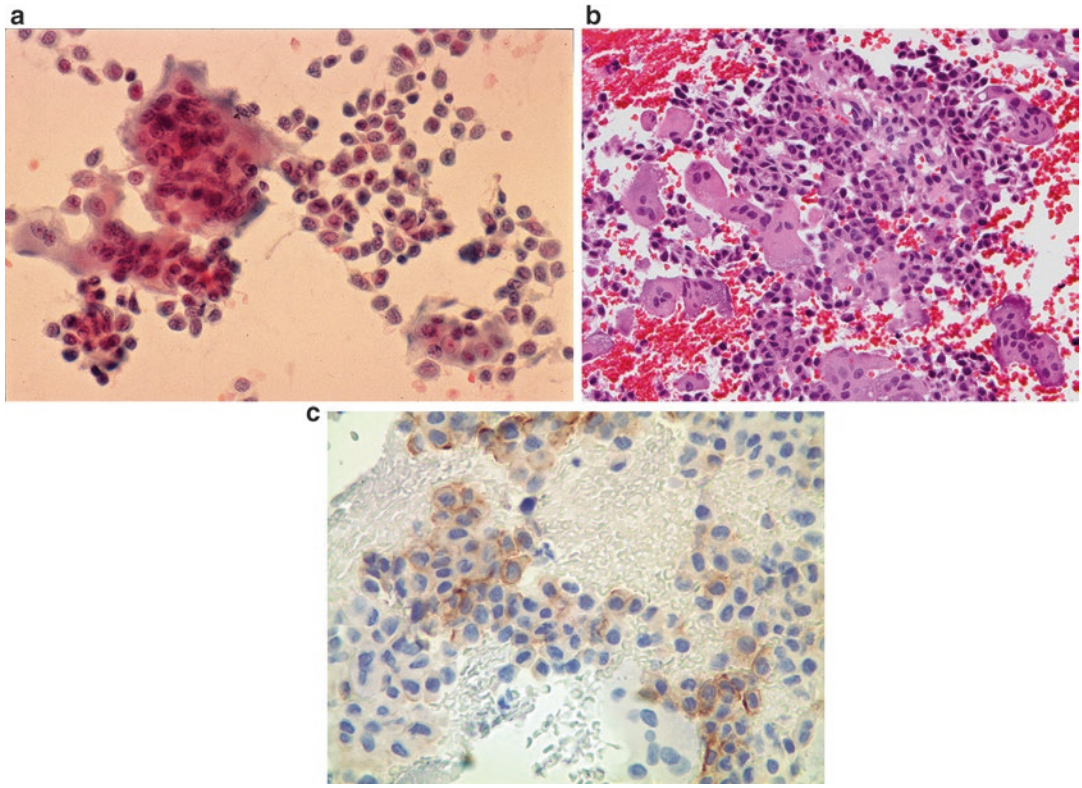


**Fig. 5.5** Chondroblastoma (**a**. Papanicolaou stain, high power; **b**. Cell block, H&E stain, high power; **c**. Cell block, DOG1 immunoperoxidase stain, high power). Chondroblastoma is comprised of mononuclear cells admixed with multinucleated giant cells. The cells occur singly and in small loosely cohesive aggregates. Nuclei in the mononuclear cells are ovoid with finely dispersed chromatin, small nucleoli, and nuclear grooves (**a**). The cell block shows mononuclear cells with nuclear grooves interspersed with multinucleated giant cells (**b**). An immunoperoxidase stain for DOG1 is positive in a subset of the mononuclear cells in this cell block preparation (**c**). (Image of DOG1 immunoperoxidase stain courtesy of Dr. Jeffrey Goldstein).

cells in a "chicken-wire" pattern, with or without calcification, may be present and are virtually diagnostic of this entity.

#### Differential Diagnosis

The main differential diagnostic consideration is giant cell tumor of bone (GCT). Although GCT can occur in the pediatric population, it is more common in skeletally mature individuals. In contrast to CB, mononuclear cells of GCT lack nuclear grooves and their nuclei resemble those of the multinucleated giant cells. In addition, the giant cells in GCT typically have many more nuclei (sometimes greater than 50) than those of CB. The mononuclear cells in CB are positive for DOG1, a feature that can help to confirm the diagnosis (Fig. 5.5).

#### Pearl

Cell block preparations can help to demonstrate the characteristic chicken-wire calcifications.

### 5.2.2.4 Chondrosarcoma

#### Clinical Features

Chondrosarcoma (CS) usually occurs in patients older than 40 years of age, and is rare in persons under 20 years of age. Usually, there is a history of pain that may be of long duration. Rest pain or night pain is not uncommon. CS may be primary, or arise in a previously benign lesion, such as osteochondroma or enchondroma. Patients with osteochondromatosis or enchondromatosis are at increased risk for secondary CS. Mesenchymal chondrosarcoma (MCS) is a rare variant of CS,

comprising 3–10% of tumors, and has a uniformly dismal prognosis. MCS tends to occur at a younger age than conventional CS, with a peak incidence in the second and third decades of life.

### Location

More than three quarters of primary chondrosarcomas are located in the axial skeleton (especially the pelvis), and the proximal femur and humerus. The most common sites of involvement by intraosseous MCS are the craniofacial bones, ribs, ilium, and vertebrae. MCS may also develop extraskeletally in the soft tissues of the head, neck, and lower extremities, and occasionally in the meninges.

### Radiographic Appearance

CS appears as a poorly demarcated, lytic lesion that erodes or destroys the cortex. In large lesions, extension into soft tissue is common. A periosteal reaction is usually absent in low grade CS, but present in high grade tumors. Speckled calcification may be present, but is less than seen in the typical EC and decreases in amount with increasing grade of tumor. MCS tends to be less heavily mineralized than conventional CS.

### Cytological Features

The cytological appearance varies with the grade of the tumor. FNA of low grade CS yields variably cellular smears in which malignant chondrocytes occur singly, in small clusters, and embedded within chondroid matrix (Fig. 5.6) [13]. Individually dispersed cells are round, oval, or polygonal with abundant vacuolated or granular cytoplasm. Nuclei are relatively uniform, round to oval, and have fine to coarse, evenly dispersed chromatin. Nucleoli may be absent, and when present, are small, round, and regular. Binucleated forms may occur. Within the matrix, cells occur singly, as doublets or in small clusters within lacunar spaces. Cells are plump, and tend to fill lacunar spaces. The chondroid matrix is dense or opaque, and has an amorphous quality. Foci of myxoid degeneration may be present, and impart a fibrillar or stringy quality to the matrix.

In contrast, FNA of high grade CS typically yields moderately to highly cellular smears in which cellular and nuclear pleomorphism are readily apparent. Nuclei are enlarged and hyperchromatic, with irregular contours and prominent, often irregular nucleoli. Variable numbers of anaplastic cells are present and can be the predominant cell type. Mitotic figures, including abnormal forms, are present and may be abundant. Myxoid degeneration and/or necrosis may be evident. The amount of chondroid matrix may be scant in high grade lesions.

Aspirates from MCS yield highly cellular smears dominated by small, round cells that occur singly and in loosely cohesive aggregates (Fig. 5.7). These cells have scant or moderate amounts of granular cytoplasm, distinct cellular borders, and central, round to oval nuclei with coarsely granular chromatin and small nucleoli. The nuclear

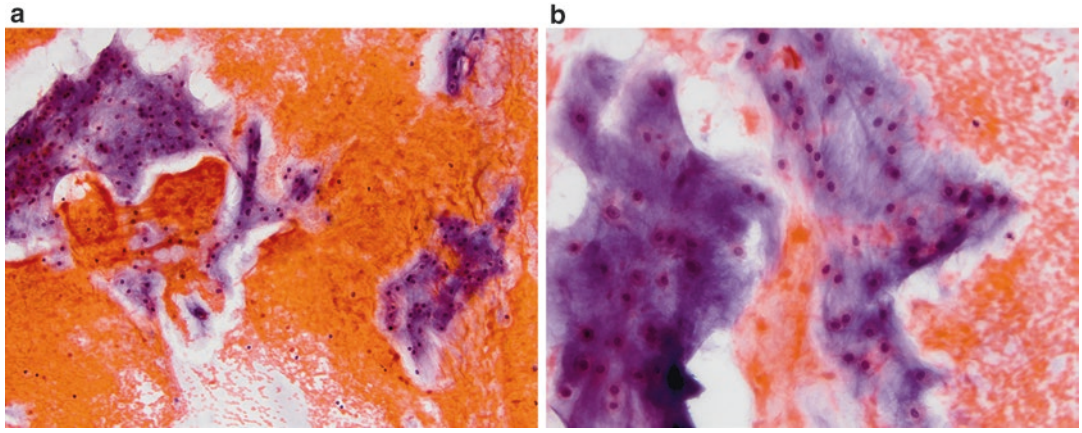


**Fig. 5.6** Chondrosarcoma, grade 2 (**a**. Papanicolaou stain, medium power; **b**. Papanicolaou stain, high power). Irregular fragments of hypercellular cartilaginous matrix, as well as scattered single cells, are present in this smear from a low grade chondrosarcoma (**a**). At high magnification, mild cytologic atypia is evident. Overt anaplasia is absent (**b**).

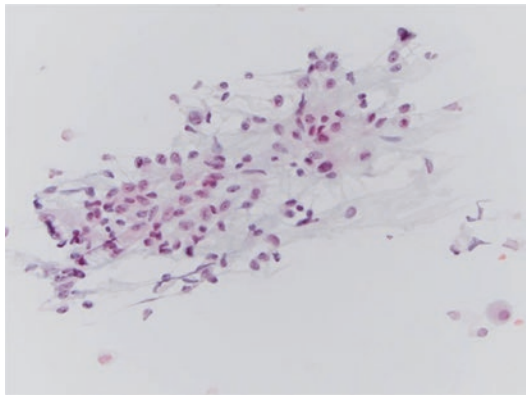

**Fig. 5.7** Mesenchymal chondrosarcoma (Papanicolaou stain, high power). Chondroid matrix is usually present in mesenchymal chondrosarcoma but can scanty and focal. In this field the tumor cells are embedded in pale chondroid matrix that has a frayed, stringy appearance.

membranes are smooth and thickened, and longitudinal nuclear grooves may be present. A chondroid component indistinguishable from usual CS is usually present, but may be extremely scant or absent, making distinction from other small round cell tumors difficult. Necrosis may be present.

#### Differential Diagnosis

In low grade CS, the primary differential diagnostic consideration is enchondroma. Features that help to distinguish these lesions are summarized in Table 5.4. In high grade CS, conventional osteosarcoma is the main consideration. The presence or absence of osteoid distinguishes these lesions from each other. MCS must be distinguished from Ewing sarcoma and metastatic small cell tumors. The presence of matrix helps to distinguish MCS from other small round cell tumors, but when matrix is absent immunoperoxidase stains can be used to confirm the diagnosis. Cells in the chondroid component are positive for S100, while those in the small cell component are positive for SOX9 and negative for FLI-1.

#### Pearls

The distinction between low grade CS and EC may be difficult or impossible on cytologic preparations. Radiographic correlation is essential; however, when imaging studies are equivocal a core or open biopsy should be considered. In practice, a cytologic diagnosis of "low grade cartilaginous neoplasm" may suffice, as treatment for both EC and low grade CS is complete curettage. The distinction between high grade CS and chondroblastic OS is more problematic, as high grade CS is treated by surgical resection, whereas treatment for OS is neoadjuvant chemotherapy followed by surgical resection. In the absence of convincing osteoid in an FNA, a core or open biopsy is needed to resolve the differential diagnosis.

**Table 5.5** Fibrous lesions without associated bone formation

| Benign lesions | Malignant lesions |
|---|---|
| Desmoplastic fibroma of bone (desmoid tumor of bone) | Fibrosarcoma |
| Non-ossifying fibroma/benign fibrous histiocytoma of bone | Adamantinoma |
| Giant cell reparative granuloma | |
| Brown tumor of hyperparathyroidism | |

### 5.2.3 Fibrous and Fibrohistiocytic Lesions Without Associated Bone Formation

A number of fibrous and fibrohistiocytic lesions of bone without associated bone formation occur in the pediatric population as summarized in Table 5.5. However, FNA is rarely used for the evaluation of these lesions. Non-ossifying fibroma, giant cell reparative granuloma, and adamantinoma each has a characteristic radiographic appearance that obviates the need for pathologic diagnosis prior to definitive treatment in most cases. Similarly, brown tumor of hyperparathyroidism can be suspected based on clinical history and in the absence of unusual radiographic features is unlikely to undergo FNA or small biopsy. Desmoplastic fibroma is a locally aggressive tumor that is most common in adolescents and young adults, but is vanishingly rare (less than 0.1 % of bone tumors). Fibrosarcoma of bone is a rare and controversial entity, the hallmark of which is absence of differentiation other than fibroblastic. Most previously reported examples of this tumor likely represent other

**Table 5.6** Fibro-osseous lesions of bone

| Benign lesions | Malignant lesions |
|---|---|
| Fibrous dysplasia | Parosteal osteosarcoma |
| Osteofibrous dysplasia (ossifying fibroma) | Adamantinoma |
| Resolving (healing) osteomyelitis | |

**Table 5.7** Giant cell lesions of bone

| Benign/inflammatory lesions | Malignant lesions |
|---|---|
| Giant cell tumor of bone | Giant cell rich fibroblastic subtype of conventional osteosarcoma |
| Brown tumor of hyperparathyroidism | |
| Chondroblastoma | |
| Giant cell reparative granuloma | |
| Langerhans cell histiocytosis | |
| Aneurysmal bone cyst | |
| Non-ossifying fibroma | |

entities. The diagnosis is one of exclusion. Given the rarity of these tumors and/or the very low likelihood of encountering these entities in cytological specimens, further discussion of these tumors is beyond the scope of this chapter.

### 5.2.4 Fibrous Lesions with Associated Bone Formation (Fibro-Osseous Lesions)

Fibro-osseous lesions of bone are uncommon overall. The most common fibro-osseous lesions encountered in the pediatric population are listed in Table 5.6. These lesions either have a characteristic radiographic appearance or are difficult to access by FNA and thus, are rarely encountered in cytologic specimens.

### 5.2.5 Lesions with a Prominent Giant Cell Component

Giant cells are a ubiquitous feature of osseous tumors, but in a small number of benign and malignant lesions, are prominent and diagnostically important. Table 5.7 lists the major giant cell lesions of bone seen in the pediatric population.

#### 5.2.5.1 Giant Cell Tumor of Bone

##### Clinical Features

Although giant cell tumor of bone (GCT) generally presents in young adults, with the peak incidence in the third decade, approximately 10% occur in the second decade of life. Lesions are almost always painful, and swelling is present in about 75% of cases. Pathologic fracture may also occur.

##### Location

More than 75% of GCT are located near the articular end of a tubular bone. Approximately 50% occur in the region of the knee. Other sites include the distal radius, proximal femur, proximal humerus, and distal tibia.

##### Radiographic Appearance

GCT of long bones invariably involves the epiphysis, usually with metaphyseal extension. The vast majority of lesions arise eccentrically, and many abut the articular cartilage. Lesions are lytic, with well-defined borders, and typically have fine to moderately coarse trabeculations. GCT is usually confined within the normal bony contour, but may occasionally erode and expand the cortex. Lesions that extend into the surrounding soft tissues are usually covered by a thin layer of periosteal new bone. True periosteal reaction is rare.

##### Cytological Features

FNA yields moderately or highly cellular smears composed of a biphasic population of multinucleated osteoclast-like giant cells and mononuclear stromal cells occurring in large, cohesive sheets, in clusters, and singly. Within cellular aggregates, giant cells are fairly evenly distributed and intimately admixed with the mononuclear stromal cells. The latter are plump, spindled cells with scant to moderate amounts of cytoplasm and nuclei with granular chromatin and regular, round to oval nucleoli. Mitotic figures are rare.

The osteoclast-like giant cells contain few to greater than 50 nuclei that are randomly distributed throughout the cytoplasm and are morphologically identical to those in the mononuclear stromal cells. The latter feature is a hallmark of GCT, and helps to distinguish it from other lesions with a prominent giant cell component.

#### Differential Diagnosis

In the context of the clinical and radiographic features, the principal differential diagnostic consideration is chondroblastoma, which was discussed in Sect. 5.2.2.3. The often high number of nuclei in the giant cells and their morphologic similarity to those of the mononuclear cells are hallmarks of GCT, and help to distinguish it from CB and other lesions with a prominent giant cell component. In some cases, GCT has an aggressive radiographic appearance that raises the possibility of malignancy. However, the cells in GCT lack the overtly malignant features seen in osteosarcoma.

### 5.2.6 Cystic Lesions of Bone

Cystic lesions of bone that are encountered in the pediatric population are listed in Table 5.8. The benign, cystic nature of simple, unicameral and ganglion cysts of bone is readily apparent on imaging studies and therefore, these lesions rarely undergo FNA or small biopsy prior to definitive treatment with curettage and bone packing. Aspirated fluid obtained at the time of surgery may be submitted for cytological evaluation. Specimens are typically paucicellular and comprised of bland spindle cells admixed with histiocytes. Rarely, small fragments of characteristic cementum-like matrix are present in intraoperative aspirates from unicameral bone cysts. In contrast to other benign cystic lesions, aneurysmal bone cyst has a more complex radiographic appearance that can raise the possibility of either aneurysmal bone cyst arising in an underlying neoplasm or telangiectatic osteosarcoma. It is these lesions with solid areas and/or aggressive features that are most likely to undergo FNA or small biopsy.

**Table 5.8** Cystic lesions of bone

| Benign lesions | Malignant lesions |
|---|---|
| Aneurysmal bone cyst<br>Primary or secondary | Telangiectatic osteosarcoma |
| Simple cyst (uncommitted cyst) | |
| Unicameral bone cyst | |
| Ganglion cyst of bone | |

#### 5.2.6.1 Aneurysmal Bone Cyst

##### Clinical Features

Aneurysmal bone cyst (ABC) is most common in children and adolescents with 75% of lesions occurring in patients under 20 years of age, and has a peak incidence in the second decade of life. Pain and swelling in the area of the involved bone are the main symptoms.

##### Location

ABC may occur in any part of any bone, but has a predilection for long bones and the vertebral column.

##### Radiographic Appearance

ABC appears as a well-demarcated, lytic lesion with a sclerotic rim and fluid–fluid levels. Although ABC can occur in any part of any bone, in long bones it most often involves the metaphysis. In rapidly growing lesions, sclerosis is usually absent and marked cortical thinning and a periosteal reaction are often present, raising concern for malignancy.

##### Cytological Features

FNA characteristically yields bloody, paucicellular smears [17]. Cellular elements include variable numbers of osteoclast-like giant cells, hemosiderin-laden macrophages, and benign spindle cells consistent with fibroblasts and myofibroblasts. In some cases, osteoblasts and osteoid are also noted. Mitotic figures may present in the spindle cells, particularly in rapidly growing lesions, but abnormal forms are absent.

### Differential Diagnosis

The main differential diagnostic considerations include secondary ABC arising in an underlying benign or malignant tumor, and telangiectatic osteosarcoma. Cytologic evidence of other bone tumors should be carefully sought to exclude an underlying neoplasm with secondary ABC. The absence of overtly malignant cells helps to exclude telangiectatic osteosarcoma. *USP6* gene rearrangements are found in approximately 70% of primary ABC but not in secondary ABC. Identification of a *USP6* rearrangement by FISH can help to confirm the diagnosis and exclude other possibilities.

### Pearl

When aggressive radiographic features are present, it is important to exclude telangiectatic osteosarcoma. Because aspirates from telangiectatic osteosarcoma are usually bloody, the diagnostic overtly malignant cells can be sparse and may be overlooked. This pitfall should be borne in mind when evaluating an FNA from a clinically suspected ABC with atypical or aggressive features.

## 5.2.7 Small Round Blue Cell Tumors and Inflammatory Infiltrates of the Marrow Space

A distinctive group of highly malignant neoplasms of bone are the so-called small round blue cell tumors (SRBCT). These include Ewing sarcoma/primitive neuroectodermal tumor (PNET), primary malignant lymphoma, mesenchymal chondrosarcoma (see Sect. 5.2.2.4), and small cell osteosarcoma (see section "Small Cell Osteosarcoma"). A number of metastatic lesions should also be considered in the differential diagnosis of SRBCT, including neuroblastoma, lymphoma, and rhabdomyosarcoma.

As SRBCTs usually consist of a monomorphous population of small, round cells with scant cytoplasm and hyperchromatic nuclei, distinction between these neoplasms may be difficult or impossible without ancillary studies. Notable exceptions include small cell osteosarcoma and mesenchymal chondrosarcoma, in which the presence of osteoid and chondroid material, respectively, allows accurate diagnosis. Unfortunately, these matrices may be scant or absent in aspirates from these lesions. Ancillary studies, including histochemical and/or immunoperoxidase stains, flow cytometry, molecular studies and electron microscopy, usually allow definitive diagnosis of a SRBCT. Of note, electron microscopy has largely been replaced by immunoperoxidase stains and is rarely used. The importance of rapid on site evaluation of aspirates from SRBCTs cannot be overstated, as it allows collection of additional material for appropriate ancillary studies, and often obviates the need for a more invasive diagnostic biopsy.

Table 5.9 lists the common neoplastic and inflammatory small cell lesions of bone seen in the pediatric population. Features that help to distinguish some of the more common SRBCT of bone are summarized in Table 5.10.

### 5.2.7.1 Ewing Sarcoma/Primitive Neuroectodermal Tumor (ES/PNET)

#### Clinical Features

Ewing sarcoma/PNET is the second most common primary malignant neoplasm of bone, and 80% of cases occur within the first two decades of life. Localized pain and swelling are the most common symptoms. Occasional patients present with systemic illness, which is usually indicative of a worse prognosis.

**Table 5.9** Small cell lesions of bone: neoplastic and inflammatory

| Benign/inflammatory lesions | Malignant neoplasms |
|---|---|
| Acute osteomyelitis | Ewing sarcoma/PNET |
| Chronic osteomyelitis | Malignant lymphoma |
| Plasma cell osteomyelitis | Small cell osteosarcoma |
| Langerhans cell histiocytosis | Mesenchymal chondrosarcoma |
| | Metastatic lesions |
| | Neuroblastoma |
| | Lymphoma |
| | Rhabdomyosarcoma |

**Table 5.10** Useful features for distinguishing between various SRBCT of bone

| Features | ES/PNET | Lymphoma | Small cell OS | MCS |
|---|---|---|---|---|
| Cytoplasm | ES: scant, indistinct borders; PNET: ± wispy extensions | Scant to moderate | Scant to moderate | Scant, distinct borders |
| Cytoplasmic glycogen (PAS + diastase digestible) | Usually prominent | Absent | Absent | Rare |
| Nuclear features | Oval to round, evenly dispersed fine chromatin to coarse, clumped chromatin, ± small nucleoli | Irregular contours; coarse or vesicular chromatin; nucleoli usually prominent | Round, oval or irregular; fine to clumped chromatin; pleomorphism may be present | Oval to spindled shaped; fine to coarse chromatin; ± nucleoli |
| Matrix | Absent | Absent | Focal osteoid, rarely chondroid | Focal chondroid (may be scant) |
| Immunoperoxidase stains | + CD99, FLI-1; ± synaptophysin, chromogranin; (−) LCA | + LCA; B-cell: + CD20, others; T-Cell: + CD3, others | ± SATB2 | + S100 in chondroid component, + SOX9 in small cell component |
| Molecular studies | *EWSR1* rearrangements | T-cell receptor rearrangements in T-cell lymphomas | Not helpful | Not helpful |
| Pattern | Single cells, loose clusters and pseudorosettes | Single cells; lymphoglandular bodies | Single cells | Single cells |
| Age range | Broad with peak in the second decade of life | Broad, rare in the pediatric population | Broad with peak in the second decade of life | Broad |
| Extraosseous mass | Usually prominent | Usually prominent | Usually prominent | Common |

### Location

ES/PNET has a predilection for the diaphysis of long tubular bones, although any portion of any bone may be affected.

### Radiographic Appearance

ES/PNET typically appears as a large, poorly defined, lytic lesion with a moth-eaten appearance. A thin rim of cortex may persist, and an "onion skin" or "sunburst" periosteal reaction is often present. Extension into the soft tissue with formation of a large extraosseous mass is characteristic. Matrix production is absent.

### Cytological Features

FNA of ES/PNET yields highly cellular smears in which cells are individually dispersed and arrayed in loosely cohesive clusters (Fig. 5.8) [18, 19]. Cells are relatively uniform, small and round to ovoid with scant cytoplasm and indistinct cellular borders. The cytoplasm is often vacuolated due to abundant glycogen and disruption of the cytoplasm may impart a tigroid appearance to the background that is best seen in air-dried, modified Giemsa-stained smears. Cytoplasmic projections may be evident in some cells and variable numbers of pseudorosettes may also be present. Nuclei are round to ovoid with finely granular, evenly distributed chromatin and inconspicuous nucleoli. In some tumors nuclei are more irregular with clumped chromatin and small nucleoli. Naked nuclei and DNA streaks (crush artifact) are common. Mitotic figures are typically present, but few in number. Necrosis is usually present and may be prominent.

### Differential Diagnosis

Differential diagnostic considerations include primary and metastatic small round blue cell tumors arising in the pediatric population, including

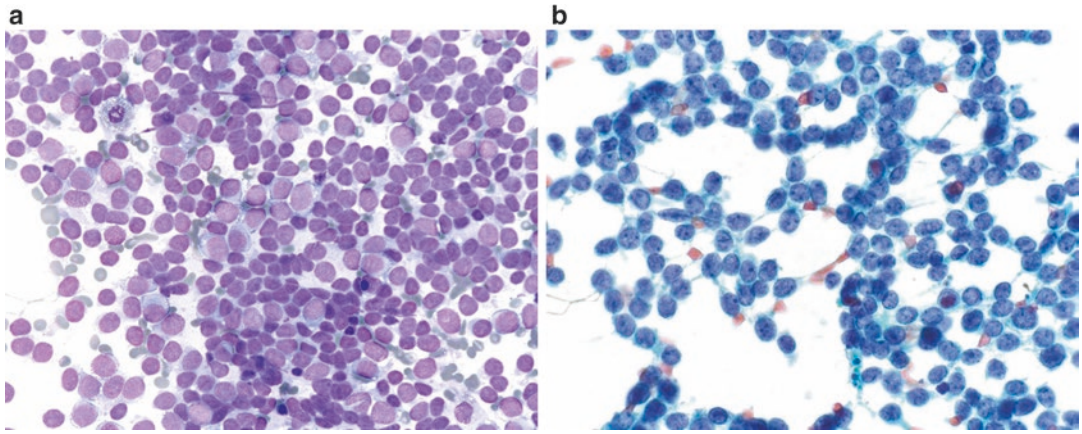


**Fig. 5.8** Ewing sarcoma (**a**. Diff-Quik stain, high power; **b**. Papanicolaou stain, high power). This hypercellular smear is composed of a relatively monotonous population of round to oval cells with scant cytoplasm and fine chromatin. Note the "light and dark" appearance of the cells in this smear (**a**). The evenly dispersed, fine chromatin and inconspicuous nucleoli are better seen in the Papanicolaou-stained preparation. Some cells have delicate cytoplasmic extensions (**b**).

lymphoma, small cell OS, MCS neuroblastoma, and rhabdomyosarcoma. Features that help to distinguish ES/PNET from other primary bone tumors are summarized in Table 5.10. Metastatic lesions can usually be distinguished from primary ES/PNET of bone on the basis of clinical history with or without confirmatory immunoperoxidase stains. Recurrent translocations, the most common of which (>95 %) involve *EWSR1*, are also characteristic of ES/PNET and can be identified using FISH or other molecular studies. Recently, Ewing-like tumors with translocations involving *DUX4* or *BCOR* have also been described.

### Pearls

- Immunoperoxidase stains and FISH are usually required for definitive diagnosis of ES/PNET, thus it is essential to submit material for cell block and when possible, prepare extra smears for FISH. *EWSR1* rearrangements are seen in a variety of tumors other than ES/PNET, and rare ES/PNETs lack *EWSR1* rearrangements, both of which can lead to misdiagnosis.
- In addition, there are now a group of Ewings-like tumors, referred to as round cell sarcomas, that have more atypical cytologic features, lack the diffuse membranous CD99 immunostaining, and are more likely to show diffuse nuclear WT1 positivity.

#### 5.2.7.2 Malignant Lymphoma of Bone

### Clinical Features

Primary lymphomas of bone may occur at any age, but are much more frequent after the second decade of life and are rare in young children. In the pediatric population, secondary involvement of bone, particularly by lymphoblastic lymphoma, is far more common than primary lymphoma of bone. Bone pain is the most common presenting symptom of both primary and secondary bony involvement.

### Location

Malignant lymphoma can occur in any part of any bone.

### Radiographic Appearance

These lesions almost always appear malignant radiographically. However, the appearances are quite variable and characteristic features that suggest the diagnosis of lymphoma are lacking.

### Cytological Features

The cytologic features vary considerably, depending on the type of lymphoma and are discussed in more detail in Chap. 3. In general, FNA of lymphoma yields highly cellular smears in which cells occur singly or in loosely cohesive pseudoepithelial clusters. Due to cytoplasmic fragility,

the background contains numerous lymphoglandular bodies that are best appreciated in air-dried, modified Giemsa-stained smears. Intact cells are generally round to ovoid, with scant to moderate amounts of cytoplasm and indistinct borders. Mild cellular and nuclear pleomorphism is usually evident. Nuclei are round to ovoid, with irregular nuclear membranes, fine to coarsely clumped chromatin, and one or more, often irregular nucleoli. Mitotic figures, including abnormal forms, may be scarce or abundant. DNA streaks are usually evident. Necrosis is variably present. Nuclear molding is absent.

#### Differential Diagnosis

Differential diagnostic considerations include other primary and metastatic small round blue cell tumors. Features that help to distinguish lymphomas from other primary bone tumors are summarized in Table 5.10. Metastasis from other small round blue cell tumors can usually be distinguished from either primary or secondary lymphoma of bone on the basis of clinical history, with or without confirmatory immunoperoxidase stains. In many cases, the lymphoid origin of the malignant cells is readily apparent at the time of rapid on site evaluation. In such cases, additional passes should be performed for flow cytometry and immunoperoxidase stains. When the cell of origin is less certain, material should also be obtained for cytogenetics and molecular studies, whenever possible.

### 5.2.7.3 Osteomyelitis

#### Clinical Features

Not infrequently, the acute phase of an aggressive infection involving bone can mimic a malignancy both clinically and radiographically. Osteomyelitis can be bacterial, fungal or possibly, viral in origin, and can result from either hematogenous dissemination or direct surgical or traumatic introduction of microorganisms.

#### Location

Osteomyelitis can involve any part of any bone.

#### Radiographic Appearance

The radiographic findings in osteomyelitis depend on the stage and activity of the disease. Alterations that are detectable on plain radiographs are not present until the disease is well established and significant destruction of bone has occurred. At this stage, acute osteomyelitis appears as a lytic lesion in which the permeative destruction of trabecular and cortical bone often mimics malignancy.

#### Cytological Features

The cytological findings reflect the stage of the disease. In general, aspirates contain inflammatory cells admixed with necrotic tissue and osteoclasts. In early lesions, neutrophils and granular, necrotic debris often dominate the smears, while necrotic trabeculae and osteoclasts are less conspicuous. Aspirates from later lesions contain a mixed population of neutrophils, macrophages, lymphocytes, and eventually plasma cells, and both necrotic trabeculae with or without conspicuous resorption lacunae and osteoclasts are present in increased numbers. Rarely, microorganisms are identified in routinely stained preparations or with histochemical stains. In resolving acute osteomyelitis, smears may be paucicellular and dominated by irregular fragments of granulation tissue.

#### Differential Diagnosis

Differential diagnostic considerations include Langerhans cell histiocytosis, which is discussed in detail in Sect. 5.2.7.4, and necrotic tumor. The abundance of neutrophils and absence of malignant cells support a diagnosis of osteomyelitis, as does the demonstration of microorganisms on a smear or cell block. However, biopsy may be warranted to exclude malignancy in cases with less prominent neutrophilic inflammation and/or conspicuous reactive endothelial or myofibroblastic cells derived from granulation tissue. Whenever possible, material should be obtained for culture and sensitivity. Polymerase chain reaction (PCR) can help to identify the causative microorganism in some cases.

### 5.2.7.4 Langerhans Cell Histiocytosis

#### Clinical Features

Langerhans cell histiocytosis (LCH) involving bone generally presents in the first two decades of life, with a peak incidence between 5 and 10 years. LCH has a broad spectrum of clinical

presentations with highly variable prognoses. Older children typically present with single or multiple skeletal lesions that usually follow a benign course and either regress spontaneously or require minimal treatment. In contrast, infants and very young children may present with multifocal, multisystem disease, which can progress to organ failure and has an aggressive or sometimes fatal clinical course. Bone lesions usually manifest as a painful swelling.

### Location

The most frequent sites of involvement are the skull, followed by long bones, flat bones, and vertebrae.

### Radiographic Appearance

Three stages have been described in the evolution of LCH, including incipient, mid, and late phases. During the incipient or early phase, lesions tend to have an aggressive radiographic appearance that is characterized by a permeative pattern of growth, indistinct borders, and a lamellated periosteal reaction. This radiographic picture overlaps with that of aggressive osteomyelitis and malignancies such as Ewing sarcoma and lymphoma, and these entities are frequently considered in the radiographic differential diagnosis. Later in the course of the disease the lesions tend to develop well-demarcated borders that are often surrounded by a rim of sclerotic bone.

### Cytological Features

FNA of LCH yields moderately to highly cellular smears composed of a polymorphous population of individually dispersed cells that include variable numbers of Langerhans cell histiocytes, eosinophils, osteoclast-like giant cells, lymphocytes, neutrophils, and plasma cells (Fig. 5.9) [20]. Langerhans cell histiocytes are characterized by moderate to abundant cytoplasm and eccentric, oval to reniform nuclei with pale, evenly dispersed chromatin and inconspicuous nuclei. Nuclear folds or grooves are characteristic, and help to distinguish these cells from ordinary macrophages by light microscopy. Definitive diagnosis of LCH usually requires immunoperoxidase stains to confirm the identity of the lesional cells. In contrast to ordinary macrophages, Langerhans cell histiocytes are immunoreactive for S100, CD1a, langerin, and CD68. The cells are negative for lysozyme and alpha-1 antitrypsin. The diagnostic ultrastructural feature of Langerhans cell histiocytes is the presence of Birbeck granules within the cytoplasm, but these structures may be difficult to find.

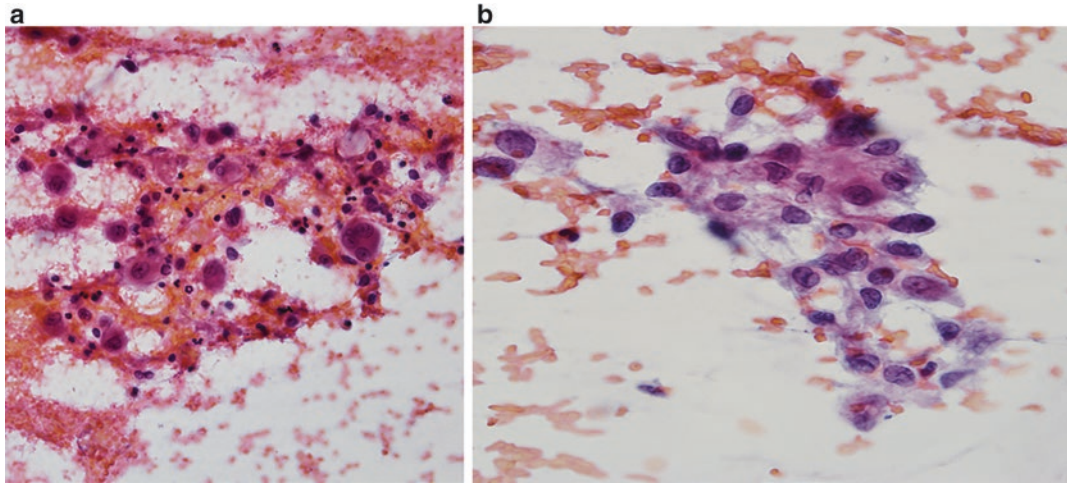


**Fig. 5.9** Langerhans cell histiocytosis (**a**, **b**. Papanicolaou stain, medium and high power). Langerhans cell histiocytosis is comprised of Langerhans cell histiocytes admixed with variable numbers of eosinophils, neutrophils, lymphocytes, and plasma cells (**a**). Multinucleated Langerhans cells, as well as osteoclast-like giant cells are also present. As seen in this cluster of Langerhans cell histiocytes, the cells have moderate to abundant cytoplasm and ovoid to reniform, grooved or folded nuclei (**b**).

### Differential Diagnosis

The main differential diagnostic consideration is osteomyelitis. The distinctive morphologic appearance of Langerhans cell histiocytes provides an important clue to the correct diagnosis which can be confirmed with immunoperoxidase stains.

## 5.3 Soft Tissue Tumors

A wide variety of benign and malignant neoplasms, as well as non-neoplastic lesions occur in the soft tissues of children and adolescents. Benign neoplasms and reactive processes are generally small and superficial. In contrast, most soft tissue sarcomas appear as bulky, deep-seated masses. Soft tissue tumors are classified based on the presumed mesenchymal cell of origin, as summarized in Table 5.11. However, a pattern-based approach, as summarized in Table 5.12, is often more practical for cytological evaluation of these lesions. Discussion of the myriad soft tissue lesions seen in the pediatric population, only some of which are included in Tables 5.11 and 5.12, is beyond the scope of this book; therefore, this chapter will focus on some of the more common soft tissue lesions seen in the children and adolescents.

### 5.3.1 Small Round Cell Tumors

Small round cell tumors are the most common primary malignant tumors of soft tissue in children and adolescents. Rhabdomyosarcoma, Ewing sarcoma/PNET, poorly differentiated (small cell) synovial sarcoma, and desmoplastic small round

**Table 5.11** Classification of pediatric soft tissue tumors based on presumed mesenchymal tissue of origin

| Origin | Benign | Locally aggressive | Malignant |
|---|---|---|---|
| Fat cells | Lipoma | Atypical lipomatous tumor | Liposarcoma |
| | Lipoblastoma | | Myxoid |
| | Hibernoma | | Round cell |
| | | | Pleomorphic |
| Fibroblasts/ myofibroblasts | Nodular fasciitis | Desmoid-type fibromatosis | Fibrosarcoma |
| | Fibrous hamartoma of infancy | Dermatofibrosarcoma protuberans (DFSP) | Infantile |
| | Digital fibroma | | Adult type |
| | Myofibroma | | |
| | Gardner fibroma | | |
| | Hypertrophic scar | | |
| So-called fibrohistiocytic tumors | Benign fibrous histiocytoma | | |
| | Tenosynovial giant cell tumor, nodular or diffuse | | |
| Peripheral nerve sheath elements | Neurofibroma | | Malignant peripheral nerve sheath tumor |
| | Schwannoma | | |
| | Granular cell tumor | | |
| Endothelial cells | Hemangioma | Epithelioid hemangioendothelioma | Angiosarcoma |
| Skeletal muscle | Rhabdomyoma | | Rhabdomyosarcoma |
| | | | Embryonal |
| | | | Alveolar |
| | | | Spindle cell/sclerosing |
| Smooth muscle | Leiomyoma | | Leiomyosarcoma |
| Uncertain | | Angiomatoid fibrous histiocytoma | Synovial Sarcoma |
| | | | Epithelioid Sarcoma |
| | | | Alveolar soft part sarcoma |
| | | | Desmoplastic small round cell tumor |
| | | | Extrarenal rhabdoid tumor |

**Table 5.12** Classification of pediatric soft tissue tumors based on pattern

| Pattern | Benign | Locally aggressive | Malignant |
|---|---|---|---|
| Small round cell | | | Rhabdomyosarcoma<br>Ewing sarcoma/PNET<br>Desmoplastic small round cell tumor<br>Poorly differentiated (small cell) synovial sarcoma<br>Extrarenal rhabdoid tumor<br>Metastatic neuroblastoma or other round cell tumor |
| Spindle cell | Nodular fasciitis<br>Fibrous hamartoma of infancy<br>Digital fibroma<br>Myofibroma<br>Gardner fibroma<br>Hypertrophic scar<br>Hemangioma<br>Leiomyoma<br>Neurofibroma<br>Schwannoma<br>Rhabdomyoma | Desmoid-type fibromatosis<br>Dermatofibrosarcoma protuberans (DFSP)<br>Angiomatoid fibrous histiocytoma | Fibrosarcoma<br>Infantile<br>Adult type<br>Synovial sarcoma<br>Spindle cell/sclerosing rhabdomyosarcoma<br>Malignant peripheral nerve sheath tumor<br>Low grade fibromyxoid sarcoma<br>Angiosarcoma |
| Epithelioid | Granular cell tumor<br>Rhabdomyoma | Epithelioid hemangioendothelioma<br>Angiomatoid fibrous histiocytoma | Epithelioid malignant peripheral nerve sheath tumor<br>Epithelioid sarcoma<br>Angiosarcoma<br>Alveolar soft part sarcoma |
| Myxoid | Myxoma | Aggressive myxoma | Myxoid liposarcoma<br>Low grade fibromyxoid sarcoma |
| Pleomorphic | | | Pleomorphic liposarcoma<br>Pleomorphic undifferentiated sarcoma |
| Clear cell | Lipoblastoma<br>Lipoma<br>Hibernoma | Atypical lipomatous tumor | Clear cell sarcoma of soft tissue |

cell tumor account for the overwhelming majority of these neoplasms. Considerable overlap exists in cytomorphologic features of these tumors and in most cases, ancillary studies are needed to confirm the diagnosis and exclude other entities. In general, additional material should be collected for a cell block and air-dried unstained smears prepared and reserved for FISH.

#### 5.3.1.1 Rhabdomyosarcoma

**Clinical Features**

Rhabdomyosarcoma (RMS) is the most common soft tissue sarcoma in the pediatric population. The majority of patients (60–70 %) present in the first decade of life, most before 5 years of age. Embryonal rhabdomyosarcoma (ERMS) can be congenital, occurs the first year of life in up to 10 % of cases, and is uncommon in children older than 10 years of age. ERMS most often arises in the head and neck and genitourinary system, and is rare in the extremities. Alveolar rhabdomyosarcoma (ARMS) can occur at any age, but is more common in adolescents than ERMS and is rare in very young children. ARMS most often arises in the extremities. Other sites include the paraspinal and perineal regions and paranasal sinuses.

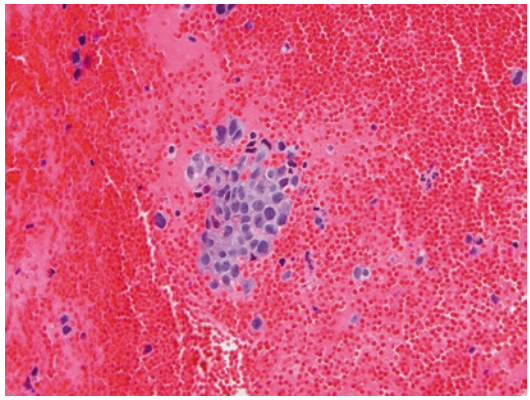

**Fig. 5.10** Alveolar rhabdomyosarcoma (Cell block, H&E stain, high power). Alveolar rhabdomyosarcoma is characterized by a relatively monotonous population of round cells with round nuclei and one or more conspicuous nucleoli.

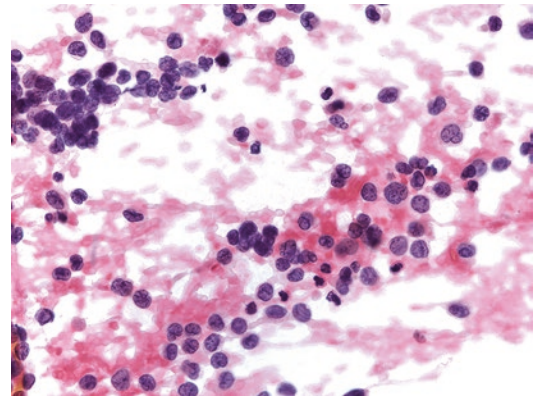

**Fig. 5.11** Embryonal rhabdomyosarcoma (Papanicolaou stain, high power). Embryonal rhabdomyosarcoma is characterized by round cells with scant cytoplasm and round to irregular nuclei with fine chromatin and inconspicuous nucleoli. The cells occur singly and in small loosely cohesive clusters.

### Cytological Features

Aspirates from RMS are usually highly cellular and are composed of relatively monotonous cells occurring singly and in small, loosely cohesive clusters. In ARMS the cells are round and have round nuclei with coarse chromatin and one or more nucleoli (Fig. 5.10). Cells with eccentric cytoplasm and multinucleated cells are present in variable numbers, and when present, are an important clue to the diagnosis. However, cells with cross striations are rare. The cells in ERMS are typically smaller than those in ARMS and have round to ovoid or irregular nuclei with fine chromatin and inconspicuous nucleoli (Fig. 5.11). Elongate or strap-like cells with cross-striations can be present and are occasionally prominent. Anaplastic cells with enlarged, hyperchromatic nuclei are present in a minority of cases. Fragments of myxoid stroma are sometimes seen in ERMS.

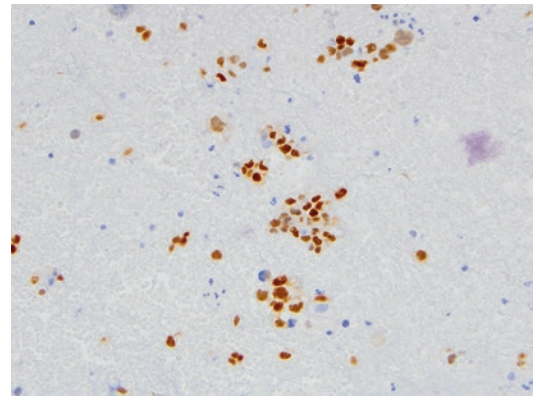

**Fig. 5.12** Alveolar rhabdomyosarcoma (Cell block, myogenin immunoperoxidase stain, medium power). Alveolar rhabdomyosarcoma (ARMS) shows strong, diffuse nuclear staining for myogenin. This pattern of staining helps to distinguish alveolar from embryonal rhabdomyosarcoma, which typically shows patchy, variable staining for myogenin.

### Differential Diagnosis

Differential diagnostic considerations include Ewing sarcoma/PNET, desmoplastic small round cell tumor, poorly differentiated (small cell) synovial sarcoma, lymphoma, neuroblastoma, and other pediatric small round cell tumors. Although the clinical history and site of involvement can help to narrow the differential diagnosis, ancillary studies are essential for confirming the diagnosis of RMS and excluding other entities. RMS shows nuclear staining for myogenin and MyoD1, which distinguishes it from other entities in the differential diagnosis, as well as cytoplasmic staining for desmin and muscle specific actin, and is usually negative for CD99, FLI-1, synaptophysin, chromogranin, epithelial membrane antigen, cytokeratin, TLE-1, and CD45. Nuclear staining for myogenin is typically strong and diffuse in ARMS (Fig. 5.12) and patchy and variable in ERMS, and

helps to distinguish these entities. Gene rearrangements involving *FOXO1* and either *PAX3* or *PAX7* are present in approximately 80 % of ARMS, but are absent in ERMS. The morphologic, immunophenotypic, and molecular genetic features of soft tissue and osseous Ewing sarcoma/PNET are identical and are discussed in Sect. 5.2.7.1. Synovial sarcoma and desmoplastic small round cell tumor are discussed below, while other entities in the differential diagnosis are discussed in detail elsewhere in this book.

**Pearl**

Although the pattern of myogenin staining helps to support a diagnosis of either ARMS or ERMS, demonstration of a *FOXO1* translocation is required to reliably distinguish these entities in cytologic specimens.

### 5.3.1.2 Desmoplastic Small Round Cell Tumor

**Clinical Features**

Desmoplastic small round cell tumor (DSRCT) is a rare tumor that predominantly occurs in children and young adults and has a male predilection. DSRCT usually presents with widespread intra-abdominal disease, involving the serosa, mesentery, omentum, retroperitoneum, and/or pelvis. However, tumors occasionally arise in the thoracic cavity and paratesticular regions, and rarely in other sites. Patients present with abdominal pain, distention, ascites, a palpable mass, and/or intestinal obstruction. DSRCT is an aggressive tumor with a poor prognosis.

**Cytological Features**

Aspirates from DSRCT are variably cellular with small to intermediate-sized round cells arrayed singly and in loosely cohesive sheets and clusters. Fragments of hypocellular fibrous stroma are variably present. The tumor cells are uniform, round to oval, and have scant cytoplasm and hyperchromatic nuclei with finely granular chromatin and inconspicuous nucleoli (Fig. 5.13). Occasional tumors are composed of larger, more pleomorphic cells. Necrosis can also be present.

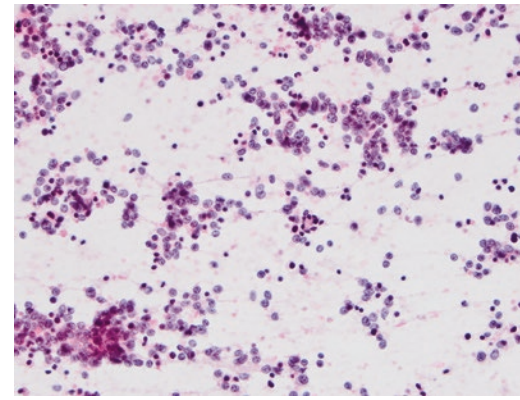

**Fig. 5.13** Desmoplastic small round cell tumor (Papanicolaou stain, medium power). The tumor is composed of small round cells lying singly and in loosely cohesive clusters. The cells have scant cytoplasm with indistinct borders and round nuclei with fine chromatin and inconspicuous nucleoli. Numerous single necrotic cells are present in the background.

**Differential Diagnosis**

Differential diagnostic considerations include Ewing sarcoma/PNET, rhabdomyosarcoma, lymphoma, poorly differentiated (small cell) synovial sarcoma, and metastasis from other pediatric small round cell tumors. In contrast to other tumors in the differential diagnosis, DSRCT is a polyphenotypic tumor and stains positively for low molecular weight cytokeratins, epithelial membrane antigen, desmin (perinuclear dot-like pattern), neuroendocrine markers, and WT1 (C-terminus). The tumors are variably positive for CD99. DSRCT is characterized by a translocation involving *EWS* and *WT1*. Ewing sarcoma/PNET and rhabdomyosarcoma are discussed in Sects. 5.2.7.1 and 5.3.1.1, respectively, and other tumors in the differential diagnosis are discussed in greater detail elsewhere in this book.

**Pearls**

Because *EWSR1* gene rearrangements are present in both DSRCT and Ewing sarcoma/PNET and DSRCT can be positive for CD99, it is essential to perform a panel of immunoperoxidase stains to confirm the polyphenotypic nature of DSRCT and avoid misdiagnosis. Confirmation of the

translocation partner is also helpful but in the context of the appropriate immunophenotype is not critical.

### 5.3.2 Spindle Cell Pattern

Spindle cell morphology is characteristic of a wide variety of benign and malignant neoplasms and non-neoplastic proliferations involving soft tissues. Some of the more common spindle cell lesions seen in the pediatric population are listed in Table 5.12. Overall, non-neoplastic reactive processes and benign neoplasms account for the majority of spindle cell lesions in children and adolescents. These lesions are usually small, superficial, and well circumscribed and treatment, if any, consists of simple excision. Because FNA is rarely used for the evaluation of these benign lesions, this discussion will focus on selected pediatric spindle cell malignancies.

#### 5.3.2.1 Synovial Sarcoma

##### Clinical Features

Synovial sarcoma can occur at any age but is most frequently seen in adolescents and young adults, with the peak incidence in the second and third decades of life. Tumors commonly involve the extremities, most often in a juxta-articular location, but can arise in virtually any anatomic site. Pain, either spontaneous or on palpation, is a frequent symptom. These tumors are typically indolent, and years may elapse between the first symptom and diagnosis. Irregular calcifications are detected in up to one-third of tumors on imaging studies.

##### Cytological Features

FNA yields moderately to highly cellular smears in which cells occur singly, and in irregular sheets and clusters (Fig. 5.14). The cytologic appearance varies with the subtype of the tumor, and may be biphasic or monophasic [21, 22]. Aspirates from biphasic lesions contain variable numbers spindle and epithelial cells, although the former usually predominate. The spindle cells are relatively uniform cells with scant, tapering cytoplasm and solitary, hyperchromatic, oval or elongate nuclei with inconspicuous nucleoli. Epithelial elements have scant to abundant cytoplasm and uniform, often eccentric, round to oval nuclei with pale, evenly distributed chromatin. Mitotic figures may be few to abundant. Monophasic tumors are comprised of either spindle or epithelial elements. Rarely, calcifications may be identified in the aspirates. When both spindle and epithelial elements are present,

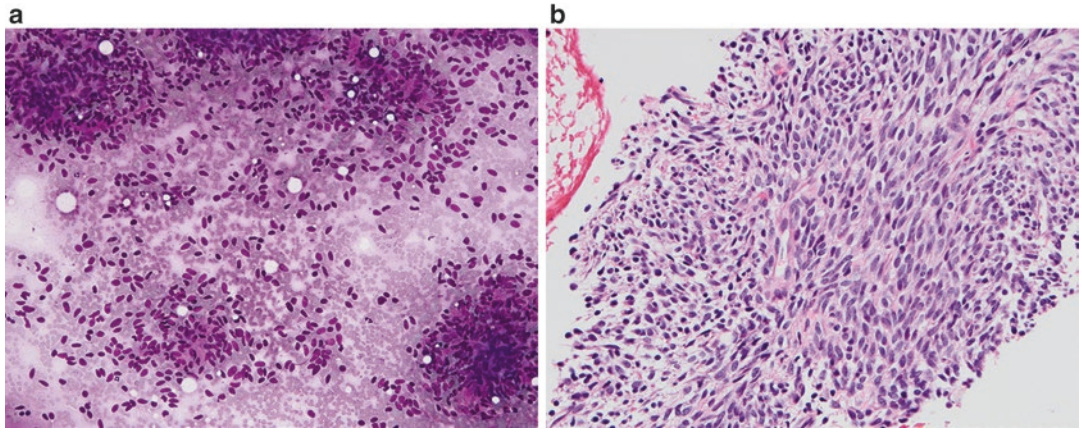


**Fig. 5.14** Synovial sarcoma (**a**. Diff-Quik stain, medium power; **b**. Cell block, H&E stain, high power). The smear is highly cellular and shows tumor cells arranged in clusters and singly. The tumor cells are uniform with spindled nuclei and evenly dispersed chromatin Cytoplasm is scant and many stripped nuclei are present (**a**). This fragment of tissue in the cell block is composed of short, bland spindle cells arrayed in fascicles. The cells have uniform nuclei with evenly dispersed chromatin and inconspicuous nucleoli. Mitoses are not apparent (**b**).

the cytologic diagnosis is usually straightforward. In contract, monophasic lesions may be difficult to distinguish from fibrosarcoma or adenocarcinoma. Rarely tumors are composed of poorly differentiated small round cells reminiscent of those in other small round cell tumors. These cells have scant cytoplasm and uniform, round to ovoid, hyperchromatic nuclei with coarse chromatin.

#### Differential Diagnosis

Differential diagnostic considerations include malignant peripheral nerve sheath tumor, fibrosarcoma, solitary fibrous tumor, and leiomyosarcoma. With the exception of malignant peripheral nerve sheath tumor, these neoplasms are rare in the pediatric age group. Immunoperoxidase stains can help to resolve the differential diagnosis. Synovial sarcoma is usually positive for epithelial membrane antigen, CD99 and TLE-1 (nuclear), variably positive for keratins and S100, and negative for CD34. Poorly differentiated (small cell) synovial sarcoma, for which the differential diagnosis is other pediatric small round cell tumors, shows a similar pattern of staining. Rearrangements involving the *SS18 (SYT)* gene are seen in over 95 % of synovial sarcomas.

#### Pearls

Because both spindle cell and poorly differentiated (small cell) synovial sarcoma can mimic other malignancies morphologically and, in some cases, immunophenotypically, demonstration of an *SS18* rearrangement is important for confirming the diagnosis.

### 5.3.2.2 Malignant Peripheral Nerve Sheath Tumor

#### Clinical Features

Malignant peripheral nerve sheath tumor (MPNST) is a rare tumor that is most often seen in adults but can be seen in children and adolescents, particularly those with neurofibromatosis type 1 (NF-1). MPNST usually arises in a preexisting neurofibroma, with the extremities and trunk being common sites of involvement. Rapid growth of an existing lesion and pain are the typical presenting symptoms.

#### Cytological Features

Aspirates from MPNST are usually highly cellular with cells arranged singly and in irregular fragments [23]. Depending on the grade of the tumor, the individual cells vary from bland and virtually indistinguishable from those of benign spindle cell lesions to highly pleomorphic with obviously malignant features. Cells have scant cytoplasm and enlarged hyperchromatic nuclei with variably prominent nucleoli. Nuclei are often wavy or comma shaped. Bizarre tumor giant cells can also be present. Mitotic figures, including abnormal forms, are usually apparent. Necrosis can also be present.

#### Differential Diagnosis

Differential diagnostic considerations vary depending on the degree of differentiation of the tumor. Low grade MPNST should be distinguished from schwannoma, atypical neurofibroma, and other bland spindle lesions. In contrast the differential diagnosis of intermediate or high grade lesions includes synovial sarcoma, malignant solitary fibrous tumor, leiomyosarcoma, spindle cell melanoma, and other malignant spindle cell sarcomas. MPNST shows staining for S100 in less than 50 % of cases and for GFAP in 20–30 %; however, nuclear positivity for SOX10 can be a helpful finding in some cases. Staining is usually focal, in contrast to the diffuse staining seen in the majority of benign peripheral nerve sheath tumors. Because MPNST can mimic a variety of spindle cell neoplasms at both ends of the spectrum of differentiation, a panel of immunoperoxidase stains is needed to exclude other entities.

#### Pearl

Immunoperoxidase stains are helpful for excluding other tumors but, in the absence of S100 staining, do not confirm the diagnosis of MPNST. In such cases, the presence a preexisting lesion and a history of NF-1 are highly suggestive of MPNST.

## 5.4 Conclusion

FNA is a valuable tool for the primary diagnosis of pediatric bone and soft tissue lesions. When correlated with the clinical presentation and

findings on imaging studies, FNA combined with the judicious use of ancillary studies can often provide information on which to base further diagnostic or therapeutic decisions. In many cases, FNA allows accurate and specific diagnosis of primary or metastatic lesions of bone and soft tissue, thereby obviating the need for a more invasive and significantly more expensive diagnostic biopsy. In other cases, although a definite diagnosis is not possible, FNA is useful for ruling out specific processes or for narrowing the diagnostic considerations, and in the appropriate clinical setting, this information may be sufficient for initiation of therapy. Although limitations and pitfalls exist, FNA represents a highly accurate and cost-effective technique for the diagnosis of pediatric bone and soft tissue tumors.

## References


1. Kilpatrick SE, Ward WG, Chauvenet AR, Pettanati MJ. The role of fine-needle aspiration biopsy in the initial diagnosis of pediatric bone and soft tissue tumors: an institutional experience. Mod Pathol. 1998;11:923–8.
2. Ward Sr WG, Kilpatrick S. Fine needle aspiration of primary bone tumors. Clin Orthop Relat Res. 2000; 373:80–7.
3. Kilpatrick SE, Cappellari JP, Bos GD, et al. Is fine-needle aspiration biopsy a practical alternative to open biopsy for the primary diagnosis of sarcoma? Experience with 140 patients. Am J Clin Pathol. 2001;115:59–68.
4. Sapi Z, Antal I, Papai Z, et al. Diagnosis of soft tissue tumors by fine-needle aspiration with combined cytopathology and ancillary techniques. Diagn Cytopathol. 2002;26:232–42.
5. Singh HK, Kilpatrck SE, Silverman JF. Fine needle aspiration biopsy of soft tissue sarcomas: utility and diagnostic challenges. Adv Anat Pathol. 2004; 11:24–37.
6. Domanski HA. Fine-needle aspiration cytology of soft tissue lesions: diagnostic challenges. Diagn Cytopathol. 2007;35:768–73.
7. Walaas L, Kindblom LG. Light and electron microscopic examination of fine-needle aspirates in the preoperative diagnosis of osteogenic tumors: a study of 21 osteosarcomas and two osteoblastomas. Diagn Cytopathol. 1990;6:27–38.
8. Venugopal SB, Prasad S. Cytological diagnosis of osteoblastoma of cervical spine: a case report with review of literature. Diagn Cytopathol. 2015;43: 218–21.
9. Dodd LG, Scully SP, Cothran RL, Harrelson JM. Utility of fine-needle aspiration in the diagnosis of primary osteosarcoma. Diagn Cytopathol. 2002;27: 350–3.
10. Akerman M, Domanski HA, Jonsson K. Cytological features of bone tumours in FNA smears I: osteogenic tumours. Monogr Clin Cytol. 2010;19:18–30.
11. Sathiyamoorthy S, Ali SZ. Osteoblastic osteosarcoma: cytomorphologic characteristic and differential diagnosis on fine-needle aspiration. Acta Cytol. 2012;56:481–6.
12. VandenBussche CJ, Sathiyamoorthy S, Wakely Jr PE, Ali SZ. Chondroblastic osteosarcoma: cytomorphologic characteristics and differential diagnosis on FNA. Cancer Cytopathol. 2016;124: 493–500.
13. Akerman M, Domanski HA, Jonsson K. Cytological features of bone tumours in FNA smears II: cartilaginous tumours. Monogr Clin Cytol. 2010;19: 31–44.
14. Sreedharanunni S, Gupta N, Rajwanshi A, et al. Fine needle aspiration cytology in two cases of chondromyxoid fibroma of bone and review of literature. Diagn Cytopathol. 2013;41:904–8.
15. Cozzolino I, Zeppa P, Zapatta A, et al. Benign chondroblastoma on fine-needle aspiration smears: a seven-case experience and review of the literature. Diang Cytopathol. 2015;43:734–8.
16. Krishnappa A, Shobha SN, Shankar SV, Aradhya S. Fine needle aspiration cytology of chondroblastoma: a report of two case with brief review of pitfalls. J Cytol. 2016;33:40–2.
17. Creager AJ, Madden CR, Bergman S, Geisinger KR. Aneurysmal bone cyst: fine-needle aspiration findings in 23 patients with clinical and radiologic correlation. Am J Clin Pathol. 2007;128:740–5.
18. Klijanienko J, Couturier J, Bourdeaut F, et al. Fine-needle aspiration as a diagnostic technique in 50 cases of primary Ewing sarcoma/peripheral neuroectodermal tumor. Institut Curie's experience. Diagn Cytopathol. 2012;40:19–25.
19. Frostad B, Tani E, Brosjo O, et al. Fine needle aspiration cytology in the diagnosis and management of children and adolescents with Ewing sarcoma and peripheral primitive neuroectodermal tumor. Med Pediatr Oncol. 2002;38:33–40.
20. Shabb N, Fanning CV, Carrasco CH, et al. Diagnosis of eosinophilic granuloma of bone by fine-needle aspiration with concurrent institution of therapy. A cytologic, histologic, clinical and radiologic study of 27 cases. Diagn Cytopathol. 1993;9:3–12.
21. Kilpatrick SE, Teot LA, Stanley MW, et al. Fine needle aspiration biopsy of synovial sarcoma: a cytomorphologic analysis of primary, recurrent, and metastatic tumors. Am J Clin Pathol. 1996;106:769–75.
22. Klijanienko J, Caillaud JM, Lagace R, Viehl P. Cytohistologic correlations in 56 synovial sarcomas in 36 patients: the Institut Curie experience. Diagn Cytopathol. 2002;27:96–102.

23. Wakely Jr PE, Ali SZ, Bishop JA. The cytopathology of malignant peripheral nerve sheath tumor. A report of 55 fine-needle aspiration cases. Cancer Cytopathol. 2012;120:334–41.

## General Resource

Fletcher CDM, Bridge JA, Hogendoorn PCW, Mertens F, editors. WHO classification of tumours of soft tissue and bone. Lyons: IARC Press; 2013.

# Lung and Mediastinum

6

Anita L. Sengupta and Sara E. Monaco

## 6.1 Introduction

Exfoliative cytology and fine needle aspiration (FNA) are valuable tools for the evaluation of pulmonary lesions. In the pediatric population, the most common cytologic specimens from the respiratory tract are bronchoscopy-acquired specimens, including bronchoalveolar lavages (BALs) and bronchial brushings/washings. Sputum specimens are infrequently seen as it is difficult or impossible to obtain an adequate sample representative of a deep cough from children. Bronchial brushings are usually performed if there is a visible, discrete lesion on bronchoscopy, whereas a washing is typically done if there is no discrete endobronchial lesion. BAL specimens are obtained by infusion and re-aspiration of sterile saline into distal areas of the lung. These specimens are typically utilized in the evaluation of suspected infection in both immunocompetent and immunocompromised patients, and for routine follow-up of lung transplant recipients to exclude unsuspected infection. Of note, up to 25 % of stem cell transplant recipients have pulmonary complications and will require evaluation to exclude a pulmonary infection [1]. In addition, BALs can be therapeutic in the setting of pulmonary alveolar proteinosis, cystic fibrosis, and asthma, to provide symptomatic relief to patients. In the setting of infection, BALs have a sensitivity of approximately 82 % and a specificity of 53 %. Although malignancy is rare in children, a variety of different conditions can lead to atypia that mimics malignancy, including reactive bronchial cells and pneumocytes in the setting of inflammation, infection, diffuse alveolar damage, bone marrow transplantation, and chemotherapy. When there is a neoplasm, a metastatic neoplasm should be considered before diagnosing a primary lung neoplasm. One study revealed that 81 % of lung neoplasms in the pediatric population are due to metastatic lesions with nephroblastoma (Wilms tumor) being the most common, followed by osteosarcoma [2]. Overall, benign and reactive changes, in addition to metastatic tumors, should strongly be considered before making a diagnosis of a primary lung malignancy in a child or adolescent. Whereas CT-guided FNA or endobronchial ultrasound (EBUS) guided transbronchial needle aspiration (TBNA) is routinely used to evaluate pulmonary and mediastinal masses in adults, aspirates from these sites are infrequently

A.L. Sengupta, MD (✉)
Department of Pathology B2279, Children's Medical Center, 1935 Medical District Dr,
Dallas, TX 75235, USA
e-mail: anita.sengupta@utsouthwestern.edu

S.E. Monaco, MD
Department of Pathology, University of Pittsburgh Medical Center (UPMC) & Children's Hospital of Pittsburgh of UPMC, Pittsburgh, PA, USA
e-mail: monacose@upmc.edu



S.E. Monaco, L.A. Teot (eds.), *Pediatric Cytopathology*, DOI 10.1007/978-3-662-53441-0_6

**Table 6.1** Pediatric pulmonary lesions encountered in exfoliative cytology and/or FNAs

| Non-neoplastic pediatric lung lesions | Neoplastic pediatric lung lesions |
|---|---|
| Reactive or prior treatment-related changes | Clear cell (sugar) tumor |
| Infection | Epithelioid hemangioendothelioma |
| Aspiration or Trauma/Fat emboli (with positive Oil Red O staining) | Inflammatory myofibroblastic tumor |
| Pulmonary alveolar proteinosis | Juvenile squamous papilloma |
| Bronchogenic cysts | Metastatic tumors |
| Hamartomas | Pleuropulmonary blastoma |
| | Salivary gland-type tumors (Mucoepidermoid carcinoma, adenoid cystic carcinoma) |
| | Carcinoid |
| | Primary adenocarcinoma |

**Table 6.2** Summary of pediatric mediastinal lesions by compartment

| Anterior/superior mediastinum (5 Ts) |
|---|
| • Thymic lesions<br>• Thyroid lesions<br>• Teratoma or germ cell tumors<br>• Terrible lymphoma<br>• Terribly common metastatic neoplasms<br>• Vascular tumors<br>• Hernia |
| **Posterior mediastinum** |
| • Neurogenic and neuroblastic tumors<br>• Bronchogenic and congenital cysts<br>• Hernia<br>• Paraspinal abscess<br>• Vertebral lesions |
| **Middle mediastinum** |
| • Lymphoma<br>• Bronchogenic cysts |

encountered in the pediatric population, in part due to the low incidence of lung cancer in children and adolescents. However, fine needle aspiration biopsy and/or core needle biopsy may be of use in cases where the clinical and radiologic picture cannot differentiate between neoplastic and infectious lesions. Some of the common, as well as uncommon, lesions encountered in cytologic specimens from the lung and mediastinum in the pediatric population are summarized in Tables 6.1 and 6.2, respectively.

## 6.2 Cytology of Normal and Benign Elements in the Lung

- Benign respiratory epithelial cells are columnar with basally oriented nuclei, terminal bars, and cilia.
- Creola bodies are hyperplastic or papillary clusters of bronchial cells with occasional vacuolization and small nucleoli that can be seen with asthma or bronchiectasis.
- Reactive atypia (mild nuclear enlargement and prominent nucleoli) can be seen with radiation, chemotherapy, or severe inflammation (Fig. 6.1).
- Reserve cell hyperplasia or proliferation is more common when there is lung injury and shedding of the normal respiratory tract epithelium. These cells appear in tightly packed clusters with small nuclei and scant cytoplasm.
- Macrophages have abundant foamy to vacuolated cytoplasm, oval to round nuclei, and occasional prominent nucleoli. The vacuolated cytoplasm may have debris or other ingested material, such as hemosiderin or anthracotic pigment. The presence of macrophages is used to confirm the adequacy of sputum samples and BALs (Fig. 6.2).
- Lipid-laden macrophages can be highlighted with an Oil Red O stain, and these cells can be elevated in patients with lipoid pneumonia, fat embolism syndrome, pulmonary aspiration, or amiodarone toxicity (Fig. 6.3).
- Curschmann spirals are coiled strands or helical casts of inspissated mucus that appears darkly stained. These are a non-specific finding, seen with excess mucus production (e.g., asthma) (Fig. 6.4).
- Charcot-Leyden crystals are small, eosinophilic to orangeophilic, rhomboid-shaped crystals that are derived from the granules of degranulated/degenerating eosinophils, usually in the setting of asthma and other causes of eosinophilia. These can be seen in allergic

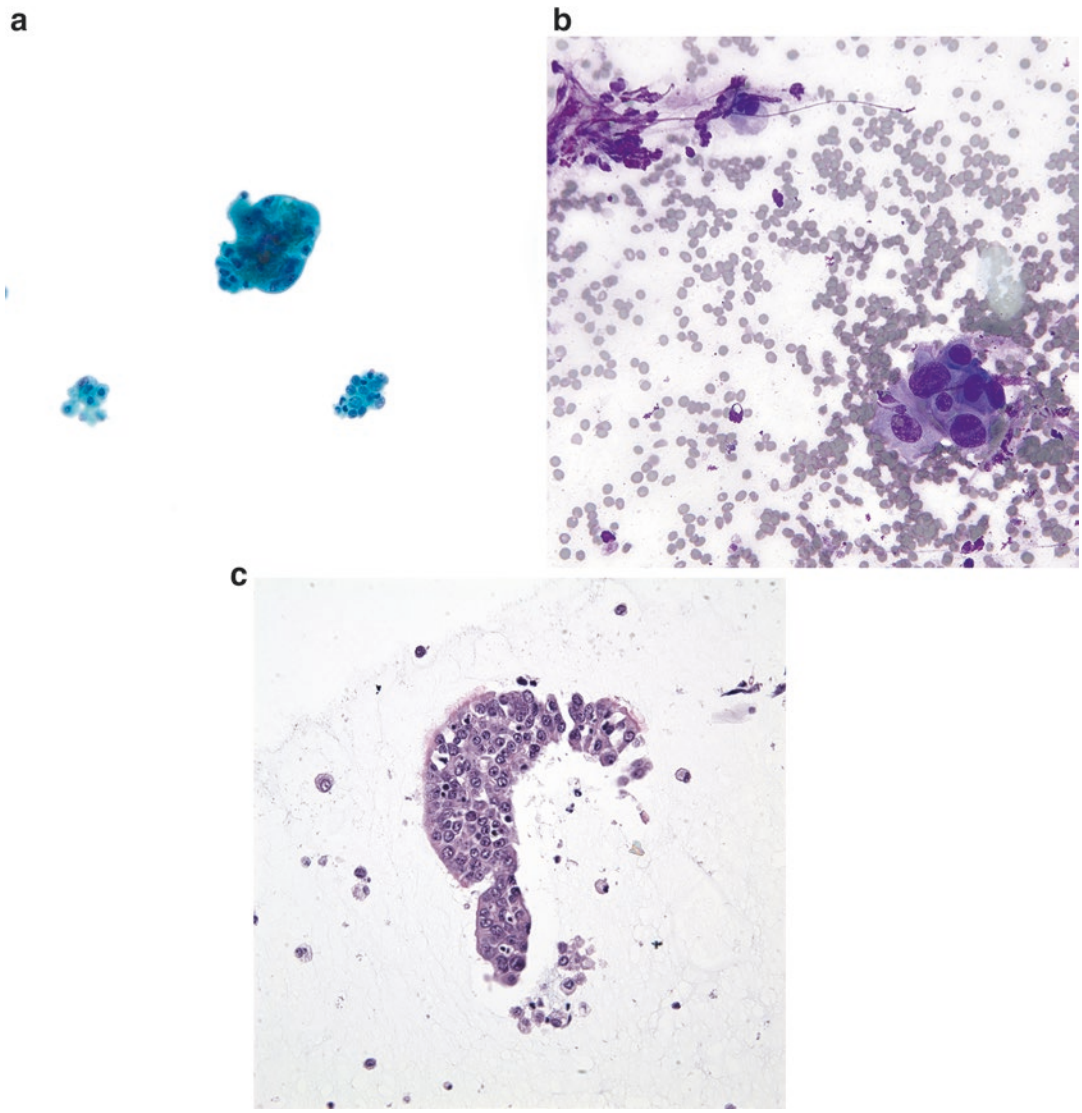


**Fig. 6.1** Reactive epithelial atypia in BAL (**a**. Papanicolaou stain, high power; **b**. Diff-Quik stain, high power; **c**. H&E stain, high power). Lung specimens from patients status post chemotherapy showing reactive pneumocytes and reactive bronchial epithelial cells. These cells have mild nuclear enlargement without irregularities, and are seen in association with benign cells, including ciliated bronchial cells on the cell block (**c**).

bronchopulmonary aspergillosis with numerous eosinophils and fungal hyphae (Fig. 6.5).

- Ciliocytophthoria appears as detached ciliary tufts, and is associated with viral infection (e.g., adenovirus) but can also be a non-specific finding (Fig. 6.6).
- In systemic disease (autoimmune, cystic fibrosis, asthma), the lung can show a variety of reactive changes. In asthma, increased eosinophils are often present within mucus. Cystic fibrosis is characterized by thick mucus plugs, often with abundant mixed inflammation. Most pulmonary specimens from these patients are obtained to evaluate for infection. Two particular infections, *Burkholderia cepacia* and *Pseudomonas aeruginosa*, are relatively common in cystic fibrosis patients and can have implications for disease progression.

- Pollen or starch granules: Starch granules appear as clear and refractile cubes with a Maltese cross appearance under polarized light. Pollen appears as spherical structures that are colorful, have a thickened wall, and may have small internal bodies or a spiked border, and can mimic large yeast forms or other infectious organisms, in addition to other contaminants.
- Drug particles: Dark black carbonaceous material can appear within histiocytes in drug users, particularly crack/cocaine smokers. Rhomboid crystals can appear with aspiration of barium sulfate.

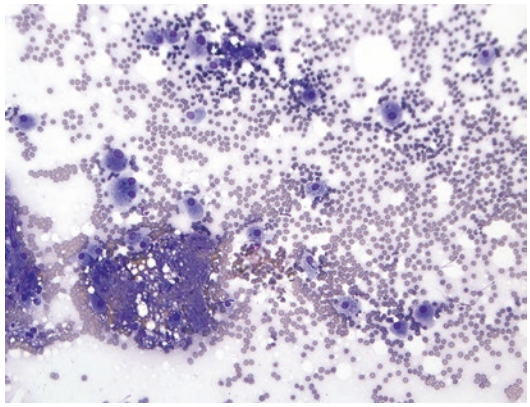

**Fig. 6.2** Non-diagnostic lung FNA in a pediatric patient showing benign macrophages (Diff-Quik stain, medium power). The aspirates show benign macrophages in a bloody background and do not characterize a mass lesion in the lung. Thus, these findings are non-diagnostic.

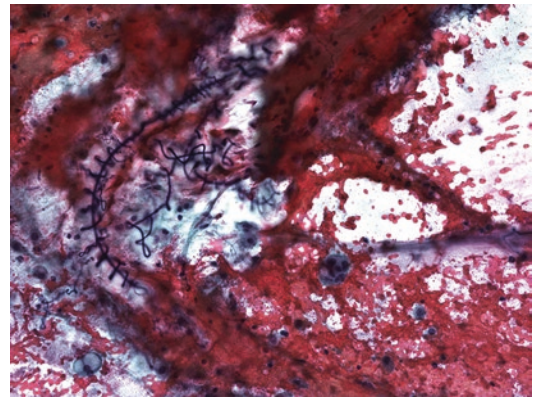

**Fig. 6.4** Curschmann spirals in a bronchial specimen (Papanicolaou stain, medium power). These darkly stained spiral shaped structures represent thick, inspissated mucus.

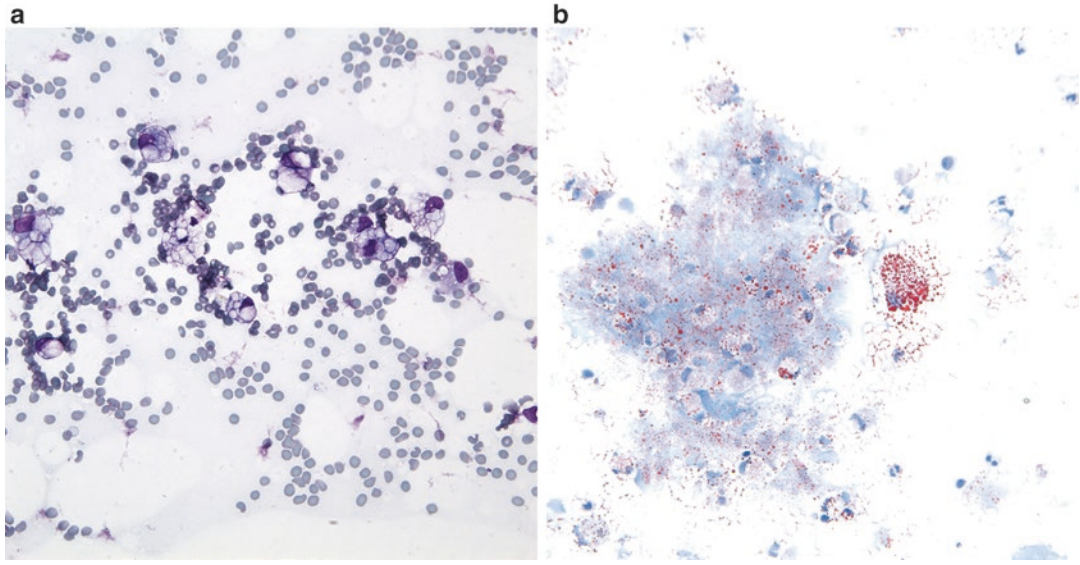


**Fig. 6.3** Lipid laden macrophages (**a**. Diff-Quik stain, high power, **b**. Oil red O stain, high power). Lipid laden macrophages are frequently a sign of aspiration, along with other etiologies, in children. Thus, identification of them is important and an Oil Red O stain can help prove their presence (**b**).

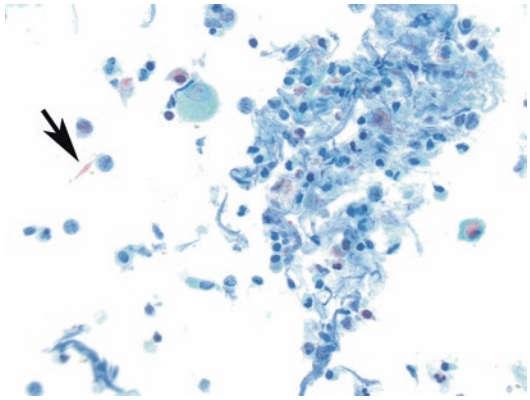

**Fig. 6.5** Charcot-Leyden crystals (Papanicolaou stain, high power). Eosinophilic rhomboidal crystals (*arrow*) are frequently seen with eosinophilic-rich infiltrates. They can be an important clue that the inflammatory cells are predominantly eosinophils given that the eosinophilic granules are hard to identify on a Papanicolaou stain.

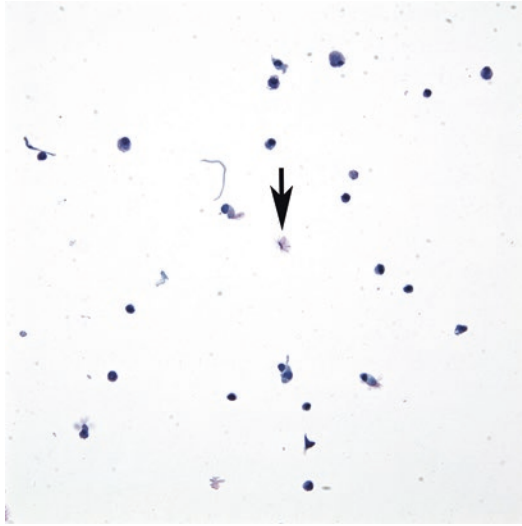

**Fig. 6.6** Ciliocytophthoria (Papanicolaou stain, medium power). Detached ciliary tufts (ciliocytophthoria) can be seen in BALs of patients with adenovirus infection and should not be confused with organisms or contaminants (*arrow*).

## 6.3 Bronchogenic Cysts

### Clinical Features

These developmental cysts arising from the foregut appear most frequently as a posterior mediastinal cyst, but can also be intrapulmonary.

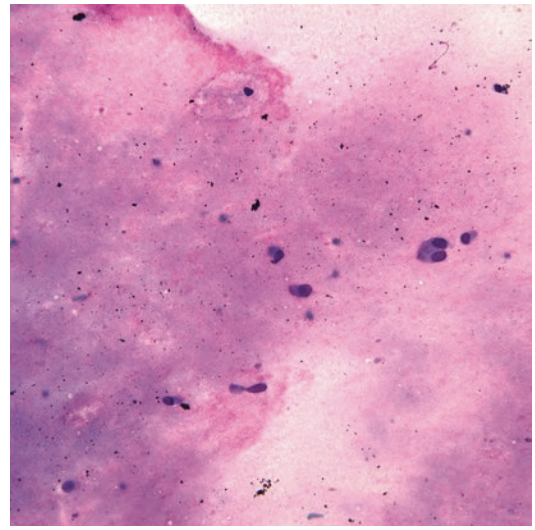

**Fig. 6.7** Bronchogenic cyst (Diff-Quik stain, low power). This bronchogenic cyst shows thickened proteinaceous fluid with a few ciliated cells.

These are rare lesions, but can compress the airway if large.

### Cytological Features

Aspirates yield thick proteinaceous to mucoid fluid with variable types of lining cells, including ciliated, squamous, or simple columnar epithelium (Fig. 6.7). Liquid-based cytology can be helpful for demonstrating the cyst lining cells and excluding thymic or neoplastic cysts (e.g., germ cell tumors with cystic change).

### Differential Diagnosis

A cystic lesion in the mediastinum or lung of a child raises the differential diagnosis of thymic cyst, mediastinal goiter, lymphangioma, cystic pulmonary airway malformation (CPAM; formerly congenital cystic adenomatoid malformation), mesenchymal cystic hamartoma, and neoplastic cysts (e.g., cystic teratoma or other germ cell tumor with cystic change). In contrast to bronchogenic cysts, most of the congenital malformations and hamartomas in this age group are within the lung and are multicystic lesions with small cysts.

### Pearls

If small lymphocytes are identified from a cystic lesion in the mediastinum in the pediatric population, the possibility of a thymic cyst should be considered. Flow cytometry and/or immunoperoxidase stains can be used to support thymic origin by identifying immature and maturing T-cells that are positive for TdT, CD1a, and CD3.

## 6.4 Infectious Disease

### Clinical Features

Fine needle aspiration biopsy has not been routinely used for the diagnosis of infectious disease in the lung. Thus, there are few studies evaluating its effectiveness. One paper in the adult literature reported a range of sensitivity of 21–47 % for FNA and 52–94 % for core needle biopsy [3]. One study in the pediatric population reported a sensitivity of 88 %, but did not separate FNA from core needle biopsy [4]. Another noted that CT-guided biopsy had a high diagnostic yield of 60 %, but only yielded organisms already isolated from peripheral blood [1]. Occasionally, FNA performed for infectious disease of the lung may reveal an undiagnosed tumor of the chest wall or mediastinum.

### Cytological Features

Infections that present as discrete masses in the lung frequently show either abscess formation, granulomatous inflammation, or a cystic fungal ball. Aspirates show abundant histiocytes with a variable numbers of small lymphocytes and neutrophils in the background (Figs. 6.8 and 6.9). Stains for fungal elements and/or acid fast bacteria can be performed on aspirate smears and may be useful; however, if there are only rare yeast or fungal elements, the possibility of specimen contamination with *Alternaria* or other fungi or oropharyngeal contamination from Candida should be considered [5] (Fig. 6.10). Well-formed granulomas with clusters of epithelioid histiocytes are suggestive of fungal or mycobacterial infection (Fig. 6.11). Fungal balls typically show abundant granular debris with fungal hyphae present. BAL is commonly used for the cytologic evaluation of suspected infection but, in the setting of a mass lesion, may not yield representative material. Depending on the etiologic agent, BALs can show neutrophils, lymphocytes, and/or histiocytes, necroinflammatory debris and reactive epithelial cells. Gram, methenamine silver, AFB and Fite stains can be helpful for identifying microorganisms on cytospins, liquid-based preparations or cell blocks from BALs. Viral infections, such as cytomegalovirus and herpes virus, can also be seen in BAL specimens (Fig. 6.12).

### Triage

Material should be submitted from the FNA or BAL for microbial cultures and special stains. When handling the specimen, care should be taken to avoid contamination. Since complications such as pneumothorax are common in lung FNA, few passes may be performed, and each pass should be triaged carefully. If the needle tip is not touched to the slide when the first drop(s) are taken for smears, the remaining specimen may be rinsed into sterile saline for microbiologic studies. If the smears show anything other than an infectious process, this rinse can be used for other ancillary studies (flow cytometry, cell block, etc.). In addition, if there is abundant hemodilution on subsequent passes, unstained smears could be prepared from the best pass and sent for special stains [5].

### Differential Diagnosis

Neoplastic disease, metastatic or primary, may mimic an infectious lung mass radiologically. Although atypical bronchial cells and/or pneumocytes can be present in the setting of infection, cytologic features of malignancy, such as increased nuclear to cytoplasmic ratios, nuclear pleomorphism, nuclear membrane irregularity, and hyperchromasia are absent. Lymphocytic infiltrates associated with infectious processes are polyclonal, in contrast to the monoclonal proliferations associated with non-Hodgkin lymphomas.

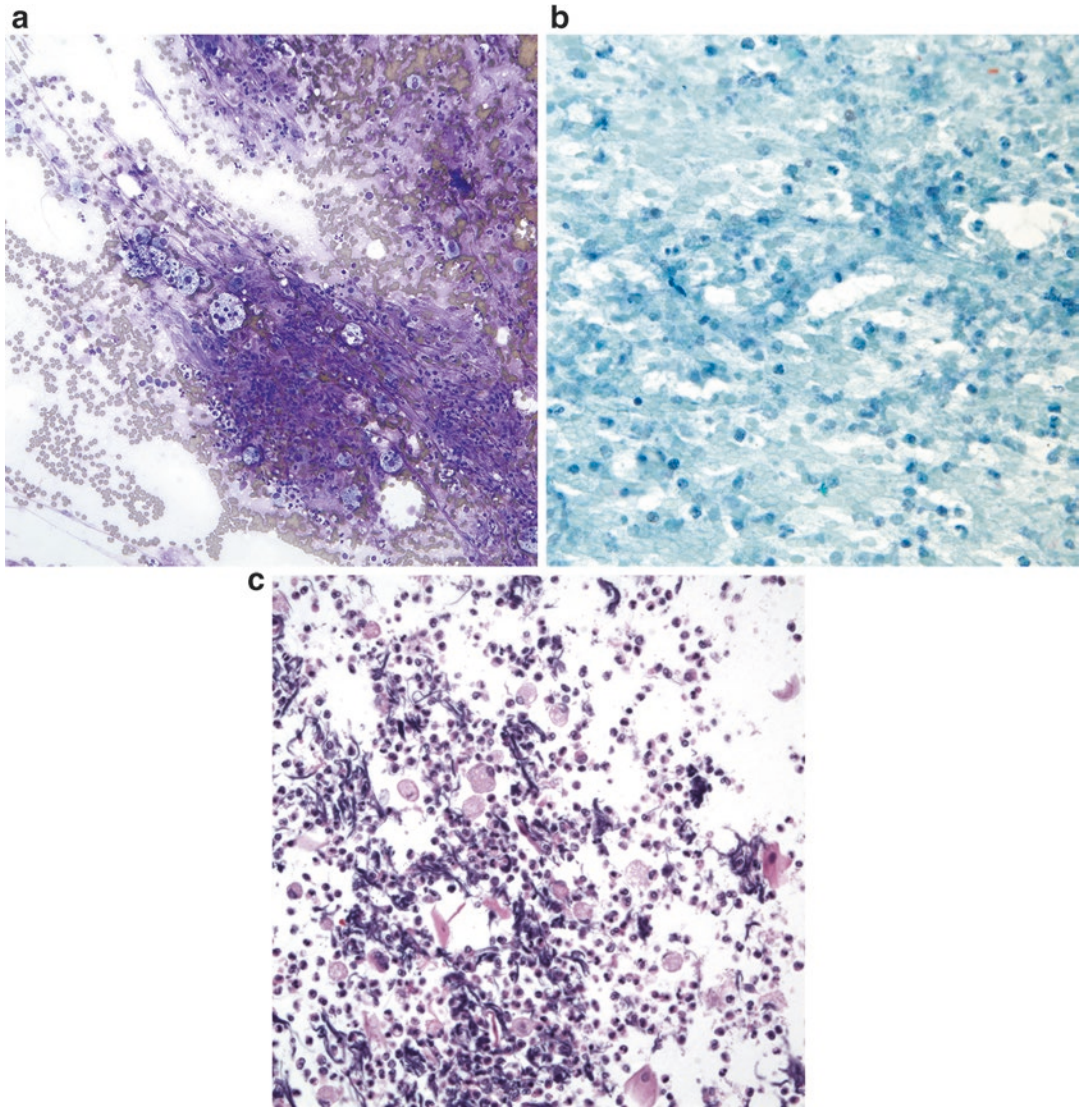


**Fig. 6.8** Lung abscess (**a**. Diff-Quik stain, medium power; **b**. Papanicolaou stain, medium power; **c**. H&E stain, high power). The aspirates show abundant neutrophils and granular debris in this FNA from a lung mass.

### Pearls

Primary lung carcinomas are exceedingly rare in the pediatric population. When atypical squamous or glandular cells are identified in an FNA or exfoliative specimen from the lung of a child or adolescent with a mass lesion, reactive atypia in metaplastic squamous cells, bronchial cells or pneumocytes secondary to infection should be excluded before considering malignancy.

## 6.5 Alveolar Proteinosis

### Clinical Features

Pulmonary alveolar proteinosis (PAP) is a rare disorder associated with impaired or dysfunctional surfactant clearance. Some cases are congenital, due to mutations in surfactant protein-B, *ABCA3* or GM-CSF receptor genes. This is in

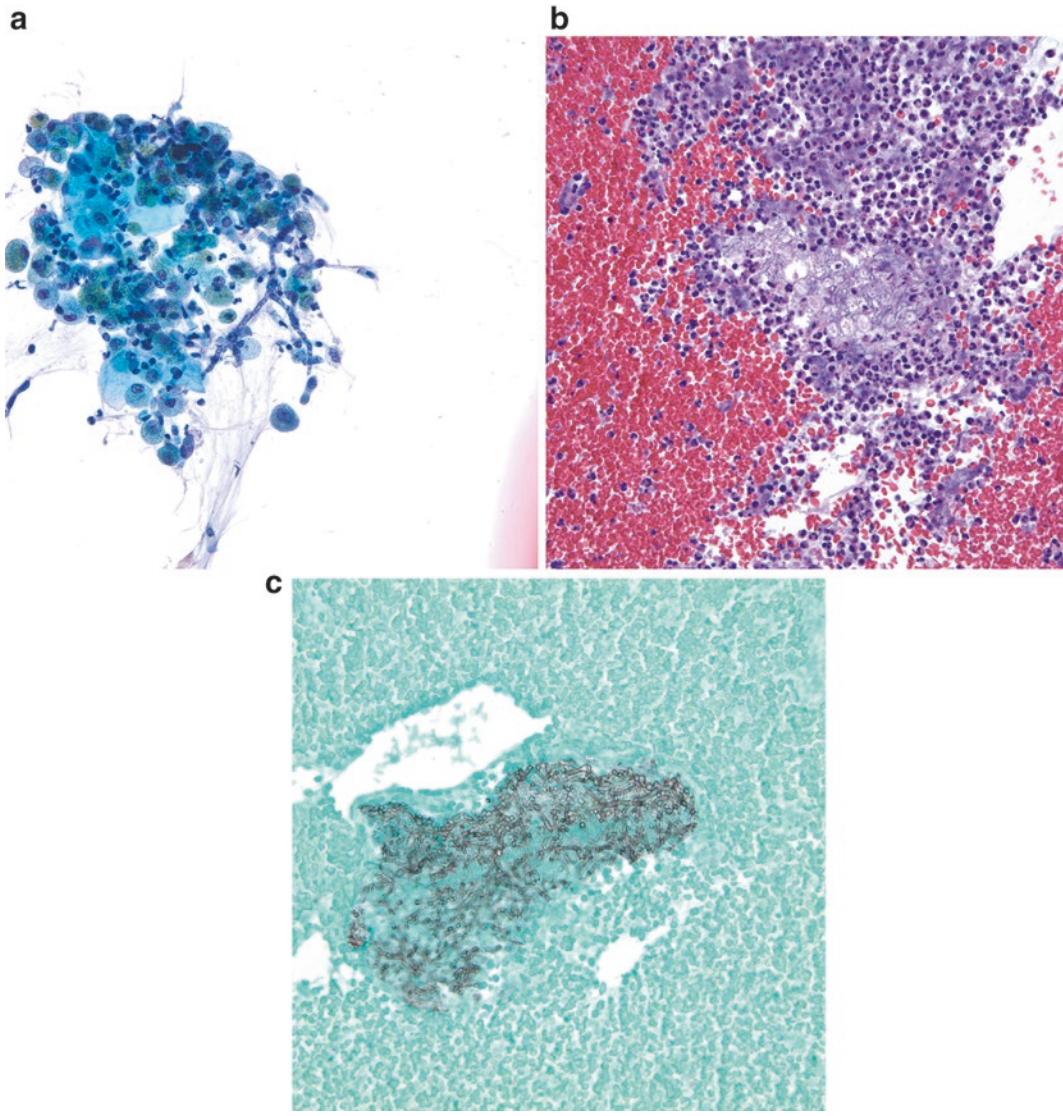


**Fig. 6.9** Fungal infection creating mass lung lesion in a young patient (**a**. Papanicolaou stain, high power; **b**. H&E stain, high power; **c**. Grocott stain, high power). The aspirates show branching fungal hyphae within a background of acute inflammation, debris, and reactive changes. The Grocott stain shows branching fungal hyphae, compatible with Aspergillus (**c**).

contrast to adults, in which most cases are acquired and due to autoantibodies to GM-CSF. Most other pediatric cases are secondary to infection, drugs, foreign material, treatment for malignancy, or idiopathic causes. PAP is characterized by accumulation of lipid-rich proteinaceous material in alveolar spaces leading to respiratory distress or failure. On imaging, patients have diffuse, bilateral, pulmonary infiltrates or opacities, without features of fibrosis or chronic lung disease. BALs can be performed in these patients for diagnosis and therapeutic purposes.

### Cytological Features

The BALs from patients with PAP have abundant, acellular, PAS-positive diastase-resistant, lipid-rich proteinaceous material, often in large globules, and pulmonary macrophages containing similar

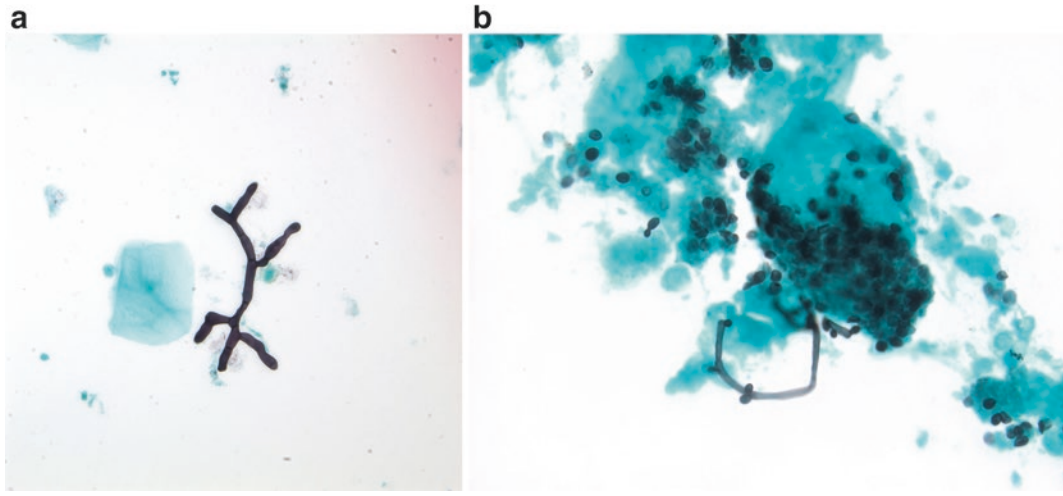


**Fig. 6.10** Other fungal organisms in children (**a**, **b**. Grocott stain, high power). *Fusarium* identified in this pediatric lung specimen was morphologically similar to Aspergillus (**a**). Candida can also be identified in BAL specimens in children and may represent contamination from the oropharynx (**b**).

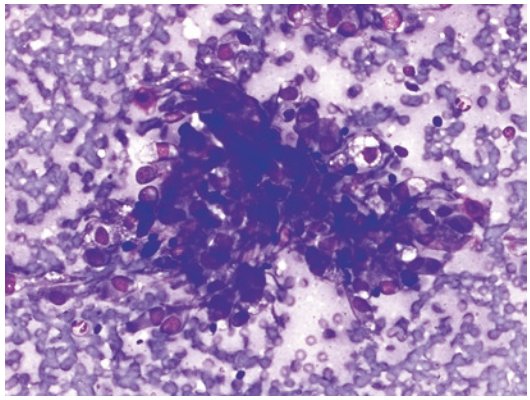

**Fig. 6.11** Granulomatous inflammation in the lung (Diff-Quik stain, high power). There are clusters of epithelioid histiocytes and scattered small lymphocytes, compatible with epithelioid granulomas.

material. Degenerating macrophages, lamellar bodies, cholesterol crystals, and reactive pneumocytes can also be present, but inflammation is usually absent (Fig. 6.13). PAS and PAS-D stains can be performed on additional cytospins, liquid-based preparations or sections from a cell block to support the diagnosis.

### Differential Diagnosis

The other possibilities to consider are mucus plugs or alveolar casts from *Pneumocystis jirovecii* infection. Mucus plugs lack the intense PAS-positivity seen in PAP but stain with mucicarmine or Alcian blue, while methenamine silver stains can help to exclude *Pneumocystis jirovecii* infection.

### Pearls

Electron microscopy shows that the lamellar bodies are proteinaceous surfactant material.

## 6.6 Primary Lung Neoplasms

Primary lung neoplasms are so rare in the pediatric population that they are frequently not included in the differential diagnosis of mass lesions. Over two-thirds of cases are malignant, the majority of which are bronchogenic in origin. Carcinoid tumor is the most common pediatric lung malignancy accounting for 33 % of malignant cases, followed by bronchogenic carcinoma (28 %), mucoepidermoid carcinoma

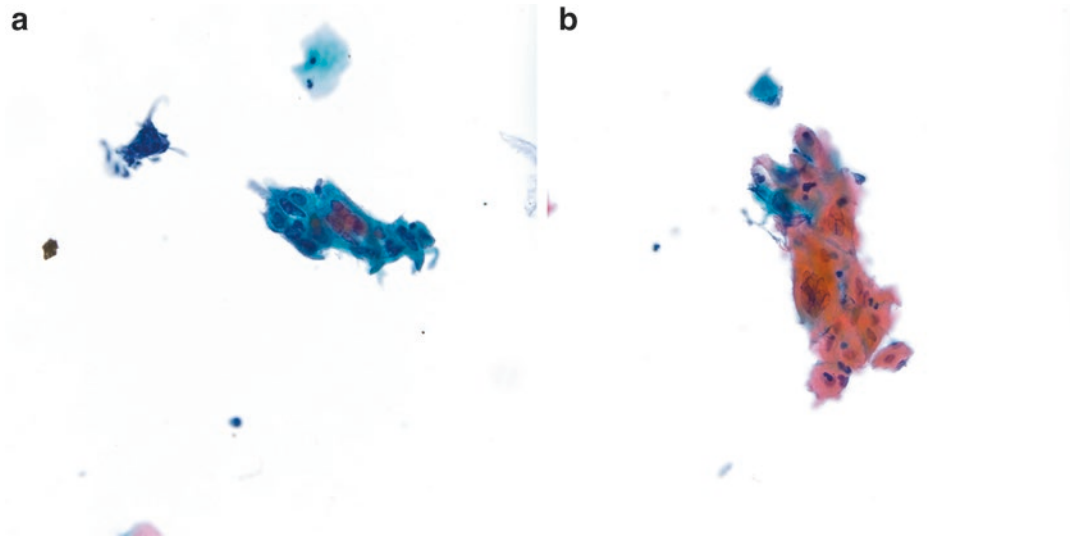


**Fig. 6.12** BAL specimen showing HSV infection in an immunocompromised child (**a**, **b**. Thin Prep, Papanicolaou stain, high power). The squamous cells in this specimen show prominent nuclear enlargement, margination of the chromatin, and multinucleation, which are clues of an HSV infection.

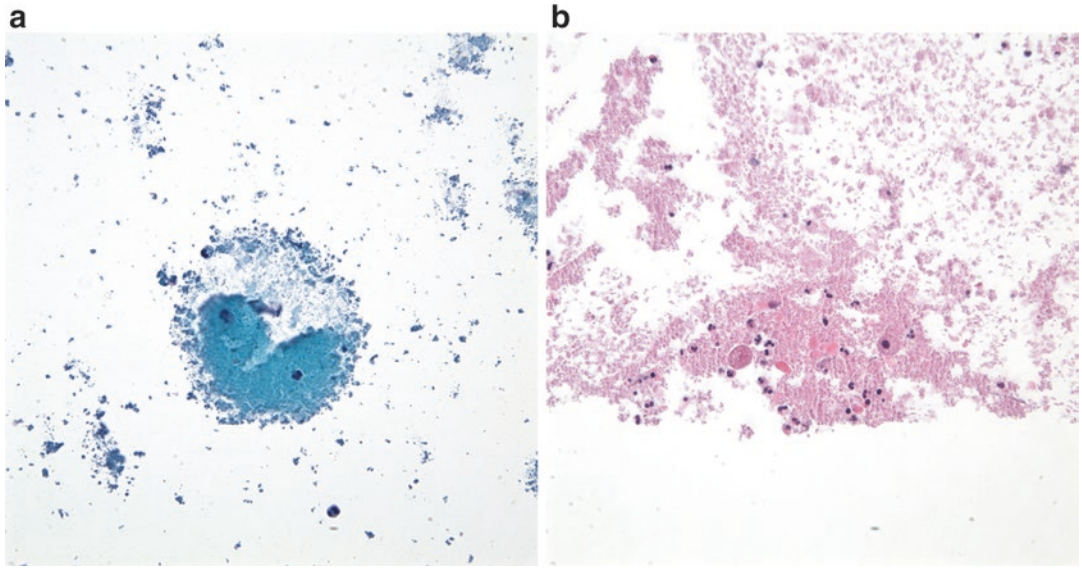


**Fig. 6.13** Pulmonary alveolar proteinosis (**a**. Papanicolaou stain, high power; **b**. H&E stain, high power). This BAL from a patient with longstanding pulmonary alveolar proteinosis shows proteinaceous acellular material forming large globules and prominent background debris.

(9 %), and pleuropulmonary blastoma (8 %). Benign tumors are more frequently located in the parenchyma with inflammatory myofibroblastic tumor accounting for 70 % of benign cases, followed by hamartoma (12 %) [6, 7]. Bronchial tumors may be amenable to transbronchial biopsy; however, this technique is rarely used in the pediatric population. Although FNA can be used in children and adolescents, the tumors seen in these patients are often difficult or impossible to diagnose with confidence given the limited cells aspirated in these cases

and the need for architectural evaluation (e.g., hamartoma or inflammatory myofibroblastic tumor).

### 6.6.1 Inflammatory Myofibroblastic Tumor

#### Clinical Features

Inflammatory myofibroblastic tumors (IMTs) are the most common lung tumors in patients under 15 years of age, and are usually found incidentally on imaging. These tumors typically present as a solitary, peripheral mass lesion and behave in a benign fashion in the majority of cases.

#### Cytological Features

The aspirates yield relatively bland, plump spindle cells arranged in sheets, clusters and singly with a background of lymphocytes, plasma cells, and myxoid matrix. Scattered lesional cells with a ganglion-like appearance and foamy xanthomatous cells can also be seen. A collagenous or hyalinized stroma can be seen on cell block or core biopsy as well. Preparation of a cell block for immunoperoxidase stains is important to confirm the myofibroblastic nature of the tumor cells (positive for smooth muscle actin, negative for S100, cytokeratin, and desmin), and to assess for the presence of ALK-1 or ROS positivity. Rearrangement of *ALK, ROS1,* and genes of other actionable kinases is present in approximately 90 % of IMTs in the pediatric population and can be assessed by FISH or other molecular techniques [8].

#### Differential Diagnosis

The differential diagnosis includes organizing pneumonia and other spindle cell neoplasms, such as solitary fibrous tumor.

#### Pearls

Immunoperoxidase staining for ALK-1 and ROS, and FISH or other molecular studies to demonstrate *ALK* or more recently described *ROS1* rearrangements in these tumors can be of therapeutic importance. Although IMT is currently classified as a tumor of intermediate malignant potential unlikely to metastasize, it can be locally aggressive and encroach on vital structures. Some of these tumors have been shown to be responsive to crizotinib.

### 6.6.2 Clear Cell (Sugar) Tumor of the Lung

#### Clinical Features

These tumors are part of the PEComa family of neoplasms, and although they are more likely to occur in adults, they are important to recognize in pediatric patients. These typically present as a solitary, well-circumscribed lesion in the periphery of the lung.

#### Cytological Features

These tumors yield cellular aspirates composed of large epithelioid and spindle cells with clear to eosinophilic or granular cytoplasm. The cytoplasm typically contains PAS-positive diastase-digestible glycogen granules. A cell block is necessary to confirm that the clear cells are positive for HMB45 and MelanA, and negative for cytokeratins and CD1a. Focal staining with S100 can be seen, but staining with macrophage markers (CD68) should be negative. A PAS stain should highlight the cytoplasmic granules. TFE3 immunostaining has been described in some PEComas [9].

#### Differential Diagnosis

The main diagnoses to consider are Langerhans cell histiocytosis (LCH), non-Langerhans histiocytosis, and vacuolated histiocytes from a reactive process (e.g., lipoid pneumonia or drug treatment). Unlike LCH, clear cell tumors are CD1a negative and do not stain with macrophage markers. Also, LCH involving the lungs is more likely to occur in adult smokers than in children. In adults, the differential diagnosis includes metastatic renal cell carcinoma (RCC). However, unless there is a history of clear cell or translocation RCC, this is not typically a consideration in the pediatric population.

#### Pearls

TFE3 immunoreactivity and gene fusions have been reported in a subset of PEComas, outside of the lung, in a small series of cases [9]. This is important to recognize given that clear cell tumors of the lung can mimic a metastatic translocation-associated renal cell carcinoma, which is also positive for TFE3.

### 6.6.3 Mucoepidermoid Carcinoma

#### Clinical Features

Mucoepidermoid carcinoma is a salivary gland-type malignancy that can arise from submucosal glands of the bronchus and is usually centrally located. Tumors are typically considered low-grade with good prognosis if excised, and although they can recur, rarely manifest in a high-grade, aggressive form.

#### Cytological Features

Aspirates from these tumors can yield a variety of cell types, including squamous cells, intermediate cells, and mucus-secreting cells. The malignant cells can be deceptively bland and the proportion of each cell type varies considerably with the degree of differentiation of the tumor. A mucin stain performed on a cell block or smear can be used to demonstrate the presence of cytoplasmic mucin. In addition, FISH studies are increasingly important as the majority of these tumors show a *MAML2* gene rearrangement due to t(11;19), and can help distinguish mucoepidermoid carcinoma from other neoplasms in the differential diagnosis [10].

#### Differential Diagnosis

The main entities to consider are adenosquamous carcinoma, adenocarcinoma, pleomorphic adenoma, and benign goblet cell metaplasia.

#### Pearls

Although uncommon, salivary gland-type tumors can occur in the lung in the pediatric population. Morphologic distinction between primary pulmonary and metastatic salivary gland-type carcinomas is not possible, and therefore clinical correlation is essential.

### 6.6.4 Juvenile Squamous Papillomas

Squamous papillomas of the lower bronchial tree are rare but can occur in children and adolescents and are HPV-positive. They appear as pedunculated lesions on bronchoscopy and consist of fibrovascular stalks covered by squamous epithelium. In some cases, atypical squamous cells with nuclear enlargement, nuclear irregularities, and features suggestive of HPV infection can also be seen in cytologic specimens (Fig. 6.14). Given the rarity of squamous cell carcinoma in pediatric patients, a papilloma should be considered before making a diagnosis of squamous cell carcinoma in this age group. Squamous papillomas can also break off and seed the lower airway or lung parenchyma, where they can attach and grow independently, resulting in more numerous lesions.

### 6.6.5 Epithelioid Hemangioendothelioma (EHE)

These are rare tumors that can occur in other locations outside of the lung, including liver, head and neck, and soft tissue/bone. EHEs typically have an indolent course. On cytology, the key feature is the presence of bland, vacuolated, epithelioid endothelial cells with intracytoplasmic lumina containing red blood cells. Immunohistochemical stains performed on a cell block demonstrate that the cells are positive for ERG, FLI-1, CD31, and CD34. TFE3 is also frequently positive. FISH studies in these tumors have shown a t(1;3) translocation of *WWTR1-CAMTA1*.

## 6.7 Metastatic Neoplasms to the Lung

#### Clinical Features

Many metastatic lesions can be confidently diagnosed based on the clinical history and radiographic features. For certain primary malignancies, including osteosarcoma, adrenal cortical carcinoma

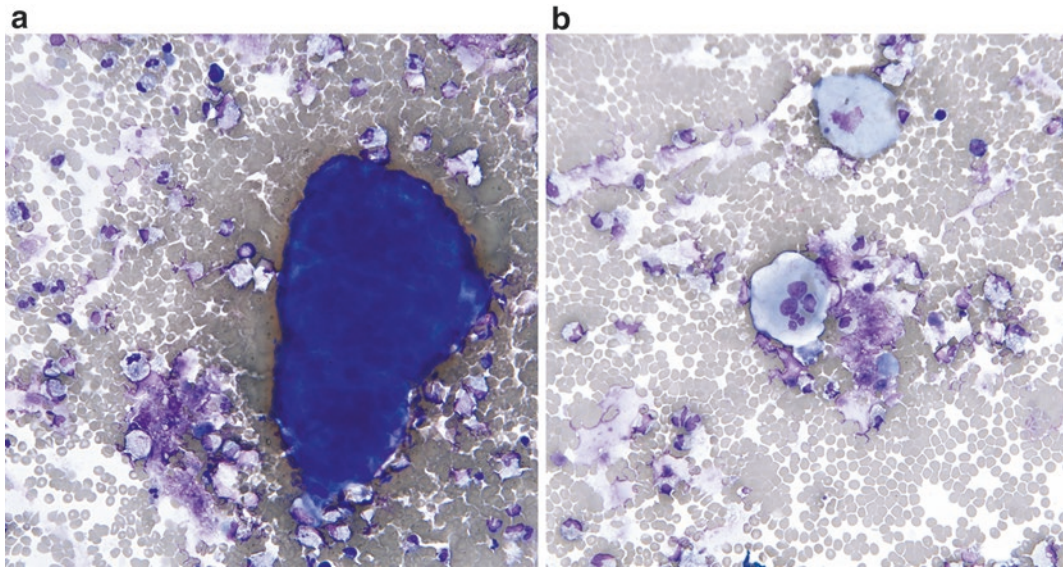


**Fig. 6.14** Juvenile papilloma of the bronchus (**a**, **b**. Diff-Quik stain, high power). Juvenile papillomas of the respiratory tract can show papillary fragments and scattered atypical squamous cells with features of HPV infection.

and hepatoblastoma, resection of the lesions remaining after chemotherapy confers a definitive survival benefit and is becoming standard of care [11]. Aspiration biopsy is only occasionally performed to confirm metastasis or resolve a question of infection vs. metastasis. Patients present with nodules detected on imaging workup. One study showed that the most significant predictors of malignancy were: (1) peripheral location, (2) lesions measuring between 5 and 10 mm, (3) lesions in the right lower lobe, and (4) a primary diagnosis of osteosarcoma, Ewing sarcoma or hepatocellular carcinoma [12].

### Cytological Features

With the exception of osteosarcoma, most lesions that metastasize to the lung release cells easily and are amenable to FNA biopsy. However, cellular yield will depend on the technique of the practitioner. The larger gauge needles needed to reach the nodules also tend to give more bloody specimens. Cellular smears show cytologic features similar to those seen in the primary neoplasms, which are addressed in more detail in other chapters. Given that many of the pediatric malignancies are small round blue cell tumors, many of these neoplasms have similar morphology and need to be distinguished from lymphoid cells as well as each other (Figs. 6.15, 6.16, and 6.17). A cell block is essential to confirm that the tumor cells are morphologically and immunophenotypically similar to the patient's previously diagnosed tumor. On-site evaluation is also critical given that the differential diagnosis often includes infection; thus, immediate evaluation can exclude infection and maximize cell block material.

### Differential Diagnosis

Differential diagnostic considerations depend on the type of tumor and are included in discussions of the primary tumors in other chapters. Histiocytes can appear as large cells with folded nuclei that may be concerning for malignancy. However, regularity of the nuclear membranes, even chromatin, and a uniform spectrum of cells without pleomorphism are clues to the correct identity of these cells.

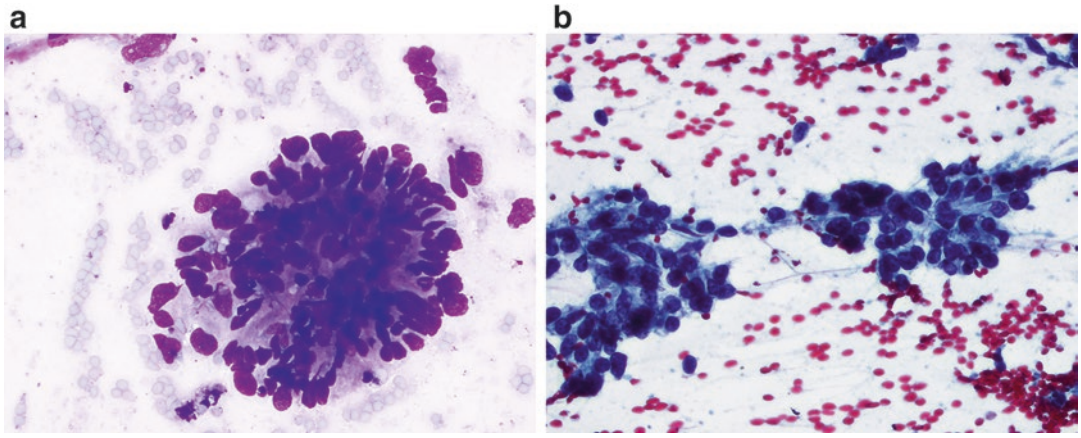


**Fig. 6.15** Wilms tumor metastatic to lung (**a**. Diff-Quik stain, high power; **b**. Papanicolaou stain, high power). This is a metastasis in a patient with a known history of Wilms tumor showing pseudorosettes of cells with large pleomorphic nuclei and prominent molding. The Papanicolaou stain highlights the irregular chromatin and small nucleoli.

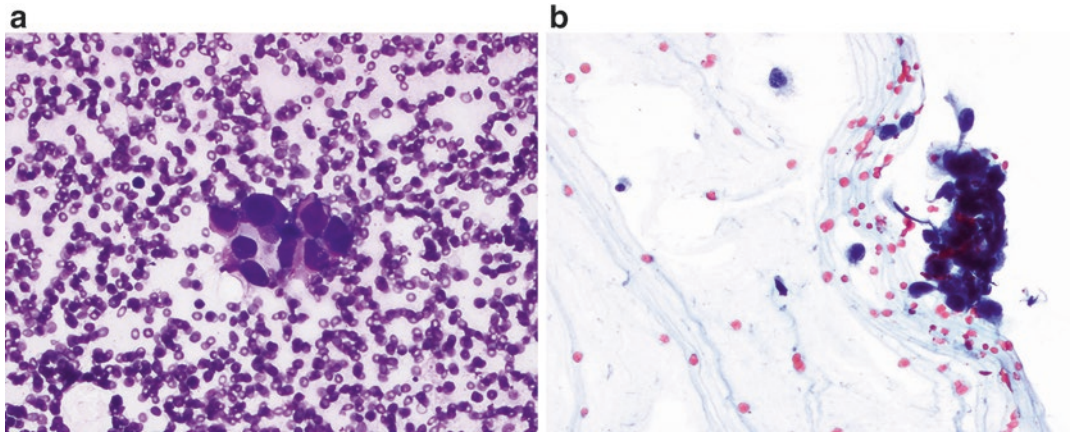


**Fig. 6.16** Osteosarcoma metastatic to lung (**a**. Diff-Quik stain, medium power; **b**. Papanicolaou stain, high power). Large pleomorphic cells with irregular nuclear membranes and moderate amounts of cytoplasm are seen. Occasional multinucleated cells may be present.

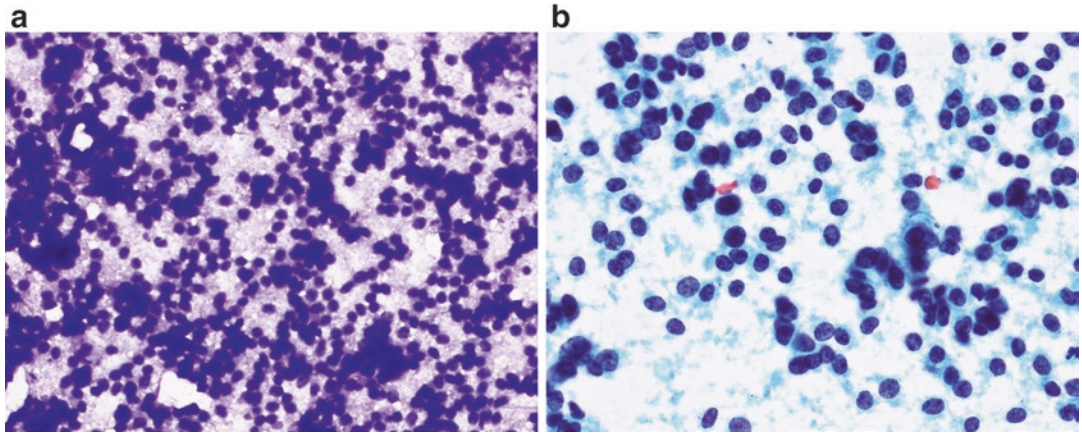


**Fig. 6.17** Ewing Sarcoma metastatic to lung (**a**. Diff-Quik stain, high power; **b**. Papanicolaou stain, high power). Dyscohesive small round blue cells with round nuclei and granular chromatin are present. The background material has a somewhat reticulated or tigroid-like appearance due to the glycogen within the tumor cells (**a**).

**Pearls**

Correlation of the cytologic features of a presumed metastatic lesion with the histologic appearance of the patient's known primary tumor is often helpful and may obviate the need for ancillary studies.

## 6.8 Mediastinum

The mediastinum consists of the tissues in the central thorax. Its boundaries are defined by the thoracic inlet superiorly, the parietal pleura bilaterally, the sternum anteriorly, the spine and ribs posteriorly, and the diaphragm inferiorly. The mediastinum is usually divided into three main compartments: anterior/superior, middle and posterior. There is a high prevalence of malignancy in pediatric mediastinal masses (37–61 %) and a large number of tumors are hematolymphoid in origin [13, 14]. Given the need for ancillary studies such as cytogenetics and flow cytometry, tissue biopsy is often necessary to obtain enough tissue for diagnosis. However, fine needle aspiration biopsy can be a useful tool at the time of surgery to localize viable lesional tissue prior to core needle biopsy and direct the distribution of material for ancillary studies. Aspirates rinsed in saline or RPMI can be sent for cytogenetics and flow cytometry and air dried smears can provide cellular monolayers for FISH studies, reducing the amount of tissue cores that need to be diverted from histology. The majority of masses that present in the anterior mediastinum are lymphomas (2/3 non-Hodgkin lymphoma, 1/3 Hodgkin lymphoma), followed by germ cell tumors. Approximately three quarters of germ cell tumors in the mediastinum are benign teratomas followed by yolk sac tumors. In the posterior mediastinum, the most common lesions are neurogenic including neuroblastoma, ganglioneuroblastoma, and ganglioneuroma [23]. A summary of pediatric mediastinal lesions is seen in Table 6.2.

### 6.8.1 Anterior/Superior Compartment

The anterior compartment of the mediastinum encompasses the area from the sternum to the anterior pericardial sac. The superior portion of the mediastinum, including tissues above the great vessels of the heart, is usually considered part of the anterior mediastinum. Tissues in the anterior compartment include the thymus, scattered lymph nodes, and loose connective tissue. Tumors of the anterior mediastinum include lymphoma, thymoma, germ cell tumors, thyroid lesions, metastases, and vascular lesions. One way to summarize the lesions of the anterior mediastinum is to use the 5 T's, which represent: thymic lesions, thyroid lesions, teratoma and other germ cells tumors, terrible lymphoma, and terribly common metastatic tumors (Table 6.2).

#### 6.8.1.1 Lymphoma

**Clinical Features**

Lymphoma is the most common malignancy in the mediastinum accounting for about half of all mediastinal malignancies. Two-thirds of lymphomas are non-Hodgkin lymphomas (e.g., lymphoblastic and large cell) and one third are Hodgkin lymphomas [13]. Most lymphomas present in multiple sites, many of which are more amenable to biopsy than the mediastinum (e.g., cervical lymph nodes, bone marrow). Also, due to the need for multiple ancillary studies, open biopsy is often a preferred method of obtaining tissue. However, FNA and small core biopsies are increasingly being used for primary diagnosis or in the setting of recurrence, given that, for many lymphomas, diagnosis is based on cytogenetic and immunophenotypic findings, rather than architecture. Patients present with symptoms of airway compression, including cough, stridor, and respiratory distress. Occasionally there are symptoms of superior vena cava obstruction and markedly elevated lactate dehydrogenase (LDH) levels. Patients with Hodgkin lymphoma also may present with B-symptoms of weight loss, night sweats and malaise.

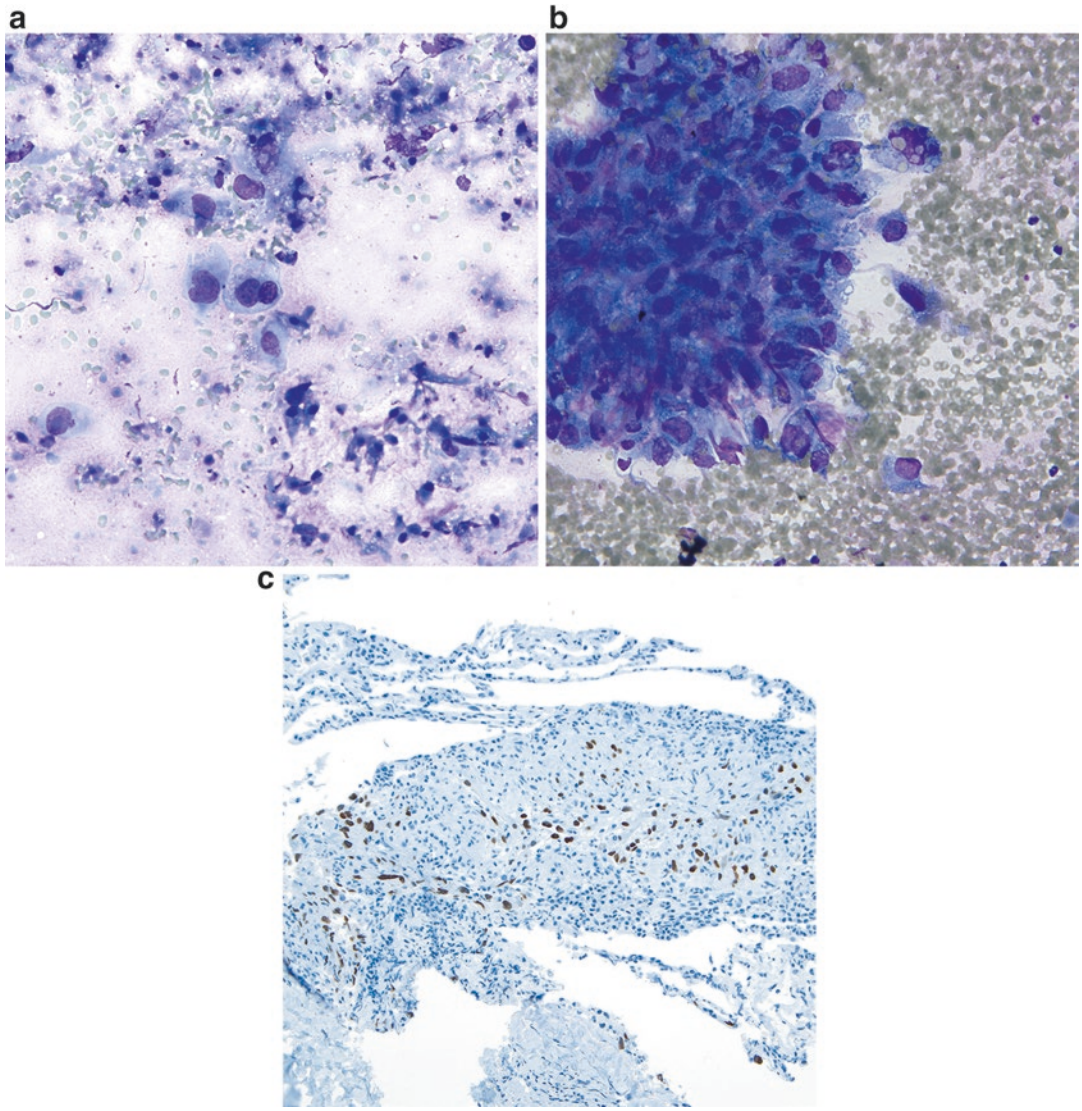


**Fig. 6.18** Metastatic yolk sac tumor to the lung (**a**, **b**. Diff-Quik stain, high power; **c**. SALL4 immunostain). This is a metastasis in a young patient with a known yolk sac tumor that metastasized to the lung, which shows loosely cohesive pleomorphic tumor cells, which are positive for SALL4 immunostaining.

### Cytological Features

The cytomorphology will depend on the type of lymphoma, as discussed below and in greater detail in Chap. 3.

- *Lymphoblastic Lymphoma*: Smears show a dyscohesive population of monotonous small lymphocytes. The lymphocytes have a high nuclear to cytoplasmic ratio and may show atypical nuclear features such as nuclear folds or membrane irregularities. The nuclear chromatin is usually fine and powdery without a conspicuous nucleolus (Fig. 6.19). The key to diagnosis is lack of variation in size and cell type. A lesser population of tingible body macrophages may be present. Subclassification of lymphoma requires flow cytometry and/or immunohistochemistry.
- *Large Cell Lymphoma*: Smears usually show large atypical cells with variable amounts of

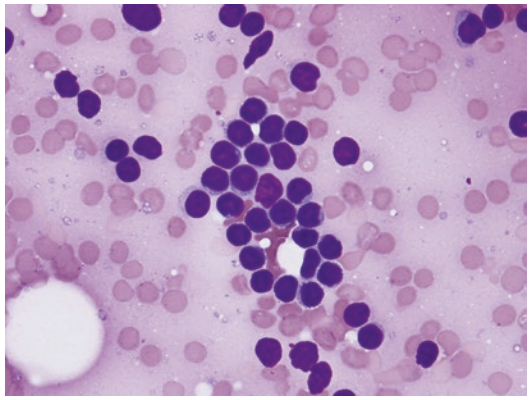

**Fig. 6.19** Lymphoblastic lymphoma (Diff-Quik stain, high power). Small to intermediate sized lymphoid cells with immature chromatin are seen in this patient with a T-lymphoblastic lymphoma/leukemia of the anterior mediastinum.

cytoplasm and large nuclei with irregular membranes. The neoplastic cells should have a nuclear size greater than that of a histiocytic nucleus (Fig. 6.20). Large cell lymphomas may present in cohesive clusters mimicking a solid neoplasm.

- *Hodgkin Lymphoma*: Smears show variable numbers of Reed–Sternberg (RS) cells and Reed–Sternberg variants in a background of mixed lymphoid cells. In the pediatric population, Hodgkin lymphomas tend to have more abundant RS cells making the diagnosis

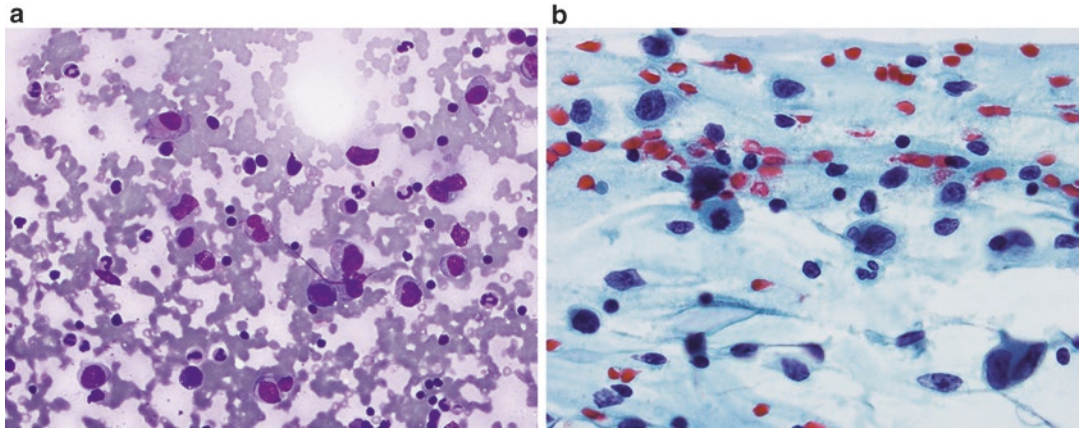


**Fig. 6.20** Anaplastic large cell lymphoma (**a**. Diff-Quik stain, high power; **b**. Papanicolaou stain, high power). These aspirates show a predominance of highly atypical large lymphoid cells with occasional boomerang or horseshoe shaped nuclei, compatible with a large cell lymphoma such as anaplastic large cell lymphoma.

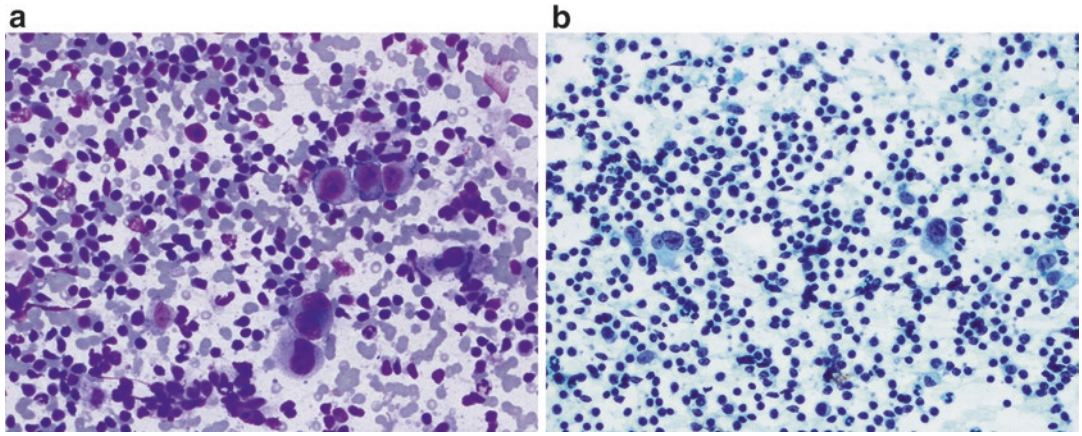


**Fig. 6.21** Classical Hodgkin Lymphoma of the mediastinum (**a**. Diff-Quik stain, high power; **b**. Papanicolaou stain, high power). The large lymphoid cells are seen in a background of small lymphocytes, and show some binucleated large cells with prominent nucleoli (Reed–Sternberg cells).

possible on FNA alone. RS cells show abundant cytoplasm and large round to oval nuclei with prominent nucleoli. The background lymphoid cells usually show intermixed eosinophils (Fig. 6.21).

On-site evaluation is usually helpful in cases of lymphoma. Flow cytometry shows a reactive pattern in classical Hodgkin lymphoma, and thus, if RS cells are seen at on-site evaluation, material may be better allocated for cell block for immunoperoxidase stains than for flow cytometry. In contrast, if a lymphoblastic or large cell lymphoma is suspected, then flow cytometry and cell block material are typically needed for a definitive diagnosis.

#### Differential Diagnosis

Malignant germ cell tumors are the second most common anterior mediastinal mass in children and can also show large atypical, dyscohesive cells within a background of smaller lymphocytes, which can mimic a large cell lymphoma. Germ cell tumors show more cohesive clusters and tend to have more abundant cytoplasm and prominent nucleoli, without conspicuous lymphoglandular bodies. Myeloid sarcoma can also mimic large cell lymphomas morphologically but can be distinguished by flow cytometry and immunoperoxidase stains. The differential diagnosis for lymphoblastic lymphomas includes reactive lymphoid tissue and small round blue cell tumors. Classical Hodgkin lymphomas, particularly those with a paucity of RS cells, can be difficult to distinguish from reactive lymphadenopathy, whereas those with abundant RS cells may mimic a large cell lymphoma, germ cell tumor, or malignant melanoma.

#### Pearls

Myeloid cells can mimic lymphomas or atypical histiocytes, and myeloid sarcoma should be considered when evaluating a cellular hematolymphoid proliferation in the mediastinum. Myeloid sarcoma is negative for lymphoid markers but positive for CD33 by flow cytometry, and MPO and CKIT on immunoperoxidase stains (Fig. 6.22).

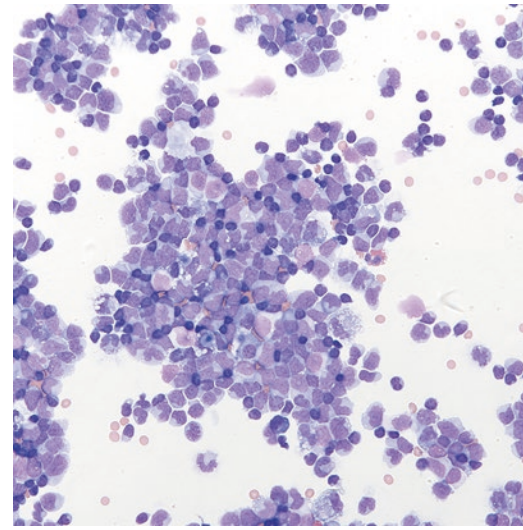

**Fig. 6.22** Myeloid sarcoma presenting as a pleural/soft tissue mass (Diff-Quik stain, high power). Immature appearing myeloid cells with powdery chromatin and irregular nuclei are present in this cellular aspirate from a soft tissue mass in a patient with a known history of acute myeloid leukemia.

### 6.8.1.2 Germ Cell Tumors

#### Clinical Features

Germ cell tumors develop from cells in the primordial germ cell crest that fail to properly migrate to the urogenital ridge. Approximately 4–18 % of germ cell tumors arise in the mediastinum which is the fourth most common site after the ovary, sacrococcygeal region, and testis [13, 15, 16]. Most mediastinal germ cell tumors are in the anterior mediastinum/thymus, although rare tumors have been reported in the pericardium/heart and posterior mediastinum [15, 16]. Benign teratomas comprise up to 70–85 % of mediastinal germ cell tumors [15, 16]. While seminoma is the most common malignant germ cell tumor in the adult population, yolk sac tumor is more common in pediatrics [17, 18]. Most patients present with respiratory symptoms, such as shortness of breath and cough; some patients additionally show weakness, loss of appetite, and/or chest pain. Benign teratoma can frequently be diagnosed by imaging and malignant components may be indicated by

serum markers (e.g., serum alpha-fetoprotein, beta-human chorionic gonadotropin). Complete surgical resection is the mainstay of treatment so patients with low stage disease are frequently taken directly to surgery; however, FNA may be used in cases that are indeterminate by imaging or that appear cystic. Patients with extensive disease and/or potential airway compromise may present for biopsy (with or without FNA) prior to neoadjuvant chemotherapy.

### Cytological Findings

The morphology depends on the predominant type of germ cell tumor seen in the lesion, as described below:

- *Teratoma*: Cystic teratomas may show predominantly cyst contents—anucleate squamous debris or mucin—with scant fragments of glandular or squamous epithelium. Neural tissues and stromal tissues are usually more cohesive and less likely to release cells on FNA. The nuclear features are usually bland, consistent with the mature nature of the tissues.
- *Yolk Sac Tumor*: Cytological findings vary corresponding to the histologic heterogeneity of yolk sac tumors. Tumors with well-formed Schiller–Duvall bodies may yield papillary fragments on FNA. Intracytoplasmic and extracytoplasmic hyaline globules may be present and can be an important clue to the diagnosis. Irrespective of histologic type, aspirates should contain cells with malignant features including increased nuclear to cytoplasmic ratios and nuclear pleomorphism, hyperchromasia, and membrane irregularities (Fig. 6.23).
- *Seminoma*: Smears show a biphasic population of large polygonal tumor cells intermixed with small lymphocytes and granulomas. The tumor cells show abundant cytoplasm with clear borders and large round nuclei with prominent nucleoli. A tigroid background can be seen in many cases on Diff-Quik-stained slides due to the presence of glycogen (Fig. 6.24).

### Differential Diagnosis

When cystic, the differential diagnosis includes foregut duplication cysts or bronchogenic cysts, mediastinal goiter, and thymic cysts, but these lesions tend to be very hypocellular. Non-cystic germ cell tumors can mimic large cell lymphomas, lymphoblastic lymphomas, or other high-grade large cell malignancies.

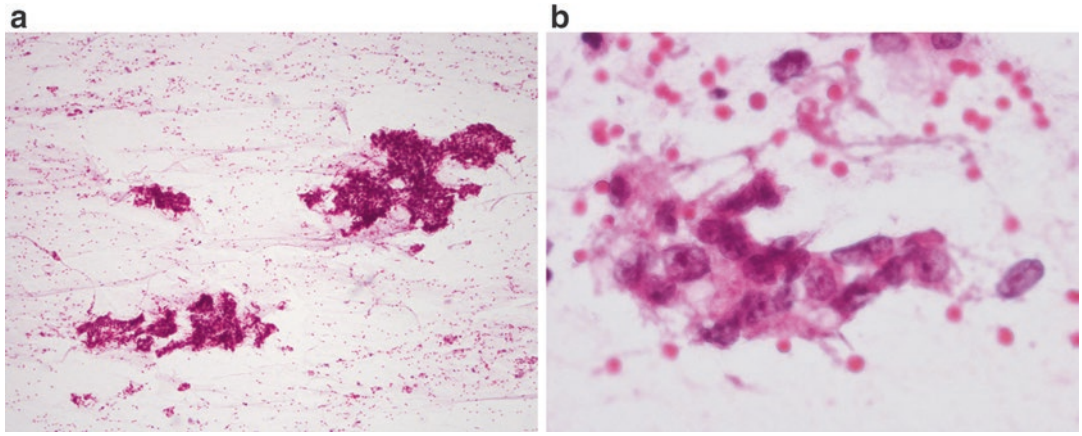


**Fig. 6.23** Mediastinal germ cell tumor with yolk sac component (**a**. H&E stain, low power, **b**. H&E stain, high power). The aspirates from this yolk sac tumor show papillary-type groups of tumor cells with cytoplasmic vacuolization, prominent nucleoli, and cytoplasmic hyaline globules.

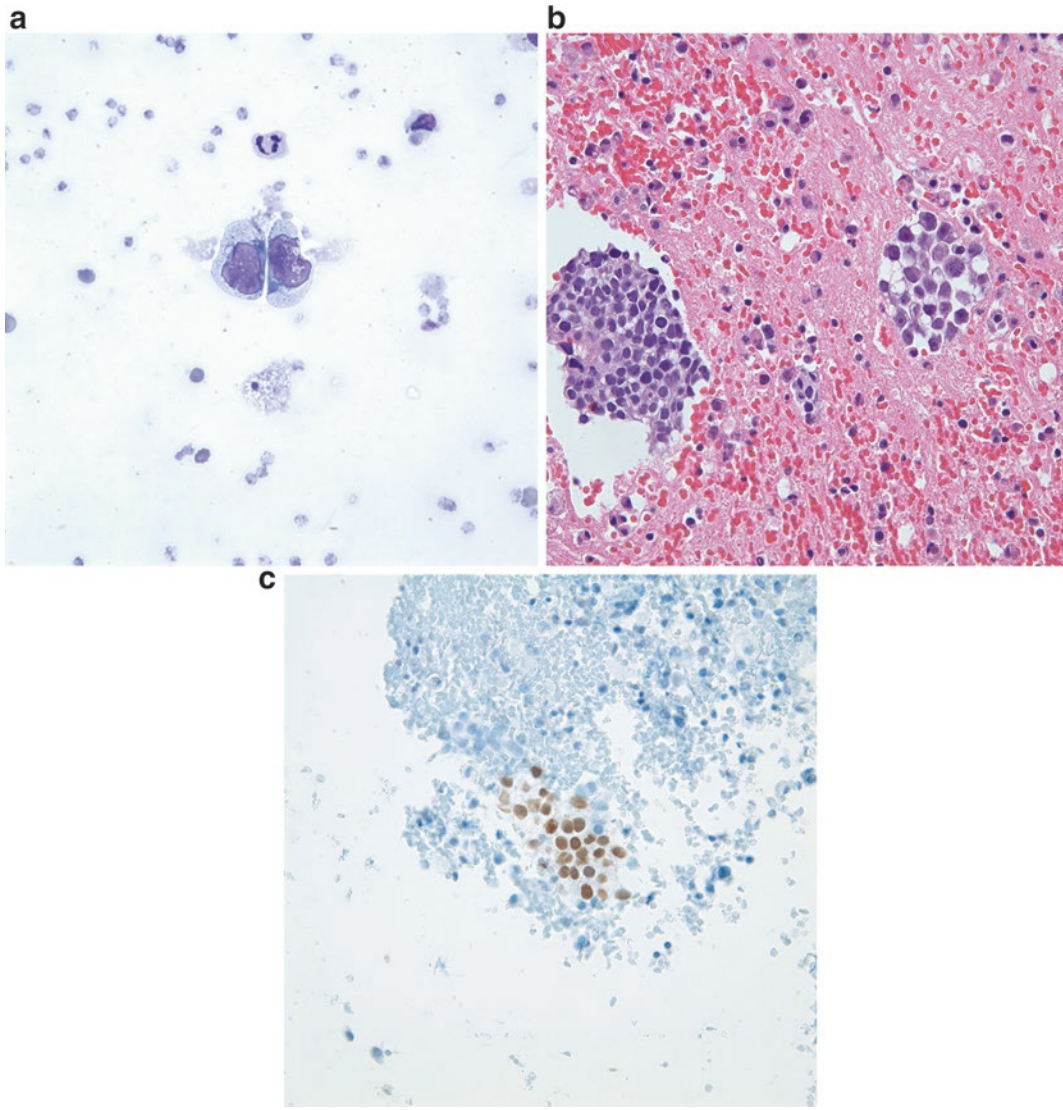


**Fig. 6.24** Metastatic seminoma involving the pleural fluid (**a**. Diff-Quik stain, high power; **b**. H&E stain, high power; **c**. OCT3/4 stain, high power). Dyscohesive large cells with centrally located nuclei, prominent nucleoli, and moderate amounts of clear cytoplasm are identified. The OCT3/4 stain shows strong nuclear staining, confirming the presence of a germ cell tumor.

### 6.8.1.3 Thymus

Lesions in the thymus include cysts, hyperplasia, and tumors. Cysts and hyperplastic lesions usually are diagnosed radiologically and do not require FNA. Solid tumors arising in and around the thymus include lymphomas, thymomas, thymic carcinomas, neuroendocrine tumors, and germ cell tumors, and these are typically amenable to biopsy for planning of further management.

#### Thymoma

#### Clinical Features

Thymomas are rare in pediatrics accounting for 1–4 % of pediatric mediastinal masses [14, 19]. However, it is the fourth most common tumor after lymphoma, germ cell tumors, and neurogenic tumors [17]. Thymomas rarely present for FNA diagnosis even in the adult population,

given that the lobulated nature and presence of fat are radiological clues to the diagnosis. Patients usually present with respiratory complaints, including cough and shortness of breath. Myasthenia gravis, which is associated with thymoma in 30 % of cases in the adult, is only associated with thymoma in 5 % of pediatric cases [17].

#### Cytological Features

Aspirates of thymoma vary depending on the histology of the lesion. Lymphocytic thymomas (type B) are the most common and are the only type reported in pediatrics [20]. On histology, these lesions show varying amounts of epithelial clusters in a background of small lymphocytes. Concordantly, aspirates show abundant small lymphocytes with a variable population of epithelial cells. The recognition of the latter is necessary to distinguish thymoma from reactive lymphoid tissue. These epithelial cells usually present in tightly clustered fragments of bland cells with round to oval nuclei and finely granular chromatin [21]. Flow cytometry and/or immunoperoxidase stains on a cell block can be helpful to confirm the presence of thymic T-lymphocytes, which are positive for CD3, TdT, and CD1a. In addition, thymic epithelium can be confirmed with p63 and cytokeratin, and a thymic carcinoma can be excluded with a CD5 immunostain given that thymic carcinomas are CD5-positive.

#### Differential Diagnosis

The differential diagnosis includes small cell lymphoma, classical Hodgkin lymphoma with a paucity of RS cells, and small round blue cell tumors.

#### Pearls

Newer immunoperoxidase stains can also help mark thymic epithelium, including CKIT and PAX8. PAX8 can be particularly helpful given that it is a nuclear stain, and typically only stains thyroid, renal, Müllerian, and thymic lesions.

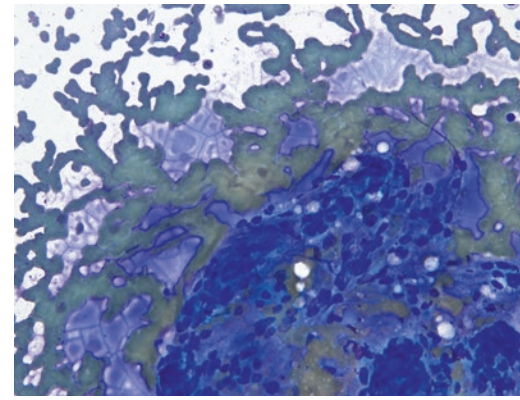

**Fig. 6.25** Mediastinal goiter (Diff-Quik stain, medium power). Mediastinal thyroid tissue can show features of a benign colloid nodule, and an important clue is the cracking of the watery colloid in the background.

### 6.8.1.4 Vascular Malformations

Vascular malformations, including lymphangiomas/cystic hygromas and hemangiomas, account for 3–6 % of mediastinal tumors in children [13]. These are usually easily diagnosed by radiology and are generally not amenable to FNA. Rarely lesions with thrombosis may mimic a solid neoplasm. Cytology shows old blood, fibrin and hemosiderin laden macrophages.

### 6.8.1.5 Mediastinal Goiter or Thyroid Tissue

Thyroid tissue can also extend into the anterior mediastinum and show the spectrum of changes seen in the normal thyroid, ranging from benign colloid nodules to malignant papillary thyroid carcinoma. Mediastinal goiters usually present as large cystic masses that can radiologically mimic bronchogenic cysts. A combination of colloid and follicular epithelial cells are important for the diagnosis (Fig. 6.25). If cystic, liquid-based cytology can be helpful to identify the thyroid follicular cells, which will also stain positive for TTF1 and thyroglobulin. PAX8 is not as helpful given that thymic epithelium will also be PAX8 positive and is in the differential diagnosis of a cystic anterior mediastinal mass.

### 6.8.2 Posterior Compartment

The posterior compartment consists of the tissues between the posterior pericardial sac and the spine/chest wall. This includes the descending aorta, esophagus, sympathetic chain of the nervous system, trachea, and lymph nodes. A summary of posterior mediastinal lesions is seen in Table 6.2.

#### 6.8.2.1 Congenital Cysts

Congenital cysts include bronchogenic cysts, esophageal duplication cysts, and enteric cysts which are malformations/remnants of the embryonic foregut. These are usually diagnosed radiographically and are not subject to FNA. If aspirated, liquid-based cytology and immunoperoxidase stains can be helpful to try to identify and characterize the cyst lining cells. Unfortunately, some cases just show cystic fluid or histiocytes and cannot be definitively diagnosed.

#### 6.8.2.2 Lymph Nodes

Most lymph nodes in the mediastinum are located along the trachea and great vessels of the heart. These are frequently involved and enlarged in systemic diseases, including infections, lymphoma, and widely metastatic neoplasms. In the adult population, endoscopic ultrasound guided biopsy of lymph nodes may be performed via the trachea or the esophagus. This has also been performed successfully in the pediatric population [22]; however, most children present with widespread disease that has other lymph nodes/sites that are more readily accessible.

#### 6.8.2.3 Neuroblastoma Spectrum

##### Clinical Features

Tumors of the neuroblastoma spectrum (neuroblastoma, ganglioneuroblastoma, ganglioneuroma) are the most common tumors in the posterior mediastinum and the most common mediastinal tumor in children under 2 years old [23]. Only 11–26 % of pediatric neuroblastoma cases present in the thoracic cavity. These tumors tend to have a better prognosis, although the reasons are not fully understood. Thoracic neuroblastoma frequently presents with localized disease (66 % stage I and II vs 45 % in other sites) and is less frequently *MYCN* positive [23]. Of the patients who present with opsoclonus-myoclonus, up to 50 % have been found to have a slowly growing chest tumor [24]. Patients frequently present with a mass discovered on an X-ray performed to evaluate upper respiratory symptoms. Younger patients with aggressive tumors may have symptoms of chest pain, paraplegia, and Horner's syndrome. Adolescent patients occasionally have incidental findings on routine X-rays. As with lymphoma, patients with meta-

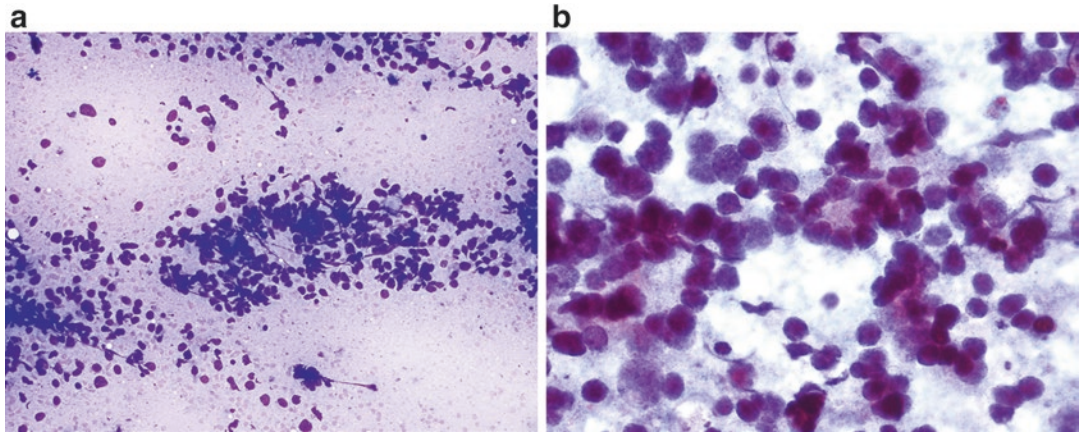


**Fig. 6.26** Neuroblastoma in the posterior mediastinum (**a**. Diff-Quik stain, high power; **b**. Papanicolaou stain, high power). The aspirates are cellular and reveal a small round blue cell tumor with immature granular chromatin, nuclear molding, and rosette formation.

static neuroblastoma may have more accessible lymph nodes for biopsy in the cervical region.

### Cytological Features

Smears from neuroblastoma show abundant small round blue cells with prominent nuclear molding. Occasional Homer Wright rosettes or balls of cells may be present. Fibrillary neuropil may be present, but can be difficult to identify. On Papanicolaou stain, the neuroblastic nuclei show fine granular chromatin without prominent nucleoli (Fig. 6.26). Occasional maturing ganglion cells may be seen. Ganglioneuromas are less amenable to FNA as they are less cellular and less prone to release cells, but will show large epithelioid ganglion cells with prominent nucleoli, abundant cytoplasm, and Nissl substance within a background of bland comma-shaped spindled Schwann cells. Biopsies from ganglioneuroblastoma show variable findings depending on the area sampled; however, even without a neuroblastic component identified on FNA, these tumors are typically excised to completely exclude a component of neuroblastoma. A cell block or core biopsy can be helpful for performing immunoperoxidase stains to confirm neuroblastic, Schwannian, or gangliocytic origin of cells. While FNA biopsy may be diagnostic of neuroblastoma, the mitotic karyorrhectic index (MKI) cannot be calculated on aspirate smears. If a minimally invasive procedure is planned, every effort should be made to obtain at least one tissue core for complete staging.

### Differential Diagnosis

The differential diagnosis depends on the predominant cell type. For cases with abundant spindle cells, mesenchymal tumors are in the differential diagnosis. For tumors with a more prominent gangliocytic component, epithelioid tumors, large cell lymphomas, melanoma, and germ cell tumors enter the differential diagnosis. If there is a prominent neuroblastic component, then other small round blue cell tumors, including lymphoblastic lymphoma, Ewing sarcoma, and rhabdomyosarcoma enter the differential diagnosis.

## 6.9 Conclusions

The mediastinum and lung contain a wide spectrum of entities to consider when a mediastinal or thoracic lesion is identified on imaging. Given the variety of ancillary studies required for a definitive and accurate diagnosis, FNA and small biopsies can play a powerful role in triage and management by helping to confirm which lesions require surgery (e.g., primary lung neoplasm) and which can be better managed in non-surgical ways (e.g., lymphoma, infection, metastatic tumor).

## References

1. Qualter E, Satwani P, Ricci A, Jin Z, Geyer MB, Alobeid B, et al. A comparison of bronchoalveolar lavage versus lung biopsy in pediatric recipients after stem cell transplantation. Biol Blood Marrow Transplant. 2014;20:1229–37.
2. Cohen MC, Kaschula ROC. Primary pulmonary tumors in childhood: a review of 31 years' experience and the literature. Pediatr Pulmonol. 1992;14:222–32.
3. Uruga H, Takaya H, Hanada S, Beika Y, Miyamoto A, Morokawa N, et al. Diagnostic efficacy of CT-guided transthoracic needle biopsy and fine needle aspiration in cases of pulmonary infectious disease. Jpn J Radiol. 2012;30:589–93.
4. Kropshofer G, Kneer A, Edlinger M, Meister B, Salvador C, Lass-Flörl C, et al. Computed tomography guided percutaneous lung biopsies and suspected fungal infections in pediatric cancer patients. Pediatr Blood Cancer. 2014;61:1620–4.
5. Silowash R, Monaco SE, Pantanowitz L. Ancillary techniques on direct-aspirate slides: a significant evolution for cytopathology techniques. Cancer Cytopathol. 2013;121:670.
6. Hancock BJ, Di Lorenzo M, Youssef S, Yazbeck S, Marcotte J, Collin P. Childhood primary pulmonary neoplasms. J Pediatr Surg. 1993;28:1133–6.
7. Welsh JH, Maxson T, Jaksic T, Shahab I, Hicks J. Tracheobronchial mucoepidermoid carcinoma in childhood and adolescence: case report and review of the literature. Int J Pediatr Otorhinolaryngol. 1998;45:265–73.
8. Antonescu CR, Suurmeijer AJH, Zhang L, et al. Molecular characterization of inflammatory myofibroblastic tumors with frequent *ALK* and *ROS1* fusions and rare novel RET gene rearrangement. Am J Surg Pathol. 2015;39:957–67.
9. Argani P, Aulmann S, Illei PB, Netto GJ, Ro J, Cho HY, Dogan S, Ladanyi M, Martignoni G,

Goldblum JR, Weiss SW. A distinctive subset of PEComas harbors TFE3 gene fusions. Am J Surg Pathol. 2010;34:1395–406.
10. Garcia JJ, Hunt JL, Weintreb I, McHugh J, Barnes EL, Cieply K, Dacic S, Seethala R. Fluorescence in situ hybridization for detection of *MAML2* rearrangements in oncocytic mucoepidermoid carcinomas: utility as a diagnostic test. Hum Pathol. 2011;42:2001–9.
11. Kayton ML. Pulmonary metastasectomy in pediatric patients. Thorac Surg Clin. 2006;16:167–83.
12. Murrell Z, Dickie B, Dasgupta R. Lung nodules in pediatric oncology patients: a prediction rule for when to biopsy. J Pediatr Surg. 2011;46:833–7.
13. Jaggers J, Balsara K. Mediastinal masses in children. Thorac Cardiovasc Surg. 2004;14:201–8.
14. Petroze R, McGahren ED. Pediatric chest II, benign tumors and cysts. Surg Clin N Am. 2012;92:645–58.
15. Billmire D, Vinocur C, Rescorla F, Colombani P, Cushing B, Hawkins E, et al. Malignant mediastinal germ cell tumors: an Intergroup study. J Pediatr Surg. 2001;36:18–24.
16. Yalçin B, Demir HA, Çiftçi AO, Orhan D, Varan A, Akyüz C, et al. Thymomas in childhood: 11 cases from a single institution. J Pediatr Hematol Oncol. 2012;34:601–5.
17. Yalçin B, Demir HA, Tanyel FC, Akçören Z, Varan A, Akyüz C, et al. Mediastinal germ cell tumors in childhood. Pediatr Hematol Oncol. 2012;29: 633–42.
18. Schneider DT, Calaminus G, Reinhard H, Gutjahr P, Kremens B, Harms D, et al. Primary mediastinal germ cell tumors in children and adolescents: results of the German Cooperative Protocols MAKEI 83/86, 89, and 96. J Clin Oncol. 2000;18: 832–9.
19. Wright CD. Mediastinal tumors and cysts in the pediatric population. Thoracic Surg Clin. 2009;19:47–61.
20. Travis WD, Brambilla E, Müller-Hermelink HK, Harris CC, editors. World Health Organization classification of tumors: pathology and genetics of tumors of the lung, pleura, thymus and heart. Lyon: IARC Press; 2004.
21. Wakely PE. Fine needle aspiration in the diagnosis of thymic epithelial neoplasms. Hematol Oncol Clin N Am. 2008;22:433–42.
22. Atilla T, Adler DG, Hilden K, Faigel DO. EUS in pediatric patients. Gastrointest Endosc. 2009;70:892–8.
23. Häberle B, Hero B, Berthold F, von Schweinitz D. Characteristics and outcome of thoracic neuroblastoma. Eur J Pediatr Surg. 2002;12:145–50.
24. Alexander F. Neuroblastoma. Urol Clin N Am. 2000;27:383–92.

# Kidney, Adrenal Gland, and Retroperitoneum

7

Pamela Michelow and Michelle Dubb

## 7.1 Kidney

Renal lesions in children and adolescents can be due to cystic or inflammatory etiologies, in addition to neoplasms. Renal tumors are among the most common solid organ malignancies in children due to the peak incidence of Wilms tumor in this age group. Other kidney tumors, including conventional renal cell carcinoma (RCC) of the clear cell type seen in adults, are rare in children. One of the most important factors to know is the age of the child, as some pediatric renal tumors are seen more often in certain age groups (Table 7.1).

### 7.1.1 Cysts

#### Clinical Features

Renal cysts in children and adolescents are due to a variety of causes and can be single or multiple, unilateral or bilateral. Autosomal recessive polycystic kidney disease, which is due to a mutation in the *PKHD1* gene on chromosome 6 (fibrocystin protein), is characterized by enlarged, diffusely echogenic kidneys with multiple, bilateral cysts and typically presents in the neonatal period or infancy. In countries with widespread use of prenatal ultrasound, it is increasingly recognized in utero. In contrast, autosomal dominant polycystic kidney disease is due to mutations in genes encoding polycystin-1 (*PKD1* on chromosome 16) or polycystin-2 (*PKD2* on chromosome 4) and is a late-onset disorder characterized by progressive, bilateral renal enlargement due to multiple cysts. It usually becomes symptomatic after the third decade of life but may also present in adolescents or children. Other diseases associated with renal cysts include, but are not limited to, tuberous sclerosis, von Hippel–Lindau syndrome, Ehlers–Danlos syndrome, Zellweger syndrome, Meckel–Gruber syndrome, Beckwith–Wiedemann syndrome, short rib-polydactyly syndrome, renal dysplasia, and calyceal diverticula [1–5]. Acquired simple cysts, which are the most common cysts encountered in adults, are uncommon in children. Current imaging techniques allow accurate assessment of the risk of malignancy in many cystic renal lesions, precluding the need for fine-needle aspiration (FNA) except in cases with indeterminate findings or for decompression of a benign cyst.

#### Cytological Features

FNA of a renal cyst usually yields clear or blood-stained fluid with macrophages, cyst-lining cells, and occasional inflammatory cells. Renal tubular cells and Liesegang rings are infrequently observed. Benign cysts of various etiologies cannot be distinguished from each other on FNA.

P. Michelow, MBBCh, MSc (Med Sci) (✉)
M. Dubb, MBBCh, FCPath, FRCPath
Cytology Unit, Department of Anatomical Pathology, Faculty of Health Sciences, University of the Witwatersrand and National Health Laboratory Service, Johannesburg, South Africa
e-mail: pamela.michelow@nhls.ac.za; mdubb@telkomsa.net



S.E. Monaco, L.A. Teot (eds.), *Pediatric Cytopathology*, DOI 10.1007/978-3-662-53441-0_7

**Table 7.1** Pediatric renal tumors according to age

| **Congenital and under 6 months** | **Under 5 years** |
|---|---|
| Mesoblastic nephroma | Clear cell sarcoma |
| | Rhabdoid tumor |
| | Intrarenal neuroblastoma |
| | Ossifying renal tumor |
| **Older children, adolescents, young adults** | **All pediatric age groups** |
| Translocation-associated renal cell carcinoma | Nephroblastoma (Note: Although seen throughout childhood, the majority are diagnosed before 5 years of age) |
| Renal medullary carcinoma | |
| Ewing sarcoma/primitive neuroectodermal tumor (PNET) | |

### Triage

Cyst fluid may benefit from liquid-based cytology to decrease obscuring blood in hemorrhagic cyst contents and to increase the ability to find cyst-lining cells, to exclude malignancy.

### Differential Diagnosis

Neoplasms that undergo cystic degeneration are the main consideration but usually have greater cellularity and more atypia. Cyst contents with macrophages may also mimic granulomatous infections (mycobacterial or fungal) or the xanthomatous histiocytes of xanthogranulomatous pyelonephritis.

### Pitfalls

Misinterpretation of reactive atypia or degenerative changes in cyst-lining cells can lead to a false-positive diagnosis of malignancy. Conversely, a hypocellular specimen with few or no malignant cells can result in a false-negative diagnosis in a cystic neoplasm.

## 7.1.2 Infections

### Clinical Features

Pyelonephritis is caused by a variety of bacterial, viral, fungal, and parasitic organisms. Infection can be blood-borne or ascending and in children less than 6 years of age is associated with vesicoureteral reflux in up to 50 % of cases. The most common causes of pyelonephritis are bacteria, such as *E. coli*, *Proteus mirabilis*, *Klebsiella* spp., *Enterobacter* spp., *Enterococcus faecalis*, *Staphylococcus* spp., and others. Fungal pyelonephritis usually occurs in the context of systemic infection with opportunistic or pathogenic organisms, such as *Candida spp, Aspergillus spp, Cryptococcus spp, Histoplasma capsulatum, Coccidioides immitis*, and others and, although more common in immunocompromised patients, can also affect otherwise healthy individuals. Viruses, especially BK virus and cytomegalovirus, are associated with clinically significant renal infection in immunocompromised patients, particularly those with renal allografts. Pyelonephritis due to parasitic infiltration of the renal parenchyma is rare but can be seen in schistosomiasis, leishmaniasis, and malaria. In addition, schistosomiasis can cause obstructive uropathy at the level of the bladder and/or ureter with consequent ascending pyelonephritis due to other organisms. Mycobacterial infection of the kidney is usually due to *M. tuberculosis*. Infection may be due to disseminated infection or be localized within the urinary tract. Xanthogranulomatous pyelonephritis occurs in children, albeit infrequently, and is associated with kidney stones and persistent urinary tract infection [1, 2, 6].

### Cytological Features

The cytomorphology of these various infections is similar at whatever body site they occur. In the setting of mycobacterial infection, the aspirates show necrotizing granulomatous inflammation (Fig. 7.1a) Immunosuppressed children may present with an FNA comprised almost entirely of necrosis or a more suppurative picture with a moderate number of neutrophils in a necrotic background. A complication of infection, especially bacterial, is a renal abscess, and the FNA yields purulent material with numerous neutrophils, scattered histiocytes, and debris. Xanthogranulomatous pyelonephritis shows vacuolated histiocytes, acute and chronic inflammatory cells, multinucleated giant cells, cholesterol crystals, and necrotic debris (Fig. 7.1b). Rare cases of aspergillosis involving the kidney with fungal balls eliciting ureteral obstruction have been described [6].

### Triage

A portion of the aspirate should be submitted for microbial cultures and cell block if infection is suspected. Special stains, such as Grocott, AFB,

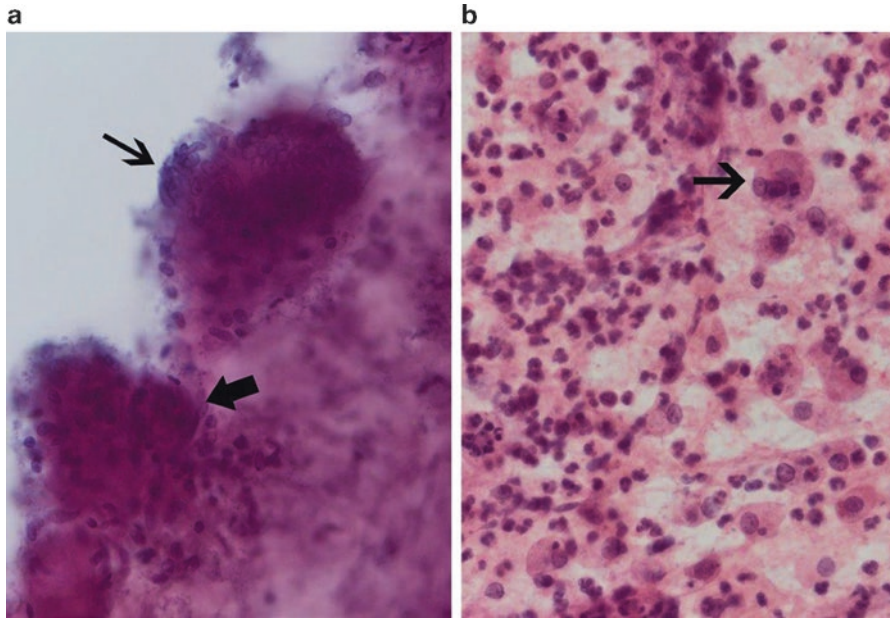


**Fig. 7.1** Renal Infections (**a**, **b**. Papanicolaou stain, high power; **b**. H&E stain, high power). Mycobacterial infection in the kidney of a 4-year-old girl showing epithelioid histiocytes (*thick arrow*) and Langhans-type giant cells (*thin arrow*) in a necrotic background (**a**). Xanthogranulomatous pyelonephritis diagnosed by FNA of the kidney in a 6-year-old boy. The aspirates showed acute inflammatory cells, vacuolated histiocytes (*arrow*), and debris (**b**).

and gram stains can be performed on the cell-block material. In addition, if there is limited inflammatory or cellular material, extra unstained smears can be prepared and used for key special stains, in the event there is scant material on the cell block [7]. In cases in which special stains or culture results are negative but clinical suspicion for mycobacterial infection is high, molecular diagnostic techniques can be performed on the FNA material for identification and subtyping.

#### Differential Diagnosis

In infectious cases dominated by macrophages, the differential diagnosis includes cyst contents.

#### Pearls

In case of suspected infection, it is important to preserve fresh material for microbial cultures and antibiotic sensitivities.

### 7.1.3 Miscellaneous Nonneoplastic Conditions

Amyloidosis, renal infarct, sarcoidosis, extramedullary hematopoiesis, and malakoplakia have all been described, albeit infrequently, in the kidneys of children (Fig. 7.2). The cytomorphology is identical to that seen in the FNA of similar conditions in adult kidneys. FNA is not usually utilized in the diagnosis and management of glomerulonephritis. However, cytology plays an important role in the identification of red cell casts in pediatric urine specimens, which may be a clue in the diagnosis of glomerulonephritis.

### 7.1.4 Renal Neoplasms

Children with renal tumors may present symptomatically, e.g., hematuria, abdominal pain or mass, or the tumor may be an incidental finding. A wide variety of renal neoplasms, both benign and malignant, are described in children. These include Wilms tumor, nephrogenic rests and nephroblastomatosis, cystic partially differentiated nephroblastomatoma, metanephric neoplasm, mesoblastic nephroma, clear cell sarcoma, rhabdoid tumor, renal cell carcinoma (in particular translocation-associated and renal medullary), angiomyolipoma and ossifying renal tumor of infancy.

### 7.1.4.1 Angiomyolipoma

#### Clinical Features

These benign tumors are rare and occur more often in adults but can be seen in young adults and children with tuberous sclerosis. Tuberous sclerosis is an autosomal dominant syndrome due to alterations of the *TSC1* gene on chromosome 9q34 or the *TSC2* gene on chromosome 16p13, which is associated with hamartomas of the brain (subependymal giant cell tumor), cutaneous angiofibromas, rhabdomyomas, lymphangioleiomyomatosis, and angiomyolipomas.

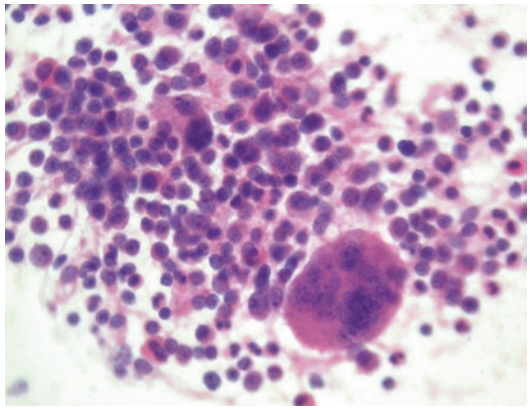

**Fig. 7.2** Extramedullary hematopoiesis (Papanicolaou stain, high power). Megakaryocytes and immature myeloid precursor cells, consistent with extramedullary hematopoiesis, in a 4-year-old girl who presented with anemia and renal mass.

#### Cytological Features

FNA yields a proliferation of thickened blood vessels, sheets and bundles of perivascular spindle and epithelioid cells, and adipose tissue in varying proportions. Fat globules can be seen in the background. In some cases the epithelioid cells show a striking degree of cytologic atypia and pleomorphism. Most imaging studies can identify adipose tissue within a tumor rendering an FNA diagnosis unnecessary; thus, it is the angiomyolipomas with scant fat that typically present for FNA biopsy (Fig. 7.3).

#### Triage

The epithelioid cells co-express melanocytic markers (HMB45, MART1) and smooth muscle markers (calponin, muscle specific actin). CD117, hormone receptors (PR, less often ER), and occasionally desmin can also be positive.

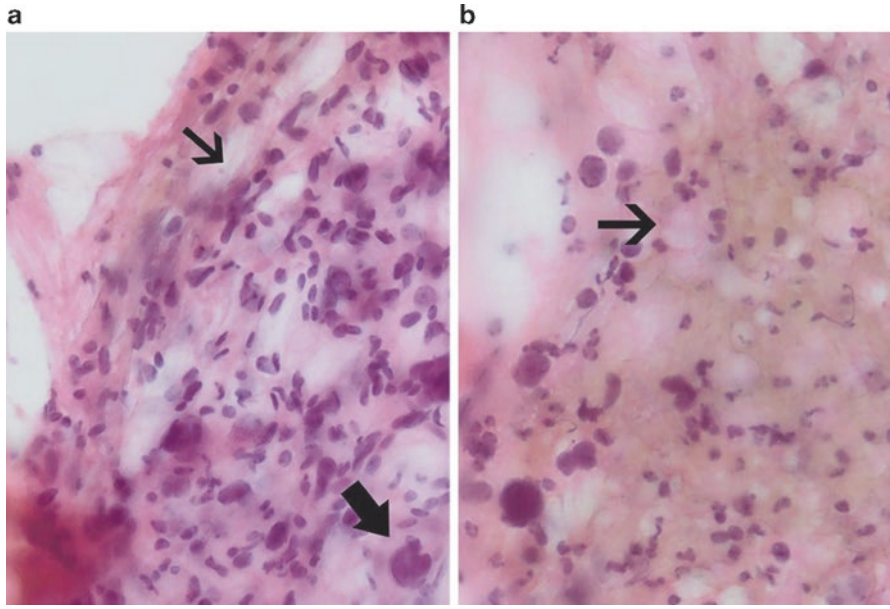


**Fig. 7.3** Angiomyolipoma in kidney (**a**, **b**. Papanicolaou stain, high power). Aspirates from this renal mass in a 12-year-old girl show thick-walled blood vessels (**a**, *thin arrow*) and naked nuclei of smooth muscle cells (**a**, *thick arrow*) with fat globules (**b**, *arrow*).

### Differential Diagnosis

When aspirates contain few or no HMB45-positive epithelioid cells, angiomyolipoma may be mistaken for sampling of normal kidney and surrounding soft tissue. When epithelioid cells predominate and/or have significant cytologic atypia and pleomorphism, differential diagnostic considerations include carcinoma and metastatic melanoma. Soft tissue neoplasms (e.g., lipoma) form part of the differential diagnosis.

### Pearls

Positivity for melanocytic markers is characteristic of angiomyolipoma and should not be misinterpreted as evidence of melanoma.

## 7.1.4.2 Wilms Tumor (Nephroblastoma)

### Clinical Features

Wilms tumor is among the most common solid organ tumors of childhood and the most common pediatric renal tumor. It occurs throughout childhood but is usually diagnosed before the age of 5 years and occurs equally in both sexes. Wilms tumor can be sporadic or occur with nephroblastomatosis, or in children with syndromes such as Beckwith–Wiedemann, WAGR (Wilms tumor, Aniridia, Genitourinary abnormalities, and mental Retardation due to chromosome 11p13 (*WT-1* gene) deletion), and Denys–Drash syndromes. Children usually present with a painless flank or abdominal mass or abdominal pain. Hematuria, elevated blood pressure, or fever may be observed [1, 4].

### Cytological Features

The cytomorphology of Wilms tumor recapitulates the embryologic development of the kidney, represented by blastema, mesenchyme, and epithelium (Figs. 7.4 and 7.5).

- Blastemal component: Blastema yields a cellular background of small round blue cells. The cells are small and primitive, about twice the size of a lymphocyte, with a high nuclear cytoplasmic (N/C) ratio and minimal, scanty, fragile cytoplasm. The nuclei have finely granular chromatin with inconspicuous nucleoli. Nuclear molding may be seen. Necrosis may be present in the background (Fig. 7.4).
- Epithelial component: The epithelial component is best identified on scanning power as aggregates of tumor cells forming ill-defined clusters, tubules, and nests. The epithelial component has well-defined edges. The cells are larger than the background blastemal cells, with more cytoplasm, and may be attached to metachromatic basement membrane-like material. Tubules may demonstrate branching [1]. Occasionally, rosettes are seen; however, unlike neuroblastoma, there is no associated eosinophilic fibrillary neuropil. Glomeruloid-like bodies can be observed. These are made up of tumor cells, not the bland-appearing balls of cells that make up normal glomeruli (Fig. 7.5).
- Mesenchymal component: The mesenchymal spindle cell component is comprised of bland fibroblast-like cells set in fibrous or metachromatic myxoid stroma. Occasionally, smooth muscle or skeletal muscle differentiation may be seen.
- One, two, or three components may be present. If only blastema is aspirated, differentiation from other small round cell tumors is based on immunoperoxidase stains. A variety of heterologous elements, such as squamous or mucous epithelium, endocrine cells, neuroglial components, osteoid, and cartilage, can be also present, and such tumors are referred to as teratoid Wilms tumor.
- Anaplasia: Approximately 4% of Wilms tumors demonstrate a triad of microscopic features diagnostic of anaplasia. These changes can be focal or diffuse and thus may not be seen in the aspirate due to sampling. The features of anaplasia, which can be seen even under scanning at low power, are as follows: enlarged nuclei (at least three times the size of adjacent tumor nuclei), nuclear hyperchromasia, and abnormal or multipolar mitotic figures. All three features must be present for the diagnosis of anaplasia (Fig. 7.6). Although definitive classification of anaplasia as focal or diffuse is not possible in cytologic prepara-

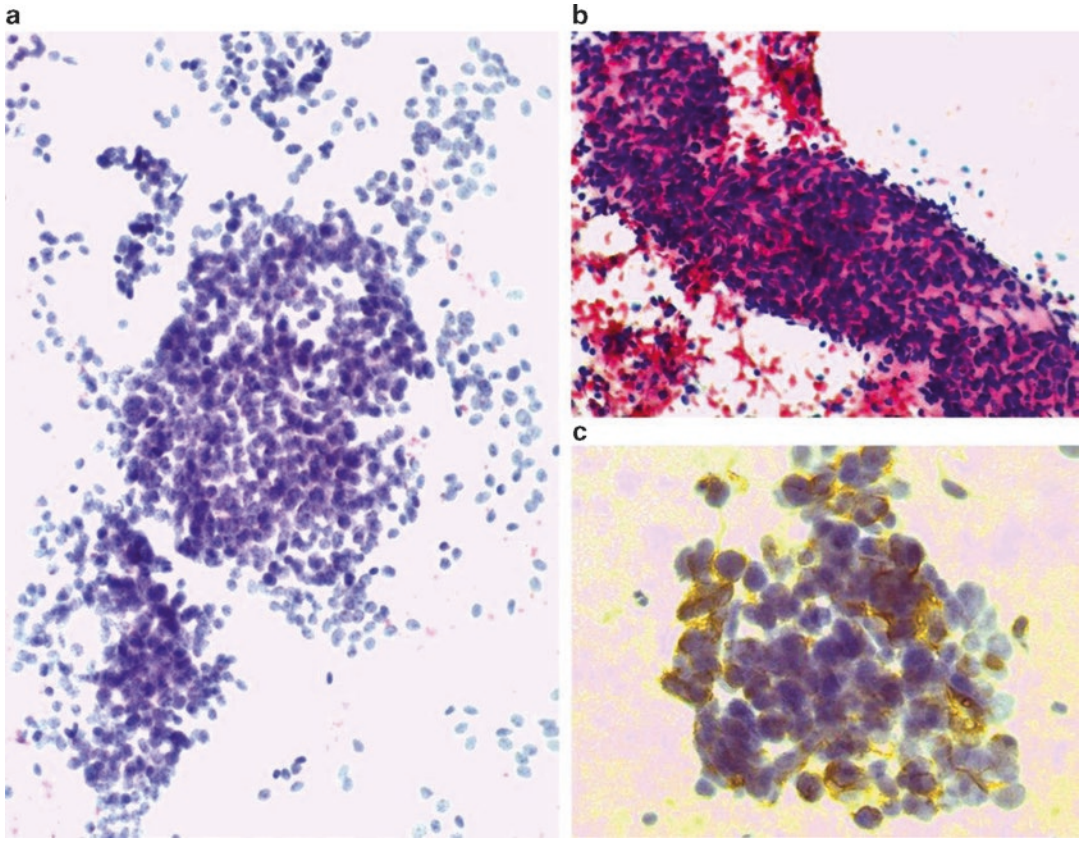


**Fig. 7.4** Wilms tumor (**a**. Papanicolaou stain, medium power; **b**. H&E stain, medium power; **c**. WT1 immunoperoxidase stain, high power). The aspirates show a blastemal component comprised of small round cells with minimal cytoplasm (**a**). Bland spindle cells (**b**) that constitute the mesenchymal component can also be seen. Positive WT1 immunostaining is demonstrated in the blastemal component (**c**).

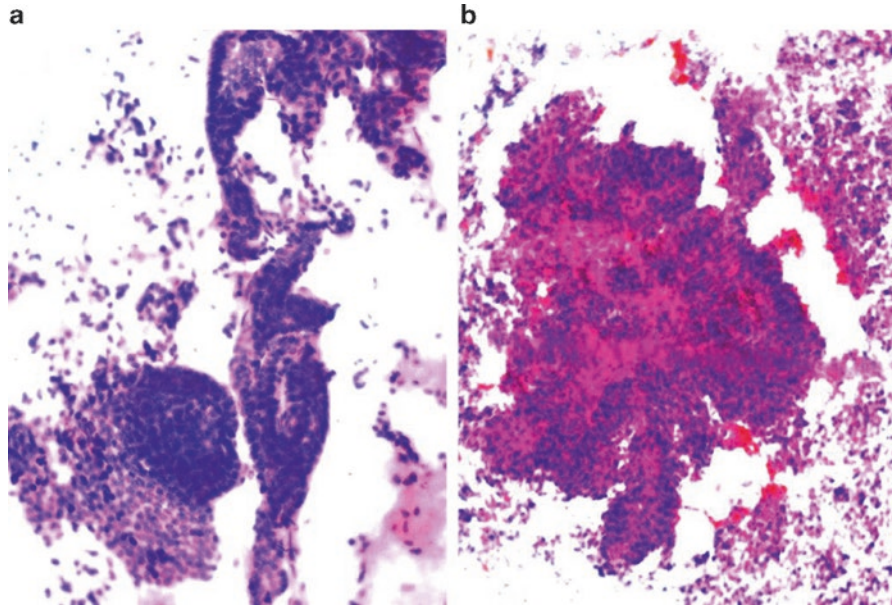


**Fig. 7.5** Wilms tumor with prominent epithelial component (**a**. Papanicolaou stain, medium power; **b**. Diff-Quik stain, medium power). The epithelial component can form tubules (**a**), and the cells may be attached to a metachromatic, basement membrane-like material (**b**). Please note the well-defined edges of the epithelial component.

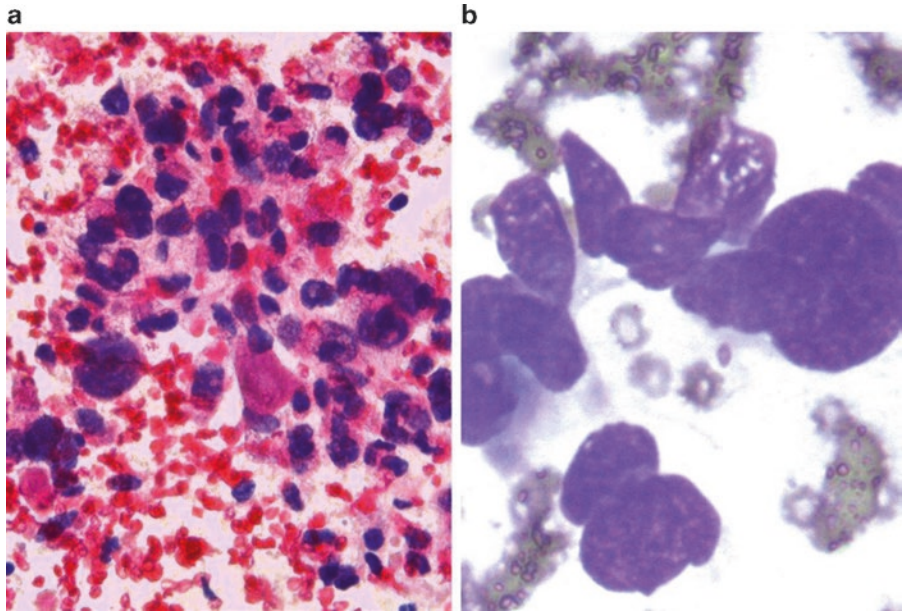


**Fig. 7.6** Wilms tumor showing anaplasia (**a**. Papanicolaou stain, high power; **b**. Diff-Quik stain, high power). Enlarged and hyperchromatic nuclei are observed in this Wilms tumor with anaplasia.

tions, it is important to recognize and comment on the presence of any anaplasia, thereby alerting the oncologist to the possibility of diffuse anaplasia which is associated with a worse prognosis.

## Triage

Ancillary studies are helpful, particularly if the blastemal component predominates, in order to exclude other small round blue cell tumors. All components of a Wilms tumor may show nuclear positivity for WT1, albeit weak in the stromal component. However, WT1 expression is not seen in all Wilms tumors and is not restricted to Wilms tumors. The blastemal component is also positive for vimentin and may show positivity (±) for neuron-specific enolase (NSE), desmin, cytokeratin, and CD56. The epithelial component is positive for EMA and cytokeratin. Staining of the mesenchymal component varies according to its morphologic appearance and differentiation. For example, cells with skeletal muscle differentiation are usually myogenin positive. Material can also be submitted for cytogenetic studies to demonstrate abnormalities of the Wilms tumor (*WT*) genes 1 (chromosome 11p13) and 2 (chromosome 11p15). Mutations in *TP53* are seen with high frequency in the anaplastic subtype of Wilms tumor. Electron microscopy can also be used to demonstrate epithelial differentiation (such as intercellular junctions, basement membrane-like material, oligocilia, and microvilli) and exclude other small round cell tumors, such as neuroblastoma and rhabdomyosarcoma, by demonstrating a lack of neurosecretory granules and muscle fibrils, respectively.

## Differential Diagnosis

The differential diagnosis, particularly for those tumors with a predominant blastemal component or round blue cell morphology, is presented in Table 7.2. Wilms tumor cannot be distinguished cytologically from nephroblastomatosis and nephrogenic rests, which are aggregates of persistent primitive metanephric tissue. When microscopic in size, these aggregates are termed rests and, when large, nephroblastomatosis. As the metanephric tissue is primitive, aspiration of nephroblastomatosis will be indistinguishable from nephroblastoma on cytology. Children with nephroblastomatosis are at a markedly increased risk for the development of nephroblastoma. The diagnosis is made by radiological confirmation

**Table 7.2** Differential diagnosis of small round cells on renal and perirenal FNA

| | Cytomorphology | Ancillary tests | Comments |
|---|---|---|---|
| Wilms tumor | Blastema: ±rosettes, no neuropil, bland unless anaplasia present.<br>Epithelial component: tubules, aggregates, glomeruloid bodies.<br>Stroma: bland, fibroblast-like, ±smooth, or skeletal muscle differentiation ±heterologous elements. | Immunostains: WT1+ (weak in stroma), EMA+ (epithelial component), desmin (blastemal component). Stromal stains according to differentiation.<br>Cytogenetics: *WT1* or *WT2* gene abnormalities. | Blastema can be CD56+, vimentin+, desmin+. Both Wilms tumor and neuroblastoma can demonstrate CD56 positivity. |
| Neuroblastoma | Background neuropil, ±calcification. Single-lying cells, syncytia, rosettes, ±ganglion cells, ±Schwann cells. | Immunostains: +neuroendocrine markers (e.g., synaptophysin, chromogranin, CD56) and +PGP9.5.<br>Cytogenetics: ±*MYCN* amplification. | Clinically patients present with more systemic symptoms and appear ill, compared to a child with Wilms tumor.<br>Compared to Ewing/PNET: younger age, neuropil, and rosettes more frequent, ganglion cells, no tigroid background, -CD99. |
| Rhabdomyosarcoma | Single cells and syncytial fragments, bi- and multinucleation, ±cells with more abundant cytoplasm, ±strap cells. | Immunostains: +desmin, myogenin, myoD1.<br>Cytogenetics: t(2;13) and t(1;13) in alveolar subtype. | Exclude muscle differentiation in Wilms tumor. Can show focal immunopositivity for neuroendocrine markers, CK, actin, CD99. |
| Ewing sarcoma/PNET | ±Tigroid background, dyscohesive and loose/tightly cohesive groups, vacuolated cytoplasm, ±rosettes, ±neuropil. | Immunostains: +neuroendocrine markers, +CD99, +FLI-1. Cytogenetics: *EWSR1* translocations, such as t(11;22)(q24;q12) | Less neural differentiation than neuroblastoma. |
| Desmoplastic small round cell tumor | Metachromatic stromal fragments, cytoplasmic vacuoles, ±oval-spindle cells. | Immunostains: +epithelial (EMA), neural (NSE) and muscle (desmin with dot-like staining) markers, and +WT1.<br>Cytogenetics: t(11;22)(p13;q12). | Tend to occur in males, second to fourth decade. |
| Hematolymphoid malignancies | Includes non-Hodgkin lymphomas, Hodgkin lymphomas, and leukemias. Morphology depends on type, but typically shows dyscohesive cells with lymphoglandular bodies. | Immunostains: +lymphoid markers, ±EMA. Flow cytometry, cytogenetics, other stains depend on type. | Dyscohesion and presence of lymphoglandular bodies help distinguish from other small round cell tumors. |
| Synovial sarcoma (round cell variant) | Oval, hyperchromatic nuclei, ±bean-shaped nuclei, coarse chromatin, multiple nucleoli. | Immunostains: +CK, +EMA, +TLE1, ±CD99.<br>Cytogenetics: t(x;18). | Any age but more common in late adolescence/young adults. |
| Osteosarcoma (small cell variant) | Small-/intermediate-sized cells, cytoplasmic vacuoles, mitotic figures, karyorrhectic debris. | Immunostains: ±CD99, most others including FLI1 are negative.<br>Cytogenetics: lack of *EWS* gene rearrangement | Osteoid may be scanty or absent on FNA. |
| Myxopapillary ependymoma | Background myxoid material, papillary fragments, ±rosettes, bland cells. | Immunostains: +GFAP, +S100, +EMA, ±CK, −synaptophysin. | Seen more frequently in adults compared to classic ependymoma which is seen in children. |
| Small-cell neuroendocrine tumor | Granular chromatin, occasional larger cells ("endocrine atypia"), nuclear molding. | Immunostains: +neuroendocrine markers, −muscle and −epithelial markers. | Older age group. |
| Metanephric neoplasm | Small bland cells, high nuclear-to-cytoplasmic ratio, tight clusters, ±glomeruloid bodies, ±psammoma bodies, ±rosettes, ±metachromatic stroma. | Immunostains: +CK, +vimentin, ±WT1, +CD57, PAX2. Cytogenetics: *BRAF* V600E mutation | Usually seen in adult females but has been described in children. |

of the subcapsular location and diffuse nature of the process. It is noted that 30 % of kidneys containing Wilms tumor have foci of nephroblastomatosis, which also show *WT-1* mutations.

#### Pearls

FNA of a flank mass in a child is usually performed via the flank or posterior approach since the kidney is a retroperitoneal structure. Theoretically, it is possible that an anterior approach may lead to the spread of tumor to the peritoneum and upstage a potentially curable childhood neoplasm.

Another tumor in the differential diagnosis, particularly in older patients is metanephric adenoma, which shows positivity for BRAF V600E mutations, and is less likely to have a triphasic morphology.

### 7.1.4.3 Cystic, Partially Differentiated Nephroblastoma

#### Clinical Features

This is a rare, cystic neoplasm occurring in early infancy or young children, almost always under the age of two. It has low malignant potential. It is also known as multilocular cystic nephroma, multicystic nephroma, or multilocular cyst. This entity may represent a fully differentiated variant of Wilms tumor. Patients commonly present with a mass lesion or ureteral obstruction. Radiological evaluation reveals a large, solitary, well-circumscribed multilocular cystic mass.

#### Cytological Features

Aspirates tend to be of low cellularity with variable representation of epithelial, stromal, and nephroblastomatous elements. Benign-appearing epithelial cells are arranged singly and in sheets. Bland spindle cells, with or without skeletal muscle differentiation, are generally present in sparse numbers. The background stroma can be myxoid in nature, or have other mesenchymal components such as cartilage and fat.

#### Triage

Electron microscopy reveals epithelial cells with long cilia suggestive of collecting tubular cells, while cytogenetics shows nonrandom X-chromosome inactivation. Liquid-based cytology may be of benefit in these cases to concentrate the cells available for evaluation in this cystic neoplasm.

#### Differential Diagnosis

Benign or hemorrhagic cysts of the kidney or retroperitoneum should be considered.

#### Pearls

The presence of any solid nodules radiologically favors cystic Wilms tumor rather than cystic, partially differentiated nephroblastoma or cystic nephroma [1].

### 7.1.4.4 Clear Cell Sarcoma

#### Clinical Features

This is an uncommon but aggressive childhood renal tumor with a poor prognosis. It comprises approximately 5 % of childhood renal tumors, with a peak incidence at 2–3 years of age, and is seen more frequently in boys [1, 4]. It has a propensity to spread to bones, often skull, as well as to soft tissue, orbit, and brain. Children usually present with an abdominal mass. Abdominal pain, fever, hematuria, and hypertension may also be noted. Radiological imaging shows a renal tumor, usually in the medulla or central region.

#### Cytological Features

These tumors are well circumscribed and commonly show cystic change. Several variants of this tumor are noted; thus, the cytomorphology varies accordingly (Fig. 7.7). In general, the aspirates are cellular and show two cell types, including stellate or spindled tumor cells (“septal cells”) arranged singly in a myxoid background and polygonal tumor cells (“cord cells”) in clusters with pale cytoplasm. Nuclei are generally bland, round, oval, or reniform with finely granular chromatin and inconspicuous nucleoli. Nuclear grooves, when present, are a useful clue to the diagnosis. Myxoid or mucoid material may be seen in the background [8, 9].

#### Triage

On immunocytochemistry, these tumors are positive for vimentin and bcl-2 and negative for WT1,

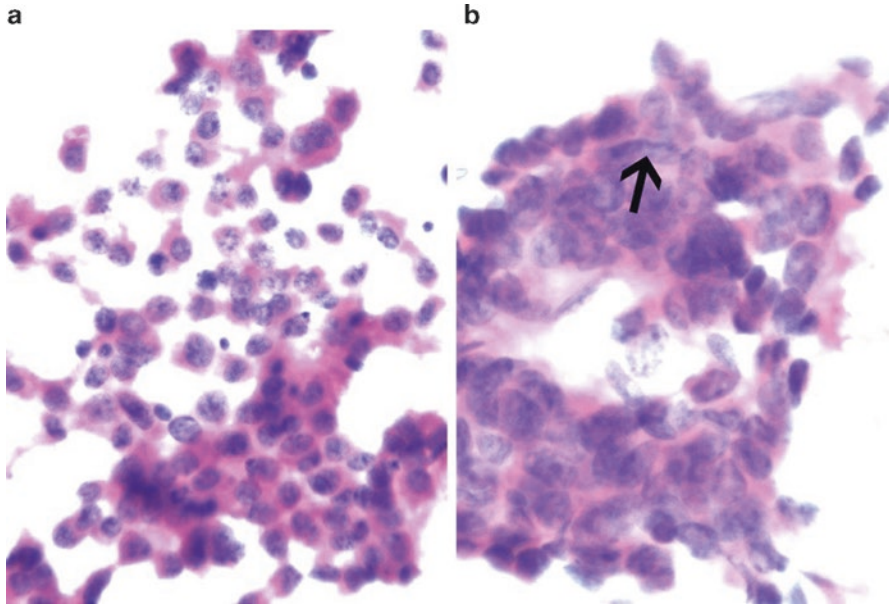


**Fig. 7.7** Clear cell sarcoma of the kidney (**a**. Papanicolaou stain, medium power; **b**. Papanicolaou stain, high power). The aspirates show dyscohesive and cohesive clusters of stellate and polygonal cells, in addition to bare nuclei. The nuclei are round to oval with very occasional nuclear grooves (**b**, *arrow*).

EMA, CD34, S-100, desmin, CD99, and synaptophysin. Ultrastructurally, the tumor cells have a high nuclear-to-cytoplasmic ratio, with thin complex cytoplasmic extensions surrounding extracellular matrix. Intermediate filaments are present in the cytoplasm. Fluorescent in situ hybridization (FISH) studies may show a t(10;17) translocation or a chromosome 14q deletion [10].

#### Differential Diagnosis

Tumors in the perirenal area that may exhibit nuclear grooves include clear cell sarcoma, renal cell carcinoma, renal medullary carcinoma, Langerhans cell histiocytosis, epithelioid hemangioendothelioma, and metastases to the kidney (e.g., papillary thyroid carcinoma, granulosa cell tumor, and solid pseudopapillary neoplasm of the pancreas). Given the variations in morphology of clear cell sarcoma, a wide variety of tumors enters the differential diagnosis, although, in practice, many of these are unlikely based on age at presentation or other clinical considerations. A summary of the differential diagnostic considerations is listed in Tables 7.2, 7.3, and 7.4.

### 7.1.4.5 Mesoblastic Nephroma

#### Clinical Features

Mesoblastic nephroma is the most common renal tumor of infancy. It can be seen within a few days of birth, with most diagnosed before 6 months of age. The vast majority are cured by nephrectomy alone. Age at diagnosis (<3 months old) and adequate surgical resection are the most important favorable prognostic features rather than the presence or absence of a cellular subtype on microscopic evaluation. Patients usually present with an abdominal mass. Radiological studies confirm a kidney tumor, often in the region of the hilum. These tumors are commonly well circumscribed and solid. However, infiltration of adjacent renal parenchyma or perirenal fat, hemorrhage, necrosis, and cystic change can occur, particularly in the cellular variant [1, 4].

#### Cytological Features

Three main subtypes are described: classic, cellular, and mixed (Fig. 7.8). Smears are generally paucicellular, comprised of spindle cells lying both singly and in cohesive clusters. The prolifer-

**Table 7.3** Differential diagnosis of cells with moderate to abundant cytoplasm on renal and perirenal FNA

| | Cytomorphology | Ancillary tests | Comments |
|---|---|---|---|
| Clear cell sarcoma | Background mucoid/myxoid, polygonal-to-stellate or spindle cells, pale cytoplasm, round, oval or reniform nuclei, nuclear grooves. | Immunostains: +vimentin, +bcl-2, −WT1, −EMA, −CD34, −desmin, −synaptophysin. | Propensity to spread to bones, especially skull. |
| Rhabdoid tumor | Well-defined abundant cytoplasm, cytoplasmic rhabdoid inclusion, large eccentric nuclei, prominent nucleoli, bare nuclei. | Immunostains: +vimentin, +desmin, +EMA, +keratin, −INI1, −WT1<br>Cytogenetics: *INI1* mutations/deletions. | Cytoplasmic inclusions can trap antibodies, resulting in false-positive immunostaining. |
| Rhabdomyosarcoma | Small round cells with minimal cytoplasm in addition to larger, more pleomorphic cells with moderate to abundant orangeophilic cytoplasm, spindle and strap cells, bi- and multinucleation. | Immunostains: +desmin, myogenin, myoD1.<br>Cytogenetics: t(2;13) or t(1;13) in alveolar subtype. | Cytoplasmic cross-striations should be looked for in rhabdomyosarcoma to help distinguish it from rhabdoid tumor where cross-striations are lacking. Cytoplasm is dense rather than granular/vacuolated as seen in several other tumors in this area. |
| Renal cell carcinoma | Nests, trabeculae, papillary structures, low N/C ratio, abundant clear or orangeophilic cytoplasm, granular chromatin, prominent nucleoli. | Immunostains: +CD10, +RCC marker, +CA IX, ±TFE3, ±vimentin, ±AE1/AE3.<br>Cytogenetics: t(X;17)(p11.2;q25.3) or t(X;1)(p11.2; q21) in translocation RCC. | Many pediatric RCC are Xp11.2 translocation RCC. |
| Renal medullary carcinoma | Inflammation and necrosis in background, single cells and loose clusters, vacuolated cytoplasm, hyperchromatic irregular nuclei, neutrophils. | Immunostains: +CK7, -CK20, +vascular endothelial growth factor, +nuclear p53. | Associated with sickle cell trait. Seen most often in adolescent - young adult males. |
| Adrenal cortical neoplasm | Clean/foamy background, naked nuclei, cells with abundant vacuolated cytoplasm lying singly and in loosely cohesive structures, occasional larger, pleomorphic cells. | Immunostains: +inhibin, +Melan A, +calretinin, +vimentin, ±synaptophysin, −chromogranin. | CD10, inhibin, Melan A, and calretinin are useful markers to distinguish adrenal cortical neoplasms from renal cell carcinoma. |
| Pheochromocytoma | Background of blood, necrosis, or cystic degeneration. Single-lying cells, loose clusters, syncytia, ±rosettes. Cells round to spindled, variable amounts of granular cytoplasm. Red cytoplasmic granules may be seen on Diff-Quik stain, granular chromatin, occasional larger pleomorphic cells. | Immunostains: +synaptophysin, +chromogranin, −inhibin, −Melan A, −calretinin, ±vimentin. | Can demonstrate ganglion cells but does not have a blastemal component seen in neuroblastoma. |
| Ganglioneuroblastoma | Large, polygonal-shaped cells, abundant granular cytoplasm, large hyperchromatic nuclei, prominent nucleoli, ±bi- or multinucleated. Small round cell component and Schwann cells may be seen. | Immunostains: +Synaptophysin, +chromogranin, +CD56. | Ganglion cells may also be seen in ganglioneuromas, gangliocytic paragangliomas, pheochromocytoma, neural ganglia. |
| Angiomyolipoma | Epithelial cells, adipocytes, thick-walled blood vessels, smooth muscle cells. | Immunostains: +HMB45, +Melan A, +smooth muscle markers, −CK. | Can be associated with tuberous sclerosis. |

**Table 7.4** Spindle cells in the renal and perirenal area

| | Cytomorphology | Ancillary tests | Comments |
|---|---|---|---|
| Wilms tumor (mesenchymal predominant) | Bland fibroblast-like cells, fibrous or metachromatic myxoid stroma. Variable smooth or skeletal muscle differentiation. | Immunostains: ±WT1, staining according to differentiation (e.g., skeletal muscle, +myogenin; smooth muscle, +SMA). | Blastema or epithelial component usually observed, albeit in small quantities. |
| Mesoblastic nephroma | Two patterns: Classic (paucicellular, spindle cells lying singly and in cohesive clusters, bland nuclei, scanty eosinophilic cytoplasm. The proliferating cells can acquire features of fibroblasts, myofibroblasts, or smooth muscle cells) and cellular (increased cellularity, atypia, ±hemorrhage, ±necrosis). | Immunostains: +vimentin, +actin, ±WT1, −desmin, −CD34, −keratin Cytogenetics: classic variant is diploid, while the cellular variant shows t(12; 15) (p13; q25). | The two patterns (classic and cellular) can co-exist. |
| Rhabdomyosarcoma | Spindle and strap cells, dense cytoplasm, ±cross-striations in cytoplasm. | Immunostains: +desmin, +myogenin, +myoD1+, −CK, −neuroendocrine. | Look for small round cell component. |
| Renal cell carcinoma (sarcomatoid variant) | Striking pleomorphism, irregular nuclear outlines, granular chromatin, conspicuous nucleoli, osteoclast-like giant cells. | Immunostains: +CK, +vimentin, +CD10, +PAX8, +RCC marker. | Any renal cell carcinoma can undergo sarcomatoid change. Usually see “epithelioid” renal cell carcinoma together with spindled cells. |
| Ossifying renal tumor | Composed of osteoid, osteoblasts, and spindle cells. | Immunostains: +EMA, +vimentin, −CK. | Extremely uncommon. Hematuria usually present. |
| Metanephric renal tumors | Range from pure spindle to pure epithelial components Epithelial component: bland, high N/C ratio, tubules/papillae/glomeruloid bodies, ±psammoma bodies Stromal component: bland, pointed hyperchromatic nuclei, ill-defined cell borders. | Immunostains: Epithelial: +WT1, +CK, +CD57, −EMA, −AMACR Stroma: +vimentin, +fibronectin, +CD34, −actin, −desmin. | Include metanephric adenoma (epithelial), metanephric stromal tumor (stromal), metanephric adenofibroma (mixed epithelial-stromal). |
| Clear cell sarcoma (spindle cell variant) | Myxoid stromal fragments, arborizing vasculature, septal cells. | Immunostains: +vimentin, +bcl-2, −WT1, −EMA, −CD34, −desmin, −synaptophysin Cytogenetics:±t (10; 17), ±14q deletion. | Look for blastema and epithelial component to distinguish from mesenchymal predominant Wilms tumor. Cells appear more sarcomatous compared to mesoblastic nephroma. |
| Synovial sarcoma (monomorphic fibrous variant) | Cohesive and dyscohesive, high N/C ratio, hyperchromatic, irregular nuclear outlines, multiple nucleoli, ±comma-shaped nuclei (Fig. 7.11) | Immunostains: EMA+ (epithelioid cells), bcl-2+ (spindle cells), CD99+. Cytogenetics: t(X:18). | Need to distinguish from sarcomatoid renal cell carcinoma and other sarcomas. |
| Ganglioneuroma | Schwann (spindled cells with wavy nuclei) and ganglion cells in a fibromyxoid or collagenous background. | Immunostains: +NSE, +synaptophysin, +S100, −CK, −actin. | Neuroblasts, necrosis, and mitotic figures are absent. |

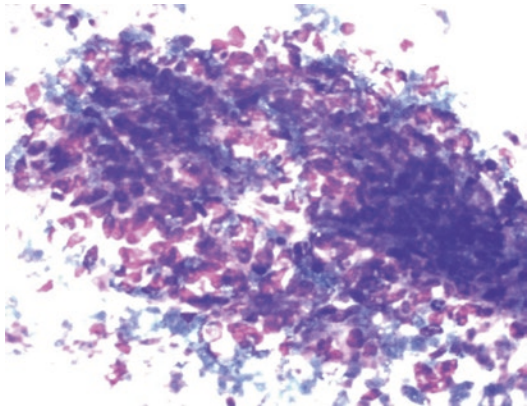

**Fig. 7.8** Mesoblastic nephroma (Diff-Quik stain, high power). Cohesive clusters of spindle cells with bland nuclear features and scanty cytoplasm are seen in this FNA in a 40-day-old girl with mesoblastic nephroma.

ating cells can acquire features of fibroblasts, myofibroblasts, or smooth muscle cells. The spindle cells have bland nuclei and scant eosinophilic cytoplasm with ill-defined borders. The nuclei show minimal atypia and coarse chromatin. On the Diff-Quick stain, a small amount of fibromyxoid material can usually be seen. Rarely, heterologous elements such as cartilage may be present. Cellular mesoblastic nephroma is a variant of mesoblastic nephroma showing increased cellularity and atypia. Hemorrhage and necrosis can be observed.

#### Triage

On immunoperoxidase staining, mesoblastic nephromas are positive for vimentin, actin, and occasionally WT1. Desmin, CD34, and keratin are negative. Features of fibroblasts or myofibroblasts are seen on electron microscopy. The classic mesoblastic nephroma is diploid, while the cellular variant shows t(12;15) (p13;q25), which results in a fusion of the *ETV6* and *NTRK3* genes. This is also seen in infantile fibrosarcoma, but is not present in fibromatosis. This supports the analogy between cellular mesoblastic nephroma and infantile fibrosarcoma, and between classic mesoblastic nephroma and infantile fibromatosis.

#### Differential Diagnosis

Table 7.4 highlights other pediatric renal tumors that can show a predominance of spindled cells.

#### Pearls

Entrapped or adjacent benign tubules or glomeruli may be aspirated together with the mesoblastic nephroma and should not be over-interpreted as an epithelial component of a Wilms tumor.

### 7.1.4.6 Rhabdoid Tumor

#### Clinical Features

This is a rare, but aggressive, childhood tumor of the kidney. Rhabdoid tumors can be renal or extrarenal. The mean age at diagnosis is 1 year, with the vast majority of patients presenting by 2 years of age. Patients commonly present with hematuria, fever, or metastases. Tumors are typically large and circumscribed with extensive hemorrhage and necrosis and almost always involve the medullary region [1, 11].

#### Cytological Features

The aspirate is usually cellular with tumor cells arranged singly or in clusters. The cell population tends to be a monomorphic population of round, oval, or spindled cells. Occasional multinucleated giant cells or a component of small, round, undifferentiated cells may be seen. The nuclei are characteristically large, single, and eccentric with vesicular chromatin and prominent macronuclei. Naked nuclei are common. The cytoplasm is well-defined and abundant. Variable numbers of characteristic "rhabdoid" inclusions, comprised of large, intracytoplasmic, dense eosinophilic hyaline globules, are present. These abut and displace the nucleus laterally resulting in a plasmacytoid appearance.

#### Triage

On immunoperoxidase staining, rhabdoid tumor is positive for vimentin, desmin, EMA, and keratin. The tumor cells are negative for INI1 and WT1. However, the whorls of intracytoplasmic filaments that make up the hyaline inclusions can cause nonspecific trapping of antibodies and give a wide range of false-positive results on immunocytochemistry. Cytogenetic studies show deletions or mutations of the *SMARCB1*

*(INI1)* gene. The intracytoplasmic inclusion consists of whorls of intermediate filaments on electron microscopy.

#### Differential Diagnosis

Table 7.3 highlights other pediatric renal tumors that can have large epithelioid cells.

#### Pearls

Intracytoplasmic inclusions occur in a wide variety of other tumors, including Wilms tumor, mesoblastic nephroma, rhabdomyosarcoma, renal medullary carcinoma, and renal cell carcinoma, and are not specific for rhabdoid tumor. Loss of INI1 nuclear staining has also been reported in renal medullary carcinomas and is therefore not entirely specific for rhabdoid tumors, although these tumors are unlikely to be confused clinically or cytologically [12].

### 7.1.4.7 Renal Cell Carcinoma (RCC)

#### Clinical Features

Renal cell carcinoma is the second most common kidney neoplasm in the pediatric population, especially older children and adolescents. Many of these are translocation-associated RCC (approximately 20–54 %), with less common variants including papillary (approximately 20 %), clear cell (approximately 15 %), and chromophobe (approximately 5 %) [11, 13, 14]. Translocation-associated, RCC usually involves the *TFE3* gene on chromosome 11 or much less frequently the *TFEB* gene on chromosome 6. Translocation RCCs have a better prognosis compared with non-translocation RCCs and are sometimes referred to as microphthalmia transcription factor (MiT) family translocation carcinomas [13, 14]. One-third of RCCs are associated with either tuberous sclerosis, neuroblastoma, or other syndromes. Signs and symptoms include abdominal pain, hematuria, and a mass lesion.

#### Cytological Features

- Translocation-associated RCC tends to mimic clear cell or papillary renal cell carcinoma. Cells are arranged in nests, trabeculae, and papillary structures. Psammoma bodies can be seen. The cells have a low N/C ratio with abundant eosinophilic, granular, or foamy cytoplasm. In some cases, the tumor cell nuclei appear as naked nuclei due to the fragility of the vacuolated cytoplasm (Fig. 7.9a). Metachromatic material and transgressing vessels can also be seen (Fig. 7.9a, b). The nuclei contain granular chromatin and prominent nucleoli. Rare cases may show melanin pigment.
- Papillary RCC can have less cytoplasm that appears basophilic (type 1) or more abundant cytoplasm imparting an eosinophilic or oncocytic appearance (type 2).

#### Triage

On immunoperoxidase staining, TFE3 and CD10 are positive, while vimentin and AE1/AE3 staining is variable. TFE3 should show nuclear positivity (Fig. 7.9c). The negative or focal staining for epithelial markers (e.g., EMA and cytokeratin) and vimentin in a vacuolated epithelioid kidney tumor should raise the possibility of translocation-associated RCC, given that other types of RCC are typically positive for both [1, 14]. Papillary RCC is positive for CK7, which helps to distinguish it from Wilms tumor and metanephric adenoma.

#### Differential Diagnosis

Tables 7.3 and 7.4 list other pediatric renal tumors in the differential diagnosis.

#### Pearls

Clear cell sarcoma of the kidney should be distinguished from renal cell carcinoma of the clear cell type and is TFE3 negative.

### 7.1.4.8 Renal Medullary Carcinoma

#### Clinical Features

This is an uncommon tumor, most often described in adolescent and young adult African American males with sickle cell trait. It is aggressive with a poor prognosis. Patients present with hematuria, abdominal pain, weight loss, fever, and a mass lesion in the kidney [1, 11].

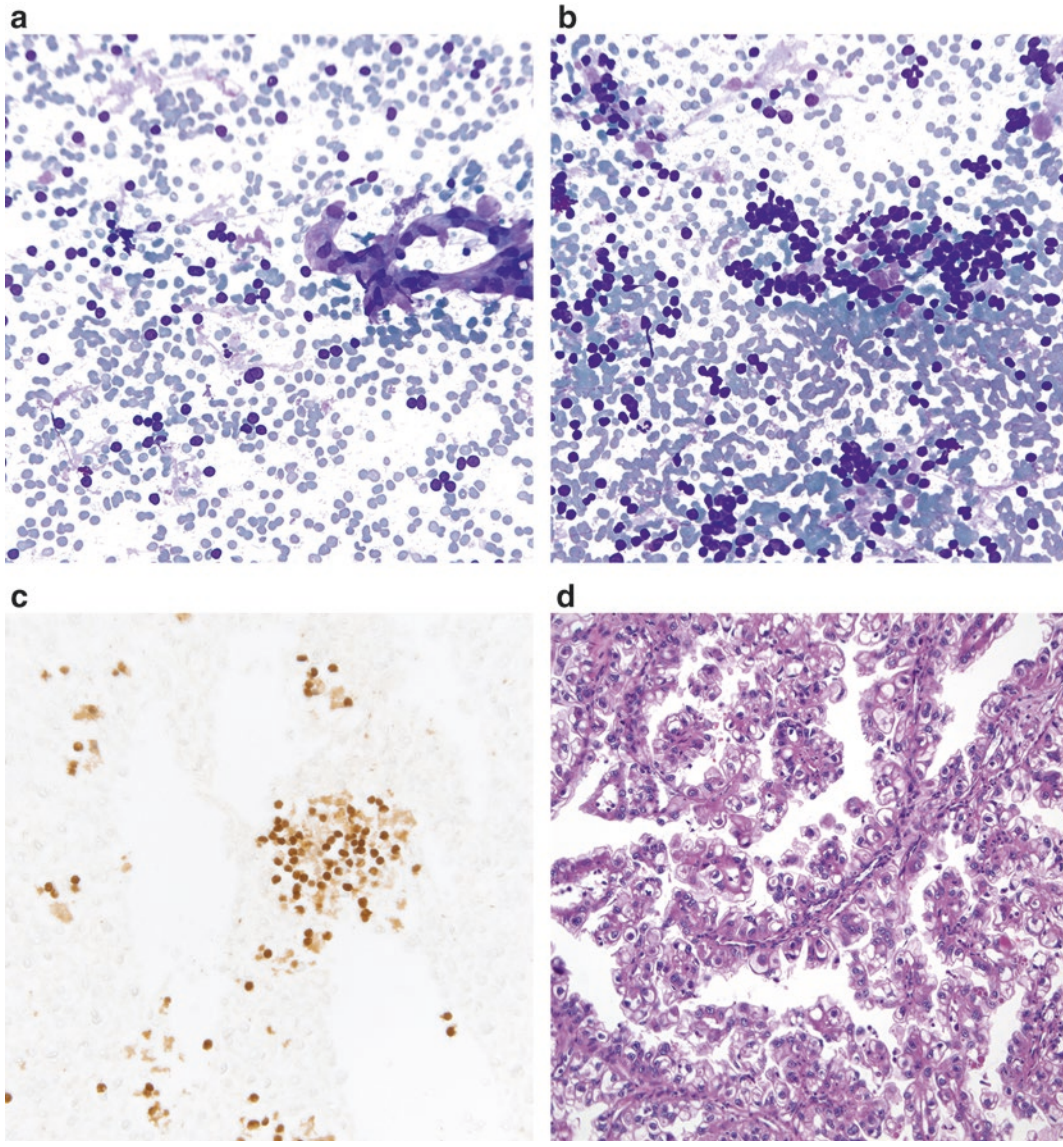


**Fig. 7.9** Renal cell carcinoma associated with translocation Xp11.2/TFE gene fusion (**a**, **b**. Diff-Quik stain, high power; **c**. TFE3 immunostain, high power; **d**. H&E stain, high power). Translocation-associated RCC shows papillary fragments or cohesive clusters of tumor cells with abundant vacuolated cytoplasm that can be stripped off creating naked nuclei (**a**). There is also usually metachromatic material (**b**), and transgressing blood vessels (**a**). A TFE3 immunostain shows nuclear positivity (**c**). Histological follow-up shows a papillary renal tumor with tumor cells having abundant clear-to-vacuolated cytoplasm (**d**). (Image courtesy of Dr. Sara Monaco).

### Cytological Features

The aspirates reveal a marked inflammatory cell infiltrate with intratumoral neutrophils. Tumor cells are seen in loosely cohesive groups or as single cells. The cells have a high N/C ratio, and the cytoplasm is vacuolated. The nuclei are hyperchromatic and irregular in shape with reniform nuclei indented by the cytoplasmic vacuoles. Nuclear grooves and rhabdoid features have also been described. Prominent, sometimes multiple, nucleoli can be seen. A variety of growth patterns can be observed including tubular, solid, yolk sac-like, adenoid cystic-like and micropapillary. Sickled red blood cells may be noted.

### Triage

Although there are no definitive immunoperoxidase stains for this renal tumor, a cell block is helpful to confirm positivity for cytokeratin and vimentin. In addition, some renal medullary carcinomas, particularly high-grade variants with rhabdoid features, can have loss of nuclear staining for INI1, as is seen in rhabdoid tumors [12]. A TFE3 stain should be negative.

### Differential Diagnosis

Table 7.3 highlights some other tumors to consider in the differential diagnosis.

### Pearls

The positivity for cytokeratin and vimentin, and negativity for TFE3, can be helpful to exclude a translocation-associated RCC. In addition, the morphology and clinical history can usually help to exclude a rhabdoid tumor in the cases of renal medullary carcinomas that show loss of nuclear staining for INI1 [12].

## 7.1.5 Secondary Tumors to the Kidney

Neuroblastoma and non-Hodgkin lymphoma are the most frequently described tumors to metastasize to the kidney in children. Lymphomas are important to recognize, as they usually do not require surgical excision (Fig. 7.10). However, many other childhood tumors (e.g., germ cell tumors) can involve the kidney, either by contiguous spread or from distant metastases. An example would be germ cell tumors metastasizing to the kidney, which can mimic certain primary renal tumors, such as renal medullary carcinoma. Spindle cell tumors, such as synovial sarcoma, can also be metastatic in the kidney and mimic a renal tumor with predominance of spindle cells (Table 7.4) (Fig. 7.11).

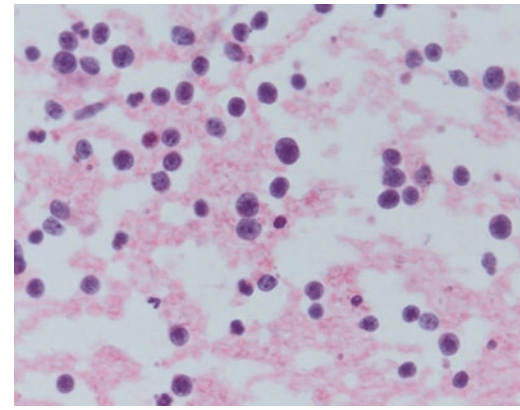

**Fig. 7.10** Diffuse large B-cell lymphoma in the kidney (Papanicolaou stain, high power). Dyscohesive malignant lymphocytes are seen in this kidney FNA in a 14-year-old girl with a known diagnosis of diffuse large B-cell lymphoma.

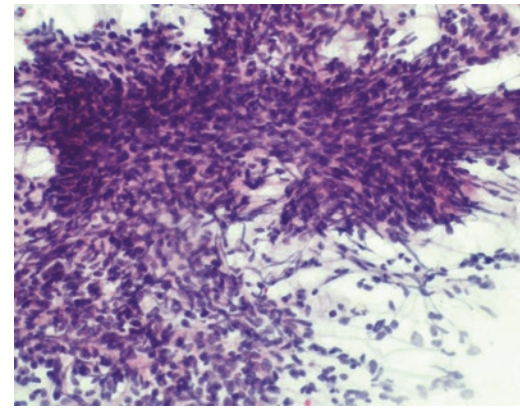

**Fig. 7.11** Metastatic synovial sarcoma in the kidney (Papanicolaou stain, medium power). The cellular aspirates from this metastasis show dyscohesive single cells and clusters of oval spindle cells, some with comma-shaped nuclei.

## 7.2 Adrenal Gland

There are two adrenal glands situated in the retroperitoneum in close proximity to each of the kidneys. The adrenal gland has a cortex and medulla. The cortex secretes glucocorticoids, mineralocorticoids, and androgens, while the medulla produces catecholamines. Adrenal disorders in children include congenital abnormalities, hyper- and hypoplasia, cysts, and inflammatory lesions and tumors, both benign and malignant. Adrenal "incidentaloma" refers to adrenal masses over 1 cm in size detected, unexpectedly, on radiological imaging. These may be functional (i.e., secrete adrenocortical or medullary hormones) or nonfunctional [1, 4].

### 7.2.1 Congenital Adrenal Lesions

Congenital adrenal lesions include congenital adrenal hyperplasia, an autosomal recessive disorder, usually due to mutations on chromosome 6p21, in addition to adrenal cytomegaly, adrenal hypoplasia, and storage diseases. Diagnosis, including neonatal screening, is typically based on biochemical assay not FNA biopsy. Some disorders are also associated with adrenal abnormalities, such as enlargement, which may raise concern for malignancy. One such example is Beckwith–Wiedemann syndrome, which is sometimes associated with adrenal enlargement and demonstrates large pleomorphic cells with cytoplasmic nuclear inclusions.

### 7.2.2 Adrenal Cysts

Adrenal cysts are not often seen in children. Symptoms of adrenal cysts include abdominal pain and palpable mass but are often asymptomatic. Adrenal cysts are occasionally functional. Several types of adrenal cysts are described:

- Endothelial or simple cysts: These are usually less than 2 cm in size and lined by flattened endothelial cells. Aspiration yields a clear or milky fluid.
- Pseudocysts: These are unilocular cysts, the cyst lining being fibrous tissue without identifiable epithelial cells. These mainly occur in children following neonatal adrenal infarction but usually resolve spontaneously within a few months. Pseudocysts may also arise in adrenal neoplasms following necrosis and hemorrhage.
- Epithelial cysts: These are lined by epithelium and may represent retention cysts, cystic adenomas, or embryonal cysts.
- Parasitic cysts: These are usually due to echinococcal (hydatid) disease.

### 7.2.3 Adrenal Infections

Various infections of the adrenal gland have been described. These include viral (e.g., herpes family of viruses), bacterial (e.g., staphylococcal spp, mycobacterial), fungal (e.g., histoplasmosis, cryptococcosis), and parasitic (e.g., strongyloidiasis, echinococcosis, amebiasis). The cytomorphology of these infections, and host response, is similar to that found elsewhere in the body. The most frequently encountered infection of the adrenal gland in children is bacterial.

### 7.2.4 Adrenal Myelolipoma

#### Clinical Features

This benign neoplasm is usually noted in older adults but has, on occasion, been described in children [15]. These are benign and can be managed conservatively without surgery, unless symptomatic.

#### Cytological Features

FNA demonstrates mature adipose tissue together with hematopoietic elements that may include erythroid and myeloid precursor cells and megakaryocytes. Large neoplasms can exhibit necrosis, calcification, and hemorrhage.

#### Differential Diagnosis

The differential diagnosis includes angiomyolipoma (fat cells, smooth muscle, thick-walled vessels, no hematopoietic precursor cells, HMB45-positive epithelioid cells), extramedullary hematopoiesis (lack of adipose tissue), teratoma (mature and immature elements of cell types other than erythroid and myeloid precursor cells), and liposarcoma (lipoblasts, no hematopoietic precursor cells).

#### Pearls

Megakaryocytes can mimic multinucleated malignant cells or giant cells, leading to a misdiagnosis of malignancy or granulomatous inflammation, respectively.

### 7.2.5 Adrenal Cortical Neoplasms

#### Clinical Features

Adrenocortical neoplasms are rare in children, comprising approximately 0.2 % of all pediatric

neoplasms. Adrenal cortical neoplasms are encountered more frequently in children with Beckwith–Wiedemann and Li–Fraumeni syndromes. Most occur in children under the age of 8 years with a female preponderance. Many adrenal cortical tumors in childhood are functional, the most common presentation being virilization. Less common manifestations are Cushing syndrome and feminization [1, 4].

### Cytological Features

Adrenal cortical hyperplasia and adenoma show identical cytomorphology. However, hyperplasia is bilateral, while adenoma usually presents as a unilateral, solitary mass. The background can be clean or foamy, without necrosis (Fig. 7.12). FNA yields a cellular specimen comprising naked nuclei and cells with low N/C ratio and abundant vacuolated cytoplasm lying singly and in loosely cohesive clusters. The nuclei are round with regular nuclear outlines, finely granular chromatin, and inconspicuous nucleoli. Occasional large, pleomorphic nuclei (so-called endocrine atypia) may be found. Adrenal cortical carcinomas tend to be unilateral and large at time of presentation. Necrosis, hemorrhage and calcification are noted in the background. Arborizing blood vessels are described. Compared to adrenal cortical adenoma, adrenal cortical carcinoma demonstrates cells that have denser, rather than finely vacuolated, cytoplasm and a less frothy background. The nuclei exhibit somewhat more pleomorphism. Fewer naked nuclei are encountered. Cells are arranged singly and in loosely cohesive groups. The cells are cuboidal, polygonal, or plasmacytoid in shape with central to eccentrically situated nuclei and variable amounts of cytoplasm. Intranuclear cytoplasmic inclusions, irregular nuclear membranes, granular chromatin, and nucleoli and mitotic figures may all be seen.

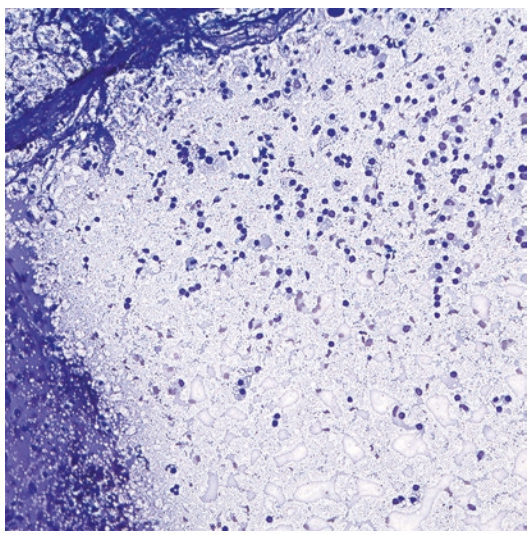

**Fig. 7.12** Adrenal cortical hyperplasia (Diff-Quik stain, low power). The aspirates from adrenal cortex typically have this abundantly vacuolated background imparting a "foamy" appearance.

### Triage

On immunoperoxidase staining, both adenomas and carcinoma are positive for inhibin, Melan A, calretinin, and vimentin. Synaptophysin is variably positive, while chromogranin is negative. Whorls of smooth endoplasmic reticulum are seen on electron microscopy.

### Differential Diagnosis

See Table 7.3. Of note, prominent cytoplasmic vacuolization is typically seen with RCC and some Burkitt lymphomas; however, in adrenal lesions, the vacuoles are more often seen in the background.

### Pearls

- It may not be possible, on cytomorphology and immunostaining, to distinguish adrenocortical hyperplasia, adenoma, and carcinoma. The term "adrenal cortical lesion/neoplasm" should then be used. The presence of metastatic disease is indicative of a carcinoma.
- Chromogranin is more helpful than synaptophysin for distinguishing an adrenal cortical tumor from pheochromocytoma, as both adrenal cortex and pheochromocytoma can be synaptophysin positive, whereas adrenal cortex is usually negative for chromogranin.
- Proliferation index, Ki-67, is much higher in adrenal cortical carcinoma, as compared to adenoma.
- Loss of heterozygosity on chromosome 11p is seen in most pediatric adrenal cortical carcinomas.

### 7.2.6 Pheochromocytoma

#### Clinical Features

Pheochromocytomas are infrequent in children but are the most common pediatric endocrine neoplasms. They arise from the chromaffin cells of the adrenal medulla (intra-adrenal paraganglioma) or extra-adrenal sympathetic or parasympathetic paraganglia (extra-adrenal paraganglioma). Many tumors secrete catecholamines and their metabolites. Compared with those in adults, pheochromocytomas in children are more likely to be familial, extra-adrenal, bilateral, and multifocal. Pheochromocytomas are associated with multiple endocrine neoplasia (MEN) type 2, von Hippel–Lindau syndrome, neurofibromatosis type 1, and familial paraganglioma syndrome. The average age of presentation in children is 11 years, and there is a male preponderance. Some children with pheochromocytoma are asymptomatic, while others present with hypertension, palpitations, headache, excessive sweating, pallor, and anxiety [1, 4].

#### Cytological Features

Blood, necrosis, or cystic degeneration can be seen in the background. The cells are seen as single cells, loose clusters, syncytia, and occasional rosettes. They are round to spindled with variable amounts of granular cytoplasm. Red cytoplasmic granules may be seen on the Diff-Quik stain. The nuclei are central or eccentrically located with granular chromatin. Multinucleation, intranuclear inclusions, and mitotic figures may be seen. Occasional nuclear pleomorphism is described; however, even in neoplasms showing very mild nuclear pleomorphism, occasional larger hyperchromatic nuclei can be noted ("endocrine atypia"). Ganglion cells that are polygonal in shape with abundant cytoplasm and prominent nucleoli may be encountered (Fig. 7.13). Amyloid is sometimes seen.

#### Triage

On immunoperoxidase stains, pheochromocytomas are positive for synaptophysin and chromogranin, while negative for inhibin, Melan A, and calretinin. There is variable vimentin staining. GATA3 is also positive in these tumors. Membrane-bound secretory granules are noted on electron microscopy. Biochemical tests include urinary and plasma catecholamines and metabolites.

#### Differential Diagnosis

Table 7.3 lists the differential diagnosis.

#### Pearls

FNA is contraindicated if a pheochromocytoma is suspected due to the risk of hypertensive crisis or hemorrhage. However, the complication rate is rare in those patients who have had an inadvertent FNA of a pheochromocytoma. The biologic behavior of a pheochromocytoma cannot be determined on cytomorphology.

### 7.2.7 Neuroblastic Tumors

#### Clinical Features

Neuroblastoma is the most frequently encountered extracranial, solid malignancy in childhood. It develops from neural crest cells in autonomic ganglia or paraganglia along the sympathetic chain, with 35 % arising in the adrenal medulla, 35 % in the extra-adrenal retroperitoneum, and 20 % in the posterior mediastinum. Other sites include cervical, paravertebral and pelvic areas. Given that the primary mass is rarely aspirated, the most common aspirates are from metastatic neuroblastoma, which commonly involves the skin, liver, bone marrow, or lymph nodes. Neuroblastoma is most often seen in children under the age of 4 years, and congenital neuroblastoma is well described. Neuroblastoma is associated with neurofibromatosis type 1, Hirschsprung disease, and Beckwith–Wiedemann syndrome. The prognosis varies greatly, depending on a number of factors including age, mitotic-karyorrhectic index (MKI), histopathologic classification (e.g., favorable vs unfavorable histology), stage of disease, *MYCN* status, and ploidy (Table 7.5). Presentation depends on the location of the tumor (e.g., mass lesion at primary tumor site), presence of secondary deposits (e.g., cutaneous metastases resulting in a "blueberry muffin" appearance, periorbital edema, and hemorrhage), secretion of catecholamines and metabolites (e.g., hypertension), and paraneoplastic phenomena (e.g., cerebellar ataxia).

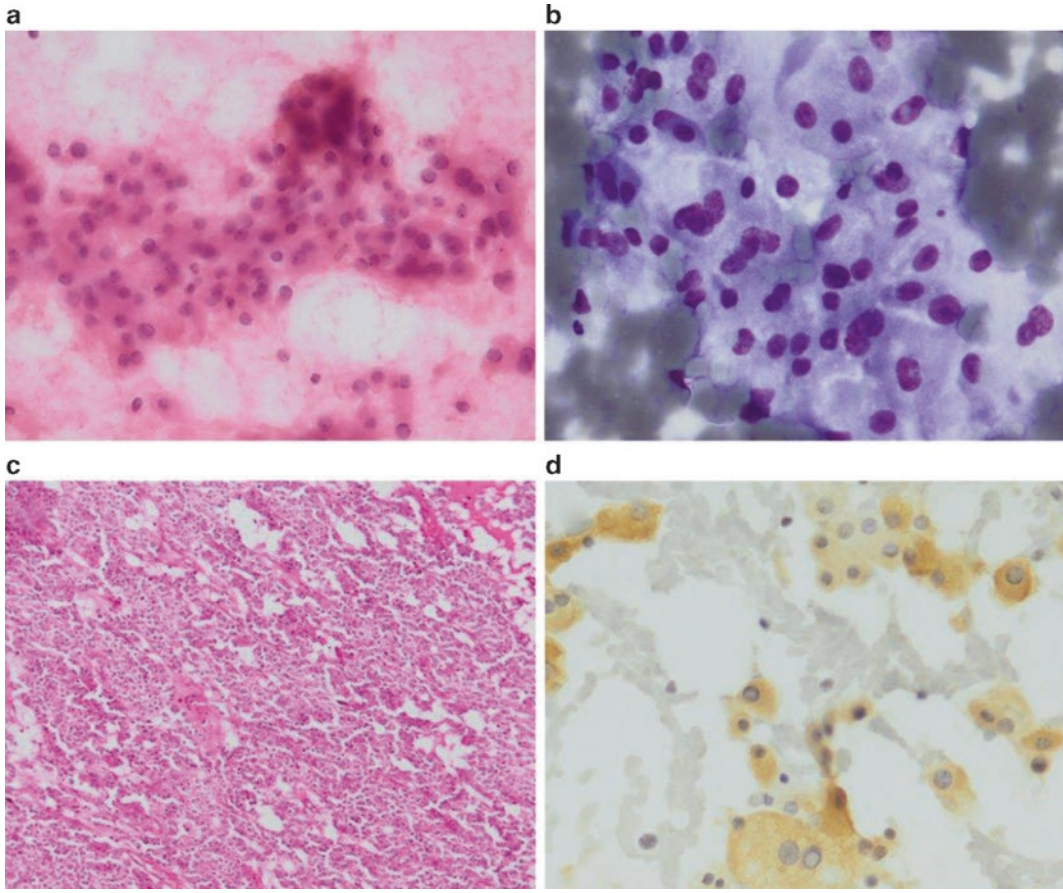


**Fig. 7.13** Adrenal pheochromocytoma (**a**. Papanicolaou stain, medium power; **b**. Diff-Quik stain, high power; **c**. H&E stain, medium power; **d**. Synaptophysin immunoperoxidase stain, high power). FNAs of pheochromocytoma show loose clusters and single cells with abundant cytoplasm (**a**, **b**), recapitulating the histomorphology (**c**). Occasional larger nuclei are present. A solid arrangement of polygonal to spindle cells with abundant, eosinophilic cytoplasm can also be seen. Positive staining for synaptophysin within tumor cells is shown (**d**).

**Table 7.5** Prognostic factors in neuroblastic tumors [1, 4, 16]

| | Risk Category | | |
|---|---|---|---|
| Factor | Low | Intermediate | High |
| Age | <1 year | Usually <1 year | 1–5 years old |
| Stage | 1, 2, 4S | Usually 3 or 4 | Usually 3 or 4 |
| Tumor morphology | Cellular differentiation or maturation, cystic variants, MKI[a] <100 or 2 % | MKI 100–200 or 2–4 % | More undifferentiated tumors, higher MKI of >200 or >4 %, positive metastases in lymph nodes on contralateral side from primary tumor |
| *MYCN* status | Normal | Normal | Amplified (>10 copies per diploid genome) |
| Ploidy | Hyperdiploid or near triploid | Near diploid or near tetraploid | Near diploid or near tetraploid |
| 17q gain | Rare | Common | Common |
| 1p LOH | Rare | Uncommon | Common |
| Overall 3-year survival | >90 % | 30–50 % | <20 % |

[a]Mitosis-karyorrhexis index (MKI) is defined as the number of tumor cells with mitotic figures and the number of cells undergoing karyorrhexis relative to the cellularity of the tumor. Usually expressed as the number of mitotic or karyorrhectic cells per 5,000 tumor cells or as a percent (<2 %, 2–4 %, or >4 %)

In congenital forms, the baby often presents as a "blueberry muffin" baby with the bluish-red cutaneous lesions and features of hydrops fetalis. A key clinical finding that can suggest a neuroblastic tumor is the presence of elevated urinary metabolites of catecholamines (vanillylmandelic acid, homovanillic acid) [1, 4, 16].

### Cytological Features

These tumors yield cellular smears with small round blue cell morphology with rosette formation (Fig. 7.14). Homer Wright rosettes appear as tumor cells surrounding a small area of neuropil. The cells are small but slightly larger than a lymphocyte, have inconspicuous nucleoli, and have scant cytoplasm, which may cause them to have nuclear molding (Fig. 7.14). The background material may reveal variable amounts of neuropil that appears as granular or fibrillary extracellular material that stains pink on Papanicolaou stain. Necrosis and calcification may also be seen. Other features to look for are comma-shaped spindle cells with cytoplasmic processes to indicate Schwannian stroma or large epithelioid polygonal-shaped cells with prominent nucleoli to indicate a gangliocytic component (Fig. 7.15). In general, neuroblastic tumors form a spectrum ranging from tumors with neuroblasts and scant-to-absent Schwannian stroma (neuroblastoma) to tumors with neuroblasts, in addition to ganglion cells and Schwannian stroma (ganglioneuroblastoma), and tumors dominated by Schwannian

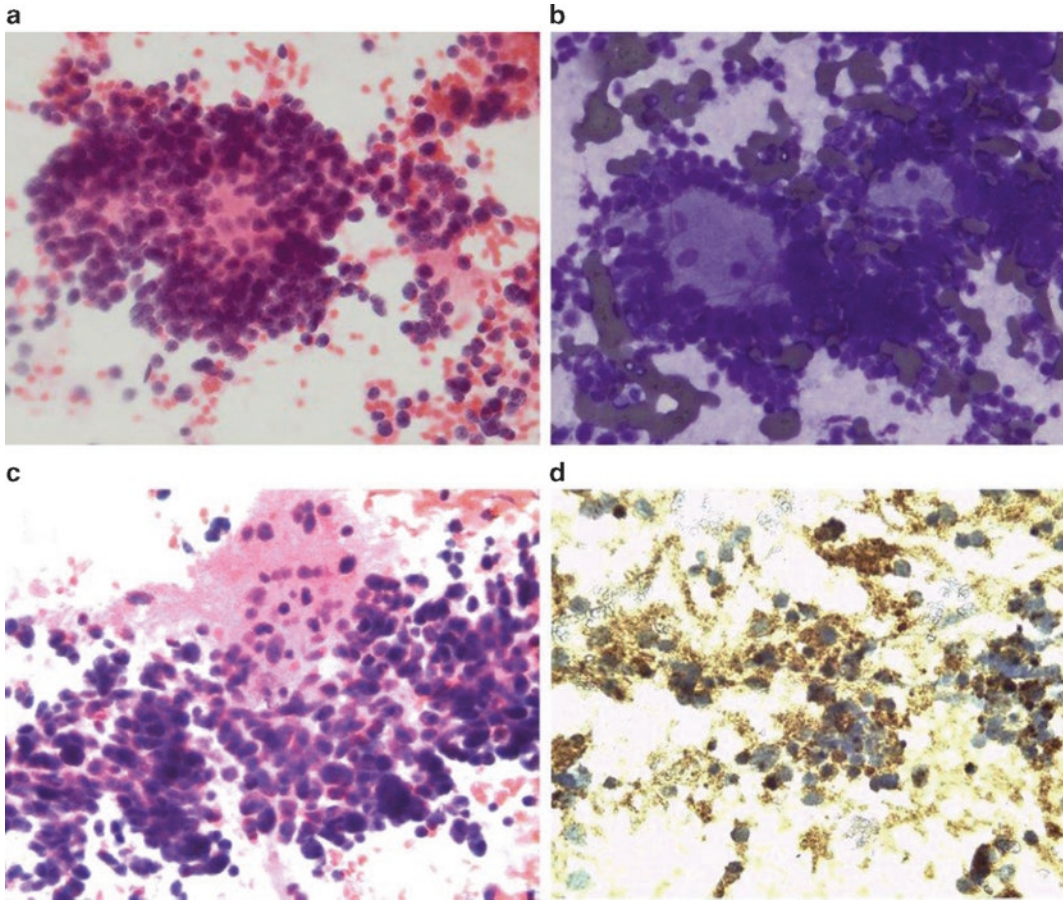


**Fig. 7.14** Neuroblastoma (**a**, **c**. Papanicolaou stain, high power; **b**. Diff-Quik stain, high power; **d**. Synaptophysin immunoperoxidase stain, high power). This FNA from an adrenal neuroblastoma in a 15-month-old boy shows Homer Wright rosettes consisting of neuropil surrounded by tumor cells (**a**, **b**). Tumor cells are also seen in a background of granular, pink neuropil (**c**). Tumor cells show positive synaptophysin immunostaining (**d**).

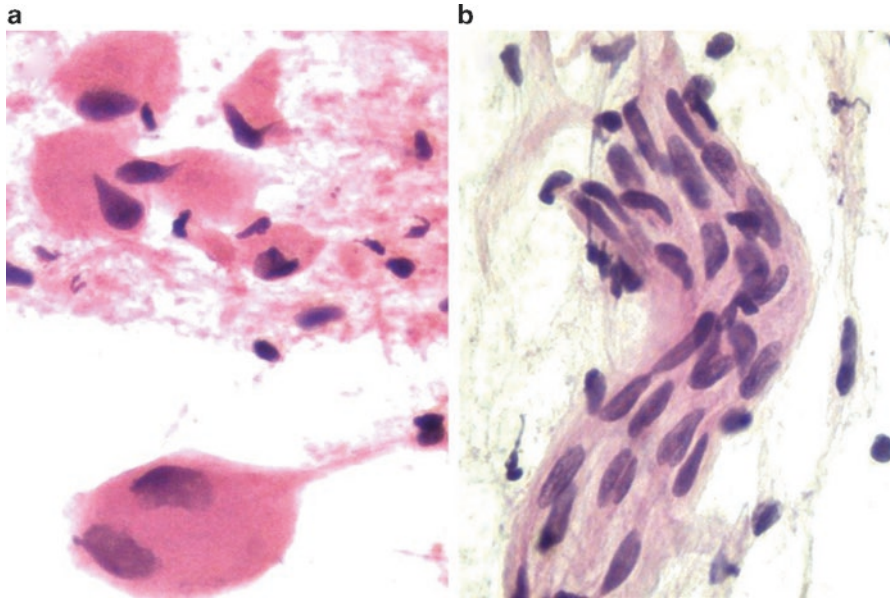


**Fig. 7.15** Primary adrenal ganglioneuroma (**a**, **b**. Papanicolaou stain, high power). Large, polygonal ganglion cells with abundant granular cytoplasm are seen and should not be mistaken for malignancy (**a**). Spindled Schwann cells with ill-defined cytoplasmic borders and nuclei with inconspicuous nucleoli are also observed (**b**). No neuroblastic component is evident.

stroma without neuroblasts (ganglioneuroma). Ganglioneuroma is a fully differentiated, benign, neuroblastic tumor that has Schwann and ganglion cells in a fibromyxoid or collagenous background without neuroblasts, necrosis, or mitotic figures (Fig. 7.15). Neuroblastomas can also be subclassified as undifferentiated, poorly differentiated, or differentiating.

## Triage

Neuroblastomas and ganglioneuroblastomas exhibit positive immunostaining for synaptophysin, chromogranin, and CD56. In addition, newer antibodies for NB84 and PGP9.5 are also positive in the neuroblastic cells. Neuroblasts tend to be negative for vimentin, desmin, myogenin, cytokeratin, WT1, CD45, and CD99. *MYCN* amplification can be demonstrated in some neuroblastomas by fluorescence in situ hybridization and is associated with a poorer prognosis. Neurosecretory granules are noted on electron microscopy. There are increased levels of catecholamines and metabolites on biochemical testing.

## Differential Diagnosis

The differential diagnosis includes other small round blue cell tumors when the tumor has a predominance of neuroblastic component (Tables 7.2, 7.3, and 7.4).

## Pearl

Neuroblastoma is divided into favorable or unfavorable histology based on the Shimada classification, which requires calculation of MKI. As defined in the Shimada classification, MKI cannot be calculated on cytologic specimens. Given that the Shimada classification is important for risk stratification and determination of therapy, a core or open biopsy is needed for appropriate management of these patients. Similarly, it may not be possible to distinguish between a ganglioneuroblastoma and neuroblastoma on cytomorphology alone, or to exclude a neuroblastic component in ganglioneuromas, so most of these lesions will be biopsied or excised for complete histological evaluation.

### 7.2.8 Metastases

The adrenal gland may be involved by contiguous spread from a renal, adrenal, or retroperitoneal tumor or metastases. Careful attention to cytomorphology and judicious use of ancillary investigations are required in this regard (Tables 7.2, 7.3 and 7.4).

## 7.3 Retroperitoneum

The retroperitoneum is a complex area that contains many vital organs, including kidneys, adrenal glands, ureters, bladder, duodenum (excluding first segment), colon (excluding transverse component, sigmoid, and cecum), pancreas (excluding tail), aorta, inferior vena cava, para-aortic lymph nodes, nerve trunks, ganglion plexuses, adipose tissue, and skeletal muscle. The retroperitoneum can be the site of diverse disease processes in children including cysts, infections, and neoplasms, both benign and malignant. The retroperitoneal space is relatively large, and symptoms of disease in this area often present at a late stage.

### 7.3.1 Cysts

#### Clinical Features

Retroperitoneal cysts in childhood can be neoplastic or nonneoplastic. Nonneoplastic cysts include pancreatic pseudocyst, lymphocele, urinoma, and hematoma. Hydatid cyst, tailgut cysts, and bronchogenic cysts have also been described [3]. Neoplastic cysts include cystic lymphangioma, cystic teratoma, Müllerian cyst, cystic changes in solid tumors (e.g., neuroblastoma), and benign multicystic peritoneal mesothelioma. Mesenteric, omental, and retroperitoneal cysts are typically endothelial- or mesothelial-lined cysts. They present in young children with abdominal mass, intestinal obstruction, volvulus, and abdominal pain. Benign multicystic peritoneal mesothelioma presents as multiple, nonadherent cysts with abdominal distention or as an incidental finding on laparotomy but is more common in young, reproductive-age women than in children [17].

#### Cytological Features

The fluid specimens usually show cyst contents with varying quantities of mature lymphocytes, histiocytes, and debris. Occasionally endothelial-lining cells or mesothelial cells will be seen. Mesothelial cells can show marked atypia in the setting of reactive conditions or benign multicystic mesothelioma. Cyst-lining cells are the most helpful for classification of these cystic lesions but are infrequently seen. In the case of bronchogenic cysts, ciliated cells are usually seen [3].

#### Triage

Liquid-based cytology is usually preferred for cystic lesions, particularly benign hypocellular fluid specimens, to concentrate the cells present.

#### Differential Diagnosis

The other entities to consider are cystic lesions arising from the ovary, kidney, or other solid organs in this region, that compress or distort other structures, and may be misinterpreted as a primary retroperitoneal mass.

#### Pearls

A variety of malignancies can undergo cystic degeneration, so ensuring adequate sampling of any solid components is essential in order to exclude malignancy. Given that ovarian and mesothelial-lining cells are positive for WT1, other stains, such as calretinin (for mesothelial origin) and ER or PAX8 (for ovarian origin), can be helpful.

### 7.3.2 Infections

Most retroperitoneal infections in children are bacterial, the most common infectious agent being *Staphylococcus aureus*. Other bacteria in this regard include *E. coli* and other gram-negative enteric bacteria, gastrointestinal anaerobes, *Actinomyces*, and mycobacteria. *Paracoccidioides*, *Cryptococcus*, and *Histoplasma* are causes of retroperitoneal fungal infections and abscesses, while parasitic sources of infection include hydatid disease. These infections may show a granulomatous or histiocytic response. One example would be xanthogranulomatous pyelonephritis from the kidney

showing prominent foamy histiocytes and debris. Viruses may cause para-aortic lymphadenopathy, and the corresponding aspirates will typically show reactive lymphadenopathy with a shift to more immunoblastic cells and occasionally features of viral cytopathic effect. In immunosuppressed children (e.g., transplant, HIV/AIDS), unusual infectious agents may be encountered. The cytomorphology will depend on the type of infection and host response. Ancillary tests (e.g., special stains, PCR, culture) can aid in accurate identification of the causative organism.

### 7.3.3 Lesions and Tumors of the Retroperitoneum with a Predominant Small Round Cell Pattern

Tumors located in the retroperitoneum that consist predominantly of small round cells are highlighted in Table 7.2 and include extra-adrenal neuroblastoma and ganglioneuroblastoma, desmoplastic small round cell tumor, rhabdomyosarcoma, Ewing sarcoma/PNET, and lymphoid lesions, including reactive lymphadenopathy and lymphoma. It is estimated that 35 % of neuroblastomas and ganglioneuroblastomas occur in the retroperitoneum. Rhabdomyosarcoma can arise in the retroperitoneum. In addition, paratesticular or bladder rhabdomyosarcoma can invade the retroperitoneum. Retroperitoneal and para-aortic lymph nodes may exhibit hyperplasia due to various stimuli, in addition to involvement by lymphoma. Burkitt lymphoma not infrequently involves the mesenteric and retroperitoneal lymph nodes.

#### 7.3.3.1 Desmoplastic Small Round Cell Tumor

**Clinical Features**

Desmoplastic small round cell tumor (DSRCT) is a rare but aggressive tumor, usually located intra-abdominally and in the pelvis, but it can also be found in the retroperitoneum, thorax, and central nervous system. It usually affects adolescent and young adult males.

**Cytological Features**

Aspirates from DSRCTs yield small round cells with varying amounts of stromal fragments that stain metachromatically on Diff-Quik preparations. The cells can also be signet-ring type,

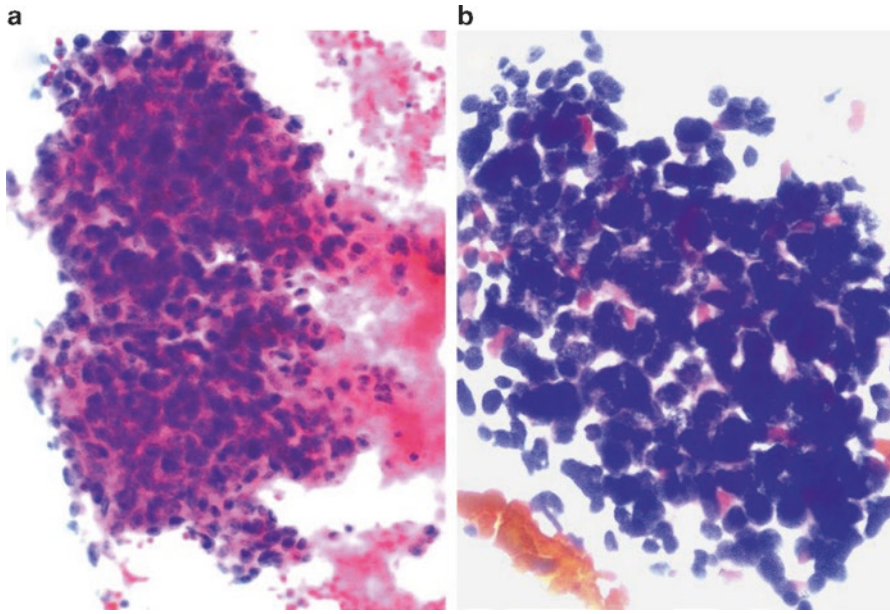


**Fig. 7.16** Desmoplastic small round cell tumor (**a**. Papanicolaou stain, medium power; **b**. Diff-Quik stain, medium power). These aspirates from a retroperitoneal DSRCT show small round cells with very high nuclear-to-cytoplasmic ratios in a necrotic background (**a**). Small round cells with some attempt at rosette formation are noted (**b**).

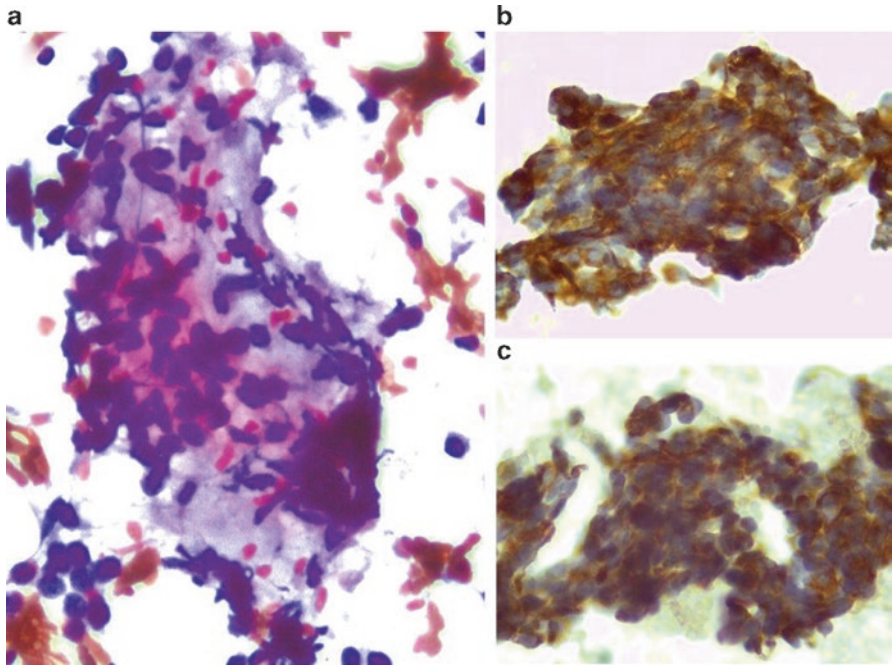


**Fig. 7.17** Desmoplastic small round cell tumor in a 7-year-old boy (**a**. Papanicolaou stain, high power; **b**. AE1/AE3 stain, high power; **c**. Desmin stain, high power). Small fragments of collagenous stroma can be noted within a small round blue cell tumor (**a**). The polyphenotypic nature of this tumor can be demonstrated by both positive AE1/AE3 and desmin staining (**b**, **c**).

rhabdoid, epithelioid, or spindled (Figs. 7.16 and 7.17). The background typically shows necrosis, karyorrhexis, and cystic debris. This tumor is described in more detail in Chap. 9 on body fluid cytopathology. On histology, small round cells organized in nests and solid areas are found in a desmoplastic stroma, while on aspirates, the small round blue cell component is more pronounced than the fibrotic component [18].

### Triage

Immunoperoxidase stains are helpful to demonstrate co-expression of epithelial markers (EMA, cytokeratin), neural markers (S100, NSE), and mesenchymal markers (vimentin and dot-like perinuclear staining for desmin). The WT1 stain using an antibody directed to the carboxy-terminus also shows nuclear positivity. This tumor demonstrates a translocation t(11;22)(p13;q12) with fusion of the *EWSR* and *WT1* genes.

### Differential Diagnosis

See Table 7.2. One of the most difficult tumors to distinguish from DSRCT is blastemal predominant Wilms tumor, given that both tumors show poorly differentiated morphology with immunopositivity for desmin and cytokeratin. Even the dot-like positivity for desmin can be seen in both tumors. Thus, the best way for distinguishing DSRCTs is to demonstrate that the tumor cells have the *EWSR1-WT1* rearrangement and show selective immunoreactivity to the WT1 carboxy-terminus. In contrast, Wilms tumors are typically positive with antibodies directed to both the WT1 amino-terminus and carboxy-terminus [19].

### Pearls

A variety of tumors in addition to DSRCTs have *EWS* gene rearrangements that can be detected by FISH using *EWS* break-apart probes. Thus, morphology and immunophenotype and/or identification of the translocation partner by FISH,

RT-PCR, or other molecular methods is necessary for a definitive diagnosis.

#### 7.3.3.2 Ewing Sarcoma/Primitive Neuroectodermal Tumors (EWS/PNET)

**Clinical Features**

This is a small round blue cell tumor originating in soft tissue, including retroperitoneum, and bone. Despite differences in morphology and immunophenotype which reflect the degree of neural differentiation, EWS and PNET share cytogenetic features and, thus, are considered a single entity. This tumor is seen most frequently in older children and adolescents. The most common presentation is that of a painful mass. Ewing sarcoma typically occurs in long bones, while the soft tissue PNET is usually located in the chest wall, paraspinal region, and head and neck. Very occasionally a PNET can arise in an organ (e.g., kidney, lung) [1, 4, 20].

**Cytological Features**

The background comprises variable amounts of blood, necrosis, apoptosis, and mitotic figures. A tigroid background, due to intracellular glycogen, is a feature in some tumors. Cells are arranged in sheets, loose and tight clusters, single cells, and occasional rosettes. The cells usually have a high nuclear-to-cytoplasmic ratio with a small amount of cytoplasm. The cytoplasm contains glycogen vacuoles, which are best seen on Diff-Quik-stained material. Occasionally, somewhat larger cells with more abundant cytoplasm are seen, imparting a light (cells with increased cytoplasm) and dark (cells with less cytoplasm or degenerating cells) pattern on aspirates. The nuclei are round to oval with mildly irregular borders and finely granular chromatin. Nucleoli may be inconspicuous, single, or multiple. Nuclear molding may be seen. Neural differentiation, in the form of fibrillary neuropil and rosettes, can be seen in varying quantities. This tumor is discussed in greater detail in Chap. 5 with images.

**Triage**

Immunocytochemistry is positive for CD99/O13 and FLI-1. Neuroendocrine and broad spectrum epithelial markers are variably positive. Muscle and lymphoid markers are negative. Glycogen can be demonstrated using PAS stains with and without diastase. Several cytogenetic aberrations involving the *EWS* gene on chromosome 22q12 are described in EWS/PNET, the most common being t(11;22)(q24;q12). Others include t(21;22)(q12q12), t(7;22)(p22;q12), t(17;22)(q12;q12), and t(2;22)(q33;q12).

**Differential Diagnosis**

See Table 7.2. One of the main entities in the differential diagnosis is undifferentiated (Ewing-like) round cell sarcoma, which typically has cells with paler cytoplasm than in EWS/PNET, more atypia, shows a *CIC-DUX4* rearrangement t(4;19), and is WT1 positive.

**Pearls**

Other tumors that show the *EWS* (chromosome 22) gene rearrangement include clear cell sarcoma, desmoplastic small round cell tumor, extraskeletal myxoid chondrosarcoma, myoepithelial tumors, and angiomatoid fibrous histiocytoma. Thus, morphology and immunophenotype and/or identification of the translocation partner by FISH, RT-PCR, or other molecular methods is necessary for a definitive diagnosis.

### 7.3.4 Lesions and Tumors of the Retroperitoneum with a Predominant Spindle Cell Pattern

Various spindle cell soft tissue tumors, including but not limited to those highlighted in Table 7.4, can involve the retroperitoneum in childhood. These include muscle tumors [e.g., rhabdomyosarcoma (Fig. 7.18), leiomyoma, and leiomyosarcoma (Fig. 7.19)], fibrotic lesions (e.g., fibrosarcoma), vascular lesions (e.g., Kaposi sarcoma), neural lesions (e.g., schwannoma, ganglioneuroma), and synovial sarcoma. Soft tissue tumors are described in greater detail in Chap. 5.

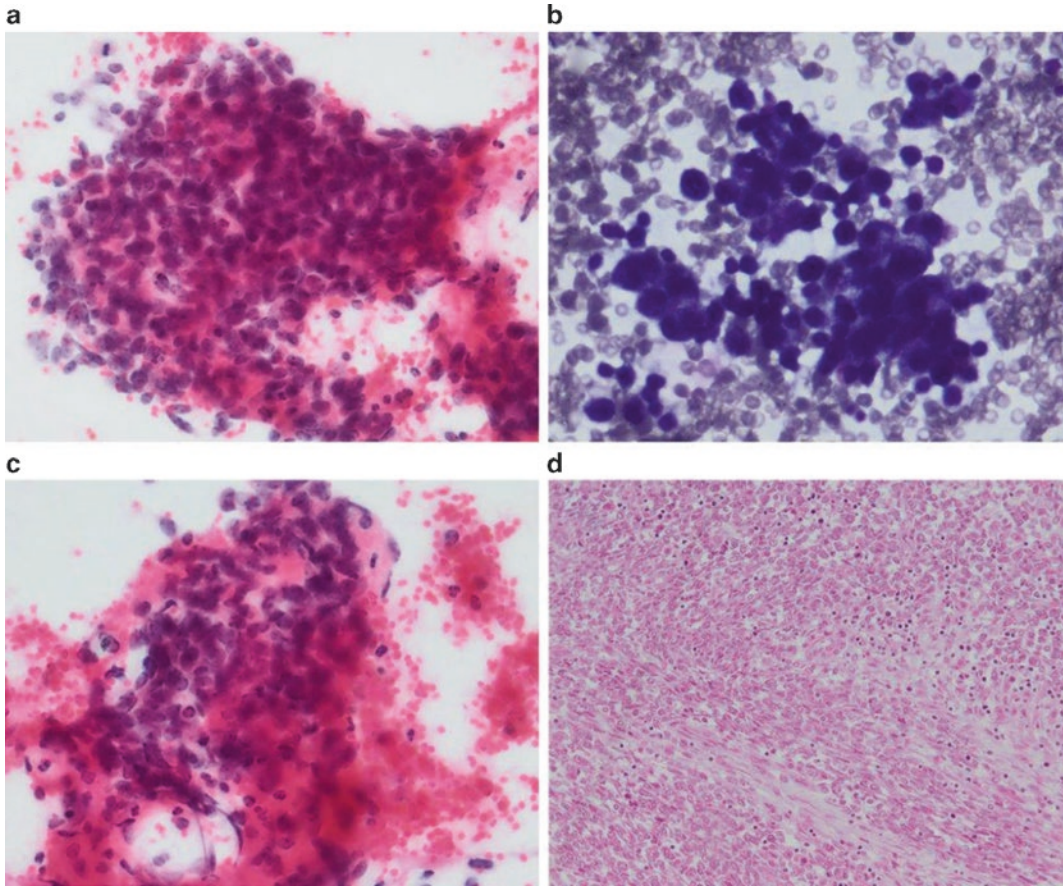


**Fig. 7.18** Primary retroperitoneal alveolar rhabdomyosarcoma (**a**, **c**. Papanicolaou stain, high power; **b**. Diff-Quik stain, high power; **d**. H&E stain, medium power). The aspirates show features of a small round cell tumor (**a**, **b**), with some cells containing more abundant, dense, orangeophilic cytoplasm (**c**). The corresponding histologic section is shown (**d**).

#### 7.3.4.1 Fibroblastic-Myofibroblastic Lesions

Lesions of this type seen in the pediatric retroperitoneum include inflammatory myofibroblastic tumor, solitary fibrous tumor, and fibrosarcoma. Inflammatory myofibroblastic tumor comprises spindle and inflammatory cells, including plasma cells and eosinophils. These tumors demonstrate chromosomal rearrangements of the 2p23 locus. Solitary fibrous tumor presents with uniform spindle cells which show variable CD34 and vimentin positivity. Fibrosarcoma (infantile and adult-type) can be seen in the retroperitoneum. Infantile fibrosarcoma comprises small or large spindle cells that may demonstrate marked pleomorphism in a hemorrhagic or necrotic background. The majority exhibit translocation t(12;15)(p13;q26). The adult type of fibrosarcoma may occasionally be seen in older children and adolescents. This comprises spindle cells in a background of variable amounts of collagen.

### 7.3.5 Lesions and Tumors of the Retroperitoneum Comprising Cells with Moderate to Abundant Cytoplasm

Angiomyolipoma, PEComa, germ cell tumors, chordoma, and ganglioneuroblastoma may all

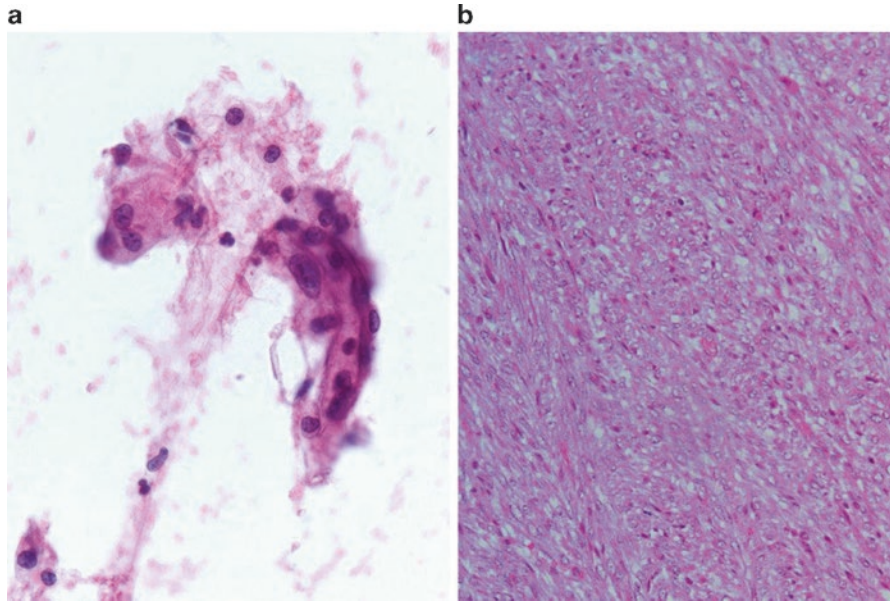


**Fig. 7.19** Retroperitoneal smooth muscle tumor in an HIV-positive child (**a**. Papanicolaou stain, high power; **b**. H&E stain, medium power). The aspirates show spindle cells with ill-defined cell borders, blunt-ended nuclei, irregular nuclear borders, and prominent nucleoli (**a**). Fascicles of spindle cells are also observed in the resection specimen (**b**).

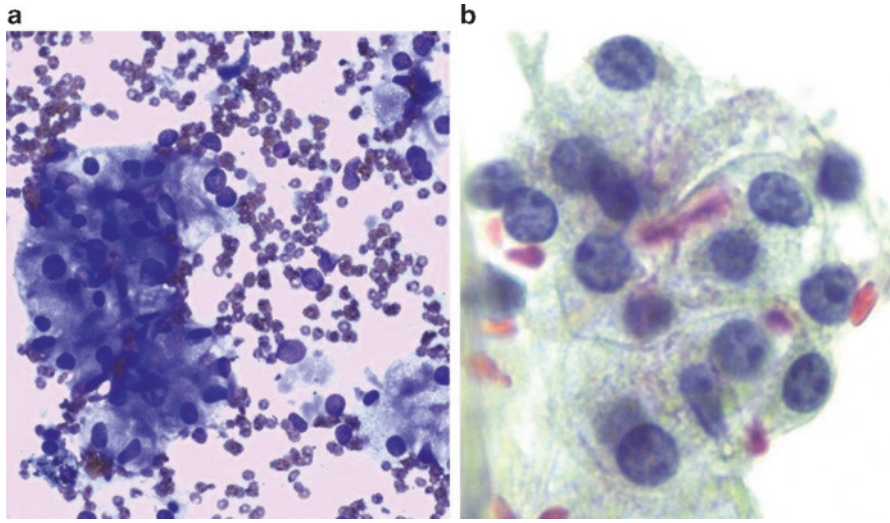


**Fig. 7.20** PEComa (**a**. Diff-Quik stain, medium power; **b**. Papanicolaou stain, high power). FNA from a renal melanotic PEComa shows cells with abundant vacuolated cytoplasm containing melanin pigment.

occur in the retroperitoneum. These lesions consist of cells with fairly abundant cytoplasm. Most germ cell tumors found in the retroperitoneum are metastases, and it is currently controversial whether the entity of primary extragonadal germ cell tumors of the retroperitoneum exists. PEComas arise from the perivascular epithelioid cell and express both muscle and melanocytic markers (Fig. 7.20). There are several tumors that form part of the PEComa family of tumors including angiomyolipoma, sugar tumor, and lymphangioleiomyomatosis. Chordoma and parachordoma are very uncommon in children. Cytologically, physaliferous cells are present in a

background of myxoid material. Physaliferous cells have abundant vacuolated cytoplasm and pleomorphic nuclei that can show scalloped nuclear contours. On immunoperoxidase stains, these tumors are positive for S100, EMA, and brachyury. Table 7.3 highlights some of the differential diagnostic considerations.

### 7.3.6 Metastases to the Retroperitoneum

Many tumors of childhood can spread to the retroperitoneum, either directly or metastatic, from a more distant site. A thorough clinical history and physical examination, in addition to careful attention to cytomorphology and the results of ancillary studies, is required to make the correct diagnosis.

## 7.4 Urine Cytology

### 7.4.1 Urine Collection

Toilet-trained children, depending on age, may be able to provide a urine sample. To collect a urine sample in younger children, the use of urine bags, disposable diapers, urine collection pads, catheterization, or suprapubic aspiration is required. The collection method also depends on the type of test to be performed (e.g., a urine sample for culture and sensitivity should be collected in a way that minimizes contamination). Cleaning the perineum and genital area before collecting urine may help reduce contamination.

### 7.4.2 Urinary Inflammation

Bacterial infection is the most common infection seen in urine. However, viral, fungal, and parasitic diseases may cause cystitis. In addition, medications, especially chemotherapeutic agents, can cause cystitis, including hemorrhagic cystitis.

- Viral infection: Cytomegalovirus (CMV) and BK virus (a polyomavirus) are the most common viral infections seen in urine cytology, especially in immunosuppressed children. The cytopathic effect of CMV includes a large cell with a prominent eosinophilic intranuclear inclusion and small intracytoplasmic inclusions. BK virus infection can cause renal transplant rejection. The cytomorphology of BK viral cytopathic effect includes urothelial cells with eccentrically situated nuclei containing a large basophilic intranuclear inclusion that imparts a "smudgy" look to the nucleus. The cells are usually seen as single cells (Fig. 7.21). The diagnosis of BK viruses can be confirmed on PCR, electron microscopy, immunostaining for the SV40 antibody, and tissue biopsy. Herpes simplex infection can be seen in the form of multinucleated cells with nuclear molding and peripheral condensation of chromatin (Fig. 7.21).
- Bacterial infection: In children, there may be an association between bacterial infection of the urinary tract, vesicoureteral reflux, and renal scarring. The causative bacteria are most often gram-negative bacteria, especially *Escherichia coli*. *Staphylococcal* spp. are associated with bladder instrumentation. Cytologic evaluation reveals a marked acute inflammatory cell infiltrate, red blood cells, reactive urothelial cells, and debris. Bacterial colonies may be noted. Gram stain and culture are ancillary investigations that can be performed.
- Fungal infection: Fungal cystitis is unusual in children and is usually associated with immunosuppression or bladder instrumentation. *Candida* spp., *Cryptococcus*, and *Aspergillus* are some examples of causative agents. Fungal casts may be identified, in addition to inflammatory cells, blood, and urothelial cells. Special stains (e.g., GMS, PAS) and fungal culture will aid in identification of the fungus.
- Parasitic infection: Schistosomiasis, especially *S. haematobium*, is the most important cause of parasitic infection of the bladder. *Schistosoma* ovum is large and oval in shape, measuring 150 × 50 μm surrounded by a chitinous shell with a terminal spine, as in the case of *S. haematobium* (Fig. 7.21). *Trichomonas vaginalis* causes cystitis and urethritis. In urine, they often appear more degen-

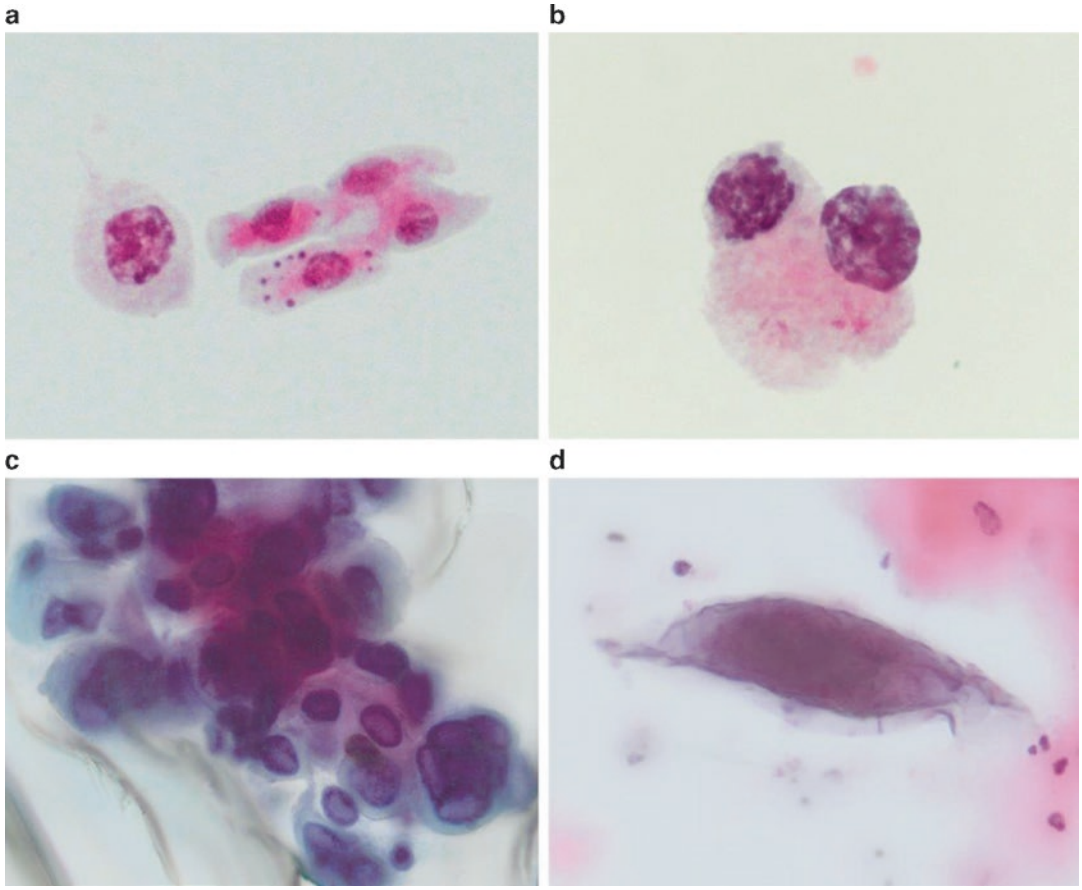


**Fig. 7.21** Urine cytology in children (**a**–**d**. Papanicolaou stain, high power). Decoy cells due to polyomavirus in the urine from a 17-year-old girl who had undergone renal transplant (**a**, **b**). Multinucleated cells with nuclear molding and margination of chromatin due to herpes simplex virus infection in urine from a 19-year-old girl (**c**). *Schistosoma haematobium* ovum in urine from a 9-year-old boy (**d**).

erate and smaller than on cervical cytology, in a background of marked inflammation. Their presence in urine may indicate onset of sexual activity in adolescents or sexual abuse.

### 7.4.3 Miscellaneous Conditions

Xanthogranulomatous pyelonephritis has been described in children. Urine cytomorphology reveals nonspecific inflammation or blood. Urine culture is usually negative. Lipid storage disorders (e.g., Niemann–Pick disease) have been diagnosed on urine cytology in the presence of cells with numerous small vacuoles, combined with special stains (e.g., PAS, Sudan stains). A high proportion of columnar cells are seen in children with cystitis cystica et glandularis.

### 7.4.4 Neoplasia

The most common childhood tumor to exfoliate into urine is the rhabdomyosarcoma, especially the embryonal and botryoides subtypes. Presentation includes hematuria, abdominal pain, and recurrent urinary tract infection. Cytologic examination of urine is associated with a low diagnostic yield of tumor cells. When present, the tumor cells exfoliate singly and in small clusters. The cells are often degenerate and smaller than seen on FNA, with high nuclear-to-cytoplasmic

ratios. More differentiated cells such as strap cells or cells with cross striations have, very occasionally, been reported in urine. Immunoperoxidase stains such as desmin, myoD1, and myogenin are usually positive. The alveolar subtype will show translocation t(2; 13)(q35;q14) or t(1;13)(p36;q14). Other small round cell tumors that have been described on urine cytology include nephroblastoma, non-Hodgkin lymphoma, and EWS/PNET. Other neoplasms, like inflammatory myofibroblastic tumors, can also occur.

## References


1. Husain AN, Stocker JT, editors. Color atlas of pediatric pathology. New York, NY: Demos Medical Publishing; 2011.
2. Kini S. Color atlas of differential diagnosis in exfoliation and aspiration cytopathology. 2nd ed. Philadelphia, PA: Wolters Kluwer/Lippincott Williams & Wilkins; 2011.
3. Yang D, Jung D, Kim H, Kang J, Kim S, Kim J, Hwang H. Retroperitoneal cystic masses: CT, clinical and pathologic findings and literature review. Radiographics. 2004;24:1353–65.
4. Stocker J, Dehner L, editors. Pediatric pathology. 2nd ed. Philadelphia, PA: Lippincott, Williams and Wilkins; 2001.
5. Khalbuss W, Monaco S, Pantanowitz L. Quick compendium of cytopathology. Chicago: ASCP Press; 2013.
6. Shohab D, Hussain I, Khawaia A, Jamil I, Raia NU, Ahmed F, Akhter S. Primary renal aspergillosis and xanthogranulomatous pyelonephritis in an immune-competent toddler. J Coll Physicians Surg Pak. 2014;24:S101–3.
7. Silowash R, Monaco SE, Pantanowitz L. Ancillary techniques on direct-smear aspirate slides: a significant evolution for cytopathology techniques. Cancer Cytopathol. 2013;121:670.
8. Iyer V, Agarwala S, Verma K. Fine needle aspiration cytology of clear cell sarcoma of the kidney: study of eight cases. Diagn Cytopathol. 2005;33:83–9.
9. Portugal R, Barroca H. Clear cell sarcoma, cellular mesoblastic nephroma and metanephric adenoma: cytological features and differential diagnosis with Wilms tumor. Cytopathology. 2008;19:80–5.
10. Brownlee NA, Perkins LA, Stewart W, Jackle B, Pettenati MJ, Koty PP, Iskandar SS, Garvin AJ. Recurring translocation (10;17) and deletion (14q) in clear cell sarcoma of the kidney. Arch Pathol Lab Med. 2007;131:446–51.
11. Sharifah N. Fine needle aspiration cytology characteristics of renal tumors in children. Pathology. 1994;26:359–64.
12. Cheng JX, Tretiakova M, Gong C, Mandal S, Krausz T, Taxy JB. Renal medullary carcinoma: rhabdoid features and the absence of INI1 expression as markers of aggressive behavior. Mod Pathol. 2008;21:647–52.
13. Schinstine M, Filie A, Torres-Cabala C, et al. Fine needle aspiration of Xp11.2 translocation/TFE3 fusion renal cell carcinoma metastatic to the lung: report of a case and review of the literature. Diagn Cytopathol. 2006;34:751–6.
14. Ramphal R, Pappo A, Zielenska M, Grant R, Ngan BY. Pediatric renal cell carcinoma: clinical, pathologic, and molecular abnormalities associated with the members of the mit transcription factor family. Am J Clin Pathol. 2006;126:349–64.
15. Barman S, Mandal KC, Mukhopadhyay M. Adrenal myelolipoma: an incidental and rare benign tumor in children. J Indian Assoc Pediatr Surg. 2014;19:236–8.
16. Davidoff A. Neuroblastoma. Semin Pediatr Surg. 2012;21:2–14.
17. Durell J, Dagash J, Eradi B, Nour S. Pediatric benign cystic mesothelioma. J Pediatr Adolesc Gynecol. 2016;29:e33–4.
18. Crapazano J, Cardillo M, Lin O, Zakowski M. Cytology of desmoplastic small round cell tumor. Cancer. 2002;96:21–31.
19. Arnold MA, Schoenfield L, Limketkai BN, Arnold CA. Diagnostic pitfalls of differentiating desmoplastic small round cell tumor (DSRCT) from Wilms tumor (WT): overlapping morphologic and immunohistochemical features. Am J Surg Pathol. 2014;38:1220–6.
20. Tsokos M, Alaggio R, Dehner L, Dickman P. Ewing sarcoma/peripheral primitive neuroectodermal tumor and related tumors. Pediatr Dev Pathol. 2012;15(1 Suppl):108–26.

# Liver, Bile Ducts, and Pancreas

# 8

Sara E. Monaco and Lisa A. Teot

## 8.1 Introduction

Cytological evaluation can be a useful diagnostic tool for assessing hepatic, biliary, and pancreatic masses in pediatric patients, particularly when the lesions are difficult to sample by other means or when obtaining a larger core or open biopsy poses undue risks. The best example is biliary tract lesions, from which samples are usually obtained by endoscopic brushing, aspirate, or small biopsy. As in other sites, a cytological diagnosis can help to guide medical and/or surgical treatment of hepatobiliary and pancreatic masses, as well as avoid unnecessary or inappropriate surgical procedures, such as pancreaticoduodenectomy, which can result in dramatic morbidity.

In contrast to those in adults, many of the tumors that occur in the liver and biliary tree in the pediatric population are either "blastomas" (e.g., hepatoblastoma (HB), metastatic neuroblastoma), or primary or metastatic small round blue cell tumors (e.g., rhabdomyosarcomas (RMSs), lymphoproliferative disorders, neuroendocrine neoplasms, malignant rhabdoid tumors, and others). Similarly, whereas ductal adenocarcinomas comprise the vast majority of pancreatic tumors in adults, many of the tumors that arise in the pediatric population are bland epithelioid neoplasms, such as neuroendocrine tumors, solid pseudopapillary tumors, acinar cell carcinomas, and serous cystadenomas. Moreover, some of the tumors arising in the liver, biliary tree, or pancreas occur in the context of a genetic syndrome that may or may not be evident at the time of diagnosis. Thus, knowledge of these syndromes and associations is very important when evaluating cytological specimens from pediatric patients.

The main differential diagnostic considerations for hepatobiliary and pancreatic mass lesions in the pediatric population are listed in Table 8.1.

S.E. Monaco, MD (✉)
Department of Pathology, University of Pittsburgh Medical Center (UPMC) & Children's Hospital of Pittsburgh of UPMC, Pittsburgh, PA, USA
e-mail: monacose@upmc.edu

L.A. Teot, MD
Department of Pathology, Boston Children's Hospital, Harvard Medical School,
300 Longwood Avenue, Boston, MA 02115, USA
e-mail: lisa.teot@childrens.harvard.edu

## 8.2 Liver

A variety of nonneoplastic and neoplastic processes produce hepatic masses that are amenable to cytological evaluation. Nonneoplastic causes of hepatic masses include infections, cysts, hamartomas, hyperplastic or regenerative nodules,



S.E. Monaco, L.A. Teot (eds.), *Pediatric Cytopathology*, DOI 10.1007/978-3-662-53441-0_8

**Table 8.1** Main differential diagnosis for pediatric hepatic or pancreatobiliary lesions based on location

| Location | Main differential diagnosis |
|---|---|
| Liver | Infection |
| | Cysts |
| | Vascular lesions |
| | Mesenchymal neoplasms |
| | Focal nodular hyperplasia |
| | Hepatic adenoma |
| | Hepatoblastoma |
| | Hepatocellular carcinoma |
| | Metastatic tumors |
| Bile duct | Infection |
| | Cholangitis, pancreatitis, or other inflammatory changes |
| | Reactive atypia (from a stent, cholangitis, or infection) |
| | Choledochal cysts |
| | Dysplastic or metaplastic changes |
| | Rhabdomyosarcoma |
| | Cholangiocarcinoma (rare) |
| Pancreas | Pseudocyst |
| | Pancreatitis (acute, chronic, autoimmune) |
| | Serous cystadenoma, microcystic type |
| | Solid pseudopapillary tumor |
| | Acinar cell carcinoma |
| | Pancreatic neuroendocrine tumor |
| | Pancreatoblastoma |
| | Mucinous neoplasms (e.g., mucinous cystic neoplasms, intraductal papillary mucinous neoplasms) |

and vascular malformations. Neoplasms can be benign or malignant and primary or metastatic. Primary malignant hepatic neoplasms are rare in the pediatric population; however, in this age group, they comprise a greater proportion of malignancies involving the liver than in adults. The types of primary hepatic malignancies seen in the pediatric population also vary with age. In children less than 5 years of age, hepatoblastoma predominates, whereas in older children and adolescents, hepatocellular carcinoma (HCC) is more common. Of the HCCs arising in pediatric patients, the fibrolamellar variant is seen only in children older than 5 years of age and has a better prognosis than non-fibrolamellar HCC [1].

### 8.2.1 Normal Liver

Aspiration of the normal liver adjacent to a mass lesion may yield benign hepatocytes, benign ductal cells, and/or fibrous stromal fragments, as well as scattered Kupffer cells and endothelial cells. Benign hepatocytes appear in small, loosely cohesive clusters and have abundant granular cytoplasm, round nuclei, and small nucleoli and may also have intranuclear inclusions. Cytoplasmic lipofuscin, the so-called aging pigment, and glycogenated nuclei are features that are typically seen in adults, not children, but can be seen in patients with childhood diabetes and obesity. An abundant amount of lipofuscin pigment or glycogenated nuclei in the pediatric liver can also be seen with Wilson's disease, an autosomal recessive condition resulting in excess copper accumulation. Naked nuclei are usually present in the background. Benign ductal epithelium appears as small glandular cells with uniform, round nuclei and scant cytoplasm arrayed in flat, honeycomb sheets. Fibrous stroma derived from the portal triads is usually sparse or absent and appears as small, irregular fragments of hypocellular collagenous tissue.

### 8.2.2 Infections

#### Clinical Features

Infections involving the liver may result in abscess formation, cysts, and granulomatous or miliary lesions. In developed countries, most hepatic abscesses are bacterial in origin, whereas worldwide the most common cause of hepatic abscesses is amebic infection, usually with *Entamoeba histolytica*. Some fungi can also give rise to abscesses, particularly in immunocompromised patients. Hydatid cysts are caused by the larvae of the canid tapeworm *Echinococcus granulosus*, following ingestion of ova. Granulomatous and miliary lesions may be due to mycobacterial or fungal infections. Symptoms vary depending on the type of infection and location of the mass lesion within the liver and may include fever, nausea and vomiting, abdominal pain or fullness, hepatomegaly, jaundice, and weight loss. Leakage or rupture of hydatid cysts produces

**Table 8.2** Main types of infections causing hepatic masses in pediatric patients

| Disease | Etiology | Cytomorphologic clues |
|---|---|---|
| Amebic abscess | Infection of the liver by trophozoites following ingestion of cysts of the protozoan *Entamoeba histolytica* | Trophozoites have well-defined cell membranes, bubbly cytoplasm, a single eccentric round nucleus with a distinct karyosome, and ingested erythrocytes |
| Pyogenic abscess | Various bacteria, including *Actinomyces israelii*, and fungi | Gram-positive or negative rods or cocci depending on organism<br>Branching colonies (granules) with delicate, Gram-positive filaments and granular basophilic centers in *Actinomyces israelii* infection<br>Yeast, pseudohyphae, or hyphal elements depending on organism |
| Hydatid cyst | Larva of the canid tapeworm *Echinococcus granulosus*, following ingestion of ova | Hooklets, scoleces (bags of hooklets), or fragments of the laminated wall |
| Granulomatous inflammation | Mycobacteria tuberculosis, atypical mycobacteria, fungi | Acid-fast bacilli, yeast, pseudohyphae, or hyphal elements depending on organism |

allergic reactions ranging from urticaria to anaphylaxis. Table 8.2 summarizes hepatic infections that result in mass lesions in children and adolescents.

### Cytological Features

Aspirates of bacterial and fungal abscesses typically yield turbid, thick, yellow fluid that is easy to smear. Microscopically, the smears are comprised of abundant neutrophils in a background of granular necroinflammatory debris. In some cases, microorganisms may be identified on routinely stained smears or with Gram, methenamine silver (GMS), or other special stains. *Actinomyces* has a distinctive filamentous appearance and may form large aggregates known as sulfur granules (Fig. 8.1). Amebic abscesses yield thick brown fluid, often likened to anchovy paste. Smears are characterized by mixed inflammation with eosinophils and Charcot-Leyden crystals in a background of necroinflammatory debris. Although rarely identified in fluid from the central cavity, trophozoites may be seen when the wall of the abscess is sampled and appear as round, blue bodies with well-defined cell borders, bubbly cytoplasm, single eccentric nuclei with a central karyosome, and engulfed erythrocytes. Aspirates of granulomatous lesions are characterized by clusters of epithelioid histiocytes, usually accompanied by lymphocytic inflammation in mycobacterial infections and by neutrophilic or mixed inflammation in fungal infections. Cavitary lesions may also yield necrotic debris. In aspirates from immunocompetent hosts, mycobacteria are usually rare or absent, whereas in those from immunocompromised hosts, mycobacteria may be numerous and appear as intracellular or extracellular negative images on modified Giemsa-type stains. Acid-fast or fluorescent Auramine O stains may be helpful for identifying the organisms. Fungal elements may be detected with routine GMS or periodic acid Schiff (PAS) stains. Hydatid cysts often have a characteristic appearance on imaging studies and, due to concern for anaphylaxis, are rarely aspirated for diagnostic purposes. When these cysts are aspirated, either accidentally or during a therapeutic PAIR (puncture, aspirate, inject [scolicidal solutions], re-aspirate) procedure, they typically yield sandy or grainy fluid with scoleces and hooklets from the tapeworm. Laminated membrane fragments may also be seen.

### Triage

Special stains, such as Gram, GMS, PAS, and acid fast, performed on smears or sections from cell blocks, can be helpful for confirming an infectious etiology. In cases with limited material, an unstained smear from a diagnostic pass can be reserved for special staining in the event that the cell block has scanty or inadequate material. In addition, polymerase chain reaction (PCR) studies can be performed on material from a cell block or from frozen abscess fluid to detect the presence of microbial organisms and/or for speciation of mycobacteria. Microbial cultures may help to identify the causative

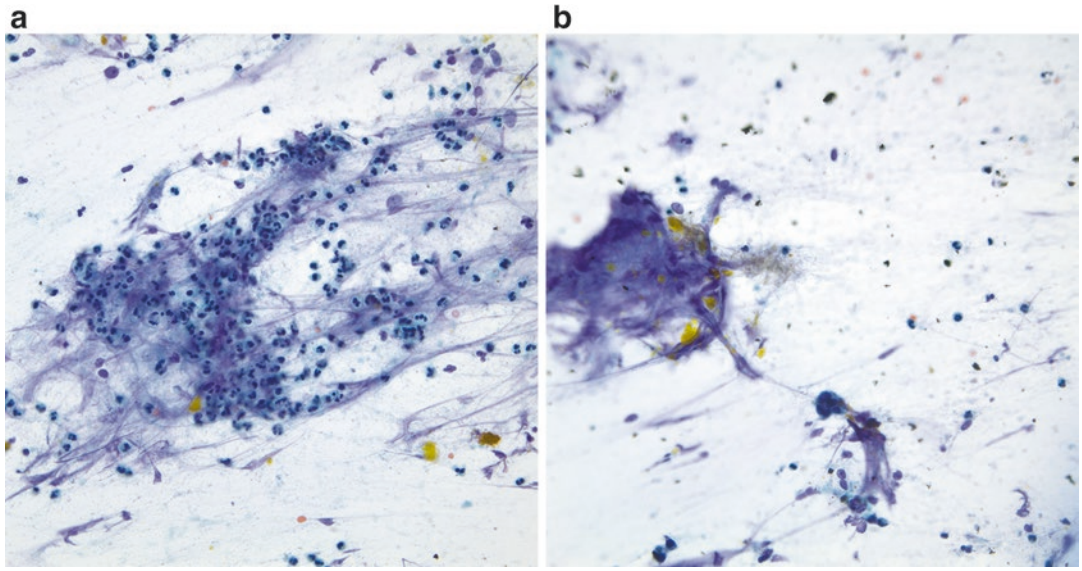


**Fig. 8.1** *Actinomyces* (**a**. Papanicolaou stain, high power; **b**. Papanicolaou stain, high power). (**a**) Numerous neutrophils and debris with bile are seen in this bile duct brushing from a patient with *Actinomyces* infection. (**b**) Clumped, filamentous bacteria are identified, compatible with *Actinomyces* infection. With the exception of the obvious presence of bile in the ductal brushings, these features are very similar to those seen in smears from pyogenic hepatic abscess due to *Actinomyces*.

microorganism(s) and determine sensitivities to antimicrobial agents.

### Differential Diagnosis

Bacterial and fungal abscesses can have similar cytologic appearances, as can granulomatous lesions due to mycobacteria and fungi. In the absence of informative special stains, PCR, and/or cultures, the etiology of some abscesses and granulomatous lesions remains unknown. Necrosis and associated inflammation involving a primary or metastatic tumor may mimic an abscess both on imaging studies and cytologically. Malignant cells may be obscured, particularly when few in number, but are the key to the correct diagnosis. Pseudocysts and other cystic lesions in the peripancreatic and peribiliary region may also mimic an infectious cyst or abscess involving the liver.

### Pearls

When adequate material is available, microbial cultures should be submitted to identify the infectious agent and define antimicrobial sensitivities for treatment. An indirect hemagglutination test or other serologic tests can be done to confirm the diagnosis of an amebic abscess, given that the trophozoites are difficult to identify unless the wall is aspirated.

## 8.2.3 Focal Nodular Hyperplasia

### Clinical Features

Focal nodular hyperplasia (FNH) is the most common cause of benign hepatocytic tumors in children over the age of 5 years. Although it is usually seen in young reproductive-age women, up to 15% of cases occur in the pediatric age group. Usually FNH is asymptomatic given its slow growth. The lesion can be quite large when detected and on imaging appears as a well-circumscribed mass with a characteristic central stellate scar with vessels.

### Cytological Features

The aspirates show benign hepatocytes, in addition to some ductal epithelium, fibroblasts, and/or fibrous tissue fragments. The fibrous tissue

fragments may make the aspirate difficult to smear and may also lead to nondiagnostic aspirates, necessitating a core needle biopsy for evaluation.

#### Triage

A cell block or unstained smears are helpful for performing routine histochemical stains, such as reticulin, iron, PAS, and PAS with diastase, to exclude other benign disorders of the liver, as well as well-differentiated or fibrolamellar hepatocellular carcinoma (HCC).

#### Differential Diagnosis

Definitive cytological diagnosis of FNH can be difficult or impossible given the fact that the aspirates show overlapping features with the normal liver, regenerative nodule, hepatic adenoma, well-differentiated and fibrolamellar HCC, and vascular lesions/neoplasms. If the cytopathologist is confident that the aspirate is representative of lesional tissue, the presence of ductal epithelium helps to exclude hepatic adenoma and HCC. Imaging studies should help to exclude sampling of the benign hepatic parenchyma adjacent to or admixed with a vascular lesion.

#### Pearls

Correlation with findings on imaging studies, particularly the presence of a central stellate scar with vascularity, and associated rapid enhancement in the arterial phase and rapid washout in the portal venous phase, can be very helpful. Distinction between hepatic adenoma and FNH can be very difficult on aspirates, and thus, larger core needle biopsies are often performed.

### 8.2.4 Hepatic Adenoma

#### Clinical Features

Hepatic adenomas typically occur in adolescents and young adults and have been associated with oral contraceptive use (typically more than 5 years of use). They are usually solitary masses and may rupture giving rise to retroperitoneal hemorrhage. Upon discontinuation of oral contraceptives, the lesions may decrease in size or disappear.

#### Cytological Features

Aspirate smears show benign hepatocytes with absent or exceedingly rare ductal epithelium and fibrous tissue, corresponding to the key histologic finding of benign hepatic tissue without conspicuous portal tracts or bile ducts. The intact reticulin meshwork may make aspirates difficult to smear. Central necrosis and/or calcifications may be present in these lesions and be seen in the background of smears or in sections from the cell block.

#### Triage

Reticulin stain should be performed on a smear or section of a cell block to exclude well-differentiated HCC.

#### Differential Diagnosis

Hepatic adenomas can be difficult or impossible to distinguish from the normal liver, regenerative nodules, FNH, and well-differentiated HCC on cytologic preparations. Correlation with clinical presentation, serum alpha-fetoprotein (AFP), and imaging studies, as well as reticulin stain and the presence or absence of ductal epithelium, can help to resolve the diagnosis. However, core biopsy may be required.

#### Pearls

Given the difficulty in distinguishing hepatic adenoma, FNH, and well-differentiated hepatocellular carcinoma on aspirates and core biopsies, correlation with the imaging findings is crucial.

### 8.2.5 Hepatoblastoma

#### Clinical Features

Hepatoblastoma (HB) typically occurs in children under 3 years of age and, although rare, is the most common malignant tumor of the liver in pediatric patients, comprising about half of hepatic malignancies in this population. These tumors can be congenital and usually are sporadic; however, some genetic diseases, particularly germline *APC* mutations (familial adenomatous polyposis) and Beckwith-Wiedemann syndrome, predispose to the development of HB. Patients typically present

with abdominal enlargement and, less often, pain. On imaging, HB appears as a solitary or multifocal liver mass with or without stippled and/or coarse calcifications in a non-cirrhotic liver. Many tumors are considered unresectable at diagnosis due to large size and bilobar involvement. Metastases to the lung are present in up to 20 % of patients at diagnosis. Patients usually have elevated serum alpha-fetoprotein (AFP) and anemia, and may also have thrombocytosis.

### Cytological Features

The cytomorphology depends on whether the tumor is epithelial, mixed epithelial and mesenchymal, or small cell undifferentiated, as well as on the type(s) of epithelial component(s) present [2]. The majority of HB is of the epithelial type with fetal and/or embryonal components, and smears are usually highly cellular [2]. Fetal cells are arranged in orderly cohesive sheets, in three-dimensional clusters, and singly and may show a light and dark pattern due to the variable amounts of glycogen or fat in the cells. The cells are uniform and round to polygonal with moderate amounts of eosinophilic, vacuolated, or clear cytoplasm and round nuclei with fine chromatin and small nucleoli (Fig. 8.2). Extramedullary hematopoiesis can also be seen. Embryonal cells are arranged singly and in loosely cohesive, disorganized sheets and glandular or acinar arrays with crowded, overlapping nuclei. They are smaller than fetal cells and pleomorphic and have scant cytoplasm, oval to irregular hyperchromatic nuclei, inconspicuous nucleoli, and high nuclear-to-cytoplasmic ratios (Fig. 8.2). Recapitulating the histologic features of HB, the fetal and embryonal elements are often intermixed, and moreover, cells intermediate between fetal and embryonal may be present making the distinction between these cell types difficult. Stripped nuclei are usually present in the background. In mixed epithelial and mesenchymal HB, the mesenchymal component is usually focal and may not be represented in the aspirate smears. When a mesenchymal component is present, it usually appears as fragments of fibromyxoid tissue with stellate mesenchymal cells, osteoid, or cartilage. Small cell undifferentiated (SCUD) HB is rare and appears as discohesive, uniform, small round cells with round, hyperchromatic nuclei and high nuclear-to-cytoplasmic ratios. These cells are difficult or impossible to distinguish from those of other small round cell tumors of childhood without the assistance of immunoperoxidase stains, and recent evidence suggests that the majority of tumors classified as SCUD HB may represent extrarenal malignant rhabdoid tumors [3, 4].

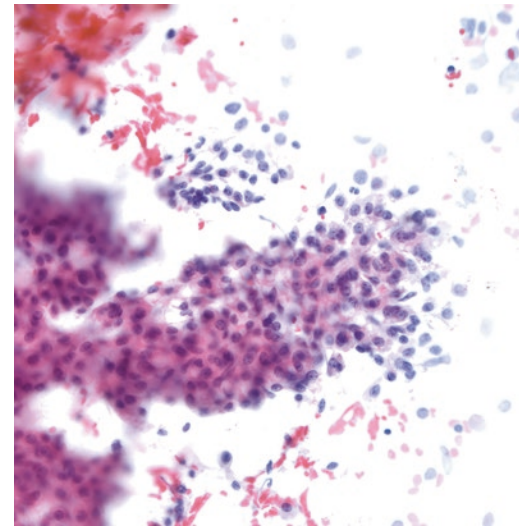

**Fig. 8.2** Hepatoblastoma (Papanicolaou stain, medium power). This aspirate is comprised of fetal and embryonal epithelial elements. The embryonal element is a minor component in this smear and appears as a discohesive cluster of small cells with dark, oval to irregular nuclei and scant cytoplasm in the upper center of the field. The fetal elements comprise a second, predominant population of cells with more abundant eosinophilic cytoplasm and round nuclei with pale chromatin and prominent nucleoli. The fetal elements are arranged in a large cohesive sheet and closely resemble normal fetal hepatocytes. (Image taken from slides provided by Dr. Pam Michelow).

### Triage

Immunoperoxidase stains can be used to confirm the diagnosis of HB and help to distinguish fetal HB from well-differentiated HCC and embryonal HB from other poorly differentiated or blastemal tumors of childhood. The malignant cells in fetal and embryonal HB are positive for low molecular weight cytokeratins (Cam5.2, CK8/18), AFP, beta-catenin (nuclear ± cytoplasmic), glypican-3,

and HepPar1. The SCUD variant of hepatoblastoma is positive for pankeratin, CK8/CK18, vimentin, and beta-catenin in a nuclear pattern, but is negative for glypican-3 and HepPar1 [3]. In addition, nuclear staining for INI-1 is lost the majority of SCUD HB. The immunophenotype and molecular evidence of *INI-1/SMARCB1* deletion suggest that these tumors may actually represent extrarenal rhabdoid tumors [3, 4].

#### Differential Diagnosis

The other entities to consider when making the diagnosis of HB are well-differentiated HCC (more pleomorphism, lack of extramedullary hematopoiesis), yolk sac tumor (positive for germ cell markers such as SALL4), adrenal cortical neoplasm (positivity for adrenal cortical markers, such as Melan-A, calretinin, and inhibin), paraganglioma, and metastatic small round blue cell tumors.

#### Pearls

This is the most common type of liver malignancy in children and should be considered before making a diagnosis of HCC in a young person. The SCUD type may actually represent extrarenal rhabdoid tumor and can mimic small cell carcinoma or any small round cell tumor of childhood.

### 8.2.6 Hepatocellular Carcinoma

#### Clinical Features

The second most common liver tumor in children is HCC, which is typically seen in older children from 5 to 15 years of age. Risk factors include cirrhosis, viral hepatitis, cholestatic liver disease, such as type 2 progressive familial intrahepatic cholestasis, and inborn errors of metabolism, such as tyrosinemia and type 1 glycogen storage disease. In contrast to classic HCC, the fibrolamellar variant of HCC (FL-HCC) usually develops de novo in adolescence or young adulthood in the setting of a noncirrhotic liver. Patients with HCC usually present with hepatomegaly, abdominal pain, and weight loss. Serum AFP is often elevated, but may be normal or only slightly elevated in well-differentiated HCC and FL-HCC. On imaging HCC typically appears as a hypervascular mass with or without necrosis and/or vascular invasion. Advanced HCC may be multinodular. FL-HCC is also characterized by a central scar, thereby mimicking FNH.

#### Cytological Features

Aspirates from classic HCC are usually highly cellular with cells arranged in sheets, in clusters, in acinar arrays, and singly with numerous naked nuclei in the background (Fig. 8.3a). In well- and moderately differentiated HCCs, thickened trabeculae (greater than three cells thick) with endothelial wrapping, tissue fragments with transgressing vessels, and nuclear crowding and overlapping are characteristic and help to distinguish these malignancies from benign hepatocellular proliferations (Fig. 8.3). Well- and moderately differentiated HCCs are characterized by relatively monotonous populations of polygonal cells with moderate to abundant, eosinophilic cytoplasm and enlarged, round, centrally placed nuclei with prominent nucleoli. Cytoplasmic lipid vacuoles, bile, hyaline globules and/or Mallory bodies, and intranuclear pseudoinclusions can also be present. The nuclear-to-cytoplasmic ratio is usually increased, although this feature can be subtle in some well-differentiated tumors. In smears from poorly differentiated FL-HCC, the cells are often arranged in loosely cohesive clusters or singly and bear little or no resemblance to hepatocytes. Cytologic and nuclear atypia and pleomorphism can be marked, and bizarre spindle and giant cells may be present. In smears from FL-HCC, the cells are often arranged singly or in loosely cohesive clusters. The cells are larger and have lower nuclear-to-cytoplasmic ratios than normal hepatocytes and those of well-differentiated HCC due to the abundant, granular (oncocytic) cytoplasm, large round nuclei, and macronucleoli. Hyaline globules and/or pale bodies can be seen in some cells (Fig. 8.4). Fragments of dense fibrous stroma with parallel arrays of spindled nuclei are present and, in some cases, prominent and correspond to the lamellar bands of fibrous tissue seen histologically (Fig. 8.4). Extramedullary hematopoiesis is usually not seen in classic or FL-HCC, in contrast to HB.

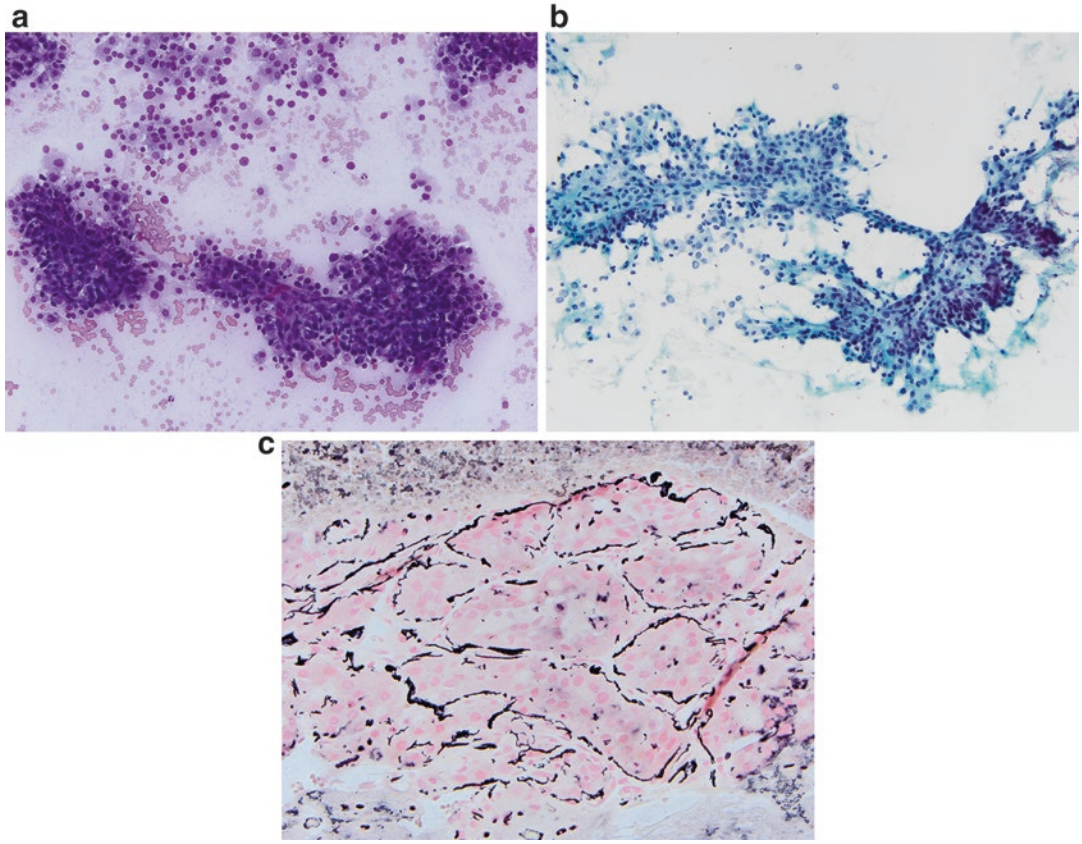


**Fig. 8.3** Hepatocellular carcinoma (**a**. Diff-Quik stain, medium power; **b**. Papanicolaou stain, medium power; **c**. Reticulin stain, high power). The aspirate shows malignant cells in sheets, in clusters, and singly with stripped nuclei in the background (**b**). The hepatocellular nature of the cells is evident. Transgressing vessels are apparent (**a**, **b**). A reticulin stain performed on the cell block highlights thickened trabeculae (>3 cells thick) (**c**).

### Triage

Immunoperoxidase stains can help to confirm the diagnosis of HCC. The tumor cells show cytoplasmic positivity for AFP, glypican-3 (GPC-3), arginase-1 (ARG-1) and HepPar1 [5], and canalicular staining for CD10 and polyclonal CEA. Stains for AE1 and nuclear beta-catenin are typically negative. A histochemical stain for reticulin is very helpful for demonstrating the loss of normal hepatic cords two cells in thickness and the presence of thickened trabeculae, particularly on a cell block with tissue fragments or on a concurrent core needle biopsy (Fig. 8.3).

### Differential Diagnosis

The entities to consider in the differential diagnosis include regenerative nodules, FNH (see Sect. 8.2.3), hepatic adenoma (see Sect. 8.2.4), hepatocellular dysplasia, HB (see Sect. 8.2.5), and metastatic oncocytic or poorly differentiated neoplasms, germ cell tumors, or renal cell carcinomas. Immunoperoxidase stains can be used to distinguish HCC from other malignancies.

### Pearls

Poorly differentiated HCCs bear little or no resemblance to hepatocytes and, in addition, can be negative for HepPar1 and AFP making them difficult to distinguish from other poorly differentiated malignancies. The combination of GPC-3 and ARG-1 is highly sensitive for confirming the hepatocellular origin of poorly differentiated HCC [5], thereby allowing a definitive diagnosis. It is important to note that no immunohistochemical

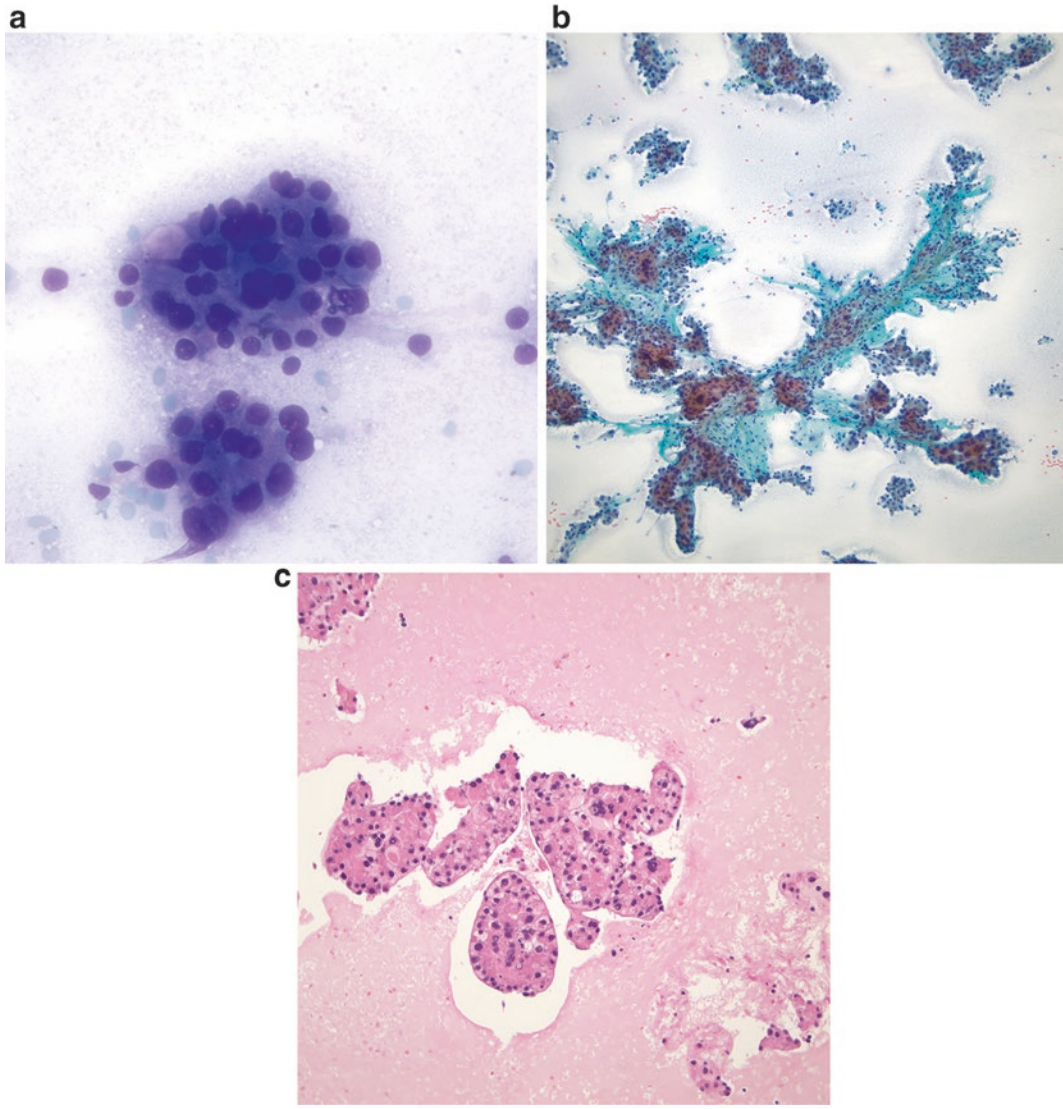


**Fig. 8.4** Hepatocellular carcinoma, fibrolamellar variant (**a**. Diff-Quik stain, high power; **b**. Papanicolaou stain, low power; **c**. H&E stain, medium power). The tumor cells are arranged in small clusters with scattered stripped nuclei in the background (**a**). The cells have round to oval nuclei and relatively abundant cytoplasm. A pale body is evident in one cell. Nodules of malignant cells are separated by fibrous stroma with parallel spindled nuclei (**b**). Clusters of large oncocytic cells are seen in the cell block (**c**).

stain reliably distinguishes malignant from benign hepatocytes. Of the hepatocellular markers, GPC-3 is usually negative in benign lesions but is also negative in up to 50 % of well-differentiated HCCs [6], limiting its usefulness for differentiating between these entities. Similarly, while reticulin stains are useful for highlighting thickened trabeculae in HCC, some well-differentiated HCCs are comprised predominantly of trabeculae less than three cells thick and, thus, are architecturally indistinguishable from benign processes. In such cases, a definitive cytological diagnosis of HCC is difficult or impossible, and core biopsy should be recommended.

### 8.2.7 Vascular Lesions

#### Clinical Features

Hepatic vascular lesions are a heterogeneous group of benign and malignant neoplasms and nonneoplastic malformations. They can be focal, multifocal, or diffuse and span the clinical spectrum from asymptomatic to life-threatening. Hemangiomas are common incidental findings in the liver in children and are classified as benign vascular tumors, according to the 2014 International Society for the Study of Vascular Anomalies (ISSVA) classification scheme [7]. Focal hepatic hemangiomas are solitary lesions and correspond to cutaneous rapidly involuting congenital hemangiomas (RICH). The lesions may be detected on prenatal ultrasound, are fully formed at birth, undergo rapid involution, and are associated with self-limited neonatal anemia and thrombocytopenia or occasionally a high-output cardiac state or overt cardiac failure [8].

Multifocal hepatic hemangiomas, which correspond to cutaneous infantile hemangiomas (IHs), consist of multiple discrete lesions separated by normal hepatic parenchyma [8]. Like their cutaneous counterparts, they appear within the first few weeks of life, grow rapidly, and then regress. Complications of multifocal hepatic hemangiomas include high-output cardiac failure and hypothyroidism. Diffuse hepatic hemangiomas likely represent coalescence of untreated multifocal hemangiomas, extensively replace the liver, and lead to significant morbidity or mortality due to severe acquired hypothyroidism, high-output cardiac failure, hepatic failure, and/or abdominal compartment syndrome secondary to massive hepatomegaly [8]. Overall, hemangiomas are the most common benign hepatic tumors in pediatric patients and comprise about 12–15 % of liver tumors in this population.

Epithelioid hemangioendothelioma and angiosarcoma are uncommon malignant vascular tumors that comprise less than 1 % of all primary hepatic malignancies. Most of these tumors occur in adults, but very rare examples are encountered in the pediatric population. Patients present with abdominal distention, pain, and weight loss. Imaging studies are diagnostic or at least highly suggestive of a particular type of vascular lesion in many cases.

#### Cytological Features

Benign vascular tumors typically yield bloody aspirates with scant cellular material. The presence of spindled endothelial cells or vascular fragments on a cell block can be helpful, when they are seen. Fibrous tissue fragments and hemosiderin-laden macrophages may also be present. Epithelioid hemangioendothelioma yields variably cellular aspirates composed of atypical epithelioid and spindle cells and fragments of fibromyxoid to fibrous stroma [9]. The epithelioid cells are large with abundant cytoplasm, round to irregular nuclei, and prominent nucleoli. Intracytoplasmic lumina with or without erythrocytes may be seen in some cells and, when present, are an important clue to the vascular nature of the lesion. Aspirates from angiosarcomas are usually bloody and, depending on the degree of differentiation of the tumor, are comprised of spindle, epithelioid, and/or anaplastic cells arranged singly or in loosely cohesive clusters. Anastomosing vascular structures and/or concentric whorls of spindle cells indicative of vascular formation can be present, particularly in well-differentiated tumors. Cytoplasmic hemosiderin and intracytoplasmic lumina with or without erythrocytes are often present and provide important diagnostic clues.

#### Triage

Immunoperoxidase stains, including CD34, CD31, FLI-1, and ERG, can be used to confirm the endothelial origin of vascular lesions, but do not distinguish benign from malignant proliferations. FLI-1 and ERG show crisp nuclear staining and can be particularly helpful. Infantile hemangiomas are GLUT1 positive, whereas congenital hemangiomas and benign vascular malformations are negative [10].

#### Differential Diagnosis

FNAs of benign vascular neoplasms tend to be nondiagnostic. However, when hepatic and/or fibrous tissue fragments with prominent vessels are seen, entities to consider include HCC and FNH. HCCs are characterized by thickened trabeculae with endothelial wrapping and clusters or sheets of tumor cells with transgressing vessels, whereas the hepatic tissue accompanying benign vascular tumors has preserved architecture with

cords less than three cells thick and lacks transgressing vessels.

**Pearl**

Correlation with radiological imaging is critical in the evaluation of vascular tumors. Hemangiomas usually show hypoattenuation in comparison to the background liver on non-enhanced CT scans and Doppler flow on ultrasound examination. In many cases, the diagnosis can be made on imaging alone, reducing the need for FNA or core biopsy.

### 8.2.8 Other Mesenchymal Neoplasms

**Clinical Features**

Other primary benign and malignant mesenchymal neoplasms are rare in the pediatric population [3]. Mesenchymal hamartoma is the most common nonvascular mesenchymal tumor, whereas malignant entities include undifferentiated embryonal sarcoma, rhabdomyosarcoma, and leiomyosarcoma. Malignant rhabdoid tumor is a rare, highly aggressive, polyphenotypic tumor that primarily affects infants.

**Cytological Features**

The cytologic appearance depends on the type of tumor and the background material. Mesenchymal hamartoma is comprised of bland spindle to stellate cells, myxoid to fibromyxoid matrix, and clusters of benign ductal epithelial cells. Most sarcomas are characterized by loosely cohesive or discohesive malignant cells arranged in sheets, in clusters, or singly. Undifferentiated embryonal sarcoma is composed of large, highly pleomorphic spindle to epithelioid cells including bizarre anaplastic and multinucleated tumor giant cells, in a myxoid matrix. Intracytoplasmic hyaline globules are present. Rhabdoid tumors are composed of epithelioid cells with moderate to abundant cytoplasm and eccentric nuclei with pale chromatin and prominent nucleoli. Cytoplasmic inclusions comprised of whorls of intermediate filaments are present. Of note, some rhabdoid tumors are comprised of small round cells with scant cytoplasm with inconspicuous inclusions, high nuclear-to-cytoplasmic ratios, and round to ovoid, hyperchromatic nuclei with coarse chromatin and variably conspicuous nucleoli. Most primary rhabdomyosarcomas of the liver and biliary tract are of the embryonal type and are composed of primitive round to short spindle cells with scant, pale cytoplasm and round, oval, or irregular nuclei with clumped chromatin and small nucleoli. Cells with small cytoplasmic globules, cytoplasmic tails, and/or striations may be present and are indicative of rhabdomyoblastic differentiation. Leiomyosarcomas typically appear as spindle cells with moderate to abundant cytoplasm, sometimes with a perinuclear cytoplasmic vacuole, and elongate nuclei with rounded ends.

**Triage**

Immunoperoxidase stains can help to confirm the diagnosis and exclude other entities in the differential diagnosis. Cytogenetics, FISH, or other molecular studies are also useful for the diagnosis of some tumors. Mesenchymal hamartoma and undifferentiated embryonal sarcoma share a 19q13.4 rearrangement and t(11;19) translocation, and rhabdoid tumors show mutations or deletions of *SMARCB1* [3].

**Differential Diagnosis**

Depending on the type of tumor and cytomorphology, other entities to consider include vascular neoplasms, hepatoblastoma, HCC, and hepatic involvement by lymphoma or metastatic sarcomas, melanoma, or poorly differentiated carcinoma.

**Pearl**

Some sarcomas, most notably leiomyosarcoma and angiosarcoma, can show cytokeratin positivity; thus, a panel of immunoperoxidase stains is essential for resolving the differential and excluding poorly differentiated carcinoma or sarcomatoid carcinoma.

### 8.2.9 Metastases and Other Neoplasms

**Clinical Features**

A variety of small round cell tumors, including neuroblastoma, Wilms tumor, and lymphoma, as well as melanomas, carcinomas, and sarcomas,

can metastasize to the liver in the pediatric population. Metastatic lesions can be asymptomatic and picked up on staging or surveillance imaging studies. However, depending on the location and extent of hepatic involvement, patients can present with elevated liver enzymes, obstructive jaundice, hepatomegaly, abdominal distention, ascites, abdominal pain, and/or weight loss. In most instances, the primary malignancy is known.

### Cytological Features

Most lesions that metastasize to the liver release cells easily and are amenable to FNA biopsy. Cellular smears show cytological features similar to those seen in the primary neoplasms, which are addressed in more detail in other chapters. Melanomas appear as discohesive pleomorphic epithelioid or spindle cells with prominent nucleoli and intranuclear pseudoinclusions (Fig. 8.5).

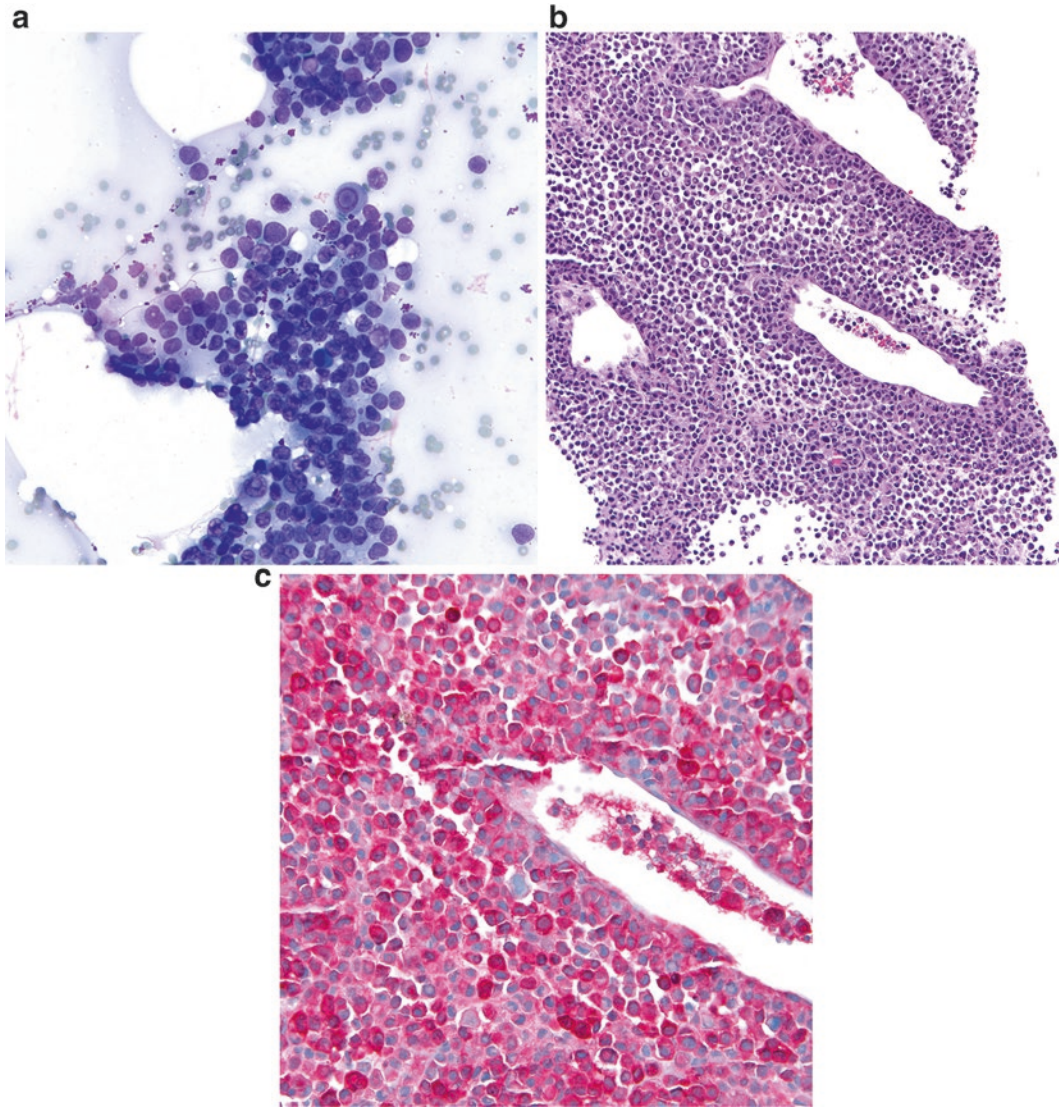


**Fig. 8.5** Metastatic melanoma in the liver (**a**. Diff-Quik stain, high power; **b**. H&E stain, medium power; **c**. S100 immunoperoxidase stain, medium power). This patient with a history of malignant melanoma with small cell features was found to have multiple liver lesions. The aspirate smear is composed of discohesive and loosely cohesive tumor cells with scant eccentrically-placed cytoplasm. Rare intranuclear inclusions are seen (**a**). The concurrent core biopsy highlights the small cell morphology (**b**). The tumor cells are positive for melanoma markers, including S100 (**c**).

Binucleate and multinucleated cells are often present, and cytoplasmic melanin pigment can be identified in some cases. Metastatic small round blue cell tumors are comprised of primitive appearing cells that can mimic embryonal or small cell primary hepatoblastoma or rhabdoid tumor. Lymphoproliferative disorders, including B-cell lymphomas, show a prominent discohesive pattern with lymphoglandular bodies (Fig. 8.6).

### Triage

Obtaining adequate material for a cell block is important to confirm that the tumor cells are morphologically and immunophenotypically similar to the patient's previously diagnosed tumor. S100, Melan-A, HMB45, MiTF, and tyrosinase are positive in metastatic melanoma. Lymphoid markers, including CD20, CD3, and additional markers as appropriate, can be used to resolve the differential diagnosis of a lymphoproliferative process. If there is a suspicion of lymphoma at the time of FNA, obtaining additional material for flow cytometry is advised.

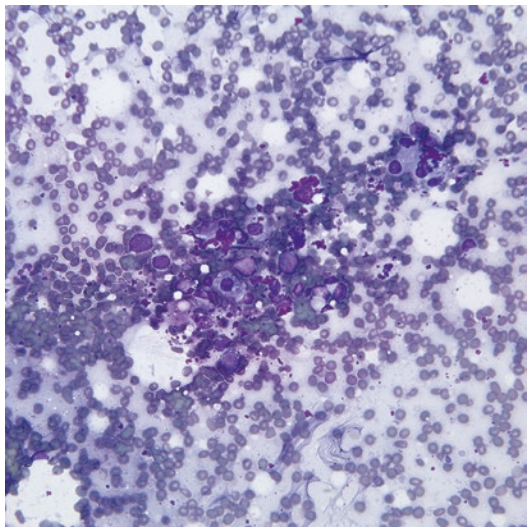

**Fig. 8.6** Large B-cell lymphoma involving the liver (Diff-Quik stain, high power). The aspirate from this lesion shows scattered large discohesive cells with scant cytoplasm in a background of benign hepatocytes. This was a large B-cell lymphoma occurring in a liver transplantation patient.

### Differential Diagnosis

Given that many of the pediatric malignancies are small round blue cell tumors, many of these neoplasms have similar morphology and need to be distinguished from lymphoid cells as well as each other. HCC and hepatoblastoma should be excluded, before rendering a diagnosis of metastatic carcinoma.

### Pearl

In the pediatric setting, hepatic metastases are usually detected in patients with a known malignancy. Thus, a good clinical history is essential in these cases and can help to limit the number of immunoperoxidase stains needed for diagnosis. In many cases, correlation with histologic material from the primary tumor can obviate the need for ancillary studies.

## 8.3 Bile Duct

In children, most lesions of the extrahepatic biliary tree present as obstructive jaundice, clay-colored stool, and/or abdominal distention. Imaging studies help to identify and distinguish between strictures and masses and also to determine whether a mass is intrinsic or extrinsic and solid or cystic. This information is used to assess the need for further diagnostic studies, including pathological evaluation. The differential diagnosis of biliary lesions based on the imaging characteristics is summarized in Table 8.3.

Cytological brushings and small biopsies are used for pathological evaluation of strictures or

**Table 8.3** Cases of obstructive jaundice in children based on imaging

| Imaging characteristics | Differential diagnosis |
|---|---|
| Cystic | Choledochal cyst |
| | Infection (e.g., hydatid cyst) |
| | Enteric duplication cyst |
| Solid or non-cystic | Cholelithiasis |
| | Congenital abnormalities of the pancreatobiliary system |
| | Post-ERCP or iatrogenic trauma |
| | Primary or metastatic tumor: Obstruction by an intrinsic mass itself or by extrinsic compression |

masses of the biliary tree and are typically acquired during endoscopic retrograde cholangiopancreatography (ERCP). Brushings can be used for smears, cytospins, liquid-based preparations, and/or a cell block. Neoplasms of the biliary tree are rare in the pediatric population and include rhabdomyosarcoma, neuroendocrine tumors, inflammatory myofibroblastic tumor, and metastases. In children and adolescents, biliary adenocarcinoma due to either primary cholangiocarcinoma or direct spread of pancreatic adenocarcinoma is rarely encountered. Overall, the sensitivity of bile duct brushings tends to be lower than for brushings of the gastrointestinal tract, largely due to sampling errors; however, the specificity is high. The use of a biliary brushing in combination with biopsy usually maximizes the sensitivity and specificity of the procedure. In some scenarios, particularly strictures, cytological brushings may sample the stenotic area better than a biopsy and thus may have a higher diagnostic sensitivity.

### 8.3.1 Nonneoplastic Biliary Lesions

In brushings from a normal bile duct, the epithelium is columnar with small uniform nuclei and appears as two-dimensional honeycomb sheets (Fig. 8.7). The ductal cells can undergo reactive and metaplastic changes due to inflammation and/or irritation. The background frequently has bile pigment (green to yellow refractile or crystalline material) and occasional contaminants from the gastrointestinal tract (Fig. 8.7).

Nonneoplastic entities seen in the bile duct include infection, inflammation from cholangitis, and reactive changes. Hydatid cysts can be seen in the biliary region and are discussed in greater detail in Sect. 8.2.2.

Reactive atypia can occur, particularly in the setting of biliary stones, an infectious or inflammatory process, primary sclerosing cholangitis, stricture, or extrinsic compression of the duct. In reactive atypia, cells are mildly to moderately enlarged with preserved nuclear-to-cytoplasmic ratios and often have prominent nucleoli (Fig. 8.7). The cells are cohesive and predominantly appear as clusters rather than as single cells. When evaluating biliary epithelial atypia, the presence of an inflammatory background or inflammatory cells within the epithelial clusters and/or a history of biliary stent merits caution to avoid an erroneous diagnosis of dysplasia or malignancy. Dysplasia is characterized by a greater degree of atypia, as well as nuclear crowding and overlapping, but in contrast to malignancy, single cells and marked pleomorphism are absent.

Rare benign neoplasms and mass lesions reported in the biliary tree include granular cell tumors, carcinoid tumors, adenomyosis, and cholesterol, inflammatory, or hyperplastic polyps.

### 8.3.2 Rhabdomyosarcoma

#### Clinical Features

Rhabdomyosarcomas (RMSs) are more commonly seen in the head and neck area, but can occur in the bladder, vagina, or biliary tract. In the biliary tract, RMS usually has a polypoid, multicystic, or grapelike gross appearance similar to sarcoma botryoides in the vagina and may mimic choledochal cysts on imaging. Biliary RMS is most often of the embryonal type and tends to occur in infants and young children (<5 years of age). These tumors are difficult to excise completely, leaving them prone to recurrences. About 30 % of patients may present with metastases, warranting careful evaluation of the biliary tree when metastatic RMS of unknown primary origin is discovered.

#### Cytological Features

Brushings or aspirates from these tumors are composed of primitive-appearing round or short spindle cells in clusters and singly. Occasional cells may have eccentric cytoplasm with small inclusions imparting a rhabdoid appearance, cytoplasmic tails, or cross striations indicative of skeletal muscle differentiation. Occasional intranuclear cytoplasmic inclusions may be seen. The background is typically myxoid or granular. If there are tissue fragments on the cell block, a cambium layer may be seen where the tumor

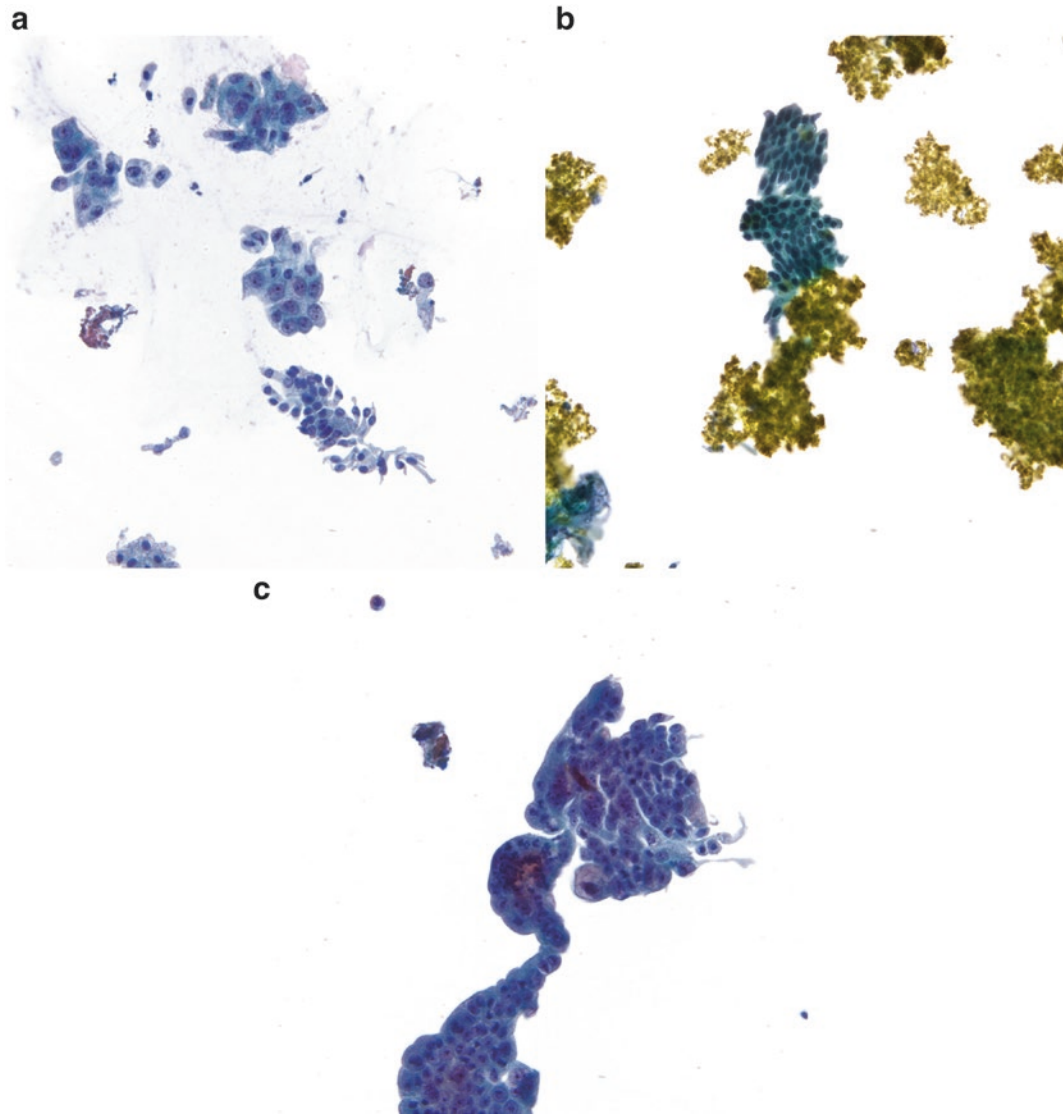


**Fig. 8.7** Benign and reactive biliary epithelial cells (**a**–**c**. Papanicolaou stain, high power). In this biliary brushing from a patient with primary sclerosing cholangitis, normal and reactive bile duct cells disposed in two-dimensional groups are seen. The normal epithelial cells are small and columnar, while the reactive cells are enlarged and have prominent nucleoli (**a**). This bile duct brushing shows bland epithelial cells arrayed in a flat, honeycomb sheet. Bile pigment is present in the background (**b**). Brushings from patients with stents or cholangitis can show marked reactive atypia; however, the presence of infiltrating neutrophils within the atypical epithelium warrants cautious interpretation. These benign cells are arranged in a cohesive cluster without nuclear overlapping (**c**).

cells form a hypercellular band below the normal bile duct epithelium (Fig. 8.8).

### Triage

Immunoperoxidase stains can confirm the diagnosis and show positivity for myoD1, myogenin, and desmin. Of note, myogenin positivity is patchy and variably intense in embryonal RMS, in contrast to the strong and diffuse staining seen in alveolar RMS. The cells are typically negative for neuroendocrine markers and S100. FISH studies for a *FOX01 (FKHR)* rearrangement can also be

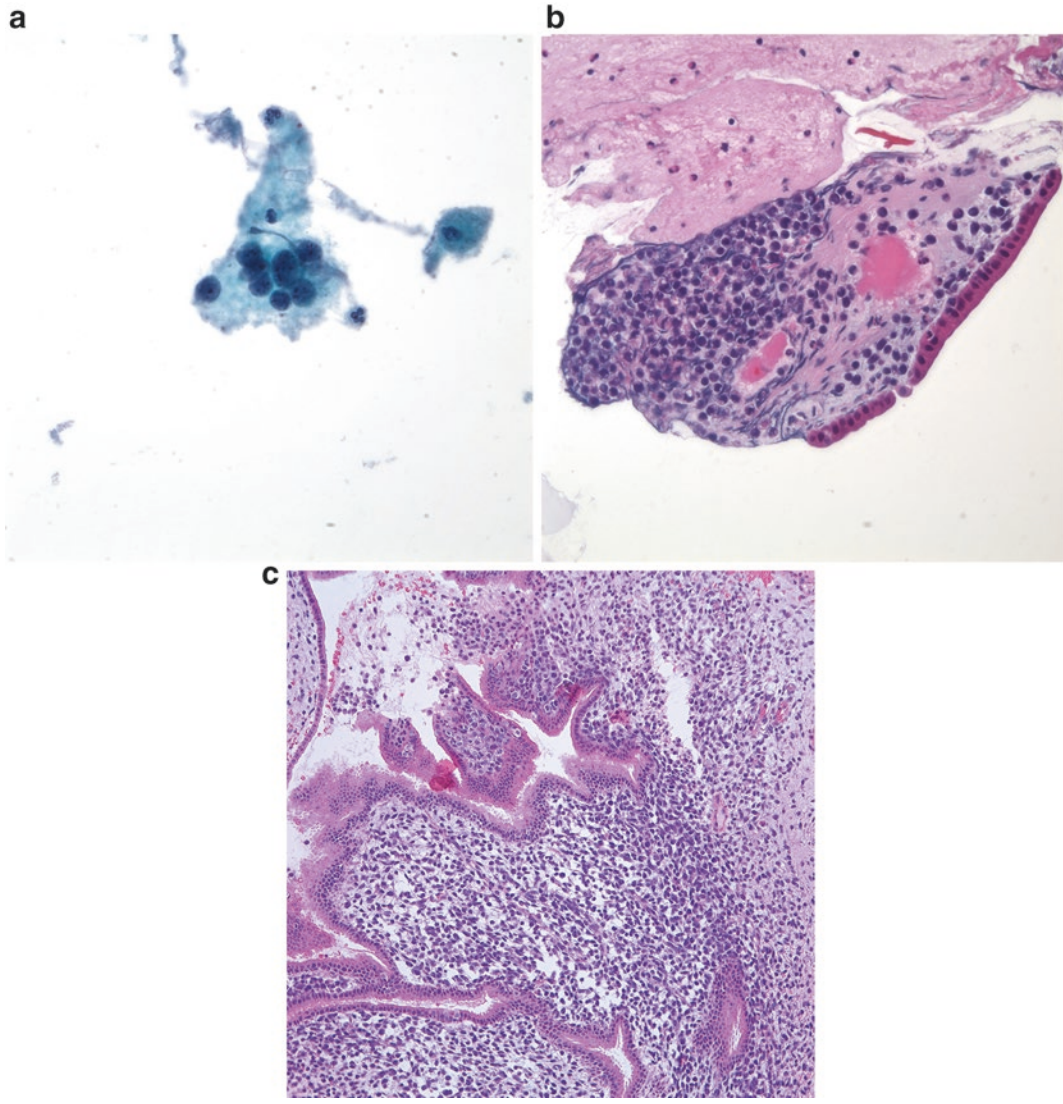


**Fig. 8.8** Embryonal rhabdomyosarcoma, botryoid type, of the biliary tree (**a**. Papanicolaou stain, high power; **b**, **c**. H&E stain, medium power). (**a**) The bile duct brushing in this specimen showed loosely cohesive clusters of small, round cells with scant, indistinct cytoplasm and round nuclei with finely clumped chromatin and variably conspicuous nucleoli (**a**). A fragment of tissue in the cell block has a hypercellular band of cells beneath unremarkable bile duct epithelium which recapitulates the histologic features observed in the resection (**b**, **c**).

done and will be positive in approximately 80 % of alveolar RMS but negative in embryonal RMS.

## Differential Diagnosis

Neuroendocrine neoplasms of the pancreas or biliary tree are rare, but can be cystic and mimic a choledochal cyst or RMS [11]. Other small round blue cell tumors, including lymphoma and metastases from neuroblastoma, Wilms tumor, Ewing sarcoma/primitive neuroectodermal tumor, and embryonal hepatoblastoma, should also be considered.

## Pearls

Tissue fragments in a cell block from a biliary brushing specimen from a young child can provide important morphologic clues to the

diagnosis, as well as material for ancillary studies. Thus, preparation of a cell block from the residual Thin Prep specimen can be helpful, if not done routinely.

### 8.3.3 Other Neoplasms

- Inflammatory myofibroblastic tumors have been reported within the extrahepatic biliary tree and can give rise to obstructive jaundice in children [12].
- Hematolymphoid malignancies, melanoma, and neuroendocrine tumors can involve the bile duct as primary or metastatic lesions (Fig. 8.9). Some neuroendocrine tumors primary to the bile duct may also be cystic and mimic a benign choledochal cyst [11].
- Carcinoids and neuroendocrine tumors (ranging from well to poorly differentiated or small cell carcinoma) can arise in the ampulla and, rarely, the bile duct (Fig. 8.10). Of the locations in the GI tract, the appendix is the most common site, followed by the small intestine, rectum, and stomach. Cytological features of these tumors include monomorphic cells in loosely cohesive clusters or as single plasmacytoid cells and stripped nuclei. The nuclei have stippled chromatin without conspicuous nucleoli. Usually the cells are seen along with small blood vessels. The clear cell variant can resemble a xanthoma. The differential diagnosis of carcinoid and other neuroendocrine tumors includes lymphoid cells from chronic inflammation or non-Hodgkin lymphoma (background has lymphoglandular bodies and cells have less cytoplasm), small cell carcinoma (more nuclear pleomorphism and molding), and adenocarcinoma.
- Metastases can rarely involve the biliary tree giving rise to obstructive jaundice, similar to that seen with pancreatobiliary primaries. Metastases can arise from almost any tumor, and in children are most often from small round blue cell tumors.

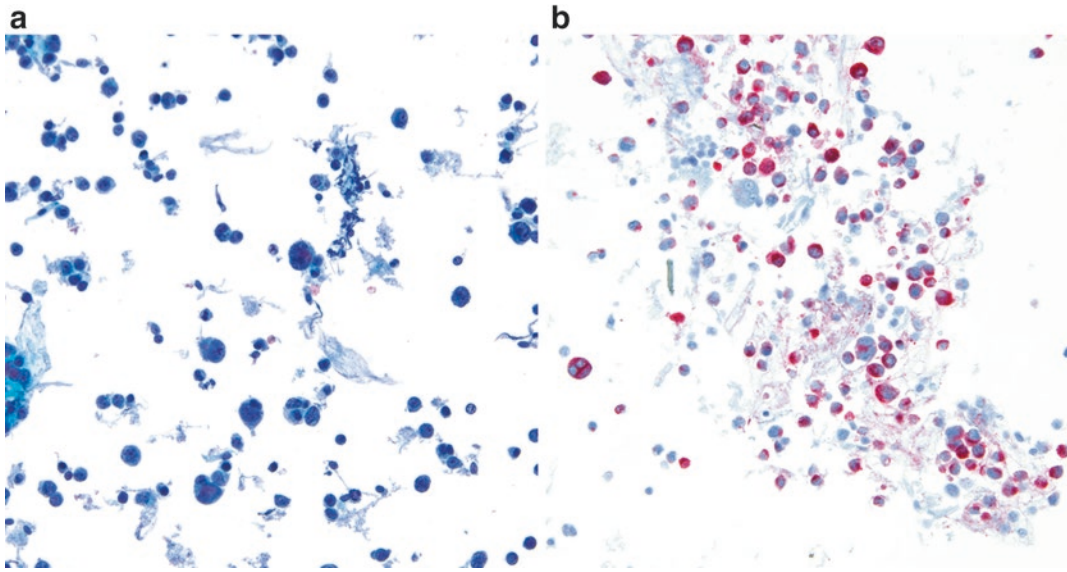


**Fig. 8.9** Melanoma involving the biliary tract (**a**. Papanicolaou, high power; **b**. Melan-A immunoperoxidase stain, high power). This bile duct brushing shows discohesive pleomorphic tumor cells with prominent nucleoli, compatible with melanoma (**a**). A Melan-A immunoperoxidase stain confirmed the diagnosis. The presence of bi- and trinucleate tumor cells is also more apparent in the Melan-A stain (**b**).

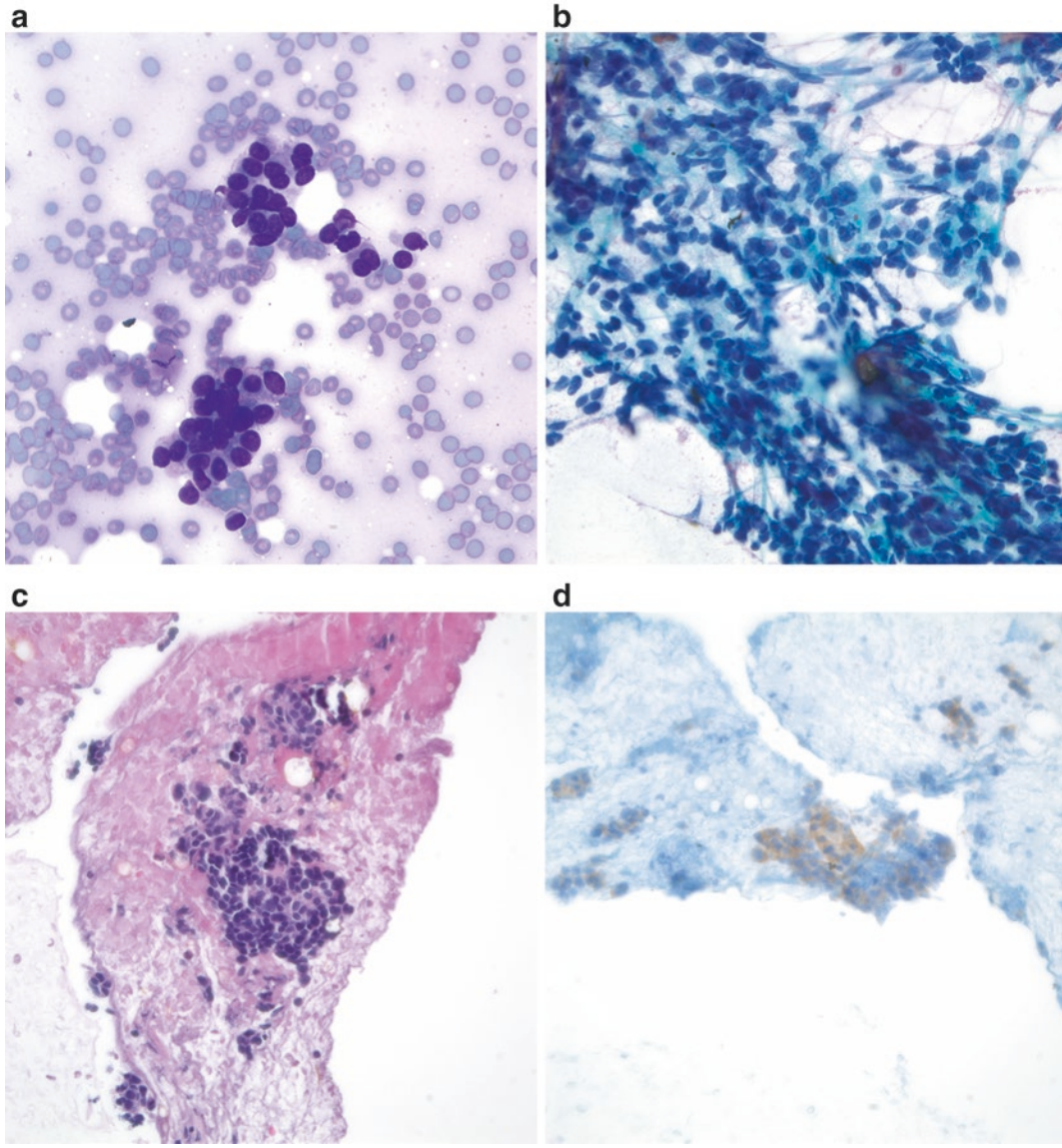


**Fig. 8.10** Well-differentiated neuroendocrine tumor of the ampulla (**a**. Diff-Quik stain, high power; **b**. Papanicolaou stain, high power; **c**. H&E stain, high power; **d**. Synaptophysin immunoperoxidase stain, high power). This aspirate from an ampullary mass shows uniform tumor cells in small clusters with a hint of pseudorosette formation (**a**). Sheets of bland tumor cells with arborizing vessels are also present (**b**). The cell block shows small, uniform tumor cells with scant cytoplasm arrayed in clusters with vague pseudorosettes (**c**). The tumor cells are positive for synaptophysin (**d**).

## 8.4 Pancreas

Similar to cholangiocarcinoma, ductal adenocarcinoma of the pancreas is exceedingly rare in children. The incidence of pancreatic cancer is estimated at 0.2 % of pediatric malignancies [13]. In a study of pancreaticoduodenectomies that were performed for malignancy in children, there were only five patients in 3 years, of which two had acinar cell carcinoma, one had a solid pseudopapillary tumor, and two had extrapancreatic rhabdomyosarcoma of the biliary tree [14].

The most common tumors are pancreatic neuroendocrine tumors (panNETs), which can occur anywhere in the pancreas and usually have a favorable prognosis. In addition, pancreatoblastoma, solid pseudopapillary, and acinar cell tumors are also seen in children.

Enteric duplication cysts can occur in association with the pancreas. When they are connected to the main pancreatic duct, they can mimic cystic neoplasms of the pancreas or pseudocysts. In addition, they can cause symptoms of pancreatitis and abdominal pain and may even be associated with pancreatic cancer [15].

One of the difficulties in interpreting pancreatic EUS-guided FNAs is that gastrointestinal contamination is common and should be distinguished from truly lesional material. One of the hallmarks is the goblet cells, creating a clearing within the two-dimensional group (Fig. 8.11).

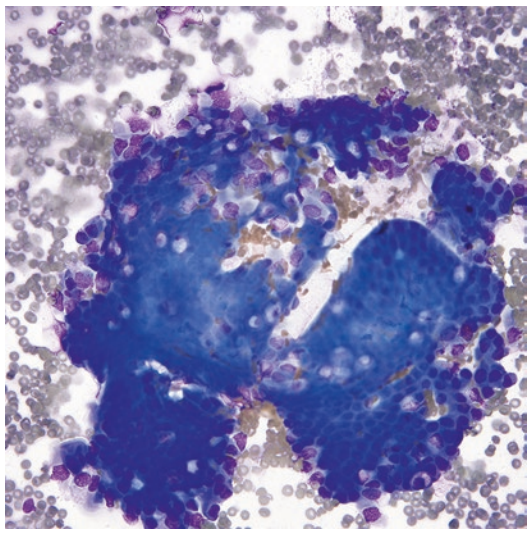

**Fig. 8.11** Gastrointestinal contamination in an endoscopic ultrasound (EUS)-guided FNA of the pancreas (Diff-Quik stain, high power). Gastrointestinal contamination frequently occurs in endoscopic pancreatic FNAs and should be distinguished from lesional material. The identification of goblet cells with cytoplasmic clearing is very helpful in distinguishing these sheets of cells from pancreatic ductal epithelium or neoplastic cells.

### 8.4.1 Pancreatoblastoma

#### Clinical Features

Pancreatoblastomas are rare tumors that can occur in children, usually infants under the age of 3 months. They can arise from any area in the pancreas and have also been reported outside of the pancreas, likely arising in ectopic pancreatic tissue. Although they can be sporadic, they can also occur in association with Beckwith-Wiedemann syndrome or familial adenomatous polyposis syndrome [16]. In general, children tend to have a better prognosis than adults with this tumor.

#### Cytological Features

Pancreatoblastoma is comprised of epithelial cells with acinar, ductal, neuroendocrine, and/or squamous differentiation. Aspirates are cellular with tumor cells arranged in sheets, in clusters, and singly in a background of metachromatic collagenous stromal fragments. Cells with acinar differentiation usually have moderately abundant, granular cytoplasm. Squamoid cells often appear in cohesive nests or corpuscles and are an important clue to the diagnosis. Foci of keratinization may also be identified.

#### Triage

Immunoperoxidase stains reveal positivity for AE1/AE3 cytokeratin, CK19, and neuron-specific enolase (NSE). Usually the tumor cells are negative for PAS and alpha-1 antitrypsin, which are positive in acinar cell carcinoma. Positivity for neuroendocrine markers, such as synaptophysin, can also be seen. In addition, these tumors can show nuclear positivity for beta-catenin, which make them difficult to distinguish from solid pseudopapillary tumor of the pancreas in some cases [16].

#### Differential Diagnosis

The differential diagnosis includes primary or metastatic neuroendocrine tumors, acinar cell carcinoma, and solid pseudopapillary tumor.

#### Pearls

These tumors are known to have a great deal of heterogeneity, which can make them difficult to diagnose in limited cytological samples. Squamoid corpuscles are an important clue to the correct diagnosis, but when these are not identified, pancreatoblastoma can easily be confused with other pancreatic neoplasms.

### 8.4.2 Solid Pseudopapillary Tumor

#### Clinical Features

Solid pseudopapillary tumors are uncommon tumors of unclear origin and typically occur in young women. They are rare in the pediatric population and may be seen in the setting of syndromes, such as Beckwith-Wiedemann syndrome or isolated hemihypertrophy. The tumors usually arise in the body or tail of the pancreas and on imaging appear as hypodense, well-circumscribed masses. They can also occur in the pancreatic head, necessitating pancreaticoduodenectomy [14].

#### Cytological Features

Aspirates from these tumors are cellular and have a characteristic low power appearance with several layers of tumor cells aligned along branching transgressing vessels, imparting a papillary appearance that resembles Chinese characters (Fig. 8.12). The background typically contains foamy histiocytes, hyaline globules, calcifications, and cholesterol crystals. The neoplastic cells are relatively monotonous, round to oval cells with finely granular chromatin, inconspicuous nucleoli, and nuclear grooves. The cells can also have cytoplasmic tails, imparting a cercariform appearance reminiscent of urothelial carcinomas [17]. Reddish granules have been described in the cytoplasm.

#### Triage

Immunoperoxidase stains reveal positivity for CD10, CD56, PR, vimentin, CD99, alpha-1 antitrypsin, and beta-catenin (nuclear) (Fig. 8.12). Negative or only weak staining for synaptophysin and chromogranin can be seen. Recently, LEF1 immunostaining has also been shown to be a reliable nuclear marker for solid pseudopapillary tumors [18].

#### Differential Diagnosis

The other entities to consider include primary or metastatic neuroendocrine neoplasms, acinar cell carcinoma, serous cystadenoma, pancreatoblastoma, and well-differentiated or papillary adenocarcinoma.

#### Pearls

The presence of nuclear grooves is one of the most helpful morphologic features for distinguishing solid pseudopapillary tumors from other pancreatic neoplasms with prominent vasculature, such as pancreatic neuroendocrine tumors. Solid pseudopapillary tumors typically have activating mutations of beta-catenin. Although rare, these tumors may be seen with Beckwith-Wiedemann syndrome or isolated hemihypertrophy; however, the risk of Wilms tumor, adrenocortical carcinoma, and hepatoblastoma is higher in these syndromes [19].

### 8.4.3 Pancreatic Neuroendocrine Neoplasms

#### Clinical Features

Pancreatic neuroendocrine tumors (panNETs) typically arise in the body or tail of the pancreas and on imaging appear as well-circumscribed, highly vascular tumors. In the pediatric population, these may occur in association with genetic disorders, such as Von Hippel-Lindau (VHL) syndrome in which 15% of patients develop panNETs [20], and may also result in syndromes associated with functional tumors, such as Verner-Morrison syndrome (watery diarrhea, hypokalemia, and achlorhydria from VIPoma) and Zollinger-Ellison syndrome (multiple, refractory peptic ulcers from gastrinoma).

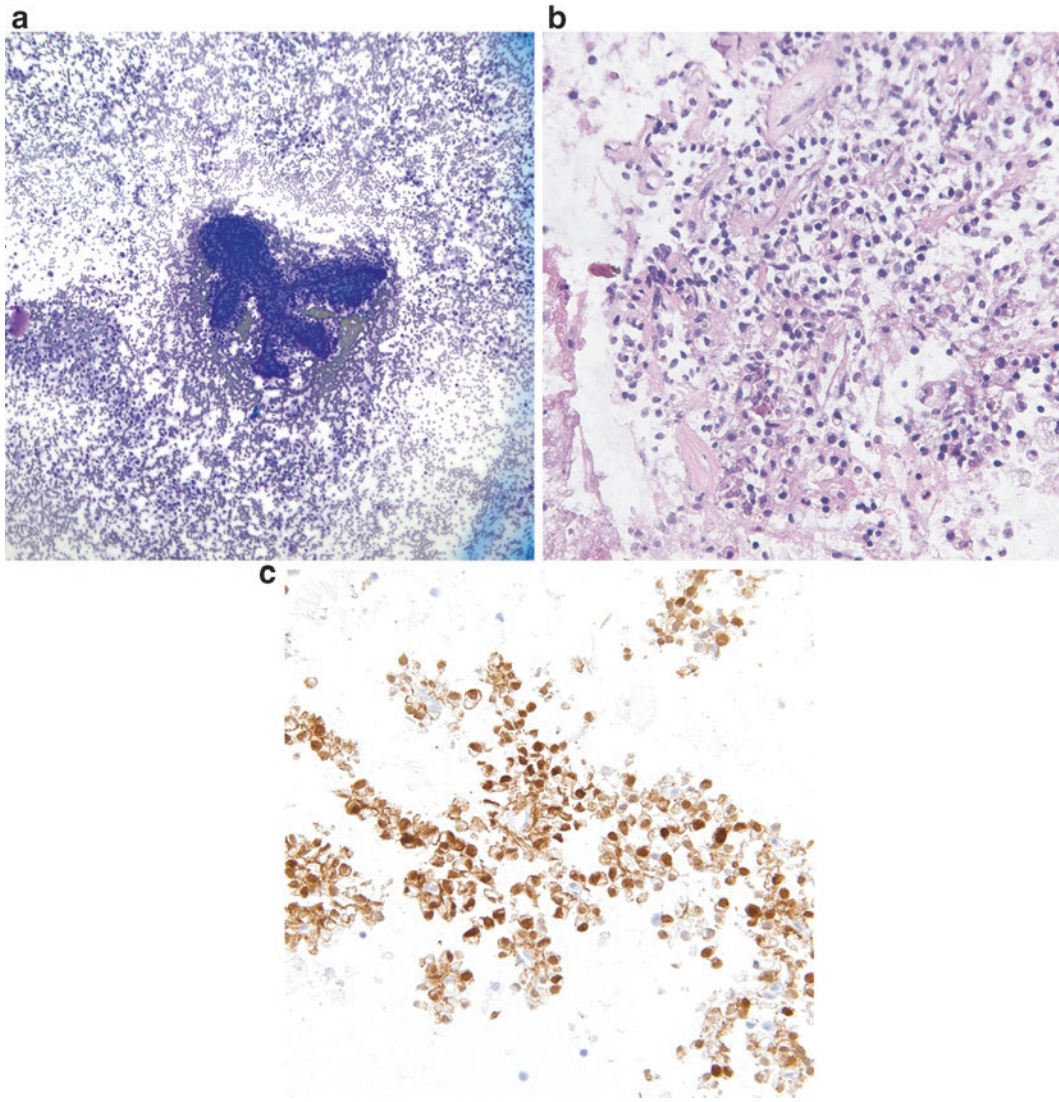


**Fig. 8.12** Solid pseudopapillary tumor of the pancreas (**a**. Diff-Quik stain, low power; **b**. H&E stain, medium power; **c**. Beta-catenin stain, high power). At low power, these tumors show arching vessels overlaid by multiple layers of epithelioid cells imparting a "Chinese character" appearance. Discohesive single cells are also noted in the background (**a**). The tumor cells show nuclear indentation or irregularities and cytoplasmic vacuoles (**b**). Nuclear positivity for beta-catenin is characteristic in these neoplasms (**c**).

### Cytological Features

Aspirates from these tumors are cellular and composed of uniform round cells with stippled chromatin, inconspicuous nucleoli, and moderate amounts of granular cytoplasm (Fig. 8.13). Some of the tumor cells appear as stripped nuclei or as plasmacytoid cells. Nuclear grooves, as seen in solid pseudopapillary tumor, are absent. In some tumors, the cells may have discrete clear cytoplasmic vacuoles, similar to those seen in renal cell carcinomas [21]. Transgressing small blood vessels can be seen within clusters of tumor cells. The background is clean, but often bloody.

### Triage

Immunoperoxidase stains for synaptophysin and chromogranin are helpful to confirm the diagnosis. Markers for specific peptide hormones,

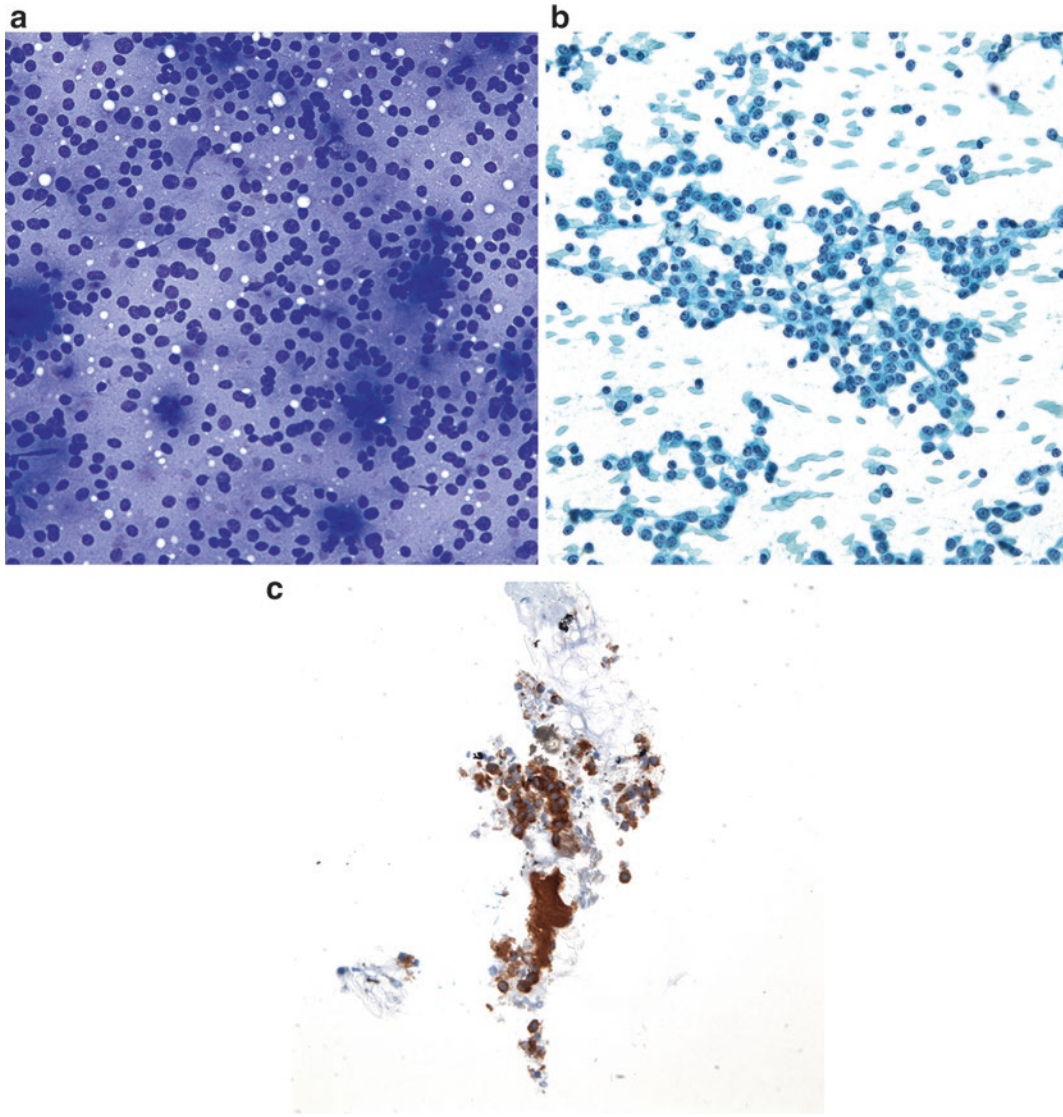


**Fig. 8.13** Pancreatic neuroendocrine tumor (**a**–**b**. Diff-Quik and Papanicolaou stain, high power; **c**. CD56 immunoperoxidase stain, high power). Aspirates from this pancreatic tail mass in an 18-year-old girl showed a monotonous population of single or loosely cohesive epithelioid cells with round nuclei and indistinct or stripped cytoplasm. Vague rosettes are also present (**a**). The cells are round to plasmacytoid and have uniform round nuclei with stippled chromatin and small nucleoli (**b**). The cells are positive for neuroendocrine markers, including CD56 (**c**).

including insulin, gastrin, somatostatin, and glucagon, are variably positive. A Ki67 stain can be very helpful for grading panNETs in cytological specimens, but should be interpreted with caution in specimens with low or modest cellularity.

## Differential Diagnosis

The other diagnoses to consider include solid pseudopapillary tumor, acinar cell carcinoma, serous cystadenoma, well-differentiated adenocarcinoma, and lymphoproliferative or plasmacytic disorders. Lipid-rich variants of panNETs can mimic clear cell carcinoma of the kidney, adrenal cortical neoplasms, or adenocarcinoma of the pancreas.

## Pearls

Given the rich vascularity of panNETs, aspirates may be nondiagnostic with a predomi-

nance of blood. In such cases, the proceduralist should consider avoiding aspiration, but rather using the needle-only (fine needle nonaspiration) technique to decrease the peripheral blood dilution and optimize the ability to see the neoplastic cells. Another difficulty can be the grading of neuroendocrine tumors, given that the 2010 WHO Classification of Neuroendocrine neoplasms uses a Ki67 of <3% for G1 tumors, 3–20% for G2, and >20% for G3 tumors.

### 8.4.4 Serous Cystadenomas

#### Clinical Features

These are very rare benign tumors that appear as a spongelike or microcystic mass in the pancreas and typically occur in elderly patients. However, these tumors can also occur in younger patients, including adolescents, with VHL who have been reported to have simple cysts (47% of patients), serous cystadenomas (11% of patients), and neuroendocrine tumors (15% of patients) (Fig. 8.14) [20].

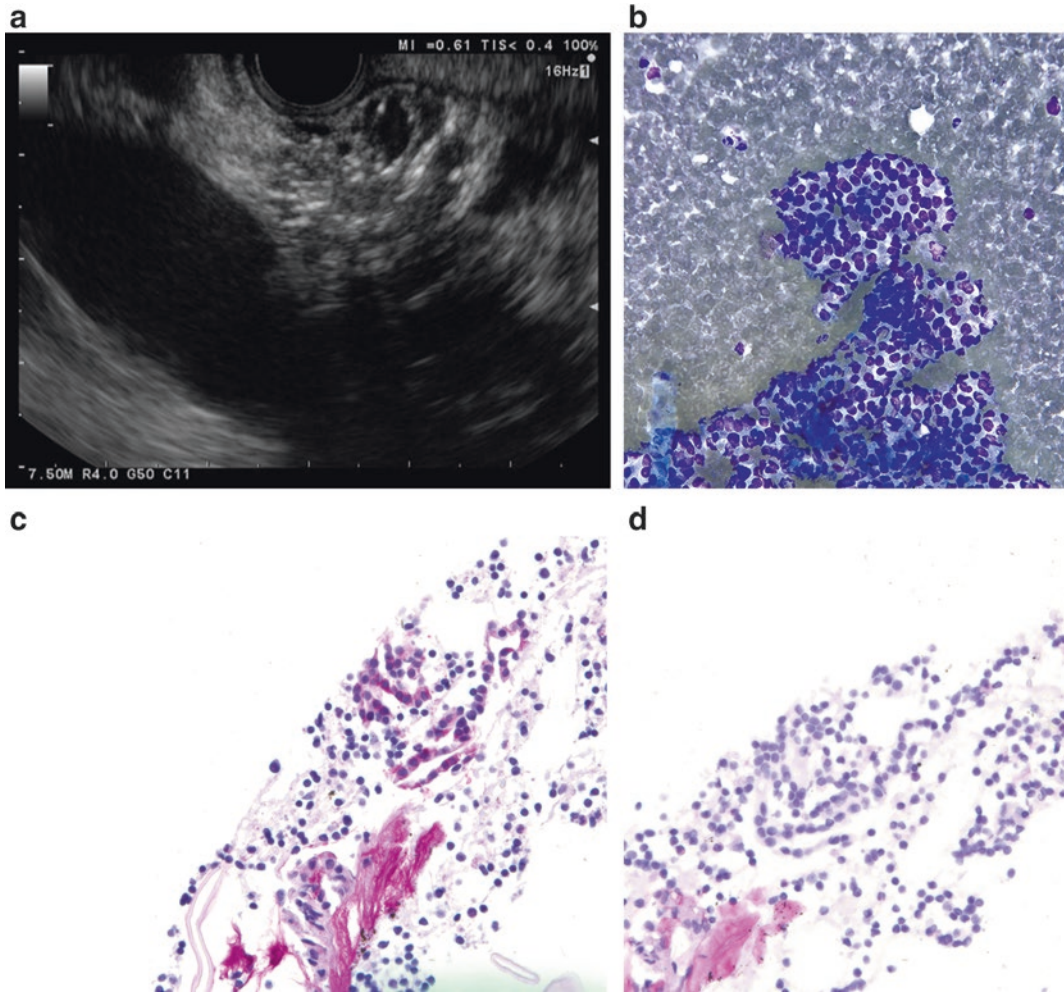


**Fig. 8.14** Serous cystadenoma in Von Hippel-Lindau syndrome (**a**. Ultrasound image; **b**. Diff-Quik stain, high power; **c**. PAS stain, high power; **d**. PASD stain, high power). This young male with Von Hippel-Lindau syndrome presented with multiple multicystic lesions of the pancreas (**a**). Aspirates yielded flat sheets of small monotonous cells with clear cytoplasm and small round nuclei (**b**). (**c**) The cytoplasm showed PAS positivity that was sensitive to digestion with diastase (**d**), confirming the presence of glycogen.

### Cytological Features

Aspirates are typically hypocellular with uniform, small, round cells and stripped nuclei, in a background of proteinaceous fluid or blood (Fig. 8.14). The cells are arranged in flat sheets or clusters and have scant, clear, finely vacuolated cytoplasm and small, round nuclei with inconspicuous nucleoli. Strips of neoplastic cells may be seen on the cell block.

### Triage

PAS and PASD special stains can be performed to confirm the presence of cytoplasmic glycogen, which is bright pink on the PAS stain and digested with diastase (negative with PASD) (Fig. 8.14).

### Differential Diagnosis

Definitive diagnosis is often difficult or impossible on FNA due to the paucity of cells. Other diagnostic entities to consider include neuroendocrine tumors, lymphoproliferative disorders, solid pseudopapillary tumors, acinar cell carcinoma, benign pseudocyst, and well-differentiated adenocarcinoma.

### Pearls

On imaging, these spongelike or multicystic tumors can also have a central scar and central calcifications, which are helpful diagnostic clues. If molecular testing is done on the aspirate fluid from a serous cystadenoma associated with VHL, there is usually a mutation in the *VHL* gene on chromosome 3, and a lack of mutations that are seen in ductal neoplasms (e.g., *KRAS, SMAD4,* and *GNAS*). This is helpful in cases with insufficient material for PAS/PASD staining.

## 8.4.5 Acinar Cell Carcinoma

### Clinical Features

Acinar cell carcinomas are rare primary pancreatic malignancies that usually occur in adults and are more common in males. However, approximately 6% of these tumors occur in patients under 20 years of age. In some patients, these tumors may be seen in association with a lipase hypersecretion syndrome, resulting in pancreatitis, panniculitis, and polyarthritis, but usually this is seen in older patients. Serum AFP elevations have been seen in young patients with this tumor. Overall, acinar cell carcinomas have a poor prognosis; however, pediatric patients may have a better prognosis than adults.

### Cytological Features

These tumors yield cellular aspirates composed of malignant acinar cells in loosely cohesive sheets and clusters, in acinar arrays, and singly. The cells have granular cytoplasm, round to oval nuclei, and prominent nucleoli. In some tumors, the cells have prominent cytoplasmic vacuoles or droplets. Stripped nuclei and zymogen granules are usually present in the background. Features that distinguish acinar cell carcinoma from benign acinar cells are discohesion and the prominence of the nucleolus in the malignant cells.

### Triage

Immunoperoxidase and histochemical stains are important for confirming the diagnosis and excluding other entities in the differential diagnosis. Acinar cell carcinoma is positive for trypsin, as well as alpha-1 antitrypsin and other pancreatic exocrine enzymes, and PASD. The tumors stain for cytokeratins, while neuroendocrine markers are usually negative.

### Differential Diagnosis

Neuroendocrine tumors, lymphoproliferative disorders, normal pancreatic acinar tissue, pancreatoblastoma, and well-differentiated adenocarcinoma are entities to consider in the differential. Metastatic small round blue cell tumors, such as neuroblastoma, can also be seen in or around the pancreas and morphologically mimic acinar cell carcinoma or other neoplasms with hyperchromatic, round nuclei without abundant cytoplasm (Fig. 8.15).

### Pearls

These tumors can occur in combination with a neuroendocrine tumor or adenocarcinoma, but should not comprise more than 25% of the neoplasm. Such cases can be cytologically ambiguous as morphology varies depending on sampling.

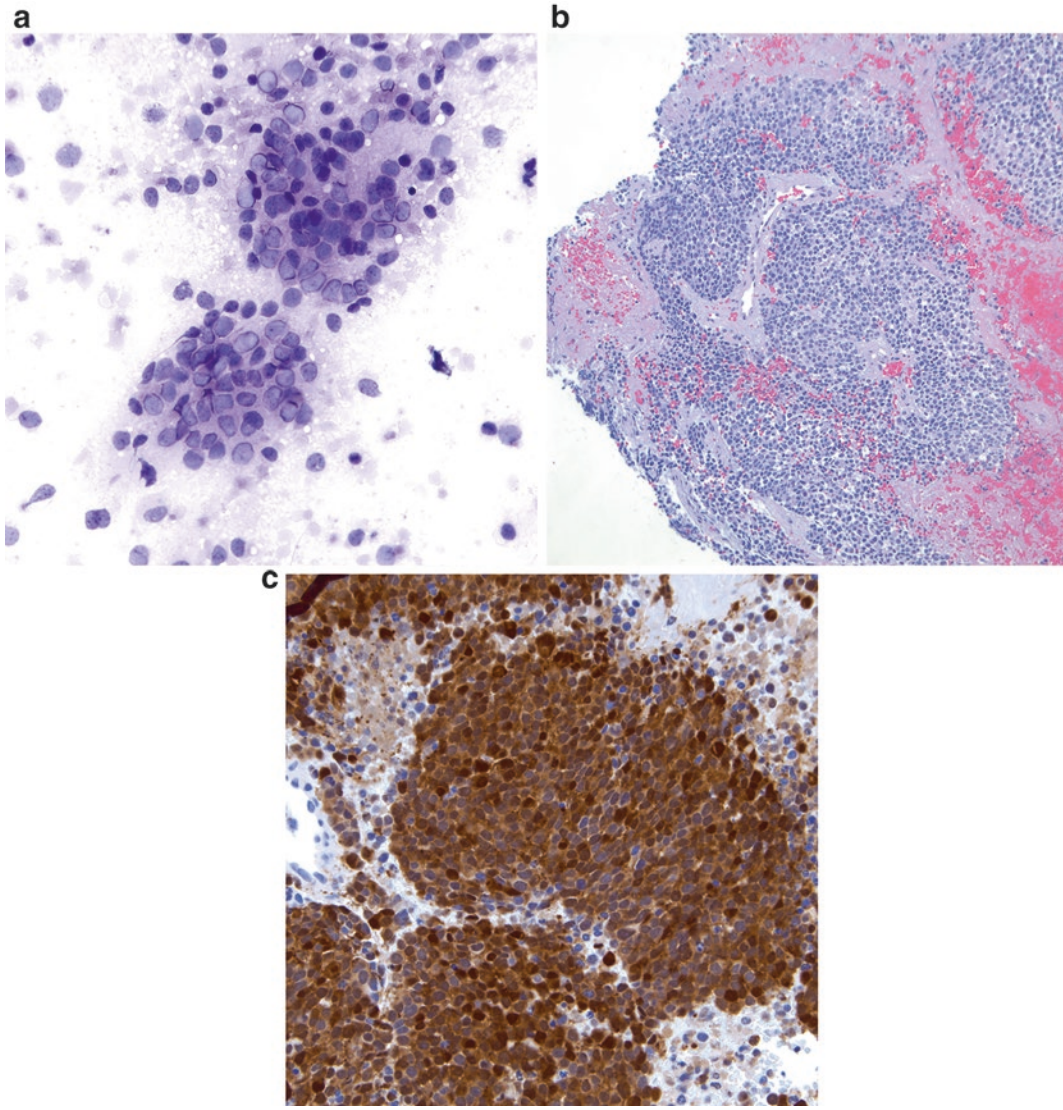


**Fig. 8.15** Metastatic neuroblastoma in the peripancreatic region (**a**. Giemsa stain, high power; **b**. H&E stain, low power; **c**. PGP9.5 immunoperoxidase stain, medium power). This specimen is from a 3-year-old patient with a history of neuroblastoma, who presented with a peripancreatic mass, which was found to be neuroblastoma. The smear shows clusters of small round cells with scant cytoplasm and round, ovoid or irregular nuclei with nuclear molding. Scant fibrillary material suggestive of neuropil is present (**a**). The corresponding biopsy shows a round cell tumor with neuropil (**b**). The tumor cells are positive for PGP9.5 (**c**).

## 8.5 Conclusions

Tumors of the liver, biliary tree, and pancreas are not as common in children and adolescents as they are in adults, and moreover, the types of neoplasms that occur in these populations differ. For example, in the pediatric population, hepatoblastomas outnumber hepatocellular carcinomas, solid pseudopapillary tumors and pancreatic neuroendocrine tumors outnumber ductal adenocarcinomas, and biliary rhabdomyosarcomas are more common than in adults. Some tumors, such as pancreatoblastoma, have a better prognosis in children than in adults. Aspirates and/or cytological brushings can be used to establish a diagnosis or narrow the differential diagnosis and thereby guide appropriate management. Ancillary studies play a critical role in accurate and specific diagnosis of these lesions.

## References


1. Allan BJ, Wang B, Davis JS, Parikh PP, Perez EA, Neville HL, Sola JE. A review of 218 pediatric cases of hepatocellular carcinoma. J Pediatr Surg. 2014;49:166–71.
2. Barwad A, Gupta N, Gupta K, Rajwanshi A, Marwaha RK, Rao KL, Dey P, Srinivasan R, Nijhawan R. Hepatoblastoma—an attempt of histological subtyping on fine-needle aspiration material. Diagn Cytopathol. 2013;41:95–101.
3. Lopez-Terrada D, Alaggio R, de Davila MT, et al. Towards an international pediatric liver tumor consensus classification: proceedings of the Los Angeles COG liver tumors symposium. Mod Pathol. 2014;27:472–91.
4. Vokuhl C, Oven F, Haberle B, et al. Small cell undifferentiated (SCUD) hepatoblastomas: all malignant rhabdoid tumors? Genes Chromosomes Cancer. 2016;55:925–931.
5. Nguyen T, Phillips D, Jain D, Torbenson M, Wu TT, Yeh MM, Kakar S. Comparison of 5 immunohistochemical markers of hepatocellular differentiation for the diagnosis of hepatocellular carcinoma. Arch Pathol Lab Med. 2015;139:1028–34.
6. Shafizadeh N, Ferrell LD, Kakar S. Utility and limitations of glypican-3 expression for the diagnosis of hepatocellular carcinoma at both ends of the spectrum. Mod Pathol. 2008;21:1011–8.
7. Wassef M, Blei F, Adams D, Alomari A, Baselga E, Berenstein A, Burrows P, Frieden IJ, Garzon MC, Lopez-Gutierrez JC, Lord DJE, Mitchel S, Powell J, Prendiville J, Vikkula M, ISSVA Board and Scientific Committee. Vascular anomalies classification: recommendations from the international society for the study of vascular anomalies. Pediatrics. 2015;136, e203-14.
8. Hsi Dickie BH, Fishman SJ, Azizkhan RG. Hepatic vascular tumors. Semin Pediatr Surg. 2014;23:168–72.
9. Jurczyk M, Zhu B, Laskin W, Lin X. Pitfalls in the diagnosis of hepatic epithelioid hemangioendothelioma by FNA and needle core biopsy. Diagn Cytopathol. 2014;42:516–20.
10. Hernández F, Navarro M, Encinas JL, López Gutiérrez JC, López Santamaría M, Leal N, Martínez L, Patrón M, Tovar JA. The role of GLUT1 immunostaining in the diagnosis and classification of liver vascular tumors in children. J Pediatr Surg. 2005;40:801–4.
11. Tonnhofer U, Balassy C, Reck CA, Koller A, Horcher E. Neuroendocrine tumor of the common hepatic duct, mimicking a choledochal cyst in a 6-year-old child. J Pediatr Surg. 2009;44:E23–5.
12. Büyükyavuz I, Karnak I, Haliloglu M, Senocak ME. Inflammatory myofibroblastic tumour of the extrahepatic bile ducts: an unusual cause of obstructive jaundice in children. Eur J Pediatr Surg. 2003;13:421–4.
13. Perez EA, Gutierrez JC, Koniaris LG, et al. Malignant pancreatic tumors: incidence and outcome in 58 pediatric patients. J Pediatr Surg. 2009;44:197–203.
14. d'Ambrosio G, del Prete L, Grimaldi C, Bertocchini A, Lo Zupone C, Monti L, de Ville de Goyet J. Pancreaticoduodenectomy for malignancies in children. J Pediatr Surg. 2014;49:534–8.
15. Chiu AS, Bluhm D, Xiao SY, Waxman I, Matthews JB. Enteric duplication cyst of the pancreas associated with chronic pancreatitis and pancreatic cancer. J Gastrointest Surg. 2014;18:1054–8.
16. Hammer ST, Owens SR. Pancreatoblastoma: a rare, adult pancreatic tumor with many faces. Arch Pathol Lab Med. 2013;137:1224–6.
17. Samad A, Shah AA, Stelow EB, Alsharif M, Cameron SE, Pambuccian SE. Cercariform cells: another cytologic feature distinguishing solid pseudopapillary neoplasms from pancreatic endocrine neoplasms and acinar cell carcinomas in endoscopic ultrasound-guided fine-needle aspiration. Cancer Cytopathol. 2013;121:298–310.
18. Singhi AD, Lilo M, Hruban RH, Cressman KL, Fuhrer K, Seethala RR. Overexpression of lymphoid enhancer-binding factor 1 (LEF1) in solid-pseudopapillary neoplasms of the pancreas. Mod Pathol. 2014;27:1355–63.
19. Nichols-Vinueza DX, Veintemilla G, Perez-Atayde AR, Gutierrez A. Letter to the editor: pseudopapillary tumor of the pancreas in a child with hemihypertrophy and a history of Wilms tumor. Pediatr Blood Cancer. 2014;61:1901–2.
20. Charlesworth M, Verbeke CS, Falk GA, Walsh M, Smith AM, Morris-Stiff G. Pancreatic lesions in von Hippel-Lindau disease? A systematic review and meta-synthesis of the literature. J Gastrointest Surg. 2012;16:1422–8.
21. Levy GH, Finkelstein A, Harigopal M, Chhieng D, Cai G. Cytoplasmic vacuolization: an underrecognized feature in endocrine tumors of the pancreas. Diagn Cytopathol. 2013;41:623–8.

# Body Fluids

# 9

Pamela Michelow and Michelle Dubb

## 9.1 Introduction

The four main body cavities (left and right pleural, pericardial and peritoneal) are lined by parietal and visceral membranes, composed of blood and lymphatic vessels in loose connective tissue stroma covered by mesothelial cells, with a film of fluid in between for lubrication. Any accumulation of fluid within this potential space is termed an effusion and is always pathological. Effusions may be noninflammatory, inflammatory, infectious, or neoplastic, benign or malignant. Common causes of effusions in adults include cirrhosis, heart failure, pneumonia, and metastatic carcinoma, all of which are rare in children and adolescents. As a consequence, body cavity fluids from the pediatric population represent a small minority of all effusions sent for cytological evaluation and raise different diagnostic considerations than those from adults [1–6].

P. Michelow, MBBCh, MSc (Med Sci) (✉)
M. Dubb, MBBCh, FCPath, FRCPath
Cytology Unit, Department of Anatomical Pathology, Faculty of Health Sciences, University of the Witwatersrand and National Health Laboratory Service, Johannesburg, South Africa
e-mail: pamela.michelow@nhls.ac.za; mdubb@telkomsa.net

## 9.2 Categorization of Body Fluids

- Effusions can be divided into transudates and exudates. Transudates are ultrafiltrates that are low in protein and typically accumulate due to physiological abnormalities, such as increased fluid pressures. Exudates imply damage to the serous membranes and leakage of protein, due to an underlying inflammatory or neoplastic process. Whereas the cause of a transudate is often known, the etiology of an exudate may be unknown or require confirmation to initiate appropriate therapy. Therefore, exudates are more likely to be sent for cytological evaluation.
- The vast majority of effusions in children are benign; however, they are not common cytological specimens and usually contain a smaller volume of fluid than those in adults. Although the primary purpose of effusion cytopathology is to identify a neoplastic effusion, it can be useful in the identification of inflammatory and other conditions.
- Parapneumonic effusions are pleural effusions that occur in patients with pneumonia, lung abscess, or bronchiectasis. Cardiac failure should also be ruled out in a child presenting with an effusion if there is no evidence of neoplasia or infection.



S.E. Monaco, L.A. Teot (eds.), *Pediatric Cytopathology*, DOI 10.1007/978-3-662-53441-0_9

## 9.3 Gross Appearance of Fluid

On receipt of an effusion, the laboratory should note the amount of fluid and the gross appearance. This includes the following descriptions, which can help in categorizing the fluid specimen [5]:

- *Clear straw colored*: The vast majority of effusions are serous in nature and appear clear or straw colored, even if some blood is present.
- *Milky white*: Chylous effusions are cloudy and milky in appearance. They may be due to the accumulation of chylomicrons which can be idiopathic or due to blockage or injury of the thoracic duct. Tuberculosis of a body cavity can also present with a chylous-appearing effusion, as can hematologic malignancies.
- *Metallic gold*: This implies a pseudochylous effusion due to the presence of cholesterol crystals. This color is associated with long-standing effusions, often in association with tuberculosis, rheumatoid lung disease, or myxedema.
- *Yellow purulent*: This is due to the presence of a marked acute inflammatory infiltrate, often secondary to an underlying pneumonia or perforated organ. When a purulent fluid is received in the cytology laboratory, a portion should be submitted for microbial cultures at the time of processing if that was not done at the point of collection.
- *Green*: Bile-stained effusions are usually due to a perforated bile duct or secondary to acute pancreatitis.
- *Bloody dark brown*: This may be due to trauma, infarction, endometriosis, or malignancy. As blood can be seen in both benign and malignant conditions, it is relatively nonspecific.

## 9.4 Benign Conditions

As previously mentioned, effusions in the pediatric population are most commonly due to non-neoplastic or benign causes.

### 9.4.1 Transudates

Common causes of transudates include congestive heart failure, cirrhosis, nephrotic syndrome, hypoalbuminemia due to malnutrition, and hypothyroidism. These are paucicellular specimens with scattered lymphocytes, histiocytes, and mesothelial cells. The mesothelial cells appear singly and in small clusters. Intercellular windows may be evident. The cells have well-defined cell borders with a peripheral cytoplasmic "lacy skirt," centrally situated nuclei with smooth nuclear borders, and finely granular chromatin.

### 9.4.2 Reactive Mesothelial Cells

Reactive mesothelial cells occur in the context of a wide variety of injuries, infections, and neoplasms. The fluid contains increased numbers of mesothelial cells appearing singly, in monolayered strips, and in sheets. The clusters have "knobby" borders, papillary-like structures, and "cell-in-cell" arrangements. The cells are round with dense cytoplasm and central to eccentrically situated nuclei. The nucleus has a well-defined membrane and uniform granular chromatin. Nucleoli may be apparent. Binucleation and multinucleation are not uncommon. Stimulation of the mesothelium by a variety of factors, including but not limited to uremia, dialysis, liver disease, and drugs, can cause exfoliation of markedly atypical mesothelial cells that may mimic malignancy. Immunocytochemistry may be required to make this distinction.

### 9.4.3 Inflammatory Effusions

The presence of inflammatory cells in effusions is due to a wide variety of infectious and noninfectious etiologies. Table 9.1 lists the most common causes of effusions associated with various types of inflammatory cells (Figs. 9.1, 9.2, 9.3, and 9.4).

#### 9.4.3.1 Infectious Etiologies

Effusions result from a wide variety of infections. While cultures or clinical context may be needed for a specific diagnosis, the constituent inflammatory

**Table 9.1** Differential diagnosis for inflammatory effusions based on the predominant type of cells identified

| Predominantly neutrophils | Predominantly eosinophils |
|---|---|
| Acute pneumonia (empyema)<br>Acute peritonitis<br>Fungal infection<br>Mycobacterial infection<br>Penetrating injury<br>Perforated viscera or intrathoracic rupture of esophagus<br>Neoplasm<br>Mimic: Karyorrhectic debris from high-grade lymphomas or other small round blue cell tumors involving a body cavity can mimic the multilobulated nuclei of neutrophils | Chest tubes<br>Thoracotomy<br>Pneumothorax<br>Parasites<br>Allergies<br>Pneumonia<br>Malignancy<br>Autoimmune disease<br>Pulmonary embolus<br>Mimic: Eosinophils may be mistaken for neutrophils in an effusion, since the eosinophilic granules are not easily seen on Papanicolaou-stained slides |
| Predominantly lymphocytes | Predominantly plasma cells |
| Mycobacterial infection<br>Autoimmune disease<br>Trauma<br>Peritoneal dialysis<br>Chylous effusion<br>Leukemia and lymphoma<br>Other neoplasms<br>Mimic: Karyorrhectic or apoptotic debris from small round blue cell tumors involving a body cavity can mimic lymphocytic effusions | Autoimmune disease<br>Mycobacterial infection<br>Neoplasia<br>Mimic: Plasmacytoid neoplasms such as melanoma, and neuroendocrine neoplasm can mimic a plasmacytic effusion |
| Predominantly histiocytes | |
| Inflammation<br>Mechanical irritation<br>Histiocytic and mesothelial hyperplasia<br>Neoplasia | |

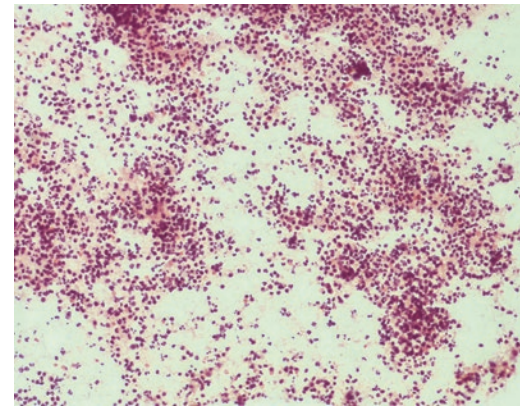

**Fig. 9.1** In this pleural fluid from a child with pneumonia, there are numerous neutrophils, scattered lymphocytes, and histiocytes, consistent with an empyema (Papanicolaou stain, medium power).

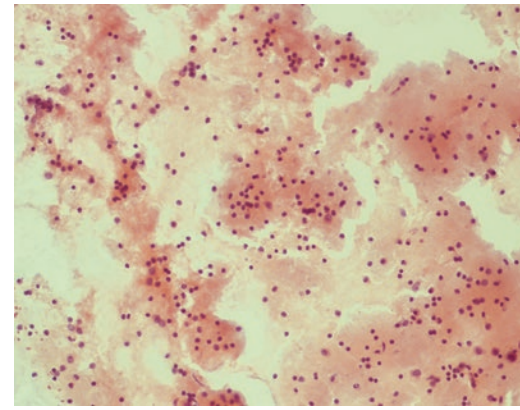

**Fig. 9.2** In this pleural fluid from a 10-year-old boy with a mycobacterial infection, a moderate number of lymphocytes are present in a serous background (Papanicolaou stain, medium power). The culture grew *M. tuberculosis*.

cells provide an important clue to the differential diagnostic considerations:

- *Viral infection*: Many viral infections including, but not limited to, influenza, parainfluenza, adenovirus, respiratory syncytial, and mumps result in serous effusions. Variable numbers of chronic inflammatory cells are noted. Very occasionally, a viral cytopathic effect can be identified in mesothelial cells.
- *Bacterial infection*: Infection due to streptococci, staphylococci, haemophili, and other bacteria can lead to empyema, acute peritonitis or pericarditis. The fluid is macroscopically purulent, with numerous neutrophils and inflammatory debris noted microscopically (Fig. 9.1). Bacteria, within neutrophils and/or histiocytes or extracellularly, may be noted. Ancillary microbiological tests can help to identify the organism and to determine antimicrobial sensitivities.
- *Mycobacterial infection*: Fluid from a tuberculous serositis is typically shiny green macroscopically. Microscopically, there is a dearth of mesothelial cells with scattered to moderate numbers of lymphoid cells in a serous background [1, 2, 6]. Very occasionally, caseous necrosis and granulomas may be seen.

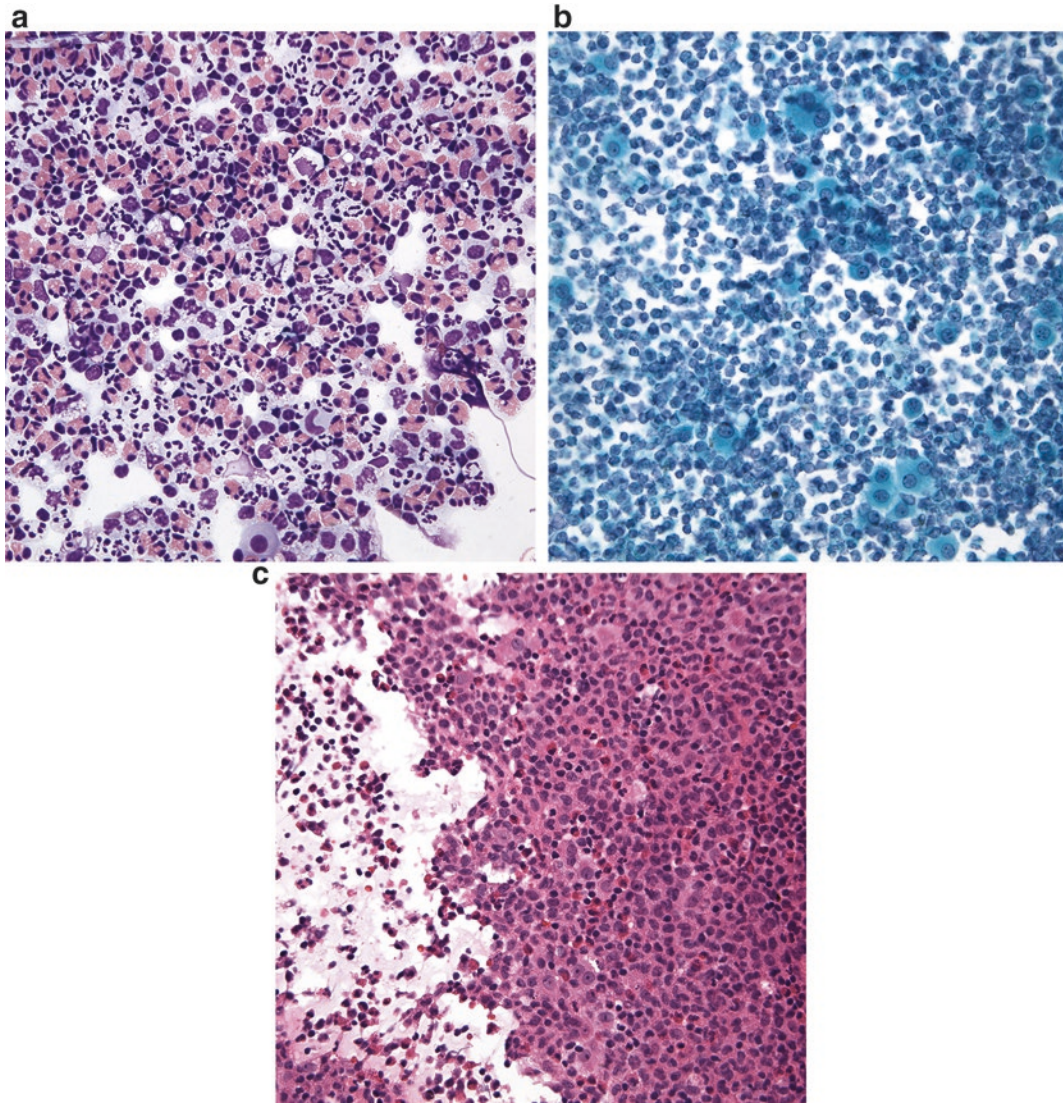


**Fig. 9.3** This eosinophilic effusion taken after repeated chest tubes has numerous eosinophils with bilobed nuclei and cytoplasmic granularity (**a**. Diff-Quik stain, medium power; **b**. Papanicolaou stain, medium power; **c**. H&E stain, medium power). The eosinophilic granules are not as easily seen on the Papanicolaou stain, compared to Diff-Quik and H&E stains. (Images courtesy of Dr. Sara Monaco).

Mycobacterial infection can, on occasion, cause an acute inflammatory infiltrate (Fig. 9.2). Adenosine deaminase (ADA) and gamma-interferon (IFN) levels are raised. Routine acid fast stains can be used on direct smears made from the centrifuged 'pellet' of the fluid. A cell block can also be produced on which ancillary tests for mycobacterial infection can be performed.

- *Fungal infection*: Fungal serositis is encountered most frequently in immunosuppressed children. A predominance of neutrophils is seen with a varying amount of debris. The most common fungi in this regard are candida spp, cryptococcus spp, and *Pneumocystis jirovecii*. Special stains, such as PAS, GMS, and mucicarmine, highlight the morphologic features of the organisms and, thus, may aid in identification.
- *Parasitic infection*: Many parasites have been reported in serous effusions including paragonimiasis, amebiasis, echinococcosis, ascariasis, and schistosomiasis (Fig. 9.4).

### 9.4.3.2 Autoimmune and Rheumatologic Disease

Effusions are most often seen with systemic lupus erythematosus (SLE) and rheumatoid arthritis, but can be associated with other autoimmune and rheumatologic disorders.

#### Rheumatoid Arthritis

- Pleural effusions are most commonly seen, but peritoneal and pericardial effusions have been described. Arthritis is typically present before pleuritis develops.
- The fluid is yellow to green with a metallic shine (pseudochylous).
- The cytomorphology mimics that seen in a rheumatoid nodule. Variable amounts of granular debris and acute inflammatory cells are observed in the background. Mesothelial cells are sparse. Histiocytes are noted and can assume a variety of unusual shapes (e.g., spindled). These spindle cells have well-defined cell borders, dense cytoplasm, and pyknotic nuclei. Multinucleated histiocytes and cholesterol crystals can also be observed (Fig. 9.5).
- Biochemical analysis reveals an exudate with low glucose and pH levels, high lactic dehydrogenase levels (LDH), and high rheumatoid factor titers.

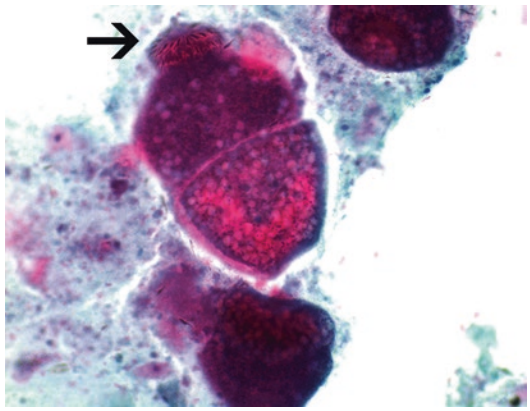

**Fig. 9.4** Protoscolex of *Echinococcus* in a background of hydatid sand from an intra-abdominal cyst in an 11-year-old boy (Papanicolaou stain, medium power). An *arrow* indicates the collar of hooklets.

#### Systemic Lupus Erythematosus (SLE)

- An effusion is a very unusual presentation for SLE, but effusions often develop during the course of the disease. Pleural effusions are more often encountered, but peritoneal and pericardial serositis may be observed.
- Under the microscope, variable numbers of neutrophils and lymphocytes are noted. Two different cell types have been described in asso-

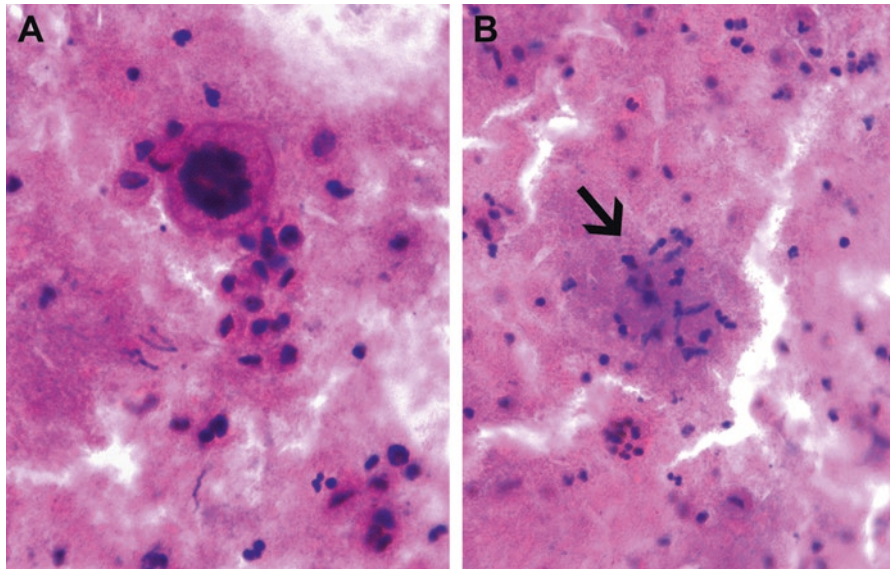


**Fig. 9.5** This pleural fluid from a 17-year-old girl with rheumatoid arthritis shows multinucleated cells (**a**) in a granular, inflamed background with degenerating epithelioid histiocytes (**b**, *arrow*) (Papanicolaou stain, high power).

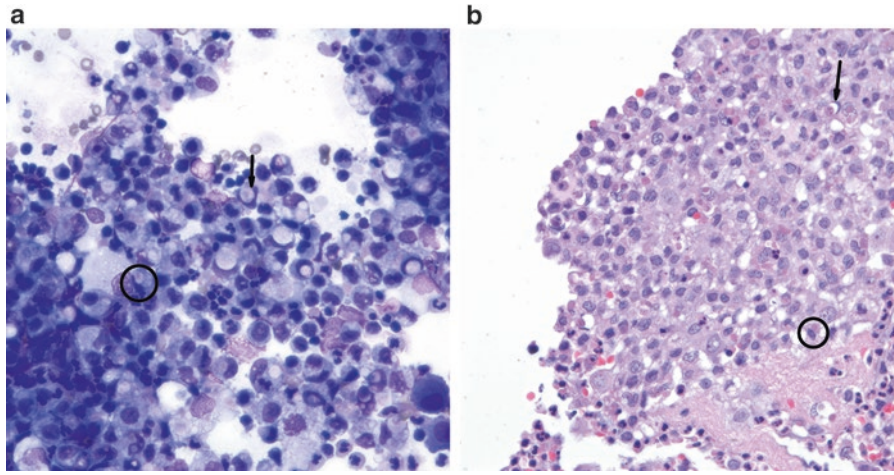


**Fig. 9.6** A pleural effusion from a young woman with a history of systemic lupus erythematosus shows degenerating cells in various stages, including those within neutrophils and histiocytes (**a**. Diff-Quik stain, high power; **b**. H&E stain, medium power). The LE cells typically have completely degenerated cells with no discernible chromatin (*circles*), whereas the tart cells contain engulfed cells in various states of degeneration, but with intact chromatin visible (*arrow*). (Images courtesy of Dr. Sara Monaco).

ciation with effusions in SLE. The LE cell is a neutrophil or macrophage with a large, homogeneous cytoplasmic inclusion that pushes the nucleus to one side of the cell. The nucleus becomes crescentic in shape [7]. This inclusion, referred to as a hematoxylin body, represents the denatured nucleus of a phagocytosed cell. Tart cells have phagocytosed material that is smaller than a hematoxylin body, is nonhomogeneous, and does not displace the nucleus. Tart cells are thought to represent the initial stages of degeneration of the phagocytosed cell, when the nuclear morphology is still visible and precedes the completely denatured and homogenized form seen in LE cells (Fig. 9.6).

- Biochemically, lupus effusions are exudates with normal glucose levels. Antinuclear antibody titers are positive in both serum and effusion fluid.

#### 9.4.3.3 Miscellaneous Lesions

- *Hepatitis and uremia*: Both of these conditions can cause reactive mesothelial cells that should not be confused with neoplasia. There are increased numbers of mesothelial cells lying singly, in monolayered sheets and in three-dimensional clusters with a knobby or flowerlike border. The cells are round with a well-defined cell border, dense cytoplasm, and central or eccentrically located nucleus. The cytoplasm has a peripheral "lacy skirt" appearance. The nuclei have smooth nuclear borders with fine to moderately coarse chromatin. Nucleoli can be prominent [1, 6].
- *Dialysis*: In children undergoing peritoneal dialysis, mesothelial cells ranging from mildly reactive to markedly atypical can be observed. Varying numbers of lymphocytes are seen, although eosinophilia has also been described.
- *Radiation and chemotherapy*: Increased numbers of mesothelial cells are noted in a hemorrhagic background. The mesothelial cells demonstrate enlargement of the nucleus and cytoplasm, but the overall nuclear-to-cytoplasmic (N/C) ratio is maintained. Other features include cytoplasmic vacuoles, nuclear hyperchromasia, and multinucleation. Degenerative changes in neoplastic cells include nuclear enlargement or reduction in size, karyorrhexis, karyolysis, and pyknosis, in addition to necrosis and apoptosis (Fig. 9.7).
- *Chylous effusion*: This is the accumulation of chyle within a serous cavity, most often the pleural cavity. It can occur in neonates with abnormal thoracic duct development, in children of all ages after surgery or trauma, or be idiopathic. Chylous fluid is a milky white. Numerous small lymphoid cells are seen on cytological evalua-

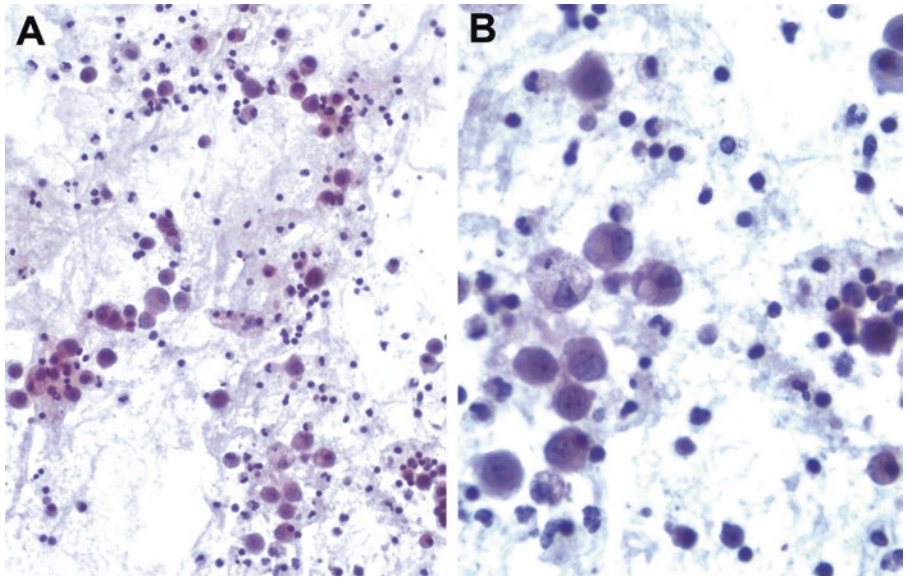


**Fig. 9.7** Benign and reactive mesothelial cells from a pleural fluid in a 2-year old male who developed a pleural effusion while undergoing chemotherapy for retinoblastoma (**a**, **b**. Papanicolaou stain, low power and high power).

tion. Biochemistry reveals chylomicrons and high triglyceride levels. These effusions can have features similar to tuberculous effusions or effusions seen in autoimmune disorders.

- *Meconium peritonitis*: This is seen soon after birth and is caused by intestinal tract perforation and leaking of meconium into the peritoneum. Cytologically, debris, hemosiderin, anucleate squamous cells, and inflammation are observed [2].
- *Endometriosis and endosalpingiosis*: These entities are rare in fluid specimens. When present, they are usually seen in peritoneal washings in female adolescents, but are occasionally encountered in pleural fluids. In endometriosis, small clusters of endometrial cells are noted in a hemorrhagic background. The cells are tightly clustered and cuboidal with eccentrically situated nuclei. Hemosiderin-laden macrophages and stromal cells may, on occasion, be seen. CD10 immunochemistry may be used to indicate an endometrial stromal component. Endosalpingiosis presents with ciliated or non-ciliated columnar cells lying in clusters and papillary-like arrangements. Psammoma bodies may be seen in endosalpingiosis but hemosiderin-laden macrophages are lacking. Endosalpingiosis demonstrates B72.3, estrogen receptor and progesteron receptor positivity.
- *Extramedullary hematopoiesis*: While the myeloid precursor cells may be difficult to appreciate in effusion cytology, the presence of megakaryocytes should alert one to the diagnosis of extramedullary hematopoiesis. Megakaryocytes are large cells with multilobulated nuclei and granular chromatin.
- *Kawasaki disease*: This is a disease of unknown etiology that produces a systemic vasculitis. It is seen most often in children under the age of 5 years. It may, on occasion, be associated with hemorrhagic pleural or pericardial effusion. Cytology reveals a blood-stained effusion with scattered lymphoid cells.
- *Nodular mesothelial and histiocytic hyperplasia*: This is a benign hyperplasia of mesothelial cells and histiocytes that can mimic malignancy and potentially cause false-positive diagnoses in fluid cytology. Although it was originally described in hernia sacs and pericardial fluids, it can occur in the pleural or peritoneal cavities as well and is thought to be the result of focal irritation by trauma, tumor, or inflammation. Cytologically, there are distinct cellular clusters of mesothelial cells and histiocytes without pleomorphism, in addition to a background of chronic inflammation [8].

## 9.5 Malignancies in Fluid Cytology

Most effusions in the pediatric population have a benign etiology. However, primary and secondary malignancies need to be actively excluded when examining serous fluid from a child or adolescent. Most malignant effusions in the pediatric population are due to involvement by a hematolymphoid process. Other small round cell tumors, primary or metastatic, are the next most common cause of malignant effusion in this clinical setting. Although most of these patients have a known history of malignancy, in a subset of patients, the malignant effusion is the initial presentation, and in these cases, ancillary testing is important for arriving at an accurate and specific diagnosis [9].

### 9.5.1 Primary Malignancies

#### 9.5.1.1 Desmoplastic Round Cell Tumor (DRCT)

**Clinical features**

DRCT is a rare but aggressive tumor, which is usually located intra-abdominally and in the pelvis but can be found in the retroperitoneum, thorax, and central nervous system. The tumor is most often seen in young males aged 8 to 38 years, but has been described in females. Patients typically present with abdominal pain or abdominal mass, and may have ascites. Prognosis is poor.

**Cytological features**

The specimen is often cellular with tumor cells in loosely cohesive groups or tighter clusters, without any distinct architecture. The presence of sphere-like clusters without a stromal core is a helpful feature, although this can morphologically mimic adenocarcinoma in fluids [9, 10]. Sporadic single cells and rosettes may also be seen. The cells have a high N/C ratio with minimal cytoplasm and occasional cytoplasmic vacuoles. The nuclei are round to oval with moderately granular chromatin and may show nuclear molding. Nucleoli can be prominent or inconspicuous. The background is typically hemorrhagic or necrotic. Despite the characteristic alternating round cell and stromal components observed on histology, metachromatic stromal fragments are seldom seen in the effusions, although scattered spindle cells may be present.

**Triage**

DRCT exhibits polyphenotypic immunostaining for epithelial (AE1/AE3, CK5/CK6, EMA, and/or others), muscle (desmin), and neural (NSE, synaptophysin, and/or others) markers. WT1 is usually positive, while FLI1 is negative. DRCT is characterized by a recurrent translocation t(11;22)(p13; q12) with fusion of the *EWSR* and *WT1* genes which can be demonstrated by cytogenetics or reverse transcriptase-polymerase chain reaction (RT-PCR). An *EWSR* translocation can also be identified by fluorescence in situ hybridization (FISH), although this is not specific for DRCT. Electron microscopy shows intermediate filaments located near the nucleus.

**Differential diagnosis**

The differential diagnosis includes other round cell tumors, and immunostains and FISH and/or RT-PCR studies are critical for establishing a correct diagnosis. Nephroblastoma or Wilms' tumor has cytological features of tubules, blastema, and stroma, which are more prominent than in DRCT, but both are positive for epithelial markers and WT1. DRCT stains with antibodies to the carboxy terminus of WT1, whereas dual immunoreactivity for the carboxy and amino terminuses is seen in Wilms tumor. Neuroblastoma occurs in a younger age group, has neuropil, and lacks metachromatically staining stromal fragments but similar to DRCT can demonstrate rosettes and positive immunostaining for neuroendocrine markers. Rhabdomyosarcomas tend to have dense cytoplasm and hyperchromatic nuclei, may show evidence of rhabdomyoblastic differentiation, such as more abundant eccentric cytoplasm or strap cells, and are immunoreactive for myogenin and myoD1, in addition to desmin. Of note, aberrant staining for epithelial and neuroendocrine markers occurs in a minority of rhabdomyosarcomas and may lead to diagnostic confusion; however, in contrast to DRCT, rhabdomyosarcomas lack *EWSR1* translocations. Ewing sarcoma/primitive neuroectodermal tumor (PNET) is typically negative for desmin, cytokeratin, EMA, and WT1, and has *EWSR1* translo-

cations that involve partners other than *WT1*. Lymphoid malignancies are characterized by lack of cellular cohesion, the presence of lymphoglandular bodies, and positivity for lymphoid markers. A less common tumor in the differential diagnosis includes extramedullary ependymoma of the myxopapillary type that may arise in the sacrum or abdominopelvic region and is positive for GFAP and S100. Small cell carcinomas and mesotheliomas are rare in the pediatric age group.

#### Pearls

DRCT overlaps cytomorphologically with other small round cell tumors of childhood. Thus, it is essential to use a panel of immunostains, in addition to FISH and/or RT-PCR to exclude other small round cell tumors of childhood and arrive at the correct diagnosis. RT-PCR has an advantage over the break-apart FISH probe for *EWSR1*, in that the *EWSR1-WT1* translocation detected by RT-PCR is specific for DRCT, whereas the break-apart probe for *EWSR1* is positive in a variety of tumors, including Ewing/PNET (*EWSR1-FLI1 and EWSR1-ERG*), extraskeletal myxoid chondrosarcoma (*CHN-EWSR1*), clear cell sarcoma (*EWSR1-ATF1*), and desmoplastic small round cell tumor (*EWSR1-WT1*) [6].

### 9.5.1.2 Pleuropulmonary Blastoma (PPB)

#### Clinical features

PPB is a rare intrathoracic neoplasm that occurs predominantly in children under the age of 4 years, but is the most common tumor seen in the cancer predisposition syndrome associated with germline *DICER1* mutations. It may be cystic, solid and cystic, or solid and, except for purely cystic tumors, follows an aggressive course. It is distinct from pulmonary blastoma. Patients present with respiratory symptoms, including cough, dyspnea, hemoptysis, and/or recurrent pneumonia, and some develop pleural effusions. Radiologically, these tumors can appear as low-attenuation masses in the pleural cavity with some high-attenuation areas, which can mimic an empyema [8].

#### Cytological features

PPB shows varying proportions of primitive blastema and sarcomatous elements and, in cystic lesions, benign epithelium. Lipoblastic, chondroblastic, and rhabdomyoblastic differentiation of the sarcomatous component has been described. The blastema is negative, on immunostaining, for CD99. Cytogenetic studies often show gains in chromosome 8q, and molecular studies reveal germline mutations in *DICER1* in approximately 50–70 % of patients with PPB.

#### Differential diagnosis

The differential diagnosis includes other small round cell tumors of childhood, malignant teratoma, synovial sarcoma, rhabdomyosarcoma, and infantile fibrosarcoma. Cases of pleuropulmonary blastoma can mimic an empyema of the pleural space on radiological imaging and thus awareness of this entity is important [11].

### 9.5.1.3 Primary Effusion Lymphoma

#### Clinical features

Primary effusion lymphoma (PEL) is a human herpesvirus 8 (HHV8)-positive lymphoma that manifests as an effusion, usually without a solid component. However, extracavitary or solid variants have been described. It is strongly linked to infection with HHV8 and variably related to infection with EBV. It usually occurs in young patients with advanced human immunodeficiency virus (HIV) disease or other immunocompromised patients, such as those with solid organ transplants, but has also been diagnosed in HIV-negative, elderly patients. Usually only one serous cavity is involved, mostly the pleura, and the prognosis is poor.

#### Cytological features

The specimen is usually cellular and composed of a pleomorphic, intermediate to large lymphoid population with features overlapping with immunoblastic diffuse large B-cell lymphoma, anaplastic lymphoma, and Burkitt lymphoma [12] (Fig. 9.8). The cytoplasm is basophilic and may be vacuolated or show perinuclear clearing. Nuclei are large and hyperchromatic with irregular nuclear contours and prominent nucleoli. Mitotic figures, bi- or multinucleation with Reed-Sternberg-like cells, and apoptosis are usually apparent.

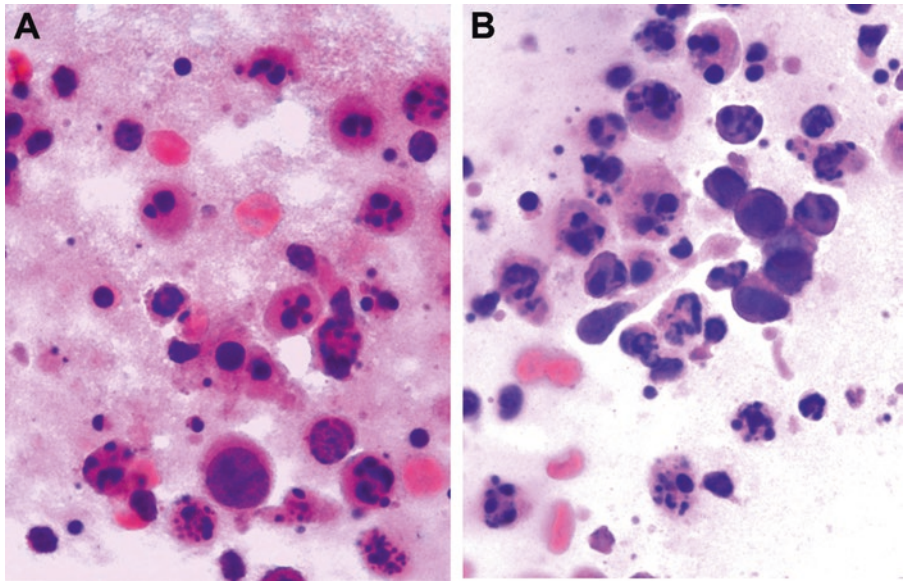


**Fig. 9.8** Peritoneal fluid from an HIV-positive 17-year-old with primary effusion lymphoma (**a**, **b**. Papanicolaou stain, high power with oil magnification). Pleomorphic, malignant lymphoid cells are noted in an apoptotic background.

### Triage

Fluid should be sent for flow cytometry, in addition to making a cell block for immunostains and in situ hybridization. This lymphoma generally does not express the usual B- and T-cell antigens, but usually expresses LCA, CD30, EMA, CD38, and CD138, while being negative for CD20, CD19, PAX5 and CD79a. The tumor cells show nuclear positivity for HHV8, and in situ hybridization sometimes reveals Epstein-Barr virus (EBV)-encoded RNA (EBER) nuclear positivity.

### Differential diagnosis

The differential diagnosis includes other intermediate to large cell lymphomas or leukemias in children, including diffuse large B-cell, plasmablastic, and anaplastic large cell lymphomas, all of which are negative for HHV8. Burkitt lymphoma is positive for *C-MYC* gene rearrangement, and lymphoblastic lymphomas/leukemias are positive for TdT. Post-transplant lymphoproliferative disorders should also be considered in immunocompromised patients, but these are negative for HHV8 and positive for EBV. Other pediatric nonlymphoid large cell malignancies should also be considered, including metastatic malignant melanoma and poorly differentiated carcinoma.

### Pearl

HHV8 infection is also associated with Kaposi sarcoma and multicentric Castleman's disease, but in lymphomas involving the body cavity, the presence of HHV8 is relatively specific for PEL. In the absence of HHV8 positivity, lymphomatous effusions are usually secondary to diffuse large B-cell lymphoma (including DLBCLs associated with chronic inflammation or pyothorax), anaplastic large cell lymphoma, or Burkitt lymphoma, depending on the immunophenotypic findings.

## 9.5.1.4 Malignant Mesothelioma

### Clinical features

Malignant mesothelioma is extremely uncommon in children. Most appear to be unrelated to asbestos exposure. Table 9.2 lists features of malignant mesothelioma and compares them to those of metastatic epithelial and germ cell tumors, which comprise the major differential diagnostic considerations in the pediatric population [13].

**Table 9.2** Comparison of malignant mesothelioma and metastatic epithelial and germ cell tumors

| | Malignant mesothelioma | Metastatic epithelial and germ cell tumors<br>Note: Morphology depends on the particular tumor |
|---|---|---|
| Frequency | Very uncommon | Uncommon but may be seen in children with germ cell tumors and adenocarcinoma of the breast, ovary, liver, colon, and other sites |
| Background | Cellular specimen, blood, necrosis, inflammation | Variable cellularity, blood, inflammation, necrosis, mucus (mucinous adenocarcinomas), tigroid (germ cell tumors with component of seminoma or dysgerminoma) |
| Architecture | Single-lying morula clusters with "knobby" borders, three-dimensional clusters, papillae, intercellular windows | Single-lying, two-dimensional, and three-dimensional clusters, acini, papillae |
| Cytoplasm | Round cells, dense two-tone cytoplasm, "lacy skirt," vacuoles usually multiple | Cuboidal to columnar shape, vacuolated or granular cytoplasm, single to multiple vacuoles |
| Nucleus | Centrally situated, bi- and multinucleation, irregular nuclear borders, granular chromatin, prominent nucleoli, normal-to-moderately increased N/C ratio | Central to eccentrically situated, irregular nuclear outlines, chromatin varies from hyperchromatic to vesicular, prominent nucleoli, moderate to marked increase in N/C ratio |
| Triage | *Immunostains*: calretinin+, CK5/CK6+, D2-40+, WT1+, CK7+, CK20−, CEA−, BerEP4−, B72.3−, MOC31−<br>*Ultrastructure*: long microvilli<br>*FISH*: *p16* deletion | *Immunostains*: BerEP4+, MOC31+, B72.3+, CEA+, CK profile depends on origin of carcinoma, calretinin−, CK5/CK6−, WT1−in metastatic carcinoma. Germ cell markers positive according to tumor type<br>*Ultrastructure*: short microvilli, cytoplasmic mucin, or other secretory products |
| Pearl | Shows a spectrum from benign to atypical to malignant mesothelial cells | Look for two different cell populations—benign reactive mesothelial cells and a foreign population of malignant cells |

### 9.5.2 Secondary Malignancies

In adults, an important diagnostic quandary is to distinguish reactive mesothelial cells from metastatic adenocarcinoma, whereas in children, the challenge is differentiating small cell neoplasms from inflammatory cells. Many different tumors can spread to body cavities during the course of disease. It is important to distinguish a primary versus secondary neoplastic process as the treatment and prognosis differ. The most common tumors seen in the body cavities, particularly the pleural fluid, of young patients are hematolymphoid (Table 9.3), small round cell tumors of childhood, particularly neuroblastoma and nephroblastoma, and round and spindle cell sarcomas [2, 14]. Approximately 20–30 % of Hodgkin and non-Hodgkin lymphomas involve the pleural fluid, especially if there is mediastinal involvement [15]. In peritoneal fluid, hematolymphoid malignancies, neuroblastoma, and germ cell tumors, particularly those arising from the ovary, predominate (Table 9.3) [2]. In children with a nonlymphoid neoplasm aged less than 4-9 years, metastatic neuroblastoma or Wilm's tumor is the most common secondary malignancy while in those over 9 years of age, the metastasis is most likely to have arisen from a sarcoma or germ cell tumor [2]. Nonlymphoid neoplasms metastatic to the body cavities are usually distinguished based on the presence of a foreign population of cells that appear different to the background lymphocytes and mesothelial cells (Table 9.4). Sarcomas tend to round up in fluids, and the characteristic cell shapes (spindled, round, or pleomorphic) and architectural patterns, such as vascular arrangements, seen in fine needle aspirates of these lesions may not be apparent in the exfoliative cytological specimens [16]. In addition, sarcomas tend to exfoliate sparsely compared with lymphomas, small round cell tumors, and carcinomas. In rare cases, spindle cells may be observed, and these may be due to primary or metastatic neoplasms (Table 9.5).

**Table 9.3** Most common malignancies in pediatric fluid cytology

| Pleural fluid | Peritoneal fluid | Pericardial fluid |
|---|---|---|
| Hematolymphoid malignancies (lymphomas, leukemias) | Hematolymphoid malignancies (lymphomas, leukemias) | Hematolymphoid malignancies (lymphomas, leukemias) |
| Neuroblastoma | Neuroblastoma | |
| Sarcoma (rhabdomyosarcoma, osteosarcoma, Ewing sarcoma/PNET) | Nephroblastoma | |
| | Germ cell tumors | |

**Table 9.4** Hematolymphoid malignancies in serous fluids

| Tumor | Cytomorphology | Triage |
|---|---|---|
| Acute leukemia | Blasts with immature powdery chromatin can be tightly packed together, especially in centrifuged preparations. Lymphoblastic leukemias tend to be round, intermediate-sized cells with scant cytoplasm, whereas myeloid leukemias usually have more lobulated nuclei and moderate amounts of granular cytoplasm. | Flow cytometry<br>Immunohistochemical stains |
| Lymphoblastic leukemia/ lymphoma (Fig. 9.9) | Intermediate-sized cells with scant cytoplasm, irregular nuclear contours, and variable nucleoli. Ancillary studies reveal a T- or B-cell population with positive CD10 and TdT immunostaining (Fig. 9.10). | Flow cytometry<br>Immunohistochemical stains |
| Burkitt lymphoma | Intermediate-sized cells with moderate amounts of vacuolated basophilic cytoplasm (best seen in Romanowsky-type preparations) and round monomorphic nuclei with immature chromatin. Abundant mitotic figures, apoptosis, karyorrhectic debris, and tingible body macrophages. | Flow cytometry<br>Immunohistochemical stains<br>FISH studies to confirm t(8;14) or variant translocations of *C-MYC* (t(2;8) and t(8;22)) |
| Diffuse large B-cell lymphoma | Large cells with moderate to abundant cytoplasm, irregular nuclear outlines, and variable nucleoli. Karyorrhectic debris and mitotic figures may be apparent. | Flow cytometry<br>Immunohistochemical stains |
| Primary effusion lymphoma (Fig. 9.8) | Large malignant cells with pleomorphism and a karyorrhectic background. | Flow cytometry<br>Immunohistochemical stains |
| Hodgkin lymphoma | Reed-Sternberg (RS) cells with a mixed background including inflammatory cells, mesothelial cells, and histiocytes. | Immunohistochemical stains |

One approach to the evaluation of tumors in body cavity fluids from children and adolescents is to determine whether the cells are small and round with minimal cytoplasm, larger with moderate to abundant cytoplasm, or spindled (Tables 9.4, 9.5, and 9.6). Based on the general morphology, the residual fluid can be triaged for flow cytometry and/or a cell block for immunostains, FISH, and/or RT-PCR.

### 9.5.2.1 Hematolymphoid Malignancies

#### Clinical features

Hematolymphoid malignancies are the most common tumors to be seen in body cavity fluids in the pediatric population. These tumors can be diagnostically challenging due to the morphological overlap with chronic inflammatory cells,

**Table 9.5** Differential diagnosis of serous effusions in children comprising cells with moderate to abundant cytoplasm

| Tumor | Cytomorphology | Triage |
|---|---|---|
| Germ cell tumor (Figs. 9.14, 9.16, and 9.17) | Single-lying and small clusters, high N/C ratio, ± vacuolated cytoplasm, round nucleus, and prominent nucleoli [17] | IHC: variable positivity for germ cell markers (PLAP, AFP, SALL4, HCG, CD117, OCT3/4, CD30) |
| Hepatocellular carcinoma (Fig. 9.18) | Single and clustered large malignant cells with eosinophilic cytoplasm, ± cytoplasmic bile pigment, prominent nucleoli, intranuclear cytoplasmic inclusions | IHC: positive for Hepar1, Glypican3, AFP; negative for CK7 and CK20 |
| Papillary thyroid carcinoma | Papillary fragments, psammoma bodies; nuclear features of papillary thyroid carcinoma may not be apparent | IHC: positive for TTF1, PAX8, thyroglobulin, CK7 |
| Serous tumors (ovary, peritoneum), mucinous tumors | Papillary fragments, psammoma bodies, ± mucin (mucinous tumors), large secretory vacuoles | HC: positive for WT1, PAX8, CA 125, CK7. Mucinous ovarian tumors can be CK7 negative, and CDX2, villin and CEA positive |
| Translocation-associated renal cell carcinoma (Fig. 9.19) | ± Papillary fragments, hemosiderin, moderate to abundant dense to granular cytoplasm, ± prominent nucleoli | IHC: positive for vimentin, CD10, PAX8, TFE3; may be negative for MOC31 and BerEP4<br>FISH: *TFE3* gene rearrangements |
| Solid pseudopapillary tumor of pancreas | Papillae, round cuboidal shape, ± hyaline cytoplasmic granules, ± nuclear grooves, finely granular chromatin | IHC: positive for vimentin, synaptophysin, β-catenin, α1-antitrypsin, CD56, CD10 |
| Rhabdomyosarcoma (Fig. 9.13) | Small round cells with minimal cytoplasm in addition to larger, more pleomorphic cells with moderate to abundant eosinophilic cytoplasm, spindle and strap cells, bi-and multinucleation | IHC: positive for desmin, myogenin, myoD1<br>FISH: Alveolar rhabdomyosarcoma has *FOXO1* translocations [t(1;13) or t(2;13)] |
| Ganglioneuroblastoma | Small round cell with minimal cytoplasm in addition to larger, more pleomorphic polygonal cells; abundant, granular cytoplasm; eccentrically to centrally situated nuclei; hyperchromatic, large nuclei; prominent nucleoli; bi- and multinucleation | IHC: positive for neuroendocrine markers<br>FISH: to determine *N-MYC* amplification status |
| Osteosarcoma (Fig. 9.20) | Large pleomorphic cells, variable amount of eosinophilic cytoplasm, hyperchromatic, prominent nucleoli which may be multiple, giant cells. Osteoid is not usually seen in fluids. | IHC: No specific markers and cells may stain with multiple mesenchymal markers, confounding the diagnosis. Known history of osteosarcoma is helpful. |
| Sex cord/stromal tumor | Small, uniform cells, bland nuclear features, nuclear grooves. scanty cytoplasm. Call-Exner bodies rarely seen in effusions. | IHC: positive for inhibin, calretinin, pankeratin |
| Malignant mesothelioma | Morulae; clusters with "knobby" borders; intercellular windows; dense, biphasic cytoplasm with a "lacy skirt"; bi- and multinucleation; granular chromatin | IHC: positive for calretinin, CK5/CK6, D2-40, WT1, CK7; negative for CK20, CEA, BerEP4, B72.3.<br>FISH for *p16* deletion |
| Multicystic mesothelioma | Single and clusters, monotonous-appearing mesothelial cells | IHC: positive for calretinin, CK5/CK6, D2-40, WT1, CK7; negative for CK20, CEA, BerEP4, B72.3 |
| Hodgkin lymphoma | Very occasional Hodgkin Reed-Sternberg (HRS) cells, lymphocytes, plasma cells, neutrophils, ± eosinophils | IHC: HRS cells positive for CD15, CD30, ±CD20, ±BLIMP1; negative for LCA, TIA1, CD3 |
| Epithelioid hemangioendothelioma | Round to oval cells, vacuolated eosinophilic cytoplasm, usually bland nuclear features, ± prominent nucleoli. Vascular architecture is not well seen in fluids. | IHC: positive for CD10, factor VIII, CD31, CD34, FLI1 |
| Malignant melanoma (Fig. 9.21) | Single-lying and loose clusters, round to oval plasmacytoid to spindle, varying amounts of cytoplasm, ± melanin pigment, central to eccentric nucleus, granular chromatin, prominent nucleoli, intranuclear cytoplasmic inclusions | IHC: positive for HMB-45, MelanA, S100, MiTF, tyrosinase |

**Table 9.6** Differential diagnosis of serous effusions in children comprising spindled cells

| Tumor | Cytomorphology | Triage |
|---|---|---|
| Embryonal or spindle cell rhabdomyosarcoma (Fig. 9.13) | Small round cells with minimal cytoplasm in addition to larger, more pleomorphic cells with moderate to abundant eosinophilic cytoplasm, spindled and strap cells, bi- and multinucleation | IHC: positive for desmin, myogenin, and myoD1; usually negative for cytokeratins and neuroendocrine markers |
| Desmoplastic round cell tumor | Small round cells with minimal cytoplasm in addition to sporadic spindle cells, ± stromal fragments | IHC: positive for desmin, neural markers, cytokeratins, EMA, vimentin, MOC31, WT1; myoD1 may be positive after treatment with chemotherapy<br>FISH: *EWSR1* translocation<br>RT-PCR: *EWSR1-WT1* fusion [t(11;22)(p13; q12)] |
| Nephroblastoma | Spindle cells as part of the stromal component, unusual for all three cells types to be seen when metastatic to serous cavity | IHC: Staining profile of stroma according to morphologic appearance (e.g., positive for desmin and myogenin in rhabdomyoblastic differentiation) |
| Pleuropulmonary blastoma | Primitive blastema and sarcomatous elements. ± lipoblastic, chondroblastic, and rhabdomyoblastic differentiation | IHC: Negative for CD99<br>Cytogenetics: ± gains in chromosome 8q<br>Molecular: ± germline *DICER1* mutations |
| Synovial sarcoma | Monophasic/biphasic, sparse cytoplasm, irregular nuclear borders, prominent nucleoli | IHC: positive for EMA (may be weak in spindle cells), bcl-2+ (spindle cells), CD99+<br>FISH: *SS18* translocation [t(X:18)] |
| Angiosarcoma | Bloodstained fluid, single cells and loose clusters, ill-defined cell borders, finely vacuolated cytoplasm, irregular nuclear borders, hyperchromatic, prominent nucleoli. May also present with more abundant cytoplasm resembling metastatic carcinoma | IHC: positive for factor VIII, CD31, CD34, VEGF, FLI1 |
| Malignant peripheral nerve sheath tumor | Wavy nuclei, hyperchromatic | IHC: positive or negative for S100 (not well demonstrated in alcohol-fixed smears) |
| Kaposi sarcoma | Bloodstained fluid, single and small clusters, bland spindle cells, scanty cytoplasm | IHC: positive for CD31, CD34, D2-40, HHV8 |
| Malignant melanoma (Fig. 9.21) | Single-lying and loose clusters, round to oval to plasmacytoid to spindled, varying amounts of cytoplasm, ± melanin pigment, central to eccentric nucleus, granular chromatin, prominent nucleoli, intranuclear cytoplasmic inclusions | IHC: positive for HMB-45, MelanA, MiTF, S100, tyrosinase; negative for cytokeratins and LCA |
| Leiomyosarcoma | Single-lying, round, dense cytoplasm, bi-and multinucleation, coarse chromatin | IHC: positive for SMA, desmin, calponin, caldesmon |

which are normally present in effusions. However, non-Hodgkin lymphomas (NHLs), excluding primary effusion lymphoma, and leukemias rarely present as an effusion without a prior history of malignancy. In addition, small cell lymphomas, which are difficult to distinguish from lymphocytic inflammation without ancillary studies, are uncommon in children, in contrast to the adult population.

### Cytological features

The key features of a malignant hematolymphoid proliferation is the presence of a uniform population of discohesive cells with slight to marked nuclear enlargement, abnormal chromatin, which varies with the type malignancy, lymphoglandular bodies, and karyorrhectic debris. Although malignant lymphoid cells may artifactually clump, there is less cellular cohesion as com-

pared to other small round cell tumors of childhood. Immersion in a fluid medium can cause cytoplasmic vacuoles, and thus, the presence of cytoplasmic vacuoles alone should not lead to a diagnosis of Burkitt lymphoma. Blasts and immature myeloid precursors can also be seen when a leukemia involves the fluid, and in these scenarios, it is important to correlate with the amount of peripheral blood dilution and the peripheral blood blast count to determine if the blasts are from true fluid involvement or peripheral blood contamination (Figs. 9.8, 9.9, 9.10, and 9.11). Hodgkin lymphomas can also be present in pleural fluids, particularly if there is mediastinal involvement, and typically show HRS cells in a heterogeneous background mixed with mesothelial cells and histiocytes [15]. A summary of the hematolymphoid malignancies to consider in a fluid specimen is seen in Table 9.4.

### Triage

Triage for flow cytometry, immunohistochemical stains, in situ hybridization or PCR is recommended for accurate immunophenotyping of the cells and to confirm malignancy. These studies are used to prove clonality, assess proliferative activity, and arrive at a differential and definitive diagnosis.

### Differential diagnosis

Non-Hodgkin lymphoma must be distinguished from other small round cell tumors of childhood and from benign causes of a lymphocytosis, such

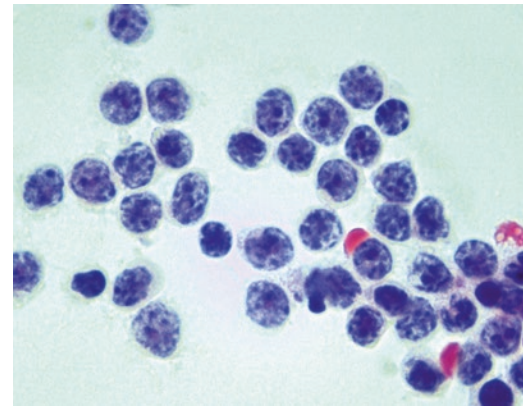

**Fig. 9.9** This pleural fluid from a 16-year-old girl with T-lymphoblastic lymphoma shows numerous malignant lymphocytes with high nuclear-to-cytoplasmic ratios, irregular nuclear contours, and finely granular chromatin (Papanicolaou stain, high power with oil magnification).

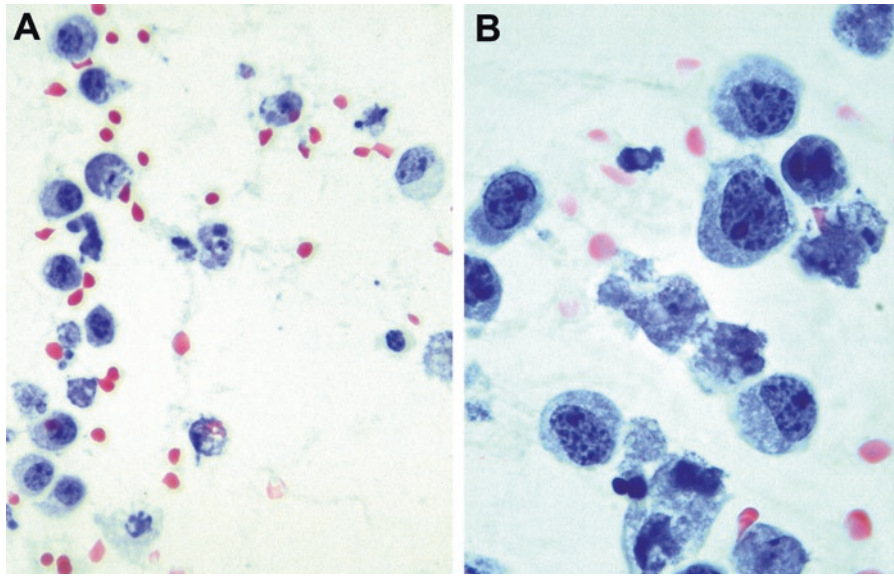


**Fig. 9.10** This pleural fluid from an HIV-infected, 8-year-old boy with plasmablastic lymphoma shows pleomorphic, single-lying cells with eccentric nuclei, coarsely clumped chromatin, and moderate amounts of basophilic cytoplasm (**a**. Papanicolaou stain, medium power; **b**. Papanicolaou stain, high power with oil magnification).

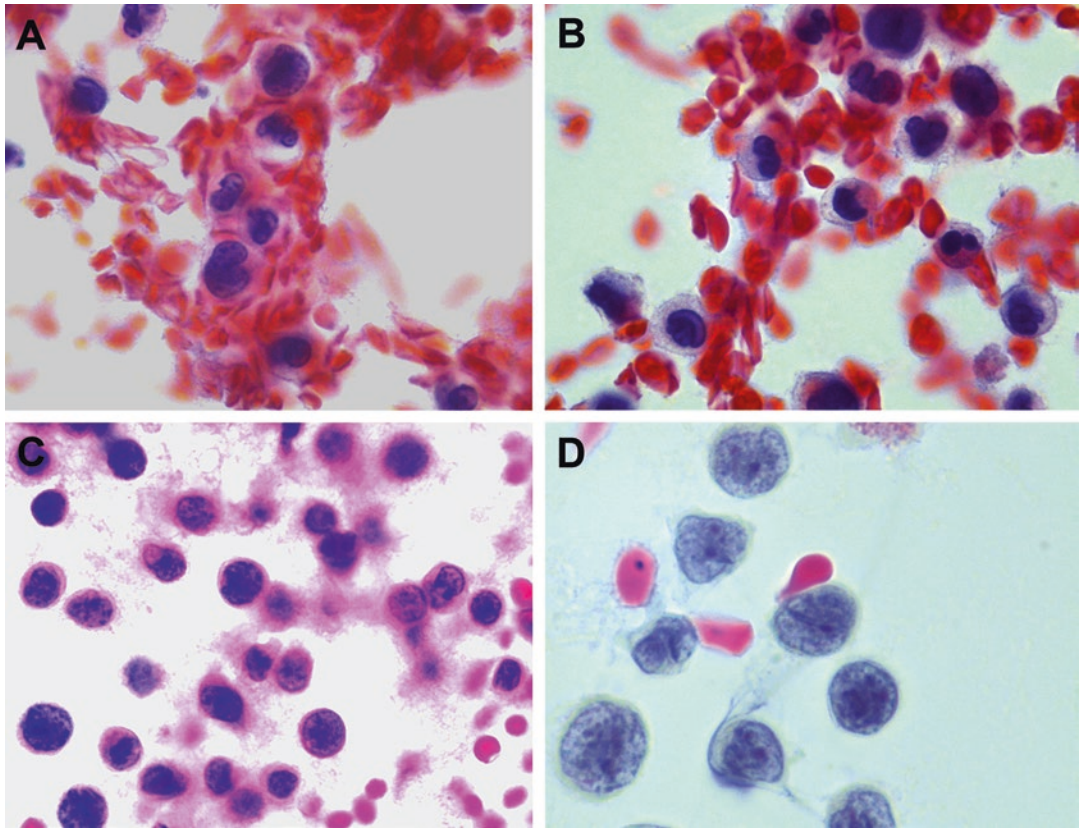


**Fig. 9.11** (**a**, **b**) A pleural fluid from an 11-year-old girl with chronic myeloid leukemia showing myeloid precursor cells in a bloodstained background. (**c**, **d**) A pleural fluid from a 4-year-old girl with acute myeloid leukemia (**a**, **b**, **d**. Papanicolaou stain, high power; **c**. H&E stain, high power). Blasts are characterized by very high nuclear-to-cytoplasmic ratios, vesicular chromatin, and prominent nucleoli.

as tuberculous effusion or chylothorax. Although small lymphocytes may predominate, reactive lymphocytosis shows a polymorphous population of lymphoid cells, ranging from small, mature lymphocytes to immunoblasts, whereas malignant lymphoid populations tend to be monomorphic, such as Burkitt and lymphoblastic lymphomas, or highly pleomorphic, such as anaplastic large cell lymphoma or primary effusion lymphoma. Malignant lymphoid cells also tend to have more nuclear contour and chromatin irregularities compared to benign lymphoid cells. However, ancillary tests, including flow cytometry, immunocytochemistry, and molecular studies, may be required to accurately make this distinction in challenging cases. Acute and chronic leukemia has also been described in effusions.

## Pearls

Flow cytometry is best performed on the residual, fresh fluid specimen as soon as possible to minimize degeneration. Ideally, the laboratories that receive body cavity fluid specimens should work together to ensure that aliquots of the specimen are sent to the appropriate laboratories for the requested tests, such as cell counts, chemical analysis, morphological assessment, flow cytometry, and/or microbial cultures. When patients are on chemotherapy at the time of fluid collection, marked degenerative changes and/or cytologic atypia may be present.

### 9.5.2.2 Metastatic Nonlymphoid Small Round Blue Cell Tumors of Childhood

#### Clinical features

Body cavity fluids are not usually the presenting site of non-hematolymphoid small round cell tumors, and, in addition, these tumors are less common in effusions than hematolymphoid malignancies. The age and gender of the patient may provide helpful clues to the differential diagnosis, as certain small round cell tumors are seen more often in effusions from patients of particular ages and/or genders (e.g., neuroblastoma in children under the age of 4 years, desmoplastic round cell tumors in adolescent and young adult males).

#### Cytological features

The key features of a nonlymphoid malignant small round cell tumor include more conspicuous cohesion and an absence of lymphoglandular bodies. In nephroblastoma metastatic to serous cavities, it is very unusual for all three cell types to be observed. Occasional rosettes may be seen in metastatic neuroblastoma (Fig. 9.12), while rhabdomyosarcoma may contain small round cells with minimal cytoplasm, binucleated cells, and cells with more abundant orangeophilic cytoplasm, with variable nuclear pleomorphism (Fig. 9.13). A checkerboard appearance of light and dark cells with a tigroid background on air-dried, Diff-Quik-stained material is observed in Ewing sarcoma/PNET, while papillary groups, rosettes, and myxoid material are more common in myxopapillary ependymoma. The immature neuroblastic elements of an immature teratoma also resembles a small round cell tumor (Fig. 9.14). Judicious use of ancillary investigations can help to confirm metastases from a known malignancy or establish an accurate, specific diagnosis in metastases of unknown primary origin.

#### Triage

Based on cytomorphology alone, it is usually not possible to distinguish the various types of small round cell tumors; however, prior history and/or ancillary studies are helpful for arriving at an accurate diagnosis. Triaging material for immunohistochemical stains is helpful for confirming the type of tumor. Due to the expected or aberrant immunoreactivity of multiple tumors to the same antibody (e.g., CD99), a panel of antibodies is usually employed.

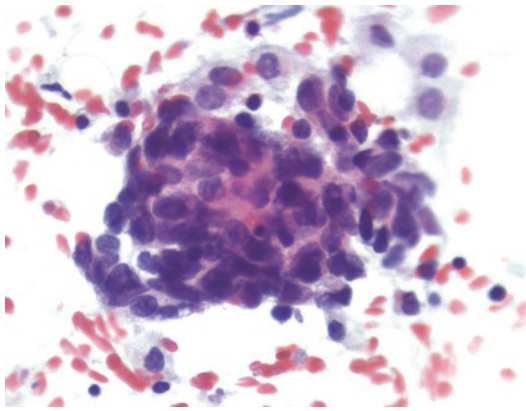

**Fig. 9.12** Peritoneal fluid from a 4-year-old girl with neuroblastoma (Papanicolaou stain, high power). An ill-defined rosette with a suggestion of neuropil in the center is noted within this cohesive cluster of small round to oval dark cells with scant cytoplasm.

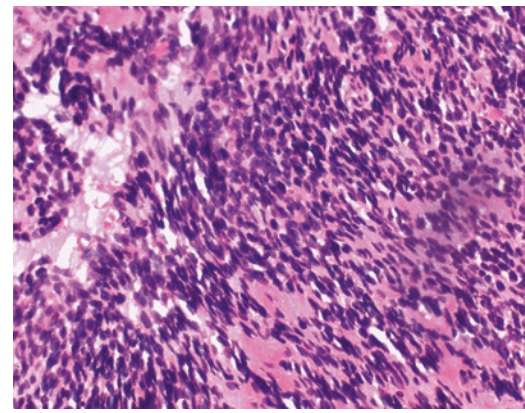

**Fig. 9.13** A cell block from the peritoneal fluid in a 7-year-old girl with embryonal rhabdomyosarcoma (H&E, medium power). Spindled nuclei, some with moderate amounts of dense cytoplasm, are noted.

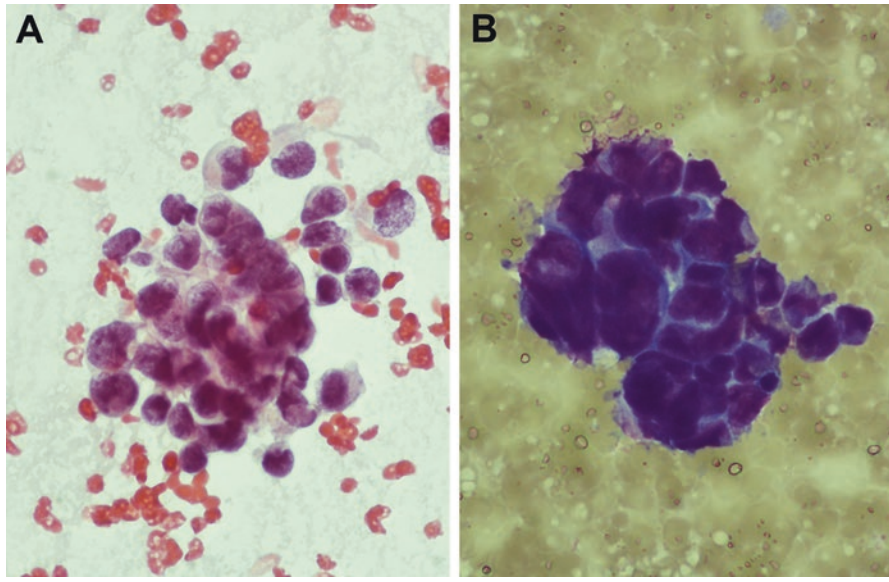


**Fig. 9.14** Clusters of poorly differentiated cells with elevated nuclear-to-cytoplasmic ratios are present in this peritoneal fluid from a 19-year-old female with an immature teratoma (**a**. Papanicolaou stain, high power; **b**. Diff-Quik stain, high power).

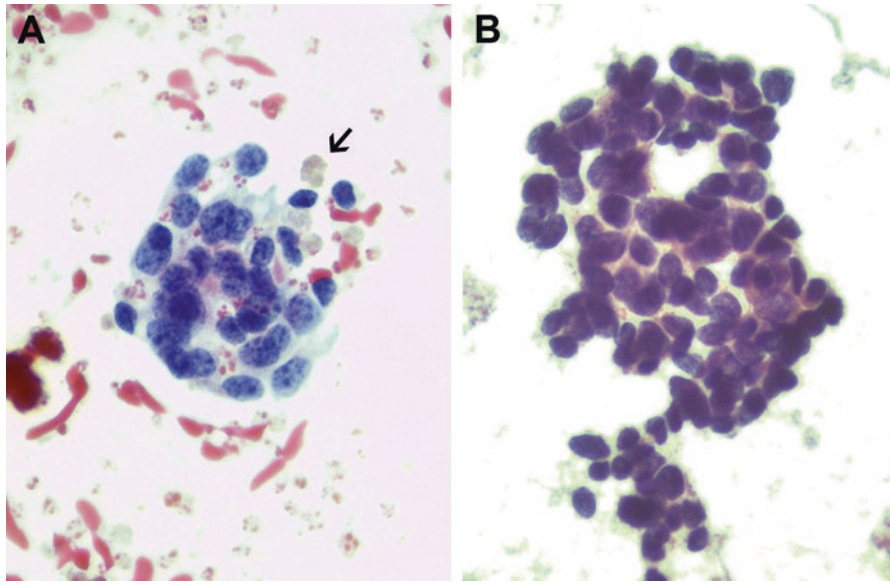


**Fig. 9.15** The differential diagnosis of small round cell tumors in serous effusions includes endometriosis (**a**) in the peritoneal washings from a young female, where clusters of epithelial cells are observed in a bloodstained background with hemosiderin (*arrow*) (Papanicolaou stain, high power). In addition, it includes metastatic neuroendocrine carcinomas (**b**), particularly well-to-moderately differentiated neuroendocrine carcinomas of the pancreas, lung, or other origins, whereby there are clusters of cells with increased nuclear-to-cytoplasmic ratios and nuclear molding.

### Differential diagnosis

Benign chronic effusions and malignant hematolymphoid tumors are the main differential diagnostic considerations from nonlymphoid small round cell malignancies (Table 9.4). Other entities with cohesive small cells with minimal cyto-

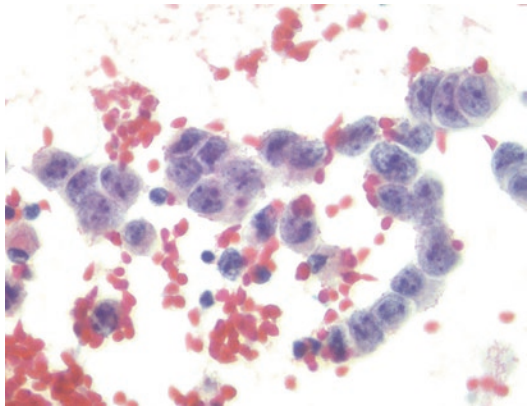

**Fig. 9.16** Loosely cohesive cells with moderate amounts of vacuolated cytoplasm, large round nuclei, vesicular chromatin, and prominent nucleoli are observed in this peritoneal fluid from a 15-year-old female with dysgerminoma (Papanicolaou stain, high power).

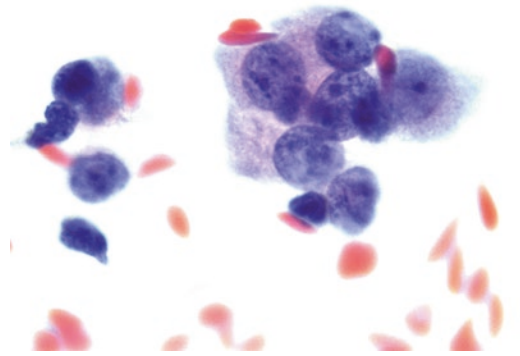

**Fig. 9.17** A cluster of cells with moderate amounts of vacuolated cytoplasm, vesicular chromatin, and multiple nucleoli are present in this peritoneal fluid from a 5-year-old boy with a history of metastatic yolk sac tumor involving the liver (Papanicolaou stain, high power).

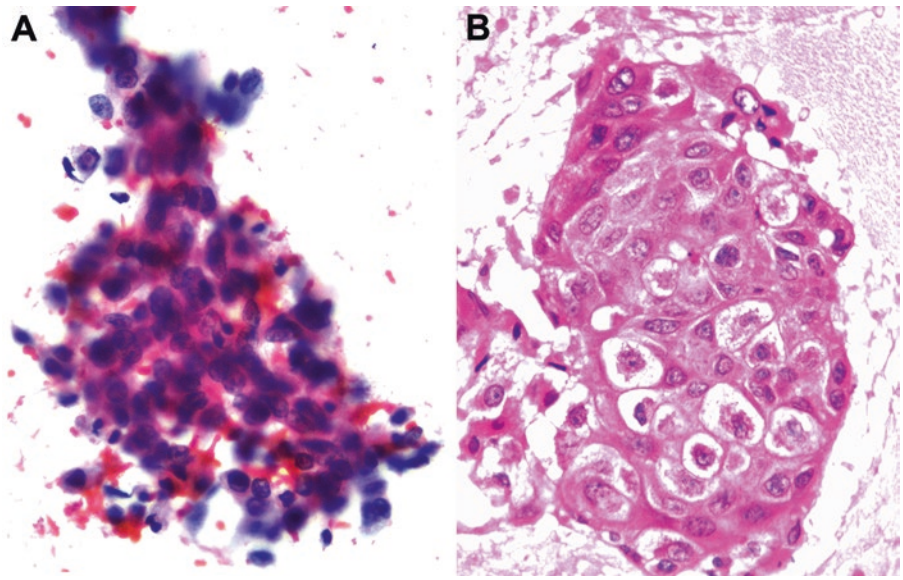


**Fig. 9.18** This peritoneal fluid from a 19-year-old male with metastatic hepatocellular carcinoma shows hepatocytes arranged in a crowded trabecular arrangement with moderate amounts of granular cytoplasm and malignant nuclei (**a**). The cell block shows malignant cells with eosinophilic granular cytoplasm within thickened trabeculae lined by some endothelial cells (endothelial wrapping) (**b**) (**a**. Papanicolaou stain, high power; **b**. H&E stain, medium power).

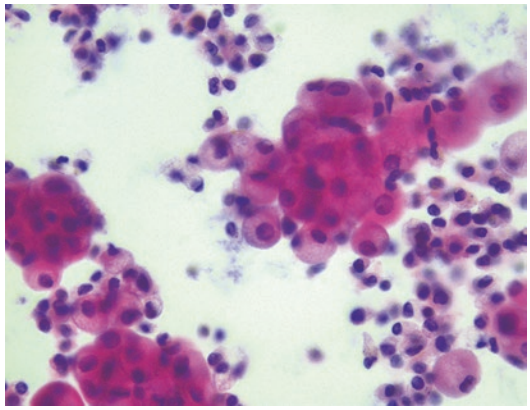

**Fig. 9.19** Bland-appearing tumor cells with a low nuclear-to-cytoplasmic ratios and abundant vacuolated cytoplasm are seen in cohesive groups within an inflamed background in this peritoneal fluid from a young woman with renal cell carcinoma (Papanicolaou stain, high power).

plasm, such as endometriosis in young females, and neuroendocrine carcinomas can also mimic small round cell tumors (Fig. 9.15). The differential diagnosis for effusions with epithelioid cells having more abundant cytoplasm is presented in Table 9.5 (Figs. 9.16, 9.17, 9.18, 9.19, 9.20, and 9.21), and that for effusions with a predominance of spindle cell are seen in Table 9.6.

**Pearl**

Clinical history is helpful in evaluation of these effusions, particularly for determining how to triage residual fluid from limited specimens most appropriately for ancillary studies.

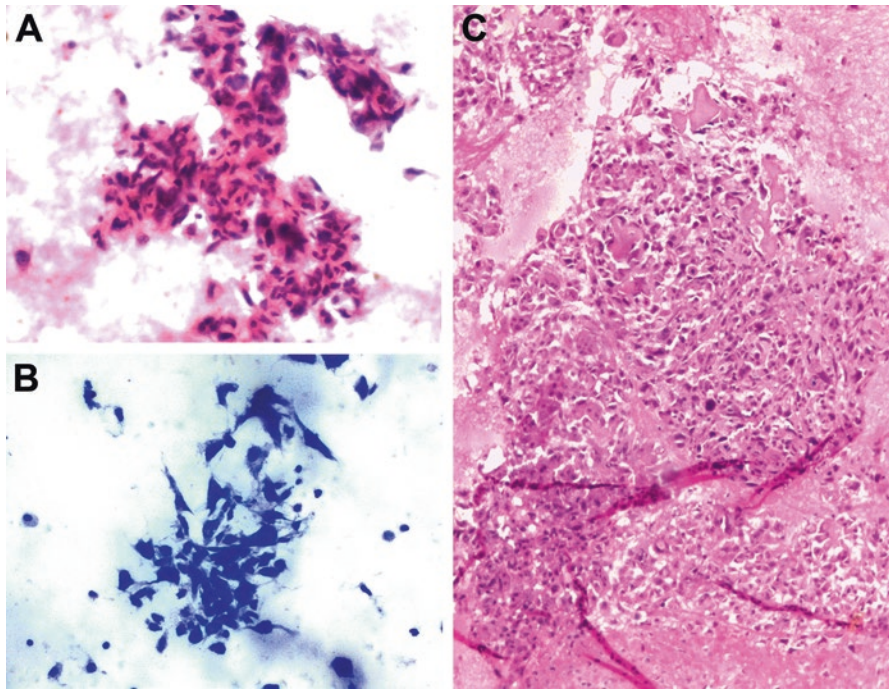


**Fig. 9.20** This is a peritoneal fluid from a young girl who had undergone amputation of her left leg 1 year previously for osteosarcoma. The fluid shows loose clusters of spindle cells with moderate amounts of wispy cytoplasm and hyperchromatic nuclei (**a**, **b**). The cell block shows pleomorphic spindled cells with moderate to abundant cytoplasm, giant cells, and osteoid (**c**) (**a**. Papanicolaou stain, high power; **b**. Diff-Quik stain, high power; **c**. H&E stain, medium power).

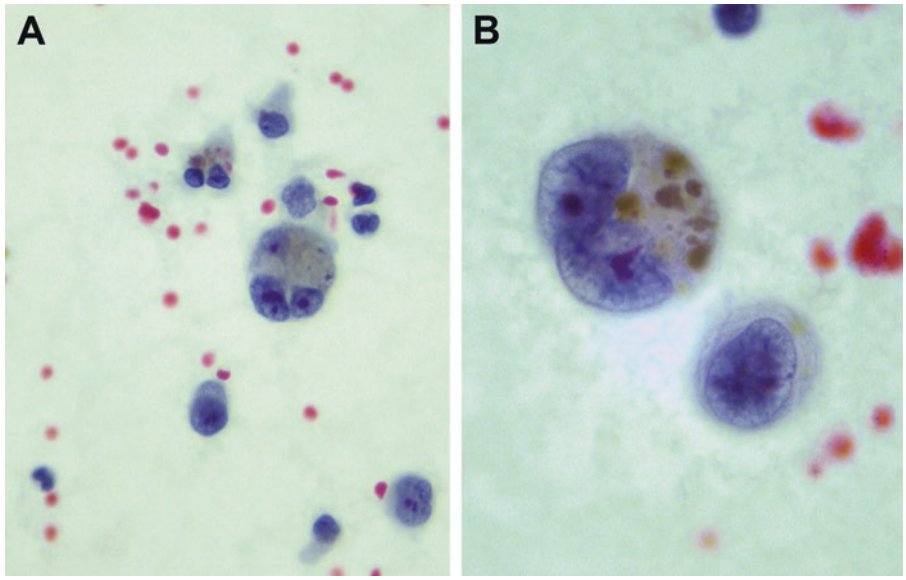


**Fig. 9.21** In this pericardial fluid from a 21-year-old female with metastatic malignant melanoma, there are discohesive cells with eccentrically located, pleomorphic nuclei with prominent nucleoli and cytoplasm showing melanin pigment (**a**. Papanicolaou stain, medium power; **b**. Papanicolaou stain, high power).

## References


1. Ali S, Cibas E. Serous cavity fluid and cerebrospinal fluid cytopathology. New York, NY: Springer; 2012.
2. Geisinger K, Silverman J, Wakely P. Pediatric cytopathology. Chicago, IL: ASCP Press; 1994. p. 99–125.
3. Wong J, Pitlik D, Abdul-Karim F. Cytology of pleural, peritoneal and pericardial fluids from children. A 40-year summary. Acta Cytol. 1997;41:467–73.
4. Helson L, Krochmal P, Hajdu SI. Diagnostic value of cytologic specimens obtained from children with cancer. Ann Clin Lab Sci. 1975;5:294–7.
5. Khalbuss W, Monaco S, Pantanowitz L. Quick compendium of cytopathology. Chicago, IL: ASCP Press; 2013.
6. Kini S. Color atlas of differential diagnosis in exfoliative and aspiration cytopathology. 2nd ed. Baltimore, MD: Lippincott, Williams & Wilkins; 2011.
7. Naylor B. Cytological aspects of pleural, peritoneal and pericardial fluids from patients with systemic lupus erythematosus. Cytopathology. 1992;3:1–8.
8. Chikkamuniyappa S, Herrick J, Jagirdar JS. Nodular histiocytic/mesothelial hyperplasia: a potential pitfall. Ann Diagn Pathol. 2004;8:115–20.
9. Oliveira MJ, de Almeida LP, Wengerkievicz AC, Siqueira SA, Antonangelo L. From conventional fluid cytology to unusual histological diagnosis: report of four cases. Diagn Cytopathol. 2013;41:348–53.
10. Hattori Y, Yoshida A, Sasaki N, Shibuki Y, Tamura K, Tsuta K. Desmoplastic small round cell tumor with sphere-like clusters mimicking adenocarcinoma. Diagn Cytopathol. 2015;43:214–7.
11. Sharif K, Alton H, Clarke J, Desai M, Morland B, Parikh D. Paediatric thoracic tumours presenting as empyema. Pediatr Surg Int. 2006;22:1009–14.
12. Das DK. Serous effusions in malignant lymphomas: a review. Diagn Cytopathol. 2006;34(5):335–47.
13. Arora S, Srinivasan R, Nijhawan R, Bansal D, Menon P. Malignant biphasic peritoneal mesothelioma in a child: fine needle aspiration cytology, histopathology and immunohistochemical features along with review of literature. Diagn Cytopathol. 2012; 40:1112–5.
14. Geisinger K, Hadju S, Helson L. Exfoliative cytology of nonlymphoreticular neoplasms in children. Acta Cytol. 1984;28:16–28.
15. Alexandrakis MG, Passam FH, Kyriakou DS, Bouros D. Pleural effusions in hematologic malignancies. Chest. 2004;125:1546–55.
16. Abadi M, Zakowski M. Cytologic features of sarcomas in fluids. Cancer. 1998;84:71–6.
17. Rodriguez E, Monaco S, Khalbuss W et al. Abdominopelvic washings: A comprehensive review. CytoJournal 2013;10:7.

# CSF and CNS Cytology

# 10

Samir B. Kahwash and Christopher R. Pierson

## 10.1 CSF Cytology

### 10.1.1 Introduction

The cerebral spinal fluid (CSF) is normally a clear fluid that circulates between the ventricles and the subarachnoid space of the central nervous system (CNS). Most of it is excreted by ultrafiltration from the choroid plexus of the ventricles. From there, it circulates through the ventricular foramina to the subarachnoid space of brain and spinal cord, where it is resorbed. The intact epithelium of the choroid plexus and the underlying capillary endothelium function together to form the so-called blood-brain barrier (BBB).

The CSF functions to protect and support the brain, as well as maintain electrolyte balance, provide nutrients, and remove waste products [1]. Total CSF volume ranges from 10 to 60 mL in the neonate to 90–150 mL in an adult [1]. The total CSF volume is replaced every 5–7 h [2].

### 10.1.2 Indications for Lumbar Puncture (LP) in Children

Most commonly, lumbar puncture (LP) is performed in the pediatric patient for one of the following indications:

1. Suspected CNS infection (e.g., meningitis, encephalitis)
2. Suspected subarachnoid hemorrhage (e.g., trauma, child abuse)
3. Evidence of sepsis in a newborn (e.g., fever above 100.4 F)
4. Staging of hematopoietic neoplasms, primary CNS malignancies, or metastatic tumors.

The specimen is usually collected in three tubes. The first tube is used for chemical and/or immunologic tests, the second for microbiologic studies, and the third for cell counts with differential and microscopic examination.

S.B. Kahwash, MD (✉)
Department of Pathology and Laboratory Medicine, Nationwide Children's Hospital, 700 Children's Drive, Columbus, OH 43205, USA

Department of Pathology, The Ohio State University College of Medicine, Columbus, OH 43210, USA
e-mail: Samir.Kahwash@nationwidechildrens.org

C.R. Pierson, MD, PhD
Department of Pathology and Laboratory Medicine, Nationwide Children's Hospital, 700 Children's Drive, Columbus, OH 43205, USA

Department of Pathology, The Ohio State University College of Medicine, Columbus, OH 43210, USA

Department of Biomedical Education and Anatomy, The Ohio State University College of Medicine, Columbus, OH 43210, USA



S.E. Monaco, L.A. Teot (eds.), *Pediatric Cytopathology*, DOI 10.1007/978-3-662-53441-0_10

### 10.1.3 The CSF Specimen

- Sources: Most of the CSF specimens in children are obtained via a lumbar puncture or spinal tap. However, specimens from other sources can be seen in this age group, including CSF derived from a shunt placed for chemotherapy, or other reasons (e.g., Ommaya reservoir), and, rarely, an intraoperative washing specimen.
- Gross examination: The initial processing of CSF includes a description of volume, color, clarity, and consistency of the specimen. Cloudy or turbid fluids may signify a high white blood cell count. Pink or red color usually indicates the presence of significant amount of blood (Fig. 10.1a). The latter may be related to a traumatic tap or can be a result of subarachnoid or cerebral hemorrhage. Table 10.1 lists some helpful features that can aid in separating traumatic tap from pre-procedural hemorrhage.
- Chemical analysis and tumor marker tests: Includes proteins, electrolytes, and pH levels along with $pO_2$ and $pCO_2$ levels for some indications. Increased total protein is the most common CSF abnormality and may serve as a nonspecific indicator of meningeal or CNS

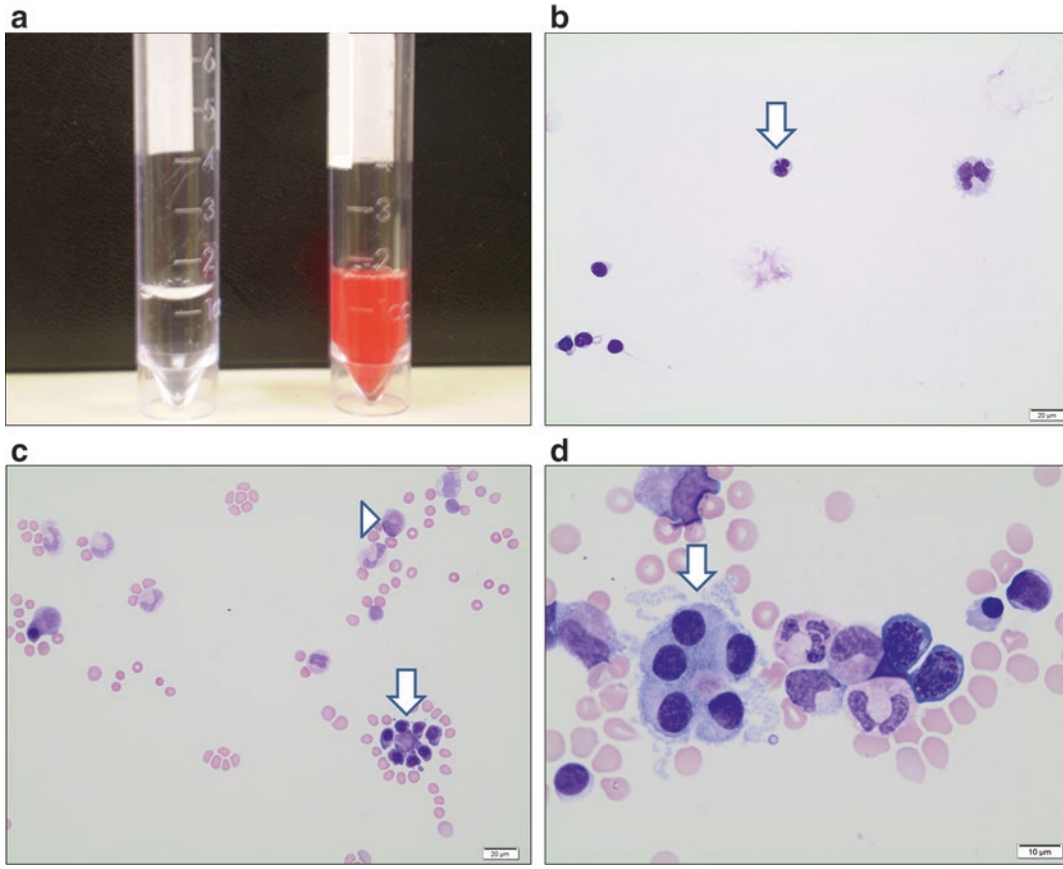


**Fig. 10.1** Common findings of normal and contaminated CSF. (**a**) Gross appearance of CSF. Normal (*left*) and blood-diluted (*right*) cerebrospinal fluid. (**b**) (Wright-Giemsa stain, high power). Normal CSF. Normal CSF in children shows the low cellularity and cellular composition (e.g., mostly lymphocytes and monocytes). Note that the centrifugal force used to prepare cytospin slides may deform nuclei of some normal cells and give a false impression of larger volume (*arrow*). (**c**) (Wright-Giemsa stain, high power). Peripheral blood and bone marrow contamination. Blood- and bone-marrow-contaminated CSF specimens showing red blood cells, erythroid precursors (*arrow*), and myeloid precursors (*arrowhead*). (**d**) (Wright-Giemsa stain, high power). Ependymal lining cells. CSF fluid showing an incidental finding of ependymal lining cells (*arrow*) with bland-appearing, round nuclei, moderate amounts of cytoplasm.

**Table 10.1** Comparison of CSF findings of traumatic tap with preexisting true CNS hemorrhage

| Feature | Traumatic tap | CNS hemorrhage |
|---|---|---|
| Bloody discoloration | Color intensity progressively decreases from tube 1 to tube 3 | Consistently similar in all three tubes |
| Post-centrifugation | Clear supernatant | Xanthochromic supernatant |
| Clot formation | May occur | Not encountered |
| D-dimer | Negative | Positive |
| Microscopic examination | No RBC-laden or hemosiderin-laden macrophages | RBC-laden (erythrophagocytosis) and/or hemosiderin- or hematoidin-laden macrophages present |

abnormality [1]. Testing for tumor markers (e.g., beta human chorionic gonadotropin, alpha fetoprotein, and carcinoembryonic antigen) may be helpful in certain clinical settings. Testing for angiotensin-converting enzyme and oligoclonal bands may be helpful in central nervous system sclerosis and multiple sclerosis, respectively.

- Microbiologic studies: The second tube collected is usually sent for microbiologic testing and must be handled immediately upon receipt. The CSF fluid is centrifuged, and the pellet is planted directly on appropriate solid culture media (for aerobic bacteria) or placed in broth culture media (for anaerobes). Other culture media may be used as indicated. A gram-stained cytospin slide is routinely examined on samples sent for cultures. Tests utilizing nucleic acid amplification methods are increasingly used in testing for viruses, bacteria, and mycobacteria.
- Microscopic examination: Cell counts include white blood cell (WBC) count, red blood cell (RBC) count, and total count. Most institutions use hemocytometers to perform these counts. Differential cell count is usually performed on a Giemsa-stained cytospin slide, following cytocentrifugation of a portion of the fluid sample. No dilution is needed if the WBC count is 500 per mL or lower. Progressive dilution with Hank's Balanced Salt Solution (HBBS) may be used when dilution is needed.

### 10.1.4 Expected and Incidental Findings

- The normal leukocyte cell count varies in children from 0 to 30 cells per mL in neonates to the adult level of 0–5 cells per mL in the older child; however, most patients without infection have counts on the lower end of the spectrum, which make these specimens quite hypocellular [1]. The cell counts are highest in neonates and monocytes usually predominate over lymphocytes. As the child gets older, there is a decrease in the number of white blood cells, and lymphocytes start to predominate over monocytes. In addition to the rare lymphocytes and monocytes (mononuclear cells), rare neutrophils can also be seen in the normal CSF (Fig. 10.1b). However, the presence of plasma cells is almost always associated with a disease process [3, 4].
- Incidental findings in normal CSF include anucleate squamous cells from the skin (most common), blood and bone marrow cells (Fig. 10.1c), ependymal lining and choroid plexus cells (Figs. 10.1d and 10.2a), capillary vessels (Fig. 10.2b), and osteoclasts and osteoblasts (Fig. 10.2c, d). These findings tend to be seen more in samples obtained from neonates and infants. Evidence of bone marrow contamination is usually heralded by the presence of immature cells from all hematopoietic lineages, particularly nucleated red blood cell precursors (e.g., basophilic or polychromatophilic normoblasts), or cartilage (dense metachromatic material with chondrocytes in lacunae), given that cases with bone marrow contamination are from lumbar punctures rather than shunt specimens. Megakaryocytes (large cells with abundant cytoplasm and multilobulated nuclei) are very rarely seen with bone marrow contamination in the CSF. In intraoperative washing specimens and specimens obtained during shunt placement, it is not uncommon to see glial fibrillary elements

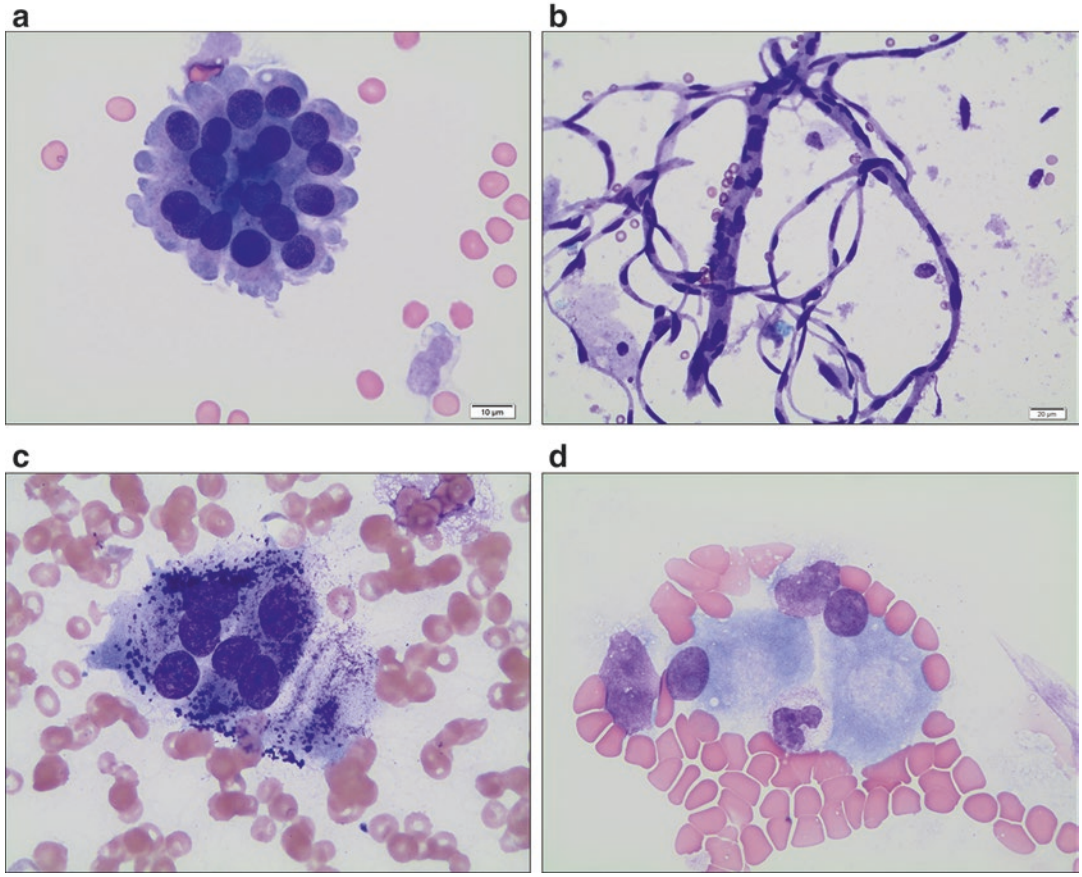


**Fig. 10.2** Common normal and incidental findings of CSF. (**a**) (Wright-Giemsa stain, high power). Choroid plexus cells. Clusters of cells with round nuclei, columnar appearance, and low nuclear-to-cytoplasmic ratios. (**b**) (Wright-Giemsa stain, high power). Capillary blood vessels. Spiderlike web of vessels with endothelial lining can be seen in some specimens. (**c**) (Wright-Giemsa stain, high power). Osteoclasts. Osteoclasts appear as multinucleated cells without atypia and can be seen from bone sampling in a lumbar puncture. (**d**) (Wright-Giemsa stain, high power). Osteoblasts. Osteoblasts have eccentrically placed nuclei, akin to plasma cells, but the cytoplasmic clearing is separate from the nucleus (not perinuclear), and the nucleus appears to extrude from the cell. These cells can also be seen from bone sampling in a lumbar puncture.

or neurons with prominent nucleoli. When interpreting these specimens, it is important not to misinterpret neurons, megakaryocytes, or chondrocytes as malignant cells.

- Ventricular lining cells (e.g., ependymal or choroid plexus cells): These are uncommonly seen in CSF specimens and have similar cytomorphology. Usually they are seen as clusters of bland-appearing columnar cells with basally oriented, round nuclei. The overall nuclear-to-cytoplasmic ratio is low and nucleoli are not typically seen. Sometimes the clusters will form round aggregates so that the columnar nature is not evident in the CSF.
- Trauma versus traumatic tap: Blood dilution of a CSF sample is more commonly caused by a traumatic tap related to the procedure than a subarachnoid hemorrhage. The possibility of subarachnoid hemorrhage due to accidental trauma, child abuse, or other causes may be in the differential diagnosis in certain pediatric patients. In general, neutrophils are not considered a normal cellular component of CSF; thus, the presence of neutrophils should raise concern for meningitis. However, in a bloody specimen, the significance of a few neutrophils is diminished given the possibility of peripheral blood

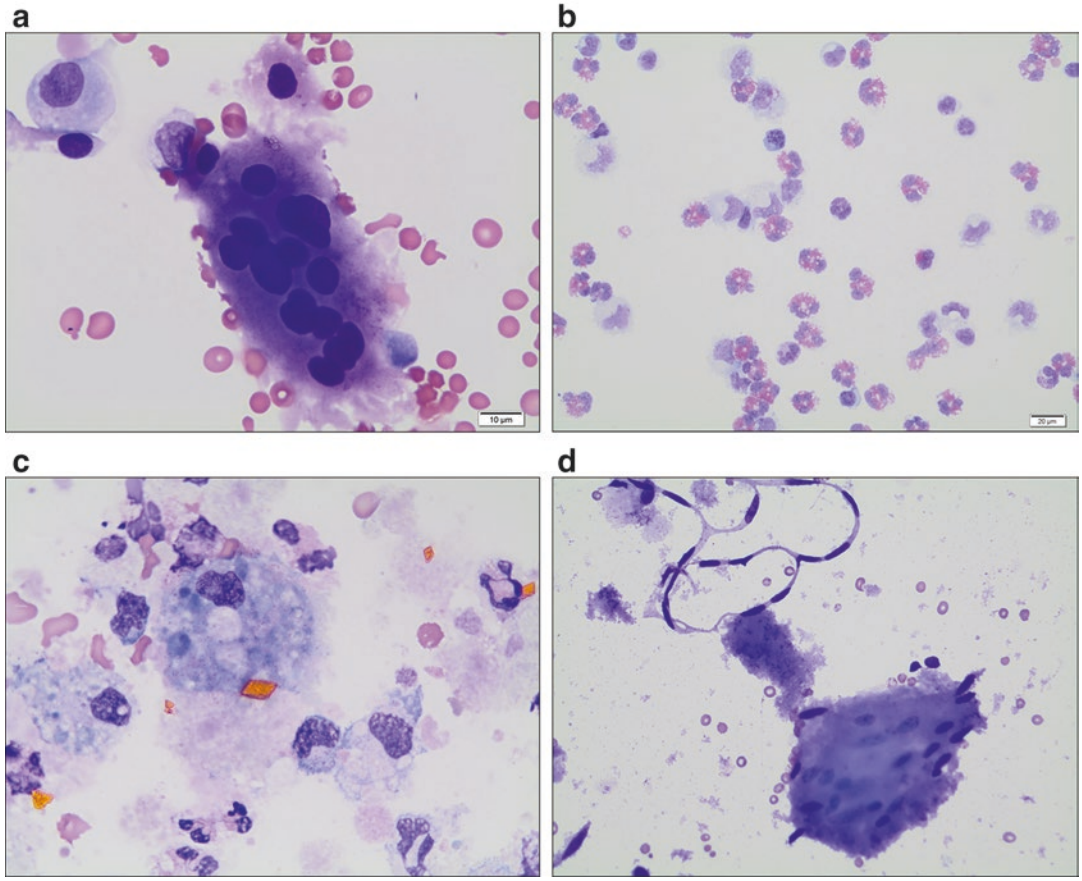


**Fig. 10.3** Common microscopic findings of shunt CSF fluid. (**a**) (Wright-Giemsa stain, high power). Multinucleated giant cells. Multinucleated foreign-body giant cells in a CSF from a child with a cerebral ventricle shunt. (**b**) (Wright-Giemsa stain, high power). Eosinophilia in CSF specimens. This CSF shows an increase in eosinophils with bilobed nuclei from a shunt fluid. (**c**) (Wright-Giemsa stain, high power). Subarachnoid hemorrhage. This CSF shows hemosiderin-laden and hematoidin-laden macrophages. (**d**) (Wright-Giemsa stain, high power). Brain material in CSF. Fragments of brain white matter and a capillary blood vessel from a shunt fluid.

contamination and the fact that mild pleocytosis can be seen in infants without CNS infection [3, 4]. One study suggested that a white blood cell (WBC) to red blood cell (RBC) ratio of less than or equal to 0.01 is considered not infected [3]. Table 10.1 compares cytologic findings of CSF in CNS hemorrhage versus traumatic tap.

### 10.1.5 Cerebral Ventricle Shunt Fluid

CSF cytology in patients with implanted shunt tubes usually reflects the cellular inflammatory reaction to the foreign material. Findings may include multinucleated giant cells (Fig. 10.3a), eosinophils (Fig. 10.3b), hemosiderin-laden and hematoidin-laden macrophages (Fig. 10.3c), and brain tissue fragments (Fig. 10.3d).

### 10.1.6 CSF in CNS Infections

- Common infections (viral and bacterial): Viral infections (Fig. 10.4a, b) are more common than bacterial infections (Fig. 10.4c, d) in the CSF of children, especially in the absence of prior surgical intervention and/or intraventricular shunt placement. Viral infections typically manifest with a predominance of lymphocytes

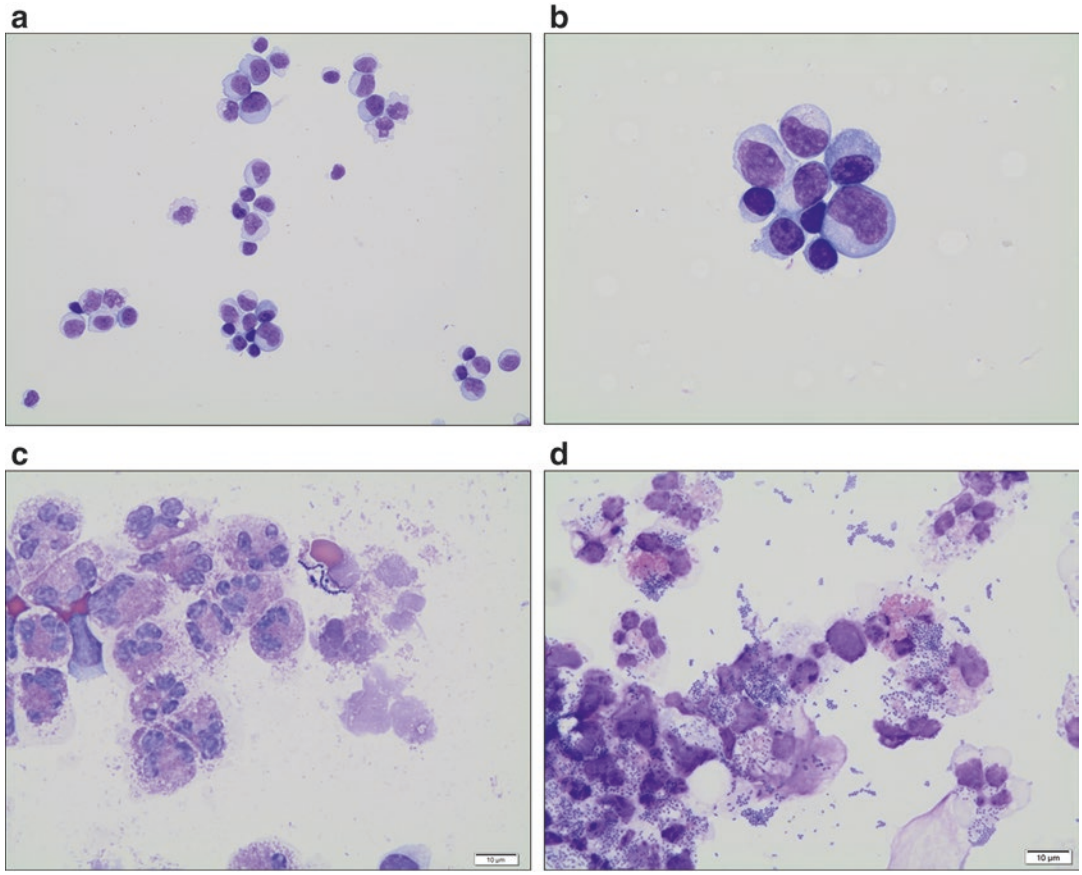


**Fig. 10.4** Common microscopic findings of CSF in viral and bacterial meningitis. (**a**, **b**) (Wright-Giemsa stain, high power). Variably sized reactive lymphocytes in a CSF from a child with aseptic/viral meningitis. (**c**, **d**) (Wright-Giemsa stain, high power). Bacterial meningitis. The CSF in bacterial meningitis typically has numerous neutrophils and occasionally intracellular bacteria.

or a lymphomonocytosis. Many of these cases will not have a pathogen detected by usual studies (e.g., culture, gram stain) and are considered "aseptic meningitis." In some viral infections, particularly herpes simplex virus (HSV) meningitis, the monocytes can have lobulated nuclei imparting a "footprint in the sand" appearance, which are called "Mollaret cells" [5]. The cytologic predominance of neutrophils is seen in the majority of bacterial meningitis, and this predominance is not limited to the first 24 h of disease [6]. CSF abnormalities associated with bacterial meningitis are rarely obscured by blood contamination from a traumatic tap [7]. Specific types of bacteria predominate in certain age groups. In a recent study by Nigrovic et al., Group B streptococcus, *Streptococcus pneumoniae*, and *Neisseria meningitidis* predominated in children 1–3 months, 3 months to 10 years, and 10–19 years of age, respectively [8]. Other organisms include gram-negative bacilli (enteric pathogens) and *Listeria* in the first 2 months of life, in addition to group B streptococcus. *Haemophilus influenzae type b* has dramatically decreased given the effective vaccination against this organism.

- Less common infections (fungal): Fungal infections of CSF are extremely rare, except in two patient groups:
  1. Patients with shunt devices may develop *Candida* infections (Fig. 10.5a).

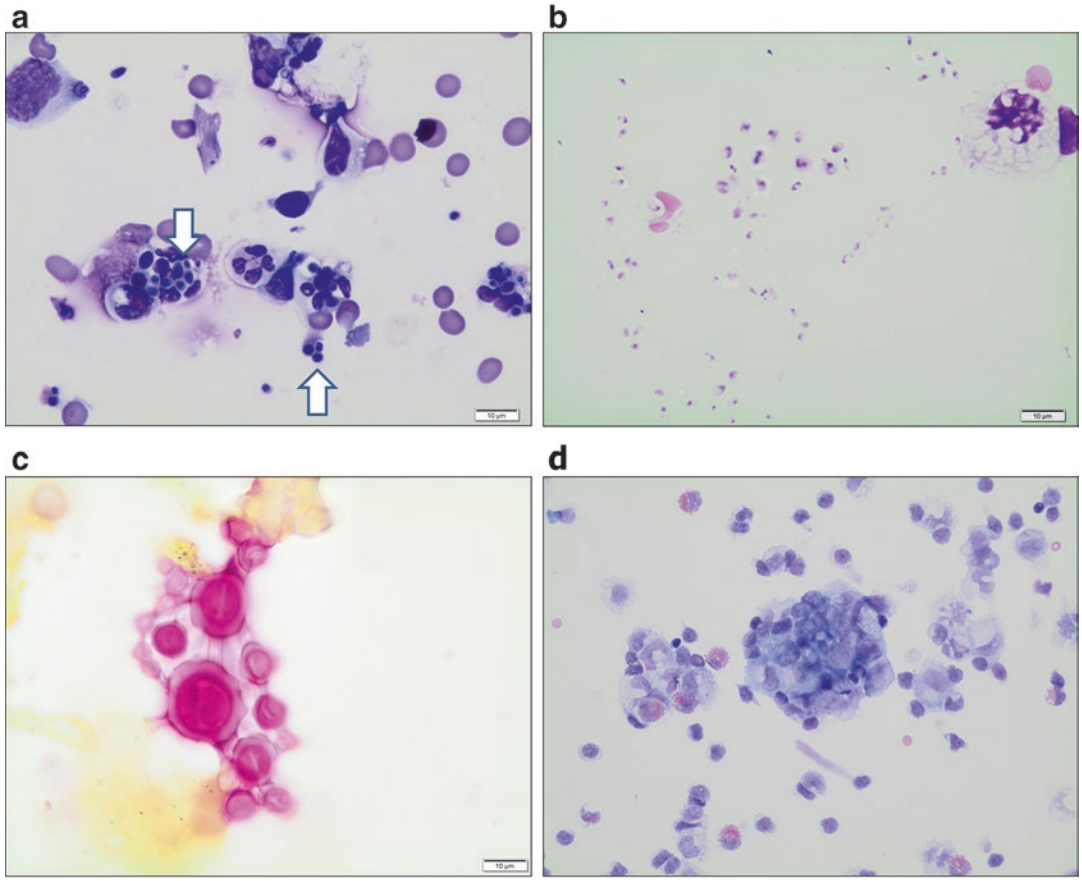


**Fig. 10.5** Common microscopic findings of CSF in fungal meningitis. (**a**) (Wright-Giemsa stain, high power). Candida. The budding yeasts (*arrows*) of *Candida parapsilosis* are seen in this CSF. (**b**) (Wright-Giemsa stain, high power) and (**c**) (mucicarmine stain, high power). *Cryptococcus neoformans* meningitis shows encapsulated yeast forms, which are more prominent where the background stain shows the clearing around the yeast forms. (**d**) (Wright-Giemsa stain, high power). Inflammatory cells clumping. Inflammatory cells can cluster in these specimens in dense aggregates.

2. Immunosuppressed patients are prone to opportunistic infection by *Cryptococcus* (Fig. 10.5b, c).

- Ancillary studies: Gram stain, microbial culture, and PCR or other molecular studies for identification of pathogens.
- Pearls: Neutrophils and other inflammatory cells start to degenerate quickly, within 2 h of collection; thus, immediate preparation of the specimen is critical. Some cases of bacterial meningitis may not have a neutrophil predominance and show more of a pleocytosis or lymphocytosis. The mixed inflammatory cells seen in bacterial infection may include clumps of reactive monocytes that may mimic the appearance of neoplastic cells (Fig. 10.5d).

### 10.1.7 CSF in Neoplasia

- Hematopoietic tumors, especially lymphoblastic leukemia, represent the most commonly encountered neoplasms involving the CSF of children. Primary CNS tumors constitute the second most common group of tumors (e.g., medulloblastoma, ependymoma, etc.) (refer to Sect. 10.2). Other small blue cell tumors of childhood may involve the CSF due

**Table 10.2** Comparison of cytologic findings in hematopoietic versus non-hematopoietic tumors

| Feature | Hematopoietic neoplasms | | Non-hematopoietic neoplasms |
|---|---|---|---|
| | Lymphoid | Myeloid | |
| Cellular clumps and/or nuclear molding | Absent | Rare | Common |
| Spindle cells | Absent | Absent | Encountered |
| Cytoplasmic fragments (lymphoglandular bodies) | Present | Absent | Absent |
| Nuclear fragments | Absent | Absent | Present |
| Ancillary diagnostic procedures | Flow cytometry<br>Immunohistochemistry (e.g., TdT) | Flow cytometry | Immunohistochemistry |

to direct extension or metastasis but are least commonly encountered.

- It is important to make every effort to separate hematopoietic from non-hematopoietic neoplastic cells based on morphology early in order to triage the specimen accordingly, especially in CSF specimens with scant volume or low cellularity. Table 10.2 compares the features of the two groups of neoplasms.

#### 10.1.7.1 Hematopoietic Neoplasms

Acute lymphoblastic leukemia is the most common neoplasm to involve the CSF (Fig. 10.6a). Acute myeloid leukemias are encountered in the CSF as well (Fig. 10.6b, c). Pediatric lymphomas are less likely to involve the CSF; however, Burkitt lymphomas and anaplastic large cell lymphoma may spread to the CSF (Fig. 10.6d).

##### Clinical Features

CSF sampling is performed routinely for staging and hence forth periodically following the diagnosis of all high-grade pediatric hematopoietic tumors. The patient may be asymptomatic or show symptoms of increased intracranial pressure (e.g., headache, nausea, etc.) or symptoms related to focal involvement.

##### Cytological Features

Cells are non-cohesive, usually with high nuclear to cytoplasmic ratios, irregular nuclear contours, and smooth chromatin with variably conspicuous nucleoli. Nuclear molding is generally absent. Rare exceptions are seen when cell counts are very high, especially in myeloid leukemias and in cases with artifactual clustering with cytospin preparation.

##### Differential Diagnosis and Ancillary Testing

The differential diagnosis includes acute leukemias and high-grade lymphomas of childhood, in addition to benign/reactive pleocytosis. The immunophenotypic workup is commonly performed on other sites of involvement (e.g., blood, bone marrow, lymph nodes, etc.) in cases worrisome for a hematolymphoid proliferation. In rare cases, the CSF is the only site of involvement, particularly at relapse, in the unlikely setting of a primary CNS lymphoma or rarely at first presentation. In such cases, a full workup, including immunophenotyping, cytogenetics, and molecular genetic studies, needs to be performed on the CSF. Table 10.3 shows a summary of preferred ancillary tests and key markers utilized.

#### 10.1.7.2 Non-hematopoietic Neoplasms

These are generally divided into primary tumors of the CNS (e.g., medulloblastoma, pineoblastoma) and metastatic solid tumors of childhood (e.g., rhabdomyosarcoma, rhabdoid tumors, CNS embryonal brain tumors).

##### Clinical Features

CSF examination is not routinely performed at initial diagnosis of non-hematopoietic solid tumors. However, exceptions include proximity of the primary site to the CNS, widely disseminated tumors, or clinical or radiologic suspicion of CNS involvement, in which cases CSF sampling is usually performed.

##### Cytological Features

Cells are generally larger than hematopoietic neoplastic cells, with more cohesion and nuclear

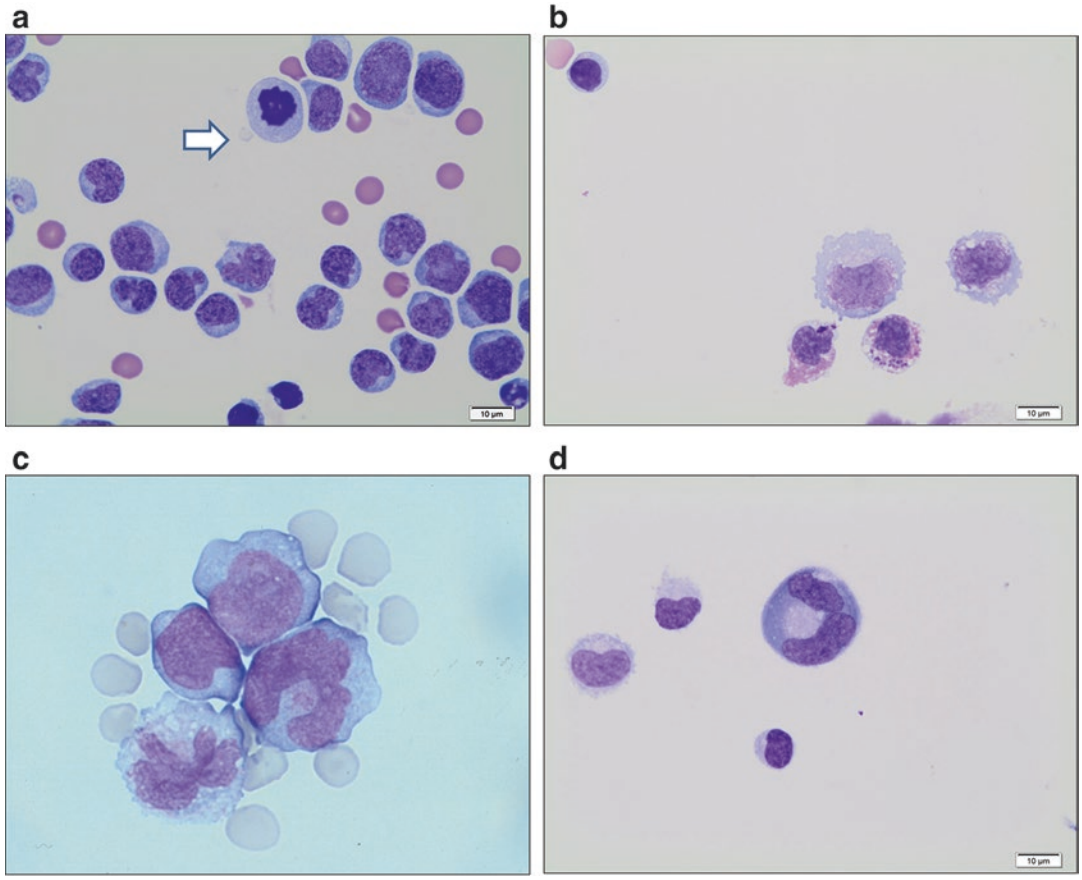


**Fig. 10.6** Examples of hematopoietic neoplasms in CSF. (**a**) (Wright-Giemsa stain, high power). Acute lymphoblastic leukemia (ALL). ALL in CSF showing small to medium-sized lymphoblasts with high nuclear cytoplasmic ratios and irregular nuclear contours. The *arrow* points to a lymphoglandular body, which is another clue to the lymphoid nature of the process. (**b**) (Wright-Giemsa stain, high power). Monoblasts and abnormal eosinophils in CSF of a patient with acute myeloid leukemia with abnormal eosinophils and chromosome 16p inversion. (**c**) (Wright-Giemsa stain, high power). Abnormal early monocytes and monoblasts from a case of acute monoblastic leukemia with t(10,19). (**d**) (Wright-Giemsa stain, high power). Large abnormal "hallmark" cell of anaplastic large cell lymphoma (ALCL). Note the size of malignant lymphoid cell compared with a neighboring normal lymphocyte.

molding. When present, nucleoli are usually larger than seen in hematopoietic proliferations. Certain formations (e.g., cellular rosettes) may be present and help narrow the differential diagnosis. There is usually an absence of lymphoglandular bodies on Romanowsky-stained material; however, a reactive lymphomonocytosis can accompany metastases or tumor involvement in the CSF, so lymphoglandular bodies could be seen in these scenarios.

### Differential Diagnosis

The main differential diagnosis includes retinoblastoma (Fig. 10.7a), CNS embryonal brain tumor (Fig. 10.7b, c), rhabdomyosarcoma (Fig. 10.7d), neuroblastoma (Fig. 10.8a), and rhabdoid tumor (Fig. 10.8b–d).

### Ancillary Testing

In cases with known primary tumors, a limited panel of key markers is utilized for confirmation

**Table 10.3** Preferred methods for confirming malignancy and key markers useful in immunophenotyping of childhood neoplasms that may involve CSF

| Neoplasm | Preferred method | Key markers |
|---|---|---|
| Acute leukemia, lymphoblastic | Flow cytometry | TdT: positive, most helpful in confirming lymphoblasts versus lymphocytes<br>CD19: most specific for B lineage<br>CD3 (surface or cytoplasmic): most specific for T-cell lineage |
| Acute leukemia, myeloid | Flow cytometry | Myeloperoxidase, other markers in certain subtypes (e.g., CD61, CD41, CD42b for megakaryoblastic leukemia)<br>Cytochemical stains (e.g., nonspecific esterase) help confirm monocytic lineage |
| Burkitt lymphoma | Flow cytometry | TdT: negative; Surface Ig positive with κ or λ light chain restriction |
| Lymphoblastic lymphoma/leukemia | Flow cytometry | TdT: positive |
| Anaplastic large cell lymphoma | Immunohistochemistry | CD30, Alk-1, CD3 |
| Metastatic solid tumors | Immunohistochemistry | See Table 10.4 |

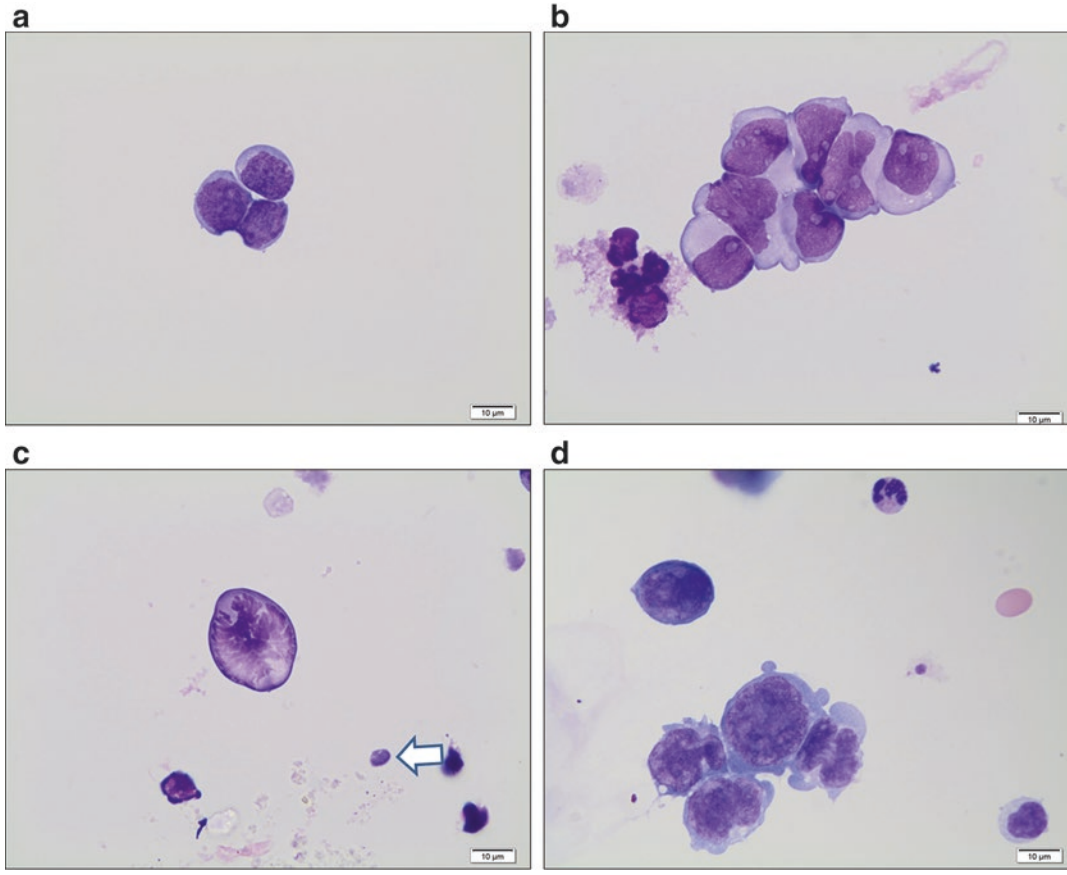


**Fig. 10.7** Examples of non-hematopoietic neoplasm in CSF. (**a**) (Wright-Giemsa stain, high power). Retinoblastoma. Small round blue cells with scant cytoplasm and conspicuous clustering with vague rosettes. (**b**, **c**) (Wright-Giemsa stain, high power). CNS embryonal brain tumor. Tumor cells in CSF show nuclear molding in (**b**) and nuclear fragments in (**c**) (*arrow*). (**d**) (Wright-Giemsa stain, high power). Alveolar rhabdomyosarcoma. This will also appear as a small round blue cell tumor with more clustering and pleomorphism than a hematolymphoid proliferation.

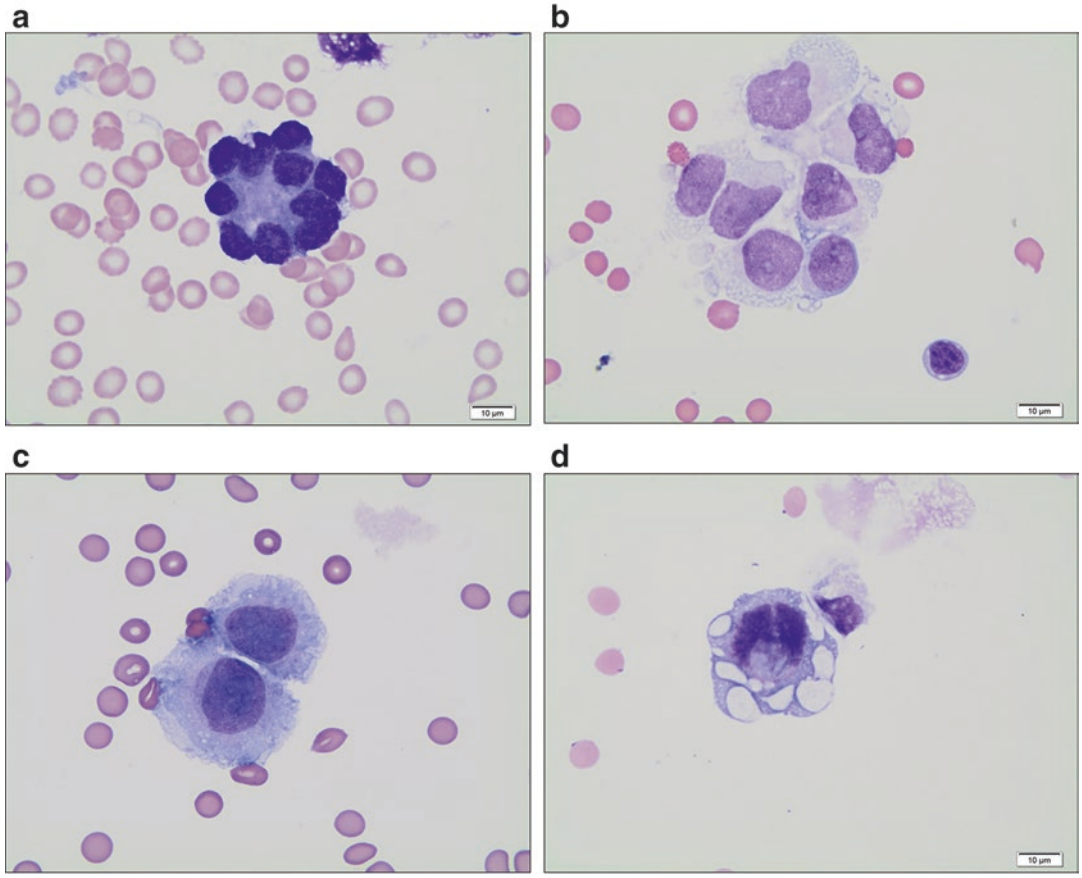


**Fig. 10.8** Examples of non-hematopoietic neoplasm in CSF. (**a**) (Wright-Giemsa stain, high power). Neuroblastoma. A"rosette" of neuroblasts around neurofibrillary center in a case of metastatic neuroblastoma. (**b**, **c**) (Wright-Giemsa stain, high power). Rhabdoid tumor. Malignant rhabdoid tumor cells are large and show unusually large nucleoli. (**d**) (Wright-Giemsa stain, high power). Cytoplasmic vacuoles. Vacuoles can be seen in non-hematopoietic tumors, in addition to Burkitt lymphomas, but the vacuoles are usually larger and are seen within pale cytoplasm.

purposes. If the primary tumor is unknown or not sufficiently studied, then a full workup, including immunohistochemical staining, molecular, and cytogenetic studies, is necessary, similar to the workup of a biopsy specimen. Individual labs should have established protocols for immunohistochemical staining of cytology specimens, including time of fixation and methodology (e.g., cell block versus cytospins). In a sample with limited cellularity and limited volume, a few additional cytospins may be more helpful than a cell block to perform a limited panel of key immunostains (e.g., LCA, cytokeratin, synaptophysin). Table 10.4 provides an abbreviated list of markers widely used in the evaluation of common small round cell tumors of childhood.

### Diagnostic Pitfalls

The cytologic findings in cases of aseptic meningitis and other inflammatory conditions may be brisk and almost exclusively lymphoid, mimicking a lymphoid malignancy. In addition, the intense cellular reaction, together with cell distortion caused by centrifugal force upon spinning, may occasionally mimic a lymphoid malignancy (Figs. 10.9 and 10.10a). Close attention to the

**Table 10.4** Abbreviated immunohistochemical panel for common childhood non-hematopoietic small round cell tumors

| Tumor | Immunohistochemical panel |
|---|---|
| Rhabdomyosarcoma | Desmin, actin, MyoD1, myogenin |
| Ewing sarcoma/ embryonal brain tumor | CD99, FLI-1, synaptophysin |
| Neuroblastoma | NSE-M, NB-84, PGP9.5, tyrosine hydroxylase |
| Desmoplastic round cell tumor | Cytokeratin, desmin, EMA, NSE, WT-1 |

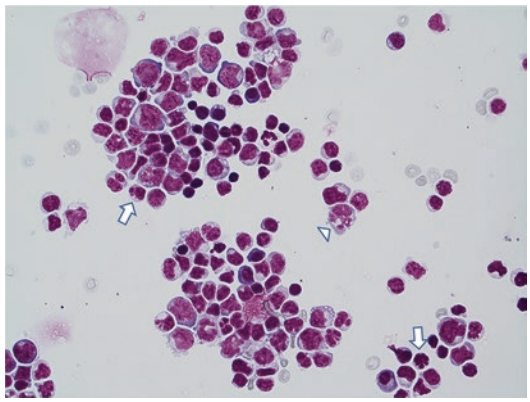

**Fig. 10.9** Brisk lymphoplasmacytic and monocytic cellular reaction from a case of lupus cerebritis (Diff-Quik stain, medium power). Lymphocytes are designated by *arrows* and a monocyte is designated by an *arrow head.* (Image courtesy of Dr. Sara Monaco).

nuclear features (smooth nuclear membrane, clumped chromatin, and low nuclear to cytoplasmic ratio) and the variability of lymphocyte shapes and sizes will help in excluding a malignant process.

A rare form of aseptic meningitis, called Mollaret meningitis, is caused in most cases by viral infections, such as HSV, and characterized by recurrent episodes of meningitis. Cytologically, atypical monocytes (i.e., Mollaret cells) with nuclei having the appearance of a "footprint in the sand" are frequently seen [5, 9]. These cells, although characteristic in this clinical context, are nonspecific.

In some cases of bacterial meningitis and reactive pleocytosis, especially in the context of a reaction to shunts, clusters of histiocytic cells or white blood cells may be seen and should not be confused with a neoplastic process (Fig. 10.10b).

Extreme prematurity predisposes to germinal matrix hemorrhages that may be accompanied with the shedding of normal germinal matrix neuroblasts to the CSF. The latter cells are morphologically difficult to distinguish from hematopoietic blasts, metastatic medulloblastoma, or neuroblastoma (Fig. 10.10c, d); however, germinal matrix neuroblasts tend to be scant in number and more cohesive. The age of the child, absence of tumor radiologically, and the clinical history are most helpful in this determination.

## 10.2 CNS Tumor Cytology/ Smear Preparations

### 10.2.1 Introduction

- Neuropathologists routinely evaluate frozen sections in conjunction with a cytological preparation at the time of intraoperative consultation. The frozen section and cytological preparation provide necessary information and complement each other in formulating a diagnosis. The frozen section is important for providing architectural detail and is essential in determining how a disease process interfaces with the surrounding tissue (e.g., infiltrative or discrete lesion). However, given the crushed nature of small specimens on frozen section and the artifactual distortion, cellular morphology is usually not ideal. Cytological preparations allow assessment of morphologic details, such as nuclear features, background fibrillarity, and presence or absence of lymphoglandular bodies; which are important for the evaluation of many brain tumors.
- Neurosurgical intraoperative consults should always be performed with knowledge of the patient's age, clinical presentation, and an understanding of the neuroimaging findings. Since many conditions tend to involve particular neuroanatomical sites and affect patients in certain age groups, having this information allows significant refinement of the differential diagnosis before the specimen is even

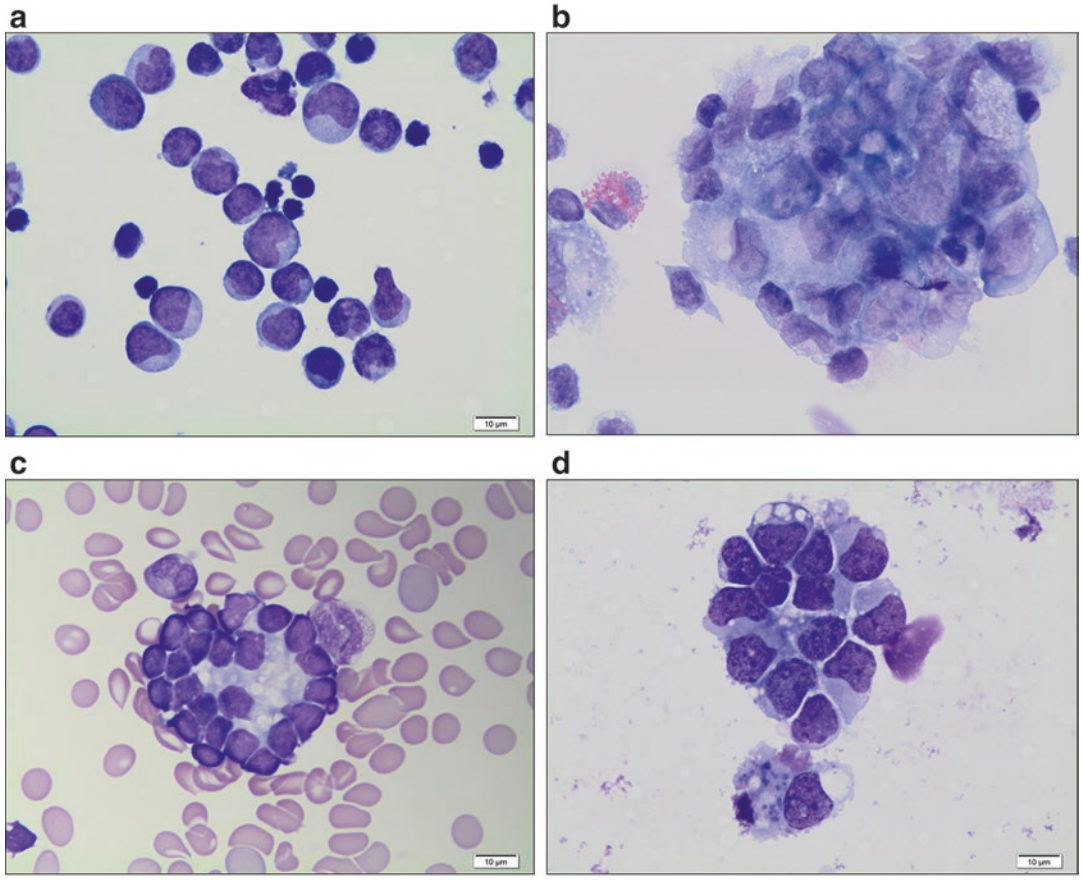


**Fig. 10.10** Benign mimickers of malignant cells in CSF. (**a**) (Wright-Giemsa stain, high power). Reactive lymphocytes. The atypical reactive lymphocytes in viral meningitis have cytologic changes that may be striking and can closely mimic a lymphoid malignancy. (**b**) (Wright-Giemsa stain, high power). Clumping of inflammatory cells in bacterial meningitis may be dominated by macrophages with prominent nucleoli, which may resemble clumps of neoplastic cells. (**c**, **d**) (Wright-Giemsa stain, high power). Germinal matrix primitive neurons may shed into CSF due to hemorrhagic infarcts in premature babies and can mimic metastatic neuroblastic tumors.

received. This approach is detailed in many neuropathology textbooks, and the main patterns will be highlighted in this chapter [10, 11].

## 10.2.2 Intraoperative Cytological Evaluation of CNS Tumors

### 10.2.2.1 Types of Preparations

Although a variety of techniques can be used to make a cytological preparation, the majority of sampled brain lesions are received as minute fragments of soft, fragile material and are thus best suited to being smeared. Smears are quickly and easily prepared by placing multiple small (1–3 mm) tissue fragments on a glass slide and firmly squashing them with another slide while drawing the tissue out to the end of the bottom slide. Immediate fixation reduces the impact of air-drying artifact, which can alter the appearance of the chromatin, as well as the size and shape of cells. An intraoperative washing specimen is rarely utilized and may require a smear preparation for immediate evaluation, but more often is processed similar to a CSF specimen.

**Table 10.5** Background material and differential diagnosis in CSF cytology

| Clean or bloody | Necrotic | Fibrillary | Myxoid or chondroid | Inflammatory |
|---|---|---|---|---|
| Nerve sheath tumors | Benign (infection, radiation necrosis) | Glial or astrocytic tumors | Myxopapillary ependymoma | Germinoma (tigroid, granular; lymphohistiocytic) |
| Meningioma | High-grade tumors (metastatic SRBCTs, hematolymphoid malignancies) | Pineocytoma | Dysembryoplastic neuroepithelial tumor | Demyelinating lesions (inflammatory with plasma cells, granular) |
| Choroid plexus papillomas | Glioblastoma | Ependymal tumors | Chordoma | Infection |
| Vascular tumors (hemangioblastoma, choriocarcinoma) | Germ cell tumors (embryonal, yolk sac, non-germinomatous) | Oligodendroglial and astrocytic tumors | Chordoid meningioma | |
| Metastatic melanoma | Craniopharyngioma (dirty cystic debris with cholesterol crystals and keratin) | | Metastatic sarcomas or matrix-producing tumor | |

#### 10.2.2.2 Types of Staining

Hematoxylin and eosin (H&E) staining is frequently used because eosin nicely resolves glial cell fibrillarity, and most of neuropathologists evaluating these specimens are more comfortable evaluating material stained with H&E as opposed to other cytochemical stains. However, other stains can be used depending on individual preference. When a hematolymphoid proliferation is suspected, Romanowsky-type stains are helpful for recognizing lymphoglandular bodies and can enhance triaging of the specimen for flow cytometry and fluorescence in situ hybridization (FISH) studies. The figures in this section consist primarily of H&E-stained preparations.

#### 10.2.2.3 Approach to the cytomorphology

The background material in a smear preparation can be visualized at low magnification and provides important information to guide one's differential diagnosis, as shown in Table 10.5. In general, a fibrillary background is usually seen in primary glial or astrocytic tumors, pineocytomas, and ependymal tumors. In contrast, a necrotic background is more often indicative of a glioblastoma, high-grade small round blue cell tumor, germ cell tumor, or benign necrosis related to treatment or infection. A tigroid background is typically associated with germinoma, a type of CNS- germ cell tumor.

In addition to the background material, the cellular features at high magnification are also helpful, as shown in Table 10.6. Spindle or oval/fusiform nuclei are typically seen with nerve sheath tumors, spindle cell variants of tumors (particularly melanoma and meningiomas), and sarcomas. In contrast, rounder epithelioid cells are seen with gangliocytic tumors, oligodendrogliomas, meningiomas, melanoma, germ cell tumors, and lymphoproliferative disorders.

A few CNS tumors have particular cytological features that can be important clues to the diagnosis, such as the whorling of cells in an onion skin-like fashion, intranuclear inclusions seen in meningiomas, and the presence of rosettes and papillary formation in other tumors. Differential diagnostic considerations raised by these and other features are highlighted in Table 10.7.

### 10.2.3 Glial Tumors

Gliomas, such as astrocytomas, are characterized into two types based on their growth pattern in histological specimens, which includes discrete lesions that do not widely infiltrate brain or infiltrative lesions that invade the adjacent brain tissue. Although the interface with adjacent brain tissue is not evident on cytological

**Table 10.6** Cell type and differential diagnosis in CSF cytology

| Polygonal/rounded | Spindle/fusiform | Long processes | Small round blue cells |
|---|---|---|---|
| Gangliocytic tumors | Nerve sheath tumors | Glial or astrocytic tumors (e.g., pilocytic astrocytoma) | Metastatic SRBCT (e.g., neuroblastoma) |
| Oligodendroglioma | Spindle cell variants of tumors (e.g., spindle cell melanoma, spindle cell or fibrous meningioma, sarcomatoid carcinoma) | Ependymal tumors | Medulloblastoma |
| Meningioma | Sarcomas | Oligodendroglial- or astrocytic tumors | CNS embryonal tumor not otherwise specified (NOS) |
| Lymphoma | Mimics: endothelial cells in microvascular proliferations, artifactual distortion and stretching of cells | | Pineoblastoma |
| Germ cell tumor/germinoma | | | Retinoblastoma |
| Metastatic melanoma | | | Any "blastoma" |
| Small round blue cell tumors (metastatic, blastomas) | | | |
| Craniopharyngioma | | | |
| Choroid plexus tumors | | | |

preparations, the tumors are grouped this way given that the radiological findings can usually be correlated.

#### 10.2.3.1 Pilocytic Astrocytomas

##### Clinical Features

Pilocytic astrocytomas are WHO grade I tumors of children and young adults [12]. Typical sites of occurrence are the cerebellum or optic nerve/chiasm and hypothalamus, but pilocytic astrocytomas can arise anywhere in the CNS. Neurofibromatosis 1 patients can have optic nerve involvement. MRI shows a generally discrete tumor with minimal edema that enhances heterogeneously. A cystic component is common and can be prominent in cerebellar and spinal cord tumors. Calcifications can occur, especially in cerebral tumors.

##### Cytological Features

Histologically, these tumors are biphasic with compact areas of bipolar astrocytes accompanied by Rosenthal fibers and more loosely textured areas with microcysts and eosinophilic granular bodies. The biphasic pattern is often not recognized in smears, but fibrillary tissue fragments and individual tumor cells with long bipolar processes emanating from each pole of a spindle-shaped nucleus are seen (Fig. 10.11a). The edge of tissue fragments is a good place to look for Rosenthal fibers, which appear glassy and torturous (Fig. 10.11b). Nuclei are uniform and bland in these tumors.

##### Pearls

Degenerative atypia and multinucleation are more common in older children, in addition to vascular proliferation, and do not upgrade a pilocytic astrocytoma (Fig. 10.11c).

##### Differential Diagnosis

Piloid gliosis, pilomyxoid astrocytoma, diffuse astrocytoma grade II, ganglioglioma with piloid glial component, dysembryoplastic neuroepithelial tumor, glioblastoma, and ependymoma.

#### 10.2.3.2 Subependymal Giant Cell Astrocytoma (SEGA)

##### Clinical Features

SEGAs are discrete, WHO grade I tumors that tend to occur in the lateral ventricles often near the foramen of Monro in tuberous sclerosis complex patients and can cause obstruction of CSF

**Table 10.7** Specific cytological features with definition and differential diagnosis

| Cytological Feature | Definition | Differential diagnosis |
|---|---|---|
| Whorls | Tight, cohesive clusters with onion skin or concentric wrapping around the edges | Meningioma<br>Papillary tumors (e.g., papillary craniopharyngioma, choroid plexus papillomas)<br>Schwannoma<br>Mimics (e.g., endothelial cells and blood vessels) |
| Intranuclear inclusions | Rounded inclusions with a distinct rim seen within the nucleus and generally the same color as the cytoplasm | Meningioma<br>Artifacts (e.g., air drying, frozen section artifacts) |
| Papillary tufts | Cohesive fragments of cells arranged around a fibrovascular core | Papillary primary CNS tumors (papillary meningioma, papillary ependymoma, choroid plexus papilloma)<br>Metastatic papillary tumor<br>Mimics (germ cell tumors, such as yolk sac tumors; arborizing vascular tumors, such as hemangioblastoma) |
| Pseudorosettes (Homer Wright) | Circular cluster of fibrillary neuropil processes concentrated in the center with cells arranged on the periphery (pink center) | Neuroblastoma<br>Pineocytoma<br>Neurocytoma<br>Medulloblastoma<br>CNS embryonal tumor NOS |
| True rosettes (Flexner-Wintersteiner and ependymal) | Circular cluster of cells radially arranged around a central lumen | Ependymoma<br>Pineoblastoma<br>CNS embryonal tumor NOS<br>Retinoblastoma |
| Perivascular pseudorosettes | Cells arranged on the periphery with cell processes extending inward in the cluster around a centrally located vessel (red blood cells and endothelial lining in center) | Ependymoma<br>Subependymal giant cell astrocytoma<br>Astrocytoma, including pilomyxoid or anaplastic astrocytoma<br>Papillary tumors |
| Melanin | Brown or dusty pigment within the cytoplasm | Melanoma<br>Melanotic neuroectodermal tumor of infancy (bullet-shaped melanin)<br>Melanotic schwannoma<br>Gangliocytic tumors with neuromelanin<br>Other melanotic tumors (e.g., melanotic medulloblastoma, melanotic choroid plexus tumors, melanotic ependymoma) |
| Eosinophilic cytoplasmic bodies | Small, rounded, eosinophilic inclusions | Pilocytic astrocytoma<br>Gangliocytic tumors<br>Xanthoastrocytoma<br>Dysembryoplastic neuroepithelial tumor |

flow. Neuroimaging shows a well-circumscribed enhancing mass that can be lobulated. SEGAs can be calcified.

### Cytological Features

Large pyramidal-shaped cells with abundant eosinophilic cytoplasm and neuron-like nuclei that are round with open chromatin and prominent nucleoli (Fig. 10.11d, e). Calcifications can be abundant (Fig. 10.11f).

### Pearls

Other features of tuberous sclerosis are frequently present; thus, a detailed clinical history of tuberous sclerosis and tumor location is critical to the diagnosis [12].

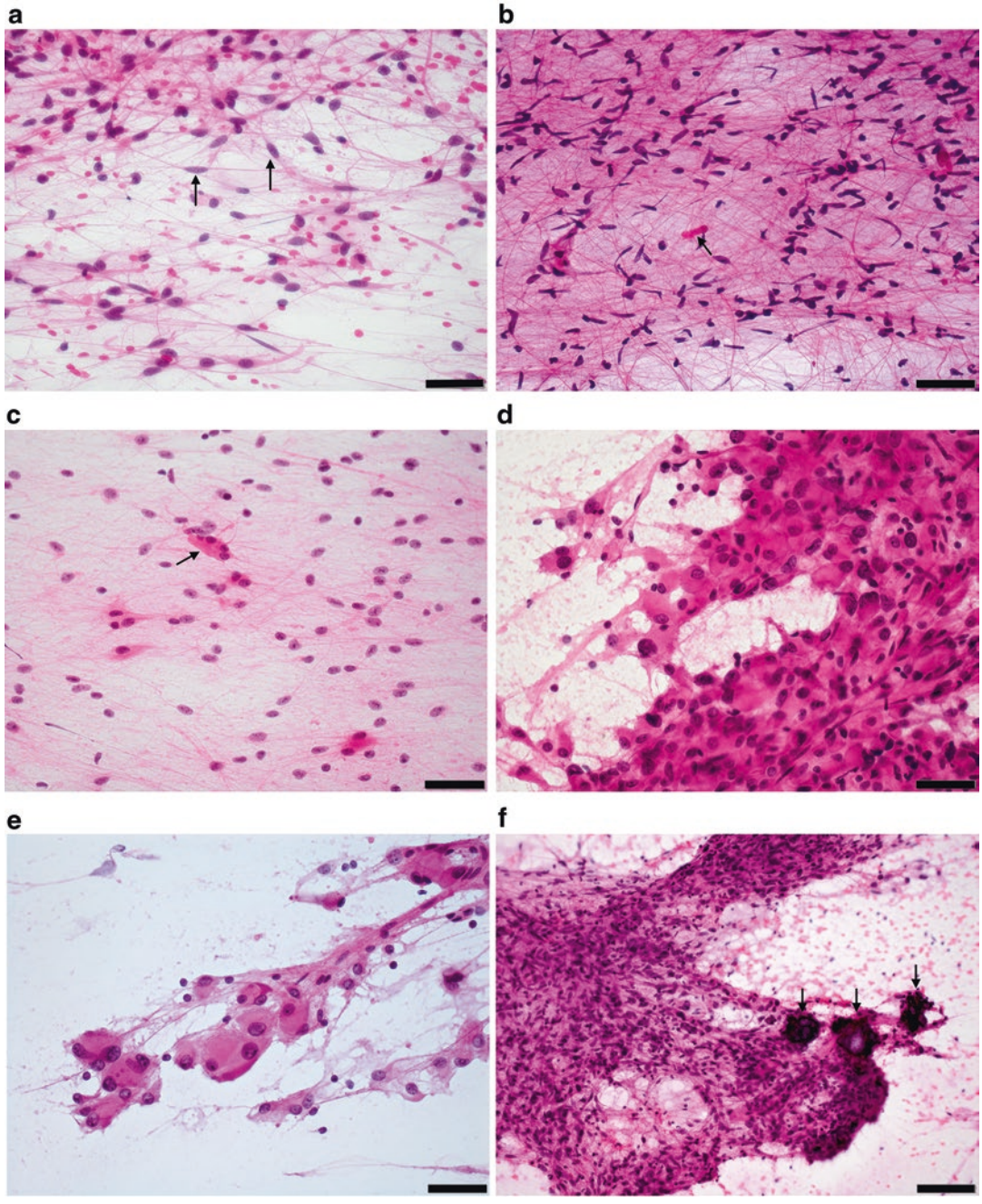


**Fig. 10.11** Discrete gliomas. (**a**–**c**) (H&E stain, high power). Pilocytic astrocytoma. The typical cell encountered in pilocytic astrocytomas is the bipolar astrocyte, which has slender glial processes that appear to extend from each pole of a spindle-shaped nucleus (*arrows*). (**b**) Rosenthal fibers are glassy-appearing, irregular structures found in glial cell processes (*arrow*). Multinucleation and degenerative atypia (**c**) can be seen in pilocytic astrocytoma (*arrow*), especially in older patients. (**d**–**f**) (H&E stain, high power). Subependymal giant cell astrocytoma. Smears show tissue fragments with large cells (**e**) that are variable in size, and many have abundant eosinophilic cytoplasm. Calcifications (**f**) are often present (*arrows*) and can be abundant, making these tumors gritty and difficult to smear.

#### Differential Diagnosis

Gemistocytic astrocytoma, ependymoma, ganglion cell tumor, and pilocytic astrocytoma.

### 10.2.3.3 Infiltrative Astrocytomas

#### Clinical Features

Infiltrative astrocytomas can arise at any age and at any site; however, the pons and thalamus are commonly involved in children, whereas the spinal cord and cerebellum are less commonly affected. The clinical presentation is variable and includes seizures, mass effect, or focal neurologic deficits. These tumors represent a spectrum from WHO grade II (diffuse astrocytoma) to grade III (anaplastic astrocytoma) and up to grade IV (glioblastoma). Neuroimaging may show a deceptively discrete-appearing lesion with variable mass effect. Grade II tumors do not enhance, but grade III tumors may focally enhance. Grade IV tumors characteristically show ring enhancement in adults, but this may not be encountered in young children [12].

#### Cytological Features

Smears of grade II astrocytomas result in fragments of tissue and dispersed individual cells. Tumor cells have extensive fibrillary processes and variable amounts of cytoplasm (Fig. 10.12a–c). The nuclei are irregular and sometimes naked with no associated cytoplasm (Fig. 10.12c). Grade III astrocytomas tend to show greater cytological atypia (Fig. 10.12d). Increased mitotic activity is used to distinguish grade III from grade II astrocytomas, but this feature is difficult to recognize in smears. Cytological atypia is even more pronounced in glioblastoma; however, it most commonly shows small cells with hyperchromatic nuclei and fine processes (Fig. 10.12e), and the cytological features can be diverse and include large epithelioid, gemistocytic, or multinucleated giant cells. Necrosis and microvascular proliferation (Fig. 10.12f) are characteristic of grade IV tumors and help distinguish them from grade III tumors.

#### Pearls

CSF spread and positive CSF specimens are more common in higher-grade astrocytomas. One should use caution when communicating intraoperative findings to the neurosurgeon. A tumor reported as low grade initially may actually be high grade when additional sections are examined; thus, consider using "infiltrating glial tumor" as a preliminary diagnosis, and do not provide a grade. If the neurosurgeon insists, indicate that a particular grade is favored based on the material examined, and carefully document this limitation.

#### Differential Diagnosis

Oligodendroglioma grades II and III, pilocytic astrocytoma, dysembryoplastic neuroepithelial tumor, and ependymoma. Reactive conditions such as an infarct or abscess can have a granular or necrotic background and are included in the differential diagnosis of high-grade gliomas.

### 10.2.3.4 Oligodendroglioma

#### Clinical Features

Oligodendrogliomas are rare in children, but can affect adolescents. These tumors characteristically occur in the cerebrum, tend to involve the cortex, and present with seizures, focal neurological deficits, or mass effects. Neuroimaging shows a bright, well-circumscribed white matter mass in T2 and FLAIR images that is often associated with thickened cortex. Calcifications may be present. Grade II lesions do not enhance and

**Fig. 10.12** (continued) tend to show increased nuclear pleomorphism. Microvascular proliferation (**f**) is encountered in glioblastoma smears. (**g**, **h**) (H&E stain, high power). Oligodendrogliomas. These tumors are cellular, show round cells with less nuclear hyperchromasia than encountered in astrocytic tumors, and show delicate capillaries. Minigemistocytes are cells (**h**) with a tongue of eosinophilic cytoplasm and an eccentrically situated nucleus, may be encountered in grade III oligodendroglioma. Nuclei in oligodendrogliomas are not as dark and hyperchromatic as seen in astrocytomas.

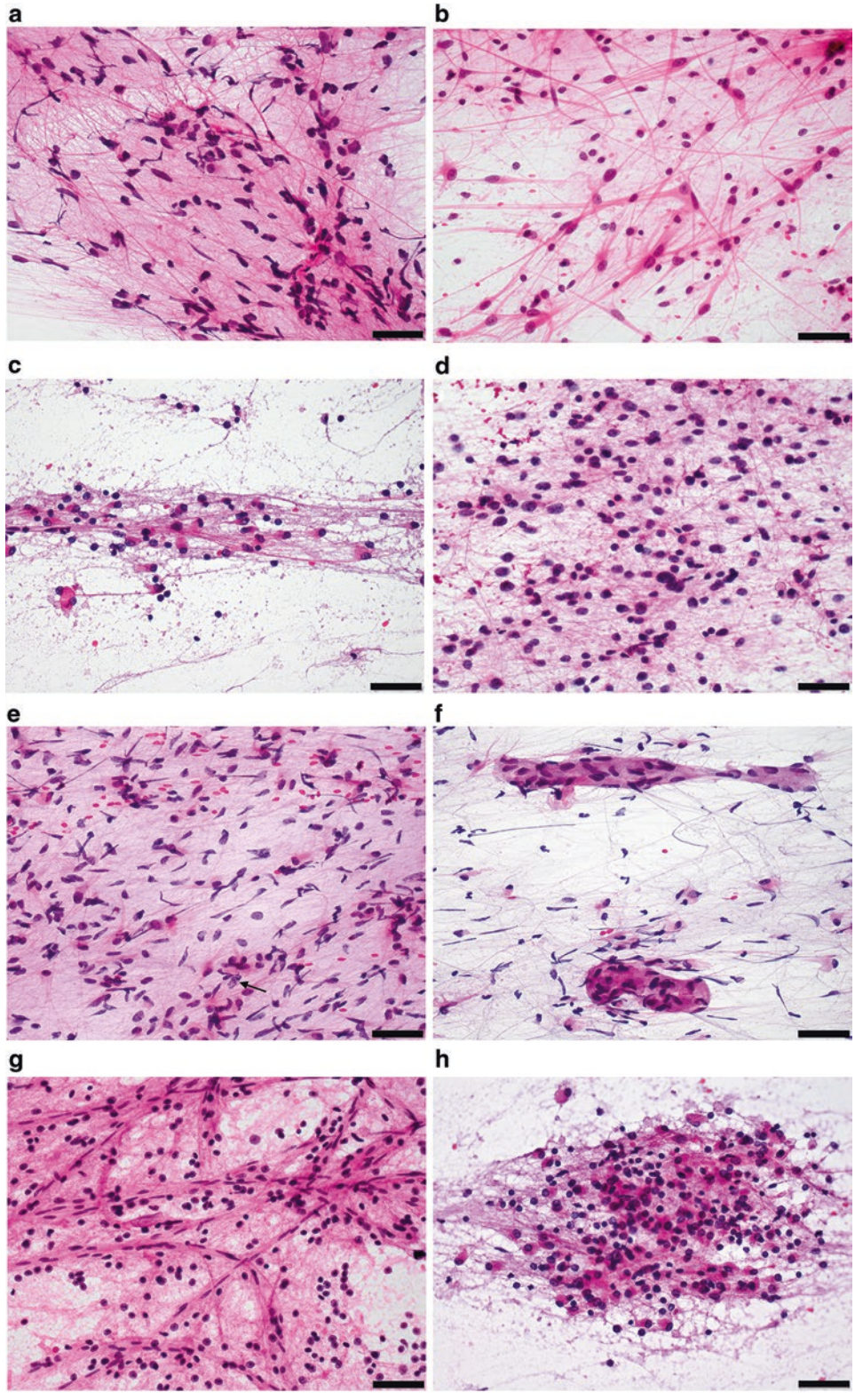


**Fig. 10.12** Diffuse glioma. (**a**–**f**) (H&E stain, high power). Diffuse astrocytomas. Smears are fibrillar with ill-defined cell borders and pleomorphic nuclei. Bare nuclei (**b**) may be apparent as the cytoplasm may be lost during smearing. Smears provide an opportunity to examine cell cytoplasm and some astrocytic tumors show eccentric nuclei (**c**). High-grade astrocytomas, such as grade III anaplastic tumors (**d**) or grade IV glioblastomas (**e**),

grade III tumors show variable enhancement, but it is not ringlike, as seen in glioblastoma. Long-standing tumors may erode the inner table of the skull [12].

#### Cytological Features

Smears show tissue fragments and individual cells. Cells from oligodendrogliomas show less fibrillarity than cells found in astrocytomas (Fig. 10.12g), whereas fibrillarity can be pronounced in oligoastrocytomas. Nuclei are round with delicate chromatin, but in grade III lesions, nuclei are hyperchromatic with coarse chromatin (Fig. 10.12h). Distinct nucleoli may be seen. Delicate "chicken wire" vasculature is often found (Fig. 10.12g). WHO grade II lesions have cells that are morphologically similar to oligodendrocytes, while grade III anaplastic oligodendrogliomas show increased cellularity, nuclear atypia, and pleomorphism. Grade III lesions may have vascular proliferation.

#### Pearls

The so-called "fried egg" appearance is not seen in smears as it is an artifact of formalin fixation. Discerning astrocytoma from oligodendroglioma can be accomplished using smears. Smears can resolve tumor cytology better than frozen sections, and are optimal for revealing cell fibrillarity and nuclear hyperchromasia, both of which are more prominent in astrocytomas than oligodendrogliomas. Consider preparing multiple smears from infiltrating gliomas. In general, 1p and 19q abnormalities are rare in pediatric oligodendrogliomas, but these molecular studies can be done on touch preps, if indicated [13].

#### Differential Diagnosis

Diffuse astrocytomas, dysembryoplastic neuroepithelial tumor, and neurocytic tumors.

### 10.2.4 Ependymoma

#### Clinical Features

Ependymomas can occur throughout the CNS. Grade II ependymoma is generally slow growing, while grade III lesions often grow aggressively, as is reflected in their characteristically high mitotic rate. Grade III lesions may also have microvascular proliferation and pseudopalisading necrosis. In children, ependymomas tend to arise in the posterior fossa and can obstruct CSF flow, so patients can present with signs and symptoms of increased intracranial pressure, and brainstem compression. Posterior fossa tumors tend to be discrete and are usually centered in the fourth ventricle where they mold to the shape of the ventricle and can extend out of the foramina. Supratentorial ependymomas present with mass effect and focal neurological deficits and are frequently paraventricular and cystic. Both posterior fossa and supratentorial tumors can be calcified and show heterogeneous enhancement.

Ependymomas of spinal cord parenchyma are more common in adults than children and are associated with neurofibromatosis 2. Myxopapillary ependymomas tend to occur in young adults and adolescents and arise in the filum terminale or as a sacral extradural mass. The myxopapillary variant is grade I and characteristically presents with pain [12]. Ependymomas growing in the spinal cord are discrete and often enhance; they can be cystic and associated with a syrinx. The myxopapillary variant is a well-circumscribed, enhancing lesion.

#### Cytological Features

Smear cytology shows fibrillary tissue fragments with fine glial processes. Some tissue fragments consist of glial cells covering vessels in papillary-like structures (Fig. 10.13a). Where cells are dispersed in grade II–III lesions, the nuclei appear ovoid, and show coarser chromatin and more nuclear irregularities (Fig. 10.13b, c). It is uncommon to identify true ependymal or pseudovascular rosettes and intracytoplasmic lumina in smears. Smears of myxopapillary ependymomas show fibrillary tissue fragments (Fig. 10.13d) with clusters of cells admixed with myxoid material (Fig. 10.13e), which is a distinctive feature. Degenerative atypia in the form of scattered large, irregular hyperchromatic nuclei is not uncommon in myxopapillary ependymoma (Fig. 10.13f), but infrequent in grade II and III ependymomas.

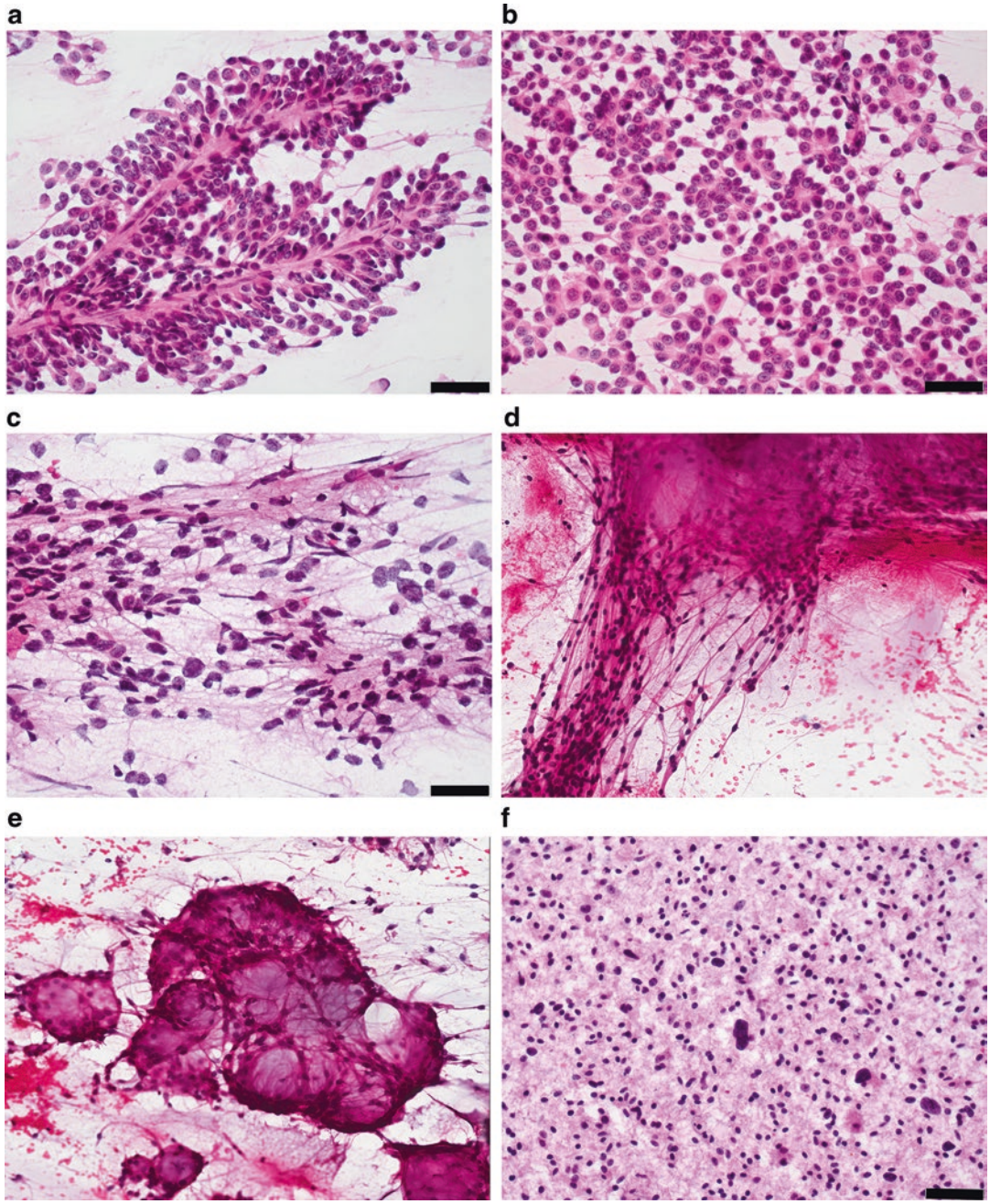


**Fig. 10.13** Ependymomas. (**a**–**c**) (H&E stain, high power). Grade II and III ependymoma. Smears tend to show fragments of tissue with papillary-like structures containing a central vessel lined by glial cells such as seen in grade II ependymoma (**a**). Cells can also be more dispersed (**b**) into little clusters. Grade III ependymoma (**c**) shows more nuclear atypia and pleomorphism. (**d**–**f**) (H&E stain, high power). Myxopapillary ependymoma. Smears show fibrillary areas (**d**) and tumor cells intimately associated with myxoid material (**e**) which can have degenerative changes in the form of dramatic nuclear pleomorphism and pronounced hyperchromasia (**f**).

#### Pearls

Grading ependymomas is fraught with difficulties; however, mitotic counts of four or more per ten high-powered fields are associated with outcome [14]. Bizarre atypia is not uncommon in myxopapillary ependymomas, in contrast to other ependymomas.

#### Differential Diagnosis

Medulloblastoma, pilocytic astrocytoma, atypical teratoid/rhabdoid tumor, and choroid plexus papilloma. For lesions arising in the filum terminale and cauda equina: metastatic or primary myxoid mesenchymal tumors, schwannoma, and paraganglioma.

### 10.2.5 Embryonal Tumors

#### 10.2.5.1 Medulloblastoma

#### Clinical Features

Medulloblastoma is a grade IV tumor of the cerebellum that shows predominately neuronal differentiation and has a tendency to metastasize via CSF (i.e., "drop metastases"). Medulloblastoma tends to affect children who present with cerebellar dysfunction, mass effects, and/or CSF obstruction. Turcot and Gorlin syndrome patients are at increased risk of developing medulloblastoma. Neuroimaging often shows a large, variably enhancing mass in the cerebellum, which can extend into the fourth ventricle. Subarachnoid spread is noted at presentation in some cases, especially those of the large cell/anaplastic subtype. The subtype with extensive nodularity tends to arise in infants and can appear as a multinodular mass [12].

#### Cytological Features

Smearing medulloblastoma disperses the tumor into individual cells and small tissue fragments. Tumor cells have round nuclei and little to no cytoplasm (Fig. 10.14a). Homer Wright rosettes are characteristic but uncommon or vague in smears (Fig. 10.14a). All cases show some degree of nuclear pleomorphism, but it is most pronounced in the anaplastic variant, which also shows frequent mitotic activity, increased apoptosis, and nuclear molding with cell-cell wrapping. The large cell variant shows prominent nucleoli, which are typically indistinct in most medulloblastomas.

#### Pearls

Be cautious and do not overinterpret granule cells of normal cerebellar cortex as tumor cells. Granule cells are uniform, small cells without atypia (Fig. 10.14b). There is no mitosis or apoptosis, and occasionally granule cells will be accompanied by Purkinje cells or fragments of the molecular layer in smears.

#### Differential Diagnosis

Ependymoma, pilocytic astrocytoma, atypical teratoid/rhabdoid tumor, and choroid plexus papilloma. Diffuse gliomas uncommonly arise in the cerebellum; however, an extension of a pontine glioma into the cerebellum via the cerebellar peduncle can occur. Exclude the possibility of normal granule cells of the cerebellum, as mentioned above. In general, it is rare for a neuroblastoma to present with metastatic CSF involvement; however, patients with rhabdomyosarcomas, particularly those of the head and neck region, can have positive CSF specimens.

**Fig. 10.14** (continued) Smears from these tumors are variable and can show cells with variable cytoplasm, pale pleomorphic nuclei and prominent nucleoli (**c**), or a small blue cell component (**d**) that is reminiscent of CNS embryonal tumor not otherwise specified (NOS) or medulloblastoma. Rhabdoid cells (**e**) and mitoses (**e**, *arrow*) can be seen, but may be sparse or even absent. (**f**) (H&E stain, high power). CNS embryonal tumor NOS. CNS embryonal tumor NOS is now recognized to represent tumors that were referred to as PNET. Smears show patternless sheets of small poorly differentiated blue cells. (**g**) (H&E stain, high power). Ganglioneuroblastoma. Smears show ganglion cells with ample cytoplasm and large pale nuclei admixed with a small blue cell component and finely fibrillar neuropil-like material. (**h**, **i**) (H&E stain, high power). Embryonal tumor with multilayered rosettes (ETMR). This is an embryonal tumor that has different molecular alterations than CNS embryonal tumor NOS despite the common morphologic appearance of small blue cells (**h**, **i**) admixed with neuropil-like material (**h**).

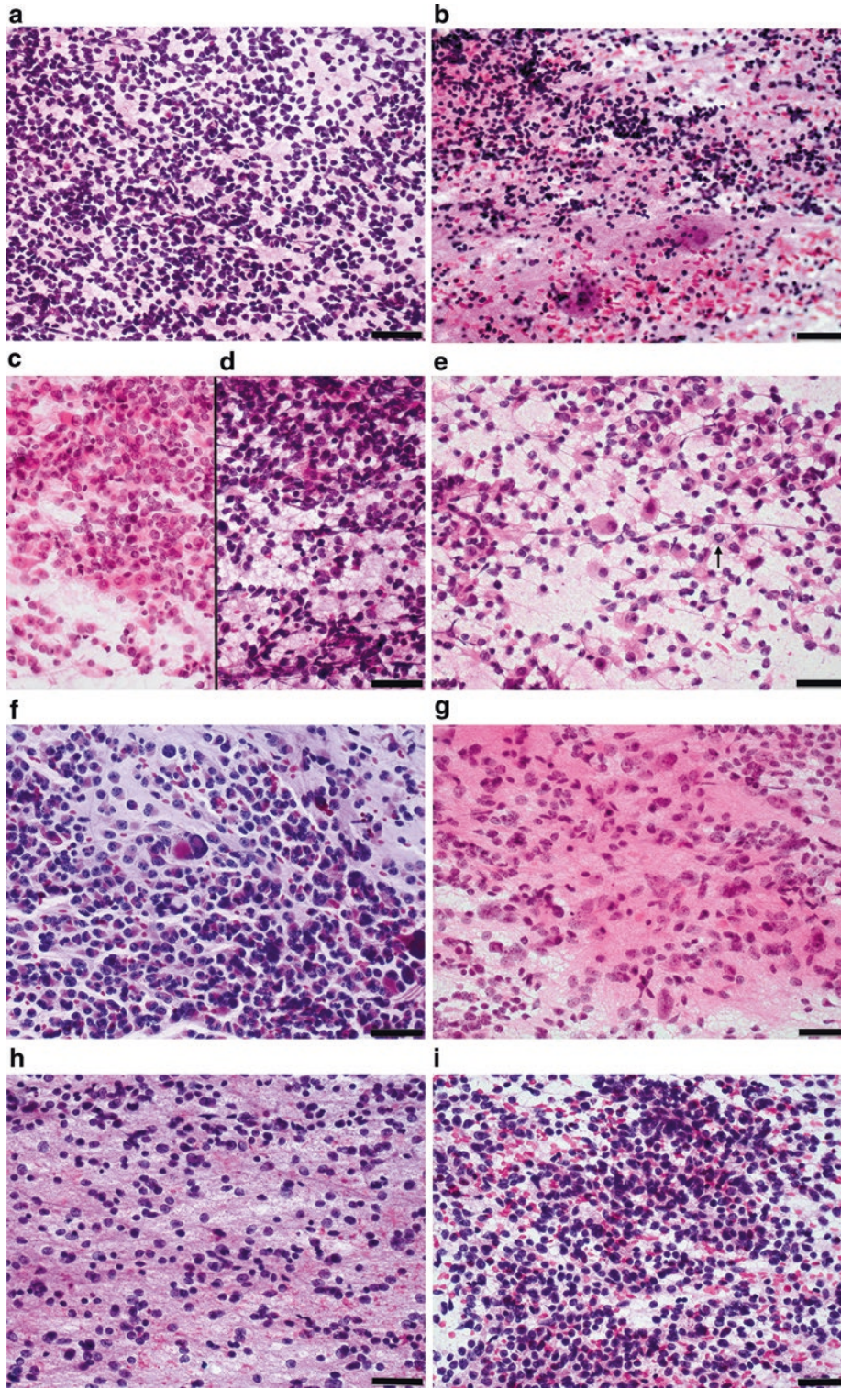


**Fig. 10.14** Embryonal tumors and mimics. (**a**) (H&E stain, high power). Medulloblastoma. Smears show patternless sheets of poorly differentiated small cells, with rare absent Homer Wright rosettes. (**b**) (H&E stain, high power). Cerebellar granule cells. The internal granule cells have uniformly round and regular nuclei, compared to the tumor cells in image (**a**). Granule cells are often accompanied by Purkinje cells, which appear as large neurons and fragments of fine fibrillar molecular layer. (**c**–**e**) (H&E stain, high power). Atypical teratoid/rhabdoid tumor (AT/RT).

#### 10.2.5.2 Atypical Teratoid/Rhabdoid Tumor (AT/RT)

**Clinical Features**

AT/RT typically arises in young children; most patients are less than 3 years of age and many are infants. AT/RT can arise anywhere but most occur in the posterior fossa. Virtually all cases are associated with *SMARCB1* mutations and loss of protein expression [12]. Neuroimaging shows a large, heterogeneously enhancing mass with a variable appearance that can be necrotic, hemorrhagic, or cystic.

**Cytological Features**

Smears typically show a heterogeneous population of tumor cells with variable amounts of cytoplasm and pleomorphic nuclei with prominent nucleoli. However, a small blue cell component that mimics medulloblastoma or CNS embryonal tumor NOS can predominate (compare Fig. 10.14c, d). The presence of rhabdoid cells (Fig. 10.14e) is variable and they may be absent. AT/RTs can feature divergent differentiation along glial, neuronal, mesenchymal, or epithelial lineages.

**Pearls**

Immunohistochemistry is essential to determine SMARCB1 (INI1) protein expression, which is lost in AT/RT, but retained in other neoplasms that make up the differential diagnosis. Performing SMARCB1 (INI1) immunohistochemistry on all embryonal brain tumors is wise, especially in infants and young children and aids in the diagnosis of AT/RTs that lack rhabdoid cells. Genetic testing should be considered to test for rhabdoid predisposition syndrome.

**Differential Diagnosis**

Medulloblastoma, ependymoma grade III, CNS embryonal tumor NOS, embryonal tumor with multilayered rosettes (ETMR), choroid plexus carcinoma, glioblastoma, and gangliocytic tumors given the prominence of the nucleoli.

#### 10.2.5.3 CNS Embryonal Tumor NOS

**Clinical Features**

CNS embryonal tumor NOS is the preferred term for what were previously known as PNETs. These tumors represent 2 % of all pediatric neuroepithelial tumors and present at a mean age of 5 years. CNS embryonal tumor NOS are a heterogeneous group of tumors that arise in the cerebrum, brainstem, or spinal cord, and are populated by undifferentiated neuroepithelial cells that show glial or neuronal differentiation [15]. Molecular studies have shown important differences among the embryonal tumors that were formerly classified as PNETs. Embryonal tumor subtypes include: CNS neuroblastoma, for those that show only neuronal differentiation; CNS ganglioneuroblastoma, if ganglion cells are also present; and medulloepithelioma, which is thought to recapitulate neural tube formation. CNS embryonal tumor NOS patients present with signs and symptoms of mass effect and increased intracranial pressure, seizures, or focal neurological deficits. These tumors are aggressive and tend to disseminate via the CSF. Neuroimaging shows a large, well-circumscribed mass with variable enhancement. Calcification is often present [12].

**Cytological Features**

Smears from CNS embryonal tumor NOS patients tend to be highly cellular and are populated by undifferentiated cells, reminiscent of medulloblastoma, but tumor location differs and helps to refine the diagnosis (Fig.10.14f). Homer Wright rosettes are uncommon in CNS embryonal tumor NOS. Cell wrapping and collections of apoptotic cells may be seen. Ganglioneurblastoma shows ganglion cells admixed with a population of small blue cells and a finely fibrillary neuropil (Fig. 10.14g). ETMR smears often have areas of fine neuropil-like fibrillarity (Fig. 10.14h) admixed with numerous small blue cells (Fig. 10.14i).

#### Pearls

Although CNS embryonal tumor NOS resembles medulloblastoma morphologically, there are a number of differences in terms of their clinical behavior and molecular genetics that make these tumors distinct entities.

#### Differential Diagnosis

Ependymoma, high-grade gliomas, choroid plexus carcinoma, medulloblastoma, hematolymphoid malignancies, and other small round blue cell tumors.

### 10.2.6 Neuronal and Glioneuronal Tumors

#### 10.2.6.1 Ganglioglioma and Gangliocytoma

#### Clinical Features

Ganglioglioma and gangliocytomas are often slow-growing neoplasms that can occur throughout the central nervous system but are common in the temporal lobe. Frequently, these tumors involve neocortex, and can be associated with focal cortical dysplasia and medically refractory epilepsy. Gangliocytomas and most gangliogliomas are grade I. Criteria to classify grade II gangliogliomas have not been established; although, if a tumor has anaplasia in the glial component, many classify it as grade III [12]. Neuroimaging shows a well-circumscribed cystic or solid tumor that may or may not show calcification. Ganglioglioma tends to enhance, but gangliocytoma does not. Long-standing cases may erode the inner table of the skull.

#### Cytological Features

A gangliocytoma is composed largely of well-differentiated neoplastic ganglion cells, while in ganglioglioma, the ganglion cell population is admixed with neoplastic glial cells. These entities share similar cytological features and can be considered together. Smears show fairly well-differentiated ganglion cells with ample cytoplasm and large open nuclei with prominent nucleoli (Fig. 10.15a, b). Sometimes neuronal cytoplasm is lost during smearing and bare nuclei remain (Fig. 10.15b). The glial component of ganglioglioma typically consists of fibrillary or piloid astrocytes (Fig. 10.15a). Eosinophilic granular bodies or scattered lymphocytes may also be seen.

#### Pearls

Be careful not to overcall normal gray matter as ganglioglioma. The normal brain is, in fact, rather cellular. Look for scattered lymphocytes and eosinophilic granular bodies and correlate smear cytology with tissue sections.

#### Differential Diagnosis

Infiltrating glioma with entrapped neurons, SEGA, dysembryoplastic neuroepithelial tumor, gemistocytic astrocytoma, desmoplastic infantile ganglioglioma, AT/RT, and normal gray matter.

#### 10.2.6.2 Dysembryoplastic Neuroepithelial Tumor (DNT)

#### Clinical Features

DNTs are grade I lesions that tend to arise in neocortex, especially temporal lobe, and are associated with focal cortical dysplasia and medically refractory epilepsy. DNT has also been described in hippocampus, amygdala, and near the foramen of Monro [12]. Neuroimaging shows a multinodular lesion that exhibits little mass effect or peritumoral edema. Some cases show foci of strong contrast enhancement, which likely corresponds to areas of microvascular proliferation.

#### Cytological Features

DNT tends to have bland smear cytology with round, monomorphous nuclei accompanied by ganglion cells occurring in a mucinous background (Fig. 10.15c, d). Occasional cases will have eosinophilic granular bodies or microvascular proliferation, which does not increase tumor grade in DNT.

#### Pearls

It can be difficult to recognize DNT or exclude an oligodendroglioma in fragmented specimens, so clinico-radiologic correlation is important. Unlike

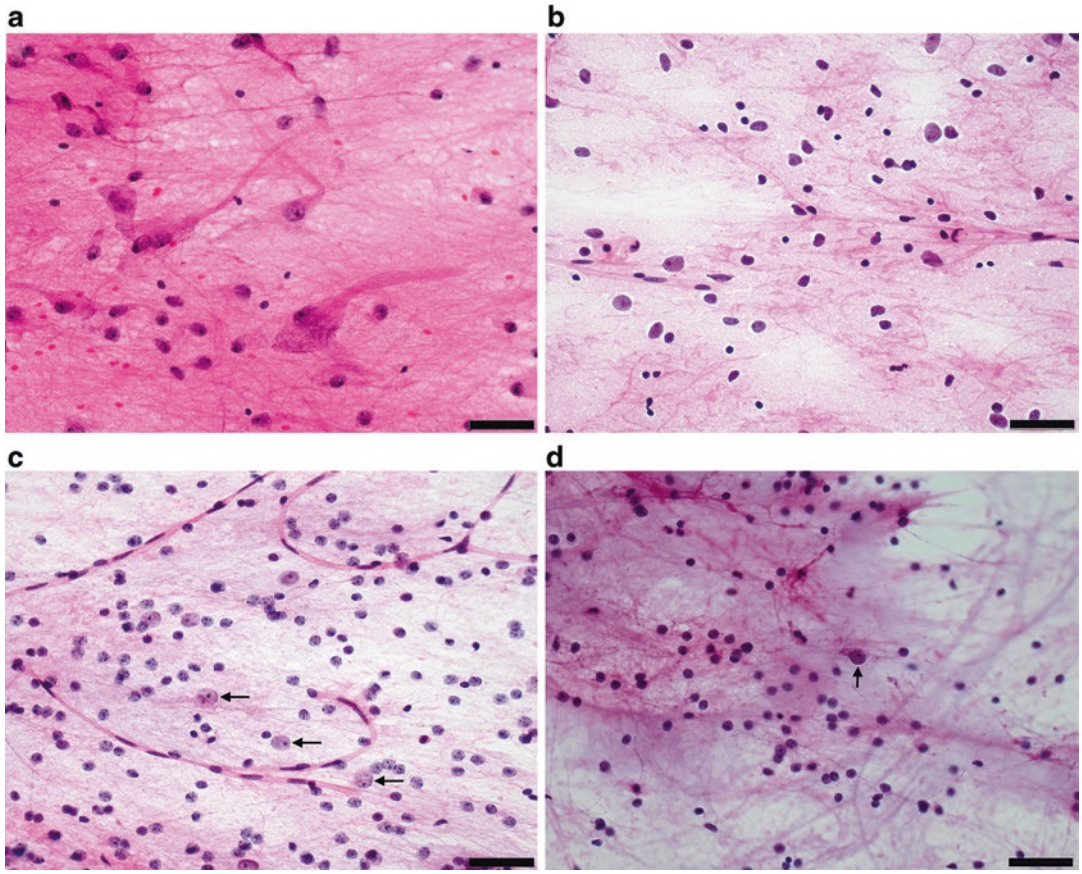


**Fig. 10.15** Neuronal and glioneuronal tumors. (**a**–**d**) (H&E stain, high power). Ganglioglioma and gangliocytoma both show large ganglion cells with abundant cytoplasm and large nuclei with open chromatin and prominent nucleoli (**a**). At times the cytoplasm is lost during the smearing process and only large nuclei remain (**b**). Gangliocytoma lacks the prominent glial component that is present in ganglioglioma, which appears as either fibrillary or piloid astrocytes. (**c**, **d**) (H&E stain, high power). DNT. The cytology of DNT is rather bland with a population of round monotonous nuclei admixed with ganglion cells (**c**, *arrows*) in a pale blue mucinous background (**d**). Ganglion cell cytoplasm may be lost and bare nuclei remain (*arrow*).

in adults, chromosome 1p and 19q tend to be intact in pediatric oligodendrogliomas, so molecular testing may not help distinguish DNT and oligodendroglioma [12].

### Differential Diagnosis

Oligodendroglioma, astrocytoma, and pilocytic astrocytoma.

## 10.2.7 Choroid Plexus Tumors

### Clinical Features

In children, choroid plexus tumors tend to arise in the lateral and third ventricles, whereas in adults, the fourth ventricle is more frequently involved [9]. The incidence peaks in the first decade. These tumors can result in hydrocephalus and macrocephaly in children with unfused cranial sutures. Choroid plexus tumors range from grade I papillomas to grade II atypical papillomas to grade III choroid plexus carcinomas. Neuroimaging reveals an intraventricular mass that is often lobulated and typically enhances brightly. Carcinomas tend to show peritumoral edema and frank invasion.

### Cytological Features

Smears of grade I lesions show papillary tissue fragments lined by cells with discrete borders and bland nuclei (Fig. 10.16a). The surface of

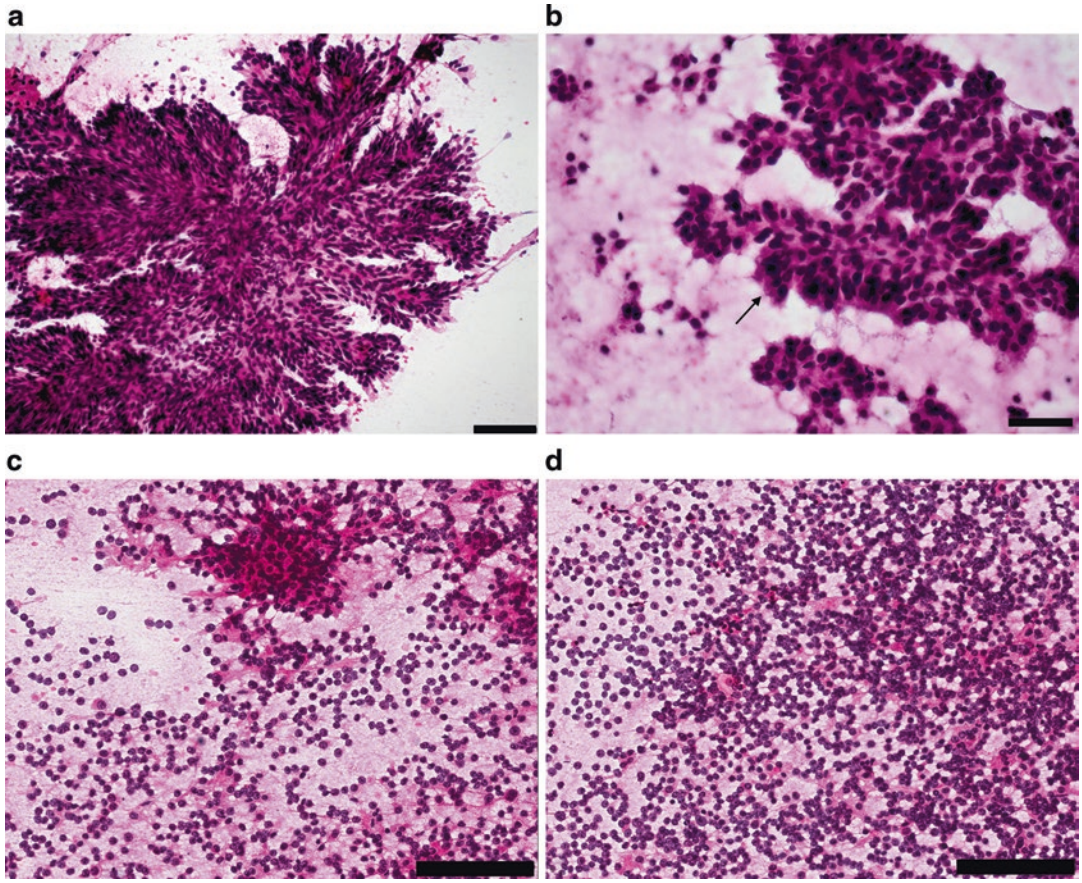


**Fig. 10.16** Choroid plexus tumors. (**a**) (H&E stain, high power). Papillomas. Smears from papillomas show papillary fragments lined by cells with discrete borders and bland nuclei. (**b**) (H&E stain, high power). Atypical papillomas. Smears show cells that appear more pleomorphic. A focal cobblestone appearance (*arrow*) may be evident on the surface of some papillary fragments. (**c**, **d**) (H&E stain, high power). Choroid plexus carcinoma. Carcinoma smears frequently yield patternless sheets of atypical or anaplastic cells and relatively few, if any, papillary structures.

some papillary fragments may have a cobblestone appearance (Fig. 10.16b). Smears from carcinomas often have fewer papillary structures and more often have patternless sheets of cells that are atypical or anaplastic (Fig. 10.16c, d). The nuclei are hyperchromatic and mitoses can be identified. Calcospherites may be present in some cases.

### Pearls

Most choroid plexus tumors arise sporadically, but papillomas can be encountered in Aicardi syndrome (defect in X chromosome, associated with partial or complete loss of corpus callosum, retinal abnormalities, and seizures) and are rarely seen in von Hippel-Lindau disease (mutation on chromosome 3, associated with hemangioblastomas, pheochromocytomas, pancreatic cysts and neuroendocrine tumors, and renal cell carcinoma). Carcinomas occasionally arise in Li-Fraumeni syndrome (tumor syndrome associated with TP53 mutations) so genetic testing may be warranted.

### Differential Diagnosis

For carcinomas, AT/RT, high-grade glioma, ependymoma, and metastatic carcinoma. For papillomas, normal choroid plexus and ependymoma.

## 10.2.8 Meningiomas

### Clinical Features

Meningiomas are populated by tumor cells with meningothelial differentiation and are attached to

the inner surface of the dura. Most meningiomas are grade I lesions and have a favorable clinical outcome, but the outcome is less favorable in atypical (grade II) and anaplastic (grade III) meningiomas. Meningiomas are diverse and encompass many subtypes. Meningiomas are uncommon in children, except for patients with neurofibromatosis 2, who can have numerous tumors. Clinical manifestations are diverse, vary by location, and include mass effect, headaches, seizures, focal neurologic deficits, hemiparesis, sensory deficits, and ataxia, to mention a few. Neuroimaging shows an enhancing tumor with a broad dural base that is isodense or hypodense to cortex in T2 images [12].

#### Cytological Features

Smears show tissue fragments, monolayers, and individual cells (Fig. 10.17a). The cells have oval nuclei with small nucleoli and cytoplasm that is thin and delicate (Fig. 10.17b). Helpful diagnostic features include nuclear pseudoinclusions, meningothelial whorls (Fig. 10.17c), and, in some cases, psammoma bodies (Fig. 10.17a). Fibrous meningiomas show elongated cells with a spindle-shaped nucleus. Grade II and III lesions have nuclear hyperchromasia and larger nucleoli (Fig. 10.17d). Scattered rhabdoid cells may be seen in meningiomas, but predominate in rhabdoid meningioma (Fig. 10.17e). Chordoid meningioma shows large cells with abundant cytoplasm admixed with a lymphoplasmacytic infiltrate and a metachromatic background (Fig. 10.17f).

#### Pearls

Meningiomas are uncommon in children but important to recognize as they can be aggressive. Meningiomas are the most common radiation-induced brain tumor. Children also may have a higher incidence of papillary meningioma, which is rare but well known to be locally aggressive and is considered to be grade III.

#### Differential Diagnosis

Hemangiopericytoma, solitary fibrous tumor, meningeal sarcoma, glioblastoma, and gliosarcoma. Different histological variants (e.g., chordoid, papillary, anaplastic, rhabdoid) can look like any other tumors of similar morphology.

### 10.2.9 Craniopharyngioma

#### Clinical Features

These tumors are classified as low-grade tumors by the WHO classification system as grade 1. They are thought to arise from the Rathke pouch epithelium and usually form cystic suprasellar masses that are partially calcified on imaging [12].

#### Cytological Features

The cyst fluid in these tumors may resemble the thick, machinery oil-type material seen with Warthin tumors of the salivary gland. The key cytological feature is the presence of keratin debris within a thick cystic background with cholesterol crystals (Fig. 10.18). The cholesterol crystals appear as rectangular flat sheets with the corners cut out, forming staircase-like appearance. The keratin is classically described as "wet" keratin and appears as whorls of anucleate cells with dense cytoplasm, intermixed with the epithelial cells that have glassy cytoplasm and peripheral palisading along the edges. A few variants of this tumor exist, with the adamantinomatous variant being more common in young patients (ages 5–14) and the papillary variant occurring rarely given that it is more common in adults. The adamantinomatous variant has also been associated with beta-catenin mutations.

#### Pearls

Gliosis can occur around the periphery of these tumors, so Rosenthal fibers and glial features can be seen intermixed with these tumors on cytological preparations.

#### Differential Diagnosis

Other cystic lesions (e.g., Rathke cleft cysts), germ cell tumors with a teratomatous component, and squamous cell contamination from the skin. Glial tumors, like pilocytic astrocytoma, may enter the differential diagnosis if the surrounding gliosis is sampled or predominates in the cytological material.

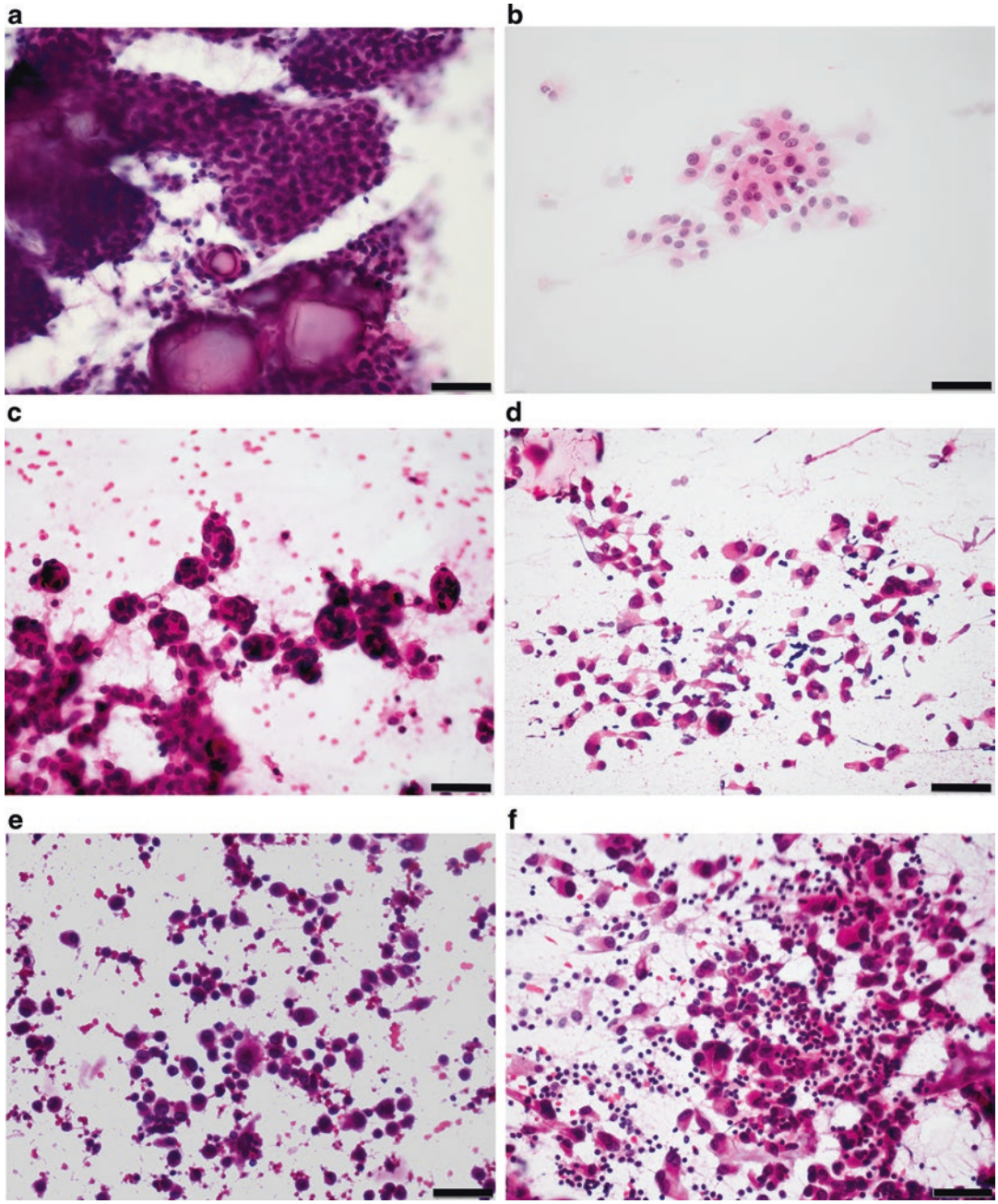


**Fig. 10.17** Meningiomas (H&E stain, high power). Smearing a meningioma often results in sheetlike fragments of cells as these tumors can be difficult to smear and often contain mineralized psammoma bodies (**a**). Other parts of the smear show aggregates of cells with abundant delicate cytoplasm and monotonous nuclei (**b**). Meningothelial meningiomas commonly have the classic whorls (**c**). Nuclear pleomorphism and hyperchromasia are characteristics of grade II and grade III meningiomas (**d**). Rhabdoid cells are noted in rhabdoid meningioma (**e**), a grade III tumor, while smears of chordoid meningioma, a grade II tumor, show large tumor cells admixed with lymphocytes (**f**).

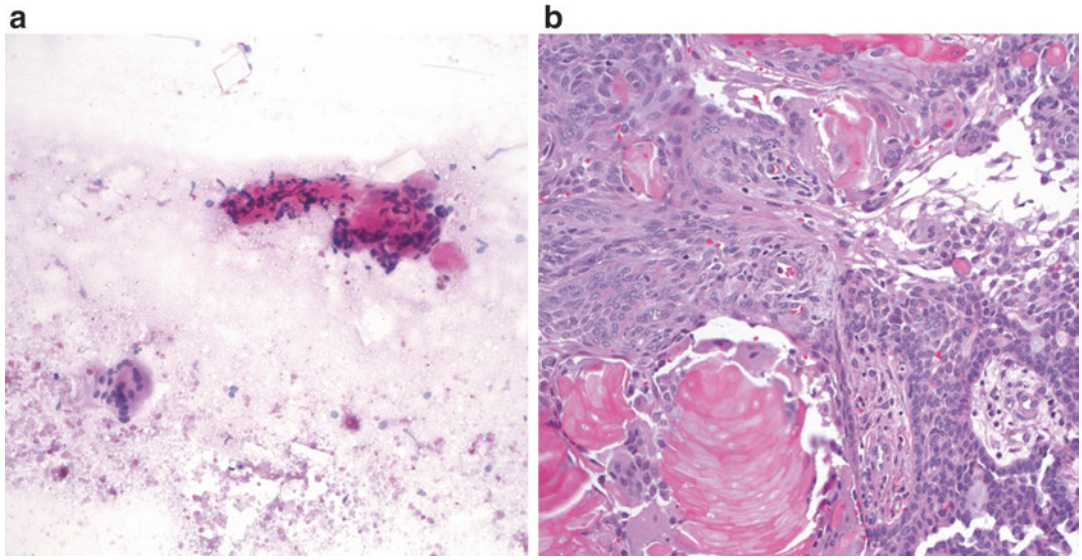


**Fig. 10.18** Craniopharyngioma (**a**. smear preparation, H&E stain, high power; **b**. surgical excision, H&E stain, high power). The smears from this suprasellar brain tumor show granular debris with numerous negative images of cholesterol crystals, in addition to multinucleated giant cells and squamoid-appearing cells with dense cytoplasm (**a**). The biopsy shows characteristic features of a craniopharyngioma (**b**). (Images courtesy of Dr. Sara Monaco).

## 10.3 Conclusions

Overall, the cytological examination of CSF and CNS lesions plays a pivotal role in the diagnosis and management of CNS diseases and neoplasms in the pediatric population. In contrast to the adult population where metastatic carcinoma predominates, children differ in that primary CNS tumors and infection are more common. Furthermore, prompt evaluation and accurate interpretations are essential as patients can be acutely ill with infectious, neoplastic, or other disorders.

## References

1. McPherson RA, Pincus MR, editors. Henry's clinical diagnosis and management by laboratory methods. 21st ed. Saunders Elsevier; 2007, Chapter 28 by Joseph A. Knight and Carl R. Kjeldsberg. p. 426–37.
2. Wood JH. Neurobiology of CSF. New York: Plenum; 1980.
3. Mazor SS, McNutty JE, Roosevelt GE. Interpretation of traumatic lumbar punctures: who can go home? Pediatrics. 2003;111:525–8.
4. Portnoy JM, Olson LC. Normal cerebrospinal fluid values in children: another look. Pediatrics. 1985;75:484–7.
5. Teot LA, Sexton CW. Mollaret's meningitis: case report with immunocytochemical and polymerase chain reaction amplification studies. Diagn Cytopathol. 1996;15:345–8.
6. Negrini B, Kelleher KJ, Wald ER. Cerebrospinal fluid findings in aseptic versus bacterial meningitis. Pediatrics. 2000;105:316–9.
7. Bonadino WA, Smith DS, Goddard S, Burroughs J, Khaja G. Distinguishing cerebrospinal fluid abnormalities in children with bacterial meningitis and traumatic lumbar puncture. J Infect Dis. 1990;162:251–4.
8. Nigrovic LE, Kuppermann N, et al. Children with bacterial meningitis presenting to the emergency department during the pneumococcal conjugate vaccine era. Acad Emer Med. 2008;15:522–8.
9. Cibas E, Ducatman B. Textbook of cytology, diagnostic principals and clinical practice. Elsevier Health Sciences; 2009. p. 178.
10. Fuller GN. Intraoperative consultation and optimal processing. In: Perry A, Brat DJ, editors. Practical surgical neuropathology: a diagnostic approach. Philadelphia: Elsevier; 2010. p. 35–45.
11. Burger PC. Smear and frozen sections in surgical neuropathology: a manual. Baltimore: PB Medical Publishing; 2009.
12. Louis DN, Ohgaki H, Wiestler OD, Cavenee WK, editors. WHO classification of tumours of the central

nervous system (revised 4th edition). Lyon: IARC; 2016 .
13. Kreiger PA, Okada Y, Simon S, Rorke LB, Louis DN, Golden JA. Losses of chromosomes 1p and 19q are rare in pediatric oligodendrogliomas. Acta Neuropathol. 2005;109:387–92.
14. Godfraind C, Kaczmarska JM, Kocak M, Dalton J, Wright KD, Sanford RA, Boop FA, Gajjar A, Merchant TE, Ellison DW. Distinct disease-risk groups in pediatric supratentorial and posterior fossa ependymomas. Acta Neuropathol. 2012;124:247–57.
15. Perry A, Miller CR, Gujati M, Scheithauer BW, Zambrano SC, Jost SC, Raghavan R, Qian J, Cochran EJ, Huse JT, Holland EC, Burger PC, Rosenblum MK. Malignant gliomas with primitive neuroectodermal tumor-like components a clinicopathologic and genetic study of 53 cases. Brain Pathol. 2009;19: 81–90.
16. Lacruz CR, Saenz de Santamaria J, Bardales RH. Central nervous system intraoperative cytopathology. New York, NY: Springer; 2014. Essentials in Cytopathology Series.

# Artifacts, Contaminants, and Mimics in Cytology

11

Samir B. Kahwash

## 11.1 Introduction

Artifacts and contaminants can be minimized, but cannot be completely eliminated from cytologic preparations, and, when present, are potential sources of diagnostic errors. Degenerative changes and preparation artifacts that alter and/or obscure cytomorphology can cause benign cells to appear malignant or, conversely, can mask features of malignancy. A variety of contaminants, as well as intrinsic elements, can mimic infectious organisms. Familiarity with these potential diagnostic pitfalls can help guide judicious use of ancillary studies, avoid unnecessary tests, and prevent interpretive errors.

Although distinguishing artifacts and contaminants from true pathologic findings in cytologic specimens is sometimes challenging, there is a dearth of published references on this topic [1, 2]. This chapter is a modest attempt at providing such a resource. Artifactual changes related to preparation and procedures, contaminants, and extrinsic and intrinsic mimics of infectious organisms are discussed and illustrated. Table 11.1 lists the major types of artifacts, contaminants, and mimics encountered in, but not limited to, cytologic specimens from children and adolescents.

S.B. Kahwash, MD (✉)
Department of Pathology and Laboratory Medicine, Nationwide Children's Hospital, 700 Children's Drive, Columbus, OH 43205, USA

Department of Pathology, The Ohio State University College of Medicine, Columbus, OH 43210, USA
e-mail: samir.kahwash@nationwidechildrens.org

## 11.2 Artifacts

### 11.2.1 Artifacts Related to Preparation

- Preservation, fixation, and staining: Delay in specimen preparation and fixation can result in poor preservation and suboptimal cytologic detail (Fig. 11.1a, b). This is particularly true of cerebrospinal fluid (CSF) specimens, in which cells rapidly degenerate at room temperature, making interpretation difficult or impossible. Cytomorphology is also affected by differences in fixation and staining techniques. As illustrated in Fig. 11.1c, d, the nuclear and cytologic features of the cells in the alcohol-fixed Giemsa-stained preparation differ from those of the cells in the air-dried Giemsa-stained preparation from the same specimen. Moreover, an examiner accustomed to one method may view differences related to preparation by another method as artifacts [2]. Table 11.2 compares cytomorphologic features of fresh alcohol-fixed and air-dried preparations.
- Thick preparations: Thick smears or cytospins with excess material can result in poorly fixed



S.E. Monaco, L.A. Teot (eds.), *Pediatric Cytopathology*, DOI 10.1007/978-3-662-53441-0_11

**Table 11.1** Overview of artifacts, contaminants, and mimics in cytology

| | | |
|---|---|---|
| Artifacts | Preparation artifacts | Preservation, fixation, and/or staining artifacts<br>Smearing or cytospin artifacts<br>Degenerative changes<br>Air and/or water bubbles |
| | Procedure-related artifacts | Dilution with blood and/or bone marrow<br>Crush artifact<br>Obscuring necrotic debris<br>Thermal and/or chemical factors |
| Contaminants | | Stain precipitate<br>Bacterial overgrowth<br>Ultrasound gel or lubricant<br>Synthetic material<br>Desquamated squamous cells<br>Dust and/or pigment<br>Plant or vegetable material |
| Mimics | Extrinsic and intrinsic mimics of organisms | Synthetic fibers<br>Tissue fibers (e.g., elastic or collagen)<br>Fibrin strands, red blood cells, and platelets<br>Detached cilia<br>Cytoplasmic immunoglobulin<br>Cytoplasmic debris and vacuoles<br>Cytoplasmic tails or granularity<br>Calcifications<br>Mucus |

and poorly stained areas that are difficult or impossible to evaluate morphologically. Moreover, even in areas with adequate fixation and staining, cytologic features may be partly or completely obscured (Fig. 11.2).

- Cytospin preparation artifact: The centrifugal force used in cytospin preparations can result in cellular distortion, including nuclear irregularity, cellular molding (Fig. 11.3a, b), and edge artifact (Fig. 11.3c).
- Degenerative changes: In some specimens, particularly urine, degenerative changes can result in nuclei with glassy or smudged chromatin that mimic viral inclusions. Similarly, mononuclear inflammatory cells with degenerative changes can mimic small round blue cell tumors, and degenerating benign epithelial and mesenchymal cells can be misinterpreted as malignant due to dark, condensed chromatin, nuclear irregularities, and increased nuclear to cytoplasmic ratios. Loss of chromatin detail, breaks in the nuclear membrane, and vacuolated or disrupted cytoplasm provide important clues for distinguishing degenerative changes from viral infection and/or malignancy.
- Air bubbles and water bubbles: Air bubbles can result from hasty coverslipping or areas of thick, unevenly distributed cytologic material. Water bubbles can be a result of mounting a wet slide (Fig. 11.3d).

### 11.2.2 Artifacts Related to Procedure

- Dilution with blood and/or contamination with bone marrow: Excessive dilution with blood reduces the number of lesional cells and may delay fixation. Bone marrow or extramedullary hematopoietic cells in CSF and other specimens can create diagnostic difficulties, as early myeloid and/or erythroid precursors may be misconstrued as malignant cells (Fig. 11.4a, b). Usually megakaryocytes are not seen in CSFs with bone marrow contamination; however, in specimens with extramedullary hematopoietic cells, megakaryocytes are known mimickers of malignant cells, due to their large size and hyperchromatic, lobated nuclei.
- Necrosis and crush artifact: "Naked nuclei" and distorted and crushed cells are features of

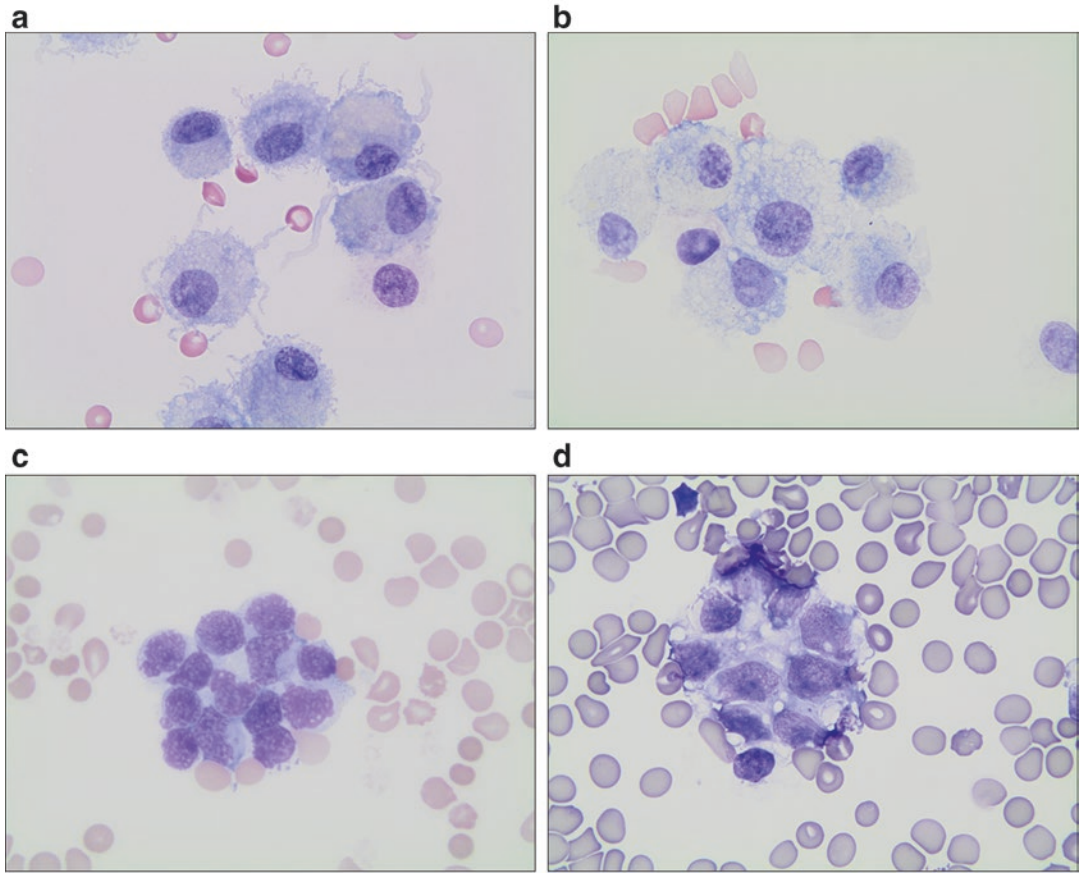


**Fig. 11.1** (**a**, **b**) (Giemsa stain, high power). Comparison of immediate and delayed processing. Well-preserved macrophages from a CSF processed soon after the time of collection (**a**). Macrophages from the same specimen as depicted in (**a**), processed hours after collection have swollen, vacuolated cytoplasm, and blurred cytoplasmic membranes (**b**). (**c**, **d**) (Giemsa stain, high power). Comparison of alcohol fixation and air drying. In this CSF from a child with meningitis, the clumped macrophages are smaller and have greater nuclear detail in the alcohol-fixed preparation (**c**), as compared to those in the air-dried preparation (**d**) from the same specimen. Cytoplasmic vacuoles are more conspicuous in the air-dried preparation.

**Table 11.2** Comparison of findings in fresh alcohol-fixed and air-dried (Diff-Quik or Giemsa stained) cytologic specimens

| Fresh alcohol fixed | Air dried |
|---|---|
| Cells appear smaller | Cells appear larger |
| Better nuclear details (chromatin, parachromatin, and nucleoli) | Better delineation of cytoplasmic details (vacuoles, granules) |

cellular fragility, but can also be present in necrosis. Apoptotic and degenerative changes are often present in necrosis and tend to be more striking in specimens with delayed processing (Fig. 11.4c). Necrosis can also appear as a background of acellular amorphous or granular debris on the stained slide.

- Thermal factors: Lasers or cold knives are used in some surgeries and produce characteristic artifacts in tissue that may confound interpretation of touch and squash/smear preparations from these specimens. Figure 11.4d illustrates freezing artifact in a case of mesenchymal chondrosarcoma. Fragmentation and microspherocytes of red blood cells can also be a clue to thermal artifact (Fig. 11.5).

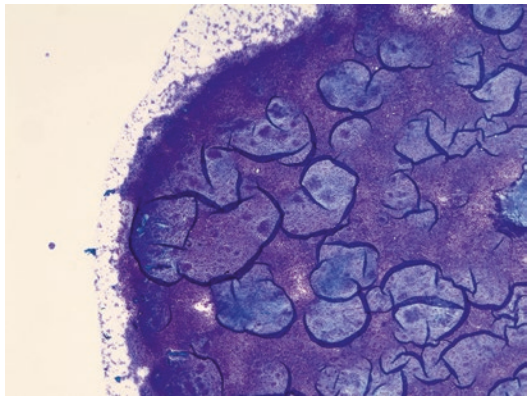

**Fig. 11.2** (Giemsa stain, low power). This cytospin preparation from an aspirate of a child's lymph node is too thick for the evaluation of the cytomorphology. Areas of poor fixation and staining appear pale (Image courtesy of Dr. Sara Monaco).

## 11.3 Contaminants

- Stain precipitate: Precipitates form as staining solutions age and are commonly encountered in daily practice (Fig. 11.6a). Filtering or replacing staining solutions is usually helpful in reducing precipitates. In stains that are used for processing slides from ultrasound-guided fine-needle aspirations, the ultrasound gel can also build up in the stains, which should be filtered or replaced to remove this contaminant.
- Bacterial and yeast overgrowth: Various species of bacteria and/or nonpathogenic fungi are able to grow in staining solutions and/or instruments used for cytologic preparations and may be misinterpreted as true pathogens (Fig. 11.6b–d).

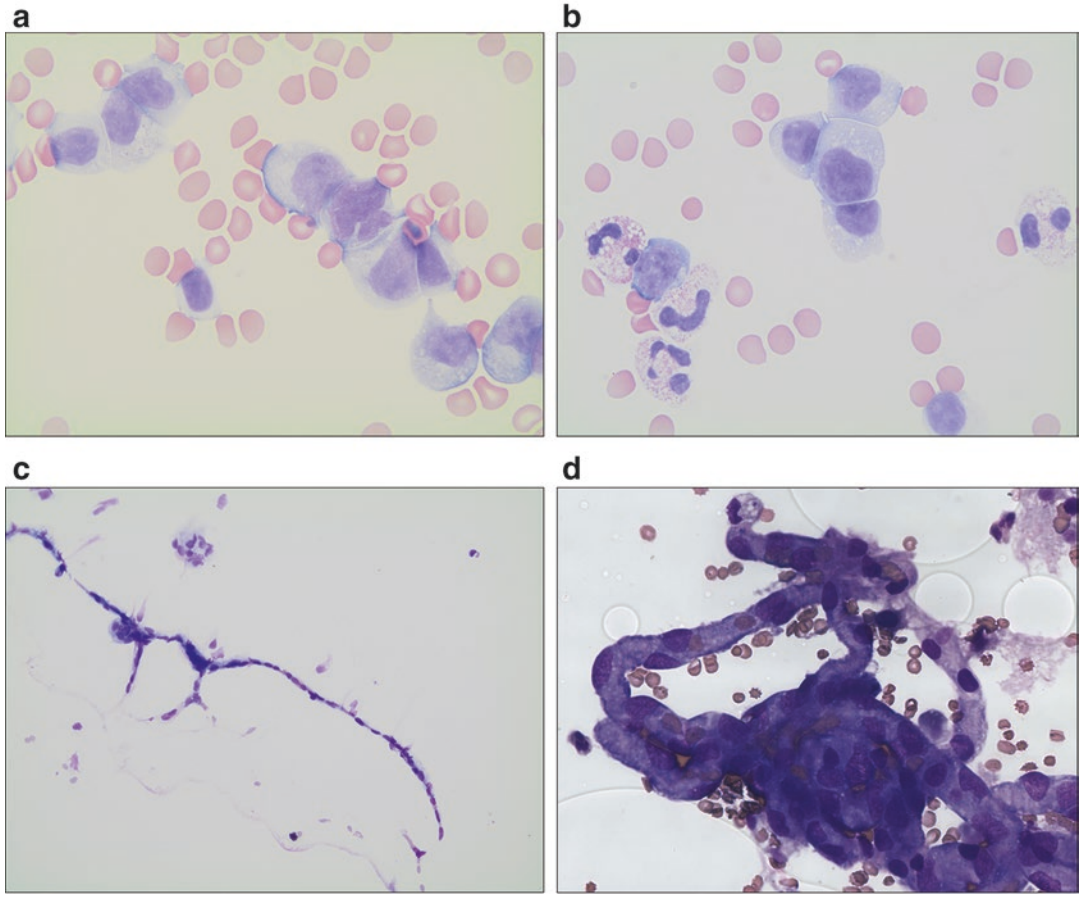


**Fig. 11.3** (**a**, **b**) (Giemsa stain, high power). Mononuclear cells from CSF fluid of a child with viral meningitis. The nuclear molding and cellular distortion are attributed to cytospin effect. The abundant cytoplasm and smooth nuclear contours are compatible with a benign process. (**c**) (Giemsa stain, medium power). Edge artifact, which is characterized by curvilinear collections of crowded, markedly distorted cells, is evident in this cytospin. (**d**) (Diff-Quik stain, high power). In this field, which shows a network of capillary vessels, the perfectly round, optically clear areas represent water droplets.

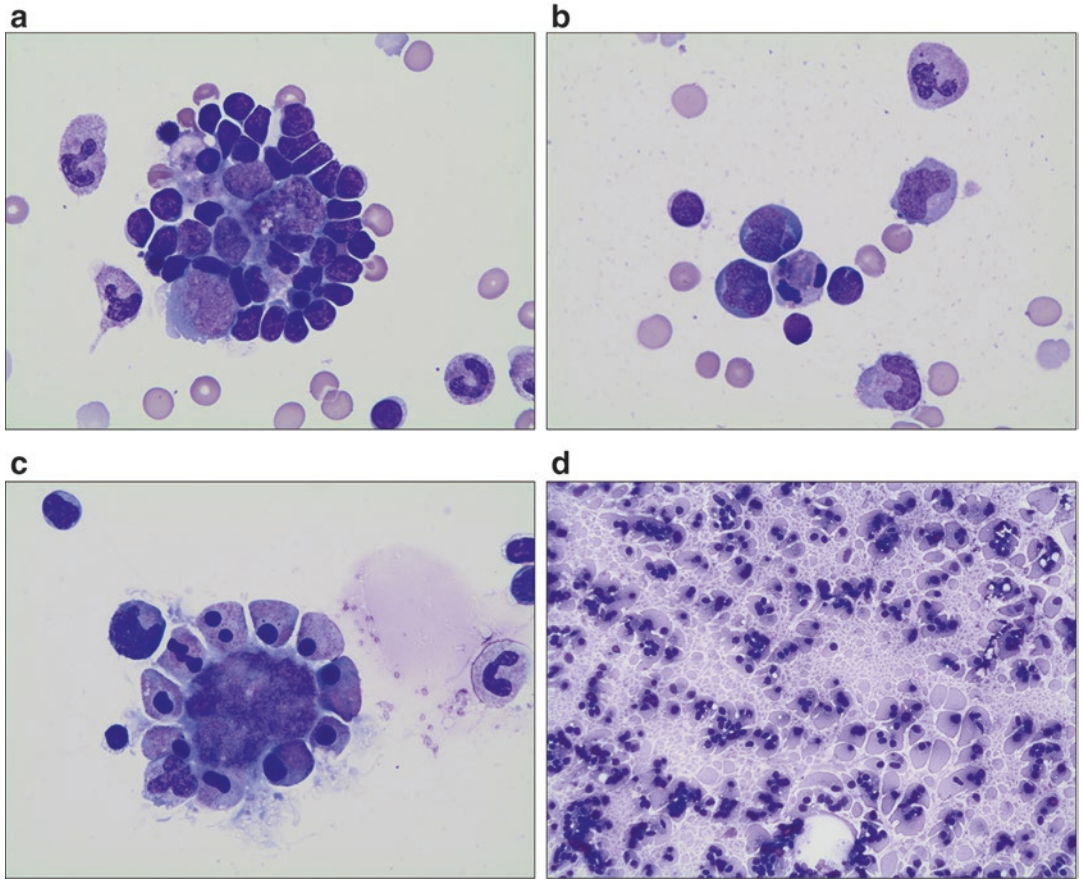


**Fig. 11.4** (**a**, **b**) (Giemsa stain, high power). Bone marrow contaminants are present in this CSF obtained by lumbar puncture. The early myeloid cells and hematogones (**a**) and early erythroid precursors (**b**) may be misconstrued as malignant cells. (**c**) (Giemsa stain, high power). Apoptotic cells in this specimen are the result of delayed processing. (**d**) (Giemsa stain, high power). The tumor cells of this mesenchymal chondrosarcoma show freezing artifact characterized by swelling and fragmentation of the cytoplasm and dark, shrunken nuclei.

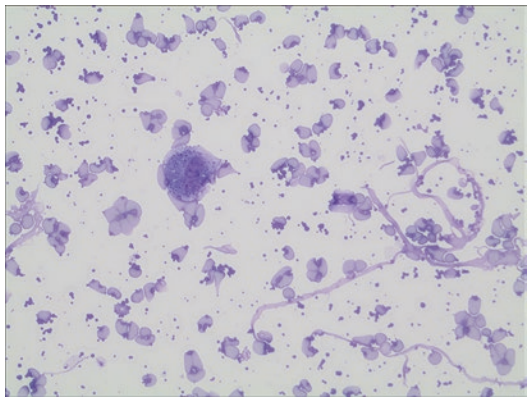

**Fig. 11.5** (Giemsa stain, medium power). Thermal artifact can appear as fragmentation of red blood cells, as seen in this field.

- Biomedical synthetic material, starch, and others: Synthetic material, such as gauze fibers, often contaminates cytologic specimens. Features such as geometric shape, absence of nuclei, and lack of septation help to distinguish these contaminants from "real" findings (Fig. 11.7a, b). Examination under polarized light is also helpful in some cases.
- Desquamated squamous epithelial cells and sneeze droplets: Squamous cells, with or without associated inflammatory cells and bacteria, are often present in bronchial washings and bronchoalveolar lavages and, in those specimens, usually represent contaminants from the patient's oral cavity and/or upper

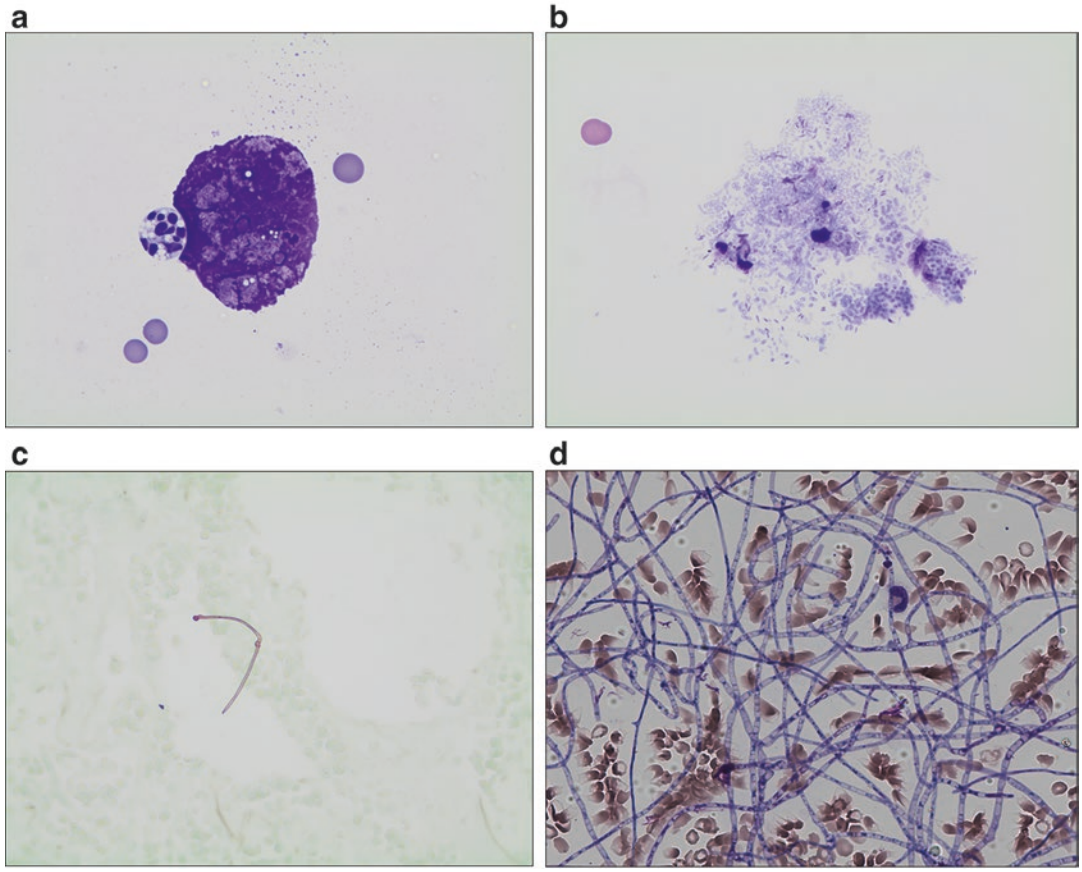


**Fig. 11.6** (**a**) (Giemsa stain, high power). Stain precipitate is present in the center of the field adjacent to an apoptotic cell. (**b**) (Giemsa stain, high power). Bacterial contamination is present in this CSF specimen. (**c**) (GMS stain, high power). Extraneous mold is present on this GMS-stained slide. (**d**) (Giemsa stain, high power). This preparation is contaminated by numerous fungal elements from overgrowth in the staining solution. The absence of an inflammatory response helps to distinguish contaminants from true pathogens (**b–d**).

respiratory tract. Extrinsic squamous contaminants, which can be present in cytologic specimens from any site, include cells exfoliated from the fingers or, rarely, sneeze droplets from personnel involved in obtaining or preparing the sample (Fig. 11.7c, d).

- Dust, pigments, and plant material: Dust and particulate matter from pollutants and tobacco smoke may be present as inhaled elements in respiratory specimens or introduced as contaminants into cytologic specimens from any site. Inhaled particles can appear as extracellular material, intracellular material engulfed by macrophages, or both. Deposition of carbon particles on the surface of respiratory epithelial cells is a characteristic of inhalation of smoke from a fire (Fig. 11.8a, b). The most commonly encountered pigment in cytologic specimens is hemosiderin, which is usually correctly recognized on routine stains (Giemsa, Diff-Quik, and Papanicolaou). However, bile pigment (Fig. 11.8c) appears very similar to hemosiderin on Giemsa and Diff-Quik stains and represents a potential pitfall for the unwary examiner. Iron stains, such as Prussian blue, stain hemosiderin but not bile and, thus, can be helpful for distinguishing these pigments in difficult cases.
- Plant or vegetable material contamination: Pieces of plant leaves or plant seeds are rarely

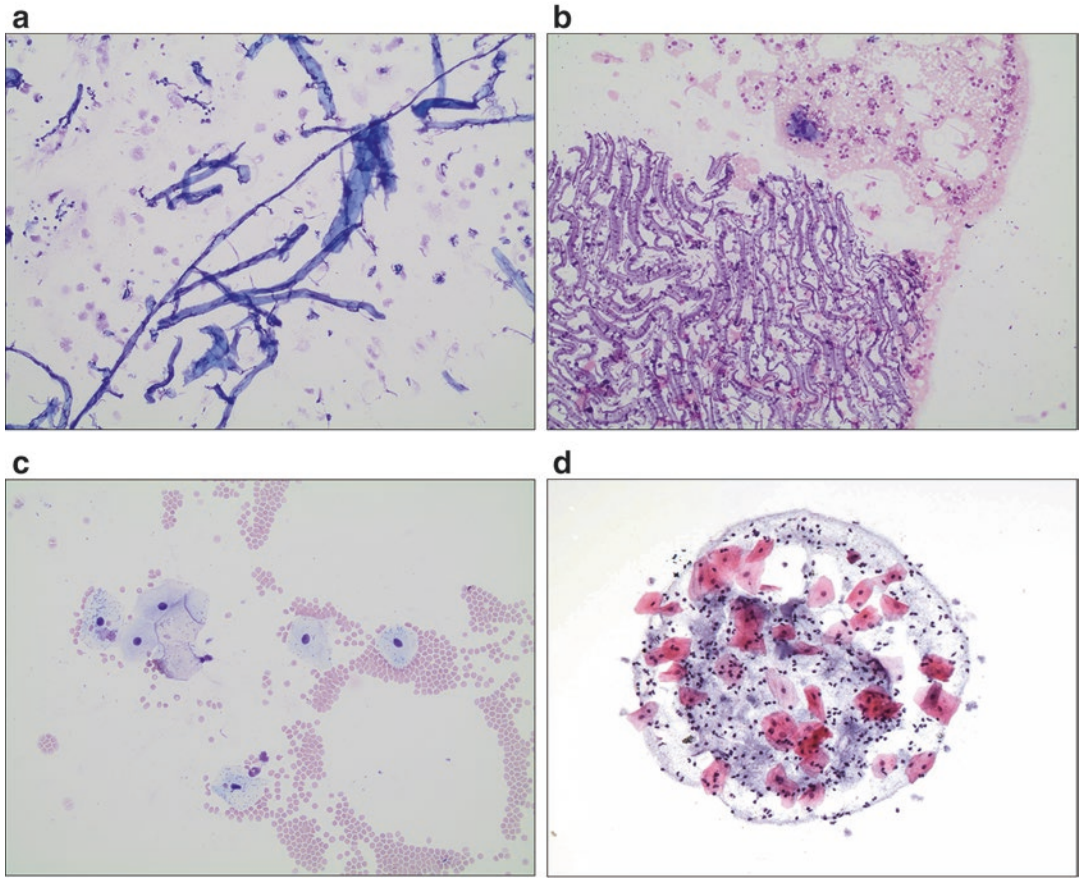


**Fig. 11.7** (**a**) (Giemsa stain, low power). The synthetic fibers in this field are recognized by their large size, sharp ends, and lack of septation. (**b**) (Giemsa stain, low power). The sheetlike aggregate of synthetic material likely represents gauze. (**c**) (Giemsa stain, low power). Squamous cells with and without overlying bacteria represent contaminants in this CSF. (**d**) (Papanicolaou stain, low power). A sneeze droplet, composed of squamous cells, neutrophils, and bacteria, is present on this slide.

encountered in cytologic specimens, but can be seen as contaminants in laboratories with plants near the preparation area or with the open windows (Fig. 11.8d). Vegetable material can be encountered as a normal finding in brushings from the gastrointestinal tract or as an aspirated or introduced contaminant in respiratory specimens and should not be misinterpreted as a parasitic organism.

- Ultrasound gel or lubricant: Materials used for a procedure, such as lubricants for endoscopic and cystoscopic examinations and ultrasound gel, can contaminate specimens obtained during those procedures. Ultrasound gel appears as metachromatic amorphous and granular material that can mimic bacteria or platelets (Fig. 11.9), whereas lubricant lacks granularity and simulates thick mucin.

## 11.4 Cytological Mimics

### 11.4.1 Mimics of Organisms

- Synthetic or tissue fibers: Lint and other synthetic fibers are common contaminants in cytologic specimens and staining solutions and can resemble fungal hyphae or parasitic worms under the microscope (Fig. 11.10a). Their sharp ends and lack of septation helps to

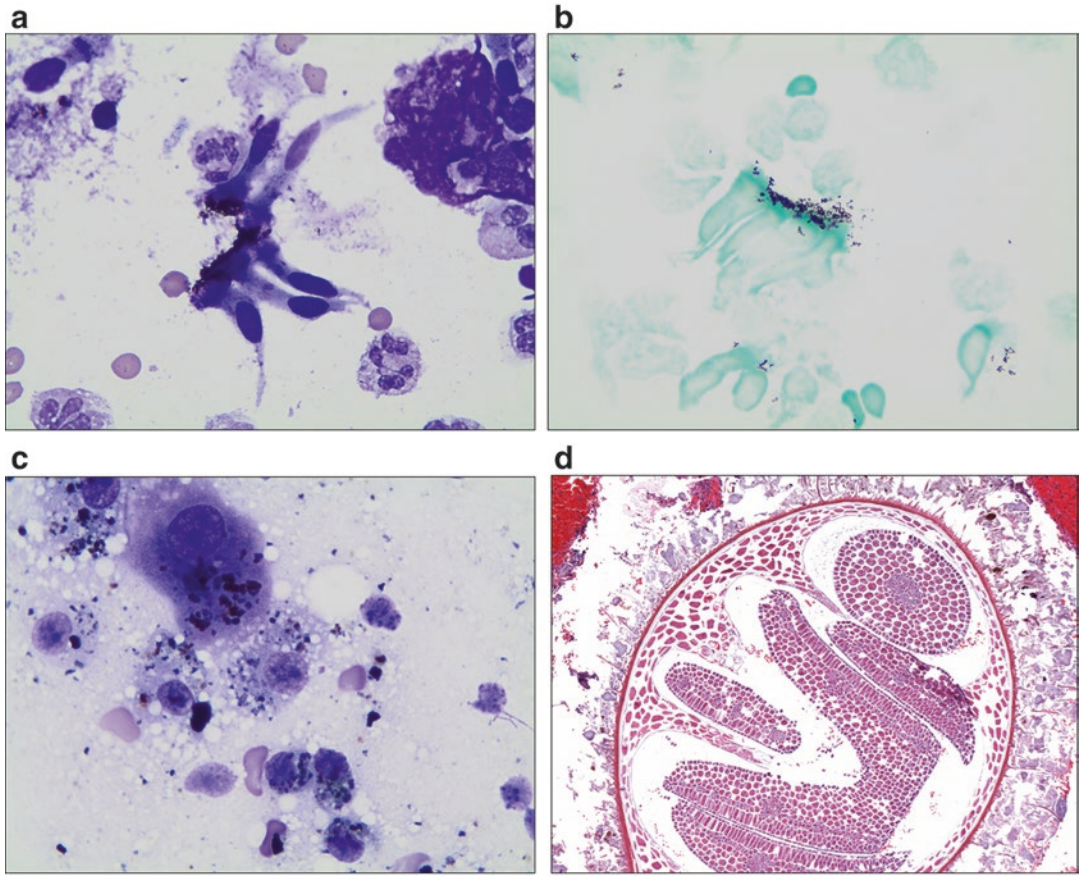


**Fig. 11.8** (**a**) (Giemsa stain, high power) and (**b**) (GMS stain, high power). Carbon particles are present on the surface of sloughed respiratory epithelial cells in this BAL from a burn victim with smoke inhalation. (**c**) (Diff-Quik stain, high power). In this touch imprint from a liver biopsy, bile pigment mimics hemosiderin in appearance. An iron stain was negative. (**d**) (H&E stain, low power). A cross section of a plant seed is present in this histologic section. Pollen and other plant or vegetable material may contaminate cytologic specimens or cell block preparations and should not be confused with parasites.

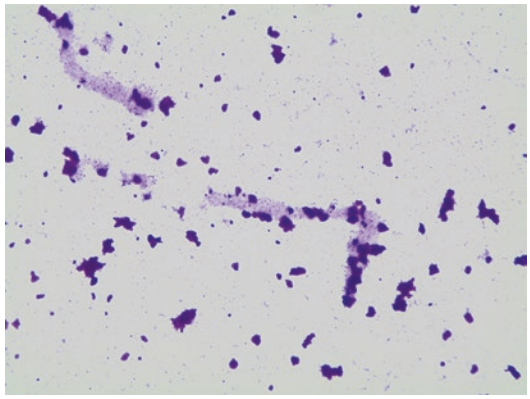

**Fig. 11.9** (Giemsa stain, low power). Clumps of metachromatic, granular material characteristic of ultrasound gel partly obscure the slide.

separate them from hyphae. Examination under polarized light may also be helpful, as some fibers are birefringent (Fig. 11.10b). Elastic and/or collagen fibers in specimens obtained by vigorous brushing or fine-needle aspiration may also mimic fungal hyphae but usually have rounded contours, which are not characteristic of fungus.

- Fibrin strands and red blood cells: Fibrin strands can resemble bacilli, fungal hyphae, or parasites (Fig. 11.10c). Features that help to distinguish fibrin from infectious organisms are its variability in size and shape, lack of structure, and thin fibrillary morphology. Red blood cell (RBC) ghosts can also mimic yeast

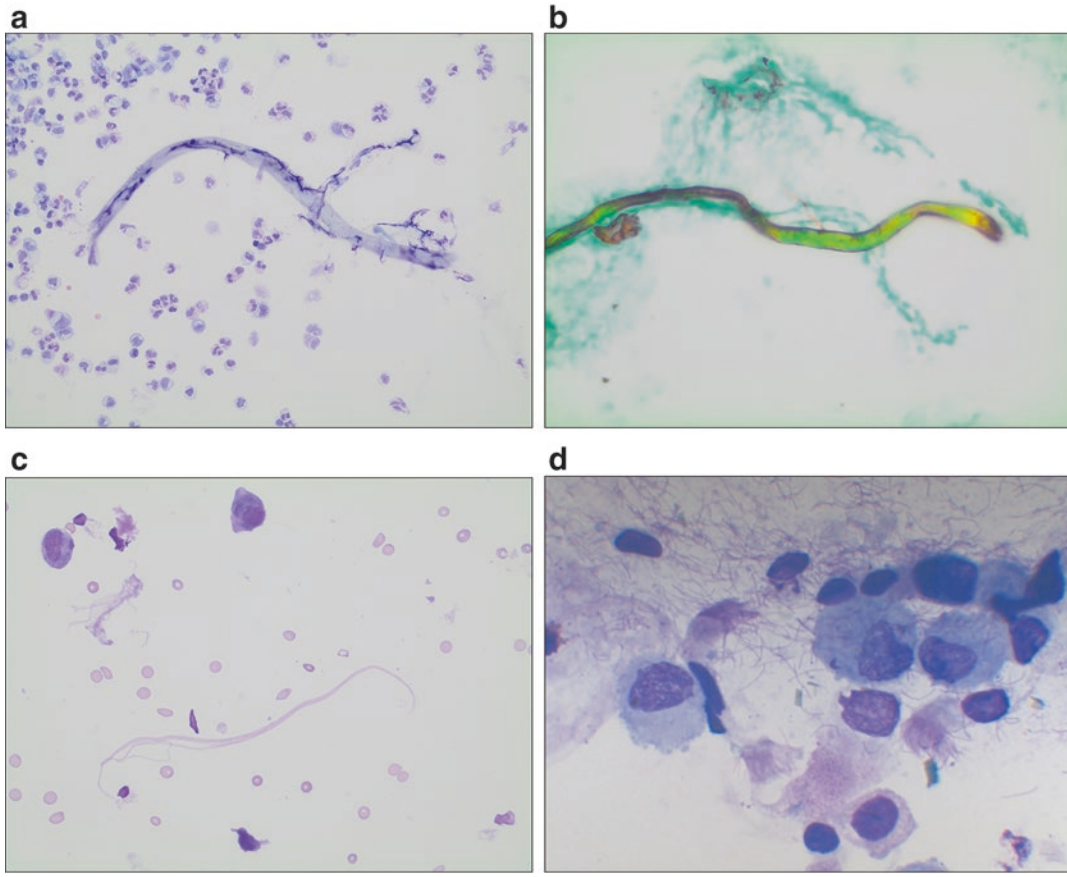


**Fig. 11.10** (**a**) (Giemsa stain, low power). A synthetic fiber in a BAL specimen mimics a fungal element or parasite. (**b**) (GMS stain, low power). A synthetic fiber is birefringent under polarized light, helping to distinguish it from fungi and parasites. (**c**) (Giemsa stain, medium power). Fibrin strands can mimic chains of bacteria or fungal hyphae. Characteristics of fibrin that help to distinguish it from microorganisms are its variability in size and shape, lack of structure and fibrillary morphology. (**d**) (Giemsa stain, high power). Detached cilia, as seen in this BAL from a patient with status asthmaticus, can mimic bacterial rods or ciliocytophthoria.

forms, particularly in erythrophagocytosis or dehemoglobinized specimens, such as ThinPrep™ preparations; however, in contrast to yeast, they should not stain with methenamine silver stains, such as GMS. Aberrant staining of RBCs with GMS occasionally occurs, but these cells lack the structure of true yeast and, when compared to the normal RBCs in the specimen, are morphologically similar.

- Detached cilia and ciliocytophthoria: Torn, detached cilia may be seen in great numbers in cytologic specimens from the respiratory tract, especially in asthmatic patients, and may be confused with bacterial rods (Fig. 11.10d) [3]. Detached cilia should be distinguished from ciliocytophthoria, which is seen in association with viral infections and is characterized morphologically by cellular degeneration and separation of entire ciliary tufts from degenerated cells.
- Plasma cell immunoglobulin: Russell bodies and immunoglobulin within Mott cells can stain with GMS and, thus, may mimic yeast [4], especially when the inclusions are multiple, in the same cell, or in cells in close proximity of each other, thereby resembling budding yeast (Fig. 11.11a, b).
- Other cytoplasmic material: Other cytoplasmic structures, such as mast cell granules,

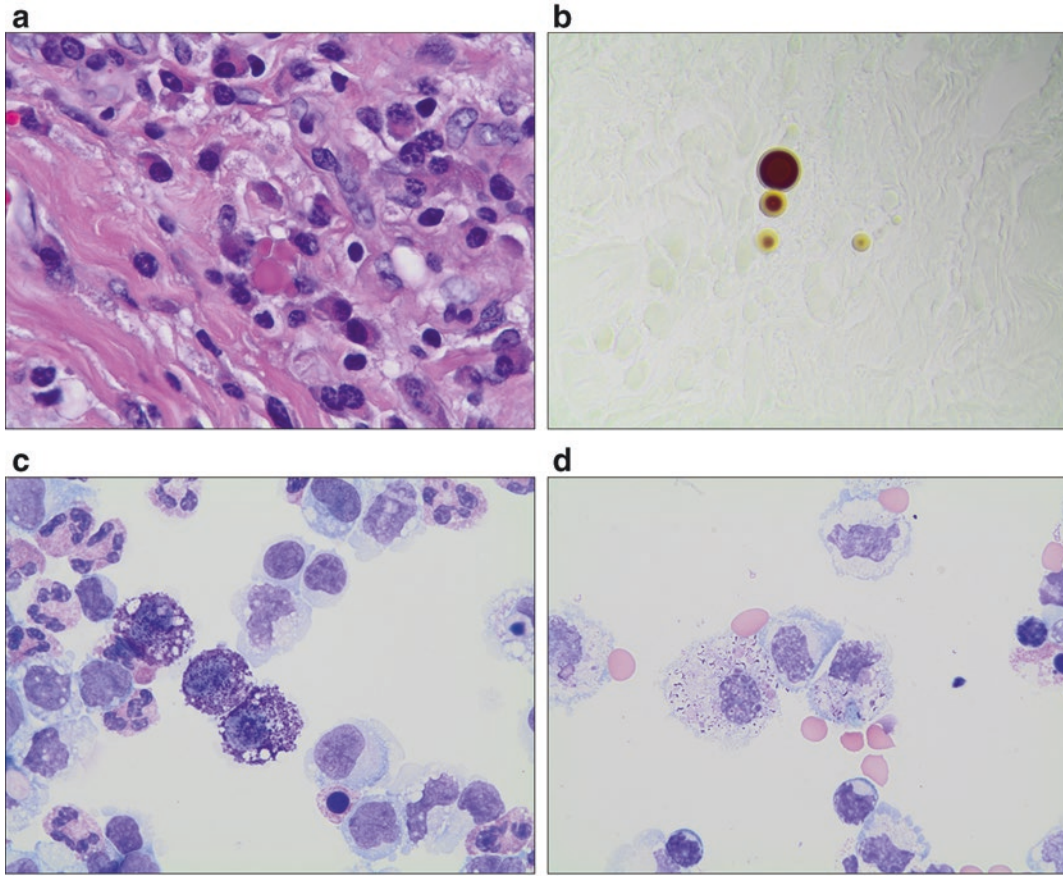


**Fig. 11.11** (**a**) (H&E stain, high power) and (**b**) (GMS stain, high power). Russell bodies appear as homogeneous, glassy, eosinophilic inclusions in plasma cells and usually easily recognized with routine stains (**a**). However, they also stain with GMS, and in GMS-stained preparation may mimic budding yeast, especially when they are multiple and close together. (**c**) (Giemsa stain, high power). Mast cells have coarse granules that mimic intracellular bacterial cocci. (**d**) (Giemsa stain, high power). Cellular debris and cytoplasmic granules within macrophages can also mimic organisms, such as bacteria or yeast.

basophil granules, and phagocytized cell debris, may mimic the appearance of bacteria (Fig. 11.11c, d).

- Cytoplasmic tails or "panhandle" distortion: Some cells (e.g., monocytic cells) possess abundant cytoplasm, which may appear elongated, mimicking fungal hyphae (Fig. 11.12a).
- Calcifications: Calcifications within some lesions (e.g., chondroblastomas) can be thin and delicate (so-called "chicken-wire" calcification) and mimic branching fungal hyphae (Fig. 11.12b).
- Mucus: Curschmann spirals from mucus in respiratory specimens can sometimes mimic parasites, synthetic fibers, tissue fibrils, or fungal hyphae. However, they are typically metachromatic and spiral shaped, features that are usually not seen in infectious organisms and synthetic fibers, and, moreover, lack the flat or frayed edges of fibers and the structure of fungal hyphae and parasites.

### 11.4.2 Atypical or Altered Morphology of Organisms

- Dying and degenerated bacteria: Dying bacteria, especially those with a capsule, may swell and appear larger (Fig. 11.13a). This may lead to confusion with fungal yeast forms. Exposure

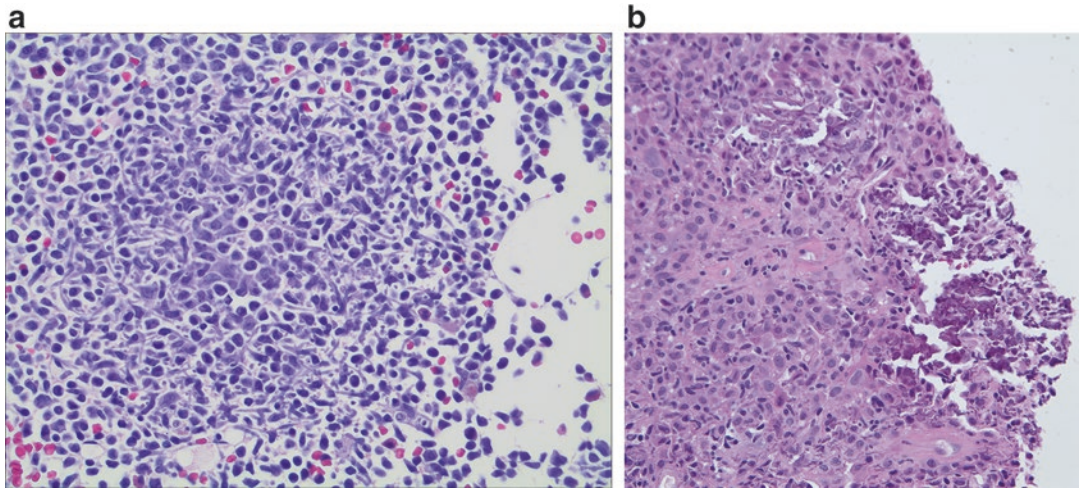


**Fig. 11.12** (**a**) (H&E stain, medium power). The distorted monoblasts from a case of acute myelomonocytic leukemia have long cytoplasmic tails or "pan-handles" that mimic fungal hyphae, while round fragments of disrupted cytoplasm mimic yeast forms. (**b**) (H&E stain, medium power). Chicken-wire calcifications, as seen in this chondroblastoma, can also mimic branching fungal hyphae. (Image courtesy of Dr. Sara Monaco).

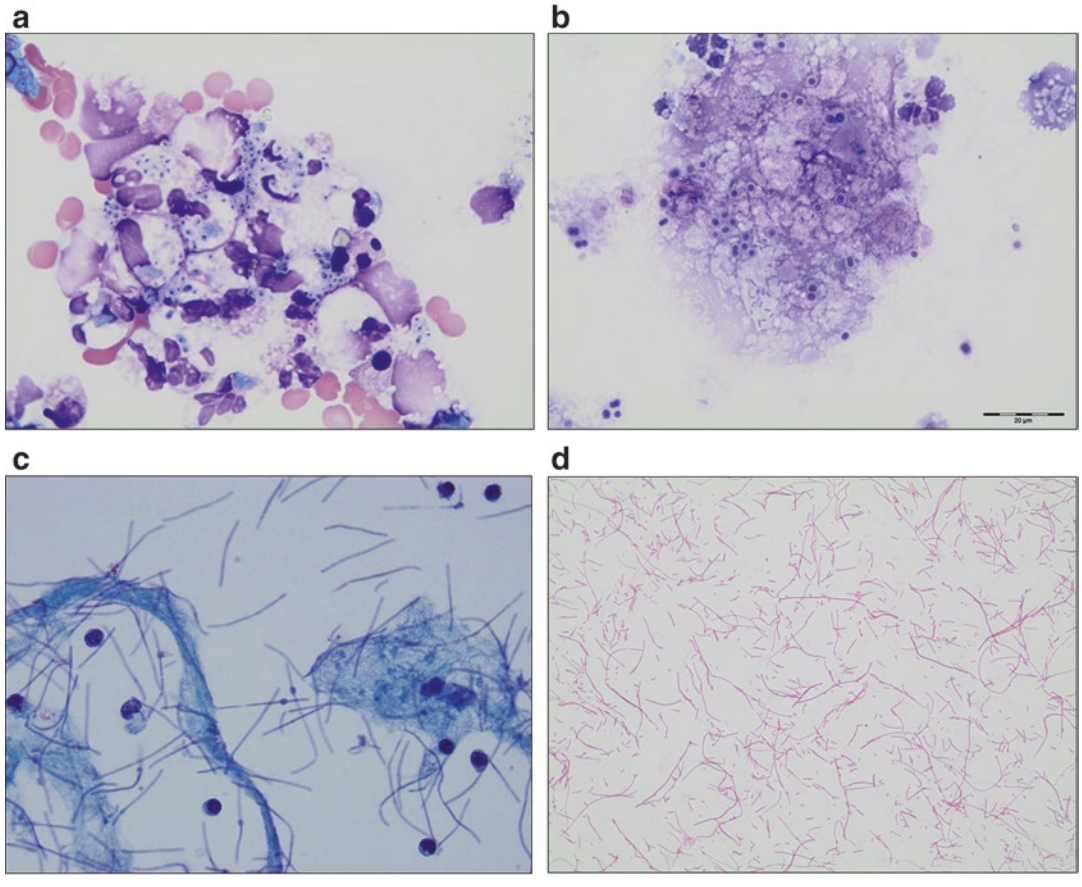


**Fig. 11.13** (**a**) (Giemsa stain, high power). The swollen, dead, or dying bacterial cocci, many of which are within macrophages and neutrophils, mimic small yeast forms. (**b**) (Diff-Quik stain, high power). Following exposure to antibiotics, some of the bacteria retain the rod-shaped morphology characteristic of viable *Pseudomonas aeruginosa*, while the large, round altered bacteria with prominent capsules mimic yeast forms. (**c**) (Gram stain, high power). Gram negative rods after exposure to a beta-lactam antibiotic appear filamentous, and some have round node-like structures. (**d**) (Gram stain, medium power). After exposure to antibiotics, these *E. coli* have filamentous morphology.

to antibiotics may also result in dramatic morphological changes in bacteria, including some rods appearing coccoid (Fig. 11.13b) and others appearing filamentous (Fig. 11.13c, d) due to the inability to divide [5].

### 11.4.3 Organisms with Morphological Overlap

- Hyphae vs. pseudohyphae: Pseudohyphae of some yeast, such as *Candida* (Fig. 11.14a, b), can be misconstrued as true hyphae of *Aspergillus* or other fungal organisms (Figs. 11.14c and 11.15). Table 11.3 lists morphologic features that can help separate hyphae from pseudohyphae [6]. In difficult cases, an immunostain for *Aspergillus* may help to confirm or exclude the presence of that organism.
- Bacteria-mimicking hyphae: Some filamentous bacteria bear a morphologic resemblance to fungi (Fig. 11.12d). In addition, antibiotic treatment may cause bacteria to replicate without complete division and simulate fungi [7].
- *Histoplasma* vs. *Pneumocystis*: In the context of respiratory specimens, *Histoplasma capsulatum* and *Pneumocystis* may be difficult to distinguish from each other (Fig. 11.13). Table 11.4 lists major characteristic features of both organisms [8].

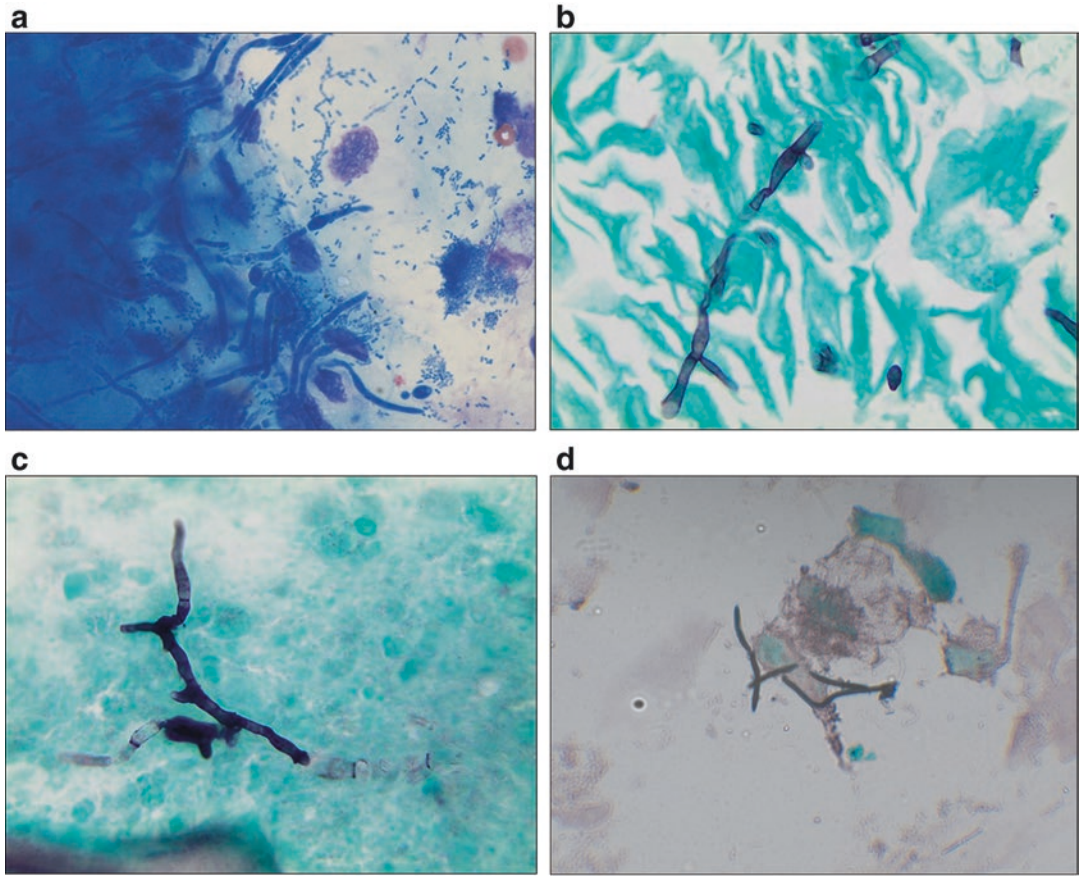


**Fig. 11.14** (**a**) (Diff-Quik stain, high power). The pseudohyphae of *Candida* can mimic the septate hyphae of *Aspergillus*. (**b**) (GMS stain, high power). Pseudohyphae of *Candida* showing the "sausage-link" constrictions and folding that mimic septation. (**c**) (GMS stain, high power). Branching septate hyphae of *Aspergillus* have uniform width and parallel walls. (**d**) (GMS stain, high power). Bacterial rods can mimic fungal hyphae on a GMS stain.

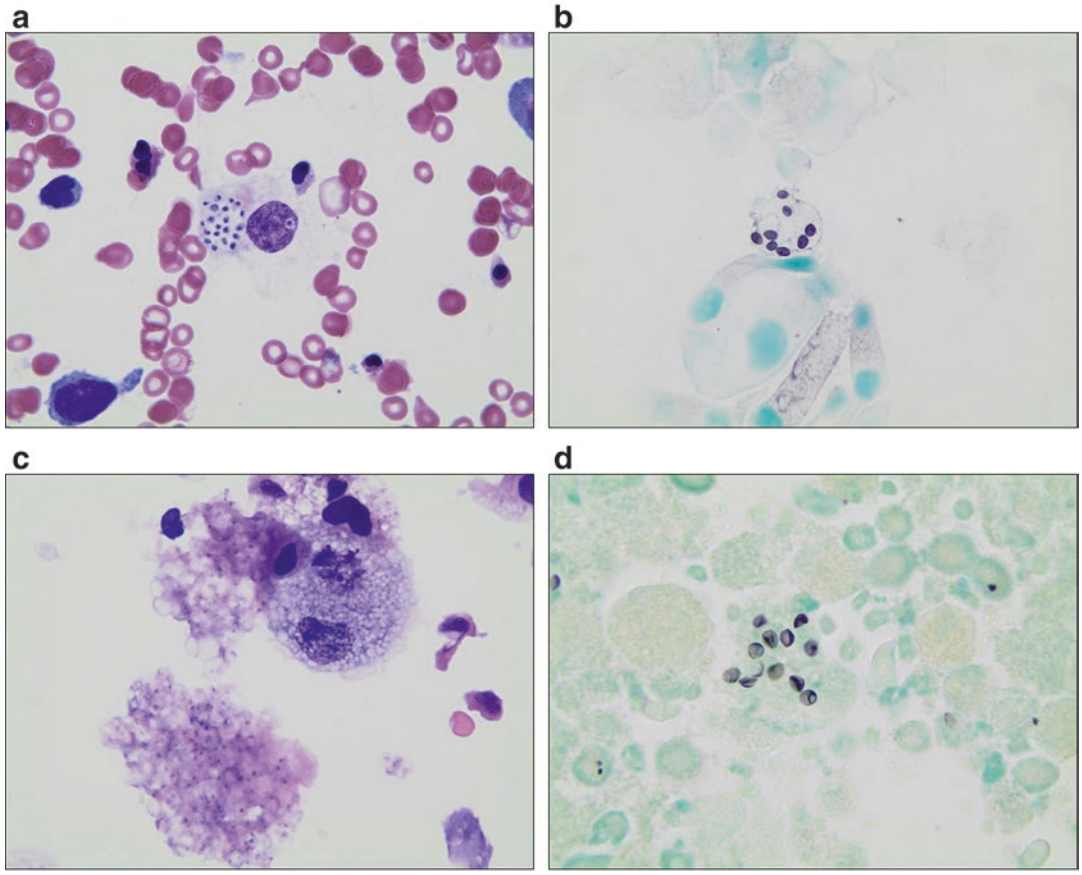


**Fig. 11.15** (**a**) (Giemsa stain, high power) and (**b**) (GMS stain, high power). Yeast forms of *Histoplasma capsulatum* are present within the cytoplasm of macrophages. These organisms are small (2–4 $\mu$m) and are almost always intracellular. (**c**) (Giemsa stain, high power) and (**d**) (GMS stain, high power). On the Giemsa stain (**c**), the cysts of *Pneumocystis* appear as optically clear spaces or foamy casts. Cysts appear cup shaped on GMS stain (**d**), which highlights the cyst walls.

**Table 11.3** Morphologic comparison between hyphae and pseudohyphae

| Hyphae of *Aspergillus* | Pseudohyphae of *Candida* |
|---|---|
| Regular width with parallel walls | Variable width due to constrictions/budding |
| Regular septation | Irregular pseudohyphae with constriction at pseudosepta (sausage-link appearance) |
| Branching at 45° angles | Irregular budding that mimics branching |
| GMS positive | GMS positive |
| Aspergillus immunostain positive | Aspergillus immunostain negative |

**Table 11.4** Cytologic features of *Histoplasma capsulatum* and *Pneumocystis*

| *Histoplasma capsulatum* | *Pneumocystis* |
|---|---|
| Round or oval organisms (from 2 to 4 μm) | Round, oval to crescent-like (4–7 μm) |
| Pseudocapsule and/or buds | No buds or capsule |
| Predominantly intracellular (macrophages) | Extracellular |

## 11.5 Conclusion

Artifacts, contaminants, and mimics can make the evaluation of cytologic specimens challenging and may necessitate secondary review by another pathologist or further workup with ancillary studies to exclude a true pathogen or abnormality. Awareness of these potentially confounding elements and their morphological appearance can help to prevent diagnostic errors, as well as unnecessary testing and/or additional sampling.

## References

1. Almarzooqi S, Leber A, Kahwash S. Artifacts and organism mimickers in pathology: case examples and review of literature. Adv Anat Pathol. 2010;17:277–81.
2. Boggio RR, Zaorske DA, Powers CN. Fresh fixed versus air dried FNA biopsy specimen. Lab Med. 1999;30:18–9.
3. Almarzooqi S, Kahwash SB. Detached respiratory cilia: an organism mimicker in BAL specimens. Adv Anat Pathol. 2011;18:414.
4. Haensch R, Seeliger H. Problems of differential diagnosis of blastomyces and Russell bodies. Arch Dermatol Res. 1981;270:381–5.
5. Healy DP, Gardner JC, Puthoff BK, Kagan RJ, Neely AN. Antibiotic-mediated bacterial filamentation: a potentially important laboratory phenomenon. Clin Microbiol Newsl. 2007;29:22–4.
6. Koneman EW. The appearance of fungi in tissues. Lab Med. 2002;12:927–34.
7. Sutton BJ, Parsons AC, Palavecino EL. Filamentous bacteria masquerading as fungi: a diagnostic pitfall in direct smear interpretation with report of two cases. J Clin Pathol. 2011;64:927–9.
8. Larone DH. Medically important fungi: a guide to identification. 5th ed.; ASM Press 2011. p. 48–9 and 59.

# Index





S.E. Monaco, L.A. Teot (eds.), *Pediatric Cytopathology*, DOI 10.1007/978-3-662-53441-0